NANOTR-20

20th NANOSCIENCE AND NANOTECHNOLOGY CONFERENCE

26 - 28 August 2026, İzmir Institute of Technology, İzmir, Türkiye



Book of Abstracts

Prof. Dr. Suna Timur
Conference Co-Chair
Ege University

Prof. Dr. Cem Çelebi
Conference Co-Chair
İzmir Institute of Technology

Organizers

NanoTR-20 Book of Abstract

Publisher	: İzmir Institute of Technology (IZTECH)
Edited by	: Prof. Dr. Suna Timur, Prof. Dr. Cem Çelebi
Composition	: Arber® Congress Solutions
Content	: The Abstract submission, reviewer evaluation and content process has been handled by ***MeetingHand Online Event Management Software*** https://meetinghand.com

The organizers do not have any legal liability for the contents of the abstracts.

Plenary Speakers



Mete Atatüre

University of Cambridge



Luis Lorenzo Sánchez-Soto

Universidad Complutense de Madrid (UCM)



Gerd Leuchs

Friedrich-Alexander-Universität Erlangen-Nürnberg



Ali Çırpan

Middle East Technical University (METU)

Invıted Speakers



Çekdar Vakıf Ahmetoğlu

Technical University of Berlin



Ülkü Anık

Mugla Sitki Kocman University



Selmiye Alkan Gürsel

Sabancı University & SUNUM



Derya Baran

King Abdullah University of Science and Technology (KAUST)



Remzi Becer

University of Warwick



Levent Beker

Koç University



Julie Marie Bekkevold

Thermo Fisher Scientific



Arif E. Çetin

İzmir Biomedicine and Genome Center



Fabienne Dumoulin

Acıbadem University



Erçin Çağan Duran

Istanbul Technical University



Özgür Duygulu

TUBITAK MAM



Batur Ercan

Middle East Technical University



Emre Erdem

Sabancı University



Ceyda Öksel Karakuş

İzmir Institute of Technology (IZTECH)



Ali Koşar

Sabancı University



Alina Manshina

St. Petersburg State University



Özgür E. Müstecaplıoğlu

Koç University



Mustafa Ordu

Bilkent University, UNAM



Sibel A. Özkan

Ankara University



Onur Parlak

Karolinska Institutet



Khaled Nabil Salama

King Abdullah University of Science and Technology (KAUST)



Giovanni Scala

Politecnico di Bari



Y. Eren Suyolcu

Max Planck Institute



H. Emrah Ünalan

Middle East Technical University



M. Selim Ünlü

Boston University, IRIS Kinetics, & Istanbul Atlas University



Funda Yağcı Acar

Koç University



Yasemin Yüksel Durmaz

İstanbul Medipol Univesity

NANOTR-20® SPECIAL EVENT

Advanced Electron Microscopy Workshop

Journey to the world of atoms



Julie Marie Bekkevold

Thermo Fisher Scientific

4D-STEM: Expanding the Analytical Capabilities of STEM



Özgür Duygulu

TUBITAK MAM, Türkiye

HRTEM Investigations on Magnesium Alloys



Erçin Çağan Duran

Istanbul Technical University, Türkiye

Sharper Eyes, Deeper Insights: Advances in TEM Electron Diffraction for Nanoscale Crystallography



Y. Eren Suyolcu

Max Planck Institute for Solid State Research, Germany

Atomic-Scale Insights into Oxide Heterostructures via Aberration-Corrected STEM

Special Program: Visit to the IZTECH Integrated Research Centers & Live Electron Microscopy Demo

Hands-on demonstration on the most advanced Electron Microscope in Türkiye at the IZTECH Central Research Laboratory. Attendees will observe live imaging of nanoscale specimens and interact with the instrument operators.

INCLUDED IN

Workshop Program

SPONSORED BY

TEKAFOS TEKNOLOJİK SİSTEMLER

NANOTR-20® SPECIAL EVENT

QuantumTR Symposium

From Theory to Cutting-edge Technologies



Luis Lorenzo Sánchez-Soto

Universidad Complutense, Spain
Max-Planck-Institut, Germany
Chapman University, USA

Experimental evidence-based sub-Rayleigh source discrimination



Gerd Leuchs

Friedrich-Alexander-Universität, Germany
Max-Planck-Institut, Germany
University of Ottawa, Canada

For every weak light field one can detect the quantum nature - measuring the commutator of the field operators



Alina Manshina

St. Petersburg State University, Russia

Bridging Light and Medicine: advances in photoswitchable and bioactive molecules and their luminescent nanohybrids



Özgür Esat Müstecaplıoğlu

Koç University, Türkiye

Design Strategies for Quantum Sensor Networks in Thermometry and Magnetometry



Giovanni Scala

Politecnico di Bari, Italy

Entanglement Certification from Randomized Measurement

Organizing Committee

- Oğuz Gülseren, Bilkent University, NanoTR Community Chair
- Antonio Di Bartolomeo, University of Salerno
- Coşkun Kocabaş, University of Manchester
- Emine Güler Çelik, Ege University
- Esat Arber, MeetingHand
- Figen Zihnioğlu, Ege University
- Filiz Kuralay, Hacettepe University
- H. Emrah Ünalan, Middle East Technical University
- Kemal Davut, İzmir Institute of Technology
- Kerem Tok, Ege University
- Mehmet Polat, İzmir Institute of Technology
- Mehmet Z. Baykara, University of California
- Ömer Aydın, Erciyes University
- Onur Büyükçakır, İzmir Institute of Technology
- Özgür Müstecaplıoğlu, Koç University
- Saniye Söylemez, Necmettin Erbakan University
- Steven R. Schofield, University College London
- Şerife Tozan Rüzgar, Ege University

Scientific Committee

- Adil Denizli, Hacettepe University
- Ali Koşar, SUNUM, Sabancı University
- Alpan Bek, Middle East Technical University
- Amitav Sanyal, Boğaziçi University
- Arif Engin Çetin, İzmir Biomedicine and Genome Center
- Ayşe Bayrakçeken, Ataturk University
- Ayşegül Uygun Öksüz, Süleyman Demirel University
- Batur Ercan, Middle East Technical University
- Binnur Aydoğan Temel, Bezmiâlem Vakıf University
- Bora Garipcan, Bogaziçi University
- Burcu Akata Kurç, Middle East Technical University
- Caner Ünlü, İstanbul Technical University
- Cem Sevik, University of Antwerp
- Ceylan Zafer, Ege University
- Emrah Özensoy, Bilkent University
- Ender Suvacı, Eskişehir Technical University
- Engin Durgun, UNAM - Bilkent University
- Erdem Alaca, Koç University
- Erem Bilensoy, Hacettepe University
- Erol Yıldırım, Middle East Technical University
- Evren Mutlugün, Abdullah Gül University
- Fabienne Dumoulin, Acıbadem University
- Fatih İnci, Bilkent University
- Feridun Ay, Eskisehir Technical University
- Filiz Kuralay, Hacettepe University
- Gökhan Demirel, Gazi University
- Göknur Cambaz, Drexel University
- Gülay Ertaş, Middle East Technical University
- H. Volkan Demir, Bilkent University
- Hakan Usta, Abdullah Gül University
- Umut Bulut, Acıbadem University
- Hatice Duran, TOBB Economy & Technology University
- Hatice Kaplan Can, Hacettepe University
- İskender Yılgör, Koç University
- İsmet İnönü Kaya, Sabancı University
- Levent Trabzon, Istanbul Technical University
- Lokman Uzun, Hacettepe University
- Mehmet Özsöz, Near East University
- Mehmet Yağmurcukardeş, İzmir Institute of Technology
- Memed Duman, Hacettepe University
- Mehmet Sarıkanat, Ege University
- Metin Ak, Pamukkale University
- Mustafa Çulha, Sabancı University
- Mustafa Kemal Sezginturk, ÇOMU
- Muhammet U Kahveci, İstanbul Technical University
- Nurdan Demirci Şankır, University of Economics & Technology
- Osman Barış Malcıoğlu, Middle East Technical University
- Özgür Birer, ASELSAN
- R. Tuğrul Senger, İzmir University of Economics
- Recep Yüksel, Eskişehir Osmangazi University
- Said Ergoktas, University of Bath
- Şefik Süzer, Bilkent University
- Salih Özçubukçu, Middle East Technical University
- Selim Hanay, Iberian Nanotech. Lab. & Bilkent University
- Selmiye Alkan Gürsel, Sabancı University
- Serdar Önses, Erciyes University
- Serpil Tekoğlu, Johannes Kepler University of Linz
- Süleyman Özçelik, Gazi University
- Talha Erdem, Abdullah Gül University
- Taner Akbay, Yeditepe University
- Taner Yıldırım, National Institute of Standards and Technology (NIST)

Sponsors

Platin Sponsor











Gold Sponsors









Bag Sponsor



Exhibitors













Academic Access Sponsorships













Preface

Dear Colleagues,

It is our great pleasure to welcome you to the **20th International Nanoscience and Nanotechnology Conference (NanoTR-20)**, held at the **İzmir Institute of Technology, Gülbahçe–İYTE Campus, Urla, İzmir**, on **26–29 August 2026.**

Since its first meeting in 2005, the NanoTR series has grown into the principal annual gathering of the nanoscience and nanotechnology community in Türkiye, and into a meeting point for colleagues from across the region and beyond. Reaching the twentieth edition is a milestone that belongs to everyone who has contributed to the series over the past two decades — the researchers who presented their work, the institutions that hosted the meetings, and the students who found their first scientific audience here.

This volume brings together the abstracts accepted for NanoTR-20. The programme comprises more than 460 oral and poster presentations from over 600 registered participants, spanning nanomaterials, nanophotonics, nanobiotechnology, energy and environmental applications, computational approaches, and characterization methods. Alongside the main parallel sessions, the conference hosts the QuantumTR Symposium, dedicated to quantum science and technologies, and the Advanced Microscopy Workshop, a new side event chaired by Assoc. Prof. Dr. Kemal Davut. Our plenary programme features Mete Atatüre, Luis L. Sánchez-Soto, Gerd Leuchs, and Ali Çırpan, whose lectures frame the breadth of the field represented in these pages.

Every abstract in this book was reviewed by members of the Scientific Committee, and we are grateful to them for the care they gave to that work. We also thank İzmir Institute of Technology for hosting the conference, our sponsors and supporters for making it possible, and the Organizing Committee and student volunteers whose efforts are visible in every detail of these four days.

Above all, we thank you, the authors and participants. The value of a conference lies in the conversations it starts, and we hope that the abstracts collected here will be the beginning of many of them.

We wish you a productive and enjoyable meeting in İzmir.

With warm regards,

On behalf of the Organizing CommitteeOn behalf of the Organizing Committee



Prof. Dr. Suna Timur

Conference Co-Chair
Ege University



Prof. Dr. Cem Çelebi

Conference Co-Chair
İzmir Institute of Technology

Table of Contents

Multifunctional Conjugated Organic Materials for Energy Harvesting, Energy Storage, and High-Performance OLED Applications
Ali Çırpan 1

Measuring quantum properties of thermal light
Gerd Leuchs 2

Interferometric Sensing: From Multiplexed Affinity to Digital Detection of Biomolecules
M. Selim Ünlü 3

The Role of Nanomorphology in Organic Semiconductors for Electronic Devices
Derya Baran 4

Cavitation on a Chip Devices with Functional Surfaces and Emerging Applications
Ali Koşar 5

Nanozing phthalocyanines for health and environment
Fabienne Dumoulin 6

Bridging Light and Medicine: advances in photoswitchable&bioactive molecules and their luminescent nanohybrids
Alina Manshina, Gulia Bikbaeva, Anastasia Egorova, Ilya Kolesnikov, Tatiana Dolenko, Anna Pilip 7

Nanoscale Mimicry of Virus–Host Interactions: Redefining Biosensing Strategies for Infectious Disease Diagnostics
Ülkü Anık 8

SiOC Aerogels: Impact of Nanoscale Porosity on Properties
Cekdar Vakif Ahmetoglu 9

Fiber-Based Nanogenerators for Advanced Wearable Technologies
Mustafa Ordu 10

4D-STEM: Expanding the Analytical Capabilities of STEM
Julie Marie Bekkevold 11

HRTEM Investigations on Magnesium Alloys
Özgür Duygulu, Gizem Oktay Irmak, Ömür Can Odabaş 12

Sharper eyes, deeper insights: Advances in TEM electron diffraction for nanoscale crystallography
Ercin Cagan Duran 13

Hybrid Nanomaterial-Molecularly Imprinted Polymer Platforms for Advanced Electrochemical Sensing
Sibel A. Özkan 14

Triboelectric Nanogenerators for Wearable Electronics, Self-Powered Sensing, and Sustainable Energy Harvesting
Hüsnü Emrah Ünalan 15

Third-Order Local Randomized Measurements for Finite-size Entanglement Certification
Giovanni Scala 16

Biomedical Applications of Nanotechnology: Current Status and Future Directions
Ceyda Öksel Karakuş 17

Shaping Green Hydrogen Technologies: Graphene-Based Electrocatalysts and Transition Metal–Modified Iridium Oxides for PEM Fuel Cells and Electrolyzers
Selmiye Alkan Gürsel, Hamza Arslan, Bahadır Patır, Büşra Çetiner, Naeimeh Rajabalizadeh Mojarrad, Begüm Yarar Kaplan, Alp Yürüm, Navid Haghmoradi, Sina Abdolhosseinzadeh, Ahmet Can Kırlıoğlu, Eser Dinçer Hafızoğlu, Aysel Zahidov, Vahide Nuran Mutlu 18

From Photonics to Intelligent Lab Infrastructure
Arif E. Cetin 20

Probing Defect Structures in Nanomaterials: Insights through EPR Spectroscopy for Supercapacitor Applications
Emre Erdem 21

Epidermal Sensors for Medical Diagnostics and Therapy
Onur Parlak 22

Engineering Nanoparticles for Histotripsy: Advancing Non-Invasive Cancer Ablation and Combination Therapy
Waleed Mustafa, Sarah Hall, Mohamad Abu Chakra, Ibtisam Naser, Semih Macit, Özge Şensoy, Eli Vlaisavljevich, Yasemin Yüksel Durmaz 23

Quantum Materials by Design: Atomic-Scale Synthesis, Imaging and Spectroscopy
Y. Eren Suyolcu 24

Entanglement Generation in Qubit Networks via Collision Model
Elif Yunt 25

Toward Scalable Transmon Qubits: Fabrication and Characterization of CPWs, Josephson Junctions, and SQUIDs.
Mehmet Kahraman, Ege Selvi, Süleyman Çelik, İsmet Kaya 26

Transforming Fluorescence from Interference to Opportunity: Photonic Crystal and Hybrid Photonic–Plasmonic Platforms for Enhanced Raman Biosensing
Fatma Uysal Ciloglu, Fatma Uysal Ciloglu, Seemesh Bhaskar, Brian T. Cunningham 27

A microfluidic single-bacteria isolation, enrichment, and characterization device for probiotic strain selection
Didem Rodoplu Solovchuk, Chien-Hsun Huang, Jong-Shian Liou, Chia-Hsien Hsu 28

Electrochemical determination of insecticides and herbicides in surface waters and environmental monitoring of fluorine and chlorine halogens
Ozge Surucu 29

Cyclodextrin-Based Drug Delivery Systems for Improved Solubility and Prolonged Ocular Delivery of Hydrophobic Drugs
Monireh Esmaeili Rad, Yusuf Menceloğlu, Meral Yuce 30

Nanostructured Layer-by-Layer Hexosomes for Improving the Stability and Bioaccessibility of Omega-3 Fatty Acids
Gokce Dicle Kalaycioglu, Zahra Eskandari, Seyed Fakhreddin Hosseini, Anan Yaghmur 31

Synthesis and Characterization of Magnetic Nanoparticles and Investigation of Their Ferroptosis-Related Biological Effects on Lung Cancer Cells
Kübra Solak, Adem Kara, Ahmet Mavi 32

Development of Cationic Hydrogel Modified with Gold Nanoparticles as a Wound Dressing Material
Emine Büşra Eker, İlknur Atlı, Özgür Özay 33

Effect of Synthesis Route on Lanthanum Removal Performance of Ce/Urea-Doped Carbon Quantum Dots Derived from Pleurotus Ostreatus
Berkant Senturk, Sabriye Yusan 34

Dynamic Behaviour of Oil–Water Interfaces and Acoustic-Enhanced Waterflooding In A Reservoir-On-Chip Micromodel
Faruk Aksoy, Gurkan Yesiloz 35

Ethylenediamine and Polyethylenimine-Functionalized ZIF-8 Prepared by Wet Impregnation and Heating Reflux: Effect of Functionalization Route in CO_2 Adsorption Performance
Tuğba Çakır, Can Erkey, Hamed Yousefzadeh 36

Sub-100 nm Ti-MIL-125 Nanoparticles for Efficient Phosphate Removal From Water
Elif Gökçen Dilci, Ömer Faruk Eşit, Zeyneb Sultan Güneysu, Sarper Ozan Kelleci, Selis Önel 37

New Generation Emergency Water Purification Equipment Containing Nanotitania and The Effect of Nanomorphology Alteration on Filtration Performance
Boğaç Kılıçarslan, Merve Gültekinoğlu, Cem Bayram 38

Preconcentration and Light Scattering-Based Approach for Rapid Estimation of Marine Nanoparticle Concentrations
Naim Yağız Demir, Emre Büküşoğlu, Mustafa Yücel 39

Effect of GO Nanofiller Concentration on the Dielectric Properties of GO–PVA–AgNW Nanocomposites
Mahammad Baghir Baghirov, Mustafa Muradov 40

Thiophene- and Dicyanothiophene-Bridged Conjugated Polymers for V2O5 Nanowire-Based Asymmetric Hybrid Supercapacitor Devices
Sedanur Şahinaslan, Elif Demir Arabacı, Oğuzhan Karakurt, Eda Çevik, H. Emrah Ünalan, Ali Çırpan, Ali Çırpan, Ali Çırpan, Ali Çırpan 41

Experimental Evaluation Of Adhesion In Poly(4-vinylpyridine) Thin Films Deposited By Initiated Chemical Vapor Deposition
Çağrı Sayın, Azizeh Hosseinjany, Gözde Özaydın İnce 42

Structural and Electronic Properties of Plasmonic Metal (Al, Au, Ag) Doped CaTiO3
Dilara Köroğlu, Veli Ongun Özçelik 43

Hybrid Thermally Conductive Filler-Reinforced Polyketone Composites for Advanced Thermal Energy Management
Lutfiye Altay, Mehmet Sarıkanat, Mehmet Mete Tokgoz, Yoldas Seki 44

Fabrication of Melamine-Formaldehyde-Organic Clay Nanocomposites and Mineral-Filled Hybrid Composites
Elif Şahin, Ahmet Gürses, Salih Akpınar, Nurtaç Canpolat 45

Engineering the Local Density of Optical States for Programmable Quantum Mode Switching
Emre Ozan Polat 46

Interfacial Defect Passivation of SnO_2 Using L-Methionine toward High-Performance Perovskite Solar Cells
Mohammad Javad Azimi Igdır, Suleyman Ozel, Erdi Akman, Faruk Ozel 47

Thickness-Controlled Photoluminescence and Vibrational Signatures in Layered LiInP2S6: A DFT Study
Ömer Nevzat Kösebay, Can Çoruh, Berna Akgenc Hanedar 48

Polaronic Excitons in Quantum Well Perovskite Structures
Sinem Duman, R. Tuğrul Senger 49

A Standalone Optofluidic “Smart Analyzer” for Adaptive Multi-Chip Plasmonic Sensing
Damla Aydogan, Cem Gok, Seda Nur Topkaya, Arif E. Cetin 50

Structural and Photophysical Properties of Microwave-assisted Synthesized Mo,N Co-doped Carbon Quantum Dots
İbrahim Yağız Coşkun, Caner Ünlü 51

Dopant-Controlled Reversible Carrier-Polarity Switching in SnSe Thermoelectric Materials
Mehmet Ozdogan, Thomas Iken, Carlos Munoz, Deniz Cakir, Nuri Oncel 52

Cyano-Modified Ethynyl-Bridged Carbazole Emitters for Efficient Blue Oleds
Esra Yenidoğan, Ozan Tekin, Erol Yıldırım, Selçuk Gümüş, Gönül Hızalan Özsoy, Erkan Aksoy, Ali Çırpan, Ali Çırpan, Ali Çırpan, Ali Çırpan 53

Potassium-Ion Redistribution and Resistive Switching in Ultrathin KxWO3 Single-Crystal Nanobelts
Abdulsalam Aji Suleiman 54

A Novel Benzodithiophene-Based Donor Polymer for Semitransparent Ternary Organic Solar Cells
Duygu Yalvaç, Meltem Türkatar, Gönül Hızalan Özsoy, Ali Çırpan, Ali Çırpan, Ali Çırpan, Ali Çırpan 55

Enhancing the Tribological Performance of Al2O3 Ceramics via MOF-derived Nanocarbon Particle Additives
Umut Savacı 56

Time-Domain Mechanical Computing with Nanoelectromechanical Resonators
Filipe Alves, Humayun Ahmed, Inês Garcia, Alper Demir, Selim Hanay 57

Thermal Spreading Resistance Measurements in Microcontacts Formed by Indentation
Seda N. Sönmez, Ahmed Uluca, Graham L. W. Cross, H. Özgür Özer 58

A Knowledge-Guided, Drift-Aware Computer Vision Pipeline for Automated Pixel-Level Nanotribological Characterization in Atomic Force Microscopy
Tuana Karakoyun Barandır, Derya Gemici Deveci, Özhan Ünverdi, Cem Çelebi 59

Spatio-temporal Feedback in Active Matter: A Dynamic Activity Field Model for Brownian Swimmers
Livio Carenza, Brandon James Fasy, Marcos Gouveia, Giuseppe Negro 60

Compact FPGA-Based Voice Classification Using Physical Reservoir Computing and Posit-Based MAC Operations
Ahmet Karacali, Xu Muzhen, Yuki Usami, Hirofumi Tanaka 61

From Flat Bands to Dirac Cones: Symmetry-Tunable Electronic States in Bilayer Kagome Lattices
Taylan Görkan, Doğukan Hazar Özbey, Cem Sevik, Milorad V. Milosevic, Engin Durgun 62

Characterization of Topological Defects in Confined Nematic Liquid Crystals
Taha Andaç, Aslı Karausta, Emre Büküşoğlu, Livio Nicola Carenza 63

Dynamic High-Q Membrane Metasurfaces for Infrared Spectroscopy, Sensing, and Light–Matter Interactions
Furkan Kuruoğlu, Samir Rosas, Yihong Chen, Brijesh Kumar, Shenwei Yin, Jin-Woo Cho, David A. Czaplewski, Yuri Kivshar, Mikhail A. Kats, Filiz Yesilkoy 64

Agronomic Potential of Green-Synthesized Cellulose Nanocomposites and Metal/Metal Oxide Nanoparticles: Implications for Crop Growth and Development
Lale Aktaş, Khairul Maghfirah Hasanah, Tugba Oztekin, Yigit Kucukcobanoglu 65

Nano lanthanum oxide enhances soybean yield and seed quality through earthworm driven rhizosphere engineering
Muhmmad Adeel 66

From Bio-Based Lignin to Smart Iron Delivery: Modified Lignin Nanoformulations for Foliar Biofortification of Soybean
Burak Özdemir, Zehra Sena Behram, Umit Baris Kutman, Hayriye Ünal, Serap Hayat Soytaş 67

Sustainable Carbon Quantum Dots from Pumpkin Biomass: Synthesis, Characterization, and Potential Use in Edible Antimicrobial Food Films
Selva Bilge, Berkay Korkmaz, Ayşe Karakeçili 68

Targeted Dual Phototherapy of Prostate Cancer with ALA-loaded SPIONs
Kübra Onbaşlı 69

Terminal Skeleton Engineering in Diketopyrrolopyrrole-Based Semiconductors for Tunable Optoelectronic Applications
Hilal Kalkan, Pınar Seyitdanlıoğlu, Barış Temelli 70

Dynamic Microneedle-Based SERS Interfaces for Localized Molecular Detection
Meryem Beyza Avci, Ayfer Aytac Arslan, Emrecan Yildiz, Gokhan Demirel, Arif E. Cetin 71

MRI-Visible Polymer Coating Solutions Based on Melanin Nanoparticles for Interventional Guidewire Applications
Khawaja Faheem Shahid, Uluç Pamuk, Gizem Kaleli Can, Engin Baysoy 72

Theoretical investigations on micro-cantilever sensitivity to external forces under single- and multi-frequency excitations in nanometrological applications
Cagri Yilmaz 73

Thermally Drawn Multilayer P(VDF-TrFE)/SnO_2 Piezoelectric Fibers for Flexible Self-Powered Sensing Applications
Vishwa Pratap Singh, Naci Enes Dirican, Deniz Berk Onuralp, Nurbolat Issatayev, Yersaiyn Busharov, Gulnur Kalimuldina, Mustafa Ordu, Sk. Rahat Ali 74

A Chirped Nanoplasmonic MIM Metasurface enables Spectrometer-free Refractometric sensing
Fahd Khalid-Salako, Fahd Khalid-Salako, Zeki Semih Pehlivan, Meral Yüce, Hasan Kurt, Hasan Kurt 75

Development of ZnO/CuO Nanofibers for Gas Sensing Applications
Elif Nur Karacan, Okan Özdemir, Onur Alp Aksan, Alp Kılıç, Nuray Kızıldağ, Serkan Büyükköse, Leyla Çoklarerol Arslan 76

Particle Morphology Control Through Liquid Metal Alloy Solidification
Mert Ulusel, Orçun Dinçer, Ozan Şahin, Simge Çınar Aygün 77

MXene-Assisted Enhancement of Hydrothermally Synthesized La2O3 Electrodes for Supercapacitors
İrem Nur Demirkol, Amira Gaber, Anas Abofoul, Selva Bilge 78

Green Synthesis of ZnO-Based Photoelectrochemical Materials via Tomato Peel Extract: Effects of Zinc Precursors on Stability and Photoactivity
Ceyda Çelik, Ufuk Erdoğan, Yunus Yener, Beren Anlaş, Serra Ersoy, Cengiz Kaya 79

Investigation of the Potential of ZnBO Memristors for Neuromorphic Computing
Gökhan Ekinci, Sümeyye Veziroglu, Fatih Mehmet Coşkun 80

Ionic Liquid Functionalized Magnetic Cu-MOF Nanocomposite for the Extraction and Determination of Pb(II), Cd(II), and Zn(II) in Environmental Water Samples
Duygu Totur Pamik, Serap Seyhan Bozkurt 81

Structural and Electrical Characterization of Diamond-Like Carbon Films Deposited on Flexible Cu and Mo Foil Substrates by RF-PECVD
Ali Altuntepe 82

Atomic Layer processing: enabling next-level processing for advanced nano technology applications
Gerd Jungmann 83

Recovered-Silver-Derived Cu@Ag Core–Shell Particles for Silver-Efficient HJT Solar Cell Metallization
Behiye Demirtas, Serdar Guler, Huseyin Utkucan Kayaci, Ilknur Ozbayrak, Onur Can Yurdakul, Seda Kilickaya Unver, Doga Doganay, Sahin Coskun, Simge Cinar Aygun, Bulent Arikan, Rasit Turan, Husnu Emrah Unalan 84

Waste-Fabric-Derived Carbon/ZnO Nanocomposite For Voltammetric Determination Of Monoferrocenylcyclotriphosphazene Derivatives
Anas Abofoul, Reşit Cemaloğlu, Selva Bilge, Nuran Asmafiliz 85

Nanofibrous Single-Layered Gas Diffusion Layers for Polymer Electrolyte Membrane Fuel Cells
Mustafa Altay Karacaoğlu, Furkan Çetiner, Serife Akkoyun, Selahattin Çelik 86

In-Situ Production of LiOH and H3BO3 from Lithium Tetraborate Solution by Using Bipolar Membrane Electrodialysis-Effect of Solution Concentration and Characteristics of Ion Exchange Membranes
Pelinsu Çamcı, Senay Çubukcuoğlu, Mert Deniz, Esra Altıok, Kamil Bostancı, Tülay Güngören Madenoğlu, Müşerref Arda, Nalan Kabay 87

Polarization and Humidity Effects in Ferroelectric α-In_2Se_3 for Mo-lecular Sensing Applications
Golibjon Berdiyorov, Abdelmajid Salhi, Brahim Aissa 88

Effect of Ag, Mn, and Ni Doping on the Structural, Morphological, Optical, and Photo-luminescence Properties of ZnO Nanopowders
Hayrunnisa Özer, Büşra Mutlu, Şeyma Duman 89

Anisotropy-Driven Evolution of Skyrmion and Meron Phases in Antiferromagnetically Coupled Bilayer Nanosystems
Gülşen Doğan, Ümit Akıncı 90

Quantum Phase Mapping In A Two-Dimensional Quasiperiodic Spin-1 Bose-Hubbard Model Using Order Parameters
Süleyman Küçük, Bilal Tanatar, Saurabh Basu 91

Electrochemical Behavior of Galvonastatic and Potansiostatic Mode Electrodeposited Tungsten Oxide Thin Films for Electrochromic Applications
Nisa Damla Tekin, Gamze Atak 92

Microstructured Thermally Drawn Triboelectric Fibers for Wearable Technologies
Maliha Rahman, Mustafa Ordu 93

Biocompatible and Wearable ZnO-Coated Hemp Woven Fabrics for Lightweight Electromagnetic Shielding in Defense Applications
Melisa Atay, Metin Yurddaskal, Mehmet Korkmaz 94

Myxinidin-Loaded UiO-66-NH_2 MOFs for Enhanced Antimicrobial Activity and Wound Healing
Bilge Ölçeroğlu, Şahika Sena Bayazit, Ahmet Katı, Fırat Barış Barlas 95

Targeted Lipid–Polymer Hybrid Nanoparticles Co-Loaded with 5-Fluorouracil and Surface-Conjugated Tocilizumab for Oral Squamous Cell Carcinoma: An In Vitro Therapeutic Evaluation
Ezgi Özdemir, Demet Cansaran Duman, Tuğrul Mert Serim, Gülin Amasya, Pelin Mutlu 96

Investigation of the Effects of Niosomal Forms of Passiflora incarnata Plant Extracts on Alzheimer's Disease Under In Vitro Conditions
Şevval Çiçek, Bilge Ölçeroğlu, Alper Filiz, Pınar Siyah, Kartal Çetintürk, Fırat Barış Barlas 97

Nanoscale Adhesion Forces of Naturally Dispersed Bacteria from Biofilms of Different Ages Measured by Atomic Force Microscopy
Buse Ece Burgaz Oral, Fatma Pinar Gordesli Duatepe 98

Size-Based Protein Separation via Capillary Flow on AKD-Hydrophobized Paper Gradients: An Equipment-Free Alternative to Electrophoresis
Tolga Erdoğan, Emine Güler Çelik 99

Ionic Liquid-Based Molecularly Imprinted Magnetic Nanocomposites for Selective Biomarker Recognition
Ozge Ozufuklar, Aysenur Yardim, Veysel Ceyirdekci, Faezeh Ghorbanizamani, Hichem Moulahoum, Tuncay Goksel, Suna Timur, Emine Guler Celik 100

Magnetic Soft Composite Fibers for Actuation, and Energy Harvesting
Sk. Rahat Ali, Mustafa Ordu 101

Post-Consumer Waste-Derived Graphene Nano Sheets with Recovered Carbon Fibers from Automotive Composite Wastes and Their Reintegration into PP Composites
Ozgenur Parmaksiz, Ozgenur Parmaksiz, Havva Baskan Bayrak, Israr Ahmed, Ebrahim Al Hajri, Yarjan Abdul Samad, Yarjan Abdul Samad, Burcu Saner Okan, Burcu Saner Okan 102

Synthesis and Characterization of Boron Nitride Fibers
Yelda Yorulmaz, Onur Zırhlı, Deniz Köken, Fevzi Ç. Cebeci 103

Tuning Ionic Transport in Electrospun SPEEK Nanofiber Separators with Boron Nitride Nanostructures for Structural Lithium Batteries
Onur Zırhlı, Yelda Yorulmaz, Deniz Köken, Fevzi Ç. Cebeci 104

International Requirements for Nanomaterials in Biomaterials and Medical Devices: EN ISO 10993-22
Umut Doğu Seçkin, Aylin Şendemir 105

Plant-Derived QSH/Gelatin Scaffolds with Nanostructured Bioactive Glass for Osteogenic Biomaterials
Hilal Deniz Yılmaz Dağdeviren, Kai Zheng, Aldo Roberto Boccacini, Ahu Arslan Yıldız 106

Fabrication of Hierarchical Micro- and Nanostructured Pure Iron for Bioresorbable Orthopedic Implants
İlkim Tuana Gümüşkaya, Barkın Bayram, Mete Batuhan Durukan, Hüsnü Emrah Ünalan, Batur Ercan 107

Chitosan for Wound Dressing Applications: Controlling The Dissolution Kinetics
Ateş Batıkan Özdamar, Hürriyet Polat, Mehmet Polat 108

Development of siNRF2-Loaded Prostate Cancer Cell-Derived Extracellular Vesicles as a Targeted Therapeutic Platform for Prostate Cancer
Vedat Gündoğdu, Mustafa Kotmakçı, Bilge Debeleç Bütüner 109

3D melt electrowritten MXene-reinforced scaffolds for tissue engineering applications
Mina Namvari, Mahdiyeh Zahrabi, Mine Altunbek, Suleyman Celik, Bahattin Koc 110

Molecularly Imprinted Polymer Based Surface Acoustic Wave Gas Sensor for Indoor Air Quality
Alp Kılıç, Onur Alev, Michael Cheffena, Serkan Büyükköse 111

Synthesis of Dendritic Nickel Nanoparticles And Development of QTC-Based Flexible Pressure and Temperature Sensors
Ethem Ünal Saçlı, Batuhan Parlak, Taylan Irmak Kılıç, Doğan Sarper Ataman, Yunus Emre Sarkmaz, Faruk Oğuzhan Karman, Furkan Sarıboğa, Arif Altan Selçuk, Şeyma Özkan, Barış Oğuz Gürses 112

Using an Interferometric Imaging Sensor to Characterize Receptor Binding Affinity for Vascular Endothelial Growth Factor
Nese Lortlar Unlu, Monireh Bakhshpour-Yücel, M Selim Ünlü 113

Organ-On-Chip and Microwave Biosensor Integrated Membrane Model for Drug Screening
Gurkan Yesiloz, Faruk Aksoy, Servin Bagheralmoosavi, Fayiti Fuerkaiti 114

Broadband Photoresponse of Electrodeposited Al:NiO/Porous Silicon Photodetectors: Bias-Dependent Spectral Uniformity
Mohammed Sulaiman Mustafa Mustafa, Alper Çetinel 115

Investigation of the Wound Healing Properties of the Bioactive Regenerative Peptide BPC-157 Via a Nanocarrier System
Alper Filiz, Bilge Ölçeroğlu, Şima Mertol, Kartal Çetintürk, Şahika Sena Bayazıt, Ahmet Katı, Fırat Barış Barlas 116

Synthesis, Characterization, and Biomedical Application of Europium, Samarium Single and Co-Doped Calcium Tetraborate Nanoparticles
Huseynagha Abasov, Ayşen Yılmaz 117

Engineering Rice Husk-Derived Mesoporous Silica Nanocarriers for Enhanced Blood–Brain Barrier Penetration and Glioblastoma Therapy
Sahar Porrang, Turkan Doga Gizer, Birsen Beril Bildirici, Gulin Baran, Ahmet Baki Sahin, Nur Mustafaoglu 118

Ternary Active Layer Design Utilizing BDT-Based Novel Donor for Semitransparent Organic Photovoltaics
Elif Pınar Yılmaz, Sevgi Aydın, Gönül Hızalan Özsoy, Ali Çırpan, Ali Çırpan, Ali Çırpan, Ali Çırpan 119

Lateral metal-semiconductor homojunctions in Janus Sc2CClBr MXene: Electron transport and thermoelectric properties
Gözde Özbal Sargın 120

Bridging Research and Application in Printable Electrochromics: A Start-Up Perspective
Elif Begüm Elçioğlu, Ömür Şaylıgil 121

Advanced Nanomaterial-Based NFC-Enabled Battery-Free Electrochemical Biosensors for Point-of-Care Diagnostics
Saniye Soylemez, Dilek Soyler, Dilara Yeniterzi 122

Metrohm Hyphenated EC-Raman solution
Selin Altınapa 123

AFM Investigation of Strain Relaxation Mechanisms in Epitaxial Graphene Ridges
Özhan Ünverdi 124

Interfacial Nano-Frictional Behavior of Para-Aramid Fibers Modified with nano-Hexagonal Boron Carbide (nh-B_4C)
Erman Bilisik, Havva Esra Bakbak, Mahmut Korkmaz, Gulhan Erdogan, Kadir Bilişik 125

Bridging Atomic-Scale to Hierarchical Architecture: Neutron Techniques for Advanced Hybrid Nanomaterials
Selay Sert Çok, Zoltán Dudás 126

Strain Engineering at the Nanoscale: Computational Insights into Catalytic Materials
Mehya Mansoor, Mubashir Mansoor, Maryam Mansoor, Sina Rouhi, Onur Ergen, Kamil Czelej, Servet Timur, Mustafa Ürgen, Sebahattin Gürmen 127

Characterization of Silver Nanoparticles Synthesized from Astragalus membranaceus Extract via Green Synthesis Method: Assessment of Their Antioxidant Activity, and Antimicrobial Effects
Emir Kermen, Kader Kelle, Yagmur Kose, Emre Erden Kopar, Serife Tozan Ruzgar 128

Green Synthesis and Antibacterial Potential of N,S-Doped Carbon Dots Derived from Nettle (Urtica dioica)
Özlem Gümrah, Pınar Acar Bozkurt, Mahdi Marzi, Şeniz Özalp Yaman 129

Green Synthesis, Characterization, and Antibacterial Activity of Silver Nanoparticles Derived From Centaurea Kirmacii Aqueous Extract
Zehra Sinem Yılmaz, Hüsniye Kayalar, Tuğçe Fafal 130

One-Step Green Fabrication of AgNP-Embedded Electrospun PVA Nanofibers for Dual Antibacterial and Photocatalytic Performance
Seda Şen, Nalan Oya San Keskin 131

Development of Antibacterial Coatings on Micro-Arc Oxidized Titanium Surfaces via Chitosan-Silver Hybrid Functionalization
Sıla Özay, Tuğçe Aybüke Arıca Güvenç, Ezgi Oğur, Fatih Toptan 132

Development of Collagen Hydrolysate-Based Gel Electrolytes Derived from Leather Industry Wastes for Sustainable Supercapacitors
Halil Utku Peker, Damla Sahin, Gulsah Yılmaz, Sirin Siyahjani-Gultekin, Batikan Kavukcu, Bugra Ocak, Bahri Basaran, Burak Gultekin, Gulsah Türkmen 133

Multifunctional Electrospun Cellulose Acetate Nanofibrous Mat with Molecular Release, Biocompatibility, pH-Responsiveness and Sensor Properties
Osman Arslan, Merve Esra Üngör 134

Haptic In-Sensor Computing Device Based on CNT/PDMS Nanocomposite Physical Reservoir
Kouki Kimizuka, Ahmet Karacali, Saman Azhari, Yuki Usami, Shuhei Ikemoto, Hakaru Tamukoh, Hirofumi Tanaka 135

Highly Uniform Microfabricated 3D Ring-Shaped Electrode Arrays: From Thin Films to Mesoscale Structures
Patricia Pereira Silva, Inês S. Garcia, Filipe S. Alves, Rosana A. Dias, Mehmet Selim Hanay 136

Towards HSV Management with Minimal Invasiveness: Mechanical Integrity, Skin Penetration and Ex Vivo Deposition of Bilayer Berberine-Loaded Dissolving Microneedles
Zakaria Ouzaid, Ebru Altuntaş, Ceren Koca, Hasan Sercan Palancı 137

Microfluidically Synthesized Aprotinin Nanoconjugates for Enhanced Therapeutic Response in 3D Tumor Spheroid Model
Iqra Munir, Faiqa Nazir, Gurkan Yesiloz, Faruk Aksoy 138

Albumin Polyelectrolyte Complex Nanoparticles as a Novel Platform for Therapeutic mRNA Delivery
Aytul Gul-Mete, Aytul Gul-Mete, Sümeyra Cigdem Sözer-Demirdas, Merve Basol, Merve Basol, Ozlem Erez, Yasar Akdogan, Gulcin Cakan-Akdogan, Gulcin Cakan-Akdogan 139

Routine operando studies with Near Ambient Pressure (NAP) - XPS
Liana Socaciu-Siebert 140

Vertically Aligned Carbon Nanostructures: From Electrode Architecture to Functional Performance in Electrochemistry and Sensing
Eser Metin Akinoglu, Zijie Luo 141

EPR-Guided Defect and Particle-Size Engineering of Fe-Doped ZnO Nanostructures for Energy-Storage Applications
İpek Deniz Yıldırım, Ahmet Güngör, Oluwatosin Johnson Ajala, Emre Erdem 142

Comparison of the photoresponse characteristics for 4H–SiC Schottky barrier UV photodetector with graphene and Ni/Cr electrode
Atilla Mert Dülcel, Melike Gözek, Özhan Ünverdi, Cem Çelebi 143

Advanced Metrology based on analytical SEM for Nanofabrication Applications
Muhammed Bekin, Nezih Ünal, Sven Bauerdick, Dmitri Titko 144

From Cell to Module: Scaling-Up Effects on PM6:Y6-Based Organic Photovoltaic Performance
Bilgenur Kazancıoğlu, Gönül Hızalan Özsoy, Bahri Eren Uzuner, Selçuk Yerci, Selçuk Yerci, Selçuk Yerci, Ali Çırpan, Ali Çırpan, Ali Çırpan, Ali Çırpan 145

Investigation of the Photoanode Properties of Pulsed Voltage Electrodeposited WO_3 Thin Films
Ece Değirmenci, Gamze Atak 146

Exploiting Metal Mobility in Liquid Metals for Ammonia Production
Karma Zuraiqi 147

Superconducting diode effect and topological superconductivity in microwave-cQED embedded planar Josephson junctions
Barış Pekerten 148

Exploring Topological Properties of Two-Dimensional Materials Through Berry Curvature Analysis
Sümeyye Cörüt, Semran İpek 149

Geometry-Controlled Exciton Selectivity In Monolayer Mos2 Using Plasmonic Hollow Nanocavities
Abdullah Efe Yıldız, Emre Ozan Polat 150

Investigation of Magnetotransport Effects in Ferromagnet/Normal-Metal (FM/NM) Multilayer Thin Films
Murat Kol, Perihan Aksu, Erdem Demirci, Mustafa Öztürk 151

Theoretical Investigation of pH-Responsive Lenvatinib Release from Halloysite Nanotubes via Steered Molecular Dynamics
Celal Yıldıray Köylü, Harun Nalçakan, Müşerref Önal 152

Simulation of coupled fluid–ion transport through a biological nanopore
Maxim Solovchuk, Kumar Saurabh 153

Molecular Dynamics Simulations of the Self-Assembly Mechanisms of Antimicrobial Peptides and Their Interactions with Lipid Membranes
Emine Deniz Tekin 154

Computational Studies on the electronic, structural, and optoelectronic properties of pristine graphene, holey graphene, and their doped derivatives
Erol Yıldırım, Berrin Ayyıldız, Benan Nakipoğlu 155

Advanced Hydrogel Matrix Supporting Oxygenation and Probiotic-Derived Metabolite Release
Nermin Seda Kehr, Ulvi Süleymanzade, Tuğba Ezgi Şahin, Yağmur Damla Demir 156

Investigation of Antioxidant and In Vitro Wound Healing Potential of Electrospun Chitosan/Peo Nanofibers Containing Aronia Melanocarpa Fruit Extract
Ümran Ünüvar, Fuat Aslan 157

Design and Fabrication of Nanostructured TiNbTaZr-Hf Alloy for Biomedical Applications
Yaşar Kemal Erdoğan, Gökhan Polat, Batur Ercan 158

Synthesis of Cyclodextrin Modified Cellulose Nanocrystal Nanofibers
Kazım Köse, Yirou Wang, Akshat Verma, Jeffrey P. Youngblood 159

Ultrafast Eco-Friendly Synthesis of Functional Nanoparticles for Biomedical Applications
Güneş Kibar 160

Synthesis of 2-inch Free-Standing Polycrystalline Diamond Wafers with Controlled {110} Texture and Surface Properties to Enhance Thermal Conductivity by MPCVD
Neslihan Şişman, Yiğit Can Urlu 161

Tuning the Structural, Optical, and Electronic Properties of WS2 Thin Films via Controlled Potassium Doping
Ali Altuntepe, Güldöne Toplu, Mehmet Ali Olğar, Recep Zan 162

Fabrication of High-Purity V_2O_5 Thin Films by Pulsed Electron Deposition Technique
Sefer Haşim Burgaz, Cem Çelebi, Gökhan Utlu 163

The Role of Sodium Metavanadate Concentration in the Green Synthesis of Vanadium Oxides Using Fumaria officinalis Extract
Kübra Özlen, Tuğba Soğancı Aras, Elif Begüm Elçioğlu 164

From PET Waste to Upcycled Conductive Graphene Sheets for Reinforcement of Semi-Crystalline Thermoplastics
Nihan Birgun, Nihan Birgun, Havva Baskan-Bayrak, Semih Doğan, Israr Ahmed, Ebrahim Al Hajri, Yarjan Abdul Samad, Yarjan Abdul Samad, Burcu Saner Okan, Burcu Saner Okan 165

Investigation of the Use of Phosphate Modified rGO and rGO-Alginate Microspheres in Lanthanum and Cerium Adsorption
Nursu Aydın, Şenol Sert 166

Formation and Field Emission Behavior of Graphitic Nanosheet Networks on SiC
Erhan Gurpinar, Jose Navarrete, Marc Cahay, Marc Cahay, Goknur Cambaz Buke, Goknur Cambaz Buke, Goknur Cambaz Buke 167

Growth of Ultrathin TaC Crystals on Copper via CVD
Eren Atlı, Göknur Cambaz Büke 168

Probing CVD Graphene on Cu Foil by Simultaneous UHV AFM/STM: From Atomic Defects to Folded Nanoribbons
Feyza Nur Yıldırım, Hakan Özgür Özer 169

Quartic Energy Band Engineering in Artificial Semiconductor Honeycomb Lattices
Emre Okcu, Emre Mesudiyeli, Haldun Sevinçli, A. Devrim Güçlü 170

Development of Recycled Graphene-Based Polypropylene and PEEK Compounds Derived from Waste Tires for Automotive and Aerospace Applications
Tülin Erdal Erikli, Selin Arıcan, Burcu Saner Okan, Murat Cansever 171

Engineering Bifunctional Conjugated Polymers: Triphenylamine-Based Systems for Electrochromic Energy Storage in Asymmetric Hybrid Supercapacitor Devices
Arya Zelal Keserci, Ali Çırpan, Ali Çırpan, Ali Çırpan, Ali Çırpan 172

Controllable porosity and conductivity in graphene-polymer nanocomposite fiber as multimodal wearable sensors
Arooj Fatima, Mustafa Ordu 173

Design Parameters of PbSe Nanorod–Quantum Dot Bulk Nano-Heterojunction Platforms for Multiple Exciton Generation-Based Solar Cells
Demet Asil, İrem Kolay, Tuğba Hacıefendioğlu 174

Homoepitaxial Quantum Diamond Growth by MP-CVD: Effect of O_2 Pre-Treatment on Crystal Quality, Substitutional Nitrogen, and NV^- Center Activation
Vildan Aker, Neslihan Şişman 175

Investigation Of The Effect Of Nanoclay Incorporation On Structural, Mechanical, And Biological Properties Of Yttria-Stabilized Zirconia Bone Grafts
Doğa Memioğlu, Yiğithan Tufan, Jae-Hyung Park, Abdullah Öztürk, Jongee Park, Young-Hag Koh, Batur Ercan 176

Surface Characteristics and Antibacterial Performance of Medium-Entropy Alloys Functionalized with Dual-Functional Chimeric Peptides
Turgut Güven Tarım, Ayşe Öykü Ova, Sevgi Berfin Kıran, Ferda Soyer, Esra Şahin, Deniz Yücesoy, Benay Uzer 177

Thin Film Metallic Glass Coatings for Magnesium Implants
Kaan Yetiş, Iulian Pana, Senem Büyüksungur, Anca Constantina Parau, Mihaela Dinu, Catalin Vitelaru, Alina Vladescu Dragomir, Nesrin Hasırcı, Batur Ercan 178

Valorization of Discarded Cigarette Butts into High-Performance Carbon Electrodes for Supercapacitors
Oluwatosin Johnson Ajala, Ipek Deniz Yıldırım, Ahmet Güngör, Feray Bakan Misirlioglu, Emre Erdem 179

Investigation of the Durability and Insulation Properties of Polyurethane-Silica Nanocomposite Coatings Produced by One-Step Spray Method
Semih Pehlivan, Fatih Büyükserin 180

Development of Carbon-Based Supercapacitor Electrode Materials from Waste Wet Wipes via Hydrothermal Carbonization
Ezgi Nur Belek, Burak Dalkılıç, Anas Abofoul, Selva Bilge 181

A Shallow Plasma Nanotexturing Regime For Passivation-Compatible Silicon Surfaces
Ozan Aydın, Milad Ghasemi, Hisham Nasser, Raşit Turan 182

Recycling of $Ca_2NaNb_4O_{13}^-$ Perovskite Nanosheets: Structural Reintegration and Life Cycle Assessment
Atahan Orhon, Mine Güngörmüşler, Özge Sağlam 183

Ultra-Thin Mo_2C/W_2C Heterostructures for Tunable Electromagnetic Interference Shielding
Sina Rouhi, Mehya Mansoor, Mubashir Mansoor, Maryam Mansoor 184

Fluorine-Free Synthesis of Two-Dimensional Mo2AlB2 MBene for OLED Applications
Hilal Doğan, Aseel Zaid, Selin Piravadili, Müslüm Demir 185

Investigation of the Removal of Sr(II) and Pb(II) Ions from Aqueous Media Using Green-Synthesized Quantum Dots and Polyoxometalate-Based Biohydrogels
Zehra Sisman, Sabriye Yusan, Taha Furkan Gül, Eduardo Alberto Lopez Maldonado 186

Optimization of Electrospun PAN/Amino-MWCNT Nanocomposite Fibers for SPME: Tuning Carbon Nanotube Content for Enhanced Fire Debris Analysis
Rukiye Aslan, Mihriban Dilan Kılıç, Merve Kuloğlu Genç, Tuğçe Töngüç Yalçinkaya, Selda Mercan, Ahmet Çay, Serap Annette Akgür, Fatma Nil Ertaş 188

A Naturally Fluorescent Micellar Platform for Imaging-Guided Delivery
Esmanur Akdoğan, Zeliha Soran Erdem 189

Effect of Plasmonic Shell in Photothermal Heating in Core-Shell Nanoparticles
Seda Aygül Akyüz, Zeliha Cansu Canbek Ozdil 190

Ge-Based Thin-Film Photodiodes for Near-Infrared Detection: Structural and Optoelectronic Investigation
Koray Soydaner, Abdulsalam Aji Suleiman, Timuçin Emre Tabaru 191

In Silico Design of Peptide-dsDNA Molecular Constructs for Bioelectronic Glucose Sensing
Ravza Nur Ceran, Ersin Emre Ören 192

Novel Altermagnetic Monolayer of Vanadium Oxide with a Buckled Lieb Structure
Tamer Taşkıran, Soheil Ershadrad, Biplab Sanyal, Cüneyt Şahin 193

A Novel PEGylated Cationic Liposomal Platform for Sorafenib Delivery in Triple-Negative Breast Cancer: Design, Optimization, and In Vitro Evaluation
Esra Merve Zanbak Çotaoğlu, Kubra Kılıc, Gizem Ruya Topal 194

Monobee: Micro-Dispensing Based Flexible Electronics Platform for Printed Functional Materials
Kaan Yapıcı 195

CNC-machined Alumina Doughs as Robust Ceramic Platforms for Prototyping of Microchannels and Micromixers
Ceren Özsaltık, Öykü Yanaz, Omid Moradi, Özge Akbulut 196

Mold-Free, Dough-Based Processing of Highly Loaded Strontium Hexaferrite Ceramics for Conformal X-Band EMI Absorbers
İleyna Uvak, Batuhan Özkaya, Ozan Akdogan, Özge Akbulut 197

Theoretical Understanding of Stability in Atomically Precise Nanoclusters
Fahri Alkan 198

First-Principles Investigation of Electronic Structure and Magnetic Properties of Fe-Intercalated 2H-NbSe2
Mustafa İnanç, Abdulsalam Aji Suleiman, Aydan Yeltik 199

Theoretical Investigation of Perovskite/Polymer Heterostructures for Improved Interfacial Charge Transfer
Somayyeh Alidoust, V. Ongun Özçelik 200

Effects of Calcination Process on Crystallization of Aluminum Oxide Nanoparticles
Alp Bigalı, Elif Begüm Elçioğlu 201

Unraveling CeO_2- and FeO_x-Induced Surface Restructuring in Rh/HAP Catalysts: A Spectroscopic Mechanistic Study of Dry Reforming of Methane
Aybala Büşra Topcu, Ayse Dilay Erdali, Erdem Deniz, Yusuf Kocak, Zafer Say 202

Ultrasound-Assisted Synthesis of Morphology-Controlled Copper Hydroxy Sulfate Micro/Nanoparticles
Sibel Şentürk, Chenyang Liu, Halide Sezi Hasin, Abdurahman Aghamaliyev, Sıla Boyacıgil, Cansu Yıldırım, Hüseyin Enis Karahan 203

Green Synthesis of Silver Nanoparticles Using Turkish White Tea (Camellia sinensis) Extract: Optimization of Synthesis Parameters and Physicochemical Characterization
Danya Anbar, Berkcan Zulfikar, Osman Eksik, Nihan Aydemir 204

Sulfur-Assisted Growth and Phase Evolution of Mo-Based Carbide Crystals via Chemical Vapor Deposition
Deniz Cakir, Goknur Buke, Michael Naguib, Yury Gogotsi 205

Characterization and Evaluation of Bioactivities of Green Synthesized Silver Nanoparticles Through Tarragon (Artemisia dracunculus) Extract[
Deniz Nur Erbey, Ayşegül Öztürk, Zalike Keskin Erdoğan, Yılmaz Yürekli, Aylin Şendemir, Aylin Şendemir 206

Synthesis and Characterization of BODIPY-Modified Mesoporous Silica Nanoparticles
Eda Erdemir Tavukçu, Nisa Demirbilek, Erman Karakuş 207

Effect of Fluoride Concentration on the Morphology and Corrosion Behavior of Anodized Pure Iron
İlkim Dila Kaya, İlkim Tuana Gümüşkaya, Batur Ercan 208

Eco-Friendly synthesis of ZnO Nanoparticles Using Endemic Flora from Türkiye: Morphological, Optical and Photoelectrochemical Insights
Eylül Sude Tırpan, Betül Bibin, İrem Beyza Dolu, Serra Ersoy, Cengiz Kaya 209

Characterization, Rheological Behavior and Physical Stability Evaluation of Plant-Based Wax Nanoemulsions Produced by Ultrasonic Emulsification
Ezgi Zekiye Aktürk, Çağla Ural Aytuna, Beril Atmaca, Tolga Duran 210

In situ Chlorophyll Decoration of ZIF-8 for Structural Modulation of Porous Frameworks
Fatma Yelda Ünlü, Özge İbiş, Caner Ünlü 211

Bio-Derived SiO_2-Based Hybrid Sols for Transparent Anti-Reflective Coatings on Glass Surfaces
Fatoş Koç, Nazire Türköz, Murat Özkan, Merve Deniz Köse, Berrin İkizler, Şerife Şeref Helvacı 212

Green Synthesis of Nitrogen-Doped Carbon Dots by Hydrothermal and Sonochemical Methods
Fethi Emre Bayat, Sinemis Met Turhan, Ayşe Elif Yılmaz, Özlem Gümrah, Pınar Acar Bozkurt 213

Controlled Synthesis and Surface Modification of Magnetite Nanoparticles as Optimized Tracers for Magnetic Particle Imaging
Firdevs Aydın, Damla Alptekin Soydan, Sefa Karaca, Can Barış Top, Gökçen Birlik Demirel 214

Synthesis and Characterization of PEI Coated Iron Sulfide Nanostructures
Mine Yiğit, Gülce Özkan, Selin Şen, Ayben Top 215

Effect of Morphological and Structural Features of Silica Nanoparticles on Functional Coating Properties
Miray Kaya, Merve Çevik Eren, Hürriyet Polat, Mehmet Polat 216

Morphology-Dependent Triboelectric Performance of Ce-Doped ZnO Nanoparticles Synthesized by Thermal Decomposition and Hydrothermal Routes
Melisa Atay, Metin Yurddaskal, Neslihan Sakar 217

Defect-Engineered ZnO-Gd2O3 composites for energy storage applications
Oluwatosin Johnson Ajala, Emre Erdem 218

Effect of 355 nm Pulsed Laser Ablation Parameters on the Synthesis and EPR Characterization of NiO and Ni Nanoparticles
Omid Moradi, Ipek Deniz Yıldırım, Emre Erdem, Ali Koşar 219

Investigation of the Thermoelectric Synergistic Mechanism in Self-Powered Systems Employing MOF-Derived Carbon/MXene Heterojunctions Synthesized through Large-Scale Solar Furnace Thermal Shock
Saidov Kamoladdin, Sattorov Khurshid, Pecherskaya Mariya, Ahmedova Dilbar, Abdullaev Abdubakir, Butanov Khakimjan, Razzokov Jamoliddin, Mamatkulov Shavkat, Ruzimuradov Olim 220

Synthesis and Characterization of Carbon Quantum Dots from Organometallic Complexes
Serhat Demirci, Taha Yasin Bayram, Aslı Yılmaz, Özlem Gündoğdu Aytaç, Sertan Aytaç, Yunus Kara, Mehmet Yılmaz 221

Low-Concentration Citric Acid Catalyzed Sol-Gel Synthesis Of Mesoporous 45S5 Bioactive Glass For Dental Applications
Sevgi Berfin Kıran, Eyüp Bilgi, Ceyda Öksel Karakuş 222

Development of High-Performance Gel Electrolyte Reinforced with Waste Textile-Derived Cellulose and h-BN for Wearable Supercapacitors
Mehmet Can Göreli, Yiğit Efe Yılmaz, Eren Doğukan Kala, Tolga Bakırsoy, Serra Ersoy, Suna Avcıoğlu 223

Design and Fabrication Of Non-Toxic Bi2O3 Nanoparticles With Finite Element Method and Pulsed-Laser Ablation in Liquid Phase
Yasemin Arslan, Timuçin Emre Tabaru, Hamd Alhaj Qasem, Bülend Ortaç, Ali Karatutlu 224

Boron-Based 2D Materials for Hydrogen Storage: Synthesis and Characterization
Yıldıray Yılmaz, Mehmet Ali Gülgün, Ahmet Eymen Akşener 225

Synthesis and Characterization of Bioactive Carbon Dots Derived from Citric Acid and Hydroquinone
İdil Savru, Selin Şen, Ayben Top 226

Novel Nanocomposite Triboelectric Nanogenerators (TENG) Through Combining Thermal Drawing and Electrospinning Techniques
Ali Eren Yüksel, Vishwa Pratap Singh, Maliha Rahman, Enes Dirican, Savaş Sönmezoğlu, Tudor Braniste, Mustafa Ordu 227

Microwave-Assisted Synthesis of Co3O4/rGO Nanocomposites toward Promising Supercapacitor Electrodes
Anas Abofoul, Amira Gaber, Soliman I. El-Hout, Selva Bilge 228

Electric-Field-Assisted Facile Growth of Aligned ZnO Nanowires on Flexible Substrates for High-Performance Piezoelectric Nanogenerators
Ayşegül Demircioğlu, Eminenur Sarıtaş, Murathan Kabak, Kuzey Kaya, Mohamad Hasan Aleinawi, Omid Moradi, Emre Erdem 229

A New Quinone-Based Molecule as Cathode Material for Long-Life Aqueous Zinc-Ion Batteries
Batu Sercan Cantürk, Yasmin Geçalp, Mustafa Erdoğmuş, Onur Büyükçakır 231

Experimental and Machine Learning Investigation of the Annealing Temperature-Dependent Structural Evolution of N-Type Window Layers Used in Solar Cells
Caner İldeş, Tarık Akan 232

Ni-MOF-Based Platforms for Advanced Electrochemical Energy Storage Applications
Damla Tezcan, Umut Güzel, Ulku Anik, Ulku Anik 233

Multiphase Displacement Application of Green Nanofluid In Reservoir-on-Chip
Robab Jahangir, Faruk Aksoy, Gurkan Yesiloz 234

Sol-Gel Based High-Durability Nano Coating Technology for Solar Panel Glass Surfaces to Enhance Energy Efficiency
Orhan Alal, Duygu Kaya, Mihriban Demir 235

Synchrotron-Based X-Ray Raman Spectroscopy of a Ni-Decorated Nitrogen-Doped Graphene Quantum Dot Anode for Lithium-Ion Batteries
Kayra Ümekkan, Didem Ketenoğlu, Erdinç Öz, Georg Spiekermann, Manuel Harder, Bahadir Boyacioglu, Mustafa Yıldız 236

Cu Nanoparticle-Decorated Nitrogen-Doped Graphene Quantum Dots as High-Performance Anodes for Lithium-Ion Batteries
Mustafa Sezgin Tekkalmaz, Didem Ketenoğlu, Erdinç Öz, Yunus Emre Uyanık, Georg Spiekermann, Manuel Harder, Bahadır Boyacıoğlu, Hüseyin Ünver, Ashok Chatterjee, Mustafa Yıldız 237

Semitransparent Organic Solar Cell Applications of Thienothiophene II-Bridge based Novel Conjugated Polymer
Mürüvvet Ganız, Gizem Arslan, Gönül Hızalan Özsoy, Ali Çırpan, Ali Çırpan, Ali Çırpan, Ali Çırpan 238

Surface and Thickness Effects in Nanostructured Copper Films for CO2 Electroreduction on Gas Diffusion Electrodes
Patrycja Kolbusz, Sebastian Jarczewski, Krzysztof Mech 239

Transesterification-Based Biodiesel Production Using Micro-Nano-Sized Spinel Zinc Ferrite Particles
Yasemin Fatih Aghdaei, Gökçe Zeynep Yılmaz, Cansu Yıldırım, Hüseyin Enis Karahan 240

Synergistic Enhancement of Uranium Adsorption Kinetics and Selectivity through In Situ Growth of ZIF-8 on Amidoxime-Functionalized Polyacrylonitrile Membranes
Taha Furkan Gül, Zehra Sisman, Sabriye Yusan, Sule Aytas, Nalan Kabay 241

Co-Doped TiO_2 Nanorods for Triple-Cation Perovskite Solar Cells: From Synthesis to Device Application
Şeydanur Kaya, Andrés-Felipe Castro-Méndez, Felix Lang 242

A Conjugated Polymer-Based Asymmetric Supercapacitor With Integrated Electrochromic Functionality
Asude Gürsoy, Eminenur Baran, Elif Demir Arabacı, Ali Çırpan, Ali Çırpan, Ali Çırpan, Ali Çırpan 243

Injectable MXene-Based Composite Hydrogels for Photothermal Cancer Therapy
Berivan Polat, Gökçen Birlik Demirel 244

MXene-Based Nanocomposite Ionogels for Flexible Wearable Strain Sensors
Büşra Çevik, Gökçen Birlik Demirel 245

Design and Synthesis of A Dual-Function Phenyl-Linked Carbazole-Based Polymer for Supercapacitors
Dilan Akdeniz, Elif Demir Arabacı, Ali Çırpan, Ali Çırpan, Ali Çırpan, Ali Çırpan 246

Design and Synthesis Cyano-Functionalized Triphenylamine-Based Monomer for Supercapacitor Application
Gülten Yıldırım, Sedanur Şahinaslan, Oğuzhan Karakurt, Ali Çırpan, Ali Çırpan, Ali Çırpan, Ali Çırpan 247

Nanoadhesive Polymer Coating Development for Enhanced Grip on Complex 3D Surfaces
Melike Nur Öz, Göksu Yağız, Merve Karabıyık, Özgenç Ebil 248

Quinoline-Based Porous Organic Polymers for Enhanced CO_2 Uptake and Catalytic Conversion
Mustafa Erdogmus, Mehmet Anil Arapoglu, Batu Sercan Canturk, Yasmin Gecalp, Onur Büyükcakir 249

Fabrication And Characterization Of PVDF-HFP Nanofiber-Reinforced Composite Sponges For Biomedical Applications
Ozlem Ceren Aktas, Aylin Ziylan Albayrak, Oylum Colpankan Gunes, Taner Goktas, Neslihan Sakar 250

Injectable Hydrogels for Controlled Delivery of Allocryptopine in Alzheimer's Disease
Simge Koç, Gökçen Birlik Demirel, Belma Aslım, Mine Türktaş, Büşra Aktaş Mansuroğlu, Filiz Kardiyen, Serap Niğdelioğlu Dolanbay, Zehra Kübra Yılmaz 251

Mechanical Performance and Degradation Behavior of 3D-Printed Biodegradable Graded Gyroid Bone Scaffolds with Hierarchical Porosities
Duygu Üçüncü, Miray Dereli, Nehir Heppekcan, Sinem Gülseroğlu, Fatih Büyükserin, Mervenaz Şahin 252

Cargo Transportation via Magnetically Responsive Soft Robotic Platforms
Sudenaz Ergen, Kubra Ozkan Hukum, Gorkem Liman, Gokhan Demirel 253

Fluorine-Rich Porous Organic Polymers for Electrochemical CO_2 Conversion
Yasmin Gecalp, Mustafa Erdogmus, Batu Sercan Canturk, Onur Buyukcakir 254

Data-Driven Optimization of Experimental Design Using Machine Learning and Active Learning
Ata Gazi Kuş, Gamze Atak 255

A Drift-Aware Framework for Reliability Assessment and Spatiotemporal Interpretation of Atomic Force Microscopy Measurements
Batuhan Yenen, Seda N. Sönmez, Derya Gemici Deveci, Özhan Ünverdi, H. Özgür Özer 256

The Shape of Color: 3D Machine Learning Meets Electrochromic Nanomaterial Discovery
Derya Hazal Yıldırım, Erol Yıldırım, Levent Toppare 257

Integration of Digital Colorimetry and Machine Learning for the Evaluation of CdZnSeS Quantum Dots
Ezgi Tan, Preston T. Snee, Abdurrahim Akgündoğdu 258

A Modular CNN-Attention Framework for SEM Microstructure Classification of Nanofibrous Materials
Miray Esma Yalçın, Ahmet Emrehan Emre, Burak Alakent 259

Neural Score Models for Control of Active Dynamical Systems
Rosha Razmarafar, Francesco Cagnetta, Alessio Ansuini, Giuseppe Negro, Livio Nicola Carenza 260

Comprehensive Drift Analysis and Machine Learning-Based Predictions in Atomic Force Microscopy
Derya Gemici Deveci, Tuana Karakoyun Barandır, Özhan Ünverdi, Cem Çelebi, Lütviye Özge Temur, Doğu Çağdaş Atilla 261

Superlattice Formation of PBI_2 Passivated PBS Quantum Dots via Langmuir-Schaefer Method
Ecem Efe, İrem Kolay, Demet Asil Alptekin 262

Effect of Ligand Length on PbSe Quantum Dot Films for SWIR Photodetectors: Solution-Phase and Layer-by-Layer Ligand Exchange
Furkan Arda Koca, Demet Asil Alptekin, İrem Kolay 263

Joint Estimation of Phase-Shift And Losses in SU(2) and SU(1,1) Interferometers
Hasan Mermer 264

Development of an In-Situ Bromoplumbate Surface Passivation Protocol for Directly Synthesized PbS Quantum Dots
Mert Eray, İrem Kolay, Demet Asil Alptekin 265

Doping of ZNO Electron Transport Layers for PBS Quantum Dot Solar Cells
Sezin Şevval Acar, İrem Kolay, Demet Asil Alptekin 266

Direct Conversion of Highly Monodisperse CdS Quantum Dots into Halide-Passivated PbS INKS via In-Situ Cation Exchange
Yiğit Emre Karakaş, İrem Kolay, Demet Asil Alptekin 267

Tuning Energy Transfer Efficiency in PBSE Quantum Dot – Nanorod Heterojunctions for Enhanced Exciton Harvesting
İrem Kolay, Demet Asil Alptekin 268

Goldene/MX2N4 Metal-Semiconductor Heterostructures As Promising Platforms For High-Performance Gas Sensing
Mehmet Özcan, Berna Akgenc Hanedar 269

Strain-Dependent Evolution of Crystallographic Texture and Microstructure in Laser Powder Bed Fusion-Processed 316L Stainless Steel
Büşra İrem Türkpençesi, Kemal Davut, Mustafa Güden, Benay Uzer, Kay-Peter Hoyer 270

Development of a Flexible Carbon Fiber Supercapacitor and Integration with a Triboelectric Nanogenerator for Self-Charging Energy Systems
Kaan Yapıcı, Serap Hayat Soytaş 271

Nanoscale Friction Mechanisms of SnSe and SnSe2 Nanoflakes as Solid Lubricants
Mehmet Ozdogan, Thomas Iken, Deniz Cakir, Nuri Oncel 272

Micro Structured Surface Creation for Leidenfrost Enhancement in Low Temperatures
Monika Maziukiene, Raminta Skvorcinskiene, Lina Vorotinskiene, Ainė Antanavičė 273

Wafer-Scale Characterization of Orientation- and Doping-Density-Dependent β-Ga_2O_3 Single Crystals for Optoelectronic and Electrooptic Applications
Selen Nur Yılmaz, Ümit Doğan, Muratcan Aydoğdu, Mustafa Aydın, Şahin Yakut, Deniz Bozoğlu Parto, Hüseyin Furkan Eminoğlu, Hüseyin Furkan Eminoğlu, Ayşe Erol, Ayşe Erol, Ömer Dönmez, Ömer Dönmez 274

A Safety-by-Design Framework for Silver Nanoparticles in Biomedical Applications
Melis Kaya, Furkan Eker, Sercan Karav 275

Human Intestinal Organoid-Derived Monolayers Recapitulate Epithelial Features Relevant to Oral Nanomedicine Evaluation
Merve Ceylan, Zekai Serhan Derici, Nilay Danış, Anıl Aysal Ağalar, Sinan Güven 276

Fabrication and Characterization of PANI-DMF Based Thin Film Sensor for NH3 Gas Detection
Erdi Ağrı, Ümit Doğan, Ahmet Ünverdi, Alican Ökçün, Şule Özdilek 277

Protein A-Engineered SPR Biosensor for Real-Time IgG Capture and Purification
Ayşegül Bülbül, Fatma Yılmaz, Ateş Kara, Adil Denizli 278

Design of Biomaterial-Film-Modified Screen-Printed Platforms for Glucose Biosensing
Azra Kolukısa, Eren Polat, Zeynep Elçim Koru, Selin Yavuzhan, Gözde Duman, Büşra Başol, Buğra Gizlenci, Suna Timur 279

Development of a Mushroom-Derived Ce–N Co-Doped Carbon Quantum Dot/Alginate Biosensor for Glyphosate Detection in Water
Berkant Senturk, Burak Tas, Ozge Tuzun Ozmen, Sabriye Yusan 280

A Complete Low-Volume Electrochemical System Employing SPE for Biosensing
Damla Aydogan, Seda Nur Topkaya, Arif E. Cetin 281

Au/Co3O4 Nanoparticle-Modified Platform for Multiplex Sensing of Galantamine, Dopamine, and Uric Acid
Dilara Yeniterzi, Umut Bulut, Serdar Akbayrak, Saniye Soylemez 282

Smartphone-Assisted PAN Nanofiber-Based Fluorescent Biosensing Platform for Epidermal Growth Factor Receptor Detection
Dilek Soyler, Semih Can Çakmaktepe, Oguzhan Karakurt, Ali Cirpan, Serdar Akbayrak, Saniye Soylemez 283

Development of a Fluorescence-Based Sensor with Fe_3O_4@SiO_2 Magnetic Nanoparticles; Application in Environmental Water Samples
Zeynep Azra Demir, Doğa Yücesoy, Reyhan Selin Uysal Afacan 284

Beyond Spherical Gold Nanoparticles: Comparative Evaluation of Gold Nanolabels for Enhanced Lateral Flow Assays
Egemen Aydin, Ozge Ozufuklar, Veysel Ceyirdekci, Suna Timur, Emine Guler Celik 285

Developing a QCM-based Biosignature Detection Concept Using Molecularly Imprinted Polymeric Adsorbents Embedded in Multilayered Nanofilms
Egemen Sönmez, Yaren Özkaynak, Selin Baş, Kaan Arıduman, Cansu Yıldırım, Tuğrul Cem Bıçak, Hüseyin Enis Karahan 286

ITO-Based Dual-Mode Lateral Flow Biosensor Integrating Smartphone Imaging and Electrochemical Quantification
Ela Koçhan, Ozge Ozufuklar, Sena Yanasık, Veysel Ceyirdekci, Suna Timur, Emine Guler Celik 287

Dual Electrodes, Triple Detection: A Flexible MXene-Based Platform for Simultaneous Electrochemical Detection of Dopamine, Uric Acid, and Glucose
Esra Nur Elmas, Dilara Yeniterzi, Serdar Akbayrak, Saniye Soylemez 288

Development of Antibody-Antigen-Based Plasmonic Sensors for the Rapid, Simple, and Inexpensive Detection of the Mutant Huntington Protein (mHTT), a Biomarker of Huntington's Disease
Fatma Dalkilic, Nimet Temur, Seyma Dadi, Cemile Yilmaz, Aslihan Kiraz, Begum Unveroglu, Ismail Ocsoy 289

Amplification-Free Detection of HBV cccDNA Using CRISPR-Cas12 and Photonic Resonator Absorption Microscopy
Fatma Uysal Ciloglu, Fatma Uysal Ciloglu, My Nguyen, Lucas D. Akin, Sneha Mittal, Weinan Liu, Saurabh Umrao, Seemesh Bhaskar, Xing Wang, Daryl T. Lau, Brian T. Cunningham 290

High-Sensitivity Biothiol Detection Utilizing Gold Nanoparticle-Functionalized Fluorescent Turn-On Probe
Garen Suna, Eda Erdemir, Erman Karakuş, Songül Eğlence Bakır, Musa Şahin 291

CHIKV Lateral Flow Diagnostic Platform Enabled by Aptamer–Nanogold Conjugates
Gunes Ertemcoz, Ozge Ozufuklar, Veysel Ceyirdekci, Jagriti Narang, Suna Timur, Emine Guler Celik 292

Mo-MOF@GNR Nanohybrid-Based Electrochemical Sensors for the Detection of Bisphenol A
Havva Nur Gürbüz, Özlem Şahin, Yasemin Öztekin, Mustafa Şahin 293

Fabrication Of Laser-Induced Graphene And Screen-Printed Hybrid Electrodes For Electrochemical Sensing
Hikmet Batuhan Balki, Ezgi Kivrak, Eren Kucuk, Levent Beker 294

Fabricating Metal-Organic-Framework-Based Paper Biosensor for Colorimetric Detection of Glucose as a Vitality Biosignature
Kaan Arıduman, Selin Baş, Nil Ürküt, Cansu Yıldırım, Hüseyin Enis Karahan 295

Mip-Based Electrochemical Analytical Method for Alpha-Hederin Quantification in Complex Plant-Based Systems
M.Mesud Hürkul, Seyda Yayla, Asmin Kurt, Ahmet Cetinkaya, Sonja Jovanović, Marija Milićević, Sibel A. Ozkan 296

Polylysine-Fullerenol Nanoarchitectonics: A High-Performance Platform for PoC Biosensor Application
Mehmet Hakan Yorgancılar, Dilek Soyler, Yasin Sozer, Salih Ozcubukcu, Saniye Soylemez 297

Real-time Capture and Visualization of Whole Cell E. coli for Rapid Detection and Antimicrobial Susceptibility Testing via IRIS
Neşe Lortlar Ünlü, Monireh Bakhshpour-Yücel, Sinem Diken Gür, Neval Elgörmüş, Negin Zaraee, M Selim Unlu 298

Early Detection of HIV Using Infection Mechanism-Based Gold Nanoparticle Spectrophotometric Biosensor
Burak Ekrem Çitil, Nil Su Çaylayık, Ülkü Anık, Ülkü Anık 299

Self-Organized Nanostructure Formation through Solid-State Thermal Dewetting for Label-Free Biosensing Platforms
Sena Simsek, Meryem Beyza Avci, Tossaporn Lertvanithphol, Mati Horprathum, Khwanchai Tantiwanichapan, Chanunthorn Chananonnawathorn, Wantanee Hincheeranan, Hande Nur Yılmaz, Arif E. Cetin 300

A Computational Modeling Approach for ITO-Based Competitive Lateral Flow Assay
Sena Yanasik, Ela Kochan, Emine Guler Celik 301

Magnetic Nanoparticle-Based Reusable Electrode Surfaces: Psychostimulant Aptasensor
Veysel Ceyirdekci, Ezgi Man, Ozge Ozufuklar, Aysenur Yardim, Jagriti Narang, Serap Evran, Suna Timur, Emine Guler Celik 302

Comparative Analysis of Faradaic and Non-Faradaic Impedimetric Sensing Methods for Immunosensors Using PCB Interdigitated Electrodes
Alper Demirhan, Yagmur Ozdemir 303

Development and In Vitro Evaluation of Lipid Nanoparticle-Mediated CRISPR/Cas9 Ribonucleoprotein Delivery Targeting VEGFR, p65 and Survivin in Non-Small Cell Lung Cancer
Deniz Onan, Hasan Akbaba 304

Functional Antibody-Modified Gold Biointerface for Electrochemical Recognition of Lung Cancer Cell-Derived Extracellular Vesicles
Eren Polat, Zeynep Elcim Koru, Selin Yavuzhan, Sude Yılmaz, Didem Aksu, Kerem Tok, Figen Zihnioglu, Suna Timur 305

Transcriptomic and Proteomic Expression Level of IL-6/JAK/STAT3 Pathway Inhibition by Tocilizumab-Conjugated 5-Fluorouracil-Loaded Lipid–Polymer Hybrid Nanoparticles in Oral Squamous Cell Carcinoma
Ezgi Özdemir, Demet Cansaran Duman, Pelin Mutlu 306

Graphene-Reinforced Polyimide-Modified Electrodes for the Voltammetric Determination of Sorbic Acid
Esra Yetişkin, Fatma Bilge Emre, Süleyman Köytepe, Turgay Seçkin, Ergun Ekinci 307

Magnetic Micropatterned Platform for High-Throughput 3D Liver Spheroid Engineering and Toxicity Screening
Merve Oztas, Mehmet Ali Onur, Gunes Kibar 308

Ferroptosis-Driven Macrophage Polarization Assessed by Flow Cytometric Profiling of THP-1 Derived M1/M2 Cells
Kübra Solak, Adem Kara, Ahmet Mavi 309

Sustainable Magnetic Biochar Nanozymes
Ece Mavili, Mehmetcan Uzuner, Zeynep Elcim Koru, Eren Polat, Selin Yavuzhan, Gözde Duman, Büsra Basol, Bugra Gizlenci, Suna Timur 310

A New-Generation Approach to Tuberculosis Treatment: Synthesis, Characterization, and Investigation of the Antimicrobial Activity of Berberine-Based Nanocomplexes
Nimet Temur, Ismail Ocsoy 311

Multiplex Colorimetric Profiling of Lung Cancer Cell-Derived Extracellular Vesicles
Selin Yavuzhan, Eren Polat, Zeynep Elçim Koru, Sude Yılmaz, Kerem Tok, Emine Güler Çelik, Didem Aksu, Figen Zihnioğlu, Suna Timur, Derya Nil Kişin 312

Next-Generation Sequencing for Early Disease Diagnositcs and Targeted Therapeutics in Rare Diseases
Shams Ismayilova, Afig Berdeli 313

Amino-Functionalized Carbon Dots as a Cost- Effective Alternative to Fluorescent Dyes for Wound Healing Monitoring
Sümeyye Kozan, Havva Nur Gürbüz, Meltem Demirel Kars 314

Biological Applications of Carbon Quantum Dots Synthesized from Different Organometallic Complexes
Taha Yasin Bayram, Serhat Demirci, Ezo Palavan, Aslı Yılmaz, Özlem Gündoğdu Aytaç, Sertan Aytaç, Yunus Kara, Mehmet Yılmaz 315

Production and Characterization of Electrospun Nanofibers Containing Polycationic Polymers for Controlled Release of Anticancer Drugs
Yağmur Aktepe, Sultan Sacide Gelen, Ozan Yesiltepe, Dilek Odacı 316

ACE2-Rich Plasma Membrane-Modified Gold Interface as a Bioinspired Sensing Platform
Zeynep Elcim Koru, Eren Polat, Sude Yılmaz, Kerem Tok, Didem Aksu, Faezeh Ghorbanizamani, Hichem Moulahoum, Emine Guler Celik, Figen Zihnioglu, Suna Timur 317

Eco-Friendly ZnO Thin Films Produced via Leaf Extract-Assisted Hydrothermal Processing
Fatma Nurgül Çataklı, Beyza Sandık, Berrin İkizler 318

Development of a Novel Biomaterial for Seed Treatments Against Drought Stress
Betul Akkus, Nermin Seda Kehr 319

Design and Characterization of Ionic Liquid Functionalized Magnetic MOF-on-MOF Nanocomposite for Green Extraction Applications
Duygu Totur Pamık, Serap Seyhan Bozkurt 320

Potential of Green-Synthesized and Iodine-131 Radiolabeled Plant-Based Nanoparticles in Biomedical Applications
Duygu Tugce Baran, Rumeysa Celik, Fazilet Zumrut Biber Muftuler 321

Effect of Hydrothermal Carbonization Temperature on the Antioxidant Activity of Carbon Dots Derived from Winery Fermentation Waste
Ecem Köseoğlu, Didem Aksu, Gözde Duman Taç 322

Conversion of Nitrates into Ammonia Using Nanostructured Metal–Organic Framework-Based Catalysts
Eray Tabak, Ali Furkan Albora, Eren Özbay, Aslı Sare Gürsu, Şahika Sena Bayazit 323

From Bio-Silica to Radionuclide Sorbent: κ-Carrageenan/Diatomite Composites for Sr(II) Removal
Ikbal Gozde Kaptanoglu 324

Valorization of Grape Pomace for the Green Synthesis of TiO2 Nanoparticles as Nano-biopesticide Against Tuta absoluta
Faezeh Ghorbanizamani, Tugba Oztekin, Kerem Tok, Lale Aktaş, Ahmet Hatipoglu, Suna Timur, Figen Zihnioğlu, Hichem Moulahoum 325

Encapsulation of Peppermint Essential Oil in a Chitosan Nanosystem and Evaluation of the Particle Size of Encapsulated Nanoparticles
Rezvan Shaddel, Sara Jalaei Moghaddam, Younes Zahedi, Bahram Fathi Achachlouei 326

Carbon Dot-Loaded 3D PAN/ES Electrospun Nanofibrous Sponges for Efficient Methylene Blue Removal and Photoinduced Antibacterial Water Treatment
Timur Tongur, Altangerel Amarjargal, Viraj P. Nirwan, Rebecca Hengsbach, Amir Fahmi, Seda Demirel Topel 327

Green Synthesis of Bio-Compatible Quantum Dots and Their Interactions with Plant-Derived Photosynthetic Pigments
Özge İbiş, Caner Ünlü 328

Nanostructured Metal-Organic Framework Aerogel Composites (MOFACs) with Hierarchical Porosity for Enhanced Molecular CO2 Capture
Ayça Tüter Semercioğlu, Hamed Yousefzade, Emre Morkaya, Prof. Can Erkey 329

Identification of Organic and Inorganic Surface Contaminants on ZnS Substrates and Development of Safe Cleaning Protocols Before Photolithography
Berkay Tözendemir, Ahmet Toprak, Tolga Yelboğa, Murat Alp Şahin 330

Plasmonic Nanostructures Integrated Electrically Driven Phase Transition Soft Actuators
Elif Kose, Gokhan Demirel 331

Fabrication and Characterization of ZnBO-Based Ultrasonic Biosensors for Blood Pressure Monitoring by Destructive and Non-Destructive Methods
Gökhan Ekinci, Fatih Mehmet Coşkun, Sümeyye Veziroglu, Surhan Bozkurt 332

High-Performance Electrochemical Sensing Platform Based on MWCNT/Ni-MOF Nanocomposites for Catechol Detection
Havva Nur Guden, Saliha Mutlu, Bülend Ortaç, Ali Karatutlu, Dilek Soyler, Jelena Lillepäg, Volkan Filiz, Nergis Arsu, Sevil Savaskan Yilmaz, Saniye Soylemez 333

Interface-Engineered Diamond-Like Carbon Coatings on ZnS for Durable LWIR Applications
Murat Alp Şahin, Eylül Demir Sağıroğlu, Hasan Hüseyin Güllü, Çiğdem Toparlı 334

Encapsulative Molecule Releasing, Quantum Dot Modified Fluorescent, pH Sensitive Multifunctional Nanofiber Mats Combined by Electrospinning Method
Merve Esra Üngör, Gökçe Asan, Osman Arslan 335

Lightweight Dual-Mode CNT-Aerogel Nanocomposite Stack for Anti- / De-Icing of Sub-20 kg UAVs
Uğur Zaimoğlu 336

Applicability of Fairness, Accountability, Transparency and Ethics (Fate) to Electrospun Nanofibers In Dermal Applications
Yasin Sahin 338

Cell Phone-Based Microscopy for Life Science Applications
Bilge Can, Miktat Efe Eyibilen, Arif Engin Çetin, Zeynep Güneş Özunal 339

Light–Matter Interactions of Fluorescent Molecular Rotors Inside Resonant Microcavities
Eren Toker, Wonmi Ahn 340

Plasmon-Coupled Gold-BODIPY Nanocomposites as High-Efficiency Agents for Combined Photodynamic and Photothermal Therapy
Gülden Yıldız Şengüler, Elif Yıldız, Fazlı Sözmen, Umay Koparan, Açelya Yılmazer Aktuna, Ayhan Elmalı, Sevim Naseri, Ahmet Karatay 341

Electric Field Engineering via Floating Guard Ring Optimization for Edge Breakdown Suppression in PLANAR INGAAS/INP SAGCM APDS
Habibe Keleş, Mert Satılmış, Çağrı Tok, Aydan Yeltik, Fikri Oğuz, Ekmel Özbay 342

Fano Resonances in Metal−Organic Framework ZIF-8
Naz Ülkem, Sümeyye Meryem Çöpür, Ozan Baran Orhan, Tuğçe Küçüktartar, Sinan Balcı, Fadime Mert Balcı 343

Investigations of laser-material interactions using Finite Element Method for the creation of laser-inscribed units of photonic integrated circuits.
Okan Uslu, Mahmut Çağlayan, Timuçin Emre Tabaru, Ali Karatutlu 344

Ultrafast Lattice Dynamics of Layered Material Surfaces
Alp Akbıyık, Felix Kurtz, Hannes Böckmann, Claus Ropers 345

Ion-Implanted Silicon PIN Photodiodes: Design and Electrical Characterization
Emre Doganci, Ozan Yilmaz 346

Piezoelectric Phononic Crystal Enabled Acoustofluidics for Low-Voltage Microparticle Patterning
Nurseli Seda Genç, Ahmet Cicek, Ayşe Erol, Furkan Kuruoğlu 347

Magnetic Susceptibility and ESR Characterization of a Cu(II) Paddle-Wheel Complex with 6 Amonihexonic Acid
Onur Ercem, Simon Pasqualon, Jana Chrappová, Erik Rakovský, Dmytro Kamenskyi, Mamoun Hemmida, Hans-Albrecht Krug von Nidda, Svitlana Vitushkina 348

Different Wavelength LED Array Integrated Wireless System for Enhanced Photobiomodulation-Assisted PVA Hydrogel-Based Skin Wound Healing
Yusuf Aksu, Seda Demirel Topel 349

Controlled Synthesis and Characterization of Silver Nanoplatelets for Biosensor Applications
Emine Eflin Koç, Ülkü Anık 350

Magnetically Actuated Triboelectric Fiber for Self-Powered Sensing Applications
Sk. Rahat Ali, Mustafa Ordu 351

Innovative Biodegradable Films in Chitosan Matrix: Towards Therapeutic Dressings
Berkay Bektaş, Pelin Pehlivanoğlu, Ateş Batıkan Özdamar, Gizem Tezeren, Hürriyet Polat 352

Development of Berberine-Antibiotic Nanocomplexes and Investigation of Their In Vitro Antimicrobial Activities
Cemile Yilmaz, Ismail Ocsoy 353

Investigation of the Potential of Quercetin-Loaded Lipid Nanoparticles (LipQueNPs) to Enhance Quercetin Bioavailability and Their Applicability in Breast Cancer Treatment
Demet Yalçın, Mehmet Aytar, Gülen Melike Demirbolat, Özge Çevik 354

Investigation of The Impact of The Second Disulphide Bond In HIV-1 Capsid Binding Nanobody
Dilan İrem Açan, Gamze Terlemez, Hümeyra Taşkent Sezgin 355

Development of Gold Nanoparticle-Modified, Charge-Tunable Semi-IPN Hydrogels Based On ZEIN, 2-Hydroxyethyl Methacrylate and Vinylimidazole for Controlled Drug Delivery Systems
Elif Sultan Karabayır, Pınar Ilgın, İlknur Atlı, Hava Özay, Özgür Özay 356

A Novel Microfluidics Immunotherapy-On-Chip to Decipher Paracrine Communication Between Colorectal Cancer Spheroids and Tumor-Associated Macrophages
Gurkan Yesiloz, Eylul Tabel, Servin Bagheralmoosavi 357

Development and Characterization of Extracellular Vesicle–Liposome Hybrid Nanoparticles for Nucleic Acid Delivery
Khayala Rasulova, Deniz Bozdağ, İsmail Altıntop, Irmak Bayazıt, Irmak Bayazıt, Gülşah Erel Akbaba 358

Development of Lung Surfactant-Biomimetic Lipid Nanoparticles for Co-Delivery of Paclitaxel and Nintedanib
Melike Belenli Gümüş, Kadir Sinan Arslan, Hasan Ümit Öztürk, Müge Serhatlı, Seda Kızılel, Hilal Yazıcı Malkoçoğlu 359

Investigation of Biomedical Applications of Boron Nitride-Doped Superabsorbent Hydrogels
Nurgul Turker Yildiz, Ozgur Ozay 360

Development and Characterization of Tunable Elastin-Peg/Gelma Hydrogels for Topical Drug Delivery
Osman Doğan, Aslı Kara, Naile Öztürk, Yakup Gültekin, Şeyma Nigiz, Ceren Özkul Koçak, Naciye Dilara Zeybek, İmran Vural 361

Isotonic, hypotonic and hypertonic solutions and their differentiation with optical biosensors
İsmail Celil Haskoloğlu, Oya Akca, Melih Erol Ceyhan, A. Berk Tuzcu, Selim Unlu, Zeynep Güneş Özünal 362

Nanodelivery Systems of Thymoquinone for Enhanced Bioavailability
Rezvan Shaddel, Ali Rashidinejad, Mohammad Mahdi Karimkhani, Ozgur Tarhan, Seid Mahdi Jafari 363

Evaluation of the Bioactive Properties of Silver Nanoparticles Produced by Green Synthesis Using Hericium erinaceus (Lion's Mane Mushroom)
Selcen Çakır, Özgür Özay, İlknur Atlı 364

Biomedical Applications of Al_2O_3-Doped Hydrogels and Composites
Sema Nur Belen, Ozgur Ozay 365

Computational Analysis of Doxorubicin Release Kinetics from Carboxymethylcellulose-Modified Superparamagnetic Iron Oxide Nanoparticles
Sıla Nur Soyat, Seda Demirel Topel 366

Investigation of Biomedical Applications of N-Vinylcaprolactam-Based Hydrogels and Their Composites
Tılsım Ayris Albay, Ozgur Ozay 367

Development of Metal Organic Framework (MOF) Based Material for the Treatment of Triple Negative Breast Cancer
Zehra Canbulat Altun, Beyza Nur Karakoc, Zafer Eroğlu, Melek Sermin Ozer, Gozde Korkmaz, Onder Metin 368

Cell Count Optimization Using a Label-Free Interferometric Reflectance Imaging Sensor (IRIS)
Zg Özünal, Ae Çetin, Ab Tuzcu, S Unlu, A Bilir 369

Design and Development of Magnetic and Thermo-Responsive Polymeric Nanomaterials for Hyperthermia-Induced Controlled Drug Delivery
Muhammad Arsyik Kurniawan, Önder Topel 370

The use of poly(3-sulfopropyl acrylate-co-1-vinyl imidazole)/xanthan gum@Ag nanocomposites modified with cationic groups in wound healing
Özgür Özay, Dilara Gokkaya 371

Development of Colon-Targeted Fe3O4-Loaded Alginate Hydrogel Beads Containing Brassica oleracea L. Extract and 5-Fluorouracil for Enhanced Anticancer Activity
İlknur Atlı, Selcen Cakır, Tılsım Ayris Albay, Ozgur Ozay 372

An Innovative Approach to Opioid Overdose Emergency Intervention: Development of Naloxone-Loaded ZIF-8 Nanoplatform
İrem Avcı, Gülümsernur Can, Mustafa Nakipoglu 373

Generation of Bilayer Oxygen Delivery Antimicrobial Hydrogels for Wound Dressing Applications
Dilek Tepeli, Nermin Seda Kehr 374

Plasmonic-Enabled Edible Soft Biorobots for Targeted Sampling and Molecular Detection
Hayrettin Oner, Gorkem Liman, Gokhan Demirel 375

Interactions and Adhesion Capabilities of Extracellular Vesicles Produced by Probiotic Bacteria in Bladder Cancer Cells
Mehmet Aytar, Demet Yalcin, Gulen Melike Demirbolat, Ozge Cevik 376

Development of Gelatin-Based Hydrogel Inks Loaded with Silver Nanoparticles for 3D Printing
Melike Tuncer, Kemal Çetin, Gökalp Özmen Güler 377

Phage Display-Selected Mineral-Forming Peptides for Biomimetic Enamel Remineralization
Mert Can Akyol, Deniz Tanıl Yücesoy, Hümeyra Taşkent Sezgin 378

Development of Cellulose Nanocrystal Reinforced Hydroxyapatite/Chitosan/Gelatin Nanobiocomposite Scaffolds for Bone Tissue Engineering Applications
Nazli Buket Yilmaz, Deniz Genc, Elif Vargun 379

Anodization of Ti13Nb13Zr Alloy for Total Hip Replacement Applications
Olgu Çağan Özonuk, Muhammed Zahid Doğan, Merve Gültekinoğlu, Eylül Yarar, Cem Bayram, Batur Ercan 380

Handheld Electrospinning-Assisted In Situ Deposition of Silk Fibroin Fibrous Dressings for Wound Healing Applications
Rumeysa Bilginer Kartal, Burçin İzbudak, Ayça Bal Öztürk 381

Development of Superparamagnetic NIR Carbon Dots for Theranostic Applications
Selin Alptekin, Berke Ayevi, Alphan Sennaroğlu, H. Funda Yağcı Acar 382

Development and in vitro Analysis of Immunological Cell-Derived Nano Extracellular Vesicle Added Injectable Hydrogel
Umut Doğu Seçkin, Aylin Şendemir 383

The Effect of Cornelıan Cherry and Cısplatın-Loaded Nanofıbers on Skın Cancer Cells
Zeynep Gergin, Aysegul Tiryaki, Songul Ulag, Ali Sahin 384

Oleuropein-Rich Olive Leaf Extract-Incorporated PAN/CA Nanofibrous Membranes via Electrospinning: Characterization and In Vitro Biocompatibility for Wound Healing
Çağla McKenzie, Amarjargal Altangerel, Timur Tongur, Viraj P. Nirwan, Rebecca Hengsbach, Suray Pehlivanoğlu, Amir Fahmi, Seda Demirel Topel 385

Development and Characterization of Biocompatible Fe_3O_4 Nanoparticles for Magnetically Controlled Microrobotic Applications
Özge Akbülbül, Şeyma Özkan, Barış Oğuz Gürses, Bekir Özkan, Arif Altan Selçuk, Edin Yilmaz 386

Two-Dimensional Nanomaterial–Reinforced Hydrocarbon Membranes for High-Performance Aqueous Organic Redox Flow Batteries
Amina Ben Ayed, Rumman Zaidi, Mina Namvari, Barun K. Chackrabarti, Lukas Pachernegg-Mair, Gutmann Torsten, Stefan Spirk, Tülay Y. İnan 387

Investigation of the Layer and Substrate Dependency of the Thermal Conductivity of MoS_2
Elanur Hut, Ayşe Erol, Fahrettin Sarcan 388

Molecular Dynamics Simulation of 2D Water Confined Between Metal Surfaces
Gamze Ozgunes, Mine Ilk Capar 389

Synthesis of Large-Area Single- to Few-Layered MoS2 With Liquide Phase Mechanism
Gizem Gülistan Bozkurt Akın, Cumhur Gökhan Ünlü, Aleyna Akçay Tataroğlu, Ayten Cantaş Bağdaş, Hatice Dilay Yazıcı 390

Conductive Network Formation and EMI Shielding in MXene/PVA Composites
Nevzat Duman, Muhittin Aktaş, Göktürk Torun, Teng Zhang, Kadri Aydınol, Goknur Cambaz Buke 391

Fabrication and Optoelectronic Characterization of a Lithography-Free Gr/4H-SiC-Based UV Photodetector Array
Melike Gözek, Cem Çelebi 392

Structural Quality vs. Transferability in CVD-Grown Graphene
Oyku Sude Uluturhan, Gokturk Torun, Eren Atli, Elif Okay, Erhan Gurpinar, Emre Ozan Polat, Goknur Cambaz Buke 393

Synthesis of Molybdenum Boride (MoB) via Different Hydrothermal Routes: Structural and Morphological Characterization
Sevda Jafari Aghdam, Aytekin Uzunoglu 394

Solution-Phase Delamination of Magnesium Diboride Facilitated by EDTA
Sibel Şentürk, Cansu Yıldırım, Alara Efsun Canlı, Hale Gürbüz, Hüseyin Enis Karahan 395

MXene-Coated Glass Veil Interlayers for EMI Shielding in Lightweight Glass Fiber Composite Panels for Electrical/Hybrid Vehicles
Sinan Şen, Mert Özdoğan, Berke Kesici, Suat Bahar Baştürk, Gülnur Başer, Melisa Yeke 396

Structural Characterization of Polycarbonate+MoS_2/MWCNT Nanocomposites
Habiba Shirinova, Jeyran Sultanova, Turkan Musayeva, Huseyn Mammadov, B.G. Pashayev 397

Determination and Evaluation of Rheological Properties of Solid Lubricants on Lithium Greases
Alize Pınar, Sevda Atar, Semih Koç, İbrahim Alkaya 398

Dynamic and Electrically Tunable Electromagnetic Shielding via Phase-Engineered MoS2
Atalay Bozdoğan, Hakan Eroğlu, Muharrem Karaaslan, Mustafa Akyol 399

Fabrication and Electrical Characterization of Laterally a-Si:H Photodiodes for Scintillator-Based Radiation Imaging
Leyla Başak Büklü, Hanife Baş, Alp Osman Kodolbaş 400

Power beam combining of quantum cascade lasers using high-reflective distributed Bragg gratings for sensing and defense applications
Mahmut Çağlayan, Ali Aytaç Seymen, Timuçin Emre Tabaru, Bülend Ortaç, Ali Karatutlu 401

Development of a Photocatalytic Nano-TiO_2 Functional Coating for Self-Cleaning PVC Synthetic Leather Used in Public Transportation
Remziye Yıldız Ceyhan, Sevda Manav 402

Comparative Wear Performance and Surface Residue Characterization of Zirconia-Based Grinding Media Used in the Paint Industry
Rüştü Alper Taştekin 403

A Multiscale DFT and Ab Initio Molecular Dynamics Study of LiBOB Tuned Li+ Solvation in Multicomponent Carbonate Electrolytes, Validated by ATR-FTIR
Abdül Kahar Baruğ, Didem Ketenoğlu, Bahadır Boyacıoğlu, Hande Toffoli 404

First-Principles Investigation of CO and CO2 Capture on Group IVB Metal Diboride Monolayers
Ahmet Selim Gözükara, Duygu Şentürk, Ongun Özçelik 405

Quantum Mechanical Assessment of Adsorption Dynamics in Lisinopril-Single Walled Carbon Nanotube Complexes as Drug Delivery System
Celal Yıldıray Köylü, Harun Nalçakan, Müşerref Önal 406

Computational Surface Modeling of Lunar Ilmenite for CO_2 Capture toward In-Situ Resource Utilization
Harun Nalçakan, Celal Yıldıray Köylü, Müşerref Önal 407

Heterostructure Engineering of p- and n-Type P3HT Polymers for Enhanced Organic Photovoltaic Performance
Can Çoruh, Somayyeh Alidoust, Ali Kumralbaş, V. Ongun Özçelik 408

Mechanisms Of Kapton Polyimide Degradation Under Atomic Oxygen Exposure In Low Earth Orbit
Tugay Kaya, İrem Böbrek, Gozde Ozaydin İnce, V. Ongun Özçelik 409

Monobee: Micro-Dispensing-Based Fabrication of Flexible Heaters Using Silver and Carbon Conductive Inks
Yaren Özdemir, Kaan Yapıcı, Ömer Faruk Güleç 410

Theoretical Investigation of Size, Ligand, and Functional Effects on the Excited-State Properties of Silver Nanoclusters
Fahri Alkan, Zeynep Başocak 411

Carbazole-Based Polymers: Promising Emitters for High-Performance Solution-Processable Oleds
Dilara Naz Günaydın, Gökçe Kadeş, Semih Can Çakmaktepe, Gönül Hızalan Özsoy, Ali Çırpan 412

Development and Characterization of Isocyanate-Free Polyurethane (NIPU)-Based Hybrid Coatings Synthesized by Sol-Gel Method
Feride Demir, Ömer Kesmez 413

Opto-Electronic Properties of Carbazole-Phenothiazine Donor Polymers with Pendent Diphenyl Sulfone for Solution-Processable TADF-Based OLED Applications
Gökçe Kadeş, Dilara Naz Günaydın, Semih Can Çakmaktepe, Oğuzhan Karakurt, Ali Çırpan 414

Theoretical and Photophysical Evaluation of a Novel Ethynyl-Bridged Hot Exciton Emitter for OLEDs
Ozan Tekin, Esra Yenidoğan, Cem Maraşlıoğlu, Gönül Hızalan Özsoy, Selçuk Gümüş, Erkan Aksoy, Ali Çırpan, Ali Çırpan, Ali Çırpan, Ali Çırpan 415

Sustainable Cellulose/MXene/CuO Hybrid Composites Derived from Forestry Waste for Electromagnetic Interference Shielding Applications
Rumman Zaidi, Amina Ben Ayed, Tülay Yılmaz İnan 416

Synthesis of Fluorene-Containing DBPA-Type Polymeric TADF Emitters
Semih Can Çakmaktepe, Dilara Naz Günaydın, Gökçe Kadeş, Oğuzhan Karakurt, Ali Çırpan 417

Shrimp-Derived Chitosan-Activated Carbon Composite for Methylene Blue Removal
Hamed Yousefzadeh, Dila Selin Cubukcuoglu, Azra Zeynep Ture 418

Additive-Dependent Triboelectric Performance of Polystyrene Composites against Polytetrafluoroethylene
Ahmet Tulumtas, Ahmet Korkmaz, Barkin Bayram, Onur Demircioglu, Fatih Ozcan, Mehmet Gursoy, Husnu Emrah Unalan 419

GO/CNT-Modified DGEBA-Based Epoxy Systems: Thermal, Curing, and Spectroscopic Evaluation
Berke Sayınman, Elif Okutan 420

Multi-Analytical Characterization of Silica Nanoparticles for Paint and Coating Applications
Ece Sağkol, Seçil Sevim Ünlütürk, Adalet Ayça Biçen İbik, Necati Güdümcüoğlu 421

Correlation Between Microstructural Characteristics and Mechanical Properties of Selective Laser Melted Ti-6Al-4V Alloy Fabricated in Different Build Orientations
Uğurcan Güncan 422

Multifunctional Conjugated Organic Materials for Energy Harvesting, Energy Storage, and High-Performance OLED Applications

Ali Çırpan *

Department of Chemistry, Middle East Technical University, 06800 Ankara, Türkiye

Conjugated organic materials have emerged as versatile platforms for next-generation energy and optoelectronic technologies owing to their tunable electronic structures, solution processability, and multifunctional properties. In this work, advanced conjugated materials were designed and developed for three complementary applications: semitransparent organic solar cells (OPVs), electrochromic asymmetric supercapacitors, and thermally activated delayed fluorescence (TADF) OLEDs. For photovoltaic applications, donor–acceptor conjugated polymers and non-fullerene acceptors were synthesized through molecular engineering strategies involving halogen substitution and π-bridge modulation, leading to optimized binary and ternary OPVs with power conversion efficiencies exceeding 10% and semitransparent devices reaching 8.78%. For energy-storage applications, triphenylamine-based donor–π–acceptor polymers containing EDOT, thiophene, and thieno[3,2-b]thiophene units were electropolymerized to fabricate electrochromic asymmetric supercapacitors exhibiting enhanced electrochemical activity, broad operating voltage windows, high coloration efficiencies, rapid switching kinetics, and excellent cycling stability. In parallel, metal-free TADF emitters based on triazine- and boron-centered donor–acceptor architectures were developed for OLED applications, and the effects of oxygen, sulfur, and selenium heteroatoms on their photophysical and electroluminescent properties were systematically investigated through spectroscopic, electrochemical, theoretical, and device studies. The developed materials demonstrated efficient exciton utilization and promising OLED performance. Overall, the results highlight the power of rational molecular design in conjugated systems to simultaneously address energy harvesting, energy storage, and light-emitting applications, establishing conjugated organic materials as key building blocks for sustainable and multifunctional optoelectronic technologies.

This work was supported by the Scientific and Technological Research Council of Turkey (TÜBİTAK) under Grants 222Z151 and 124Z087 and by METU BAP under Grant ADEP-103-2025-11626.

Measuring quantum properties of thermal light

Gerd Leuchs [*] [1,2,3]

[1] *Friedrich-Alexander-Universität Erlangen-Nürnberg*
[2] *Max Planck Institute for the Science of Light*
[3] *Department of Physics, University of Ottawa*

Naïvely one might expect, that sufficient attenuation of any light field will eventually will lead to measurable quantum effects. This naïve expectation is true (!) even for thermal light when comparing measurements of different types of correlation functions:

(1) the auto correlation function obtained by measuring an intensity time series with a single detector and calculating the correlation function numerically; and

(2) the Hanbury Brown & Twiss type cross correlation function, for which the signal beam is first split, then measured with two detectors, finally correlating the two different measured intensity signals.

The difference between (1) and (2) can only be explained considering a true quantum effect: the projection associated with a quantum measurement.

More mathematically speaking, by comparing (1) and (2) one recovers the commutator of the quantum field operators (arXiv:2601.18870).

Interferometric Sensing: From Multiplexed Affinity to Digital Detection of Biomolecules

M. Selim Ünlü [*] [1,2]

[1] *Boston University, IRIS Kinetics*
[2] *Istanbul Atlas University*

We present a simple yet elegant technology – Interferometric Reflectance Imaging Sensor (IRIS) [1]. Building on multi-disciplinary innovations, IRIS technology defies the conventional wisdom that calls for enhancing the signal through complex optical resonances and exploits light interference from an optically transparent thin film—similar to a soap film that gives rainbow colors when illuminated by white light. Recent innovations in multi-parametric IRIS enables accurate, quantitative and bulk-effect free binding kinetics [2]. IRIS technology has been commercialized for ensemble biomolecular mass measurements allowing for multiplexed affinity measurements to accelerate biomolecular discovery, assay development, and translational diagnostics research.

Perhaps one of the most exciting applications of IRIS is single nanoparticle/molecule counting or digital detection, an approach that provides resolution and sensitivity beyond the reach of ensemble measurements [3,4]. Digital detection is a disruptive technology allowing most advanced tools to become available at a low cost and at the point-of-need [5]. IRIS relies on interference of light reflected from the sensor surface being modified by the presence of particles producing distinct signals that correlate to the polarizability (size) of the particle. A new modality, ‘pixel-diversity’ IRIS (PD-IRIS) [6], introduces a paradigm shift for encoding the necessary optical signature of target particles as it compresses the relevant optical information within a single image frame rather than an image stack by using camera sensors that simultaneously record multiple spectral or polarization channels. A single image can record distinct spectral responses of target particles for different excitation wavelengths (multi-spectral PD-IRIS) or the distinct scattering characteristics for linear polarization (polarization PD-IRIS). With the practical implementation of multiplexed single-molecule detection and counting, “digital detection – the ultimate biomarker analysis” is posed to shape the future of diagnostics.

References:

O. Avci, N. Lortlar Ünlü, A. Yalcin, and M. S. Ünlü, (2015) “Interferometric Reflectance Imaging Sensor (IRIS)—A Platform Technology for Multiplexed Diagnostics and Digital Detection,” Sensors, Vol. 15 (7)

M. Aslan, et al. Multi-parametric interferometric reflectance imaging sensor. Sci Rep 16, 10780 (2026). https://doi.org/10.1038/s41598-026-45282-x

D. Sevenler, et al. (2018) “Digital Microarrays: Single-Molecule Readout with Interferometric Detection of Plasmonic Nanorod Labels.” ACS nano 12 (6), 5880-5887

F. Ekiz Kanik, et al. (2022) “Attomolar sensitivity microRNA detection using real-time digital microarrays,” Scientific Reports 12 (1), 1-10

MS Ünlü, (2016) “Digital detection of biomarkers for low-cost, high-sensitivity diagnostics,” SPIE News http://spie.org/newsroom/6318-digital-detection-of-biomarkers-for-low-cost-high-sensitivity-diagnostics

MS Ünlü, I Celebi, and M Aslan, (2025) “Pixel-diversity nanoparticle detection by interferometric reflectance imaging sensor,” US Patent 12,392,721

ID: 451

The Role of Nanomorphology in Organic Semiconductors for Electronic Devices

Derya Baran *

Materials Science and Engineering Program (MSE), Physical Sciences and Engineering Divistion (PSE), King Abdullah University of Science and Technology (KAUST), 23955, Thuwal Saudi Arabia

Controlling nanomorphology of an organic semiconductor is key to achieve high performing electronic devices such as photovoltaics and thermoelectrics. In this talk, I will discuss these two types of devices for energy conversion. I will focus on strategies to control nanomorphology of organic semiconductors using thermosets for thermally and photostable photovoltaic devices in hot climates.[1,2] Further, I will show molecular interactions can be used as a design parameter to control doped conjugated polymer films across different length scales. First, I will present our work on conjugated polymer nanofiber self-assembly, highlighting how solvent–polymer interactions direct aggregation pathways toward greener fabrication of electronically active nanostructures.[3] I will then show how intermolecular-force-driven anisotropy enables preferential molecular orientation in n-type conjugated polymers, breaking the conventional trade-off between electrical conductivity and Seebeck coefficient in organic thermoelectrics.[4]

References:

Xu, H., Han, J., Babics, M. et al. Elucidating the photodegradation pathways of polymer donors for organic solar cells with seven months of outdoor operational stability. Nat. Photon. 19, 415–425 (2025).

Han J, Xu H, Sharma A., et al In situ formation of thermoset matrices for improved stability in organic photovoltaics Joule, 8, 2883-2902 (2024).

Y. Zhang, D. Rosas Villalva, O. Zapata-Arteaga, et al. “Molecular-Interactions Driven Conjugated Polymer Nanofiber Self-Assembly Toward Greener Fabrication.” Advanced Materials: e73513 (2026).

Rosas Villalva, D., Derewjanko, D., Zhang, Y. et al. Intermolecular-force-driven anisotropy breaks the thermoelectric trade-off in n-type conjugated polymers. Nat. Mater. 24, 1236–1244 (2025).

Cavitation on a Chip Devices with Functional Surfaces and Emerging Applications

Ali Koşar *

Sabanci University Nanotechnology and Applications Center (SUNUM), Center of Excellence for Functional Surfaces and Interfaces for Nanodiagnostics (EFSUN), Sabanci University, Istanbul, Türkiye

Hydrodynamic cavitation (HC) is one of the major phase change phenomena. This phenomenon incepts because of a sudden decrease in the local pressure accompanied with consequent increase, leading to a progressive cycle of vaporization, bubble generation, and bubble collapse. While its catastrophic effects on turbomachinery have been widely investigated in macro scale, it could be manipulated and exploited for specific applications in micro scale with functional surfaces.

Thanks to the advances in lab-on-a-chip, organ-on-a chip and microfabrication and 3D printing technologies, HC-on-a-chip (HCOC) has been proposed as a new research lane in micro and nanofluidics. With HCOC, it is possible to have hydrodynamic cavitation under controlled conditions and to manipulate it for energy and biomedical applications. In addition, functional surfaces such as those with micro scale roughness elements can facilitate and manipulate micro scale hydrodynamic cavitation due to dominant surface effects in micro scale. The applications of HCOC such as diagnostic tool based on different responses to cavitation, biomolecule detection, and energy efficient water treatment will be covered in the talk. Recent developments and future research directions will be also discussed.

Nanozing phthalocyanines for health and environment

Fabienne Dumoulin *

Acibadem University

Phthalocyanines are used in a wide range of applications, from photodynamic therapy [1] to the catalysis of carbon dioxide reduction [3] or methane oxidation [4]. Amongst others, such as cardiac rhythm photomodulation [5].

There are tens of thousands phthalocyanine structures reported, as their structure allows for nearly infinite structural variations.

Nanosizing phthalocyanines is a versatile and powerful manner to expand the range of their optical, catalytic and biological properties.

Our recent explorations of nanozing phthalocyanines for biomedical and environmental purposes will be presented.

[1] Pui-Chi Lo, M. Salomé Rodriguez-Morgade, Dennis K. P. Ng*, Tomas Torres*, Ravindra Pandey* and Fabienne Dumoulin*, Chemical Society Reviews, **2020**, 49, 1041-1056

[2] Min Wang, Kristian Torbensen, Danielle Salvatore, Shaoxuan Ren, Dorian Joulié, Fabienne Dumoulin, Daniela Mendoza, Benedikt Lassalle-Kaiser, Umit Işci, Curtis Berlinguette, Marc Robert, Nature Commun., **2019**, 10, 3602

[4] Ümit İşci, Abayomi S. Faponle, Pavel Afanasiev, Florian Albrieux, Valérie Briois, Vefa Ahsen, Fabienne Dumoulin,* Alexander B. Sorokin* and Sam P. de Visser*, Chem. Sci. **2015**, 6, 5063–5075

[5] Lukas Naimovičius, Mila Miroshnichenko, Ekin Opar, Helen Hölzel, Masa-aki Morikawa, Nobuo Kimizuka, Manvydas Dapkevičius, Justas Lekavičius, Edvinas Radiunas, Karolis Kazlauskas, Víctor Cilleros-Mañé, Fabio Riefolo, Carlo Matera, Kevser Harmandar, Masahiko Taniguchi, Fabienne Dumoulin, Jonathan S. Lindsey, Pankaj Bharmoria, Pau Gorostiza, Kasper Moth-Poulsen, Nature Commun., **2025**, 16, 6377.

ORCID:
Fabienne Dumoulin: 0000-0002-0388-8338

Keyword: *Phthalocyanine*

Bridging Light and Medicine: advances in photoswitchable&bioactive molecules and their luminescent nanohybrids

Alina Manshina [*1], Gulia Bikbaeva[1], Anastasia Egorova[2], Ilya Kolesnikov[1], Tatiana Dolenko[3], Anna Pilip[4]

[1] *St. Petersburg State University*
[2] *St. Petersburg State Technological Institute (Technical University)*
[3] *M.V. Lomonosov Moscow State University*
[4] *Scientific Research Centre for Ecological Safety of the Russian Academy of Sciences*

Photopharmacology is an emerging and dynamic research area at the crossroads of multiple disciplines, including synthetic chemistry, materials science, medicine, and photonics. Its core concept is to achieve precise, light-mediated regulation of a drug's therapeutic effects. Traditionally, photopharmacological compounds are created by attaching molecular switches (structures that change shape when exposed to light) to a pharmacophore (which is the molecule responsible for biological activity). When illuminated, these switches undergo a structural rearrangement, altering the molecule's 3D structure and, consequently, its biological potency. However, this approach often faces a major hurdle: finding the right combination of switch and pharmacophore is a difficult, trial-and-error process, and the resulting difference in bioactivity between the "on" and "off" states is frequently minimal.

Our work introduces a groundbreaking and more effective strategy: developing single-molecule systems where both the biological function and the light-sensitive switching capability are inherent to the same structure. To test this concept, we investigated their ability to inhibit butyrylcholinesterase, an enzyme linked to neurodegenerative conditions like Alzheimer's disease and skin disorders such as psoriasis and dermatitis. In this presentation, we will showcase several families of these intrinsically photo-responsive compounds. Some become deactivated upon light exposure, while others are activated. We discovered that this modulation of their biological effect is driven by light-induced structural changes—a "laser twist"—such as the rotation of phosphonate groups or cis-trans isomerization.

Finally, we will discuss our approach to adding another layer of functionality: the ability to track these molecules in space. This is achieved by attaching them to luminescent nanocarriers, like nanoparticles doped with rare-earth elements or carbon quantum dots [1-5]. These core@shell hybrid nanostructures are ingeniously designed to combine all the essential features for next-generation photopharmacology: (1) the ability to switch biological activity with light, (2) luminescence for visualizing where the drug goes, and (3) the capacity to determine the molecule's switching state by analyzing the luminescence characteristics. In essence, this presentation will offer a comprehensive look at the field of photopharmacology and highlight our key advances in creating versatile systems that address multiple major challenges at once.

Acknowledgment:
The study was carried out at the expense of the Russian Science Foundation No. 22-13-00082-P, https://rscf.ru/en/project/22-13-00082-P/. Authors are grateful to “Centre for Optical and Laser Materials Research”, “Centre for Magnetic Resonance”, “Nanocenter” of St.Petersburg State University Research Park.

References:
I. Kolesnikov, A. Khokhlova, D. Pankin, et al, New J. Chem., 2021, 45, 15195–15199.
D. Pankin, A. Khokhlova, I. Kolesnikov, et al, Spectrochim. Acta Part A, 2021, 246, 118979
G. Bikbaeva, A. Egorova, N. Sonin, et al., ChemPhotoChem, 2023, e202300131
G. Bikbaeva, A. Pilip, A. Egorova, et al, Nanomaterials, 2023, 13, 2409
G. Bikbaeva, A. Pilip, A. Egorova, et al, Nanoscale Advances, 2024, 6, 4417-4425

Keyword: *butyrylcholinesterase inhibition, luminescence, photoactivation of bioactivity*

ID: 44

Nanoscale Mimicry of Virus–Host Interactions: Redefining Biosensing Strategies for Infectious Disease Diagnostics

Ülkü Anık *

Muğla Sıtkı Koçman University

Biosensors possess inherent characteristics—such as practicality, robustness, and cost-effectiveness—that make them highly suitable for conversion into effective diagnostic tests.

Conventional biosensors typically rely on antigen–antibody interactions, enzymes, microorganisms, nucleic acids, or aptamers as recognition elements. However, alternative approaches have emerged, including biosensors based on virus–host interactions at the nanoscale, encompassing both protein–protein and glycan-mediated recognition mechanisms involved in viral attachment and entry.

Importantly, these interactions occur at the nanoscale, where molecular recognition is governed by spatial arrangement, multivalency, and surface chemistry. This principle can be exploited to develop biosensors that mimic viral infection mechanisms. This biomimetic strategy offers a key advantage: the ability to detect multiple virus variants without requiring frequent redesign of the recognition elements, as is often necessary in conventional biosensing systems [1].

Meanwhile, the incorporation of nanomaterials into diagnostic biosensor platforms provides several performance-enhancing benefits. These include a high surface-to-volume ratio, enabling efficient functionalization with bioactive molecules, as well as excellent electrochemical properties, conductivity, and biocompatibility. Many nanomaterials also exhibit localized surface plasmon resonance, allowing strong visible coloration and tunable optical properties for sensitive and selective detection [2]. For instance, gold nanoparticles (AuNPs) demonstrate high surface energy, promoting strong interactions with biomolecules such as proteins, lipids, and nucleic acids [2].

In conclusion, biosensors that leverage nanoscale virus-host interactions—supported by nanomaterial-enhanced platforms—offer a powerful and adaptable approach for infectious disease diagnostics. This strategy not only improves detection performance but also provides robustness against viral mutations, supporting the development of next-generation diagnostic systems.

ORCID:
Ülkü Anık: 0000-0002-3607-7208

References:
Anık, Ü., Çaylayık, N. S. Development of Epstein–Barr virus biosensor by mimicking its infection mechanism for early detection of multiple sclerosis. Scientific Reports, 2025, 15, 28089.
2. Anık, Ü., Çaylayık, N. S. Early detection of multiple sclerosis using spectroscopic Epstein–Barr virus biosensors based on infection mechanism mimicry. Analytical Chemistry, 2025, 97(37), 20466–20474.

Keyword: *Nano biosensors, nanoscale interactions, nanomaterials*

SiOC Aerogels: Impact of Nanoscale Porosity on Properties

Cekdar Vakif Ahmetoglu *

Advanced Ceramic Materials, Technical University of Berlin, BA3, Hardenbergstraße 40, 10623 Berlin

In this work, monolithic polymer, hybrid, and ceramic SiOC aerogels were synthesized via the polymer-derived ceramic (PDC) route and systematically characterized. Despite employing two distinct drying routes—ambient-pressure (ambigels) and CO_2 supercritical drying—the resulting materials displayed comparable structural characteristics, indicating that the simpler, more cost-effective ambient-pressure drying can effectively replace supercritical drying without a significant loss of performance. Beyond neat aerogels, foam–aerogel composites were fabricated by infiltrating aerogels into substrate foams, yielding lightweight monoliths that remain readily machinable into complex shapes while preserving their intrinsic properties. All aerogels and composites were primarily assessed for their thermal insulation and heat-transfer behavior, with additional features highlighting their suitability for multifunctional, thermally demanding applications.

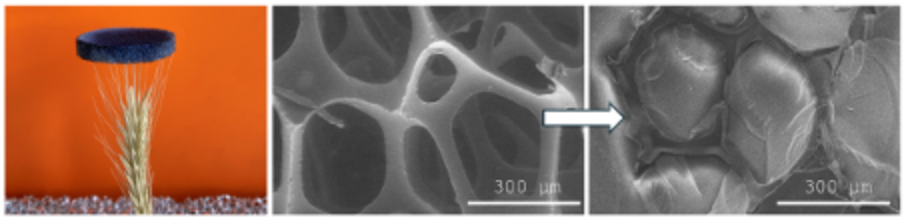


Figure: SiOC Foam-Aerogel Composite *(left)*, SEM images of neat foam before aerogel impregnation *(middle)* and after aerogel impregnation *(right)*.

ID: 13

Fiber-Based Nanogenerators for Advanced Wearable Technologies

Mustafa Ordu *

UNAM – National Nanotechnology Research Center and Institute of Materials Science and Nanotechnology, Bilkent University, Türkiye

The rapid growth of wearable technologies drives demand for real-time, battery-independent monitoring of human activities and physiological signals. Flexible piezoelectric and triboelectric nanogenerators offer a compelling solution by acting as self-powered sensors that function without external power supplies. These devices also enable energy harvesting from everyday human motion, presenting a viable alternative energy source for low-power electronics. Among them, fiber-shaped nanogenerators stand out due to their inherent flexibility, stretchability, and compatibility with textile manufacturing, allowing direct integration into wearable fabrics. This talk will present our research activities on the development of thermally drawn, fiber-based triboelectric and piezoelectric nanogenerators, highlighting their dual role as both self-powered sensors and energy harvesters. By incorporating low-dimensional materials into thermally drawn fibers, the sensing and energy conversion performances of nanogenerators are significantly enhanced. Moreover, forming highly porous media and micro/nano spheres in fibers further controls the electrical properties that can be exploited for multifunctional sensing. These smart fibers demonstrate promising capabilities for tracking physical human activities and vital signs such as heart rate, respiration, and blood pressure. Furthermore, their ability to convert mechanical energy into electricity opens pathways for powering small-scale and portable electronic devices, without the need for traditional batteries.

ID: 442

4D-STEM: Expanding the Analytical Capabilities of STEM

Julie Marie Bekkevold *

Thermo Fisher Scientific Achseweg Noord 5 | 5651 GG Eindhoven | The Netherlands

Recent advances in detector technology have enabled the routine acquisition of diffraction patterns at every probe position in a scanning transmission electron microscope (STEM). This generates a four-dimensional dataset, consisting of a two-dimensional diffraction pattern recorded at each position within a two-dimensional scan, giving rise to the term 4D-STEM. By capturing the full scattering information from the electron beam, 4D-STEM provides access to a wide range of analytical techniques, including orientation and phase mapping, strain analysis, electric and magnetic field measurements, and phase reconstruction methods such as ptychography. These capabilities allow researchers to extract significantly more information from a specimen than is possible using conventional STEM imaging alone. This presentation will introduce the principles of 4D-STEM and discuss the key detector requirements that enable efficient data acquisition, including detector speed, sensitivity, and dynamic range. Particular emphasis will be placed on the implementation of 4D-STEM on the Thermo Scientific Spectra equipped with the Ceta-S camera and Speed Enhancement technology. Application examples from materials science will illustrate how 4D-STEM can provide new insights into structure, crystallography, and nanoscale functionality.

HRTEM Investigations on Magnesium Alloys

Özgür Duygulu * **, Gizem Oktay Irmak, Ömür Can Odabaş**

TUBITAK MAM, Materials and Process Technologies, Kocaeli Turkey

Magnesium (Mg) alloys are premier candidates for structural applications due to their exceptionally low density, high specific strength and stiffness, excellent castability, superior machinability, and high energy absorption capacity. As the sixth most abundant metal on Earth, Mg also provides significant environmental benefits through its recyclability. Recently, wrought Mg-Zn alloys have gained prominent interest owing to their enhanced strength and ductility achieved via precipitation (age) hardening. This study investigates the effects of solutionizing and artificial aging heat treatments on the microstructural and mechanical evolution of extruded and rolled Mg-Zn alloys. Hardening response and aging curves were established using microhardness testing. Phase identification and macro/microstructural evaluations were conducted using X-ray diffraction (XRD), optical microscopy (OM), and scanning electron microscopy (SEM). Furthermore, advanced transmission electron microscopy (TEM) techniques including selected area electron diffraction (SAED), energy dispersive X-ray spectroscopy (EDS), and high resolution transmission electron microscopy (HRTEM) were utilized to rigorously analyze the precise size, type, morphology, and distribution of secondary phases and precipitates.

Keyword: *Magnesium alloys, HRTEM, EDS, SAED*

Sharper eyes, deeper insights: Advances in TEM electron diffraction for nanoscale crystallography

Ercin Cagan Duran *

Department of Metallurgical and Materials Engineering, Istanbul Technical University, Türkiye

The advances in detector technology significantly improved the electron diffraction data quality in transmission electron microscopes (TEM) which in turn allowed unprecedented characterisation analyses to be conducted on various materials. Traditional charge-coupled devices (CCD cameras) along with photographic films have been largely superseded by direct electron detectors (DEDs) and hybrid pixel detectors. These detectors offer much higher sensitivity, readout speeds and dynamic range as well as incredible signal-to-noise ratios. Due to the availability of these detectors, it is now possible to collect high quality electron diffraction data from beam sensitive materials (which require low electron doses) and also do very fast 4-dimensional scanning transmission electron microscopy (4DSTEM) and electron diffraction tomography experiments.

In order to showcase this, an example of precession electron diffraction tilt series experiment on La-doped $SrTiO_3$ is presented. With this approach a novel nano-scale phase was found and its crystal structure was determined. The data for that study was collected on a CCD camera but the quality was good enough to perform an accurate structure solution and refinement. In addition, a low dose continuous rotation electron diffraction tomography experiment on synthetic rhabdophane ($DyPO_4 \cdot nH_2O$) is also presented. This experiment was performed using a high-speed DED diffraction camera and due to the high data quality, it was possible to determine the disorder in the crystal structure using the diffuse background signals. And lastly, a correlated 4DSTEM/EDS study on Co_2FeSi thin films is presented to investigate the structural orderings within the material. Using a combined structural and compositional analysis approach, which is performed with the help of machine learning algorithms, the phases of the material were correctly analysed.

Hybrid Nanomaterial-Molecularly Imprinted Polymer Platforms for Advanced Electrochemical Sensing

Sibel A. Özkan *

Ankara University, Faculty of Pharmacy, Department of Analytical Chemistry, Ankara, Türkiye

Molecular imprinting technology is a creative approach to developing synthetic mimics of biological components like antibodies and enzymes. By creating and then clearing template-specific cavities, this method enables selective recognition and rebinding of target molecules. These synthetic receptors are often more stable and have higher affinities than their natural counterparts [1]. To ensure maximum performance, researchers must optimize the choice of functional monomers, crosslinkers, and their ratios, all of which depend on the specific polymerization technique used [2]. The structural integrity of the polymer and the non-covalent interactions (such as hydrogen bonds and van der Waals forces) between the template and monomer are vital to the MIP's success [1, 2]. Ultimately, MIP-based electrochemical sensors are essential tools because they provide the high selectivity that standard electrochemical sensors often lack.

Nanotechnology has become very popular in the field of sensors. It is thought that the use of such technologies and nano-sized materials could have beneficial effects on sensor performance. Nano-sized materials have been shown to have several novel and interesting physical and chemical properties. Nanomaterials, renowned for their high electron-transfer capacity and large specific surface area, are increasingly employed to modify MIP sensors. Unlike traditional electrochemical sensors, nanomaterials-based MIP sensors have excellent sensing and recognition capabilities.

Nanomaterial-based MIP sensors and miniature electrochemical transducers have proven their practicality by successfully detecting target analytes in situ. Their superior chemical and physical stability, low-cost manufacturing, high selectivity, and fast response have made nanomaterial-based MIPs an exciting field of research. Studies on electrochemical nanomaterial-based MIP sensors for the detection of pharmaceuticals, heavy metals, hormones, enzymes, and biomarkers have shown promising results. These sensors have been successfully used in biological fluids (serum and urine samples) and pharmaceutical samples, demonstrating their real-world applicability.

The increase in environmental awareness and stricter regulations for the use of chemicals and economic competitiveness are challenging the scientific community and industry to explore greener strategies in their processes, preventing pollution and reducing waste while maximizing the efficiency of the processes, and that can only be achieved by the application of green chemistry and engineering principles.

Molecular imprinting has much to gain in applying these green tools since new alternative solvents and clean technologies, combined with computational tools, can optimize both the polymer and the process.

ORCID:
Sibel A. Özkan: 0000-0001-7494-3077

References:
[1] L. Uzun, A.P.F. Turner, Molecularly-imprinted polymer sensors: realising their potential, Biosens. Bioelectron. 76 (2016) 131e144.
[2] S. Irem Kaya, Ahmet Cetinkaya, Sibel A. Ozkan, Trends in Environmental Analytical Chemistry, 37, (2023), e00193.

Keyword: *Analysis, Molecular imprinting polymer, nanomaterial*

Triboelectric Nanogenerators for Wearable Electronics, Self-Powered Sensing, and Sustainable Energy Harvesting

Hüsnü Emrah Ünalan *

Department of Metallurgical and Materials Engineering, Middle East Technical University (METU), 06800, Ankara, Türkiye

Triboelectric nanogenerators (TENGs) have emerged as versatile platforms capable of converting ubiquitous mechanical energy into electrical power while simultaneously enabling self-powered sensing. Their simple device architecture, broad material compatibility, and scalability have attracted considerable attention for applications ranging from wearable electronics to large-scale renewable energy harvesting. This presentation provides an overview of our recent research on TENGs, demonstrating how different material systems and device architectures have been engineered to address diverse application requirements. The presentation begins with wearable TENGs based on silver nanowire-functionalized fabrics laminated with thermoplastic polyurethane (TPU), where washability, Joule heating capability, and energy harvesting are integrated into flexible textile platforms for human–machine interfaces [1]. To further improve flexibility and textile compatibility, coaxially wet-spun core–shell fibers incorporating carbon black, silver nanowires, and TPU are introduced, providing stretchable electronic fibers suitable for next-generation wearable systems [2]. The incorporation of two-dimensional TiS_2 nanosheets and their oxidized TiO_2 counterparts into the triboelectric layer significantly enhances electrical output, enabling machine-learning-assisted tactile sensing in smart gloves while delivering sufficient power to illuminate 100 LEDs [3]. Beyond wearable systems, transparent triboelectric devices employing optimized silver nanowire networks are presented for self-powered droplet sensing, simultaneously enabling pH determination, chemical concentration monitoring, and transparent Joule heating within a single platform [4]. The discussion then extends to sustainable energy harvesting, where buoy-type TENGs capable of delivering stable power densities up to 1.1 W m^{-2} under simulated ocean-wave conditions are demonstrated for blue-energy applications [5]. Finally, free-standing triboelectric generators fabricated through additive manufacturing are introduced, including compact oscillating PTFE marble devices and rolling triboelectric–electromagnetic hybrid bearings that efficiently harvest rotational mechanical energy while powering LEDs, environmental sensors, and portable electronic devices [6,7]. Collectively, these studies demonstrate the versatility of triboelectric nanogenerators across wearable electronics, transparent sensors, rotational energy harvesting, and blue-energy systems. By combining advanced nanomaterials, scalable manufacturing methods, and application-driven device engineering, TENG technology continues to evolve toward practical self-powered systems capable of supporting future intelligent and sustainable electronic technologies.

References:

[1] Fabric Based Wearable Triboelectric Nanogenerators for Human Machine Interface, D. Doganay, M. O. Cicek, M. B. Durukan, B. Altuntas, E. Agbahca, S. Coskun, H. E. Unalan, Nano Energy 89 (2021) 106412.
[2] Wet Spun Core-Shell Fibers for Wearable Triboelectric Nanogenerators, D. Doganay, O. Demircioglu, M. Cugunlular, M. O. Cicek, O. Cakir, H. U. Kayaci, S. Çınar Aygün, H. E. Unalan, Nano Energy 116 (2023) 108823.
[3] O. Demircioglu, unpublished work.
[4] Post-Treatment Optimization for Silver Nanowire Networks for Transparent Droplet-Based TENG Sensors, O. Cakir, D. Doganay, M. Cugunlular, M. O. Cicek, O. Demircioglu, S. Coskun, H. E. Unalan, Nano Energy 128 (2024) 109940.
[5] Triboelectric Nanogenerators for Blue Energy Harvesting in Simulated Wave Conditions, O. Demircioglu, M. O. Cicek, D. Doganay, G. Gazaloglu, C. Baykal, S. Cinar, H. E. Unalan, Nano Energy 107 (2023) 108157.
[6] B. Bayram, unpublished work.
[7] M. Cugunlular, unpublished work.

ID: 438

Third-Order Local Randomized Measurements for Finite-size Entanglement Certification

Giovanni Scala *

Politecnico di Bari

Randomized measurements access nonlinear functionals without full tomography, yet turning third-order local single-copy data into a strong entanglement test remains difficult. We convert the reduction criterion into an experimentally measurable bipartite separability criterion by testing it on the span of the identity, the local marginals, and the state itself. This yields a 4x4 matrix built from experimentally accessible second- and third-order local invariants. Entanglement is certified when its minimum eigenvalue becomes negative. This can be inferred from single-copy randomized measurements with a finite number of shots independent on local dimensions. We show a drastic improvement beyond what can be detected via the second-order criteria. Finally, we generalized to the multipartite scenario, unveiling the underlying structure via group theory.

ID: 487

Biomedical Applications of Nanotechnology: Current Status and Future Directions

Ceyda Öksel Karakuş *

İzmir Institute of Technology (IZTECH)

Nanotechnology is reshaping the landscape of modern biomedicine by enabling innovative approaches to disease prevention, diagnosis, and treatment. Advances in nanomaterials have led to significant progress in targeted drug delivery, molecular imaging, biosensors, tissue engineering, regenerative medicine, and personalized healthcare. While numerous nanotechnology-based products have successfully reached clinical practice, many promising technologies still face challenges related to safety evaluation, regulatory approval, scalable manufacturing, and clinical translation. This keynote will provide an overview of the current state of nanotechnology in biomedicine, highlighting recent scientific breakthroughs, successful clinical applications, and emerging trends. It will also discuss the opportunities and challenges that will shape the next generation of nanomedicine, with particular emphasis on translational research and interdisciplinary collaboration. By bridging fundamental research with real-world healthcare needs, nanotechnology is expected to play a transformative role in improving patient outcomes and advancing precision medicine

Shaping Green Hydrogen Technologies: Graphene-Based Electrocatalysts and Transition Metal–Modified Iridium Oxides for PEM Fuel Cells and Electrolyzers

Selmiye Alkan Gürsel [*1,2], Hamza Arslan[1], Bahadır Patır[1], Büşra Çetiner[1], Naeimeh Rajabalizadeh Mojarrad[2], Begüm Yarar Kaplan[2], Alp Yürüm[1,2], Navid Haghmoradi[3], Sina Abdolhosseinzadeh[4], Ahmet Can Kırlıoğlu[5], Eser Dinçer Hafızoğlu[6], Aysel Zahidov[6], Vahide Nuran Mutlu[6]

[1] Faculty of Engineering and Natural Sciences, Sabancı University, Istanbul, Turkey
[2] Sabanci University Nanotechnology Research and Application Center (SUNUM), Istanbul 34956, Turkey
[3] Karlsruhe Institute of Technology, Karlsruhe, Germany
[4] Laboratory for Functional Polymers, Empa, Swiss Federal Laboratories for Materials Science and Technology, Überlandstrasse 129, CH-8600 Dübendorf, Switzerland
[5] Vlaamse Instelling voor Technologisch Onderzoek (VITO), Boeretang 200, 2400 Mol, Belgium
[6] SOCAR Türkiye R&D and Innovation Co., Aliaga, Izmir, Turkey

Hydrogen is emerging as a cornerstone of the clean energy transition, with polymer electrolyte membrane (PEM) fuel cells and PEM water electrolyzers representing two complementary technologies for sustainable energy conversion and green hydrogen production. Despite remarkable progress, the widespread deployment of these systems is still constrained by the limited activity, durability, and high cost of noble metal electrocatalysts required for the oxygen reduction reaction (ORR) in fuel cells and the oxygen evolution reaction (OER) in electrolyzers[1,2]. This invited presentation highlights our group's research on designing advanced electrocatalysts that improve performance while reducing precious metal consumption in PEM-based hydrogen technologies.

For PEM fuel cells, we developed a series of graphene-supported Pt electrocatalysts by exploiting graphene's exceptional electrical conductivity, large specific surface area, and electrochemical stability. Various graphene architectures including graphene nanoplatelets, reduced graphene oxide (rGO), functionalized graphene derivatives, and graphene-based hybrid supports were engineered to optimize Pt dispersion, charge transfer, and catalyst utilization. These materials enabled significant reductions in Pt loading while delivering enhanced ORR activity and improved fuel cell performance[3,4]. We further introduced a scalable photocatalytic deposition strategy in which transition metal ions simultaneously act as hole scavengers and surface modifiers, providing precise control over Pt nanoparticle nucleation and growth[5,6].

The second part of the presentation focuses on advanced anodic electrocatalysts for acidic PEM water electrolyzers. To reduce the dependence on iridium while enhancing catalytic performance, we synthesized pristine and transition metal (Ti, Mn, and Ni) doped IrO_2 electrocatalysts using a sol-gel method. By tailoring the thermal treatment conditions, both amorphous-like and highly crystalline rutile structures were obtained, enabling a systematic investigation of the combined effects of composition and crystallinity on the oxygen evolution reaction (OER). Comprehensive structural, morphological, and electrochemical characterization revealed that both the incorporated transition metal and the degree of structural ordering strongly influence catalytic behavior. Among the investigated catalysts, Mn incorporation produced the most significant enhancement in OER activity, while amorphous catalysts consistently outperformed their crystalline counterparts owing to their higher density of under-coordinated active sites and greater structural flexibility. In particular, the amorphous Mn-modified IrO_2 catalyst exhibited outstanding activity, delivering an overpotential as low as 287 mV at 10 mA cm^{-2} with a Tafel slope of 49 mV dec^{-1}, while maintaining stable operation for 12 h under acidic conditions. These findings demonstrate that precise control of both the electronic structures through transition metal incorporation and the catalyst crystallinity provides an effective strategy for developing durable, high-performance, and reduced-iridium OER electrocatalysts[7]. Furthermore, integrating these catalysts onto anodized TiO_2 nanotube arrays grown on Ti mesh created high-surface-area, corrosion-resistant electrodes that further enhanced catalyst utilization, activity, and operational stability in PEM electrolyzers.

Together, these studies demonstrate how rational catalyst and support engineering from graphene-based nanostructures for PEM fuel cells to transition metal-modified iridium oxides for PEM electrolyzers can simultaneously enhance activity, durability, and cost effectiveness. By combining advanced nanocarbon architecture, controlled catalyst synthesis, and electronic structure engineering, these approaches contribute to the development of scalable, high-performance materials that will help shape the next generation of green hydrogen technologies.

Acknowledgment:
This work was supported by the European Union's Horizon 2020 research and innovation program (Graphene Flagship, Grant No. 696656) and SOCAR Türkiye R&D and Innovation Co.

References:
1. Mojarrad, N. R., Kırlıoğlu, A. C., Ölmez, B., Hamedani, A. A., Buldu-Akturk, M., Zabara, M. A., Yürüm, A., Ozkan, C. S., Alkan Gürsel, S., Yarar Kaplan, B., Ozkan, M. "Advances in membranes and electrocatalysts to optimize proton-exchange membrane fuel cells." Cell Reports Physical Science, 6, 102728 (2025).
2. Yarar Kaplan, B., Kırlıoğlu, A. C., Alinezhadfar, M., Zabara, M. A., Rajabalizadeh Mojarrad, N., İskandarani, B., Yürüm, A., Ozkan, C. S., Ozkan, M., Alkan Gürsel, S. "Hydrogen production via electrolysis: Operando monitoring and analyses." Chem Catalysis, 3(5), 100601

(2023).
3. Quesnel, E., Roux, F., Emieux, F., Faucherand, P., Kymakis, E., Volonakis, G., Giustino, F., Martín-García, B., Moreels, I., Alkan Gürsel, S., et al. "Graphene-based technologies for energy applications, challenges and perspectives." 2D Materials, 2(3), 030204 (2015).
4. Kaplan, B. Y., Haghmoradi, N., Biçer, E., Merino, C., Alkan Gürsel, S. "High-performance electrocatalysts supported on graphene-based hybrids for polymer electrolyte membrane fuel cells." International Journal of Hydrogen Energy, 43(52), 23221–23230 (2018).
5. Abdolhosseinzadeh, S., Sadighikia, S., Alkan Gürsel, S. "Scalable synthesis of sub-nanosized platinum-reduced graphene oxide composite by an ultra-precise photocatalytic method." ACS Sustainable Chemistry & Engineering, 6(4), 3773–3782 (2018).
6. Haghmoradi, N., Sarı, Z. T., Kırlıoğlu, A. C., Kaplan, B. Y., Dedeoğlu, B., Zahedimaram, P., Abdolhosseinzadeh, S., Alkan Gürsel, S. "Co^{2+}, Fe^{2+}, and Ni^{2+}: Modifiers for photocatalytic deposition of highly active Pt on graphene-based supports." ACS Applied Energy Materials, 5(11), 13939–13951 (2022).
7. Arslan, H., Patır, B., Çetiner, B., Mojarrad, N. R., Yarar Kaplan, B., Yürüm, A., Alkan Gürsel, S. "Iridium-based doped electrocatalysts for water splitting in PEM electrolysers." Manuscript in preparation (2026).

ID: 11

From Photonics to Intelligent Lab Infrastructure

Arif E. Cetin *

Izmir Biomedicine and Genome Center, Balcova, Izmir, Turkey

Modern life science laboratories rely on multiple standalone instruments for imaging, incubation, liquid handling, and environmental regulation. This fragmented infrastructure increases operator dependency, limits reproducibility, and raises operational costs. Here, we present an integrated and modular laboratory automation platform engineered to unify precision liquid handling, real-time cell imaging, and controlled incubation within a compact and scalable architecture.

The system combines five-axis robotic motion, PID-controlled CO_2 and temperature regulation, automated droplet generation, and programmable fluidics in a single closed-loop framework. Integrated brightfield imaging enables real-time monitoring of cell confluency, viability, adhesion dynamics, and long-term proliferation. Automated cleaning protocols and tubing-based fluid control reduce cross-contamination risks while minimizing consumable waste. The platform supports continuous environmental stability with ±0.2 °C temperature and ±0.2% CO_2 variation, ensuring optimal cell culture conditions during extended experiments.

Compared to conventional high-cost automated imaging systems, this modular platform significantly reduces footprint and cost while maintaining analytical performance. The architecture is software-driven and AI-ready, allowing automated experimental workflows, programmable dosing strategies, and real-time data acquisition for downstream analysis. In addition, precision droplet handling enables reproducible sample preparation for fluorescence staining, drug-response assays, and functional cell studies.

This work demonstrates a shift from isolated laboratory instruments toward intelligent laboratory ecosystems. By integrating robotics, environmental control, imaging, and fluidics into a unified infrastructure, the proposed platform enhances scalability, reproducibility, and accessibility of advanced cell-based experiments. The approach provides a cost-effective pathway for distributed, high-throughput laboratory automation suitable for academic, clinical, and translational research environments.

A.E.C. acknowledges the Scientific and Technological Research Council of Turkey (TÜBİTAK) (Project No. 122E385).

References:

Meryem Beyza Avci, Furkan Kocer, Fatma Kurul, and Arif E. Cetin, “An Integrated Platform for Liquid Handling and Cell Imaging in Life Science Applications”, Nature Communications, Vol. 16, No: 11521, (2025)

Keyword: *Laboratory Automation*, *Robotics*, *Cell Imaging*

Probing Defect Structures in Nanomaterials: Insights through EPR Spectroscopy for Supercapacitor Applications

Emre Erdem *

Sabancı University, Materials Science and Nanoengineering Program, Istanbul, Turkey

Electron paramagnetic resonance (EPR) spectroscopy is a versatile and powerful technique for investigating defect structures in a wide variety of materials, particularly oxides, where defects play a key role in defining their electronic, magnetic, and optical properties. In this talk, I will provide a brief introduction to EPR spectroscopy within the context of solid-state materials science, focusing on its ability to study defects in nano-structured semiconductor materials, perovskite nanomaterials, and emerging 2D nanomaterials. EPR is not only effective in characterizing intrinsic and extrinsic defect states but is also highly sensitive to variations in crystal field parameters, which differ across material types, from nano-perovskites like $PbTiO_3$ and lead-free alternatives to semiconductor systems such as ZnO nanostructures.

Additionally, EPR offers detailed insights into the electronic states of metal ions, making it an extensive technique for determining the concentration and nature of defect ions, whether they are extrinsically doped into solids or intrinsically present. It is also capable of distinguishing between surface and volume defects, which is particularly critical at the nanoscale, where surface-to-volume ratios dominate material behavior. We will explore how EPR spectroscopy can uncover critical details such as ion substitution, charge compensation, and oxygen vacancies, and discuss how these insights contribute to the broader understanding of structure–property relationships in nanomaterials.

Finally, I will introduce ongoing research where nanostructured ZnO and lead-free perovskites are being applied as electrode materials in all-in-one supercapacitor devices for energy storage systems. We will examine the relationship between nanoscale defect structures and device performance, highlighting how EPR and complementary techniques such as photoluminescence provide extensive control over defect states, enabling a deeper understanding of the functional properties of electrode materials for sustainable energy technologies.

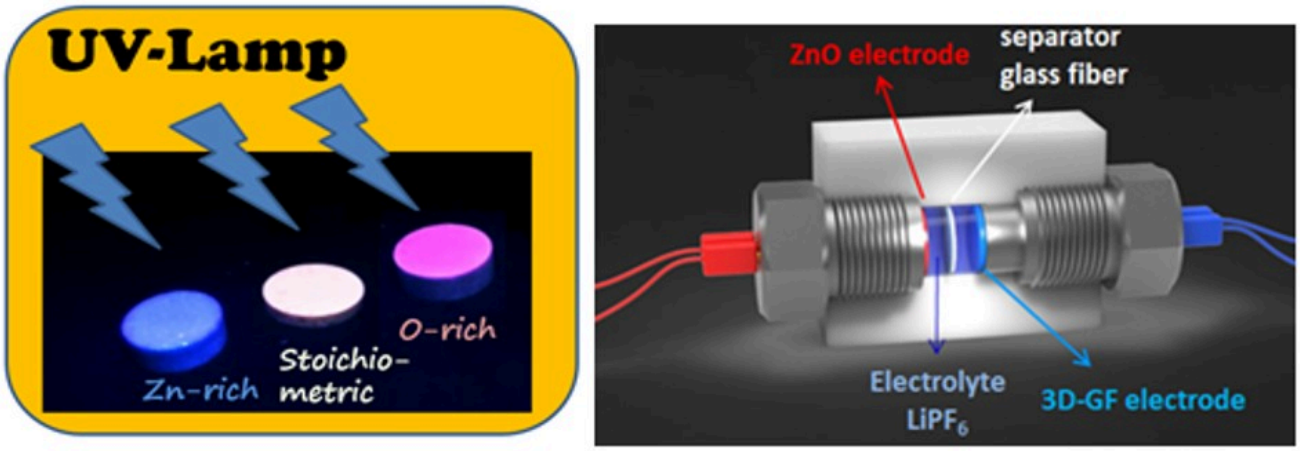


Figure 1: (left) Defect evolution of non-stoichiometric ZnO nanomaterials. (right) The supercapacitor device based on ZnO nanomaterials and 3D graphene foam electrodes.

ORCID:
Emre Erdem: 0000-0002-8395-0364

Keyword: *Defect Engineering, EPR Spectroscopy, Nanomaterials*

ID: 338

Epidermal Sensors for Medical Diagnostics and Therapy

Onur Parlak [*] [1,2,3]

[1] *Karolinska Institute, Department of Medicine, Solna, Division of Dermatology and Venereology, Stockholm, Sweden*
[2] *Center for the advancement of Integrated Medical and Engineering Sciences (AIMES), Karolinska Institutet, Stockholm, Sweden*
[3] *Center for Molecular Medicine, Stockholm, Sweden*

Epidermal bioelectronic devices show great promise in healthcare due to their ability to provide longitudinal monitoring as well as on-demand delivery to maintain optimal health status and evaluate patients' physical conditions. Epidermal biosensors are at the center of this effort and offer a vast potential to revolutionize conventional diagnostics that uses traditional laboratory tests-based evaluations, usually called 'clinical labs,' that are slow and mainly require in-person visits and frequent invasive sampling if the long-term analysis is necessary.[1]

In this presentation, I will give a brief overview of our recently developed epidermal diagnostic approaches targeting various metabolites, hormones and microorganisms as well as some of skin physical and chemicals parameters to acquire better knowledge on early diagnosis and disease progression particularly for metabolic diseases and infections.[1-5] This talk will summarize how to design epidermal sensors, integrated electronics and how to use them in clinical setting with our unique access to patient materials, which creates an unprecedented opportunity to address fundamental questions in medical diagnostics.

References:

1. N. Poursharifi, M. Hassanpouramiri, A. Zink, M. Ucuncu, O. Parlak, Transdermal Sensing of Enzyme Biomarker Enabled by Chemo-Responsive Probe-Modified Epidermal Microneedle Patch in Human Skin Tissue, Advanced Materials, 2024, 2403758.
2. S. Xu, K.D. Mahapatra, N. Maïno, O. Parlak, Dynamic monitoring of skin barrier function enabled by 3D bioelectronic human skin model, Biosensors and Bioelectronics, 2025, 117673, Biosensors and Bioelectronics, 2025, 117673.
3. Y. Song, S. Xu, O. Parlak, Bilirubin Sensing Using Organic Electrochemical Transistors: Role of Gate Materials and Operational Parameters, Advanced Healthcare Materials, 2025, e02481.
4. S. R McCuskey, J. Chatsirisupachai, E. Zeglio, O. Parlak, P. Panoy, A. Herland, G. C. Bazan, T.Q. Nguyen, 2022, Current Progress of interfacing organic semiconducting materials with bacteria, Chemical Reviews, 122, 4, 4791-4825.
5. N. Maino, S. Xu, P. Brodin, O. Parlak, Lab on a Chip, 26 (2026), 316-330.

Engineering Nanoparticles for Histotripsy: Advancing Non-Invasive Cancer Ablation and Combination Therapy

Waleed Mustafa[1], Sarah Hall[2], Mohamad Abu Chakra[1], Ibtisam Naser[1], Semih Macit[1], Özge Şensoy[1,3], Eli Vlaisavljevich[2], Yasemin Yüksel Durmaz [* 1,3]

[1] Department of Biomedical Engineering, School of Engineering and Natural Sciences, Istanbul Medipol University, 34810, Istanbul, Turkey
[2] Department of Biomedical Engineering and Mechanics, Virginia Tech, USA
[3] Research Institute of Health Science and Technologies (SABITA), Istanbul Medipol University, 34810, Istanbul, Turkey

Histotripsy is a non-invasive, non-thermal mechanical tissue ablation technique that relies on acoustic cavitation generated by high-pressure, short-duration focused ultrasound pulses. It uses pre-existing gas pockets in the tissue as cavitation nuclei to form energetic bubble clouds once the peak negative pressure exceeds the intrinsic cavitation threshold, rapidly fractionating the target into an acellular homogenate while preserving collagen-rich critical structures such as large blood vessels and bile ducts.1,2 Following its FDA approval for liver tumor ablation in October 2023, histotripsy has advanced rapidly in the clinic, and emerging evidence of abscopal immune responses has further broadened its therapeutic promise. However, the high negative pressures (>25-30 MPa) needed to initiate intrinsic cavitation, the requirement for secondary imaging guidance, and limited practicality for multifocal or deep-seated tumors remain key barriers. Nanoparticle-mediated histotripsy (NMH) addresses these limitations by employing ultrasound-active, perfluorocarbon (PFC)-based nanoparticles as exogenous cavitation nuclei that lower the cavitation threshold to 10-15 MPa and, through selective tumor accumulation, enable targeted ablation without damaging surrounding healthy tissue.3,4 This talk traces the scientific evolution of the nanoparticles engineered in our laboratory for NMH. The first-generation agents were crosslinked triblock-copolymer nanodroplets with an acoustically excitable perfluoropentane or perfluorohexane core, which markedly reduced the cavitation threshold in tissue-mimicking phantoms but were constrained by relatively large size (>200 nm), limited stability, and indeterminate PFC content.3,4 To overcome these limitations, we developed nanocone clusters (NCCs), cyclodextrin-perfluorocarbon inclusion complexes, as smaller (~40 nm), reproducible, next-generation agents whose PFC payload can be quantified and whose surface can be bioconjugated for active tumor targeting.5-7 Building on this platform, drug-loaded NCCs and a new generation of PEGylated nanodroplets were engineered to co-deliver chemotherapeutic agents such as doxorubicin, offering pH-responsive release and quantifiable PFC loading.8 In vitro and in vivo studies confirmed the feasibility of NMH, demonstrating bubble-cloud formation and tissue fractionation at reduced pressures, tumor-selective biodistribution, and enhanced cytotoxicity when ablation was combined with locally released drug. Finally, because histotripsy alone may leave viable tumor cells at the ablation margin, we present a combination strategy in which drug-loaded nanoparticles unite mechanical ablation with locally delivered chemotherapy, eliminating residual disease within the treated zone while sparing healthy tissue, as a rational route toward more complete, non-invasive cancer therapy.

References:

1. Xu Z, Hall TL, Vlaisavljevich E, Lee FT, Histotripsy: The First Noninvasive, Non-Ionizing, Non-Thermal Ablation Technique Based on Ultrasound. Int. J. Hyperthermia 2021;38(1);561–575.
2. Vlaisavljevich E, Maxwell A, Mancia L, Johnsen E, Cain C, Xu Z, Visualizing the Histotripsy Process: Bubble Cloud–Cancer Cell Interactions in a Tissue-Mimicking Environment. Ultrasound Med Biol, 2016;42(10);2466–2477.
3. Durmaz YY, Vlaisavljevich E, Xu Z, Elsayed M, Development of Nanodroplets for Histotripsy-Mediated Cell Ablation. Mol Pharm 2014;11(10);3684–3695.
4. Vlaisavljevich E, Durmaz YY, Maxwell A, ElSayed M, Xu Z, Nanodroplet-Mediated Histotripsy for Image-Guided Targeted Ultrasound Cell Ablation. Theranostics 2013;3(11);851–864.
5. Kaymaz B, Mustafa W, Hall S, Vlaisavljevich E, Sensoy O, Durmaz, YY, Experimental and Computational Investigation of Clustering Behavior of Cyclodextrin–Perfluorocarbon Inclusion Complexes as Effective Histotripsy Agents. Mol Pharm 2022;19(8);2907–2921.

Quantum Materials by Design: Atomic-Scale Synthesis, Imaging and Spectroscopy

Y. Eren Suyolcu *

Max Planck Institute for Solid State Research (MPI-FKF), Stuttgart, Germany ·

Complex transition-metal oxides host a rich landscape of quantum states – superconductivity, magnetism, and metal–insulator transitions – that emerge from the coupling between charge, spin, orbital, and lattice degrees of freedom. Because this coupling plays out at the atomic scale, understanding and controlling these materials requires both atomically precise synthesis and atomic-resolution characterization. Combining epitaxial thin film growth techniques, such as molecular-beam epitaxy (MBE) and thermal laser epitaxy (TLE), with aberration-corrected scanning transmission electron microscopy (STEM) imaging and electron energy-loss spectroscopy (EELS) makes it possible to design emergent properties and to resolve, column by column, the structure that produces them.

In epitaxial oxide heterostructures, precise flux calibration and adsorption-controlled growth enable interface engineering at the atomic-layer level: realizing the sharpest oxide interfaces [1], stabilizing filamentary superconducting interfaces down to a single monolayer [2], tuning anisotropic magnetism and superconductivity through “bi-directional” growth [3], and reaching (and in some cases exceeding) the quality of bulk single crystals in thin-film form [4]. In bulk quantum materials, specifically in the rare-earth nickelates, following the discovery of ~80 K superconductivity in $La_3Ni_2O_7$ under pressure [5], real-space STEM and EELS reveal that optical floating-zone-grown single crystals adopt an unconventional structure - dominated by alternating monolayers and trilayers of NiO_6 octahedra rather than the assumed bilayer stacking [6] – informing the ongoing debate on the nature of the superconducting phase. In the same spirit, atomic-scale imaging resolves how topotactic reduction reshapes the local structure of $LaNiO_3$ single crystals [7], the route by which oxygen control governs nickelate ground states [8].

Across both fronts, the same principle holds: macroscopic behavior is set by picometer-scale structure, and combining atomic-scale synthesis with atomic-resolution electron microscopy makes that structure both measurable and controllable.

References:

[1] Y. E. Suyolcu* et al., APL Mater. 9, 021117 (2021).
[2] Y.-M. Wu, Y. E. Suyolcu* et al., ACS Nano 15, 16228 (2021).
[3] N. Bonmassar, Y. E. Suyolcu* et al., Adv. Funct. Mater. 34, 2314698 (2024).
[4] B. Faeth*, V. Harbola*, Y. E. Suyolcu* et al., unpublished.
[5] H. Sun et al., Nature 621, 493 (2023).

Entanglement Generation in Qubit Networks via Collision Model

Elif Yunt *

Turkish German University

We consider small interacting qubit networks and investigate the pairwise entanglement over them, when in contact with a coherent environment. In order to model the interaction with the environment, we adopt two approaches, which we distinguish according to whether the environmental ancilla is reset or not. The former is the traditional collision model, and the latter we dub repeated interaction model. By proper choice of interaction, network geometry and initial states, bipartite entanglement is generated even between qubits not directly interacting with the environment. Our scheme promises scalability in specific models and provides a physically implementable way to entanglement distribution in quantum communication and metrology.

Acknowledgment:
We acknowledge support by the Scientific and Technological Research Council of Turkey (TÜBİTAK), Grant No. (125F164).

ORCID:
Elif Yunt: 0000-0001-7824-5209

References:
F. Ciccarello, Quantum Meas. Quantum Metrol. 4, 53 (2017).
V. Scarani, M. Ziman, P. Štelmachovič, N. Gisin, and V. Bužek, Phys. Rev. Lett. 88, 097905 (2002).
F. Ciccarello, S. Lorenzo, V. Giovannetti, and G. M. Palma, Physics Reports 954, 1 (2022), quantum collision models: Open system dynamics from repeated interactions
V. Giovannetti, G. M. Palma, and F. Sciarrino, Phys. Rev. A 86, 012302 (2012).

Keyword: *Entanglement Distribution, Quantum Collision Model, Qubit Network*

ID: 423

Toward Scalable Transmon Qubits: Fabrication and Characterization of CPWs, Josephson Junctions, and SQUIDs.

Mehmet Kahraman * **, Ege Selvi, Süleyman Çelik, İsmet Kaya**

Sabancı University

Superconducting transmon qubits rely critically on the fabrication quality and electrical performance of their circuit components, particularly coplanar waveguides (CPWs), Josephson junctions (JJs), and superconducting quantum interference devices (SQUIDs). In this study, we present the individual fabrication and characterization of these essential building blocks toward scalable transmon qubit development.

CPW structures were fabricated using both Aluminum (Al) and Niobium Titanium Nitride (NbTiN) superconducting thin films to evaluate material-dependent microwave performance. Their cryogenic characterization was performed at base temperature using a vector network analyzer (VNA) and FPGA-based measurement platform. Scattering parameters (S11 and S12) were analyzed through logarithmic magnitude and standing wave ratio (SWR) methods to assess transmission characteristics, impedance matching, and resonator behavior.

For nonlinear quantum elements, Josephson Junction and Superconducting Quantum Interference Device structures based on Al/AlOx/Al tunnel junctions were fabricated using two different nanofabrication approaches. The first employed the conventional Dolan bridge double-angle evaporation method with controlled thermal oxidation to form the tunnel barrier. The second utilized a Manhattan-style process incorporating alumina barrier deposition via electron-beam evaporation, enabling an alternative junction geometry and barrier formation strategy. Both fabrication methods were compared in terms of process reproducibility and electrical characteristics.

Electrical characterization of the fabricated JJs and SQUIDs was carried out through room-temperature measurements and low-temperature current–voltage (I–V) characterization in a cryogenic environment at base temperature. The extracted junction parameters, including normal resistance, critical current behavior, and superconducting switching characteristics, provide insight into device quality and suitability for transmon integration.

The results demonstrate successful fabrication and cryogenic validation of CPWs, JJs, and SQUIDs, establishing a robust process foundation for future fully integrated transmon qubit architectures.

ORCID:
Mehmet Kahraman: 0000-0002-7083-1227

Keyword: *Coplanar Waveguide (CPW) Resonators, Josephson Junction and Superconducting Quantum Interference Device (SQUID),, Transmon qubits*

Transforming Fluorescence from Interference to Opportunity: Photonic Crystal and Hybrid Photonic–Plasmonic Platforms for Enhanced Raman Biosensing

Fatma Uysal Ciloglu [*1,2], Seemesh Bhaskar[1], Brian T. Cunningham[1]

[1] *Nick Holonyak Jr. Micro and Nanotechnology Laboratory, University of Illinois at Urbana-Champaign, Urbana, Illinois 61801, USA*
[2] *Department of Biomedical Engineering, Erciyes University, Kayseri 38039, Türkiye*

Raman spectroscopy is a powerful analytical technique that enables molecular identification through unique vibrational fingerprints [1]. However, its practical application is often limited by the inherently weak Raman scattering process and by fluorescence emission originating from analytes or surrounding materials. In many Raman-based measurements, fluorescence is considered an undesirable background that can mask Raman features and reduce detection sensitivity [2]. Overcoming fluorescence-related limitations therefore remains an important challenge in the development of highly sensitive optical sensing platforms.

In this work, photonic crystal (PC) substrates were explored as a nanophotonic approach to utilize fluorescence-assisted optical enhancement mechanisms rather than suppressing fluorescence entirely [3]. Rhodamine 6G (R6G) was selected as a model fluorescent Raman reporter. The optical performance of PC substrates was compared with that of conventional glass surfaces to evaluate their ability to support enhanced signal generation at reduced analyte concentrations. Comparative measurements revealed that photonic crystal substrates maintained detectable Raman signatures at lower R6G concentrations than conventional glass substrates. To further enhance optical performance, hybrid photonic–plasmonic platforms incorporating metallic nanostructures, including silver and gold nanoparticles, were investigated. By combining plasmonic field enhancement with photonic crystal resonance effects, these hybrid architectures generated measurable Raman signals at lower reporter concentrations than those obtained on glass substrates. The results highlight the synergistic interaction between photonic and plasmonic enhancement mechanisms for improved optical sensing performance. Overall, the findings demonstrate that fluorescence, traditionally regarded as a source of interference in Raman spectroscopy, can be transformed into a useful contributor to signal amplification through appropriate nanophotonic engineering.

Acknowledgment:
F.U.C. acknowledges the support of the Scientific and Technological Research Council of Türkiye (TÜBİTAK) during her postdoctoral research.

ORCID:
Fatma Uysal Ciloglu: 0000-0001-8827-3668
Seemesh Bhaskar: 0000-0003-2714-3776
Brian T. Cunningham: 0000-0002-9681-2104

References:
[1] Ferraro, J. R. (2003). Introductory Raman spectroscopy. Elsevier.
[2] Arya, G. C., & Singh, Y. P. (2026). Advances and Challenges in Raman and Surface-Enhanced Raman Spectroscopy for Biological Systems. ACS Applied Bio Materials.
[3] Ciloglu, F. U., Bhaskar, S., Liu, L., & Cunningham, B. T. (2025). Fluorescence enabled Raman amplification using photonic crystal resonant modes. Applied Physics Letters, 127(18).

Keyword: *Raman spectroscopy, Fluorescence, Photonic Crystals*

A microfluidic single-bacteria isolation, enrichment, and characterization device for probiotic strain selection

Didem Rodoplu Solovchuk [*1], **Chien-Hsun Huang**[2], **Jong-Shian Liou**[2], **Chia-Hsien Hsu**[1]

[1] *Institute of Biomedical Engineering and Nanomedicine, National Health Research Institutes, Zhunan, 350401, Taiwan*
[2] *Bioresource Collection and Research Center, Food Industry Research and Development Institute, Hsinchu 30062, Taiwan*

Driven by the growing probiotics market, there is increasing demand for high-throughput, automated workflows for efficient microbial strain isolation and selection. The probiotic strain development workflows comprise single-colony isolation, preliminary screening, and molecular identification. However, conventional plating and microscopic imaging are labor-intensive, time-consuming, and often fail to capture rare or slow-growing strains [1-4]. Although single-cell dispenser technology allows high-throughput isolation, it lacks preliminary screening and requires high-cost instrumentation. To address these limitations, we present a microfluidic chip (SII-chip) with rapid and high-throughput isolation of single-bacteria, using a simple liquid-liquid cutting, coupled with image-based phenotypic characterization to exclude non-target bacteria, before the molecular identification.

The deeper main channel of the SII-chip enables uniform liquid isolation, while the low-depth observation chambers confine bacterial motion to the focal plane, enhancing imaging, segmentation, and phenotypic characterization. The microfluidic channel configuration and operational steps are optimized for conducting experiments in a limited space in an anaerobic hood. Preliminary morphology and motility testing are used to classify bacteria as normal-dividing, filamentous, or non-dividing [5]. The multiparametric characterization of bacteria is found useful for detecting antimicrobial-resistant bacteria and eliminating non-target pathogenic strains.

For the probiotics detection, seven different probiotic strains, one neutral strain, and one pathogenic strain are used as positive and negative control groups. For the proof-of-concept human-sample testing, gut bacteria in infant feces were isolated. We successfully isolated ~100 single-bacteria in the SII-chip using 10^4 CFU/ml under anaerobic conditions. Our device enables the isolation and cultivation of single, motile bacteria prior to single-clone retrieval. The majority of isolates exhibited phenotypic characteristics consistent with Escherichia coli, while additional isolates showed similarity to Bacillus subtilis, Lacticaseibacillus rhamnosus, and Faecalibacterium prausnitzii. Future work will focus on optimizing chamber geometries to accommodate a broader range of bacterial morphologies, particularly longer strains, and on integrating downstream molecular identification to validate on-chip phenotypic classification. This platform has the potential to reduce non-target sample processing and the overall cost and time associated with molecular analyses, thereby accelerating the discovery of novel probiotic strains.

ORCID:
Didem Rodoplu Solovchuk: 0000-0001-5052-3932
Chien-Hsun Huang: 0000-0003-2268-1161
Chia-Hsien Hsu: 0000-0002-0752-3133

References:
S. Gul, E. Durante-Mangoni, Journal of Clinical Medicine 13(5) (2024) 1436.
K. Papadimitriou, G. Zoumpopoulou, B. Foligné, V. Alexandraki, M. Kazou, B. Pot, E. Tsakalidou, Front Microbiol 6 (2015) 58.
M.-Q. X et.al., Military Medical Research 11(1)(2024) 34.
D.R. Solovchuk, C.-H. Hsu, Microfluidic Diagnostics and Drug-Delivery Platforms for the Early Diagnosis and Treatment of Bacterial Diseases,Springer Nature, (2023), pp. 201-228.
C.-H. Hsu, D.R. Solovchuk, Microfluidic chip and use thereof for continuous monitoring of bacterium intended for motion, growth, and morphology detection. U.S. Patent Application US20240384321A1 (2024).

Keyword: *single-bacteria, microfluidics, probiotics*

Electrochemical determination of insecticides and herbicides in surface waters and environmental monitoring of fluorine and chlorine halogens

Ozge Surucu *

Ege University, Faculty of Science, Department of Chemistry, 35100 Bornova, Izmir, Türkiye

Agricultural activities require the use of plant protection products to combat pests. However, the transformation of forests and other natural ecosystems into areas for livestock farming, mining, illegal logging, and increased agricultural activities directly affects surface water resources. Insecticides and herbicides are frequently preferred among plant protection products, and their use leads to significant damage to water resources. Lambda-cyhalothrin pyrethroids are highly effective insecticides used to control a wide variety of insect pests in agriculture, public spaces, and homes [1]. Lambda-cyhalothrin is highly hydrophobic, practically insoluble in water, and can cause long-term effects on beneficial soil microorganisms and aquatic species. On the other hand, 2,4-dichlorophenoxyacetic acid (2,4-D) is an herbicide classified as a newly emerging pollutant and is one of the most widely used herbicides due to its low cost and high effectiveness in weed control [2]. The presence of insecticides and herbicides with such high toxicity in surface waters will lead to the accumulation of persistent organic pollutants through human consumption, agricultural irrigation, recreation, and other activities, and consequently, the development of new methodologies for assessing water pollution is urgent. Although many analytical approaches have been developed for the determination of plant protection products, electroanalytical methods provide environmentally friendly alternatives with low energy and reagent consumption as well as short analysis time. These features, combined with the development of various nanomaterials for electrode production, have made electroanalytical methods increasingly popular for such analyses. In this respect, more reliable and environmentally friendly electrochemical techniques such as voltammetry and impedance spectroscopy have come to the forefront [3]. Within the scope of this presentation, the determination of these hazardous lambda-cyhalothrin and 2,4-D species in surface waters will be carried out electrochemically. At this stage, voltammetric techniques such as cyclic voltammetry (CV) and differential pulse voltammetry (DPV) as well as electrochemical impedance spectroscopy (EIS) will be utilized at nanomaterials modified electrodes. On the other hand, most insecticide and herbicide types contain heteroatoms, and the most common elements are fluorine (F) and chlorine (Cl) halogens, as in lambda-cyhalothrin and 2,4-D, respectively. Therefore, F and Cl halogens present in insecticide, and herbicide species will be determined using a supporting technique such as attenuated total reflectance-Fourier transform infrared (ATR-FTIR) spectroscopy. Combining the analysis of F and Cl halogen species contaminated with lambda-cyhalothrin and 2,4-D in water within a single automated system using electrochemically active materials will increase sustainability and provide green transition for environmental monitoring.

ORCID:
Ozge Surucu: 0000-0002-5618-0341

References:

Oudou, H. C., Alonso, R. M., & Hansen, H. B. (2004). Voltammetric behaviour of the synthetic pyrethroid lambda-cyhalothrin and its determination in soil and well water. Analytica Chimica Acta, 523(1), 69-74.
Gomes-Junior, P. C., Augusto, K. K., Alves, B. S., Resque, I. S., Dantas, K. G., & De Souza, J. P. (2026). Voltammetric determination of 2, 4-D (dichlorophenoxyacetic acid) herbicide in water samples from Amazonian rivers using boron-doped diamond electrode. Journal of Solid State Electrochemistry, 30(3), 1141-1155.
Anastas, P., & Eghbali, N. (2010). Green chemistry: principles and practice. Chemical society reviews, 39(1), 301-312.

Keyword: *lambda-cyhalothrin, 2,4-dichlorophenoxyacetic acid, electrochemical and environmental analysis*

ID: 480

Cyclodextrin-Based Drug Delivery Systems for Improved Solubility and Prolonged Ocular Delivery of Hydrophobic Drugs

Monireh Esmaeili Rad [*1], **Yusuf Menceloğlu**[1,2], **Meral Yuce**[1]

[1] *SUNUM, Nanotechnology Research and Application Center, Sabanci University, Istanbul, 34956, Turkey*
[2] *Faculty of Engineering and Natural Sciences, Sabanci University, Istanbul, 34956, Turkey*

Topical ophthalmic drug delivery is constrained by limited ocular bioavailability, primarily due to rapid precorneal drug elimination and the low aqueous solubility of many therapeutic agents. Cyclodextrin (CD)-based nanocarriers represent a promising approach to enhance the solubility, stability, and controlled release of hydrophobic drugs. This study investigates β-cyclodextrin (β-CD) and its derivatives as delivery systems for dexamethasone (DEX) and curcumin (CUR), two hydrophobic compounds commonly utilized in ocular therapy. Drug/CD inclusion complexes were prepared using solvent evaporation, freeze-drying, and autoclave techniques. These methods were systematically compared regarding water solubility enhancement, entrapment efficiency, loading capacity, and processing time. The autoclave method demonstrated superior overall performance and was therefore selected for preparing complexes with hydroxypropyl-β-cyclodextrin (HP-β-CD) and sulfobutyl ether-β-cyclodextrin (SBE-β-CD). Cyclodextrin derivatives significantly enhanced the aqueous solubility of both drugs. HP-β-CD increased the solubility of DEX and CUR by approximately 98.8-fold and 40.5-fold, respectively, while SBE-β-CD achieved 108-fold and 48-fold improvements. In vitro release studies indicated sustained drug release from derivative-based complexes. Among the tested formulations, DEX-SBE-β-CD demonstrated the most controlled release, with 27.47% of the encapsulated drug released within 6 hours and 64.70% after 48 hours. CUR-loaded HP-β-CD and SBE-β-CD complexes also exhibited sustained release, whereas the natural β-CD complex showed negligible drug release. These findings indicate that cyclodextrin derivatives, particularly SBE-β-CD, are promising nanocarriers for enhancing solubility and enabling controlled ocular delivery of hydrophobic drugs, thereby offering an effective platform for advanced ophthalmic drug delivery systems.

Acknowledgment:
The authors gratefully acknowledge financial support from the TÜBİTAK 2244 Industrial PhD Program (project number 118C146) and the Technology Development Foundation of Turkey (TTGV).

ORCID:
Monireh Esmaeili Rad: https://orcid.org/0000-0002-3665-5688

References:
Loftss on T, Stefánsson E (2002) Cyclodextrins in eye drop formulations: Enhanced topical delivery of corticosteroids to the eye. Acta Ophthalmol Scand 80:144 150. https://doi.org/10.1034/j.1600 0420.2002.800205.x
Saokham P, Muankaew C, Jansook P, Loftsson T (2018) Solubility of cyclodextrins and drug/cyclodextrin complexes. Molecules 23:1 15. https://doi.org/10.3390/molecules23051161
Stella VJ, Rajewski RA (2020) Sulfobutylether β cyclodextrin. Int J Pharm 583:119396. https://doi.org/10.1016/j.ijpharm.2020.119396

Keyword: *Cyclodextrin nanocarriers, Drug delivery, Controlled drug release*

Nanostructured Layer-by-Layer Hexosomes for Improving the Stability and Bioaccessibility of Omega-3 Fatty Acids

Gokce Dicle Kalaycioglu [*1,2], **Zahra Eskandari**[3], **Seyed Fakhreddin Hosseini**[3], **Anan Yaghmur**[1]

[1] *Department of Pharmacy, Faculty of Health and Medical Sciences, University of Copenhagen, Universitetsparken 2, DK-2100 Copenhagen Ø, Denmark*

[2] *Department of Chemical Engineering, Hacettepe University, Beytepe, 06800 Ankara, Turkey*

[3] *Department of Seafood Processing, Faculty of Marine Sciences, Tarbiat Modares University, Noor 46414-356, Iran*

Omega-3 polyunsaturated fatty acids (ω-3 PUFAs) offer significant nutritional and therapeutic benefits; however, their practical application is limited by poor oxidative stability and low bioaccessibility. In this study, layer-by-layer (LbL) coated hexosomes were developed as nanostructured delivery systems for ω-3 PUFA concentrate obtained from common kilka fish oil. Hexosomes were prepared using a distilled monoglyceride (Dimodan U/J) and stabilized with Pluronic F127. Surface modification was achieved through sequential deposition of chitosan and sodium alginate layers via electrostatic interactions.

The structural and morphological characteristics of the nanoparticles were investigated using synchrotron small-angle X-ray scattering (SAXS), cryogenic transmission electron microscopy (cryo-TEM), nanoparticle tracking analysis (NTA), and zeta potential measurements. SAXS analysis confirmed the preservation of the inverse hexagonal (H_2) internal structure following LbL coating. Cryo-TEM observations further demonstrated that the coated nanoparticles retained their structural integrity while exhibiting characteristic surface modifications associated with the polymer layers (Fig. 1).

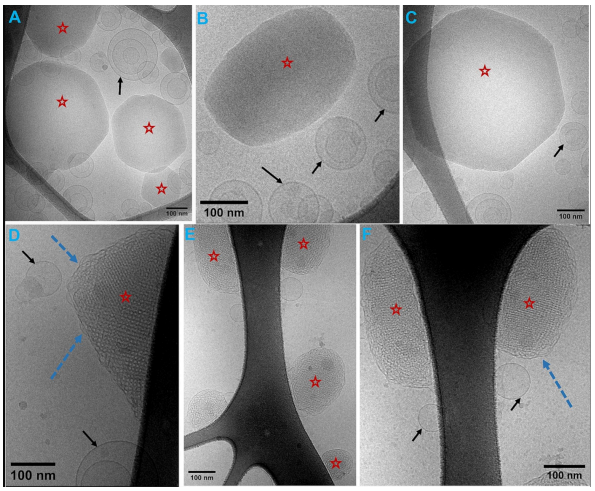


Fig. 1. Effect of LbL coating on the morphological features of Pluronic F127-stabilized nanodispersion produced from Dimodan U/J and ω-3 PUFA concentrate extracted from common kilka fish oil at weight ratio of 70:30 (sample S_1). Cryo-TEM images of the nanodispersion before (A-C) and after its coating with the first layer of CH (D-F). In all panels, the detected hexosomes (marked with red stars) coexisted with discrete vesicular structures (including relatively small spherical vesicles) that are marked with black arrows. In contrast to the uncoated hexosomes (A-C), the detected CH- and LbL-coated hexosomes (D-I) were covered with vesicular structures (marked with dashed blue arrows).

The influence of LbL coating on oxidative stability and in vitro digestion behavior was also evaluated. Encapsulation of ω-3 PUFAs within hexosomes significantly reduced the formation of primary and secondary oxidation products compared with free ω-3 PUFA concentrate. Additional improvement was achieved after chitosan–alginate coating, indicating enhanced protection against oxidative degradation. Simulated gastrointestinal digestion studies revealed that LbL-coated hexosomes provided controlled release under gastric conditions and substantially improved intestinal bioaccessibility of ω-3 PUFAs. The bioaccessibility increased to approximately 75% for coated formulations, compared with about 36% for the free ω-3 PUFA concentrate.

These findings demonstrate that LbL-coated hexosomes are promising nanocarriers for the stabilization and oral delivery of omega-3 fatty acids and may facilitate the development of advanced functional food and nutraceutical formulations.

Keyword: *Hexosomes, Layer-by-layer coating, Omega-3 polyunsaturated fatty acids*

Synthesis and Characterization of Magnetic Nanoparticles and Investigation of Their Ferroptosis-Related Biological Effects on Lung Cancer Cells

Kübra Solak [*] [1,2,3], **Adem Kara**[3], **Ahmet Mavi**[2,4,5]

[1] *Department of Molecular Biology and Genetics, Faculty of Science, Atatürk University, Erzurum, Türkiye.*
[2] *East Anatolia High Technology Application and Research Center (DAYTAM), Atatürk University, 25240 Erzurum, Türkiye.*
[3] *Department of Molecular Biology and Genetics, Faculty of Science, Erzurum Technical University, Erzurum, Türkiye.*
[4] *Department of Mathematics and Science Education, Education Faculty of Kazim Karabekir, Atatürk University, Erzurum, Türkiye.*
[5] *Department of Nanoscience and Nanoengineering, Institute of Science and Technology, Atatürk University, Erzurum, Türkiye.*

In this study, we investigated the ferroptotic effects of surface-modified Fe_3O_4 magnetic nanoparticles (MNPs) with polyethylene glycol (PEG) and branching polyethyleneimine (PEI) in a lung cancer cell model. The Fe_3O_4@PEG/PEI MNPs were prepared by a modified thermal decomposition process and characterized using SEM, TEM, FTIR, and XRD. The SEM and TEM analyses demonstrated that the obtained MNPs were spherical, with an average size of approximately 15 nm. The molecular weight of 25 kDa PEI was selected to achieve the most uniform particle distribution by limiting agglomeration through electrostatic and steric repulsion. The PEI coating was successfully applied, as evidenced by FTIR spectra. The spinel structure of magnetite was preserved, as revealed by XRD patterns. For cellular uptake studies, the A549 (lung cancer) and BEAS-2B (normal bronchial epithelium) cell lines were treated with 100 µg/ml of MNP by magnetic field-assisted methods, and intracellular iron accumulation was measured using Prussian blue staining and PGSK-probe-based flow cytometry. Cancer cells engulfed MNPs at a faster rate and in greater amounts. Cell viability assays (CCK-8) were used to determine the final experimental concentrations of 40 and 80 µg/mL. Flow cytometry with DCFDA showed significant potential for elucidating cell death. The reduced glutathione (GSH) level and the JC-1 determined change in mitochondrial membrane potential ($\Delta\Psi m$) were decreased. This suggests activation of the oxidative stress processes associated with ferroptosis. BEAS-2B cells were more susceptible to ferroptosis, while A549 cells had different mitochondrial response profiles. In trials using combinations of chemotherapeutic agents, it was found that the IC50 value can be decreased or increased by combining MNPs with doxorubicin (DOX) and mitoxantrone (MTX), depending on the medication, dose, and timing of administration. The results indicate that Fe_3O_4@PEG/PEI MNPs can induce ferroptosis-related mechanisms in lung cancer cells and serve as a suitable platform for magnetic targeting and combination chemotherapeutic strategies.

Acknowledgment:
This study was supported by Scientific and Technological Research Council of Türkiye (TUBITAK) under the Grant Number 123C327 and 224Z063. The authors thank to TUBITAK for their supports.

ORCID:
Kübra Solak: 0000-0001-6643-3368

References:
Dixon, S. J., Lemberg, K. M., Lamprecht, M. R., Skouta, R., Zaitsev, E. M., Gleason, C. E., … Stockwell, B. R. 2012. "Ferroptosis: An iron-dependent form of nonapoptotic cell death". Cell, 149(5), 1060-1072.
Jiang, Q., Wang, K., Zhang, X., Ouyang, B., Liu, H., Pang, Z., Yang, W. 2020. "Platelet Membrane-Camouflaged Magnetic Nanoparticles for Ferroptosis-Enhanced Cancer Immunotherapy". Small, 16(22).
Zhang, B., Tu, Z., Zhao, F., Wang, J. 2013. "Superparamagnetic iron oxide nanoparticles prepared by using an improved polyol method". Applied Surface Science, 266.

Keyword: *Magnetic nanoparticles, ferroptosis, chemotherapeutic combination*

Development of Cationic Hydrogel Modified with Gold Nanoparticles as a Wound Dressing Material

Emine Büşra Eker * **, İlknur Atlı, Özgür Özay**

Canakkale Onsekiz Mart University, Bioenginneering

Metal nanoparticles exhibit antibacterial, antifungal, and antiviral properties and are biocompatible offers a unique advantage in tissue engineering. The incorporation of metal nanoparticles into the hydrogel structure enhances the effectiveness of the treatment process when used as a wound dressing material [1,2]. The porous structure of hydrogels, their flexibility, high water retention capacity, biocompatibility, and their ability to exhibit drug adsorption and desorption behavior make them preferred materials for wound dressings. The presence of positively charged groups in its structure imparts antibacterial properties to the hydrogel and offers significant advantages as a wound dressing material [3,4]. Additionally, the ability to encapsulate therapeutic agents such as antibiotics, antiseptics, anti-inflammatories, and antioxidants within the hydrogel structure also enhances controlled and prolonged release behavior compared to traditional treatment methods and accelerates the wound healing process [5].

In this study, the DMAPMA (N-[3-(Dimethylamino)propyl]methacrylamide) monomer, which contains positively charged groups in a hydrogel polymeric network structure, was used. Hydrogels with cationic properties sensitive to pH changes were synthesized using the redox polymerization method. Furthermore, semi-IPN hydrogels were synthesized by incorporating gelatin, a natural polymer, into the structure to enhance biocompatibility, biodegradability, porosity, and controlled drug release behavior. The swelling behavior of the synthesized hydrogels was evaluated in different pH and ion-containing media, such as deionized water, gastric medium, PBS, and wound-healing medium (SWF). To enhance the antibacterial efficacy of the hydrogel, Au nanoparticles were incorporated into its polymeric network structure. In the synthesis of Au nanoparticles, the in-situ green synthesis method was preferred, using Hibiscus sabdariffa L. plant extract as the reducing agent [6]. Hydrogel composites were prepared by forming stable Au^0 nanoparticles in a hydrogel polymeric network structure of Au^{3+} ions. The synthesized hydrogel and composite structures were characterized by FT-IR, TGA, XRD, SEM-EDX, and TEM analyses. To enhance wound healing success, hydrogels loaded with the antibacterial agent cefazolin and the anti-inflammatory agent sodium diclofenac as model therapeutic agents were evaluated for their drug release behaviors in PBS (pH=7.40) and SWF (pH=8.00) media. Antibacterial properties were evaluated on C. Albicans, B. Cereus, B. Subtilis, E. Faecalis, P. Aeruginosa, and S. Aureus bacteria using the disk diffusion method. The antioxidant capacity of the hydrogels was determined. In addition, the biocompatibility properties of hydrogels were evaluated on 3T3 skin cell lines using in vitro MTT analysis.

Acknowledgment:
The authors sincerely thank the Çanakkale Onsekiz Mart University Scientific Research Projects Coordination Unit (COMU BAP) for financial support under Project No. FBG-2025-5131 and TÜBİTAK through the 2224-B Domestic Scientific Events Participation Support Program.

ORCID:
Emine Büşra Eker: 0000-0002-6340-5107
İlknur Atlı: 0009-0003-1804-4036
Özgür Özay: 0000-0001-6589-9844

References:
[1] X. Gu, Z. Xu, L. Gu, H. Xu, F. Han, B. Chen, X. Pan, Preparation and antibacterial properties of gold nanoparticles: a review, Environ Chem Lett 19 (2021) 167–187. https://doi.org/10.1007/s10311-020-01071-0.
[2] Y. Wang, M. Zhang, Z. Yan, S. Ji, S. Xiao, J. Gao, Metal nanoparticle hybrid hydrogels: the state-of-the-art of combining hard and soft materials to promote wound healing, Theranostics 14 (2024) 1534–1560. https://doi.org/10.7150/thno.91829.
[3] X. Lin, X. Zhang, Y. Wang, W. Chen, Z. Zhu, S. Wang, Hydrogels and hydrogel-based drug delivery systems for promoting refractory wound healing: Applications and prospects, International Journal of Biological Macromolecules 285 (2025) 138098. https://doi.org/10.1016/j.ijbiomac.2024.138098.
[4] P.G. Ferreira, V.F. Ferreira, F. de C. da Silva, C.S. Freitas, P.R. Pereira, V.M.F. Paschoalin, Chitosans and Nanochitosans: Recent Advances in Skin Protection, Regeneration, and Repair, Pharmaceutics 14 (2022) 1307. https://doi.org/10.3390/pharmaceutics14061307.
[5] S. Nasra, M. Patel, H. Shukla, M. Bhatt, A. Kumar, Functional hydrogel-based wound dressings: A review on biocompatibility and therapeutic efficacy, Life Sciences 334 (2023) 122232. https://doi.org/10.1016/j.lfs.2023.122232. [6] İ. Atli, P. Ilgin, O. Ozay, Green synthesis of multifunctional responsive hydrogel embedded with silver, based on xanthan gum, N-isopropylacrylamide, vinyl imidazole, and Luffa cylindrica for wound healing, Journal of Macromolecular Science, Part A 61 (2024) 953–965.

Keyword: *Gold nanoparticles, cationic hydrogels, wound treatment, biomaterials, drug delivery systems, nanomaterials*

ID: 260

Effect of Synthesis Route on Lanthanum Removal Performance of Ce/Urea-Doped Carbon Quantum Dots Derived from Pleurotus Ostreatus

Berkant Senturk * **, Sabriye Yusan**

Ege University, Institute of Nuclear Sciences, İzmir, Türkiye

Abstract

The increasing industrial use of rare earth elements has raised significant environmental concerns regarding lanthanum (La) contamination in aquatic systems. In this study, Ce and urea-doped carbon quantum dots (CQDs) derived from Pleurotus ostreatus biomass were investigated as sustainable nanomaterials for the removal of La ions from aqueous solutions.

Environmentally friendly synthesis procedures were employed using Pleurotus ostreatus as a renewable carbon precursor, while cerium and urea were utilized as dopant sources to enhance the structural and optical properties of the CQDs. The adsorption performance of hydrothermally synthesized CQDs toward La(III) ions was experimentally evaluated, while pyrolytic synthesis studies are currently ongoing to establish a comprehensive comparison of synthesis-route-dependent adsorption behavior.

The synthesized nanomaterials were characterized using scanning electron microscopy (SEM), X-ray diffraction (XRD), X-ray photoelectron spectroscopy (XPS), Fourier transform infrared spectroscopy (FT-IR), UV–Vis spectroscopy, and photoluminescence (PL) analysis to investigate their morphological, structural, and optical properties. The adsorption capacities of the synthesized CQDs toward La ions were investigated by varying experimental parameters including solution pH, temperature, initial La concentration, and contact time. In addition, adsorption isotherm and thermodynamic studies were conducted to better understand the adsorption mechanism. Experimental equilibrium data were evaluated using Langmuir, Freundlich, and Dubinin–Radushkevich isotherm models, while thermodynamic parameters including Gibbs free energy change (ΔG), enthalpy change (ΔH), and entropy change (ΔS) were calculated to evaluate the nature and feasibility of the adsorption process.

In our previous studies using Ce and N-doped CQD-based adsorption systems, Nd(III) removal efficiencies exceeding 90% together with a Langmuir adsorption capacity of approximately 10.6 mg g^{-1} were achieved under optimized conditions [1]. Building upon these promising findings, the present study aims to elucidate the influence of synthesis route on La(III) adsorption performance and to contribute to the development of high-performance CQD-based adsorbents for rare earth remediation.

The obtained findings are expected to provide valuable insights into the design of sustainable biomass-derived nanomaterials for advanced water treatment technologies and environmental applications.

Acknowledgment:
This study was financially supported by Ege University Scientific Research Project Unit Project No. FM-DKT-2025-32710.

ORCID:
Berkant Senturk: 0000-0002-9127-583X
Sabriye Yusan: 0000-0002-1843-8591

References:
Senturk, B., & Yusan, S. (2025). Investigation of the usability of Ce-and N-doped hybrid carbon quantum dots for the removal of neodymium ions. Journal of Radioanalytical and Nuclear Chemistry, 334(9), 6785-6802.

Keyword: *Carbon Quantum Dots (CQDs), Hydrothermal Synthesis, Adsorption*

Dynamic Behaviour of Oil–Water Interfaces and Acoustic-Enhanced Waterflooding In A Reservoir-On-Chip Micromodel

Faruk Aksoy [*] [1,2], **Gurkan Yesiloz**[1,2]

[1] *Yesiloz Research Laboratory, National Nanotechnology Research Center (UNAM) - Bilkent University, 06800, Cankaya-Ankara, Türkiye*
[2] *Institute of Materials Science and Nanotechnology, Bilkent University, 06800, Cankaya-Ankara, Türkiye*

Understanding and controlling immiscible liquid–liquid interfaces under acoustic fields is critical for advancing chemical processing [1], multiphase microfluidics [2], and enhanced oil recovery (EOR) [3]. While acoustofluidics has been extensively explored for mixing, particle manipulation, and droplet control, the dynamic behavior of sequential oil–water interfaces under traveling acoustic waves remains comparatively unexplored. Here, we report acoustically induced deformation and oscillatory dynamics of an immiscible oil-water interface confined within a microfluidic channel and demonstrate how these interfacial perturbations can be harnessed to enhance waterflooding efficiency in a reservoir-on-chip micromodel.

A stable oil-water interface was first established inside rectangular PDMS microchannels under static conditions. Upon activation of a piezoelectric transducer (PZT) operating at 4.1kHz and $95V_{pp}$, the abrupt acoustic impedance mismatch between water and oil generated acoustic radiation pressure (ARP), resulting in rapid interface deformation and displacement toward the oil phase. The influence of interface curvature was investigated by comparing wide (1300 μm) and narrow (240 μm) microchannels. The narrower geometry exhibited significantly larger initial displacement amplitudes (~290 μm) due to increased confinement and enhanced acoustic energy density near the interface. However, stronger capillary restoring forces associated with higher curvature led to slower relaxation dynamics. To further investigate temporal modulation effects, pulsatile acoustic excitation was applied at 100 mHz, 250 mHz, and 12 Hz. Results showed that low-frequency pulsation produced pronounced displacement–relaxation cycles with overshoot behavior during OFF phases, whereas high-frequency excitation approached a quasi-continuous actuation regime. These findings reveal that interface dynamics depend strongly on the relationship between acoustic cycling frequency and the interface's intrinsic mechanical relaxation timescale.

Building on these findings, we developed a heterogeneous reservoir-on-chip micromodel to investigate whether acoustically induced interface oscillations could enhance multiphase displacement in porous media analogues. Under passive waterflooding (Acoustics OFF), water preferentially followed low-resistance diagonal pathways, leaving substantial residual oil trapped in peripheral high-resistance regions. The cumulative recovery factor under passive conditions remained limited to ~41.7%. Under acoustic excitation, interface oscillations redistributed flow into previously unswept zones, significantly improving sweep efficiency and mobilizing trapped oil clusters. Results showed the regions that previously exhibited negligible invasion demonstrated substantial fluid penetration under acoustic stimulation, increasing cumulative oil recovery to ~65.3%.

This work demonstrates that acoustic waves can dynamically manipulate immiscible liquid–liquid interfaces and significantly improve multiphase transport in confined porous systems. The presented acoustofluidic approach provides a tunable and non-invasive strategy for controlling interfacial instabilities and enhancing oil recovery in reservoir-on-chip platforms, opening new opportunities for acoustically assisted multiphase flow technologies.

Acknowledgment:
Authors gratefully acknowledge the support from the Scientific and Technological Research Council of Türkiye (TUBITAK) under 118C263 and 123E157 grants. The financial support received from TUBITAK does not mean that the content of the submission is approved in a scientific sense by TUBITAK.

References:
X. Zhang et al., J. Environ. Chem. Eng., 2022, 10, 109036.
A. P. Vardin, F. Aksoy and G. Yesiloz, Chem. Eng. J., 2025, 171728.
D. Radziuk et al., Phys. Chem. Chem. Phys., 2016, 18, 21–46.

Keyword: *Acoustofluidics, Interface Dynamics, Multiphase Flow*

Ethylenediamine and Polyethylenimine-Functionalized ZIF-8 Prepared by Wet Impregnation and Heating Reflux: Effect of Functionalization Route in CO_2 Adsorption Performance

Tuğba Çakır [*1], Can Erkey[2], Hamed Yousefzadeh[1]

[1] *Department of Chemical Engineering, Yeditepe University, Ataşehir 34755, İstanbul, Türkiye*
[2] *Department of Chemical and Biological Engineering, Koç University, Rumelifeneri Yolu, Sariyer, Istanbul 34450, Türkiye*

The post-synthetic amine functionalization route used for MOFs can strongly influence their CO_2 adsorption performance. In this study, zeolitic imidazolate framework-8 (ZIF-8) was synthesized via a solvothermal method and subsequently functionalized with ethylenediamine (ED) and polyethylenimine (PEI) using two post-synthetic modification routes, namely wet impregnation (WI) and heating reflux (HR). The effects of amine type and functionalization route on the structural, textural, and CO_2 adsorption properties of ZIF-8 were systematically investigated. The prepared materials were characterized by PXRD, FTIR, TGA, SEM, and N_2 adsorption–desorption analyses. PXRD results confirmed that the crystalline structure of ZIF-8 was largely preserved after amine modification, while FTIR spectra indicated the successful incorporation of amine species. Textural analysis showed that amine functionalization reduced the surface area and pore volume of ZIF-8, with PEI causing more pronounced pore blocking than ED due to its polymeric structure. The BET surface area decreased from 370.9 $m^2\ g^{-1}$ for pristine ZIF-8 to 297.1 $m^2\ g^{-1}$ for ZIF-8-PEI-WI. Dynamic breakthrough experiments performed using a 15% CO_2/85% N_2 gas mixture at 298 K showed that ZIF-8-ED-WI exhibited the highest CO_2 adsorption capacity, increasing the uptake from 0.30 mmol g^{-1} for pristine ZIF-8 to 0.48 mmol g^{-1}. In contrast, excessive pore blockage in PEI-modified samples, particularly after reflux treatment, limited CO_2 adsorption performance. These results demonstrate that the balance between amine incorporation and pore accessibility is critical, and that ED functionalization via wet impregnation is the most effective route for enhancing the CO_2 adsorption performance of ZIF-8 under dilute CO_2 conditions.

Keyword: *Metal Organic Frameworks; CO2 capture; Amine Functionalization*

Sub-100 nm Ti-MIL-125 Nanoparticles for Efficient Phosphate Removal From Water

Elif Gökçen Dilci [*] [1,2], **Ömer Faruk Eşit**[1], **Zeyneb Sultan Güneysu**[1], **Sarper Ozan Kelleci**[1], **Selis Önel**[1]

[1] *Department of Chemical Engineering, Hacettepe University, Ankara, Turkiye*
[2] *Institute of Science, Hacettepe University, Ankara, Turkiye*

Anthropogenic industrial and agricultural activities have elevated aqueous phosphate, PO_4^{3-}, concentrations in groundwater and wastewater, inducing eutrophication and threatening ecological and public health. The performance and stability limitations of conventional water treatment technologies, including chemical precipitation via coagulants [1-3] and adsorption using macroporous amorphous rocks [1-3], microporous crystalline zeolites, or nanostructured materials [1-3], necessitate the development of advanced alternatives, such as metal organic framework (MOF) particles [4, 5].

This study evaluates Ti-MIL-125, a titanium (Ti)-based MOF crystal featuring a high surface area-to-volume ratio, tunable porosity, and enhanced stability, as a solution for water treatment. While Ti-MIL-125 is widely applicable in catalysis [6] and separation [6], this work utilizes sub-100 nm Ti-MIL-125 nanoparticles synthesized via solvothermal method for pollutant removal. Batch adsorption experiments were conducted using aqueous potassium dihydrogen phosphate (KH_2PO_4, ACS reagent grade) solutions at initial concentrations, C_i, of 7, 14, 21, 28, and 35 ppm with a fixed adsorbant dosage of 1 mg/mL across contact times of 1, 5, 10, 15, 30, 60, and 120 minutes. Residual phosphate concentrations were quantified via UV-visible spectrophotometry to determine adsorption kinetics and performance of Ti-MIL-125 nanoparticles. Maximum adsorption conditions were obtained at 120 minutes for all initial concentrations. The phosphate removal efficiency, $\eta=(C_i-C_f)/C_i$, of Ti-MIL-125 achieved with the 7 ppm solution was 92.3%. For higher phosphate concentrations, the efficiency, thus, the amount of phosphate removed, reduced linearly according to the empirical correlation $\eta=-0.6331C_i+96.5771$, reaching a minimum of 74.6% for the 35 ppm solution. Experimental data could be best modelled using the pseudo-second-order adsoption kinetics.

In conclusion, sub-100 nm Ti-MIL-125 nanoparticles offer an efficient, scalable approach for phosphate removal from contaminated water. The reduced particle size enhances mass transfer and accelerates adsorption kinetics achieving significantly high removal efficiencies. These findings support sustainable industrial process designs aligned environmental and advanced materials directives, applicable to both pollutant remediation and critical chemical recovery.

Acknowledgment:
This study is supported by TUBITAK via 1001 research project no. 220M002 and 2209-A project no. 1919B012553670 and Hacettepe University BAP via research projects FHD-2024-20812 and FYL-2026-22074.

References:
[1] O. N. H. Dursun Ş., "Evsel Atık Sudan Çökeltmeyle Fosfat Giderim Metotlarının Karşılaştırılması.," Selçuk Üniversitesi Fen Edebiyat Fakültesi Fen Dergisi, vol. 26, pp. 51-58, 2005.
[2] A. N. Onar, N. Balkaya, and T. Akyuz, "Phosphate removal by adsorption," (in English), Environ Technol, vol. 17, no. 2, pp. 207-213, Feb 1996, doi: Doi 10.1080/09593331708616378.
[3] Y. H. He, H. Lin, Y. B. Dong, and L. Wang, "Preferable adsorption of phosphate using lanthanum-incorporated porous zeolite: Characteristics and mechanism," (in English), Appl Surf Sci, vol. 426, pp. 995-1004, Dec 31 2017, doi: 10.1016/j.apsusc.2017.07.272.
[4] M. O. Usman, G. Aturagaba, M. Ntale, and G. W. Nyakairu, "A review of adsorption techniques for removal of phosphates from wastewater," (in English), Water Sci Technol, vol. 86, no. 12, pp. 3113-3132, Dec 15 2022, doi: 10.2166/wst.2022.382.
[5] I. Salahshoori, M. Golriz, M. N. Jorabchi, S. Moghari, and H. A. Khonakdar, "Recent progress in MOF-based biopolymer composites for wastewater detoxification," (in English), Coordin Chem Rev, vol. 543, Nov 15 2025, doi: 10.1016/j.ccr.2025.216919.
[6] S. N. Kim, J. Kim, H. Y. Kim, H. Y. Cho, and W. S. Ahn, "Adsorption/catalytic properties of MIL-125 and NH2-MIL-125," (in English), Catal Today, vol. 204, pp. 85-93, Apr 15 2013, doi: 10.1016/j.cattod.2012.08.014.

Keyword: *Phosphate removal from water, Metal organic framework (MOF) nanoparticles, Adsorption*

New Generation Emergency Water Purification Equipment Containing Nanotitania and The Effect of Nanomorphology Alteration on Filtration Performance

Boğaç Kılıçarslan [*1], **Merve Gültekinoğlu**[2], **Cem Bayram**[3]

[1] *Department of Nanotechnology and Nanomedicine, Faculty of Science, Hacettepe University, Ankara, TURKEY; Advanced Technologies Application and Research Center, Hacettepe University, Ankara, TURKEY*

[2] *Department of Nanotechnology and Nanomedicine, Faculty of Science, Hacettepe University, Ankara, TURKEY*

[3] *Department of Nanotechnology and Nanomedicine, Faculty of Science, Hacettepe University, Ankara, TURKEY; Advanced Technologies Application and Research Center, Hacettepe University, Ankara, TURKEY; Department of Chemical Engineering, Faculty of Engineerin*

New generation emergency water purifier equipment (EMP) are the portable and electricity-free water disinfection systems providing potable water to users during a vital survival state such as heavy floods and earthquakes. The working mechanism of the commercially available EMP are commonly based on pressure-driven dead-end membrane microfiltration, and the main purpose of EMP is the filtration of water-borne pathogens like E.coli and E.faecalis which have been proven to cause health problems like urinary tract infections, gastroenteritis and/or hemorrhagic colitis. Due to their high filtration effective surface area per unit volume and high water flux under low operating pressures, polysulfone (PSf) based nanocomposite hollow fiber membranes (HFMs) have been preferred in EMPs. Because of the economic accessibility, hydrophilicity, biocompatibility, and antibacterial properties of nanoscale titanium dioxide (TiO_2) as a nanofiller in membrane technologies, TiO_2 nanomaterials were conventionally used in HFMs for water purification applications. Even though filtration performances of the different TiO_2 nanomorphologies like nanoparticles (NPs), nanowires (NWs), nanosheets (NSs), nanoflowers (NFs) were individually researched in the literature, a comparative geometrical investigation on TiO_2 nanofiller morphology for emergency water purification purposes has not been investigated yet. In this study, 0D, 1D, 2D, and 3D TiO_2 nanomorphologies were synthesized by hydrothermal/solvothermal reaction-based industrially scalable approaches and annealed to anatase crystallinity. Furthermore, 1.0 wt% of altering anatase nanomorphologies were filled into 4:3:20 w/w of PSf:PEG:DMF dope solutions before coaxial dry jet wet spun of nanocomposite HFMs. As fabricated HFMs were sealed and tested using a 3D-printed EMP prototypes made of polyethylene terephthalate glycol (PETG) and polylactic acid (PLA). Scanning electron microscopy (SEM), energy dispersive x-ray (EDX) analysis, atomic force microscopy (AFM), x-ray diffraction (XRD), surface area measurements (BET), zeta potential analysis were performed. Biofiltration performances of all EMP prototypes were investigated after gravitational filtration. Pure water fluxes (PWFs), bovine serum albumin (BSA) rejections, flux recovery ratios (FRR) of samples were determined. E.faecalis and E.coli bacteria suspensions were filtered through the EMPs and bacterial filtration ratios were calculated after optical density measurements by UV/vis microplate reader. TiO_2 NW group samples showed PWF of 188.9 $L.m^{-}2.h^{-1}$, FRR of 94.4%, BSA rejection of 57.5% due to their highly negative zeta potential and anisotropic geometry simultaneously acting as an electrostatic repulsive electro-mechanical barrier on membrane pores for negatively charged soft and deformable bacteria which could leak through membrane pores. These findings demonstrate that morphology tuning of nanofillers is a critical parameter for designing high-performance EMP equipment.

Acknowledgment:
This study is supported by Hacettepe University Scientific Research Project Coordination Unit (FBA-2024-21435).

ORCID:
Boğaç Kılıçarslan: 0000-0001-9161-9551
Merve Gültekinoğlu: 0000-0002-1021-1915
Cem Bayram: 0000-0001-8717-4668

Keyword: *titanium dioxide, nanomorphology, water purification*

Preconcentration and Light Scattering-Based Approach for Rapid Estimation of Marine Nanoparticle Concentrations

Naim Yağız Demir [*1], **Emre Büküşoğlu**[2], **Mustafa Yücel**[1]

[1] *Middle East Technical University, Institute of Marine Sciences*
[2] *Middle East Technical University, Department of Chemical Engineering*

Quantifying nanoparticle concentrations in natural seawater remains analytically challenging because of low particle abundance and the limited detectability of dispersed particles by direct dynamic light scattering (DLS) measurements [1], [2]. In this study, a two-step workflow was developed for the rapid estimation of marine nanoparticle concentrations by combining membrane-based preconcentration with DLS-based quantification. In the first step, a three-parameter calibration model relating count rate, particle diameter, and particle concentration was established using 20, 50, 100, and 200 nm polystyrene bead standards measured in both quartz and disposable cuvettes. The quartz cuvette provided the best fit, yielding the relationship log(Count Rate) = a·log(Diameter) + b·log(Concentration) + c, with coefficients a = 4.4511, b = 0.8220, c = −14.0301 and R^2 = 0.9740. In the second step, nanoparticle suspensions were processed in a 400 mL stirred cell equipped with a 76 mm, 0.1 µm PVDF membrane under argon pressure and magnetic stirring in order to evaluate enrichment behavior and particle recovery. For 200 nm suspensions, enrichment factors after volume normalization ranged from 2.4 to 5.8 in the concentrated retentate and from 3.7 to 6.4 when filter-associated particles were included. Although overall recovery remained limited, the retained fraction became measurable by DLS after preconcentration. In contrast, the low retention observed for 50 and 100 nm particles was consistent with the nominal 0.1 µm membrane pore size and therefore reflected the expected size-selective character of the enrichment step [3]. These findings show that the stirred-cell stage functions as a selective fractionation and enrichment step, preferentially concentrating the larger nanoparticle fraction while allowing smaller particles to pass into the permeate. Overall, the proposed workflow demonstrates potential as a rapid onboard screening method for estimating the concentration of the retained larger nanoparticle fraction in marine samples, while further optimization is required to improve recovery and strengthen quantitative robustness.

This project has received funding from the European Research Council (ERC) under the European Union's Horizon Europe research and innovation programme (Grant agreement no: 101043381).

ORCID:
Naim Yağız Demir: 0000-0003-4707-7606
Emre Büküşoğlu: 0000-0002-3128-059X
Mustafa Yücel: 0000-0002-7478-902X

References:

L. Chekli et al., “Aggregation behaviour of engineered nanoparticles in natural waters: Characterising aggregate structure using on-line laser light scattering,” Journal of Hazardous Materials, vol. 284, pp. 190–200, Mar. 2015, doi: 10.1016/j.jhazmat.2014.11.003.
S. M. Tareq et al., “A Dynamic Light Scattering Approach for Detection of Nanomaterials in Tennessee River,” Water Resources Research, vol. 57, no. 8, p. e2020WR028687, 2021, doi: 10.1029/2020WR028687.
Y. Tayeh, T. M. Al-Zghoul, M. J. K. Bashir, M. Y. D. Alazaiza, and S. Abuabdou, “Membrane Technologies at the Frontier: A Review of Advanced Solutions for Microplastics and Emerging Contaminants in Wastewater,” Environments, vol. 13, no. 2, p. 118, Feb. 2026, doi: 10.3390/environments13020118.

Keyword: *Dynamic light scattering, Marine nanoparticles, Membrane preconcentration*

Effect of GO Nanofiller Concentration on the Dielectric Properties of GO–PVA–AgNW Nanocomposites

Mahammad Baghir Baghirov * **, Mustafa Muradov**

Baku State University

In recent years, multicomponent polymer-based nanocomposites have attracted considerable scientific and technological attention due to their tunable structural, electrical, optical, and dielectric properties. Among these materials, graphene oxide (GO)- and silver nanowire (AgNW)-based polymer nanocomposites are regarded as promising candidates for advanced dielectric and electronic applications because of their large interfacial area and strong interaction with polymer matrices. In the present study, the effect of GO nanofiller concentration on the dielectric properties of GO–PVA–AgNW nanocomposites was systematically investigated.

Figure 1 presents the frequency–temperature dependences of the real part of dielectric permittivity for GO–PVA–AgNW nanocomposites containing different GO concentrations. Figure 1A, B, C, and D correspond to AgNW–PVA, 0.4 wt.% GO–PVA–AgNW, 0.8 wt.% GO–PVA–AgNW, and 2 wt.% GO–PVA–AgNW nanocomposites, respectively. The results reveal that all investigated samples exhibit similar dielectric behavior. In all cases, relatively high dielectric permittivity values were observed at low frequencies. This behavior is attributed to orientational polarization associated with polar functional groups of the PVA matrix, as well as Maxwell–Wagner–Sillars (MWS) interfacial polarization arising from the incorporation of Ag nanowires and GO nanosheets. At low frequencies, charge accumulation at the interfaces between conductive fillers and insulating polymer matrix enhances interfacial polarization and increases dielectric permittivity.

The obtained results further demonstrate that the real part of dielectric permittivity decreases with increasing AC electric field frequency. This behavior is related to the inability of dipolar groups and interfacial charges to follow the rapidly alternating electric field at high frequencies. In contrast, increasing temperature leads to an enhancement of dielectric permittivity due to the thermally activated mobility of polymer chains and dipolar groups.

Comparative analysis showed that the addition of 0.4 wt.% GO decreases dielectric permittivity compared to pristine AgNW–PVA. This reduction is associated with hydrogen bonding interactions between GO functional groups and PVA chains, which restrict chain mobility and suppress dipolar polarization [1,2]. However, at 0.8 wt.% GO concentration, dielectric permittivity significantly increases due to the homogeneous dispersion of GO nanosheets and the formation of an enlarged interfacial area that enhances interfacial polarization. Further increasing the GO concentration to 2 wt.% results in a reduction of dielectric permittivity because of GO agglomeration, increased hydrogen bonding interactions, and screening effects that reduce the effective electric field inside the composite. Moreover, at GO concentrations higher than 2 wt.%, the dielectric permittivity decreases sharply, indicating deterioration of interfacial polarization efficiency and enhanced filler agglomeration within the polymer matrix.

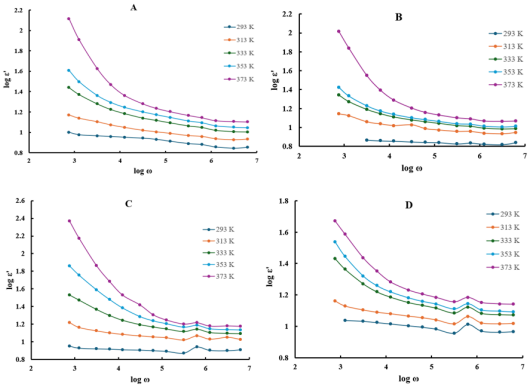


Figure 1. Frequency dependence of the real part of dielectric permittivity for (A) AgNW–PVA, (B) 0.4 wt.% GO–PVA–AgNW, (C) 0.8 wt.% GO–PVA–AgNW, and (D) 2 wt.% GO–PVA–AgNW nanocomposites at different temperatures.

ORCID:
Mahammad Baghir Baghirov: 0000-0002-0300-1856

References:

Boyrazli M, Yalcin M, Dere A, Yakuphanoglu F. Electrical and dielectric behavior of PVA nanocomposites doped with graphene oxide: Effects of doping level and frequency. Journal of Alloys and Compounds. 2025 May 11:180916.
Hurayra–Lizu KA, Bari MW, Gulshan F, Islam MR. GO based PVA nanocomposites: tailoring of optical and structural properties of PVA with low percentage of GO nanofillers. Heliyon. 2021 May 1;7(5).

Keyword: *Dielectric permittivity, concentration effect*

Thiophene- and Dicyanothiophene-Bridged Conjugated Polymers for V2O5 Nanowire-Based Asymmetric Hybrid Supercapacitor Devices

Sedanur Şahinaslan [* 1], Elif Demir Arabacı[1], Oğuzhan Karakurt[1], Eda Çevik[2], H. Emrah Ünalan[2], Ali Çırpan[1,3,4,5]

[1] Middle East Technical University, Department of Chemistry, 06800, Ankara, Turkey
[2] Department of Metallurgical and Materials Engineering, Middle East Technical University (METU), 06800, Ankara, Türkiye
[3] Middle East Technical University, Department of Polymer Science and Technology, 06800, Ankara, Turkey
[4] Middle East Technical University, ODTU GUNAM, Ankara, 06800, Turkey
[5] Middle East Technical University, Department of Micro and Nanotechnology, Ankara, 06800, Turkey

Current electrochemical energy storage technologies aim to combine high specific energy and power density with long cycle life in a single system. Supercapacitors have emerged as promising devices bridging conventional capacitors and batteries, owing to their high-power density, fast charge-discharge capability, and long cycle life. Conjugated polymers are attractive electrode materials for supercapacitors due to their π-delocalized structures, high specific capacitance, rapid redox reactions, and flexible processability.

This study aims to develop multifunctional conjugated polymer-based electrode materials integrating high capacitive performance with electrochromic functionality for asymmetric supercapacitor applications. The designed polymers incorporate triphenylamine (TPA) and 3,4-ethylenedioxythiophene (EDOT) as electroactive units, with thiophene and 3,4-dicyanothiophene serving as π-bridges. The electron-rich TPA unit enables enhanced charge storage, while EDOT contributes structural stability and the thiophene π-bridge promotes conjugation and electrical conductivity. Monomers were polymerized via electropolymerization and the resulting polymers were characterized by electrochemical and spectroelectrochemical studies. Polymer 1 (P1) demonstrated outstanding energy storage performance with specific capacitances of 26.3 mF/ cm^2 (CV) and 24.1 mF/ cm^2 (GCD), coupled with an energy density of 5.3 μWh/cm^2 and power density of 37.2 μW/cm^2. Optically, P1 exhibited 64% transmittance at 1240 nm, rapid switching (1.86 s), and high coloration efficiency (149.30 cm^2/C). An asymmetric supercapacitor device D1 was constructed using V_2O_5 nanowires and P1 as electrode materials. D1 delivered a power density of 5.02 μW/ cm^2, a b-value of 0.86 confirming predominantly surface-controlled capacitive behavior, rapid optical switching (0.45 s), and exceptional coloration efficiency (375.06 cm^2/C). Overall, this work highlights thiophene-bridged conjugated polymers as promising multifunctional materials combining capacitive and electrochromic performance.

Acknowledgment:
This study was supported by Scientific and Technological Research Council of Turkey (TUBITAK) under the Grant Number 124Z087. The authors thank to TUBITAK for their supports.

ORCID:
Sedanur Şahinaslan: 0009-0008-0539-0294
Elif Demir Arabacı: 0000-0002-3406-135X
Oğuzhan Karakurt: 0000-0002-1856-0503
Ali Çırpan: 0000-0003-3051-8380
Ali Çırpan: 0000-0003-3051-8380
Ali Çırpan: 0000-0003-3051-8380
Ali Çırpan: 0000-0003-3051-8380

References:
Cevher, D., Cevher, S. C., Toppare, L., & Cirpan, A. (2023). Enhancing electrochromic supercapacitor electrode performance through different donor compartments in DAD type conjugated polymers. Journal of Energy Storage, 74, 109501
Snook, G. A., Kao, P., & Best, A. S. (2011). Conducting-polymer-based supercapacitor devices and electrodes. Journal of power sources, 196(1), 1-12. https://doi.org/10.1016/j.jpowsour.2010.06.084
Xie, Y., Zhang, Y., Zhu, M., Huang, R., & Chao, D. (2023). High-performance electrochromic supercapacitor based on a new EDOT-triphenylamine conjugated polymer. Dyes and Pigments, 208, 110889. https://doi.org/10.1016/j.dyepig.2022.110889

Keyword: *Conjugated Polymers, Electropolymerization, Supercapacitors*

ID: 271

Experimental Evaluation Of Adhesion In Poly(4-vinylpyridine) Thin Films Deposited By Initiated Chemical Vapor Deposition

Çağrı Sayın [*1], Azizeh Hosseinjany[1], Gözde Özaydın İnce[1,2]

[1] *Materials Science and Nanoengineering Program, Faculty of Engineering and Natural Sciences, Sabancı University, Tuzla, İstanbul 34956, Türkiye*

[2] *SUNUM – Sabancı University Nanotechnology Research and Application Center, Tuzla, İstanbul 34956, Türkiye*

Adhesion of polymer thin films is an important factor for the functionality and durability of the coating. However, the adhesion behavior of polymer thin films is difficult to quantify reliably, and there is no consensus in the literature regarding the characterization of adhesion strength. In this experimental study, the adhesion strength of poly(4-vinylpyridine) (P4VP), a polymer known for its adhesive properties, is measured using a pull-off test. 4VP is deposited on silicon wafer using the initiated chemical vapor deposition (iCVD) method, and existence of the thin film is confirmed and thickness of the coating is measured using interferometry. 3D-printed studs are attached to the P4VP thin film with an epoxy-based adhesive, and the pulling force at the failure point is measured using a universal testing machine (UTM). The results provide experimental reference data for evaluating the adhesion strength of iCVD-grown P4VP polymer thin films on silicon wafers and may also provide a framework for modeling polymer-surface adhesion.

Acknowledgment:
The authors acknowledge the support of the laboratory facilities and technical staff involved in the iCVD deposition, interferometry measurements, and pull-off testing performed in this study.

ORCID:
Çağrı Sayın: 0009000886667995

Keyword: *Initiated chemical vapor deposition (iCVD), Polymer thin films, Pull-off test*

ID: 340

Structural and Electronic Properties of Plasmonic Metal (Al, Au, Ag) Doped CaTiO3

Dilara Köroğlu * **, Veli Ongun Özçelik**

Materials Science and Nano Engineering Program, Sabanci University, Istanbul, 34956, Turkey.

$CaTiO_3$ has attracted interest among perovskites since its discovery in 1839 due to its flexible structure and dielectric behavior. Chemical doping is one of the proposed methods for tuning the optoelectronic properties of $CaTiO_3$. The purpose of this study is to provide a detailed theoretical analysis using density functional theory (DFT) to evaluate how the substitution of plasmonic metals (Al, Au, Ag) with varying concentrations influences the band gap and electronic structure of $CaTiO_3$. The results show that while the combination of plasmonic metal doping and oxygen vacancy substantially narrows the band gap, it also reduces the structural stability of the system. Ag doping produces the strongest band-gap reduction, decreasing the band gap from 1.10 eV to 0.88 eV in vacancy-free systems. Ag-doped systems show the highest dopant formation energy (11-16 eV), indicating inefficient dopant integration. Au doping exhibits a concentration-dependent response, with band gaps ranging from 1.66 to 1.86 eV in vacancy-free structures. In contrast, Al doping provides a more controlled modification of the electronic structure, yielding band gaps between 1.61 and 1.83 eV without vacancies and 0.40–0.94 eV with vacancies. Moreover, Al-doped systems exhibit the lowest dopant formation energies (around 2 eV), indicating favorable thermodynamic stability and efficient dopant incorporation. Overall, Al doping offers the most favorable balance between band-gap tunability and thermodynamic stability, whereas Ag doping provides the strongest electronic modulation and Au doping preserves a stable semiconducting character at higher concentrations. These findings indicate that Al-doped $CaTiO_3$ is a promising candidate for photocatalytic and optoelectronic applications requiring tunable electronic properties.

Acknowledgment:
This work is supported by TUBITAK through grant no 2218-124C474.

References:
[1] D. Saadetnejad, R. Yıldırım, Photocatalytic hy- drogen production by water splitting over au/al- srtio3, international journal of hydrogen energy 43 (2) (2018) 1116–1122.
[2] P. Fernández de Cos, et al., Comparative study of the band structure of catio3, srtio3 and batio3 (2019).
[3]M. Rizwan, A. Shahid, T. Mahmood, A. A. Zafar, I. Aslam, N. Adnan, T. Hussain, H. Jin, C. Cao, Effect of magnesium on structural and optical properties of catio3: A dft study, Physica B: Con- densed Matter 568 (2019) 88–91

Keyword: *CaTiO3, doping, plasmonic metals, band-gap*

Hybrid Thermally Conductive Filler-Reinforced Polyketone Composites for Advanced Thermal Energy Management

Lutfiye Altay * [1], Mehmet Sarıkanat[1], Mehmet Mete Tokgoz[2], Yoldas Seki[3]

[1] Department of Mechanical Engineering, Ege University, Izmir 35100, Turkey
[2] Izmir Egitim Saglık Sanayi Yatırım A.Ş., Turgutlu, Manisa 45420, Turkey
[3] Department of Chemistry, Dokuz Eylul University, Izmir 35390, Turkey

This study presents the development of polyketone (POK)-based composites reinforced with thermally conductive fillers, including synthetic graphite (SG), carbon fiber (CF), carbon nanotubes (CNTs), and hexagonal boron nitride (BN). To further evaluate the influence of filler type, morphology, concentration, and filler interactions on thermal transport behavior, single-, binary-, and ternary-filler systems were fabricated and characterized. The in-plane thermal conductivity increased from 0.21 W/mK for neat POK to a maximum of 9.16 W/mK with 40 wt% synthetic graphite, while carbon fiber-reinforced composites reached thermal conductivities of 8.54 W/mK and 1.12 W/mK in the in-plane and through-plane directions, respectively. The individual and synergistic effects of CNTs and BN on the thermal conductivity of POK-30SG composites were systematically investigated. The incorporation of 1, 2, and 3 wt% CNT increased the in-plane thermal conductivity of POK-30SG by 42%, 82%, and 124%, respectively, while the corresponding improvements in through-plane thermal conductivity were 42%, 94%, and 273%. Similarly, the addition of 1, 2, and 3 wt% BN enhanced the in-plane thermal conductivity by 25%, 69%, and 107%, respectively, whereas the through-plane thermal conductivity increased by 92%, 135%, and 325%. The results revealed that CNTs were more effective in enhancing in-plane thermal conductivity, whereas BN exhibited superior performance in improving through-plane thermal conductivity. In addition, BN/CNT hybrid systems exhibited synergistic improvements in thermal conductivity even at relatively low filler loadings. These findings provide valuable insights into the design and optimization of lightweight, thermally conductive polymer composites for advanced thermal management applications.

Acknowledgment:
The authors are grateful for the funding from the Ege University Office of Scientific Research Projects (Project no: 28447).

ORCID:
Lutfiye Altay: 0000-0003-4946-3615

Keyword: *Carbon nanotube, carbon fiber, POK composites*

Fabrication of Melamine-Formaldehyde-Organic Clay Nanocomposites and Mineral-Filled Hybrid Composites

Elif Şahin [*1], Ahmet Gürses[1], Salih Akpınar[2], Nurtaç Canpolat[1]

[1] *Ataturk university*
[2] *Erzurum Technical University*

This study aims to fabricate, characterize, and investigate the properties of melamine-formaldehyde (MF) resin-based organo clay nanocomposites and mineral-filled hybrid composites. For this, firstly, organo-clay was prepared with the solution intercalation method using montmorillonite, a cationic surfactant and long-chain hydrocarbon material, and then was produced using a melamine formaldehyde nanocomposite with in situ synthesis using a melamine formaldehyde pre-polymer and organo-clay. Finally, hybrid composites were prepared by blending various minerals and the produced nanocomposite. For morphological and textural characterization, both FTIR spectroscopy and XRD spectra, as well as SEM and HRTEM images of the raw montmorillonite (MMT), organo-montmorillonite (OMMT), pure polymer (MF) and prepared hybrid composites, were used. The effects of adding mineral fillers such as organo clay, perlite, kaolinite, gypsum, pumice, and hollow glass spheres to the MF matrix on mechanical, thermal, and morphological properties were evaluated. It is known that organo clay forms strong interactions with the polymer matrix due to its high surface area and layered structure at the nanoscale, while mineral fillers provide cost reduction, dimensional stability, and thermal resistance. The results obtained in this study show that organoclay and mineral fillers used in appropriate ratios can significantly improve the performance of the MF resin. It is predicted that the developed hybrid composites can be used in structural materials, electrical-electronic applications, automotive parts, and areas requiring high temperature resistance.

Acknowledgment:
This study was supported by Atatürk University Scientific Research Projects Coordination Unit (BAP) (Project Code: FDK-2022-10258).The authors are grateful to Atatürk University for their financial support.

ORCID:
Elif Şahin: 0000-0003-4844-9862
Ahmet Gürses: 0000-0001-9800-0399
Salih Akpınar: 0000-0003-3247-991X
Nurtaç Canpolat: 0000-0002-0295-4823

References:
Chen, J.; Lekawa-Raus, A.; Trevarthen, J.; Gizewski, T.; Lukawski, D.; Hazra, K.; Rahatekar, S.S.; Koziol, K.K. Carbon nanotube films spun from a gas phase reactor for manufacturing carbon nanotube film/carbon fibre epoxy hybrid composites for electrical applications. Carbon 2020, 158, 282–290.
Suresha, B.; Divya, G.S.; Hemanth, G.; Somashekar, H.M. Physico-mechanical properties of nano silica-filled epoxy-based mono and hybrid composites for structural applications. Silicon 2021, 13, 2319–2335.
Toorchi, D.; Tohidlou, E.; Khosravi, H. Enhanced flexural and tribological properties of basalt fiber-epoxy composite using nano-zirconia/graphene oxide hybrid system. J. Indusrtrial Text. 2022, 51 (Suppl. S2), 238S–3252S.
Wang, M.; Fan, X.; Thitsartarn, W.; He, C. Rheological and mechanical properties of epoxy/clay nanocomposites with enhanced tensile and fracture toughnesses. Polymer 2015, 58, 43–52.
Chen, Z.; Wang, J.; Yu, F.; Zhang, Z.; Gao, X. Preparation and properties of graphene oxide-modified poly (melamineformaldehyde) microcapsules containing phase change material n-dodecanol for thermal energy storage. J. Mater. Chem. A 2015, 3, 11624–11630

Keyword: *Melamine-formaldehyde,, organo clay,, nanocomposite,.*

Engineering the Local Density of Optical States for Programmable Quantum Mode Switching

Emre Ozan Polat *

Deparment of Physics and UNAM-National Nanotechnology Research Center, Bilkent University, 06800, Ankara, Türkiye

Controlling the local density of optical states (LDOS) provides a powerful route for tailoring light–matter interaction at the nanoscale. By engineering the electromagnetic environment around quantum emitters and excitonic materials, plasmonic nanostructures can modify spontaneous emission rates, redistribute radiative and nonradiative decay channels, and selectively enhance or suppress optical transitions. This principle has recently been demonstrated in optically switchable fluorescence enhancement, where critical interparticle distances enable strong modulation of emitter–plasmon coupling [1].

Here, we present a general LDOS-engineering framework for programmable quantum mode switching using plasmonic nanocavities and hybrid low-dimensional material systems. We first discuss plasmonic toroidal nanoantennae, where strongly confined resonances and Fano-like LDOS modulation enable programmable quantum mode switching through selective control of molecular transitions [2]. This concept is further extended to toroidal plasmonic nanodimers coupled to heterostructured InP quantum dots, enabling enhanced near-infrared emission through geometry-dependent near-field localization [3]. We then apply the same design principle to monolayer MoS_2 integrated with plasmonic hollow gold nanocavities, where spectral alignment with A- and B-excitonic transitions enables geometry-controlled exciton selectivity [4].

Finally, we discuss active Fano-resonant control, where electrically tunable nanophotonic structures provide continuous and reversible modulation of fluorescent decay rates [5]. Together, these studies establish LDOS engineering as a versatile strategy for programmable control of quantum and excitonic optical modes, with potential applications in nanoscale light sources, exciton-selective photonic devices, quantum optical switches, and integrated nanophotonic platforms.

Acknowledgment:
E.O.P. acknowledges financial support from the Scientific and Technological Research Councilof Türkiye (TÜBİTAK) through Grant No. 222N308 within the CHIST-ERA program. Additional support was provided by the Turkish Academy of Sciences Outstanding Young Scientists Awards (TUBA-GEBİP) 2025.

ORCID:
Emre Ozan Polat: https://orcid.org/0000-0002-6652-059X

References:
A. Gülücü and E. O. Polat, “Optically switchable fluorescence enhancement at critical interparticle distances,” Advanced Theory and Simulations 8, e01134 (2025).
A. Gülücü and E. O. Polat, “Programmable quantum mode switches via plasmonic toroidal nanoantennae,” arXiv preprint arXiv:2512.01303 (2025).
A. Gülücü and E. O. Polat, “Toroidal plasmonic nanodimers for enhanced near-infrared emission in heterostructured InP quantum dots,” arXiv preprint arXiv:2604.14992 (2026).
A. E. Yıldız and E. O. Polat, “Geometry-controlled exciton selectivity in monolayer MoS_2 using plasmonic hollow nanocavities,” arXiv preprint arXiv:2603.07732 (2026).
E. O. Polat et al., “Continuous and reversible electrical-tuning of fluorescent decay rate via Fano resonance,” Nanotechnology 37, 165701 (2026).

Keyword: *plasmonics, nanophotonics, quantum engineering*

ID: 168

Interfacial Defect Passivation of SnO_2 Using L-Methionine toward High-Performance Perovskite Solar Cells

Mohammad Javad Azimi Igdır[1], Suleyman Ozel[2], Erdi Akman[3], Faruk Ozel [* 1]

[1] Department of Mechanical Engineering, Recep Tayyip Erdogan University, 53100 Rize, Turkiye
[2] Central Research Laboratory (BUMER), Bayburt University, 69000, Bayburt, Türkiye
[3] Department of Physics, Kamil Ozdag Faculty of Science, Karamanoglu Mehmetbey University, Karaman 70200, Turkiye

Perovskite solar cells (PSCs) have attracted considerable attention as next-generation photovoltaic technologies owing to their remarkable optoelectronic properties and potential to address future energy demands. However, their performance is often constrained by interfacial defects and charge recombination losses arising from imperfections within the device architecture. In particular, the tin dioxide (SnO_2) electron transport layer (ETL) is susceptible to surface defects, suboptimal charge extraction, and energy-level mismatches, which collectively hinder device efficiency and stability. In this work, a facile and multifunctional interfacial modification strategy is proposed through the incorporation of the amino acid L-methionine (L-Met) onto the SnO_2 electron-transparent layer (ETL). The functional groups of L-Met interact effectively with undercoordinated Sn sites, resulting in defect passivation, improved interfacial contact, enhanced electron transport, and more favourable energy-level alignment. These modifications have been shown to contribute to suppressed non-radiative recombination and more efficient charge extraction and transfer processes at the ETL/perovskite interface. Consequently, PSCs based on the L-Met-modified SnO_2 ETL demonstrate significantly enhanced photovoltaic performance in comparison with their unmodified counterparts. Furthermore, the modified devices demonstrate improved resistance to environmental degradation, leading to superior long-term operational stability under ambient conditions. The proposed approach provides a simple, cost-effective, and scalable route for interfacial engineering, offering valuable insights into the development of highly efficient and durable perovskite solar cells for future commercial applications.

Acknowledgment:
F.O. acknowledges the financial support of the Turkish Academy of Sciences (TUBA-GEBIP).

Keyword: *Perovskite solar cells, SnO_2 electron transport layer, L-Methionine*

Thickness-Controlled Photoluminescence and Vibrational Signatures in Layered LiInP2S6: A DFT Study

Ömer Nevzat Kösebay[1], Can Çoruh[2], Berna Akgenc Hanedar [* 3]

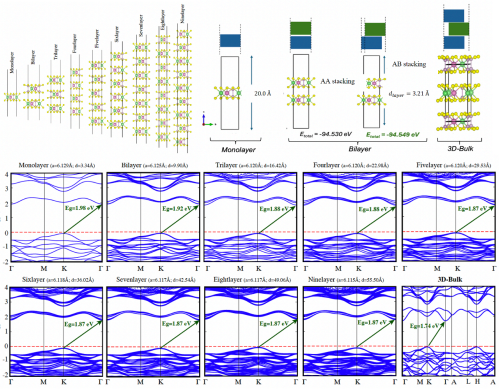
[1] *Department of Electrical-Electronics Engineering, Maltepe University, Maltepe, 34857 Istanbul, Turkey*
[2] *Department of Materials Science and Nano Engineering, Sabancı University, Tuzla, 34956 Istanbul, Turkey*
[3] *Department of Physics, Kırklareli University, 39100 Kırklareli, Turkey*

Layered metal thiophosphates have emerged as a versatile class of van der Waals semiconductors with promising applications in optoelectronics and photonics [1-2]. Among them, $LiInP_2S_6$ attracts particular attention due to its structural flexibility and tunable electronic properties. In this work, we systematically investigate the influence of thickness on the structural stability, electronic structure, lattice dynamics, Raman response, and photoluminescence (PL) characteristics of $LiInP_2S_6$ using first-principles density functional theory calculations. Structures ranging from the monolayer and ninelayer to the bulk phase were examined to reveal the evolution of material properties across different dimensionalities.

As the thickness increases, the band gap gradually decreases from 1.98 eV in the monolayer to 1.87 eV in the nine-layer structure and eventually to 1.74 eV in the bulk phase. Interestingly, despite this reduction, the overall shape of the bands near the VBM and CBM edges remains largely preserved throughout the few-layer regime. This behavior suggests that the fundamental electronic characteristics of $LiInP_2S_6$ are remarkably insensitive to thickness, with increasing layer number mainly leading to a moderate narrowing of the band gap.

Phonon dispersion calculations confirm the dynamical stability of all investigated structures through the absence of imaginary phonon modes. Increasing thickness introduces additional low-frequency interlayer shear and breathing modes, which substantially modify the vibrational spectrum and Raman-active phonon signatures. These thickness-dependent vibrational characteristics directly influence the electron–phonon coupling strength and consequently the optical emission properties.

Photoluminescence properties of $LiInP_2S_6$ were investigated within the configuration-coordinate framework. A ZPL energy of 3.13 eV, ΔR of 0.511 Å, and ΔQ of 2.66 were obtained, indicating substantial structural relaxation upon excitation. The pronounced phonon sidebands and large Huang–Rhys factor reveal strong electron–phonon coupling, suggesting that phonon-assisted transitions play a dominant role in the emission process. These findings demonstrate that lattice vibrations significantly govern the optical response of $LiInP_2S_6$.



Acknowledgment:
This work was performed at the MareNostrum 5 (MN5) at the Barcelona Supercomputing Center (BSC) and the the High Performance Grid Computing Center (TR-Grid eInfrastructure), TÜBİTAK-ULAKBİM. This study was funded by the Scientific and Technological Research Council of Turkey (TÜBİTAK) under Project No 125F626.

ORCID:
Berna Akgenc Hanedar: 0000-0002-8998-0257

References:
1. Bai, P., Xu, W., Shi, L., Wei, H., Duan, Y., Wang, R., ... & Wu, X. (2025). Two-Dimensional Direct Z-Scheme LiInP2S6/XTe2 (X= Mo and W) Heterostructures for Photocatalysis. The Journal of Physical Chemistry C, 129(25), 11698-11706.
2. Mohammadi, P., Bordoloi, A., & Singh, S. (2026). First-Principles Discovery of Novel LiInP2S6 Polymorphs with Promising Optoelectronic Responses. The Journal of Physical Chemistry C, 130(13), 4936-4944.

Keyword: *DFT, 2D Materials, Photoluminescence properties*

Polaronic Excitons in Quantum Well Perovskite Structures

Sinem Duman [*] [1], **R. Tuğrul Senger**[2]

[1] *Izmir Institute of Technology*
[2] *Izmir University of Economics*

In recent years, interest in metal halide perovskites and their lower-dimensional derivatives has grown exponentially due to their vast potential for optoelectronic applications in both bulk and low-dimensional systems **[1]**. The quantum optical properties of these highly polar materials are strongly dependent on their structural dimensionality. As the system size is reduced from the bulk form to lower dimensions, a significant increase in the band gap is observed, while quantum confinement, dielectric confinement, and polaronic effects become dominant in carrier dynamics **[1]**.

In this theoretical and numerical study, an effective Hamiltonian model is constructed to address the dielectric, quantum, and polaronic effects for bulk and quantum well perovskite structures within the framework of exciton-polaron dynamic screening. Specifically, the Hamiltonian is formulated by integrating the Pollmann–Büttner polaronic model **[2]** with the Kumagai–Takagahara formulation of dielectric confinement effect in quantum wells **[3]** and is subsequently solved by employing the variational method. A similar approach was used by Senger and Bajaj **[4]** for the case of inorganic semiconductor quantum structures. Through these calculations, physical outputs, such as the polaronic-exciton binding energy and the exciton size, are obtained as functions of the number of layers in quasi-2D perovskite crystals.

The findings derived from the model are systematically compared with traditional theoretical approaches in literature. Our results demonstrate the physical consistency of the established model compared to the simple Wannier-Mott (Rydberg) model, which ignores the dynamic response of the lattice; the Haken potential **[1, 5]** , which treats dielectric screening phenomenologically and can yield unphysical over-confinement errors at low dimensions; and ab-initio (GW-BSE) methods **[6]**, which struggle to directly incorporate electron-phonon interactions despite their high computational costs.

Our calculations reveal that as the system transitions from bulk—where the exciton binding energy is lower than the room-temperature thermal energy (k_B T) for sone materials , to quantum well structures, polaronic effects are dramatically enhanced by the static and high-frequency dielectric profiles specific to perovskite materials, alongside the quantum and dielectric confinement effects. Because of this strong interaction, it is quantitatively verified that exciton binding energies reach massive values of approximately 400–500 meV in the low-dimensional limits **[1, 5]**. This consistent approach, developed under the large polaron picture, exhibits quantitative agreement with recent experimental results **[1,5]**.

ORCID:
R. Tuğrul Senger: https://orcid.org/0000-0003-0800-1924

References:
Muhammad, Z., & Rashid, A. (2025). Exciton binding energies and polaron interplay in the optically excited state of organic–inorganic lead halide perovskites. Materials Advances, 6(1), 13-38. https://doi.org/10.1039/d4ma00454j
Pollmann, J., & Büttner, H. (1977). Effective Hamiltonians and binding energies of Wannier excitons in polar semiconductors. Physical Review B, 16(10), 4480. https://doi.org/10.1103/PhysRevB.16.4480
Kumagai, M., & Takagahara, T. (1989). Excitonic and nonlinear-optical properties of dielectric quantum-well structures. Physical Review B, 40(18), 12359-12381. https://doi.org/10.1103/PhysRevB.40.12359
Senger, R. T., & Bajaj, K. K. (2003). Binding energies of excitons in polar quantum well heterostructures. Physical Review B, 68(20), 205314. https://doi.org/10.1103/PhysRevB.68.205314
Blancon, J. C., Stoumpos, C. C., et al. (2018). Scaling law for excitons in 2D perovskite quantum wells. Nature Communications, 9(1), 2254. https://doi.org/10.1038/s41467-018-04659-x
Leppert, L. (2024). Excitons in metal-halide perovskites from first-principles many-body perturbation theory. The Journal of Chemical Physics, 160(5). https://doi.org/10.1063/5.0187213

Keyword: *Exciton Binding Energy, Quantum Well Perovskite Structures, Effective Hamiltonian Framework and Variational Calculation*

A Standalone Optofluidic “Smart Analyzer” for Adaptive Multi-Chip Plasmonic Sensing

Damla Aydogan [*1], Cem Gok[2], Seda Nur Topkaya[3], Arif E. Cetin[4]

[1] *Izmir Biomedicine and Genome Center, Balcova, Izmir, Turkey; Department of Biomedical Engineering, Faculty of Engineering and Architecture, Izmir Bakircay University, Menemen, Izmir, Turkey*

[2] *Izmir Bakircay University, Biomedical Technologies Design Application and Research Center, Menemen, Izmir, Turkey*

[3] *Izmir Biomedicine and Genome Center, Balcova, Izmir, Turkey; Izmir International Biomedicine and Genome Institute, Dokuz Eylul University, Balcova, Izmir, Turkey*

[4] *Izmir Biomedicine and Genome Center, Balcova, Izmir, Turkey; Department of Biophysics, Faculty of Medicine, Dokuz Eylul University, Balcova, Izmir, Turkey*

Plasmonic optical sensors detect minute refractive-index changes in a label-free manner, enabling applications across biomedical analysis, environmental monitoring, and food safety (Patel et al., 2023; Topor et al., 2023). However, current portable plasmonic readers share a structural constraint: they rely on fixed calibration optimized for a single chip type and cannot automatically adapt to chips with different resonance characteristics (Cetin, 2023; Yaman et al., 2023). Although linear variable filters (LVFs) enable compact spectroscopy and machine learning (ML) has advanced plasmonic spectral processing, no reported system has combined ML-guided LVF scanning to achieve automatic adaptation across distinct plasmonic chips (Corcione et al., 2021).

To address this gap, we developed and experimentally validated a portable optofluidic platform integrating LVF-based motorized spectral scanning, polydimethylsiloxane (PDMS) microfluidic flow control, and ML-assisted adaptive positioning, with all modules unified on a Raspberry Pi 5 embedded system under a single touchscreen interface. An ML-based algorithm predicts the optimal LVF position directly from the chip’s spectral response, while a CMOS camera enables real-time optical monitoring. The position–wavelength calibration exhibited high linearity ($R^2 = 0.9991$; RMSE = 2.26 nm) over a 433–689 nm window. Among five regression algorithms benchmarked under k-fold cross-validation, Ridge Regression achieved the best performance ($R^2 = 0.9999$; mean absolute error = 0.011 mm), and its adaptive generalizability across two distinct Al nanohole chip types was experimentally confirmed, eliminating the manual recalibration required by single-chip readers. A 28 µL PDMS chamber was permanently bonded via oxygen-plasma activation, and a piezoelectric micropump delivered reproducible flow with a linear voltage–flow-rate response over 85–225 Vpp. The integrated system resolved refractive-index changes with a sensitivity of S = 130.2 nm/RIU for the ethanol series. Critically, the ML model operates not as a post-hoc analysis tool but as a cognitive control layer that autonomously steers the optical hardware according to chip type, transforming the device into a standalone “smart analyzer” requiring no external computer. To our knowledge, this is the first portable plasmonic platform to simultaneously deliver portability, ML-driven adaptive multi-chip compatibility, and integrated microfluidic control.

In this study, we present the design, fabrication, and validation of the platform, with emphasis on the ML-driven adaptive readout, the comparative regression-model analysis, and the integrated microfluidic and optical performance, and discuss its pathway toward a target-specific plasmonic biosensor through surface functionalization.

Acknowledgment:
This work was supported by the Scientific and Technological Research Council of Türkiye (TÜBİTAK) under the 2210-D program (Project No. 1649B022404815).

ORCID:
Damla Aydogan: https://orcid.org/0009-0007-5095-790X
Cem Gok: https://orcid.org/0000-0002-8949-8129
Seda Nur Topkaya: https://orcid.org/0000-0002-7816-3155
Arif E. Cetin: https://orcid.org/0000-0002-0788-8108

References:
Cetin, A. E. (2023). A Portable Plasmonic Biosensor Kit for Diagnostics of Sexually Transmitted Infection. Plasmonics 2023 19:2, 19(2), 753–764. https://doi.org/10.1007/S11468-023-02035-0
Corcione, E., Pfezer, D., Hentschel, M., Giessen, H., & Tarín, C. (2021). Machine Learning Methods of Regression for Plasmonic Nanoantenna Glucose Sensing. Sensors 2022, Vol. 22, Page 7, 22(1), 7. https://doi.org/10.3390/S22010007
Patel, S. K., Wekalao, J., Alsalman, O., Surve, J., Parmar, J., & Taya, S. A. (2023). Development of surface plasmon resonance sensor with enhanced sensitivity for low refractive index detection. Optical and Quantum Electronics 2023 55:11, 55(11), 1001-. https://doi.org/10.1007/S11082-023-05265-Y
Topor, C. V., Puiu, M., & Bala, C. (2023). Strategies for Surface Design in Surface Plasmon Resonance (SPR) Sensing. Biosensors 2023, Vol. 13, Page 465, 13(4), 465. https://doi.org/10.3390/BIOS13040465
Yaman, S., Avci, M. B., Kurul, F., Topkaya, S. N., & Cetin, A. E. (2023). Handheld optofluidic platform towards binding dynamics applications in field-settings. Sensors and Actuators A: Physical, 363, 114685. https://doi.org/10.1016/J.SNA.2023.114685

Keyword: *Linear variable filter (LVF), Plasmonic sensing, Machine learning*

Structural and Photophysical Properties of Microwave-assisted Synthesized Mo,N Co-doped Carbon Quantum Dots

İbrahim Yağız Coşkun * **, Caner Ünlü**

Istanbul Technical University

The incorporation of heteroatom into carbon quantum dots (CQDs) is an effective method to modify their electronic and optical properties. In this study, molybdenum and nitrogen co-doped carbon quantum dots (Mo,N:CQDs) were synthesized through a one-step microwave-assisted method using citric acid, urea, and ammonium heptamolybdate. The research focuses on how varying the concentration of the carbon precursor (citric acid) affects the structural and photophysical characteristics of the resulting CQDs.

Detailed structural characterization techniques revealed that decreasing the carbon content significantly alters the chemical structure. XRD patterns indicated a transition from highly disordered graphenic domains with tight interlayer spacing to an expanded, multiphase structure characterized by poorly registered layers. XPS analysis showed that the reduction in citric acid leads to a marked decrease in surface carboxyl groups and induces a migration of nitrogen dopants from interior graphitic sites to pyridinic structures. Additionally, this carbon depletion drives a partial reduction of the incorporated molybdenum species from the Mo^{6+} to the Mo^{4+} state, accompanied by a transition toward direct molybdenum-oxygen coordination.

Absorbance measurements demonstrated that decreasing the carbon precursor significantly narrows the absorption profile by minimizing the absorption tail associated with surface defect states. This spectral narrowing indicates that intrinsic core absorption becomes dominant over surface-driven optical processes. Furthermore, fluorescence measurements supported this structural evolution. While samples synthesized with higher carbon content exhibited excitation-dependent emission driven by surface functional groups, the reduction of citric acid shifted the photoluminescence to an excitation-independent profile. These results establish a clear relationship between precursor stoichiometry, structural defect density, and the fundamental optical mechanisms of heteroatom-doped CQDs.

Keyword: *Carbon quantum dots, Heteroatom doping, Microwave-assisted synthesis*

ID: 65

Dopant-Controlled Reversible Carrier-Polarity Switching in SnSe Thermoelectric Materials

Mehmet Ozdogan * **, Thomas Iken, Carlos Munoz, Deniz Cakir, Nuri Oncel**

University of North Dakota

Tin selenide is a layered semiconductor with strong potential for thermoelectric and functional electronic applications because of its anisotropic crystal structure, low thermal conductivity, and highly tunable carrier transport. In this study, we examine how Bi incorporation modifies the temperature-dependent electronic transport of bulk polycrystalline SnSe and leads to reversible carrier-polarity switching in lightly doped compositions.

Polycrystalline $Sn_{1-x}Bi_xSe$ samples with x = 0, 0.02, and 0.06 were synthesized and investigated using temperature-dependent Seebeck coefficient and electrical conductivity measurements, supported by X-ray diffraction, scanning/transmission electron microscopy, energy-dispersive X-ray spectroscopy, and X-ray photoelectron spectroscopy. Structural and chemical analyses confirm that the orthorhombic SnSe phase is retained after Bi doping and that Bi is incorporated into the SnSe matrix without detectable segregation of metallic Bi. The transport response shows a strong dependence on Bi concentration. Pristine SnSe remains p-type throughout the measured temperature range, while Bi substitution introduces electron-dominated transport. In the 2% Bi-doped sample, the Seebeck coefficient is negative at low temperature, but reversibly changes sign near 550 K, indicating a transition from n-type to p-type behavior. In contrast, the 6% Bi-doped sample remains n-type up to 880 K, demonstrating that higher Bi content suppresses polarity reversal.

The origin of this behavior was analyzed using a self-consistent two-carrier transport model combined with first-principles calculations. The nonlinear Seebeck response in lightly doped SnSe cannot be described by a single-carrier model; instead, it arises from competition between electron and hole contributions whose relative weights evolve with temperature. Density-functional theory calculations show that Bi doping shifts the Fermi level toward the conduction band, while temperature-induced bandgap narrowing and band-edge evolution promote thermally activated holes at elevated temperatures. For low Bi concentration, these holes compensate and eventually dominate the Bi-donated electrons, producing the observed n-to-p transition. At higher Bi concentration, the Fermi level remains deep in the conduction band, resulting in stable degenerate n-type behavior.

These findings clarify how dopant concentration, bipolar transport, and temperature-dependent electronic structure govern carrier-polarity switching in SnSe, providing a framework for tuning transport behavior in thermoelectric semiconductors [1].

Acknowledgment:
The computer resources used in this work are provided by the Computational Research Center at UND. This work used resources of the Center for Computationally Assisted Science and Technology (CCAST) at North Dakota State University, which were made possible in part by NSF MRI Award No. 2019077. The authors acknowledge the University of North Dakota's Nanofoundry for providing access to its cutting-edge research facilities.

ORCID:
Mehmet Ozdogan: 0000-0002-2874-4787

References:
[1]. Physical Review B 113, 205202 (2026).

Keyword: *SnSe, bipolar conductivity, thermoelectric*

Cyano-Modified Ethynyl-Bridged Carbazole Emitters for Efficient Blue Oleds

Esra Yenidoğan [*1], Ozan Tekin[1], Erol Yıldırım[1], Selçuk Gümüş[2], Gönül Hızalan Özsoy[3], Erkan Aksoy[4], Ali Çırpan[1,3,5,6]

[1] *Department of Chemistry, Middle East Technical University (METU), 06800, Ankara,Türkiye*
[2] *Department of Basic Sciences, Faculty of Engineering, Architecture and Design, Bartın University, 74110, Bartın, Türkiye*
[3] *ODTU-GUNAM, Middle East Technical University, 06800, Ankara, Turkiye*
[4] *Bartın University, Rectorate, Project and Technology Office, Bartın, 74100, Türkiye*
[5] *Department of Micro and Nanotechnology, Middle East Technical University (METU), 06800, Ankara,Türkiye*
[6] *Department of Polymer Science and Technology, Middle East Technical University (METU), 06800, Ankara,Türkiye*

Solution-processable blue organic emitters are attractive materials for next-generation organic light-emitting diodes (OLEDs) due to their potential for low-cost, large-area, and flexible device fabrication. In OLEDs, high electroluminescent efficiency strongly depends on the effective utilization of electrically generated excitons, including both singlet and triplet excited states. Therefore, the development of blue emitters with efficient exciton harvesting capability, suitable energy-level alignment, balanced charge recombination, and stable electroluminescent performance remains a key challenge. In this study, a series of donor–acceptor type molecules, emitter materials, were designed by functionalizing the N-position of a carbazole donor with cyano-strengthened ethynyl-bridged acceptor units. 3,6-di-tert-butyl-substituted carbazole was selected as the donor unit owing to its high triplet energy and steric protection, while phenyl-CN-based ethynyl acceptor was introduced to enhance intramolecular charge-transfer character and support efficient blue emission. The molecular design strategy focuses on controlling the donor–acceptor geometry and spatial arrangement to tune both through-bond and through-space charge-transfer processes. The optoelectronic properties of the emitters were evaluated through optical and electrochemical characterizations, including UV–visible absorption, photoluminescence spectroscopy, cyclic voltammetry, and thermogravimetric analysis (TGA).

OLED devices were fabricated with the architecture of ITO/PEDOT: PSS/TCTA:TAPC:Emitter/TmPyPB/LiF/Al, in which PEDOT: PSS was used as the hole-injection layer, TCTA: TAPC served as the mixed-host emissive matrix, TmPyPB acted as the electron transporting layer, and LiF/Al was employed as the cathode. The emissive layer was prepared with a composition of TCTA:TAPC:Emitter = 85:10:5 wt%, where the target emitter was doped into the mixed host system to promote balanced charge recombination and efficient exciton formation. The electroluminescent properties of the fabricated OLEDs were systematically investigated through current density–voltage–luminance and electroluminescence measurements. The optimized OLED device demonstrated a turn-on voltage of 3.7 V, a maximum luminance (L_{max}) of 14.337 cd/m², and also achieved chromaticity coordinates (CIE x,y = 0.18, 0.15). These results highlight the potential of carbazole-based blue emitters in OLED technology, highlighting the importance of precise molecular engineering for enhanced device performance.

Acknowledgment:
"This study was supported by the Scientific and Technological Research Council of Turkey (TUBITAK) under the Grant Number 124F400. The authors thank TUBITAK for their support."

ORCID:
Esra Yenidoğan: 0009-0004-3713-1853
Selçuk Gümüş: 0000-0002-8628-8943
Gönül Hızalan Özsoy: 0000-0002-3308-404X
Erkan Aksoy: 0000-0002-0083-2574
Ali Çırpan: 0000-0003-3051-8380
Ali Çırpan: 0000-0003-3051-8380
Ali Çırpan: 0000-0003-3051-8380
Ali Çırpan: 0000-0003-3051-8380

Keyword: *OLED, Host–Dopant System, Solution-Processable*

Potassium-Ion Redistribution and Resistive Switching in Ultrathin KxWO3 Single-Crystal Nanobelts

Abdulsalam Aji Suleiman *

Sivas University of Science and Technology

Potassium tungsten bronze, KxWO3, is a non-stoichiometric tunnel oxide in which K+ ions occupy one-dimensional channels within a corner-sharing WO6 framework. This makes it a useful material system for studying the coupling between alkali-ion redistribution, local phase evolution, and electronic transport. Here, we report the confined solid–liquid–solid growth of ultrathin KxWO3 single-crystal nanobelts on c-cut sapphire, with thicknesses down to ~36 nm and lateral dimensions above 100 µm. The crystals exhibit sharply defined bright and dark optical domains. Spatially resolved Raman spectroscopy reveals distinct phonon fingerprints across these regions, while electron diffraction supports their assignment to potassium-dependent tungsten bronze configurations, primarily hexagonal and, to a lesser extent, more potassium-rich tetragonal phases. Two-terminal devices fabricated from individual nanobelts show reproducible bipolar resistive switching with resistance ratios of up to ~30 and gradual conductance modulation under pulsed bias. Electrical cycling also drives optical-domain homogenization, consistent with field-assisted K+ redistribution within the tunnel framework. These results indicate that ultrathin KxWO3 is a suitable platform for examining ion-mediated, phase-coupled resistive switching in open-framework transition-metal oxides.

ORCID:
Abdulsalam Aji Suleiman: 0000-0002-7087-2715

References:
https://www.sciencedirect.com/science/article/pii/S258884202500166X
https://link.springer.com/article/10.1007/s11433-023-2224-8

Keyword: *KxWO3, potassium tungsten bronze, resistive switching*

ID: 160

A Novel Benzodithiophene-Based Donor Polymer for Semitransparent Ternary Organic Solar Cells

Duygu Yalvaç [*1], Meltem Türkatar[2], Gönül Hızalan Özsoy[3], Ali Çırpan[1,2,3,4]

[1] Department of Chemistry, Middle East Technical University (METU), 06800, Ankara,Turkiye
[2] Department of Polymer Science and Technology, Middle East Technical University, Ankara, 06800, Turkiye
[3] ODTU GUNAM, Middle East Technical University, 06800, Ankara, Turkiye
[4] Department of Micro and Nanotechnology, Middle East Technical University, Ankara,06800, Turkiye

Organic solar cells (OSCs) have emerged as a promising technology for next-generation photovoltaics due to their mechanical flexibility, light weight, and chemical tunability. In particular, semitransparent organic solar cells (ST-OSCs) hold great potential for Building-Integrated Photovoltaics (BIPV) and AgriPV applications, as they can efficiently harvest solar energy while maintaining adequate visible transmittance[1]. However, achieving an optimum balance between power conversion efficiency (PCE) and average visible transmittance (AVT) remains a significant challenge in binary blend configurations. In this study, we demonstrate a highly effective ternary strategy to enhance photovoltaic performance while preserving transparency by integrating a novel donor polymer, P6, blended with Y6 and L8-BO non-fullerene acceptors. The novel P6 polymer donor incorporates benzodithiophene (BDT) and quinoxaline units with a thiophene π-bridge. The P6:Y6:L8-BO (1:1:0.2) ternary blend demonstrated enhanced photovoltaic performance in both opaque and semitransparent device configurations. The opaque ternary device achieved a high power conversion efficiency (PCE) of 10.14%, with an open-circuit voltage of 0.82 V, a short-circuit current density of 20.72 $mA.cm^{-2}$, and a fill factor (FF) of 59.91%. When integrated into a semitransparent architecture, the ternary device retained a PCE of 6.91% while delivering an average visible transmittance (AVT) of 12.70%. The results suggests that the incorporation of L8-BO enhances charge transport and extraction within the active layer without compromising optical transparency. The reason is the complementary absorption of Y6 and L8-BO which enhances infrared light harvesting while maintaining transparency[2].

This study was supported by the Scientific and Technological Research Council of TURKEY (TUBITAK) under the Grant Number 222Z151. The authors thank to TÜBİTAK for their supports.

Acknowledgment:
This study was supported by the Scientific and Technological Research Council of TURKEY (TUBITAK) under the Grant Number 222Z151. The authors thank to TÜBİTAK for their supports.

ORCID:
Duygu Yalvaç: 0009-0006-5416-6702
Gönül Hızalan Özsoy: 0000-0002-3308-404X
Ali Çırpan: 0000-0003-3051-8380
Ali Çırpan: 0000-0003-3051-8380
Ali Çırpan: 0000-0003-3051-8380
Ali Çırpan: 0000-0003-3051-8380

References:
[1] Hu, Z., Wang, J., Ma, X., Gao, J., Xu, C., Yang, K., ... & Zhang, F. (2020). A critical review on semitransparent organic solar cells. Nano Energy, 78, 105376.
[2] An, K., Zhong, W., Peng, F., Deng, W., Shang, Y., Quan, H., ... & Ying, L. (2023). Mastering morphology of non-fullerene acceptors towards long-term stable organic solar cells. Nature communications, 14(1), 2688.

Keyword: *Ternary organic solar cells, Organic photovoltaics*

ID: 186

Enhancing the Tribological Performance of Al2O3 Ceramics via MOF-derived Nanocarbon Particle Additives

Umut Savacı *

Eskisehir Technical University, Faculty of Engineering, Department of Materials Science and Engineering, Eskişehir, Türkiye

Metal-organic frameworks (MOFs) can be used as customizable precursors to generate multifunctional nanocarbon phases upon thermal decomposition, offering a potential strategy for modifying the properties and performance of ceramic matrices [1-5]. This approach aligns with the critical industrial priority of understanding and mitigating friction and wear in alumina (Al_2O_3) components to extend equipment lifespan and reduce maintenance costs in severe environments like cutting tools, aerospace, and automotive systems. To explore this pathway, the present study primarily investigates the influence of in-situ synthesized nanocarbon particles derived from a Zeolitic Imidazolate Framework-8 (ZIF-8) MOF during sintering on the tribological properties and microstructure of Al_2O_3 ceramics via pre- and post-tribological characterization to elucidate the underlying wear mechanisms. The composite samples with varying ZIF-8 contents were fabricated using spark plasma sintering (SPS) at 1500°C, during which the ZIF-8 precursor was successfully converted into carbon structures, as verified by Raman spectroscopy and XRD analyses. Tribological testing was conducted under dry sliding conditions using 3 mm Si_3N_4 ceramic and 100Cr6 steel balls in a ball-on-disc configuration. The integration of the in-situ formed nanocarbon enhanced both friction and wear properties depending on the MOF content. For the Si_3N_4 counterbody, the coefficient of friction (COF) decreased by ~10% (from 0.639 to 0.575), while an ~11% reduction (from 0.445 to 0.395) was achieved against the 100Cr6 steel ball. Remarkably, the calculated wear rate dropped by ~84%, falling from 1.33×10^{-4} mm^3/Nm to 0.21×10^{-4} mm^3/Nm. Pre- and post-tribological microstructural analyses, carried out via Scanning Electron Microscopy (SEM), revealed distinct interfacial behaviors depending on the counterbody material: three-body wear and a protective carbon tribofilm dominated the Si_3N_4 interface, whereas adhesive wear and a stable transfer film formed against the 100Cr6 steel ball to lower interfacial shear stress. Beyond wear performance, the carbon structures successfully improved the electrical conductivity and fracture toughness of the Al_2O_3 matrix. This study demonstrates the potential of MOF-derived in-situ carbon nanoparticles to comprehensively optimize the wear behavior of ceramic matrices.

ORCID:
Umut Savacı: 0000-0002-5801-9666

References:
K.G. Bayrak, E.İ. Düden, N. Cakan, et al., Enhancing Al2O3 composites: In situ synthesis and nanostructure transformation of ZIFs for mechanical and conductivity control, J Mater Res, 40 (2025) 2153-2168.
N. Cakan, A.A. Issa, H. Alsalman, et al., Enhancing the Properties of Yttria-Stabilized Zirconia Composites with Zeolitic Imidazolate Framework-Derived Nanocarbons, ACS applied materials & interfaces, 15 (2023) 58931-58939.
L. Koroglu, N. Cakan, L. Civan, et al., Bringing electrical conductivity to SiAlON ceramics by integrating zeolitic imidazolate framework-derived nanocarbons, Journal of the American Ceramic Society, 108 (2025).
L. Liu, H. Yu, J. Wang, et al., In situ carbon nanonetwork structure based on MOF-derived carbon to manufacture ceramic composites: A case study of zirconia-toughened alumina, Ceramics International, 50 (2024) 42135-42145.
U. Savacı, The effect of ZIF-8 derived nanocarbons on the mechanical and electrical properties of spark plasma sintered AlN ceramics, Ceramics International, 52 (2026) 28028-28036.

Keyword: *Al2O3 Ceramic Composite, Nanocarbon, Tribology & Microstructure Characterization*

Time-Domain Mechanical Computing with Nanoelectromechanical Resonators

Filipe Alves [*] [1], **Humayun Ahmed**[1], **Inês Garcia**[1], **Alper Demir**[2], **Selim Hanay**[1,3]

[1] *INL - International Iberian Nanotechnology Laboratory*
[2] *Koç University*
[3] *Bilkent University*

Inference on temporal signals, sequences whose interpretation depends on the history of preceding samples, requires a system that simultaneously retains memory of past inputs and applies a nonlinear transformation to them. In digital hardware these two operations are realised by recurrent or state-space architectures that store and update an explicit state at every time step, so that memory access and arithmetic persist at the sampling rate and dominate the energy budget of always-on edge devices. We instead exploit the intrinsic dynamics of a single nanoelectromechanical (NEMS) resonator to perform both operations physically, in the analogue time domain. The resonator is driven into its nonlinear (Duffing) regime, where its instantaneous displacement is a history-dependent functional of the recent input. Two physical properties supply the ingredients for temporal computation: the high quality factor sets a long ringdown time, giving an intrinsic fading memory of past excitation, while the geometric nonlinearity provides the high-dimensional, nonlinear projection that separates temporal patterns. Computation is thus a direct consequence of the equation of motion rather than an algorithm executed on the device. The resonator's transient response is read out as the computational state, and only a lightweight linear layer is trained at the output. Building on our earlier NEMS reservoir demonstration, we report time-domain processing on a single mid-Q device and characterise how the ringdown time and operating point set the accessible memory depth and nonlinearity, and how these govern performance on representative sequence tasks. indicating a route to fast, low-dissipation temporal inference under ambient conditions.

ORCID:
Filipe Alves: 0000-0002-3439-8235

References:
Kartal, E., Selcuk, Y., Ahmed, H., Kaynak, B.E., Yildiz, M.T., Erdogan, R.T., Yanik, C. and Hanay, M.S. (2025), Nanomechanical Systems for Reservoir Computing Applications. Adv. Intell. Syst., 7: 2400971.

Keyword: *nanoelectromechanical systems (NEMS), physical reservoir computing; time-domain computation; nonlinear dynamics; fading memory; energy-efficient edge inference*

Thermal Spreading Resistance Measurements in Microcontacts Formed by Indentation

Seda N. Sönmez [*1], **Ahmed Uluca**[2], **Graham L. W. Cross**[2], **H. Özgür Özer**[1]

[1] *Istanbul Technical University, Department of Physics Engineering, 34469 Maslak, Istanbul, Türkiye*
[2] *School of Physics, Trinity College Dublin, Dublin 2, Ireland*

Thermal Interface Materials (TIMs) have gained significant attention in recent decades due to the growing demand for efficient heat dissipation in miniaturized electronic devices. Conventional TIMs may have limitations in cooling microelectronics, especially under high-power operating conditions. Therefore, technological and scientific efforts have focused on developing new materials for the interface between heat-generating components and heat sinks. Owing to its extremely high thermal conductivity, diamond is considered a promising candidate for TIMs. Hence, diamond microparticles have been implemented as TIMs in various applications.

Inspired by these applications, we aimed to investigate the thermal spreading resistance of a single diamond microcontact. For this purpose, we built an indenter to enable the controlled penetration of the indenter tip into the sample while simultaneously measuring the temperature and load. A transient experimental procedure is applied to Cu, Au, and Al samples using standard indenter tips, such as cube-corner and conical shapes. During the experiments, the tip motion is defined by a square wave profile, corresponding to sudden contact during indentation and noncontact during retraction. To increase the signal-to-noise, the tip is oscillated 90 times over 4 seconds, and the resulting responses are averaged. The recorded tip temperature response showed an exponential rise and decay as the colder tip is brought into and out of contact with the hotter sample. This, in turn, allowed us to calculate thermal spreading resistance.

We investigated the thermal spreading resistance at different indentation depths and loads. The results showed that thermal spreading resistance decreased with increasing penetration depth and then approached a saturation regime at larger depths. This trend is mainly attributed to the square-root dependence of spreading resistance on contact area. A similar behavior is also observed in our finite element analysis in ABAQUS.

The dependence on load is particularly important for TIM applications, since low thermal resistance should be achieved without applying excessive force that may damage delicate microelectronic components. Therefore, the results of our study are expected to shed light on the efficient use of diamond particles as TIMs.

ORCID:
Seda N. Sönmez: 0009-0002-7019-0009

Keyword: *Thermal spreading resistance, diamond microparticles, indentation*

A Knowledge-Guided, Drift-Aware Computer Vision Pipeline for Automated Pixel-Level Nanotribological Characterization in Atomic Force Microscopy

Tuana Karakoyun Barandır [*1], **Derya Gemici Deveci**[2], **Özhan Ünverdi**[3], **Cem Çelebi**[1]

[1] *İzmir Institute of Technology, Faculty of Science, Department of Physics, Urla, 35430, İzmir, Turkey*
[2] *Institute of Graduate Studies, Department of Electrical and Computer Engineering, Altınbaş University, Istanbul, 34217, Turkey*
[3] *Yaşar University, Department of Electrical and Electronics Engineering, Bornova, 35100, İzmir, Turkey*

Atomic Force Microscopy (AFM) is a powerful tool for investigating nanoscale friction behavior; however, conventional analysis workflows remain largely manual, operator-dependent, and sensitive to measurement drift. These limitations restrict reproducibility, automation capability, and the reliable extraction of quantitative tribological data. To address this limitation, we developed a modular, knowledge-guided and drift-aware Computer Vision (CV) pipeline that treats drift as an inherent physical component of sequential AFM measurements to be tracked and accounted for. The pipeline converts raw AFM measurements into structured, machine-readable tribological outputs with minimal user intervention. Stage 1 performs preprocessing, morphological segmentation, and drift-aware SIFT–ORB–RANSAC alignment. Stage 2 applies chained point tracking to preserve surface-point identity across 0–10 nN load steps, enabling pixel-level friction force computation at spatially consistent coordinates while explicitly accounting for drift.

The proposed framework was validated on twisted bilayer graphene samples grown by Chemical Vapor Deposition (CVD) at five interlayer rotation angles ranging from 0° to 10.2°. The extracted friction coefficients showed an overall increasing trend with twist angle, consistent with the breakdown of structural superlubricity driven by atomic registry mismatch. The analysis also revealed spatially non-uniform drift, with only 18 persistent surface points remaining traceable across the full load sequence within a common observation window covering approximately 68.7% of the scan area. This highlights the need for point-identity preservation in reliable nanoscale tribological analysis [1].

By overcoming the user-dependent limitations of conventional SPM analysis workflows, the proposed pipeline provides a more objective, reproducible, and drift-aware framework for nanoscale tribological evaluation. It converts AFM datasets into structured, machine-readable outputs while preserving point identity across sequential measurements, establishing a methodological basis for next-generation automated surface characterization.

ORCID:
Tuana Karakoyun Barandır: 0009-0003-2137-7341
Derya Gemici Deveci: 0000-0003-3998-1910
Özhan Ünverdi: 0000-0001-9994-3487
Cem Çelebi: 0000-0003-1070-1129

References:
Karakoyun Barandır, T., Gemici Deveci, D., Ünverdi, Ö., Çelebi, C. (2026). A knowledge-guided, drift-aware computer vision pipeline for automated nanoscale atomic force microscope surface characterization. Ultramicroscopy, 114401. https://doi.org/10.1016/j.ultramic.2026.114401

Keyword: *Atomic Force Microscopy (AFM), Drift-aware analysis, Computer vision (CV)*

Spatio-temporal Feedback in Active Matter: A Dynamic Activity Field Model for Brownian Swimmers

Livio Carenza * [1], **Brandon James Fasy**[1], **Marcos Gouveia**[2], **Giuseppe Negro**[3]

[1] *Koç University*
[2] *Universidade de Coimbra*
[3] *University of Edinburgh*

The standard framework for Active Brownian Particles (ABP) has been instrumental in characterizing the non-equilibrium behavior of self-propelled matter, typically modeling swimmers with a constant propulsion speed along a diffusing stochastic orientation. However, real-world active systems—ranging from chemotactic bacteria to synthetic phoretic Janus particles—often inhabit complex environments where the ”fuel” or signal driving their activity is a local, finite resource.

In this work, we extend the classical ABP framework by introducing a novel model where the particle’s activity is no longer a fixed parameter but a dynamic scalar field coupled to the swimmers’ motion. In our model, the activity field evolves according to a tailored advection-diffusion-reaction equation. This field is advected by the swimmers, diffused by the solvent, and consumed at the particle’s position. This coupling creates a feedback loop: the local value of the field determines the particle’s propulsion force, while the particle’s displacement and consumption simultaneously reshape the field’s dynamics. This bidirectional coupling leads to the emergence of self-generated activity gradients and effective long-range interactions between particles.

We provide an analytical treatment of the stationary activity field for an isolated swimmer. By transforming the governing equations into the particle’s co-moving reference frame, we demonstrate that the swimmer acts as a moving multipole source. We derive the exact analytical solution for the resulting ”activity tail” using a Green’s function approach for the advected diffusion operator. Our analysis reveals that the particle acts as a monopole sink and a dipolar advective source. This analytical solution characterizes the depletion zone trailing the swimmer and the accumulation zone at its front, providing a theoretical foundation for understanding ”self-phoretic” effects. Finally, we validate our theoretical findings and explore many-body effects through large-scale molecular dynamics simulations. We have developed a custom integration protocol within the LAMMPS framework to handle the concurrent evolution of the continuum activity field and the discrete particle trajectories. This computational protocol allows us to investigate collective phenomena, such as activity-induced clustering and phase separation, in systems where the ”fuel” is a dynamic participant. Our results suggest that the inclusion of dynamic activity fundamentally alters the stability of active fluids, offering new insights into the design of responsive synthetic microswimmers and

the survival strategies of biological microorganisms.

ORCID:
Livio Carenza: 0000-0001-5996-331X

Keyword: *Active Matter, Active Brownian Particles, Micro phase separation*

Compact FPGA-Based Voice Classification Using Physical Reservoir Computing and Posit-Based MAC Operations

Ahmet Karacali [*1], **Xu Muzhen**[1,2], **Yuki Usami**[1,2], **Hirofumi Tanaka**[1,2]

[1] *Kyushu Institute of Technology , Japan*
[2] *Research Center for Neuromorphic AI Hardware*

The rapid growth of machine learning has increased the demand for energy-efficient hardware, while further performance improvements are limited by transistor scaling and power consumption. Reservoir computing provides an attractive solution by restricting training to a simple readout layer, thereby reducing computational cost and hardware complexity.

This work proposes a low-power digital platform that combines a nanomaterial-based physical reservoir computing device with posit-based digital classification. The physical reservoir is realized using Yttrium Manganese Oxide ($YMnO_3$), a ferroelectric material whose semiconductive domains and domain walls generate rich nonlinear dynamics. This device has previously demonstrated speech classification capability [1], and the present work extends its implementation toward a unified FPGA-based platform for real-time processing.

Reflected and down-sampled raw audio signals are input to the PRC device to produce 31 nonlinear outputs. These outputs are trained using linear regression to determine the weight values. The PRC outputs and weights are then converted into 16-bit posit format, and classification is performed through MAC operations. The results demonstrate that the posit-based system successfully executes the classification process without bit-level data loss. Future work will focus on implementing the complete posit classification system on FPGA for real-time operation.

ORCID:
Ahmet Karacali: 0009-0000-4695-2814
Xu Muzhen: 0009-0006-9829-1601
Yuki Usami: 0000-0002-8583-325X
Hirofumi Tanaka: 0000-0002-4378-5747

References:
[1]Xu, Muzhen, H. Tanaka et al. Small 21, e06397 (2025).

Keyword: *Material AI, Physical Reservoir Computing, Low-power consuming AI*

From Flat Bands to Dirac Cones: Symmetry-Tunable Electronic States in Bilayer Kagome Lattices

Taylan Görkan[1], Doğukan Hazar Özbey[1], Cem Sevik[2], Milorad V. Milosevic[2], Engin Durgun [* 1]

[1] UNAM-National Nanotechnology Research Center and Institute of Materials Science and Nanotechnology, Bilkent University, 06800 Ankara, Turkey

[2] COMMIT, Department of Physics and NANOlight Center of Excellence, University of Antwerp, Groenenborgerlaan 171, B-2020 Antwerp, Belgium

Flat bands (FBs) and Dirac cones represent two distinctive features of topological electronic systems [1]; however, a unified mechanism enabling transitions between them has remained elusive to date. Here, we demonstrate a symmetry-governed and tunable transition from flat bands to Dirac cones in AB-stacked bilayer kagome lattices. This transition is mediated by the interplay among destructive quantum interference (DQI), C_3 rotational symmetry, and spatial inversion symmetry. Strong interlayer coupling enhances DQI and stabilizes compact localized states that produce FBs, while weaker coupling allows C_3 and inversion symmetries to dominate, giving rise to robust Dirac nodal points. Using a minimal tight-binding model, we map the continuous evolution of topological states, including type-II and type-III Dirac cones, spin-1 Dirac nodes, and partial flat bands, as a function of interlayer coupling. We further demonstrate this transition mechanism by examining an AB-stacked bilayer derived from the experimentally synthesized Nb_3TeCl_7 structure. In particular, first-principles calculations on bilayer Nb_3TeCl_7 reveal that vertical strain (or pressure) modulates the interlayer interactions, enabling the full FB-Dirac cone transition sequence. These findings [3] establish a realistic pathway for gaining deeper insight into flat-band physics and for engineering tunable topological phases in two-dimensional materials.

Acknowledgment:
This work was supported by TUBITAK under Project No. 123F153 and the Research Foundation-Flanders (FWO-Vl).

ORCID:
Engin Durgun: 0000-0002-0639-5862

References:
F. He, Y. Zhou, Z. Ye, S.-H. Cho, J. Jeong, X. Meng, and Y. Wang, ACS Nano 15, (2021), 5944.
J.-X. Yin, B. Lian, and M. Z. Hasan, Nature (London) 612, (2022) 647.
T. Gorkan, D. H. Ozbey, C. Sevik, M. V. Milosevic, E. Durgun, Phys. Rev. B, 113, (2026), 125405.

Keyword: *Kagome Lattice, 2D Materials, Topological electronic states*

Characterization of Topological Defects in Confined Nematic Liquid Crystals

Taha Andaç [*1], Aslı Karausta[2], Emre Büküşoğlu[2,3], Livio Nicola Carenza[1]

[1] *Department of Physics, Koç University, Istanbul, Türkiye*
[2] *Department of Chemical Engineering, Middle East Technical University, Ankara, Türkiye*
[3] *Department of Micro and Nanotechnology, Middle East Technical University, Ankara, Türkiye*

Liquid crystals (LCs) are liquid-like materials that exhibit long-range orientational order while maintaining molecular mobility. However, this molecular orientational order can locally break down, leading to the formation of topological defects with nanoscopic cores [1]. In nematic LCs, these defects arise from geometric constraints and interactions with confining surfaces through surface anchoring, and may appear as point defects, disclination lines, or disclination loops.

In this work, LCs were confined within rectangular microwells with one open boundary to investigate orientational ordering and defect formation. Polarized optical microscopy (POM) images obtained from the experiments served as twodimensional references for the LC alignment and defect textures. Further investigation was performed numerically to obtain the three-dimensional orientational field and identify the defect configurations.

In the numerical simulations, the three-dimensional LC configurations were obtained by integrating Beris-Edwards equations [2]. Homeotropic and tangential anchoring conditions were imposed at the open boundary of the microwells, while the remaining surfaces were treated with ”mixed anchoring” condition. Our results show that homeotropic conditions primarily favor disclination line defects along the confining surfaces, while tangential conditions also give rise to point-like surface defects such as boojums.

Finally, simulated POM textures were generated from the numerical configurations, allowing systematic comparison with the experimental observations. Our findings highlight that confined nematic systems provide a model platform for studying how molecular orientational order, surface anchoring, and geometry collectively control topological defect formation. Future studies can extend this approach to different microwell geometries, such as triangular, circular, and square confinements, to investigate geometry-driven defect stabilization and the emergence of new defect configurations.

ORCID:
Taha Andaç: https://orcid.org/0009-0004-0270-2513

References:
Xiaoguang Wang, Young-Ki Kim, Emre Bukusoglu, Bo Zhang, Daniel S. Miller, and Nicholas L. Abbott. Experimental insights into the nanostructure of the cores of topological defects in liquid crystals. Physical Review Letters, 116:147801, 2016.
A. N. Beris. Thermodynamics of Flowing Systems: With Internal Microstructure. Oxford University Press, Oxford, 1 edition, 1994.

Keyword: *Nematic liquid crystal, Rectangular Microwell, Topological Defect*

Dynamic High-Q Membrane Metasurfaces for Infrared Spectroscopy, Sensing, and Light–Matter Interactions

Furkan Kuruoğlu [*1], Samir Rosas[2], Yihong Chen[3], Brijesh Kumar[4], Shenwei Yin[3], Jin-Woo Cho[3], David A. Czaplewski[5], Yuri Kivshar[4], Mikhail A. Kats[3], Filiz Yesilkoy[2]

[1] Department of Physics, Faculty of Science, Istanbul University, Vezneciler, 34134, Istanbul, Turkey, Department of Biomedical Engineering, University of Wisconsin-Madison, Madison, Wisconsin 53706, USA

[2] Department of Biomedical Engineering, University of Wisconsin-Madison, Madison, Wisconsin 53706, USA

[3] Department of Electrical and Computer Engineering, University of Wisconsin-Madison, Madison, Wisconsin 53706, USA

[4] Nonlinear Physics Center, Research School of Physics, Australian National University, Canberra ACT 2601, Australia

[5] Center for Nanoscale Materials, Argonne National Laboratory, Lemont, Illinois 60439, USA

Mid-infrared spectroscopy enables biochemical sensing by identifying vibrational molecular fingerprints, but it faces limitations in instrumentation portability and analytical sensitivity. Optical metasurfaces with strong mid-infrared photonic resonances provide an attractive solution towards on-chip spectrometry and sensitive molecular detection [1,2], yet their static nature hinders their anticipated impact.

Here, we introduce and demonstrate dynamically tunable silicon membrane metasurfaces exhibiting high-Q transmissive resonances in the fingerprint region. By harnessing silicon's thermo-optical properties, we achieve continuous modulation of coupling induced transparency (CIT) modes that emerge upon the interference of quasi-bound states in the continuum (q-BICs) and surface lattice modes [2,3]. We measure a spectral tuning rate of 0.06 cm^{-1} K^{-1} by continuously sweeping the sharp CIT resonances (with a maximum measured Q-factor of 230 at 1240 cm^{-1}) over a 23.5 cm^{-1} spectral range across a temperature range of 300 - 700 K. In the current proof-of-concept implementation, the dynamic transmission control enables non-contact chemical analysis of polymer films by detecting characteristic absorption bands of polystyrene (1450 and 1492 cm^{-1}) and poly(methyl methacrylate) (1730 cm^{-1}) without requiring conventional spectrometers. When analyte molecules fill the metasurface-generated photonic cavities, we demonstrate vibrational strong coupling between the poly(methyl methacrylate)’s carbonyl band and the CIT mode, manifested in a Rabi splitting of ~43 cm^{-1}.

Our results establish a new photonic platform that unites spectral precision, strong field enhancement, and reconfigurability, offering diverse potential for compact mid-infrared spectroscopy, molecular sensing, and programmable polaritonic photonics.

References:

Rosas, S., Biswas, S. K., Adi, W., Kuruoglu, F., Beisenova, A., Patankar, M. S., & Yesilkoy, F. (2025). Mass-Manufactured Gradient Plasmonic Metasurfaces for Enhanced Mid-IR Spectrochemical Analysis of Complex Biofluids. Advanced Materials, 37(47), e04355.

Rosas, S., Adi, W., Beisenova, A., Biswas, S. K., Kuruoglu, F., Mei, H., ... & Yesilkoy, F. (2025). Enhanced biochemical sensing with high-Q transmission resonances in free-standing membrane metasurfaces. Optica, 12(2), 178-189.

Kuruoglu, F., Rosas, S., Chen, Y., Kumar, B., Yin, S., Cho, J.-W., Czaplewski, D. A., Kivshar, Y., Kats, M. A., & Yesilkoy, F. (in press). Dynamically tunable membrane metasurfaces for infrared spectroscopy and strong light–matter interactions. Light: Science & Applications.

Keyword: *mid-infrared photonics, coupling induced transparency (CIT), thermally reconfigurable metasurface*

Agronomic Potential of Green-Synthesized Cellulose Nanocomposites and Metal/Metal Oxide Nanoparticles: Implications for Crop Growth and Development

Lale Aktaş * **, Khairul Maghfirah Hasanah, Tugba Oztekin, Yigit Kucukcobanoglu**

Ege University

Growing global food security concerns have accelerated the need for sustainable and multifunctional agricultural inputs capable of addressing both biotic and abiotic stresses. Green nanotechnology has emerged as a promising strategy, offering environmentally compatible nanomaterials with diverse agricultural functionalities. This study presents findings from complementary research efforts investigating the agricultural potential of green-synthesized cellulose–sodium alginate/silver nanocomposites (CNC-SA/AgNPs), biosynthesized silver nanoparticles (AgNPs), and copper oxide nanoparticles (CuO NPs), each targeting distinct but interrelated applications in crop management. All nanomaterials were produced through green synthesis routes using Laurus nobilis leaf extract and thoroughly characterized using SEM, TEM, FTIR, XRD, EDS, UV-Vis spectroscopy, particle size analysis, and zeta potential measurements. Biological evaluations included seed priming experiments with pepper (Capsicum annuum) under drought stress conditions, as well as in vitro and in vivo antimicrobial assays against economically important phytopathogens including Pectobacterium carotovorum and Verticillium dahliae. Characterization confirmed predominantly spherical nanoparticles with mean diameters of 21 nm, 24 nm, and 78–95 nm for CNC-SA/AgNPs, AgNPs, and CuO NPs, respectively. Zeta potential values between −24.2 and −27.7 mV indicated good colloidal stability across all formulations. Seed priming with CNC-SA/AgNPs at 25–100 mg L^{-1} significantly enhanced drought tolerance in pepper, as evidenced by improved photosynthetic efficiency, elevated antioxidant enzyme activities (SOD, CAT, and POX), and reduced oxidative stress markers, with root length and plant dry mass increasing by up to 38% over untreated controls ($p < 0.05$). Biosynthesized AgNPs demonstrated potent antibacterial activity against P. carotovorum (MIC = 0.0625 mg mL^{-1}) and strongly suppressed V. dahliae mycelial growth to 2.75 cm compared with 4.8–6.4 cm in controls after 14 days, with SEM analysis revealing severe hyphal deformation and spore collapse. CuO NPs exhibited broad-spectrum antibacterial and anti-yeast efficacy at 250 µg mL^{-1}. These findings present the multifunctional promise of green-synthesized nanomaterials for modern agriculture, noticing abiotic stress mitigation, phytopathogen suppression, and broad-spectrum antimicrobial protection. The results support the development of sustainable nanotechnology-based tools for precision crop management.

Acknowledgment:
The authors thank The Scientific and Technological Research Council of Turkey (TUBITAK) (Project number: 125Z250).

ORCID:
Lale Aktaş: 0000-0003-0815-8470

References:
Haseki, S., Kucukcobanoglu, Y., Ayisigi, M., Oztekin, T., & Aktas, L. Y. (2025). Influence of synthesis method on physiochemical properties and antibacterial activity of green synthesized CuO nanoparticles from Laurus nobilis L. leaf extracts. Plant Nano Biology, 11, 100128.
Cokislerel, A., Ayisigi, M., Kucukcobanoglu, Y., Gunturkun, P., & Aktas, L. Y. (2025). Antifungal effect against wilting disease factor Verticillium dahliae Kleb. by green synthesized silver nanoparticles. Exploration of BioMat-X, 2, 101329.
Ayisigi, M., Cokislerel, A., Kucukcobanoglu, Y., Yalcin, T., & Aktas, L. Y. (2020). Green synthesized silver nanoparticles for an effective control on soft rot disease pathogen Pectobacterium carotovorum and growth stimulation in pepper. Bulgarian Journal of Agricultural Science, 26(3).

Keyword: *Nanomaterial, Nano-agriculture, Cellulose, Silver Nanoparticle., CuO nanoparticle*

Nano lanthanum oxide enhances soybean yield and seed quality through earthworm driven rhizosphere engineering

Muhmmad Adeel [*] [1,2]

[1] *Beijing Normal University at Zhuhai, Zhuhai, Guangdong 519087, P. R. China*
[2] *Department of Environmental Engineering, Izmir Institute of Technology, Izmir, Turkey*

Engineered nanomaterials offer strategies to enhance crop production and nutrient use, yet the soil-fauna-driven mechanisms that shape their plant and environmental effects are still largely unresolved. To address this, we coupled earthworms (E) with nano lanthanum oxide (n- La_2O_3) in soybean, allowing us to dissect how earthworms steer the pathway from lanthanum exposure to yield gains and seed quality. Our results show that earthworms can accommodate n-La_2O_3 at the tested agronomic dose and incorporate it into casting and rhizosphere processes in a way that supports symbiotic N supply and maintains soybean yield and seed quality, rather than showing obvious toxicity or the stronger stress-associated responses seen for bulk La.

Relative to the earthworm control, n-La_2O_3+E improved reproductive yield components by 25-40% and nodulation traits by 80-160%, accompanied by a 55-70% increase in shoot and root N uptake, consistent with stronger N acquisition under this treatment. Consistently, activities of key N assimilation enzymes in shoots and roots increased by about 10 to 50%, accompanied by a 9% rise in seed protein. In earthworm-active soils, the n-La_2O_3 + E interaction was associated with greater La transfer to plant tissues, stronger symbiotic N fixation, and higher plant N pools and seed accumulation, rather than retention in residual soil pools, pointing to a potential route for more sustainable nutrient use. Seed metabolomic profile was enriched in ureide-TCA intermediates, polyamines and phenolic antioxidants, consistent with strengthened N allocation and La-related metabolic responses. Altogether, our study provides insights into the mechanistic basis of nanotechnology-enabled enhancement of soybean nutrient utilization in the presence of earthworm. Our findings underscore the nanomaterial's potential, offering a viable strategy for balancing food production and quality needs with ecological preservation.

ORCID:
Muhmmad Adeel: 0000-0002-2462-8260

References:

Wang, C.; Cheng, B.; Xiao, Z.; Ji, Y.; Zhang, J.; Zhou, R.; Yuan, X.-Z.; Kah, M.; Wang, Z.; Xing, B., Nanotechnology-driven coordination of shoot–root systems enhances rice nitrogen use efficiency. Proceedings of the National Academy of Sciences 2025, 122, (39), e2508456122.
Cao, X.; Chen, X.; Liu, Y.; Wang, C.; Yue, L.; Elmer, W. H.; White, J. C.; Wang, Z.; Xing, B., Lanthanum silicate nanomaterials enhance sheath blight resistance in rice: mechanisms of action and soil health evaluation. ACS nano 2023, 17, (16), 15821-15835.
Xiao, Z.; Fan, N.; Wang, X.; Ji, H.; Yue, L.; He, F.; Wang, Z., Earthworms drive the effect of La2O3 nanoparticles on radish taproot metabolite profiles and rhizosphere microbial communities. Environmental science & technology 2022, 56, (23), 17385-17395.
Adeel, M.; Shakoor, N.; Hussain, T.; Azeem, I.; Zhou, P.; Zhang, P.; Hao, Y.; Rinklebe, J.; Rui, Y., Bio-interaction of nano and bulk lanthanum and ytterbium oxides in soil system: Biochemical, genetic, and histopathological effects on Eisenia fetida. Journal of hazardous materials 2021, 415, 125574.
Adeel, M., et al., Bioavailability and toxicity of nanoscale/bulk rare earth oxides in soil: physiological and ultrastructural alterations in Eisenia fetida. Environmental Science: Nano, 2021. 8(6): p. 1654-1666.

Keyword: *Soybean yield, Earthworms, Rhizosphere*

ID: 390

From Bio-Based Lignin to Smart Iron Delivery: Modified Lignin Nanoformulations for Foliar Biofortification of Soybean

Burak Özdemir [*1], Zehra Sena Behram[2,3], Umit Baris Kutman[2], Hayriye Ünal[1], Serap Hayat Soytaş[1]

[1] *SUNUM Nanotechnology Research Center, Sabanci University, Tuzla, Istanbul, Turkiye*
[2] *Institute of Biotechnology, Gebze Technical University, Gebze, Kocaeli, Turkiy*
[3] *Department of Interdisciplinary Biotechnology, Graduate School, Gebze Technical University, Gebze, Kocaeli*

Iron deficiency chlorosis is a persistent limitation in crop production, particularly in alkaline soils where iron becomes poorly available to plants. Foliar fertilization offers a rapid strategy to overcome this problem; however, conventional iron formulations may suffer from limited leaf retention, weak surface interaction and inefficient uptake. In this study, lignin was chemically modified to develop a bio-based carrier system for iron delivery through foliar application. The modified lignin matrix was designed to improve surface functionality, hydrophilicity and interaction with leaf surfaces, while supporting iron complexation and controlled nutrient delivery. The synthesized lignin-based materials were characterized to confirm successful chemical modification and iron binding. Surface-sensitive analyses indicated that modification altered the chemical environment of lignin and introduced functional groups that enhanced its interaction potential. Iron complexation studies demonstrated that both native and modified lignin matrices were capable of efficiently binding iron, with modified lignin showing improved performance. Wettability experiments using a soybean leaf-wax model suggested that modified lignin-based formulations spread more effectively on leaf-like surfaces, which is a critical feature for foliar nutrient delivery. The biological performance of the developed formulations was evaluated under greenhouse conditions using iron-deficient soybean plants. Lignin-based iron formulations were compared with conventional iron sources following foliar application, and plant elemental composition was assessed by ICP-OES. The results showed that modified lignin-based nanoformulations supported iron delivery to leaves and exhibited promising foliar uptake behavior. The addition of a wetting agent further improved formulation performance, suggesting that surface interaction plays an important role in nutrient absorption. Overall, this study demonstrates that modified lignin can be transformed into a sustainable, biodegradable and functional carrier for foliar iron delivery. These findings highlight the potential of lignin-derived nanoformulations as an environmentally friendly alternative to conventional synthetic chelates for controlled micronutrient delivery and sustainable crop biofortification.

Acknowledgment:
This study was financially supported by the Scientific and Technological Research Council of Turkey (TUBITAK) under 1004 program LignoNANO (Grant No. 22AG045)

References:
Andersson, C., Lindblad, M. S., & Tjerneld, F. (2003). Surfactant-enhanced foliar uptake of pesticides—properties of surfactants used in agricultural formulations. Pesticide Science, 59(3), 266–276
Heo, J. W., Yu, Y., Kim, M. S., Kwon, M. S., Ko, H., & Kim, Y. S. (2025). Cationic lignin/silver hybrid nanoparticles with antibacterial activity as robust catalysts for hydrogenation. Industrial Crops and Products, 236, 122077
Liu, Q., Kawai, T., Inukai, Y., Aoki, D., Feng, Z., Xiao, Y., et al. (2023). A lignin-derived material improves plant nutrient bioavailability and growth through its metal chelating capacity. Nature Communications, 14, 4866
Yuan, Y., & Lee, T. R. (2013). Contact angle and wetting properties. In Surface Science Techniques (pp. 3–34). Springer
Zhao, Y., Dong, R., Wang, G., Li, W., Sui, W., Jia, H., & Si, C. (2025). Lignin-based metal chelate fertilizers: preparation, properties and applications. International Journal of Biological Macromolecules, 144108.

Keyword: *Foliar fertilization, iron delivery, Soybean*

Sustainable Carbon Quantum Dots from Pumpkin Biomass: Synthesis, Characterization, and Potential Use in Edible Antimicrobial Food Films

Selva Bilge [*1], Berkay Korkmaz[2], Ayşe Karakeçili[2]

[1] *Ankara University, Faculty of Science, Chemistry Department, Türkiye*
[2] *Ankara University, Faculty of Engineering, Chemical Engineering Department, Türkiye*

Carbon quantum dots (CQDs) are attracting attention in sustainable nanomaterial research due to their small size, surface functionality, photoluminescence properties, dispersibility in aqueous environments, and biocompatibility potential. This study aimed to convert pumpkin biomass into CQDs using an environmentally friendly hydrothermal carbonization (HTC) method and to evaluate the potential of the resulting CQDs as antimicrobial/antibacterial additives in edible food film applications. CQD synthesis was carried out at temperatures ranging from 180–260 °C for 2–8 hours. The morphological, structural, chemical, and optical properties of the synthesized CQDs were evaluated using HR-TEM, XRD, UV-vis, fluorescence, and FTIR analyses. HR-TEM images showed that the obtained CQDs have an approximate size of 9.15 nm. The broad bands observed around 9.73° and 20.99° in the XRD patterns were associated with an amorphous carbon structure rich in oxygenated functional groups and exhibiting low crystallinity. Photoluminescence analysis revealed a maximum excitation wavelength of approximately 340 nm and a maximum emission wavelength of 429 nm, indicating that CQDs exhibit blue emission characteristics. FTIR analyses supported the presence of oxygenated functional groups such as hydroxyl, carbonyl, and carboxyl groups on the CQD surface. This study primarily focuses on evaluating the antibacterial effects of pumpkin-derived CQDs on food safety-critical microorganisms such as Escherichia coli, Staphylococcus aureus, and Listeria monocytogenes using MIC/MBC analyses. Furthermore, antioxidant capacity was planned to be investigated using DPPH and ABTS methods, and biocompatibility was tested using the MTT test in the L929 fibroblast cell line. The synthesis and characterization findings have shown that CQDs produced from pumpkin biomass are a potential nanoadditive material that can be evaluated in edible film matrices for UV protective, photoluminescent, antimicrobial and biocompatible active packaging systems.

Keyword: *Renewable materials, Carbon dots, Biowaste carbon source*

ID: 225

Targeted Dual Phototherapy of Prostate Cancer with ALA-loaded SPIONs

Kübra Onbaşlı *

Istanbul Technical University, Faculty of Chemical and Metallurgical Engineering, Metallurgical and Materials Engineering Department, 34469 Maslak, Istanbul, Türkiye

Phototherapies, photothermal therapy (PTT), and photodynamic therapy (PDT) offer alternative, minimally invasive treatment options, particularly for localized cancer treatment, compared to conventional therapies like surgery, chemotherapy, and radiotherapy, which often have limitations such as systemic side effects and non-specific targeting. Nanoparticle-mediated phototherapy has emerged as a promising strategy, as nanoparticles can enhance treatment specificity and efficiency by delivering therapeutic agents directly to tumor cells and facilitating controlled activation with laser irradiation. In this study, we developed and evaluated the efficiency of 5-aminolevulinic acid (ALA)-loaded superparamagnetic iron oxide nanoparticles (ALA-PAA-SPIONs) for targeted combined PTT and PDT therapy of prostate cancer (PCa) cells. These nanoparticles utilize the selective uptake of ALA via PEPT1 and PEPT2 transporters, enhancing accumulation and therapeutic efficacy within cancer cells. Single PTT and PDT treatments resulted in limited cell death, even at high concentrations; however, their combination led to near-complete tumor cell eradication. These findings highlight the strong therapeutic potential of ALA-PAA-SPIONs as an effective dual-mode phototherapy platform for prostate cancer treatment.

Keyword: *SPION, photothermal therapy, photodynamic therapy, prostate cancer, 5-aminolevulinic acid*

Terminal Skeleton Engineering in Diketopyrrolopyrrole-Based Semiconductors for Tunable Optoelectronic Applications

Hilal Kalkan [*1], Pınar Seyitdanlıoğlu[2], Barış Temelli[2]

[1] *Department of Chemistry, Faculty of Science, Gazi University, 06500, Ankara, Türkiye*
[2] *Department of Chemistry, Faculty of Science, Hacettepe University, 06800, Ankara, Türkiye*

Diketopyrrolopyrrole (DPP)-based semiconductors offer a versatile platform for tuning organic optoelectronic properties through terminal-skeleton engineering. In this study, ten structurally diverse DPP derivatives were comparatively examined using density functional theory and time-dependent density functional theory in order to clarify how terminal fragments and π-bridges control electronic structure, optical response, excited-state character, and intrinsic charge-transport behavior. A benchmark analysis against experimental frontier orbital energies identified B3PW91/6-31+G(d,p) as a suitable computational level for the investigated series. The results showed that most molecules preserved largely planar conjugated backbones, whereas localized torsional changes modulated π-delocalization and orbital alignment. The calculated frontier orbital energies revealed a broad electronic diversity across the molecular series, indicating that terminal-skeleton modification is an effective strategy for tuning the optoelectronic behavior of DPP-based semiconductors. Furthermore, TD-DFT calculations revealed that changes in molecular structure strongly influence absorption characteristics, charge-transfer behavior, and excited-state properties. In addition, the calculated reorganization energies suggested that selected derivatives may offer favorable charge-transport tendencies. Overall, the combined electronic, optical, and charge-transport analyses demonstrate that structural engineering of the DPP framework can provide useful design principles for developing application-oriented organic semiconductor materials. By combining frontier orbital analysis, optical descriptors, CT/LE contributions, Δr, Λ descriptors, and reorganization energies, this work highlights that small terminal-structure changes can generate electronically distinct DPP subsets for application-specific organic semiconductor design.

Acknowledgment:
The calculations presented in this study were carried out using the computational resources of the Turkish Academic Network and Information Center (ULAKBIM), High Performance and Grid Computing Center (TRUBA).

References:
Li, Y., Sonar, P., Murphy, L., & Hong, W. (2013). High mobility diketopyrrolopyrrole (DPP)-based organic semiconductor materials for organic thin film transistors and photovoltaics. Energy & Environmental Science, 6(6), 1684-1710.
Molina, D., Alvaro-Martins, M. J., & Sastre-Santos, Á. (2021). Diketopyrrolopyrrole-based single molecules in photovoltaic technologies. Journal of Materials Chemistry C, 9(45), 16078-16109.

Keyword: *Optoelectronic, Small molecules, Diketopyrrolopyrrole, DFT, TD-DFT*

Dynamic Microneedle-Based SERS Interfaces for Localized Molecular Detection

Meryem Beyza Avci [*1], **Ayfer Aytac Arslan**[2], **Emrecan Yildiz**[2], **Gokhan Demirel**[2], **Arif E. Cetin**[3]

[1] *Izmir International Biomedicine and Genome Institute, Dokuz Eylul University, Balcova, Izmir, Türkiye*
[2] *Bio-Inspired Materials Research Laboratory (BIMREL), Department of Chemistry, Gazi University, Ankara, Türkiye*
[3] *Department of Biophysics, Faculty of Medicine, Dokuz Eylul University, Izmir, Türkiye*

Surface-enhanced Raman spectroscopy (SERS) is widely used for sensitive molecular detection, yet its performance depends strongly on the controlled formation of plasmonic hot-spots. Conventional SERS substrates often provide fixed nanogaps and limited control over the spatial distribution of enhanced electromagnetic fields. In this study, actuatable polymeric microneedle platforms were developed as dynamic interfaces for tunable hot-spot engineering and localized molecular sensing. Two complementary actuation strategies were examined. In the first approach, magnetic microneedles were fabricated from an Ecoflex/iron-particle composite and decorated with silver nanoparticles. Under an external magnetic field, the microneedle tips reversibly deformed and moved into closer contact, decreasing the distance between plasmonic nanoparticles and enhancing the Raman response. The magnetic platform also showed stable cyclic actuation, supporting its potential use in repeatable sensing workflows.

The second platform was based on pneumatically actuated PDMS microneedles functionalized with gold nanoparticles. When negative pressure was applied, the flexible microneedles collapsed locally and generated a larger contact region compared with the magnetic design. This deformation increased plasmonic coupling and produced stronger SERS enhancement during methylene blue detection. Experimental Raman measurements and spatial mapping confirmed that actuation changed both the intensity and the distribution of hot-spots. In addition, the pneumatic platform was integrated with independent vacuum control and robotic positioning to demonstrate selective cargo handling and localized molecular detection. Overall, these findings show that soft, deformable microneedle structures can serve as programmable SERS-active platforms. By combining mechanical actuation with plasmonic nanoparticle functionalization, the proposed strategy offers a practical route toward reconfigurable, localized, and scalable molecular sensing systems for biomedical and chemical analysis.

Acknowledgment:
This work was supported by the Scientific and Technological Research Council of Turkey (TUBITAK) (grant no: 22AG056). E.Y. also acknowledges the TUBITAK 2211-A scholarship program for financial support.

ORCID:
Meryem Beyza Avci: 0000-0001-8701-2239

Keyword: *polymeric microneedles, soft actuation, SERS*

MRI-Visible Polymer Coating Solutions Based on Melanin Nanoparticles for Interventional Guidewire Applications

Khawaja Faheem Shahid [*1], Uluç Pamuk[2], Gizem Kaleli Can[3], Engin Baysoy[2,4]

[1] *Bahçeşehir University, Institute of Bioengineering, 34353, İstanbul, Türkiye*
[2] *Center for Targeted Therapy Technologies (CT3), Boğaziçi University, Kandilli Campus, 34685, İstanbul, Türkiye*
[3] *İzmir Democracy University, Department of Biomedical Engineering, İzmir, 35140, Türkiye*
[4] *Bahçeşehir University, Department of Biomedical Engineering, 34353, İstanbul, Türkiye*

Interventional MRI (iMRI)-guided operations require real-time viewing of medical instruments, such as guidewires, within the body. Most of the conventional guidewires are not only improper due to MRI safety but also lack adequate tracking signals, limiting their use with MRI. The integration of paramagnetic particles into biocompatible polymer coatings is a promising approach to improve guidewire MRI visibility while maintaining mechanical performance.

This study involved the extraction, characterization, and initial MRI visibility performance of melanin nanoparticles (MNPs) as a biocompatible contrast agent. Scanning electron microscopy validated a spherical morphology with an average particle size of around 150 nm. MNPs were subsequently chelated with Mn^{2+} ions and integrated into 8% polycaprolactone (PCL) solutions at concentrations of 50, 100, 500, 1000, and 1200 µg/mL to assess contrast-enhancing capabilities before guidewire coating application.

Fourier transformed infrared spectroscopy results validated the successful integration of MNP-Mn^{2+} into PCL matrices at varying concentrations, as demonstrated by the preservation of melanin aromatic skeleton bands (~1600–1400 cm^{-1}) in conjunction with the characteristic PCL carbonyl (~1730 cm^{-1}) and aliphatic C-H (~2900 cm^{-1}) signatures. The expansion of the phenolic O-H stretching region (~3200–3400 cm^{-1}) in MNP-Mn^{2+} spectra compared to bare MNPs indicates Mn^{2+} interaction with catechol groups.

MRI phantom visibility investigations performed at the 7 T MRI scanner (MRS-PET/MR, MR Solutions Ltd., Surrey, UK) revealed that all MNP-Mn^{2+} included PCL solutions yielded superior contrast-to-noise ratio (CNR) values relative to the PCL control (428.01 ± 74.54) for T1-weighted (TR/TE: 300/11, slice thickness: 1 mm, FA:90^0) coronal MR images. A concentration-dependent CNR response was noted, with statistically significant increases at 50 µg/mL (844.94 ± 65.07) and 100 µg/mL (830.86 ± 65.20) compared to the control ($p < 0.05$). The progressive fall in CNR over 100 µg/mL, accompanied by significant signal dropout at 1200 µg/mL, underlines an optimal T1 shortening effect in the range of 50–100 µg/mL.

These findings delineate the ideal concentration range of MNP-Mn^{2+} for enhancing positive T1-weighted contrast in PCL-based coating solutions. Further efforts will concentrate on implementing these formulations on nitinol guidewire surfaces using dip coating and electrospinning to create MRI-visible guidewires for interventional radiology applications

Keyword: *Interventional MRI, Melanin nanoparticles, T1 contrast*

Theoretical investigations on micro-cantilever sensitivity to external forces under single- and multi-frequency excitations in nanometrological applications

Cagri Yilmaz *

Akdeniz University

Observable sensitivities of the micro-cantilevers to external forces are enhanced using single- and multi-frequency excitation schemes in nanometrological applications. Tip-sample interaction forces such as Casimir and van der Waals forces are quantified using oscillation amplitudes and phase shifts at the fundamental and higher flexural eigenmodes in multi-frequency Atomic Force Microscopy (AFM). Single-frequency excitations enable to obtain maximum amplitude responses using the micro-cantilever with a smaller effective mass when compared with multi-frequency excitations. Additionally, nonlinear observable sensitivities to van der Waals interactions are enhanced using multimodal operations depending on the elastic stiffnesses and the quality factors of the AFM micro-cantilevers. Furthermore, highly sensitive amplitude responses to acoustic forces can be explored using the computational methods. The frequencies of acoustic emissions with larger sound pressure levels within the kHz range can be detected using the analytical technique based on the Laplace transform method. In micro-rheological applications, the shifts in resonance frequencies of the micro-cantilever are used to measure the fluid properties. Sensitivities to dynamic viscosity and density can be quantified by exploiting the steady-state oscillations based on the forced van der Pol oscillator. Therefore, the vibration observables of the resonating micro-cantilevers can be utilized to quantify the sensitivities to diverse external forces for different technological applications.

ORCID:
Cagri Yilmaz: https://orcid.org/0000-0002-2976-1044

References:
Yilmaz, C. Utilizing a forced Van der Pol-Rayleigh-Helmholtz oscillator under heptamodal-frequency operations in Casimir force measurement. Indian J Phys 99, 1077–1089 (2025). https://doi.org/10.1007/s12648-024-03359-1
Yilmaz, C. Using Hexamodal-Frequency Excitation Scheme to Improve Sensitivity to Tip-Sample Interaction Forces at Flexural Eigenmodes in AFM. J. Vib. Eng. Technol. 14, 195 (2026). https://doi.org/10.1007/s42417-026-02430-x
Yilmaz, C. Using an analytical approximation to determine observable responses of the micro-cantilevers to acoustic emissions in single-and bimodal-frequency excitations. Phys. Scr. 101, 12 (2026). https://doi.org/10.1088/1402-4896/ae5001
Yilmaz, C. A multi-modal nonlinear dynamic model to investigate time-domain responses of a micro-cantilever in fluids. Eng. Res. Express. 6, 2 (2024). https://doi.org/10.1088/2631-8695/ad3c13
Okamoto, Y., Nguyen, T. -V., Takahashi, H., Takei, Y., Okada, H., Ichiki, M. Highly sensitive low-frequency-detectable acoustic sensor using a piezoresistive cantilever for health monitoring applications. Sci. Rep. 13, 6503 (2023). https://doi.org/10.1038/s41598-023-33568-3

Keyword: *Multi-frequency AFM, Acoustic force sensitivity, Microrheology*

Thermally Drawn Multilayer P(VDF-TrFE)/SnO_2 Piezoelectric Fibers for Flexible Self-Powered Sensing Applications

Vishwa Pratap Singh[1], Naci Enes Dirican[1], Deniz Berk Onuralp[1], Nurbolat Issatayev[2], Yersaiyn Busharov[2], Gulnur Kalimuldina[2], Mustafa Ordu[1], Sk. Rahat Ali [* 1]

[1] UNAM – National Nanotechnology Research Center and Institute of Materials Science and Nanotechnology, Bilkent University, Ankara 06800, Türkiye

[2] Department of Mechanical and Aerospace Engineering, School of Engineering and Digital Sciences, Nazarbayev University, Astana 010000, Kazakhstan

Piezoelectric polymer fibers have attracted significant attention for flexible electronics and self-powered sensing systems owing to their lightweight nature, mechanical flexibility, and ease of integration into wearable platforms. However, achieving high piezoelectric performance while maintaining scalable fiber fabrication remains a major challenge. Here, we report the development of thermally drawn multilayer piezoelectric fibers based on P(VDF-TrFE)/SnO_2 nanocomposites with integrated conductive polyethylene (cPE) electrodes. Unlike conventional single-layer piezoelectric fibers, the proposed multilayer architecture enables enhanced stress transfer, improved charge collection efficiency, and increased interfacial polarization, leading to superior electromechanical performance. These fibers were fabricated through a scalable thermal drawing process from a macroscopic preform while preserving the multilayer electrode–piezoelectric structure to reduced diameter. Structural characterization using X-ray diffraction (XRD) and Fourier-transform infrared spectroscopy (FTIR) confirmed enhanced electroactive β-phase formation after fiber fabrication. Incorporation of SnO_2 nanoparticles further promoted dipole alignment and polarization, resulting in β-phase-related peak ratio enhancements of approximately 72% and 58% compared to pristine polymer samples. Scanning electron microscopy and elemental mapping revealed uniform morphology and homogeneous nanoparticle distribution throughout the fiber cross-section. Electrical characterization under periodic mechanical excitation demonstrated stable piezoelectric behavior with an open-circuit voltage of approximately 12 V and a maximum output power of 9.14 μW across a 7 MΩ load resistance. The enhanced output is attributed to the synergistic effect of the multilayer architecture and nanocomposite-induced β-phase enhancement. These results demonstrate a scalable strategy for producing high-performance multilayer piezoelectric fibers with improved energy conversion efficiency, highlighting their potential for flexible self-powered sensing, smart textiles, wearable electronics, and distributed sensing applications.

Acknowledgment:
M.O. and V.P.S. acknowledges the support of the Scientific and Technological Research Council of Türkiye (TÜBİTAK) (Grant number 125M508)

ORCID:
Vishwa Pratap Singh: 0000-0003-3054-8862
Mustafa Ordu: 0000-0003-4049-9283

Keyword: *Thermal drawing, Piezoelectric fiber, P(VDF-TrFE)*

A Chirped Nanoplasmonic MIM Metasurface enables Spectrometer-free Refractometric sensing

Fahd Khalid-Salako [*] [1,2], Zeki Semih Pehlivan[3], Meral Yüce[2], Hasan Kurt[4,5]

[1] Faculty of Engineering and Natural Sciences, Sabanci University, Tuzla 34956, Türkiye
[2] Sabanci University Nanotechnology Research and Application Center (SUNUM), Tuzla 34956, Türkiye
[3] Department of Materials Science and Metallurgy, University of Cambridge, Cambridge CB30FS, United Kingdom
[4] School of Engineering and Natural Sciences, Istanbul Medipol University, Beykoz 34820, Türkiye
[5] Nanosolar Plasmonics Ltd., Gebze, 41400, Türkiye

The realities of clinical translation and industrial scale-up of biomedical diagnostic technologies are such that they have to provide highly sensitive and noise-free signal transduction, while maintaining assay simplicity, timeliness, and notably, compactness. Considering these strict requirements, optical sensing technologies have emerged as promising diagnostic options, with refractometric and vibrational sensing mechanisms among others. While optical biosensors are known for their miniaturization potential, giving them an advantage over more traditional chromatographic and mass spectrometric systems, they still suffer from bulkiness, mostly due to the spectrometer components that provide key momentum-resolved spectra. Building on recent refractometric sensing systems, this research is geared towards achieving further miniaturization through spectrometer-free biosensing, allowing on-chip spectroscopy without the need for bulky spectrometer components. Simply, the developed substrate comprises a metal-insulator-metal (MIM) layered metasurface, decorated with nanosized holes at a uniaxial periodicity gradient. The multiperiodic nanohole array (mpNHA) substrate is based on extraordinary transmission (EOT) at matching diffraction orders on a specific line element on the surface, where the EOT-transmitted light is coupled with surface-bound polaritons (SPP) within the insulator spacer, attenuating the light and causing a CMOS-observable dark mode in reflection images. Refractive index changes in the reaction medium (ϵ_d) cause EOT resonance shifts in nanohole periodicity (Λ), enabling simple CMOS-observable resonance displacement-based refractometry. This resonance shift is mathematically represented by the equation: $\lambda_{EOT} = [\Lambda/\sqrt{(i^2+j^2)}]\sqrt{[\varepsilon_d\varepsilon_m/(\varepsilon_d+\varepsilon_m)]}$

The mpNHA metasurface was designed and geometrically optimized through FDTD simulations. Nanofabrication was done by sequential thin film deposition techniques and electron-beam lithography-based nanopatterning. The metasurface was composed of a bottom Al layer, acting as a back-reflector due to its high extinction coefficient, reflectivity, and plasmonic activity in the visible spectrum; a SiO_2 spacer which supports interface SPPs enabling EOT-transmitted light attenuation and sharp dark modes; and a top Au layer decorated with nanoholes. Comprehensive characterization of the fabricated metasurface confirmed fabrication fidelity, optical properties, and congruence of experimental findings with simulations. Glycerol-based refractive index studies also confirmed the refractometric potential of the substrate and enabled biosensing performance assessments. Finally, biofunctionalization of the substrate enables binding-induced refractive index changes and ultimately, refractometric detection of target analytes in various sample media. Incorporating microfluidic flow channels for sample injection with ML models integrating segmentation and optical flow for realtime displacement tracking and dynamic binding kinetics analysis would further improve the clinical value of the developed system.

Acknowledgment:
This research was financially supported by The Scientific and Technological Research Council of Türkiye (TUBITAK) [Project ID: 22AG002].

ORCID:
Fahd Khalid-Salako: 0000000347952423
Zeki Semih Pehlivan: 0000000341412768
Meral Yüce: 0000000303931225
Hasan Kurt: 000000021677644X

References:
Kurt, H., Soylukan, C., Çelik, S., Çapkın, E., Acuner, I. C., Topkaya, A. E., & Yüce, M. (2025). Rapid and sensitive biosensing of uropathogenic E. coli using plasmonic nanohole arrays on MIM: Bridging the gap between lab and clinical diagnostics. Biosensors and Bioelectronics, 280, 117419. https://doi.org/10.1016/J.BIOS.2025.117419
Pehlivan Zeki Semih. (2022). Multi-periodical photonic array for spectrometer-free spectral refractometric sensing.

Keyword: *Multi-periodic nano-array, Metal-Insulator-Metal, Optical Biosensing*

Development of ZnO/CuO Nanofibers for Gas Sensing Applications

Elif Nur Karacan [*1], **Okan Özdemir**[2], **Onur Alp Aksan**[2], **Alp Kılıç**[1], **Nuray Kızıldağ**[2], **Serkan Büyükköse**[1], **Leyla Çoklarerol Arslan**[1]

[1] *Physics Depertmant, Gebze Technical University, 41400 Kocaeli, Türkiye.*
[2] *Nanotechnology Institute, Gebze Technical University, 41400 Kocaeli, Türkiye.*

The detection of harmful gases in industrial and environmental applications is of great importance for public health and safety [1]. In this context, there is a need for gas sensing systems with low cost, high sensitivity, and fast response time[2]. One of the sensor classes that exhibit higher selectivity and stability for detecting low gas concentrations is metal oxide semiconductor gas sensors [3-4].

In this study, one-dimensional coaxial zinc oxide (ZnO) and copper(II) oxide (CuO) heterostructured nanofibers were synthesized using a sol-gel-assisted electrospinning method, and their gas-sensing performance was investigated for various volatile organic compounds (VOCs). Nanofibers prepared at different molar ratios were coated onto SiO_2 substrates designed as interdigital transducers (IDT), and subsequently calcined at 500 °C for 5 hours under ambient atmosphere. The crystal structure of the synthesized and calcined nanofibers was determined using X-ray diffraction (XRD) technique. XRD analysis revealed that the uncalcined PVA/ZnO/CuO nanofibers exhibited an amorphous structure, while ZnO and CuO crystal phases with polycrystalline structure were observed after calcination. An improvement in the crystal structure of the material was observed with increasing molar concentration. Scanning electron microscopy (SEM) was used to determine the morphologies of the nanofibers. SEM images showed that smooth and continuous nanofiber structures were obtained before calcination. After calcination, while the fiber morphology was preserved, a decrease in nanofiber diameter and the formation of granular/agglomerated structures were observed due to the removal of the polymer and crystallization of the metal oxide phases. Elemental analysis was carried out using X-ray photoelectron spectroscopy (XPS). XPS analyses revealed the formation of strong interfacial interactions between ZnO and CuO phases and demonstrated that the heterostructure was successfully synthesized. UV-Vis optical transmission spectroscopy and Tauc plot analyses revealed that the optical properties varied depending on the composition, and the band gap energies were calculated as approximately 3.22 eV for ZnO, 2.37 eV for CuO, and 2.92 eV for ZnO/CuO nanofibers. ZnO/CuO composite nanofibers exhibited intermediate optical properties between pure ZnO and CuO, indicating the interaction between the two metal oxide phases.

Acknowledgment:
Thanks to the Gebze Technical University Research University Support Program for its financial support. ADEP, Grant No. 2025-A-113-17, ‘Ekolojik İzleme için Metal Oksit bazlı Nanolif Sensörlerin Geliştirilmesi.’ This study was also supported by the Scientific and Technological Research Council of Turkey (TÜBİTAK) 2210-C Priority Areas Scholarship Program.

References:
[1] Yang, B., Myung, N. V., Tran, T. T. 2021. "1D Metal Oxide Semiconductor Materials for Chemiresistive Gas Sensors: A Review". Advanced Electronic Materials, 7(9), 2100271.
[2] Chen, L., Yu, Q., Pan, C., Song, Y., Dong, H., Xie, X., Chen, X. 2022. "Chemiresistive gas sensors based on electrospun semiconductor metal oxides: A review". Talanta, 246, 123527.
[3] Alam, M. M., Lee, S., Kim, M., Han, K. S., Cao, V. A., Nah, J. 2020. "Ultra-flexible nanofiber-based multifunctional motion sensor". Nano Energy, 72, 104672.
[4] Lee, J., Yoon, J., Oh, S. 2024. “Electrospun nanofiber-based tri-layer separators with CuO/TiO nanowires for high-performance and long-cycle stability of lithium-ion batteries”. Journal of Industrial and Engineering Chemistry, 135, 165–174.

Keyword: *Electrospinning, ZnO/CuO Nanofiber, Metal Oxide Gas Sensor*

Particle Morphology Control Through Liquid Metal Alloy Solidification

Mert Ulusel [*] [1], Orçun Dinçer[2], Ozan Şahin[3], Simge Çınar Aygün[1]

[1] *Middle East Technical University*
[2] *Concordia University*
[3] *Advanced Research Center for Nanolithography*

Undercooled liquid metal particles have attracted significant scientific interest due to their potential applications in catalysis, sensing technologies, and drug delivery systems. They also provide an excellent platform for studying solidification processes because their confined volumes simplify the observation of microstructure evolution. In alloy solidification, the resulting morphology is primarily determined by two key phenomena: nucleation and growth. Since nucleation is inherently stochastic, controlling it in bulk materials is challenging. Nevertheless, its occurrence can be manipulated by altering the presence of catalytic sites that act as nucleation initiators. Adjusting the nucleation energy barrier, and consequently the kinetics of solidification, is a widely used strategy in metallurgical processing to achieve desired microstructures. At submicron and nanometer scales, this control can be enhanced further because individual nucleation sites can be isolated within particles derived from bulk alloys. As a result, these particles contain significantly fewer catalytic sites than their bulk counterparts, enabling the observation and exploitation of phenomena that are inaccessible in bulk systems, including undercooling levels several orders of magnitude greater. Highly undercooled alloy particles provide an ideal starting point for controlled microstructural engineering. By introducing catalytic sites and modifying solidification conditions, it becomes possible to reproducibly generate distinct particle morphologies in large quantities. In this work, we demonstrate that a variety of complex phase distributions, including Janus and triblock Janus structures, which are typically difficult to produce in metallic particles, can be fabricated at scale by tailoring solidification pathways through purely physical approaches. To accomplish this, top-down processing methods are employed to modify both the distribution and effectiveness of catalytic sites within liquid particles produced from bulk alloys. Unlike deposition or chemical techniques, which generally yield core-shell architectures, the solidification based approach promotes a more uniform phase distribution throughout the particle core, resulting in stronger anisotropic characteristics. The resulting particle morphologies are comprehensively characterized, and the relationships between processing parameters, such as thermal history and atmospheric environment, and the final particle structure are systematically investigated. These findings provide deeper insight into solidification mechanisms in confined volumes and establish a foundation for developing even more complex and unique particle architectures through future solidification-based design strategies.

Acknowledgment:
This work was supported by TUBITAK under project no. 119M306.

ORCID:
Mert Ulusel: https://orcid.org/0000-0003-1749-1646
Orçun Dinçer: https://orcid.org/0000-0001-8144-4882
Simge Çınar Aygün: https://orcid.org/0000-0003-3098-2888

Keyword: *Liquid Metal Particles, Janus Particles, Nucleation and Growth*

ID: 150

MXene-Assisted Enhancement of Hydrothermally Synthesized La2O3 Electrodes for Supercapacitors

İrem Nur Demirkol [*] [1], Amira Gaber[1], Anas Abofoul[1], Selva Bilge[2]

[1] Ankara University, Graduate School of Natural and Applied Sciences, Department of Chemistry, Türkiye
[2] Ankara University, Faculty of Science, Department of Chemistry, Türkiye

The increasing energy demand and the proliferation of portable electronic systems are driving interest in next-generation energy storage materials. In this context, supercapacitors have become a significant research area due to their complementary properties to battery systems. In this study, La_2O_3/MXene nanocomposites were developed by leveraging the synergistic effect of pseudocapacitive doping of the rare earth oxide La_2O_3 with MXene, which offers high conductivity, a hydrophilic surface, and a two-dimensional layered structure. La₂O₃ nanostructures were synthesized by hydrothermal methods. The MXene phase was obtained from the Ti_3AlC_2 MAX phase by HF removal of the Al layer, followed by washing, sonication, and freeze-drying steps. La_2O_3/MXene nanocomposites were prepared by adding 5%, 10%, and 15% MXene by weight to a La_2O_3 matrix, and the effect of different MXene ratios on the electrochemical behavior was compared. Physicochemical characterization results show that a rod-like La₂O₃ morphology is formed by hydrothermal synthesis, and a more integrated composite structure is obtained with the addition of MXene. C-TEM images reveal the distinct rod morphology of the La_2O_3 nanostructures, while in the 10% MXene/La_2O_3 sample, MXene layers were observed to be in contact with the La_2O_3 structures. XRD, Raman, FTIR, and XPS analyses supported the formation of the La₂O₃ phase, the addition of MXene, and the presence of chemical bonding interactions such as La–O, Ti–C/Ti–O, and C–C/C–O on the surface. In conclusion, the composite of hydrothermal La_2O_3 nanostructures with MXene offers a unique and efficient approach to supercapacitor electrodes by combining the pseudocapacitive character of La_2O_3 with the conductive, layered structure of MXene. In particular, the improvement in electrochemical performance with 10% MXene doping demonstrates that La_2O_3/MXene nanocomposites are promising electrode materials for high-performance energy storage systems.

Acknowledgment:
The authors would like to thank Ankara University, Department of Chemistry for providing laboratory facilities and technical support.

Keyword: *Lanthanum oxide, MXene (Ti3C2Tx), hydrothermal synthesis*

Green Synthesis of ZnO-Based Photoelectrochemical Materials via Tomato Peel Extract: Effects of Zinc Precursors on Stability and Photoactivity

Ceyda Çelik, Ufuk Erdoğan, Yunus Yener * , Beren Anlaş, Serra Ersoy, Cengiz Kaya

Yildiz Technical University Departman of Metallurgy and Materials Engineering, 34956 Istanbul, Türkiye

By lowering chemical usage and ecological effect, green synthesis techniques provide eco-friendly substitutes for the production of useful metal oxide materials. In this work, tomato peel extract was used as a bio-derived reducing and stabilizing agent to create zinc oxide (ZnO)-based photocatalysts. The effects of extract content (10 g and 20 g) and zinc precursor type (acetate vs. nitrate) on colloidal stability, crystal structure, morphology, and photoelectrochemical (PEC) performance were thoroughly examined. The hexagonal wurtzite structure of all synthesized samples was verified by X-ray diffraction examination. Compared to zinc nitrate, the usage of zinc acetate produced more consistent and regulated particle morphologies, according to scanning electron microscopy combined with energy-dispersive spectroscopy. Acetate-based production favors smaller particle sizes, as shown by UV-Vis spectroscopy, which revealed a blue shift of the typical absorption peak from 363 nm (zinc nitrate) to 356 nm (zinc acetate). The corresponding band gap values showed the impact of synthesis settings on the electrical structure, ranging from 3.08 to 3.17 eV. Dynamic and electrophoretic light scattering were used to assess colloidal characteristics. While samples containing 10 g of extract (DTS-3) displayed heterogeneous distributions and reduced stability (zeta potential: -10.3 mV, PdI: 0.407), samples containing 20 g of extract (DTS-4) showed improved stability and a monodisperse particle distribution (zeta potential: -25.2 mV, PdI: 0.075). These findings demonstrate how crucial precursor choice and extract concentration are in regulating particle agglomeration and dispersion homogeneity. Chronoamperometry was used to evaluate photoelectrochemical performance at 20 V and 365 nm light. Repeatable photocurrents up to 110 µA @ 0.3 V were shown by DTS-3 electrodes. On the other hand, because of the dense organic layer's shielding effect from the increased extract concentration, DTS-4 showed little photoactivity despite having better colloidal stability. This result highlights the need to optimize the concentration of bio-derived extracts in order to preserve access to catalytic sites, even when they improve particle stability. Overall, our work shows that extracts from agricultural waste are useful green agents for the synthesis of ZnO photocatalysts. The study highlights the promise of bio-inspired techniques in the development of sustainable materials for solar energy conversion and hydrogen generation applications by establishing clear relationships between precursor type, extract concentration, colloidal behavior, and PEC activity.

Acknowledgment:
This study was supported under the TÜBİTAK 2209-A project (project number 1919B012424064) and the Yıldız Technical University BAP LİKAP FLO-2025-7158 project.

Keyword: *biological waste, photoelectrochemical performance, transition metal nanoparticles*

Investigation of the Potential of ZnBO Memristors for Neuromorphic Computing

Gökhan Ekinci [*1], Sümeyye Veziroglu[2], Fatih Mehmet Coşkun[3]

[1] *Department of Digital Transformation Electronics, Advanced Vocational School, Dogus University, İstanbul,Türkiye*
[2] *Marmara University, Faculty of Science, Department of Physics, İstanbul, Türkiye*
[3] *Faculty of Engineering and Natural Sciences, Department of Engineering Physics, Istanbul Medeniyet University, İstanbul,Türkiye*

ABSTRACT

Humanity faces insufficient processing power in this big data age, with increasing demands for artificial intelligence and machine learning. This is because the current CMOS (complementary metal-oxide semiconductor) based computing architecture has a major inherent problem known as von Neumann bottleneck due to the physically separated structure of processor and memory units [1], [2]. Studies show that the problem of physical separation between processor and memory units can be solved by a nano-device called a memristor, and this device is attracting intense interest from researchers due to its potential and advantages in facilitating parallel computing [3]. Unlike metal oxide memristors, boron-doped memristors have advantages such as high thermal stability, precise control over potential increase, decrease and relaxation, as well as excellent mechanical stability [4].

In this study, we fabricated memristor device with a Cu/ZnBO/Cu lateral structure on a Si substrate using thin film production technique. The Sol-Gel Dip Coating Method, under carefully controlled conditions, was used in the device fabrication processes. In the fabricated memristor device, the ZnBO layer acts as the functional layer, while the Cu layers act as contacts.

Energy Dispersive X-Ray Analysis (EDX) was performed for the elemental analysis and chemical characterization of the ZnBO film structure, which is crucial for the device's operation. X-Ray diffraction analysis (XRD) was used to examine its crystal structure, and cross-sectional measurements were taken using Scanning Electron Microscopy (SEM) to determine its thickness. DC electrical measurements were performed to reveal the memristive characteristics of the device.

ORCID:
Gökhan Ekinci: 0000-0003-1918-1553
Sümeyye Veziroglu: 0000-0001-9190-4897
Fatih Mehmet Coşkun: 0000-0001-8040-8054

References:
Yongyue X., Bei J., Zihao Z., Shanwu K., Yaoyao J., Xin W., and Cong Y., ‘‘A review of memristor: material and structure design, device performance, applications and prospects’’, Science and Technology of Advanced Materials, 24:1, 2162323, 2023
Bai S, Yuanzheng C., Guangdong Z., Zelin C., ChuanY., Junmei D., Xiaoliang C., ‘’Memristor-Based Artificial Chips’’, ACSNano, 18, 14−27, 2024
Zhou G., Wang Z., Sun B., Zhou F., Sun, L., Zhao H., Hu X., Peng X., Yan J., Wang H., Wang W., Li J., Yan B., Kuang D., Wang Y., Wang L., Duan S., “Volatile and Nonvolatile Memristive Devices for Neuromorphic Computing”, Adv. Electron. Mater. 2022, 8, 2101127.
Maolin C., Yinchang M., Nabeel A., Chen L., etc, “Ultrawide-bandwidth boron nitride photonic memristors”, 20, 1633–1640 (2025).

Keyword: *Neuromorphic Computing, Memristor, ZnBO*

Ionic Liquid Functionalized Magnetic Cu-MOF Nanocomposite for the Extraction and Determination of Pb(II), Cd(II), and Zn(II) in Environmental Water Samples

Duygu Totur Pamik * [1], **Serap Seyhan Bozkurt**[2]

[1] *Dokuz Eylül University, Faculty of Engineering, Department of Environmental Engineering, İzmir, Türkiye*
[2] *Dokuz Eylul University, Faculty of Science, Department of Chemistry, Izmir, Türkiye*

In this study, a magnetically-enabled Cu-MOF (IS@Fe_3O_4@Cu-MOF) nanocomposite was synthesised. The characterisation of this synthetic nanocomposite was conducted, and the sorbent was utilised in the extraction and preconcentration of selected heavy metals from environmental water samples. The impact of the nanocomposite was also investigated. The combination of this advanced material with Fe_3O_4 nanoparticles enhances the sorption capabilities of the Cu-MOF structure, attributable to the substantial surface area. The surface and morphological properties of the synthesised nanosorbent were determined through Fourier-transform infrared spectroscopy (FTIR), scanning electron microscopy with energy-dispersive X-ray analysis (SEM-EDX), and X-ray diffraction (XRD) analyses. Furthermore, the incorporation of an ionic liquid into the structure resulted in an enhancement of both the sorption capacity and the interaction with metal ions.

The development of this sorbent was instrumental in the preconcentration of Pb(II), Cd(II), and Zn(II) ions by magnetic solid-phase extraction prior to analysis by ICP-OES. The parameters that were optimized included pH, amount of sorbent, extraction time, type and volume of desorption solution. The method has been developed under optimum conditions, resulting in expeditious magnetic properties. The separation process exhibited satisfactory reproducibility and yielded satisfactory extraction results.

The analytical performance of the method was evaluated using linearity, limit of detection (LOD), limit of quantification (LOQ), precision, and recovery values.

In summary, the developed magnetic Cu-Mof nanocomposite demonstrated strong performance in the separation, extraction and analysis of some heavy metals from environmental water samples.

Acknowledgment:
This study is supported by TÜBİTAK project number 125Z076.

ORCID:
Duygu Totur Pamik: 0000-0003-1411-3500

Keyword: *Cu-MOF; Magnetic solid phase extraction; Heavy metals; ICP-OES; Ionic liquid*

Structural and Electrical Characterization of Diamond-Like Carbon Films Deposited on Flexible Cu and Mo Foil Substrates by RF-PECVD

Ali Altuntepe *

Optical Excellence Application and Research Center, Sivas University of Science and Technology, Sivas 58000, Türkiye

Diamond-like carbon (DLC) films have attracted considerable attention in recent years due to their attractive combination of high hardness, chemical inertness, optical transmission low friction coefficient, and tunable electrical properties, making them promising candidates for flexible electronic and optoelectronic applications [1, 2]. In particular, the selection of an appropriate flexible metallic substrate plays important role in determining the microstructure, bonding characteristics, and electrical properties of DLC films [3]. In this study, DLC films were deposited on flexible Cu and Mo foil substrates using a radio-frequency plasma-enhanced chemical vapor deposition (RF-PECVD) process. The influence of various deposition conditions, such as different RF powers (50, 75, and 100 W) and chamber pressure (1, 1.5, and 2 mTorr), on the structural and electrical properties of the films was investigated.

Raman spectra exhibited the characteristic D and G bands of DLC films at approximately 1355 cm^{-1} and 1575 cm^{-1}, confirming the formation of amorphous carbon structures [4]. Variation of the I_D/I_G ratio shows changes in the sp^2/sp^3 bond structure, thereby affecting the electrical properties of the films.

SEM results showed uniform film formation on both flexible metallic substrates. However, DLC films deposited on Mo foils exhibited improved surface homogeneity, lower roughness, and fewer structural defects compared to those deposited on Cu foils. XPS analysis further confirmed a more stable carbon bonding structure on the Mo substrate, indicating enhanced film quality.

Electrical characterization demonstrated that the deposition conditions significantly affected the conductivity of the DLC films. The samples deposited at 100 W RF power and 2 mTorr pressure exhibited the most favorable electrical performance, which was attributed to enhanced plasma activity and improved carbon network formation. Among the investigated substrates, Mo foil provided superior electrical and structural characteristics, making it a promising platform for flexible DLC-based devices.

The obtained results demonstrate the potential of DLC-coated flexible metallic foils for next-generation optoelectronic systems, flexible sensors, wearable electronics, and advanced energy-related applications.

References:

[1] Tayeb HH, Ahangarani S, Rafiaei SMJERE. Mechanical and tribological performance of CVD-deposited Diamond-like carbon (DLC) coatings: challenges, strategies, and perspectives. 2025;7:042503.
[2] Rajak DK, Kumar A, Behera A, Menezes PLJAS. Diamond-like carbon (DLC) coatings: classification, properties, and applications. 2021;11:4445.
[3] Wu L, Bai Z, Hao Q, Qin JJL. Improving wear resistance of DLC-Coated metal components during service: a review. 2025;13:257.
[4] Vasilets V, Hirose A, Yang Q, Singh A, Sammynaiken R, Foursa M, et al. Characterization of doped diamond-like carbon films deposited by hot wire plasma sputtering of graphite. 2004;79:2079-84.

Keyword: *Diamond-like carbon, RF-PECVD, flexible foil*

Atomic Layer processing: enabling next-level processing for advanced nano technology applications

Gerd Jungmann *

SENTECH Instruments GmbH

As devices continue to shrink, pushing the boundaries of Moore's Law, the demand for smaller, more powerful, and energy-efficient devices has driven the need for advanced atomic layer processing (ALP). This capability is especially critical as the demand for sub-10 nm devices is steadily increasing. Consequently, there is an increasing interest and demand on an industry level for both atomic layer deposition (ALD) and atomic layer etching (ALE).

Atomic Layer Etching (ALE) is a novel etching technique that unlocks new possibilities in semiconductor manufacturing. Unlike conventional etching methods, ALE facilitates the controlled removal of material, one single atomic layer at a time. This layer-by-layer etching approach, which offers exceptional precision and repeatability, enables the fabrication of nanoscale features. The innovation of ALE lies in its ability to enable atomic-level control of etching, offering unprecedented accuracy and selectivity.

In contrast, ALD enables conformal deposition of various materials with sub-nm precision. Where typical line-of-sight deposition methods fail, ALD excels and opens up new avenues for novel device designs and manufacturing. Furthermore, its continuously expanding material library makes ALD an important asset for advanced nano-technology research.

SENTECH has over thirty years of experience in developing and manufacturing plasma process systems and thin-film metrology tools for the R&D and Industrial Production communities. Our robust systems focus on thin film deposition, dry-etching, and characterization in semiconductor technology, microsystems technology, photovoltaics, nanotechnology, and materials research.

Within the scope of this talk, we will focus on the processing of AlGaN by both ALD and ALE. AlGaN is a well-known wide-bandgap semiconductor with tunable properties. Especially, the formation of a 2-dimensional electron gas (2DEG), when placed in a junction with GaN, is a deciding factor in the fabrication of high- electron-mobility transistors (HEMTs). We will present how ALE can be used to fabricate a normally-off GaN-based HEMT device by precisely performing an AlGaN recess etch. [1,2].

In contrast to etching AlGaN, another approach is the precise growth of AlGaN by means of ALD. Therefore, an ALD super-cycle of AlN and GaN is needed. We will show how this approach has great potential for future applications. The ability to precisely control the target stoichiometry of the material without compromising the excellent thickness control typically for ALD plays a key role in further developing the HEMT technology.

In-situ monitoring is a cornerstone for the time-effective development of many types of processes. In particular, we will focus on ellipsometry, due to its non-invasive nature, measurement technique and high precision in the sub-nm range. This work will elaborate on the potential of in-situ ellipsometry for understanding surface reactions during the ALP process, process setup and process monitoring.

References:

[1] Miersch et al., J. Vac. Sci. Technol. A 42, 022604, 2024
[2] Miersch et al., J. Vac. Sci. Technol. A 43, 042603, 2025

Keyword: *atomic layer deposition, atomic layer etching, nano-technology*

Recovered-Silver-Derived Cu@Ag Core–Shell Particles for Silver-Efficient HJT Solar Cell Metallization

Behiye Demirtas [*] [1], Serdar Guler[1], Huseyin Utkucan Kayaci[2], Ilknur Ozbayrak[1], Onur Can Yurdakul[1], Seda Kilickaya Unver[3], Doga Doganay[1], Sahin Coskun[4], Simge Cinar Aygun[1], Bulent Arikan[3], Rasit Turan[3], Husnu Emrah Unalan[1]

[1] Department of Metallurgical and Materials Engineering, Middle East Technical University
[2] Department of Micro and Nanotechnology, Middle East Technical University
[3] Center for Solar Energy Research and Applications, Middle East Technical University
[4] Department of Metallurgical and Materials Engineering, Eskisehir Osmangazi University

The growing demand for silver in photovoltaic metallization poses high cost and sustainability challenges for high-efficiency solar cell technologies. Although silver-based conductive pastes are commonly used to produce low-resistance contacts in crystalline silicon solar cells, their high material cost and reliance on limited primary silver resources emphasize the need for more resource-efficient and circular metallization approaches. This need is particularly relevant for silicon heterojunction (HJT) solar cells, where low-temperature conductive pastes are required.

In this study, silver recovered from photovoltaic paste waste was utilized for the synthesis of Cu@Ag core–shell particles for HJT solar cell metallization. Silver was selectively extracted from PERC-type photovoltaic silver paste waste after removing polymeric binder, solvent residues, and glass frit components, and was subsequently converted into silver nitrate. The recovered silver nitrate was then employed as the silver source for Cu@Ag particle synthesis. In this particle design, copper was used as the conductive core to lower silver consumption, while the recovered silver formed a thin outer shell that improved electrical conductivity and provided protection against oxidation. Copper particles with an average diameter of approximately 270 nm were synthesized via wet chemical reduction and then coated with recovered silver by electroless deposition. The average particle diameter increased to approximately 317 nm after coating, indicating successful formation of the Cu@Ag core–shell structure. The particles were incorporated into a low-temperature conductive paste suitable for HJT solar cells. Their morphology, core–shell structure, and elemental distribution were examined using electron microscopy and elemental analysis, while the printed contacts were assessed through contact resistance and current–voltage measurements.

The HJT solar cell metallized with the recovered-silver-derived Cu@Ag paste achieved an efficiency of 15.74%, with a Voc of 0.710 V, a Jsc of 33.77 mA/cm2, and a FF of 65.64%. In comparison, the reference cell fabricated with commercial Ag paste reached an efficiency of 21.68%, with a Voc of 0.718 V, a Jsc of 40.62 mA/cm2, and a FF of 74.29%. The comparable Voc values suggest that the Cu@Ag contacts did not substantially affect the junction quality of the HJT cell, whereas the reduced Jsc and FF indicate that the main losses are associated with current collection and contact formation. Based on the measured core and shell dimensions, the Cu@Ag particles contain approximately 38 vol.% silver, corresponding to an estimated 60% reduction in silver usage compared with fully silver particles of similar size. By employing photovoltaic-waste-derived silver as the shell material, this approach reduces dependence on primary silver resources and contributes to a more circular metallization strategy. Overall, the findings demonstrate that recovered-silver-derived Cu@Ag core–shell particles offer a promising silver-efficient route for HJT solar cell metallization.

Acknowledgment:
This work was financially supported by the Scientific and Technological Research Council of Türkiye (TÜBİTAK) under Grant No. 222M102.

ORCID:
Behiye Demirtas: 0009-0006-3228-592X
Huseyin Utkucan Kayaci: 0000-0001-5092-9350

Keyword: *heterojunction solar cells, silver recovery, core-shell copper-silver particles*

Waste-Fabric-Derived Carbon/ZnO Nanocomposite For Voltammetric Determination Of Monoferrocenylcyclotriphosphazene Derivatives

Anas Abofoul [*] [1,2], **Reşit Cemaloğlu**[2], **Selva Bilge**[2], **Nuran Asmafiliz**[2]

[1] *Department of Chemistry, Graduate School of Natural and Applied Sciences, Ankara University, Ankara, Türkiye*
[2] *Department of Chemistry, Faculty of Science, Ankara University, Ankara, Türkiye*

Ferrocenyl-substituted cyclotriphosphazenes are redox-active hybrid compounds that combine a structurally tunable inorganic cyclotriphosphazene ring with an electrochemically active ferrocenyl group. Structurally related monoferrocenyl derivatives have also shown biological activity, including cytotoxic and DNA-binding behaviour. Because the ferrocenyl unit serves as an intrinsic redox centre, voltammetry provides a convenient approach for the electrochemical characterization and determination of these compounds and may support analytical monitoring during synthesis and derivatization studies.

Zinc oxide nanoparticles (ZnO NPs) were prepared by a solvothermal method, and a carbon material was obtained through the hydrothermal carbonization of waste fabrics. The resulting materials were combined to produce a waste-fabric-derived carbon/ZnO nanocomposite (WF-C/ZnO), which was used to modify a glassy carbon electrode (GCE). The WF-C/ZnO nanocomposite was characterized by scanning electron microscopy (SEM), transmission electron microscopy (TEM), X-ray diffraction (XRD), X-ray photoelectron spectroscopy (XPS), and Raman spectroscopy. As a representative monoferrocenylcyclotriphosphazene derivative, dichloro monoferrocenyl dispiro(N/N)cyclotriphosphazene (Fc-DSP-Cl_2) was selected as the target analyte. The effects of scan rate, pH, and supporting electrolyte on its oxidation signal were examined at the bare GCE and the WF-C/ZnO-modified GCE (WF-C/ZnO/GCE). The oxidation peak potential (E_p) and peak current (I_p) were pH-dependent, and the most pronounced signal was obtained in phosphate buffer (PB) at pH 3.00, which was selected for the analytical studies. At the bare GCE, the calibration plot was linear from 2.00×10^{-6} to 8.00×10^{-5} M. Under optimized adsorptive stripping differential pulse voltammetric (AdsDPV) conditions at the WF-C/ZnO/GCE (accumulation potential: 0.60 V; accumulation time: 60 s), the linear range extended from 8.00×10^{-8}–8.00×10^{-5} M. The WF-C/ZnO/GCE combined with AdsDPV enabled the determination of Fc-DSP-Cl_2 at lower concentrations than the bare electrode.

ORCID:
Anas Abofoul: 0000-0002-1816-2476
Reşit Cemaloğlu: 0000-0002-2802-0754
Selva Bilge: 0000-0001-5514-208X
Nuran Asmafiliz: 0000-0002-9335-4101

Keyword: *ferrocenylphosphazene; ZnO nanoparticles; waste-fabric-derived carbon; nanocomposite-modified glassy carbon electrode; adsorptive stripping differential pulse voltammetry*

Nanofibrous Single-Layered Gas Diffusion Layers for Polymer Electrolyte Membrane Fuel Cells

Mustafa Altay Karacaoğlu [*] [1], **Furkan Çetiner**[2], **Serife Akkoyun**[1], **Selahattin Çelik**[2]

[1] *Ankara Yıldırım Beyazıt University, Department of Metallurgical and Materials Engineering , 06010 Ankara, Türkiye*
[2] *Ankara Yıldırım Beyazıt University, Department of Mechanical Engineering, 06010 Ankara, Türkiye*

Proton exchange membrane fuel cells (PEMFCs) rely on gas diffusion layers (GDLs) to facilitate reactant transport, water management, and electron conduction. Conventional GDLs typically consist of a carbon fiber-based macroporous substrate combined with a microporous layer (MPL). However, the use of carbon fibers increases manufacturing costs, while the multilayer architecture introduces interfacial contact resistance that can negatively affect cell performance.

In this study, a novel single-layer GDL concept was developed to simultaneously reduce material costs and eliminate interfacial resistance between the macroporous and microporous layers. A porous poly(methyl methacrylate) (PMMA) nanofiber structure was first fabricated via electrospinning to provide the required porous network. Since PMMA is electrically insulating, the electrospun fibers were subsequently coated with intrinsically conductive polymers, namely polyaniline (PANi) and polypyrrole (PPy), through in-situ polymerization. Ammonium persulfate (APS) and ferric chloride ($FeCl_3$) were employed as oxidizing agents for PANi and PPy synthesis, respectively.

To further investigate the feasibility of their use in PEMFCs, the fabricated GDL specimens were cut into 4 cm^2 active areas and were subjected to electrochemical characterization and single-cell performance testing.

The performance of the developed single-layer structures was compared with that of conventional commercial GDL systems. PEM fuel cell testing and demonstrated stable electrochemical activity and confirmed the operational capability of the fabricated layers. The encouraging results obtained in the preliminary fuel cell experiments indicate that the proposed carbon fiber-free, integrated GDL architecture has significant potential for further development and performance enhancement. In addition, the proposed approach offers a promising pathway toward reducing manufacturing complexity and cost while supporting the large-scale production of PEM fuel cells.

Acknowledgment:
The authors acknowledge the support of TÜBİTAK under Project No. 224M281

ORCID:
Mustafa Altay Karacaoğlu: 0009-0000-5616-30939
Serife Akkoyun: 0000-0002-6676-6389

Keyword: *PEMFC, nanofibers, conductive polymers*

In-Situ Production of LiOH and H3BO3 from Lithium Tetraborate Solution by Using Bipolar Membrane Electrodialysis-Effect of Solution Concentration and Characteristics of Ion Exchange Membranes

Pelinsu Çamcı [*1], Senay Çubukcuoğlu[1], Mert Deniz[2], Esra Altıok[2], Kamil Bostancı[2,3,4], Tülay Güngören Madenoğlu[2], Müşerref Arda[3], Nalan Kabay[2]

[1] *Department of Chemical Engineering, Graduate School of Natural and Applied Sciences, Ege University, Izmir, Türkiye*
[2] *Ege University, Chemical Engineering Department, Faculty of Engineering, Izmir, Türkiye*
[3] *Ege University, Chemistry Department, Faculty of Science, İzmir, Türkiye*
[4] *Dokuz Eylul University, Torbalı Vocational School, Mining Technology Programme, İzmir*

Boron industry effluents are considered as potential secondary sources of lithium; however, the presence of both boron and lithium in aqueous streams complicates their separation and recovery [1]. Bipolar membrane electrodialysis (BMED) offers an attractive approach for simultaneous separation/recovery of both lithium and boron due to its ability to selectively transport Li^+ and $B(OH)_4^-$ ions through ion exchange membranes while generating LiOH and H_3BO_3 with the help of bipolar membranes [2]. In this study, the effect of feed solution concentration on in situ production of LiOH and H_3BO_3 from lithium tetraborate ($Li_2B_4O_7.5H_2O$) solution prepared at different concentrations was investigated using two different electrodialysis (ED) systems (PC-Cell 640 04 and MEGA EDBM-Z/4x10-0.8 models). Two membrane stacks consist of different cation and anion exchange membranes together with bipolar membranes arranged to provide acid and base production simultaneously. A schematic representation of the in situ production of LiOH and H_3BO_3 by using BMED process is shown in Figure 1. During experimental studies, electrical conductivity and pH were measured using Hach Lange HQ40d model multimeter whereas lithium and boron concentrations were analyzed by atomic absorption spectrometer (Shimadzu AA-7000 Model) and ICP-OES (Perkin Elmer Avio 200 Model), respectively. The results indicated that the feed solution concentration and the characteristics of ion exchange membranes employed have a significant influence on the performance of the BMED process. Overall, BMED was found to be an effective method for the simultaneous separation of Li^+ and $B(OH)_4^-$ ions from lithium tetraborate solution, enabling the in situ production of LiOH and H_3BO_3.

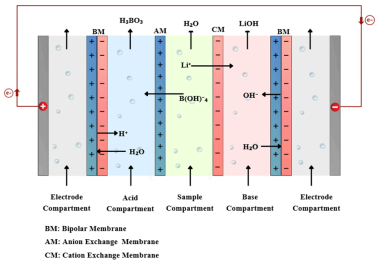


Figure 1. Flow sheet of BMED system for in situ production of LiOH and H_3BO_3

Acknowledgment:
This study was supported by Ege University Scientific Research Projects Coordination Unit (Project Number: FM-ADP-2024-32715).

ORCID:
Pelinsu Çamcı: 0009-0004-8701-4989
Senay Çubukcuoğlu: 0009-0001-2355-8803
Mert Deniz: 0009-0003-5397-8010
Esra Altıok: 0000-0001-5229-4766
Kamil Bostancı: 0000-0002-8565-1851
Tülay Güngören Madenoğlu: 0000-0001-6014-9956
Müşerref Arda: 0000-0002-1095-4831
Nalan Kabay: 0000-0001-8516-6752

References:
[1] Bunani, S., Yoshizuka, K., Nishihama, S., Arda, M., & Kabay, N. (2017). Application of bipolar membrane electrodialysis (BMED) for simultaneous separation and recovery of boron and lithium from aqueous solutions. Desalination, 424, 37–44. https://doi.org/10.1016/j.desal.2017.09.029
[2] Wang, J., Yue, X., Wang, P., Yu, T., Du, X., Hao, X., Abudula, A., & Guan, G. (2021). Electrochemical technologies for lithium recovery from liquid resources: A review. Renewable and Sustainable Energy Reviews, 154, 111813. https://doi.org/10.1016/j.rser.2021.111813

Keyword: *lithium recovery, bipolar membrane electrodialysis, resource recovery*

Polarization and Humidity Effects in Ferroelectric α-In_2Se_3 for Mo-lecular Sensing Applications

Golibjon Berdiyorov * **, Abdelmajid Salhi, Brahim Aissa**

Hamad Bin Khalifa University

The performance of two-dimensional gas sensors is strongly influenced by environmental humidity, which can modify adsorption strength and charge-transfer processes. Understanding these effects is therefore essential for the realistic assessment of sensing materials. Here, we employ first-principles density functional theory calculations to investigate the adsorption behavior of toxic gas molecules (CO, NO, NO_2, and H_2S) on ferroelectric α-In_2Se_3 monolayers under both dry and humid conditions. The humid environment is incorporated using an implicit solvation model, enabling the evaluation of solvent-induced screening effects on molecule–surface interactions. Owing to the intrinsic out-of-plane polarization of α-In_2Se_3, the two surfaces of the monolayer exhibit markedly different adsorption characteristics. For all investigated molecules, adsorption is consistently stronger on the surface where the polarization is directed outward. Among the considered gases, NO exhibits the strongest interaction, followed by NO_2, CO, and H_2S. Electronic structure analysis reveals pronounced hybridization between molecular orbitals and surface states for NO adsorption, resulting in enhanced charge transfer and stronger electronic coupling. The presence of humidity further strengthens the adsorption interaction, leading to more negative adsorption energies and increased charge redistribution between the adsorbates and the substrate. These findings demonstrate that both ferroelectric surface polarization and environmental humidity play critical roles in governing molecular adsorption on α-In_2Se_3. The results provide valuable insight into the design of high-performance two-dimensional sensing platforms capable of operating under realistic environmental conditions.

Keyword: *Ferroelectric materials, α-In_2Se_3, Molecular sensing*

Effect of Ag, Mn, and Ni Doping on the Structural, Morphological, Optical, and Photo-luminescence Properties of ZnO Nanopowders

Hayrunnisa Özer * **, Büşra Mutlu, Şeyma Duman**

Bursa Technical University

Zinc oxide (ZnO) is one of the most widely investigated semiconductor materials owing to its unique structural, optical, and luminescence properties. The incorporation of suitable dopants into the ZnO lattice provides an effective approach for tailoring its physicochemical characteristics and enhancing its potential for optoelectronic applications. In this study, Ag-, Mn-, and Ni-doped ZnO nanopowders were synthesized by sol-gel method, and their structural, morphological, optical, and photoluminescence properties were comparatively investigated. The phase composition and crystallinity of the synthesized nanopowders were analyzed using X-ray diffraction (XRD), while scanning electron microscopy (SEM) was employed to evaluate their morphology and particle characteristics. Optical properties were examined by UV–Vis spectroscopy, and photoluminescence (PL) spectroscopy was used to investigate defect-related emissions and charge carrier recombination behavior. The results revealed that all synthesized nanopowders predominantly exhibited the characteristic crystalline structure of ZnO. The incorporation of Ag, Mn, and Ni dopants significantly influenced the crystallite size, morphology, and agglomeration behavior of the powders. Furthermore, notable variations in optical absorption and photoluminescence responses were observed depending on the dopant type, indicating changes in the defect structure and electronic properties of ZnO. These findings demonstrate that Ag, Mn, and Ni doping is an effective strategy for tailoring the structural, morphological, optical, and photoluminescence properties of ZnO nanopowders, thereby expanding their potential for future optoelectronic and sensing applications.

Keyword: *ZnO, optical properties, photoluminescence properties*

Anisotropy-Driven Evolution of Skyrmion and Meron Phases in Antiferromagnetically Coupled Bilayer Nanosystems

Gülşen Doğan * **, Ümit Akıncı**

Dokuz Eylül Univesity

Topological spin textures, including skyrmions and merons, have attracted significant interest due to their potential for energy-efficient spintronic technologies. This study investigates the evolution of topological magnetic phases in an antiferromagnetically coupled ferromagnetic bilayer through Monte Carlo simulations. The model includes intralayer ferromagnetic exchange, antiferromagnetic interlayer coupling, Dzyaloshinskii–Moriya interaction, magnetic anisotropy, and external magnetic fields.

The results indicate a diverse sequence of magnetic phases governed by the interplay among these interactions. Without an external magnetic field, increasing easy-plane anisotropy suppresses skyrmionic textures and facilitates the formation of meron–antimeron crystal phases. This progression is marked by distinct transitions in reciprocal space from 1Q spiral structures to 2Q meron lattices. Under finite magnetic fields, skyrmion-related textures remain stable across a wider parameter range. Nevertheless, the competition between Zeeman energy and easy-plane anisotropy produces frustrated multi-Q states and induces dimensional crossovers among 3Q, 2Q, and 1Q phases.

A distinctive characteristic of the bilayer system is the emergence of paired topological quasiparticles with opposite chirality in the two magnetic layers, resulting from antiferromagnetic interlayer coupling. Consequently, the system's total chirality is significantly reduced, while its nontrivial local topology is maintained. These findings demonstrate that magnetic anisotropy effectively controls the topology and dimensionality of spin textures in bilayer nanostructures, offering promising strategies for designing tunable topological states in future spintronic devices.

ORCID:
Gülşen Doğan: https://orcid.org/0000-0002-8122-9290
Ümit Akıncı: https://orcid.org/0000-0002-6349-0495

References:
Tony H. R. Skyrme, Nuclear Physics 31, 556–569 (1962).
A. N. Bogdanov and A. Hubert, Journal of Magnetism and Magnetic Materials 138, 255–269 (1994).
Yoshinori Tokura and Naoya Kanazawa, Chemical Reviews 121, 2857–2897 (2021).

Keyword: *Skyrmions*, *Merons*, *Bilayer Nanostructures*

Quantum Phase Mapping In A Two-Dimensional Quasiperiodic Spin-1 Bose-Hubbard Model Using Order Parameters

Süleyman Küçük [*1], **Bilal Tanatar**[1], **Saurabh Basu**[2]

[1] *Bilkent Üniversitesi*
[2] *IIT Guwahati*

Quantum Phase Mapping In A Two-Dimensional Quasiperiodic Spin-1 Bose-Hubbard Model Using Order Parameters

We investigate the quantum phases of interacting spin-1 bosons in a two-dimensional square lattice subjected to a deterministic moiré-type quasiperiodic potential. The system is described by an extended spin-1 Bose-Hubbard model including nearest-neighbor hopping, on-site density interactions, nearest-neighbor repulsion, and on-site spin-exchange interactions. Our main objective is to identify and characterize the many-body phases of the system through appropriate order parameters. We employ a site-resolved Gutzwiller mean-field approximation with a truncated local Fock basis and solve the resulting local Hamiltonians self-consistently. For each set of model parameters, we calculate the spin-resolved condensate amplitudes, local particle densities, total condensate amplitude, spin populations, and compressibility. The spatially averaged condensate amplitude is used to distinguish superfluid and insulating regimes, while the density distribution and compressibility are used to identify incompressible and spatially modulated phases. Spin-resolved observables provide additional information on how spin-exchange interactions influence the stability and internal structure of these phases. By examining these quantities as functions of hopping strength, chemical potential, quasiperiodic potential strength, nearest-neighbor interaction, and spin-dependent interaction, we construct phase diagrams and analyze the competition between superfluid coherence, interaction-driven localization, density ordering, and quasiperiodicity. This study provides a systematic framework for mapping quantum phases in tunable spinor bosonic lattice systems.

Acknowledgment:
The numerical calculations reported in this study were performed at TÜBİTAK ULAKBİM, High Performance and Grid Computing Center (TRUBA resources).

References:
S. Tsuchiya, S. Kurihara, and T. Kimura, “Mott Insulator Transition of Spin-1 Bosons in an Optical Lattice,” Physical Review A 70, 043628 (2004).
R. V. Pai, K. Sheshadri, and R. Pandit, “Phases and Transitions in the Spin-1 Bose-Hubbard Model: Systematics of a Mean-Field Theory,” Physical Review B 77, 014503 (2008).
A. Imambekov, M. Lukin, and E. Demler, “Spin-Exchange Interactions of Spin-One Bosons in Optical Lattices: Singlet, Nematic, and Dimerized Phases,” Physical Review A 68, 063602 (2003).
T. Kimura, S. Tsuchiya, and S. Kurihara, “Possibility of a First-Order Superfluid–Mott-Insulator Transition of Spinor Bosons in an Optical Lattice,” Physical Review Letters 94, 110403 (2005).
S. S. Natu, J. H. Pixley, and S. Das Sarma, “Static and Dynamic Properties of Interacting Spin-1 Bosons in an Optical Lattice,” Physical Review A 91, 043620 (2015).

Keyword: *Spin-1 Bose-Hubbard Model, Quasiperiodic Optical Lattices, Quantum Phase Diagrams*

ID: 52

Electrochemical Behavior of Galvonastatic and Potansiostatic Mode Electrodeposited Tungsten Oxide Thin Films for Electrochromic Applications

Nisa Damla Tekin * **, Gamze Atak**

Hacettepe University, Department of Physics Engineering, Beytepe Ankara Turkiye

Electrodeposition is a technique for depositing ionic materials as a thin film onto the surface of a conductive substrate immersed in a solution containing ionic species. Notably, electrodeposition is a simple, low-cost, environmentally friendly, and versatile technique suitable for large-area fabrication. In addition, electrodeposition enables the successful synthesis of metal oxides on various conductive substrates through the control of numerous deposition parameters. By adjusting factors such as the applied potential or current during film growth, the continuous or pulsed application mode of the potential or current, deposition time, electrolyte molarity, electrolyte pH, annealing temperature, and annealing duration, the optical, structural, and electrical properties of the films can be effectively tailored [1].

In this work, using a tungsten-containing electrolyte, a three-electrode electrochemical cell was assembled consisting of FTO-coated glass as the working electrode, a platinum wire as the counter electrode, and Ag/AgCl as the reference electrode. One of the WO_3 thin films was deposited in a pulsed potentiostatic mode, consisting of deposition steps (t_{on}) at −0.7 V for 0.2 s and relaxation steps (t_{off}) at 0 V for 0.5 s. The other film was deposited in galvanostatic mode by maintaining the current density at a constant value of 5 mA/cm^2.

As part of the characterization of the prepared films, film thicknesses were measured using a profilometer (~ 200 nm); surface morphology (pore density) and microstructural properties were examined by Scanning Electron Microscopy (SEM); optical spectra was analyzed by UV–VIS spectroscopy. The influence of deposition mode on morphology, optical modulation, ion diffusion kinetics, coloration efficiency, and memory effect was comprehensively evaluated.

Acknowledgment:
The authors want to thank the Scientific and Technological Research Council of Turkey (TÜBİTAK) for financial support with Project ID 223M337 and 2209-A - Research Project Support Programme for Undergraduate Students and Hacettepe University Scientific Research Projects Coordination Unit with Project ID FHD-2024-21270 and FKB-2024-21248.

References:
[1] Kwong W. L. 2014. Synthesis of Tungsten Oxide Thin Films For Photoelectrochemical Applications, University of New South Wales, Doctor of Philosophy in Materials Science and Engineering

Keyword: *electrodeposition, electrochromic, thin films*

ID: 156

Microstructured Thermally Drawn Triboelectric Fibers for Wearable Technologies

Maliha Rahman * **, Mustafa Ordu**

UNAM – National Nanotechnology Research Center and Institute of Materials Science and Nanotechnology, Bilkent University, Ankara 06800, Türkiye

Wearable fiber-based sensors have emerged as promising candidates for next generation human-machine interfaces and self-powered sensing systems. In this work, a thermally drawn multimaterial triboelectric fiber was developed using polyvinylidene fluoride (PVDF) as the triboelectric cladding and chlorinated polyethylene (CPE) as the core electrode. To enhance charge generation, microstructured grooves were introduced onto the PVDF surface, increasing the effective contact area during mechanical deformation. The multimaterial preform was fabricated through hot pressing and machining, followed by thermal drawing to produce continuous fibers while preserving the designed architecture. Electrical characterization revealed that the microstructured fiber generated an open circuit voltage of approximately 15 V at 5 Hz, nearly twice that of the non-structured fiber (approximately 7 V). To further improve performance, hexagonal boron nitride (hBN) particles were incorporated into the PVDF matrix. Composite films containing 0.5 wt% and 1 wt% hBN exhibited the highest triboelectric output, generating approximately 50 V, which was nearly twice the output obtained from the 1.5 wt% and 2 wt% hBN loaded films (approximately 25 V). This enhancement can be attributed to the improved interfacial polarization and increased β phase formation of PVDF at lower hBN concentrations. Although low hBN concentrations improved the triboelectric performance, hBN loadings above 1 wt% resulted in a noticeable decrease in electrical output. This reduction is attributed to nanoparticle agglomeration, which restricts polymer chain mobility, suppresses β phase formation, and hinders effective charge generation within the PVDF matrix. Owing to their high electrical output, stability and self-powered operation, the developed triboelectric fibers show strong potential for wearable gesture monitoring and sign language recognition applications.

Keyword: *Thermally Drawn Fibers, Microstructured Surface, Wearable Technology*

Biocompatible and Wearable ZnO-Coated Hemp Woven Fabrics for Lightweight Electromagnetic Shielding in Defense Applications

Melisa Atay [*] [1,2], **Metin Yurddaskal**[2,3,4], **Mehmet Korkmaz**[5]

[1] *The Graduate School of Natural and Applied Sciences, Dokuz Eylul University, 35390 Izmir, Turkey*
[2] *Department of Nanoscience and Nanoengineering, Dokuz Eylul University, Izmir 35390, Turkey*
[3] *Department of Metallurgical and Materials Engineering, Dokuz Eylul University, Izmir 35390, Turkey*
[4] *Center for Fabrication and Application of Electronic Materials, Dokuz Eylul University, Izmir 35390, Turkey*
[5] *Department of Textile Engineering, Dokuz Eylul University, Izmir 35390, Turkey*

Electromagnetic interference (EMI) has become a critical challenge for modern defence platforms, including military communication systems, unmanned aerial vehicles, radar components, and wearable soldier electronics. Conventional metallic shielding materials provide high shielding effectiveness but suffer from disadvantages such as high density, corrosion susceptibility, and secondary electromagnetic reflections. In this study, a sustainable and lightweight alternative shielding textile based on hemp fabrics coated with zinc oxide (ZnO) nanoparticles was developed and evaluated for defence-oriented electromagnetic shielding applications. ZnO nanoparticles were synthesised via a sol–gel route using zinc chloride precursor and subsequently calcined at 500 °C. Structural characterisation confirmed the formation of contamination-free wurtzite ZnO nanoparticles with particle dimensions below 100 nm. Woven hemp fabrics were produced from 250 tex hemp yarns and modified through a low-temperature, environmentally friendly sol–gel finishing process. Owing to the intrinsically hydrophilic structure and high affinity of hemp fibers, ZnO nanoparticles were effectively immobilised on the textile surface without requiring complex chemical treatments. Electromagnetic shielding effectiveness (EMSE) measurements were performed in the X-band frequency range (8–12 GHz) using a vector network analyser. The untreated hemp fabric exhibited only limited shielding capability, whereas ZnO-coated hemp fabrics demonstrated a significant improvement in shielding performance. The developed nanocomposite textile achieved EMSE values ranging approximately from 37 to 39 dB across the investigated frequency range, surpassing the performance of conductive-thread-based fabrics reported within the same study. The obtained results indicate that ZnO-functionalized hemp textiles can provide effective attenuation of incident electromagnetic radiation while maintaining the lightweight, flexible, and sustainable characteristics of natural-fiber-based materials. The combination of renewable hemp fibers and nanoscale ZnO reinforcement offers a promising route toward next-generation stealth-compatible protective textiles, electromagnetic shielding garments, military shelters, and lightweight defence structures. The proposed material system demonstrates significant potential as a metal-free shielding platform for future defence and aerospace applications.

ORCID:
Melisa Atay: 0000-0003-4982-9963
Metin Yurddaskal: 0000-0001-7293-1216
Mehmet Korkmaz: 0000-0001-7000-0653

References:

Suresha, R., Chandra, J. R., Prabhu, N. N., Sachidananda, H. K., George, G., Parasuram, S., & Shivamurthy, B. (2025). Electrospun Ni-doped ZnO nanofiber coatings on carbon fabric for enhanced electromagnetic interference shielding. Scientific Reports, 15(1), 44708.
Arab, K., Sheikhzade, M. H., Fakhri, V., Naqvi, M., Dare, M. T., Jafari, A., ... & Khonakdar, H. A. (2026). Advanced conductive textiles: from nanomaterial integration to wearable applications. Advanced Composites and Hybrid Materials.
Klaykruayat, B., Pisitsak, P., Chitichotpanya, P., & Klanthip, R. (2025). In Situ Synthesis of ZnO Nanoparticles Using Soy Protein Isolate for Sustainable and Multifunctional Finishing of Hemp Fabrics. Polymers, 18(1), 116.

Keyword: *electromagnetic shielding, hemp woven fabrics, ZnO nanoparticles*

Myxinidin-Loaded UiO-66-NH_2 MOFs for Enhanced Antimicrobial Activity and Wound Healing

Bilge Ölçeroğlu [*1], Şahika Sena Bayazit[1], Ahmet Katı[2], Fırat Barış Barlas[1]

[1] *Istanbul University-Cerrahpasa, Institue of Nanotechnology and Biotechnology, Istanbul, Türkiye*
[2] *Department of Biotechnology, Institute of Health Sciences, University of Health Sciences, Istanbul, Türkiye*

The rapid increase in antibiotic-resistant pathogens has created an urgent need for alternative antimicrobial strategies, positioning antimicrobial peptides (AMPs) as promising therapeutic agents (1). Among these, Myxinidin (Myx), a short cationic AMP derived from Myxine glutinosa, exhibits broad-spectrum antimicrobial activity, high salt tolerance, and minimal hemolytic effects. However, its clinical translation remains limited due to poor stability, susceptibility to proteolytic degradation, and low bioavailability (2,3).

In this study, a nanobiotechnology-based approach was developed to overcome these limitations by covalently conjugating Myx onto UiO-66-NH_2 metal–organic frameworks (MOFs). Recombinant Myx was successfully expressed in Escherichia coli Rosetta (DE3) using the pET28(a) expression system and purified via Ni-NTA affinity chromatography. UiO-66-NH_2 nanoparticles were synthesized through a hydrothermal method and subsequently functionalized with Myx using EDC/NHS-mediated coupling, resulting in stable nanoscale conjugates. Structural and physicochemical characterization by X-ray diffraction (XRD), Fourier-transform infrared spectroscopy (FT-IR), scanning electron microscopy (SEM), and dynamic light scattering (DLS) confirmed high crystallinity, successful amine functionalization, and an increase in particle size upon peptide conjugation.

The antimicrobial activity of the developed system was evaluated against Escherichia coli and Staphylococcus aureus. Free Myx exhibited minimum inhibitory concentration (MIC) values of 9.18 µM and 6.37 µM, respectively. Notably, the UiO-66-NH_2–Myx conjugate demonstrated significantly enhanced antibacterial efficacy, with reduced MIC values of 1.71 µM for E. coli and 1.08 µM for S. aureus, along with a clear dose-dependent bactericidal effect. These findings indicate that covalent immobilization of the peptide onto the MOF surface not only stabilizes the peptide but also potentiates its antimicrobial activity.

Biocompatibility studies performed on L929 fibroblast cells revealed that while bare UiO-66-NH_2 nanoparticles exhibited cytotoxic effects, the conjugated system significantly improved cell viability and even promoted cell proliferation. Furthermore, fluorescence microscopy confirmed enhanced cellular uptake of the conjugate compared to the free peptide. In vitro scratch wound healing assays demonstrated that the UiO-66-NH_2–Myx system achieved complete wound closure within 48 hours, outperforming the free peptide and indicating a more sustained and controlled therapeutic effect.

Overall, this study presents a novel covalent AMP–MOF conjugation strategy that enhances peptide stability, antimicrobial efficacy, and wound healing capacity. The UiO-66-NH_2–Myx nanoplatform emerges as a promising candidate for combating multidrug-resistant infections while simultaneously supporting tissue regeneration, highlighting its potential for advanced biomedical and translational applications.

Acknowledgment:
The authors gratefully acknowledge the use of BioRender, VESTA 3, and Reaxys software for figure preparation, structural visualization, data analysis, and literature search. ChatGPT (OpenAI) was used to assist in language editing. This work was financially supported by The Scientific and Technological Research Council of Turkey (TÜBİTAK) under project number 22AG067. The authors thank all contributors who provided valuable input to this study.

ORCID:
Bilge Ölçeroğlu: https://orcid.org/0009-0009-4025-341X
Şahika Sena Bayazit: https://orcid.org/0000-0001-9643-4855
Ahmet Katı: https://orcid.org/0000-0002-9903-634X
Fırat Barış Barlas: https://orcid.org/0000-0001-6401-686X

References:
Ölçeroğlu, B., Filiz, A., Çiçek, Ş., Filiz, M., Katı, A., & Barlas, F. B. (2026). Nanocarrier-enabled antimicrobial peptides: Current progress, delivery strategies, and translational challenges. Colloids and Surfaces B: Biointerfaces, 265, 115679. https://doi.org/10.1016/j.colsurfb.2026.115679
Cantisani, M., Leone, M., Mignogna, E., Kampanaraki, K., Falanga, A., Morelli, G., Galdiero, M., & Galdiero, S. (2013). Structure-activity relations of myxinidin, an antibacterial peptide derived from the epidermal mucus of hagfish. Antimicrobial agents and chemotherapy, 57(11), 5665–5673. https://doi.org/10.1128/AAC.01341-13
Subramanian, S., Ross, N. W., & MacKinnon, S. L. (2009). Myxinidin, a novel antimicrobial peptide from the epidermal mucus of hagfish, Myxine glutinosa L. Marine biotechnology (New York, N.Y.), 11(6), 748–757. https://doi.org/10.1007/s10126-009-9189-y

Keyword: *Antimicrobial peptides, myxinidin, UiO-66-NH_2 metal–organic frameworks*

Targeted Lipid–Polymer Hybrid Nanoparticles Co-Loaded with 5-Fluorouracil and Surface-Conjugated Tocilizumab for Oral Squamous Cell Carcinoma: An In Vitro Therapeutic Evaluation

Ezgi Özdemir * [1], Demet Cansaran Duman[1], Tuğrul Mert Serim[2], Gülin Amasya[2], Pelin Mutlu[1]

[1] *Ankara University, Institute of Biotechnology, Ankara, Türkiye*
[2] *Ankara University, Faculty of Pharmacy, Department of Pharmaceutical Technology, Ankara, Türkiye*

Oral squamous cell carcinoma (OSCC) remains one of the most prevalent and aggressive malignancies of the head and neck, while the clinical efficacy of conventional chemotherapy is frequently limited by systemic toxicity, poor tumor selectivity, and therapeutic resistance (1, 2). Targeted nanocarrier systems capable of simultaneously enhancing drug delivery and modulating tumor-associated signaling pathways represent a promising strategy to overcome these limitations (3, 4). Therefore, this study aimed to evaluate the in vitro therapeutic effect of a lipid–polymer hybrid nanoparticle (LPHN) system encapsulating 5-fluorouracil (5-FU) and surface-conjugated with the anti-IL-6 receptor monoclonal antibody tocilizumab for targeted treatment of OSCC. Biological performance was assessed using two-dimensional cultures of human oral squamous cell carcinoma (OSC-19) cells and normal gingival fibroblasts (HGF-1). Cellular uptake, real-time cytotoxicity, flow cytometric cell viability and apoptosis, invasion and migration assays were performed to evaluate the therapeutic effect of the targeted nanocarrier. The developed nanoparticle system demonstrated efficient cellular internalization, with enhanced uptake following tocilizumab conjugation. Compared with free 5-FU, dual-functional 5-FU and tocilizumab formulation decreased the IC_{50} concentration in OSC-19 cells from 204 μM to 1.2 μM, indicating a remarkable enhancement of therapeutic potency. Moreover, the targeted formulation induced more than 90% apoptotic cell death in OSC-19 cells while causing only approximately 16% apoptosis in normal gingival fibroblasts, demonstrating pronounced cancer selectivity. In addition, the treatment significantly suppressed the invasive and migratory capacities of OSC-19 cells. These findings demonstrate that tocilizumab-conjugated 5-FU-loaded lipid–polymer hybrid nanoparticles constitute a promising targeted nanotherapeutic platform for OSCC, offering enhanced therapeutic effect, improved cancer selectivity for precision nanomedicine.

Acknowledgment:
This research was funded by the TUBİTAK Project no 124S815.

ORCID:
Ezgi Özdemir: 0009-0006-3888-6347
Demet Cansaran Duman: 0000-0001-5662-2333
Tuğrul Mert Serim: 0000-0002-7857-6232
Gülin Amasya: 0000-0002-0491-450X
Pelin Mutlu: 0000-0001-7970-880X

References:
1. Azevedo A, Coelho MP, Pinho JO, Soares PIP, Reis CP, Borges JP, et al. An alternative hybrid lipid nanosystem combining cytotoxic and magnetic properties as a tool to potentiate antitumor effect of 5-fluorouracil. Life Sci. 2024. doi:10.1016/J.LFS.2024.122558
2. Goda H, Okamoto M, Nakashiro KI, Tokuzen N, Hamakawa H. 7PAnti-interleukin-6 receptor antibody suppressed oral squamous cell carcinoma by inhibiting tumor-stroma interaction. Annals of Oncology. 2015. doi:10.1093/ANNONC/MDV517.07
3. Coletta RD, Yeudall WA, Salo T. Current trends on prevalence, risk factors and prevention of oral cancer. Frontiers in Oral Health. 2024. doi:10.3389/froh.2024.1505833
4. Chaudhary AA, Fareed M, Khan SUD, Alneghery LM, Aslam M, Alex A, et al. Exploring the therapeutic potential of lipid-based nanoparticles in the management of oral squamous cell carcinoma. Open Exploration. 2019. doi:10.37349/ETAT.2024.00272

Keyword: *Oral squamous cell carcinoma; Lipid–polymer hybrid nanoparticles; 5-Fluorouracil; Tocilizumab; Targeted drug deliver*

Investigation of the Effects of Niosomal Forms of Passiflora incarnata Plant Extracts on Alzheimer's Disease Under In Vitro Conditions

Şevval Çiçek [*1], Bilge Ölçeroğlu[1], Alper Filiz[1], Pınar Siyah[2], Kartal Çetintürk[3], Fırat Barış Barlas[1]

[1] *Istanbul University-Cerrahpaşa, Institute of Nanotechnology and Biotechnology,34500, Istanbul, Türkiye*
[2] *Bahcesehir University, School of Pharmacy, 34353, Istanbul, Türkiye*
[3] *Altium International, Inc., R&D Laboratory, Ataşehir, 34746, Istanbul, Türkiye*

Alzheimer's disease (AD) is a progressive neurodegenerative disorder characterized by multifactorial pathological mechanisms, including amyloid-beta (Aβ) plaque accumulation, tau hyperphosphorylation, oxidative stress, and neuroinflammation[1]. Current therapies are primarily symptomatic and demonstrate limited efficacy in halting or slowing disease progression, emphasizing the urgent need for safe, effective, and multi-target therapeutic strategies[2].

This study aims to evaluate bioactive compounds, particularly alkaloids and flavonoids (vitexin, isovitexin, etc.), derived from Passiflora incarnata as potential therapeutic agents for AD[3]. Comprehensive phytochemical profiling using Gas Chromatography–Mass Spectrometry (GC–MS) and Liquid Chromatography–Electrospray Ionization–Quadrupole Time-of-Flight Tandem Mass Spectrometry (LC-ESI-QTOF-MS/MS) led to the identification of 23 and 21 significant compounds, respectively. The identified constituents were predominantly phenolic compounds, along with alkaloids, vitamins (B5 and B6), phenolic glycosides, nucleosides, cyanogenic glycosides, β-blocker-like structures, dicarboxylic acids, and neuroactive secondary metabolites[3]. In silico molecular docking analyses revealed strong binding affinities of these compounds toward Monoamine Oxidase A and B (MAO-A/B), enzymes critically involved in AD pathogenesis. Several ligands demonstrated binding energies comparable to or exceeding those of standard inhibitors such as toloxatone, harmine, rasagiline, clorgyline, and pargyline. Notably, one compound exhibited a high binding affinity toward MAO-B (−9.279 kcal/mol), indicating a strong inhibitory potential. Furthermore, QSAR-based toxicity assessments predicted low cytotoxic, carcinogenic, cardiotoxic, genotoxic, and neurotoxic risks. All compounds complied with Lipinski's Rule of Five, suggesting favorable pharmacokinetic properties and oral bioavailability. Therapeutic potential predictions indicated moderate to high efficacy, particularly against AD and Parkinson's disease[4].

To overcome limitations such as low bioavailability and poor blood–brain barrier permeability, niosomal nanovesicular drug delivery systems will be developed. Alkaloid and flavonoid fractions will be extracted using optimized solvent systems, purified via column chromatography and HPLC, and encapsulated into niosomes composed of Tween 61, cholesterol, and DSPE-PEG(2000)-Amine using the thin-film hydration method. Physicochemical characterization will include particle size and zeta potential (DLS), morphology (SEM), molecular interactions (FTIR), and encapsulation efficiency (UV–Vis spectrophotometry)[5].

Biological activities will be evaluated in SH-SY5Y and U87 cell lines using assays for cell viability (MTT), apoptosis (flow cytometry), MAO-A/B inhibition (ELISA), oxidative stress (ROS measurement), cellular uptake, and scratch-wound healing. Overall, this study demonstrates the multi-target neuroprotective potential of Passiflora incarnata and proposes a nanotechnology-based approach for the development of innovative and targeted therapeutic strategies for AD.

Acknowledgment:
The author would like to express sincere gratitude to the Scientific and Technological Research Council of Türkiye (TÜBİTAK) for financial support under the 2210-C Priority Areas Scholarship Program for Master's Students, and to the Scientific Research Projects Coordination Unit (BAP) of Istanbul University-Cerrahpaşa for their valuable support.

ORCID:
Şevval Çiçek: 0009-0005-4771-9009

References:
L. A. Ahmed and H. Sharmah, "A Concise Review of Synthetic Xanthone Derivatives for Alzheimer's Disease," Brain Disord., p. 100256, Jul. 2025, doi: 10.1016/j.dscb.2025.100256.
Y. Gu, Z. Zhao, F. Xue, and Y. Zhang, "Alginate-Chitosan Coated Nanoliposomes as Effective Delivery Systems for Bamboo Leaf Flavonoids: Characterization, In Vitro Release, Skin Permeation and Anti-Senescence Activity," Antioxidants, vol. 11, no. 5, p. 1024, May 2022, doi: 10.3390/ANTIOX11051024/S1.
J. Li, H. Liu, M. S. Mazhar, S. Quddus, and H. A. R. Suleria, "LC-ESI-QTOF-MS/MS profiling of phenolic compounds in Australian native plums and their potential antioxidant activities," Food Biosci., vol. 52, p. 102331, Apr. 2023, doi: 10.1016/j.fbio.2022.102331
P. Siyah, S. Durdagi, and B. Aksoydan, "Discovery of potential PD-L1 small molecule inhibitors as novel cancer therapeutics using machine learning-based QSAR models: A virtual drug repurposing study," Biophys. J., vol. 122, no. 3, p. 144a, Feb. 2023, doi: 10.1016/j.bpj.2022.11.942
F. B. Barlas et al., "Enhancing chemotherapeutic efficacy: Niosome-encapsulated Dox-Cis with MUC -1 aptamer," Cancer Med., vol. 13, no. 15, Aug. 2024, doi: 10.1002/cam4.70079.

Keyword: *Alzheimer's Disease, Passiflora incarnata, Niosomes*

ID: 432

Nanoscale Adhesion Forces of Naturally Dispersed Bacteria from Biofilms of Different Ages Measured by Atomic Force Microscopy

Buse Ece Burgaz Oral * **, Fatma Pinar Gordesli Duatepe**

Graduate School, Bioengineering Program, Izmir University of Economics

Biofilm dispersal represents the final stage of the biofilm life cycle, during which sessile bacteria detach and re-enter a free living state. Cells released during dispersal are phenotypically distinct from both planktonic and biofilm cells [1], yet their surface properties and adhesive behavior at the nanoscale remain poorly characterized. This study investigated whether biofilm age influences the adhesion forces of naturally dispersed bacteria, as measured by atomic force microscopy (AFM) in liquid environment.

Biofilms were cultivated in well plates in Luria-Bertani broth (LB) under shaking conditions for either 17 or 24 hours. Non-adherent and loosely attached cells were removed by washing, and fresh LB medium was subsequently introduced to both groups. After an additional 24-hour incubation period to allow natural dispersal, the bacteria released into the medium were collected by centrifugation and immobilized onto poly-L-lysine (PLL) coated mica discs [2]. Single cell adhesion force measurements were performed in water using silicon nitride tips in contact mode AFM, generating force-distance curves from which adhesion forces were extracted.

The results revealed a clear age-dependent difference in nanoscale adhesion behavior. Naturally dispersed cells from 24-hour biofilms exhibited approximately 2-fold higher mean adhesion forces and approximately 3-fold higher median adhesion forces compared to those from 17-hour biofilms. These preliminary findings suggest that biofilm age significantly shapes the surface properties of dispersed cells, potentially affecting their capacity to adhere and initiate new biofilm formation on surfaces. This work is ongoing, and a larger force curve dataset is currently being analyzed to further support these results.

ORCID:
Fatma Pinar Gordesli Duatepe: 0000-0001-8129-6533

References:
Chua SL, Liu Y, Yam JK, Chen Y, Vejborg RM, Tan BG, Kjelleberg S, Tolker-Nielsen T, Givskov M, Yang L. Dispersed cells represent a distinct stage in the transition from bacterial biofilm to planktonic lifestyles. Nat Commun. 2014 Jul 21;5:4462. doi: 10.1038/ncomms5462.
Ordek A, Gordesli-Duatepe FP. Impact of sodium nitroprusside concentration added to batch cultures of Escherichia coli biofilms on the c-di-GMP levels, morphologies and adhesion of biofilm-dispersed cells. Biofouling. 2022 Sep;38(8):796-813. doi: 10.1080/08927014.2022.2131399.

Keyword: *Biofilm dispersal, Adhesion force, Atomic force microscopy*

Size-Based Protein Separation via Capillary Flow on AKD-Hydrophobized Paper Gradients: An Equipment-Free Alternative to Electrophoresis

Tolga Erdoğan [*1,2], **Emine Güler Çelik**[3,4]

[1] *Ege University, Graduate School of Natural and Applied Sciences, Department of Bioengineering*
[2] *ERAS Innovation and Advanced Engineering Technologies Inc.*
[3] *Ege University, Faculty of Engineering, Department of Bioengineering*
[4] *Ege Science Pro Scientific Research Inc.*

Traditional gel electrophoresis methods used in biomolecular separation present significant limitations, including high costs, toxic chemical requirements, and operational difficulties. To overcome these barriers, this study aimed to develop a novel paper-based microfluidic platform (µPAD) based on Alkyl Ketene Dimer (AKD) modification that utilizes capillary flow dynamics and requires no external power source. In this study, various commercial cellulose substrate materials were hydrophobized with AKD at varying concentrations to modulate their effective pore sizes. The size-based sieving capacity of the developed platform was evaluated using an AKD concentration gradient. Model proteins with distinct molecular weights (Bovine Serum Albumin and Immunoglobulin G) were utilized to test the separation efficiency. Optimization experiments demonstrated that an increase in AKD concentration successfully hydrophobized the paper surface while physically narrowing the effective pore size. Among the tested materials, the substrate providing the widest hydrophobic operating window alongside the lowest non-specific protein binding rate was selected for the gradient design. Quantitative image analysis of the designed strips revealed a distinct size-based separation pattern: larger protein molecules were retained in the early stages of the gradient, whereas smaller protein molecules were transported significantly further along the capillary flow path. This study presents a successful proof-of-concept for size-based protein separation using capillary force and surface engineering. By eliminating the need for electrical power and toxic reagents, this low-cost and portable system holds high potential as a rapid pre-screening tool in point-of-care (PoC) testing and resource-limited field conditions.

ORCID:
Tolga Erdoğan: 0000-0002-3396-6552
Emine Güler Çelik: 0000-0003-2381-9775

Keyword: *Paper-based microfluidics, alkyl ketene dimer, size-based protein separation*

Ionic Liquid-Based Molecularly Imprinted Magnetic Nanocomposites for Selective Biomarker Recognition

Ozge Ozufuklar [*1], Aysenur Yardim[2], Veysel Ceyirdekci[2,3], Faezeh Ghorbanizamani[4], Hichem Moulahoum[4], Tuncay Goksel[5], Suna Timur[4], Emine Guler Celik[6]

[1] Department of Biotechnology, Institute of Natural Science, Ege University,Izmir, Türkiye
[2] Department of Bioengineering, Institute of Natural Science, Ege University,Izmir, Türkiye
[3] Ege Science Pro Scientific Research Inc., Izmir, Türkiye
[4] Department of Biochemistry, Faculty of Science, Ege University,İzmir, Türkiye
[5] Department of Pulmonary Medicine, Faculty of Medicine, Ege University,Izmir, Türkiye
[6] Department of Bioengineering, Faculty of Engineering, Ege University,Izmir, Türkiye

Molecularly imprinted polymers (MIPs) have attracted significant attention as artificial recognition materials due to their high selectivity, chemical stability, and low-cost fabrication[1]. However, conventional MIP systems may exhibit limited conductivity, insufficient surface interactions, and reduced performance in complex biological environments[2]. To overcome these limitations, combining ionic liquids (ILs) and magnetic nanoparticles (MNPs) with MIP systems has become a promising approach for developing advanced functional nanocomposites. In this study, an IL-based molecularly imprinted MNP platform was developed as a multifunctional recognition material[3]. The designed nanocomposite integrates ionic ILs, molecular imprinting technology, and MNPs to combine selective molecular recognition with magnetic enrichment potential and enhanced surface properties. IL is expected to enhance intermolecular interactions, improve stability, and create a favorable microenvironment, while the magnetic structure enables rapid phase separation and pre-concentration[4]. All synthesized nanostructures were characterized using NMR, FTIR, and SEM analyses. In addition, the electrochemical behavior of the developed platform was investigated using electrochemical impedance spectroscopy (EIS), differential pulse voltammetry (DPV), and cyclic voltammetry (CV) techniques. In addition, ESAT-6, a well-known tuberculosis biomarker secreted by Mycobacterium tuberculosis, was used as a model template molecule to demonstrate the biomarker recognition capability of the developed nanocomposite platform. By integrating ILs, MIP technology, and magnetic nanostructures into a single platform, this approach provides reusable functional surfaces with selective recognition for advanced bioanalytical applications.

This work is supported by the TUBİTAK 2515-COST Programme (Project No: 224Z038) under the framework of COST Action CA21164 – Towards an Improvement in Diagnostics and Treatment Strategies for TB Control (ADVANCE-TB)

References:

Cui, F., Zhou, Z., Zhou, H. S. 2020. “Molecularly Imprinted Polymers and Surface Imprinted Polymers Based Electrochemical Biosensor for Infectious Diseases”. Sensors, 20(4), 996.
Hasseb, A. A., Abdel Ghani, N. D. T., Shehab, O. R., El Nashar, R. M. 2022. “Application of molecularly imprinted polymers for electrochemical detection of some important biomedical markers and pathogens”. Current Opinion in Electrochemistry, 31, 100848.
Ding, S., Lyu, Z., Niu, X., Zhou, Y., Liu, D., Falahati, M., Lin, Y. 2020. “Integrating ionic liquids with molecular imprinting technology for biorecognition and biosensing: A review”. Biosensors and Bioelectronics, 149, 111830.
Xu, W., Dai, Q., Wang, Y., Hu, X., Xu, P., Ni, R., Meng, J. 2018. “Creating magnetic ionic liquid-molecularly imprinted polymers for selective extraction of lysozyme”. RSC Advances, 8(39), 21850–21856.

Keyword: *Molecularly Imprinted Polymer (MIP), Ionic Liquid, Nanocomposite Platform*

ID: 154

Magnetic Soft Composite Fibers for Actuation, and Energy Harvesting

Sk. Rahat Ali * **, Mustafa Ordu**

UNAM – National Nanotechnology Research Center and Institute of Materials Science and Nanotechnology, Bilkent University, Ankara 06800, Türkiye

Soft magnetic actuators with high stretchability and strong magnetic responsiveness are essential for next-generation wearable devices and biomedical robotic systems. Here, we introduce a highly stretchable magnetic composite fiber fabricated using a thermal drawing technique. The fiber has a diameter of approximately 1 mm and was successfully produced with a high neodymium-iron-boron (NdFeB) magnetic filler content of up to 70 wt%. The fabricated fiber exhibits an elongation of up to 300%, demonstrating excellent mechanical compliance. Directional magnetization was achieved using an impulse magnetizer, resulting in a uniformly magnetized cylindrical fiber with an external magnetic field of nearly 30 mT. Owing to its high stretchability and magnetic loading, the fiber shows promising potential for soft robotic actuation and energy-harvesting applications. Under an external magnetic field, the fiber can be guided through complex paths. In addition, its magnetoelastic response enables the generation of an output voltage of nearly 1 V and an output current of approximately 1 µA. These results indicate that the thermally drawn magnetic composite fiber is a promising platform for future soft systems, including magnetically driven biomedical devices, wearable biomechanical sensors, and wearable energy harvesters.

Keyword: *Thermal drawing, Magnetoelasticity, Energy harvesting*

Post-Consumer Waste-Derived Graphene Nano Sheets with Recovered Carbon Fibers from Automotive Composite Wastes and Their Reintegration into PP Composites

Ozgenur Parmaksiz [* 1,2], Havva Baskan Bayrak[1], Israr Ahmed[3], Ebrahim Al Hajri[4], Yarjan Abdul Samad[3,5], Burcu Saner Okan[1,2]

[1] Sabanci University Integrated Manufacturing Technologies Research and Application Center & Composite Technologies Center of Excellence, Teknopark Istanbul, Pendik, 34906, Istanbul, Turkey

[2] Faculty of Engineering and Natural Sciences, Materials Science and Nanoengineering, Sabanci University, Tuzla, 34956, Istanbul, Turkey

[3] Department of Aerospace Engineering, Khalifa University, 127788, Abu Dhabi, United Arab Emirates

[4] Department of Mechanical Engineering Khalifa University 127788 Abu Dhabi United Arab Emirates

[5] Research and Innovation Center for Graphene and 2D Materials (RIC2D), Khalifa University, 127788, Abu Dhabi, United Arab Emirates

Plastics are deeply embedded in modern society, with annual global production exceeding 400 million tonnes. Commodity and engineering thermoplastics constitute a major share of this production and are widely used in packaging, construction, consumer goods, automotive components, and fiber-reinforced composites. Their extensive use, however, generates substantial plastic waste, emphasizing the need for sustainable recycling and upcycling strategies. In parallel, the automotive industry faces an increasing sustainability challenge associated with carbon fiber-reinforced polymer (CFRP) wastes, whose direct reincorporation into structural composites remains limited by material degradation, interfacial incompatibility, and reduced load-bearing performance. In this study, an upcycling strategy is introduced in which waste high-density polyethylene (HDPE) and waste polyamide 66 (PA66) are converted into graphene nanosheets (GNSs) through feedstock-sensitive catalytic carbonization, while carbon fibers are recovered from CFRP wastes. To demonstrate closed-loop feasibility, polypropylene (PP) compounds representative of automotive structural applications were prepared using recovered carbon fibers (rCF) and waste-derived GNSs as reinforcing additives. The incorporation of 1 wt.% (HDPE + PA66)-GNS increased the flexural strength by 15.66% compared with neat PP, while the addition of 15 wt.% rCF enhanced the tensile modulus by 70.73%, confirming their reinforcing efficiency in structural PP matrices. The structural, chemical, morphological, and thermal properties of the upcycled GNSs, rCF, and composite interfaces were evaluated by Raman spectroscopy, X-ray diffraction (XRD), X-ray photoelectron spectroscopy (XPS), scanning electron microscopy (SEM), high-resolution transmission electron microscopy (HRTEM), and thermogravimetric analysis (TGA). Finally, a cradle-to-gate life cycle assessment (LCA) was performed to quantify the carbon footprint of the proposed route. Compared with conventional reduced graphene oxide (rGO) production, the proposed upcycling route reduced the global warming potential (GWP) by approximately 99%, highlighting its strong environmental advantage for producing waste-derived (HDPE + PA66)-GNS. By transforming plastic and CFRP wastes into high-value reinforcing additives, this strategy offers a promising route toward circular and sustainable composite manufacturing.

ORCID:
Ozgenur Parmaksiz: https://orcid.org/0009-0002-1720-9567
Ozgenur Parmaksiz: https://orcid.org/0009-0002-1720-9567
Havva Baskan Bayrak: https://orcid.org/0000-0002-8635-666X
Israr Ahmed: https://orcid.org/0009-0003-3945-2055
Ebrahim Al Hajri: https://orcid.org/0000-0001-8024-6606
Yarjan Abdul Samad: https://orcid.org/0000-0001-9323-4807
Yarjan Abdul Samad: https://orcid.org/0000-0001-9323-4807
Burcu Saner Okan: https://orcid.org/0000-0002-5940-7345
Burcu Saner Okan: https://orcid.org/0000-0002-5940-7345

Keyword: *Waste-derived graphene nanosheets, recovered carbon fibers, sustainable polypropylene composites*

Synthesis and Characterization of Boron Nitride Fibers

Yelda Yorulmaz [*1], **Onur Zırhlı**[1], **Deniz Köken**[2], **Fevzi Ç. Cebeci**[3]

[1] *Faculty of Engineering and Natural Sciences Sabancı University*
[2] *Turkish Aerospace*
[3] *Faculty of Engineering and Natural Sciences Sabancı University, SUNUM Nanotechnology Research Center*

Boron nitride materials, which are structural analogues of carbon-based materials, have attracted attention due to their chemical and thermal stability, electrical insulation, thermal conductivity, low dielectric constant, mechanical strength, piezoelectric properties, and unique adsorption capabilities. Moreover, these materials can form different geometric configurations, such as nanosheets (2D), nanotubes (1D), fibers (1D), foams (3D), and nanospheres (0D) while retaining these unique properties[1, 2].

In this study, boron nitride fibers were synthesized through an established melamine–boric acid precursor route and characterized to evaluate the effect of different freeze-drying temperatures on the resulting fiber morphology, structure, and porosity. Melamine and boric acid were dissolved in deionized water, stirred at 85 °C, quenched with liquid nitrogen, and freeze-dried at either −55 °C or −97 °C to obtain melamine diborate precursor structures. The precursors were subsequently pyrolyzed at 1100 °C under argon flow to form boron nitride fibers (BNF)[2, 3]. The synthesized fibers (BNF55 and BNF97) were investigated by different characterization techniques. XRD, FTIR and Raman spectroscopy were utilized to confirm boron nitride formation. Additionally, XRD results were used for further structural analysis and results showed that synthesized fibers had different structural ordering compared to commercial h-BN. SEM images confirmed both samples exhibited fiber morphology with comparable width differences. BET analysis showed that the synthesized fibers exhibited higher specific surface areas than commercial h-BN. These results demonstrate that freeze-drying temperature is an effective processing parameter for tuning boron nitride fiber properties, making these materials promising candidates for functional nanomaterial and nanocomposite applications.

ORCID:
Yelda Yorulmaz: 0000-0003-1358-9769

References:
[1]Lu, Y., et al., Boron nitride nanotubes and nanosheets: Their basic properties, synthesis, and some of applications. Diamond and Related Materials, 2023. 136: p. 109978.
[2]Wu, C., et al., Molecular-scale understanding on the structure evolution from melamine diborate supramolecule to boron nitride fibers. Ceramics International, 2020. 46(1): p. 1083-1090.
[3]Köken, D., H-BN nanostructures; synthesis and applications.

Keyword: *Boron nitride fibers, freeze-drying-assisted synthesis*

Tuning Ionic Transport in Electrospun SPEEK Nanofiber Separators with Boron Nitride Nanostructures for Structural Lithium Batteries

Onur Zırhlı [*1], Yelda Yorulmaz[1], Deniz Köken[2], Fevzi Ç. Cebeci[3]

[1] *Faculty of Engineering and Natural Sciences Sabancı University*
[2] *Turkish Aerospace*
[3] *Faculty of Engineering and Natural Sciences Sabancı University, SUNUM Nanotechnology Research Center*

Lithium-based structural batteries require separators that maintain steady ionic transport yet stay mechanically and dimensionally intact throughout consolidation and subsequent in-service loads [1]. Polyolefin separators in commercial cells are electrically insulating but offer limited electrolyte wettability and modest thermal and dimensional stability, whereas ionomer membranes whose ion exchange capacity (IEC) is high tend to swell and soften excessively, which raises cell resistance and short-circuit risk under load [2, 3]. Nanofiber membranes electrospun from sulfonated poly(ether ether ketone) (SPEEK) are attractive candidates, since their interconnected porosity and sulfonic acid groups promote electrolyte uptake and lithium-ion transport. Boron nitride (BN) nanomaterials, which are chemically and thermally stable, electrically insulating, and mechanically robust, are available in different geometries that can reinforce the fibrous network and regulate ion transport pathways [4, 5].

In this study, nanofibrous membranes are fabricated by electrospinning of highly sulfonated SPEEK and modified with boron nitride nanosheets (BNNS), boron nitride nanofibers (BNNF), and hexagonal boron nitride (h-BN) platelets at controlled loadings to elucidate how filler geometry influences ionic transport. The basis weight and thickness of the mats are kept consistent to isolate composition effects, and the pristine SPEEK mats exhibit uniform, bead-free nanofibers that provide a reliable baseline for the BN-modified membranes. Fiber morphology and filler dispersion are examined by scanning electron microscopy (SEM) with elemental mapping, and the chemical structure is verified by Fourier transform infrared (FTIR) spectroscopy. The IEC is quantified by acid–base titration and correlated with electrolyte uptake, dimensional swelling, and porosity retention. The ionic conductivity of electrolyte-soaked membranes is evaluated by electrochemical impedance spectroscopy (EIS) between stainless-steel blocking electrodes, including its temperature dependence, while thermal shrinkage and tensile tests track dimensional and mechanical stability. Comparative evaluation of the different BN geometries is expected to reveal how filler dimensionality governs the balance among IEC, swelling, and ionic conductivity, providing design guidelines for SPEEK-based separators in structural battery laminates.

References:

1. Huang, W., et al., Mechanically-robust structural lithium-sulfur battery with high energy density. Energy Storage Materials, 2020. 33: p. 416-422.
2. Wang, X., et al., A high-safety lithium-ion battery electrospun separator with Si3N4-assisted sulfonated poly(ether ether ketone) for regulating lithium flux. Journal of Colloid and Interface Science, 2025. 678: p. 460-471.
3. Waqas, M., et al., High-performance PE-BN/PVDF-HFP bilayer separator for lithium-ion batteries. Advanced Materials Interfaces, 2019. 6(1): p. 1801330.
4. Rasul, M.G., et al., 2D boron nitride nanosheets for polymer composite materials. npj 2D Materials and Applications, 2021. 5: p. 56.
5. Yadav, V., et al., Enhancement in proton conductivity and methanol cross-over resistance by sulfonated boron nitride composite sulfonated poly(ether ether ketone) proton exchange membrane. International Journal of Hydrogen Energy, 2020. 45(34): p. 17017-17028

Keyword: *ionic conductivity, structural battery, Electrospun SPEEK nanofiber separator*

International Requirements for Nanomaterials in Biomaterials and Medical Devices: EN ISO 10993-22

Umut Doğu Seçkin [*1], **Aylin Şendemir**[2,3]

[1] *Ege University, Graduate School of Natural and Applied Sciences, Department of Bioengineering, Bornova, Izmir, 35040, Türkiye*
[2] *Ege University, Engineering Faculty, Department of Bioengineering, Bornova, Izmir, 35040, Türkiye*
[3] *Ege University, Graduate School of Natural and Applied Sciences, Department of Biomedical Technologies, Bornova, Izmir, 35040, Türkiye*

ISO 10993-22 defines the basic standards for the assessment of biocompatibility of medical devices, especially those containing nanomaterials. Biocompatibility is a critical parameter for the safety and effectiveness of medical devices that come into direct contact with the human body. The ISO 10993 series generally outlines the preclinical test methodologies required to assess whether medical devices cause adverse biological reactions. These methodologies are of even greater importance for nano-enabled medical products, especially considering the unique physicochemical properties and increased biological interaction potential of nanomaterials (Szymanski et al., 2025).

Medical devices containing nanomaterials present significant regulatory challenges compared to traditional materials. The nano-size, large surface area, and special surface properties of these devices can cause unpredictable biological responses and therefore require additional safety tests prescribed by ISO standards (Gaur et al., 2020). In this context, biocompatibility assessments in line with ISO 10993-22 can be performed at early stages of the product development process, allowing the reduction of risks that may arise from biological interactions and the fulfillment of regulatory requirements (Szymanski et al., 2025).

In particular, the global trend towards in vitro testing methodologies replacing animal experiments further highlights the role of ISO guidelines in the modern medical device safety framework (Frisch et al., 2023). The development and adoption of standards such as ISO 10993-22 enables the systematic assessment of the safety of nanotechnology-based medical devices. Such standards contribute to the harmonization of regulatory frameworks with technological developments by providing a structured approach under headings such as material selection, manufacturing processes and potential toxicological risks.

ORCID:
Umut Doğu Seçkin: 0000-0002-0123-0284
Aylin Şendemir: 0000-0003-1818-6651

References:
Szymanski, L., Kiernozek, M., Gromadka, B., Straszecka, W., Wiktorek-Smagur, A., & Matak, D. (2025). Chemical Characterization in Medical Device Evaluation: Current Practices, Regulatory Requirements, and Future Directions. Annals of Biomedical Engineering, 1-12.
Gaur, N., Sharma, N., Dahiya, A., Yadav, P., Ojha, H., Goyal, R. K., & Sharma, R. K. (2020). Toxicity and regulatory concerns for nanoformulations in medicine. The ELSI Handbook of Nanotechnology: Risk, Safety, ELSI and Commercialization, 333-357.
Frisch, E., Clavier, L., Belhamdi, A., Vrana, N. E., Lavalle, P., Frisch, B., ... & Gribova, V. (2023). Preclinical in vitro evaluation of implantable materials: conventional approaches, new models and future directions. Frontiers in Bioengineering and Biotechnology, 11, 1193204.

Keyword: *Nanomaterial, Medical device, Biocompatibility*

Plant-Derived QSH/Gelatin Scaffolds with Nanostructured Bioactive Glass for Osteogenic Biomaterials

Hilal Deniz Yılmaz Dağdeviren [*1], Kai Zheng[2], Aldo Roberto Boccacini[3], Ahu Arslan Yıldız[1]

[1] *Izmir Institute of Technology, Department of Bioengineering, Izmir, Turkey*
[2] *Engineering Research Center of Stomatological Translational Medicine, Nanjing Medical University, Nanjing, China*
[3] *Department of Materials Science and Engineering, University of Erlangen-Nuremberg, Erlangen, Germany*

Nano biomaterials with controlled surface architecture and ion-mediated bioactivity offer promising strategies for enhancing bone regeneration. In this study, quince seed hydrocolloid/gelatin (QSH/Gel)-based composite scaffolds were supplemented with either conventional 45S5 bioactive glass (BG) or mesoporous bioactive glass nanoparticles (MBGNs) to investigate how nanoscale glass architecture influences scaffold physicochemical properties and biological activities. The composites were evaluated in terms of chemical structure, morphology, porosity-related surface characteristics, swelling behavior, mechanical response, in vitro bioactivity, and long-term cellular interactions. FTIR analysis confirmed the preservation of the polysaccharide–protein scaffold network together with successful incorporation of bioactive glass phases, while SEM and elemental mapping demonstrated a relatively homogeneous distribution of silicon-, calcium-, and phosphorus-containing glass components within the scaffold matrix. Notably, MBGN incorporation resulted in a well-nanostructured and surface-active composite system, as BET analysis showed >3-fold increase in specific surface area compared with BG-containing and pristine QSH/Gel scaffolds. This enhanced surface area was associated with the mesoporous nanoscale morphology of MBGNs, which may provide more active sites for fluid uptake, ion exchange, and apatite nucleation.

All scaffold groups exhibited hydrophilic behavior; however, MBGN-containing scaffolds showed the highest swelling capacity (2094 ± 571%), nearly twice that of BG-containing composites (1105 ± 56%). Despite differences in nanoarchitecture and swelling response, MBGN- and BG-reinforced scaffolds displayed comparable elastic moduli of approximately 2330 Pa and 2140 Pa, respectively, indicating that bioactive glass incorporation preserved the soft, porous structure of the polymeric scaffold system. Long-term in vitro culture with SaOS-2 (human osteosarcoma) cells demonstrated cell viability above >70% in all composite groups, supporting their cytocompatibility. Additionally, Alizarin Red staining and SEM- elemental mapping revealed enhanced mineral deposition in MBGN-containing scaffolds, with a Ca/P ratio of 2.53, indicating a significant osteoconductive and mineralization-supportive response.

Overall, these findings suggest that MBGN-reinforced QSH/Gel scaffolds provide a bioactive nano-biomaterial platform in which mesoporous nanoscale glass features improve surface reactivity, fluid–material interactions, and mineral accumulation, highlighting their potential for bone tissue engineering applications.

Acknowledgment:
This study was financially supported by the Health Institutes of Türkiye (TÜSEB) under project no. 42980, 2024-A4-02.

ORCID:
Hilal Deniz Yılmaz Dağdeviren: 0000-0003-0412-2868
Ahu Arslan Yıldız: 0000-0003-0348-0575

Keyword: *mesoporous bioactive glass nanoparticles (MBGNs), bioactive glass (BG), composite scaffolds*

Fabrication of Hierarchical Micro- and Nanostructured Pure Iron for Bioresorbable Orthopedic Implants

İlkim Tuana Gümüşkaya [*1], Barkın Bayram[2], Mete Batuhan Durukan[3], Hüsnü Emrah Ünalan[2], Batur Ercan[1,2,4]

[1] Department of Biomedical Engineering, Middle East Technical University, Ankara, 06800, Türkiye
[2] Department of Metallurgical and Materials Engineering, Middle East Technical University, Ankara, 06800, Türkiye
[3] Helmholtz Institute Ulm (HIU), Karlsruhe Institute of Technology (KIT), Helmholtzstraße 11, 89081 Ulm, Germany
[4] BIOMATEN, Center of Excellence in Biomaterials and Tissue Engineering Research Center, Middle East Technical University, Ankara, 06800, Türkiye

Orthopedic implants play a vital role in the treatment of musculoskeletal disorders by restoring structural support and improving patients' quality of life. However, conventional permanent metallic implants may cause complications such as stress shielding, implant-associated infections, and the need for secondary removal surgeries after tissue healing [1]. To address these limitations, biodegradable metallic implants have emerged as promising alternatives, providing temporary mechanical support while gradually degrading in the physiological environment. Among biodegradable metals, pure iron has attracted considerable attention because of its excellent mechanical strength and favorable processing characteristics [2]. However, its relatively slow degradation rate and bioinert characteristics remain a major challenge that limits its clinical application [3].

In this study, hierarchical micro- and nanostructures were fabricated on pure iron through laser patterning followed by anodization to tailor its degradation behavior. Laser patterning generated microgrooves, while subsequent anodization in an ethylene glycol-based electrolyte containing ammonium fluoride produced nanotubular oxide structures on the pure iron surfaces. Hierarchical surface structures consisting of microgrooves approximately 40 μm in width and 6 μm in depth, decorated with nanotubes approximately 72 ± 14 nm in diameter, were successfully fabricated. The hierarchical micro- and nanostructured surface exhibited enhanced wettability compared with electropolished pure iron. Potentiodynamic polarization analysis revealed that the micro- and nanostructured pure iron exhibited an increased corrosion rate of 0.20 mm/year compared with 0.14 mm/year for electropolished pure iron in 1× simulated body fluid at 37 °C. Consistently, electrochemical impedance spectroscopy demonstrated a decrease in polarization resistance from approximately 3500 Ω to 250 Ω, indicating accelerated degradation after laser patterning and anodization. Furthermore, in vitro cytotoxicity assays were conducted using the MC3T3-E1 preosteoblast cell line and sample extracts prepared at 37 °C for 72 h. The micro- and nanostructured surfaces supported cellular proliferation over the 5-day culture period, demonstrating their cytocompatibility and potential for bioresorbable orthopedic implant applications. Overall, the proposed hierarchical surface engineering strategy provides a promising approach for improving the clinical potential of biodegradable pure iron implants.

Acknowledgment:
This study is financially supported by Middle East Technical University Scientific Research Coordination Unit (ODTÜ BAP) (Project ID: 11555). We also thank BIOMATEN for analytical support.

References:
[1] - Kotteda, Anil Kumar, Talari Saikumar, and Akshay A. Shreegan. "Advancements in biodegradable orthopaedic implants: a literature review." Indian Journal of Orthopaedics 59.8 (2025): 1090-1100.
[2] - Cherqaoui, Abdelhakim, Carlo Paternoster, and Diego Mantovani. "Biodegradable Metals and Corrosion Control: Challenges, Limits and New Opportunities for Innovating in Orthopedic Fixations." Materials 19.9 (2026): 1789.
[3] - Shuai, Cijun, et al. "Biodegradable metallic bone implants." Materials Chemistry Frontiers 3.4 (2019): 544-562.

Keyword: *Pure Iron, Laser Patterning, Anodization*

Chitosan for Wound Dressing Applications: Controlling The Dissolution Kinetics

Ateş Batıkan Özdamar [*1], **Hürriyet Polat**[2], **Mehmet Polat**[1]

[1] *Department of Chemical Engineering, İzmir Institute of Technology, Urla 35430, İzmir, Türkiye*
[2] *Department of Chemistry, İzmir Institute of Technology, Urla 35430, İzmir, Türkiye*

Chitosan is a promising bio-based polymer for wound dressing applications due to its biodegradability, biocompatibility, and inherent biological activity. However, controlling its dissolution under physiological conditions is essential for designing wound dressings with tailored dissolution profiles. In this study, the dissolution behavior of chitosan-based films was systematically investigated by varying solvent type/combinations, film structure, and selected formulation parameters.

Self-supporting and substrate-supported chitosan films were prepared using acetic acid (AcA), lactic acid (LA), and their combinations. Selected formulations were additionally incorporated with St. John's Wort oil, curcumin, and Pluronic 123. The resulting materials were characterized using SEM, ATR-FTIR spectroscopy, and surface wettability analysis, while their dissolution behavior was investigated in simulated body fluid at pH 7.4. Experimental dissolution profiles were further analyzed using a diffusion-controlled mass-transfer model derived from the Nernst–Brunner framework and adapted to the experimental film systems.

A pronounced solvent-dependent dissolution behavior was observed. Self-supporting LA-based films exhibited rapid dissolution, approaching complete dissolution within approximately 6 h, whereas AcA-based films reached a plateau of only approximately 15–17%. Introducing a fibrous substrate substantially retarded the dissolution of LA-based films, reducing dissolution to approximately 46% after 6 h. SEM observations further supported these findings by showing greater removal of the chitosan coating from the substrate fibers in LA-based systems than in AcA-based films.

These results demonstrate that the dissolution behavior of chitosan wound dressing films can be effectively tailored through solvent chemistry and structural architecture, providing a practical strategy for designing bio-based wound dressings with controlled persistence under physiological conditions.

ORCID:
Ateş Batıkan Özdamar: https://orcid.org/0000-0002-1850-1159
Hürriyet Polat: https://orcid.org/0000-0002-1573-0351
Mehmet Polat: https://orcid.org/0000-0002-1546-0013

Keyword: *chitosan, smart biomaterials, controlled dissolution*

Development of siNRF2-Loaded Prostate Cancer Cell-Derived Extracellular Vesicles as a Targeted Therapeutic Platform for Prostate Cancer

Vedat Gündoğdu * **, Mustafa Kotmakçı, Bilge Debeleç Bütüner**

Department of Pharmaceutical Biotechnology at the Faculty of Pharmacy, Ege University

Aberrant activation of nuclear factor erythroid 2-related factor 2 (NFE2L2/NRF2) contributes to chemoresistance, cancer stem cell properties, and tumor progression in prostate cancer, making NRF2 silencing a promising therapeutic strategy. However, effective delivery of siRNA therapeutics remains a major challenge due to their poor stability and limited cellular uptake. Extracellular vesicles (EVs) have emerged as promising biological carriers because of their intrinsic homing ability, biocompatibility, and low immunogenicity. This study aimed to evaluate the homing properties of EVs derived from prostate cancer cell lines and develop an siNRF2-loaded EV platform for efficient NRF2 silencing in prostate cancer cells.

EVs were isolated by ultracentrifugation and filtration. Physical characterization was performed by NTA, DLS, and STEM. Biochemical characterization was performed by Western blot analysis of CD9, CD81, and CD63 biomarkers. Cellular uptake of EVs was assessed by flow cytometry and fluorescence microscopy. Cell proliferation was evaluated by WST1 assay. siRNA loading was performed by ExoFect reagent and NRF-2 silencing was confirmed by qRT-PCR and Western blotting. The therapeutic effects of siNRF-2 were evaluated in the presence and absence of paclitaxel (PTX) and camptothecin (CPT) using cell viability and apoptosis assays.

EVs exhibited a spherical morphology with particle sizes ranging from 90 to 150 nm. Preferential uptake of PC3- and DU145-derived EVs by their corresponding parental cells compared with non-malignant cells was observed confirming the homing properties of cancer-cell-derived EVs. Possible proliferative effects of DU145-derived EVs were evaluated on RWPE1 normal prostate epithelial cells, and RWPE1s showed no difference in proliferation at therapeutic concentrations used for gene silencing. Successful siRNA loading into EVs were confirmed by gel electrophoresis and furthermore, siNRF2-loaded EVs reduced NRF2 expression by 37% at the transcriptional level and 24% at the protein level. NRF2 silencing enhanced the therapeutic efficacy of PTX and CPT, leading to reduced cell viability and increased apoptosis.

Prostate cancer-derived EVs exhibit intrinsic homing properties and a favorable safety profile, supporting their use as targeted drug delivery vehicles. Moreover, NRF2 silencing enhanced chemosensitivity and promoted apoptosis, highlighting the potential of siNRF2-loaded EVs as a promising strategy for overcoming chemoresistance in prostate cancer.

Acknowledgment:
This study was supported by Ege University Coordination of Scientific Projects Unit, Project No 32198

ORCID:
Vedat Gündoğdu: https://orcid.org/0000-0003-0556-756X
Mustafa Kotmakçı: 0000-0002-5593-8608
Bilge Debeleç Bütüner: 0000-0001-8112-9241

References:

• Villa, F., Quarto, R., & Tasso, R. (2019). Extracellular Vesicles as Natural, Safe and Efficient Drug Delivery Systems. Pharmaceutics, 11(11), 557. https://doi.org/10.3390/pharmaceutics11110557
• Qiao, L., Hu, S., Huang, K., Su, T., Li, Z., Vandergriff, A., Cores, J., Dinh, P. U., Allen, T., Shen, D., Liang, H., Li, Y., & Cheng, K. (2020). Tumor cell-derived exosomes home to their cells of origin and can be used as Trojan horses to deliver cancer drugs. Theranostics, 10(8), 3474–3487. https://doi.org/10.7150/thno.39434
Panieri, E., & Saso, L. (2019). Potential Applications of NRF2 Inhibitors in Cancer Therapy. Oxidative Medicine and Cellular Longevity, 2019, 8592348. https://doi.org/10.1155/2019/8592348

Keyword: *Extracellular Vesicles, Drug Delivery System, NRF2*

3D melt electrowritten MXene-reinforced scaffolds for tissue engineering applications

Mina Namvari [*] [1], **Mahdiyeh Zahrabi**[1], **Mine Altunbek**[1], **Suleyman Celik**[1], **Bahattin Koc**[2]

[1] *Sabanci University SUNUM, Istanbul, 34956, Turkey*

[2] *Sabanci University Faculty of Engineering and Natural Sciences, Istanbul 34956, Turkey, Sabanci University Integrated Manufacturing Technologies Research and Application Center, Istanbul 34906, Turkey*

2D Ti3C2Tx (MXene) is attracting significant attention in tissue engineering. The incorporation of these promising materials into conventional scaffolds remains challenging, particularly with physicochemical properties compatible with biological systems. Melt electrowriting (MEW) has emerged as a powerful additive manufacturing technique for biofabrication of customized three-dimensional (3D) scaffolds composed of bioactive materials. This study introduces MEW of 2D MXene and polycaprolactone (PCL) nanocomposite scaffolds for tissue engineering applications. First, Ti3C2Tx was functionalized using (3-aminopropyl) triethoxysilane (referred to as f -MXene) to obtain a blended nanocomposite in PCL matrix (referred to as MX/PCL). Fourier transform infrared spectroscopy revealed the nanocomposite composition. X-ray diffraction

analysis showed the reduced crystallinity in PCL after incorporation of f -MXene. Differential scanning calorimetry helped to establish the optimal MEW parameters. Thermogravimetric analysis conducted on nanocomposites containing 0.1, 0.5, and 1% (w/w) f -MXene showed the thermal stability of MXene during the MEW process. The extrudability and printability of the nanocomposites with varying concentrations was demonstrated using MEW in 0–90-degree mesh scaffolds with fine filament dimensions. Scanning electron microscopy and Energy-dispersive x-ray spectroscopy mapping showed the shape fidelity, printing accuracy, and structural integrity of 3D MEW scaffolds with uniform distribution of f -MXene, respectively. Further characterization showed the concentration-dependent enhancement in hydrophilicity and compressive modulus and yield strength of scaffolds upon integration of f -MXene. Atomic force microscopy analysis demonstrated that the topography of the 3D MEW MX/PCL scaffolds changed compared to the pristine PCL and the roughness of the surfaces increased as the concentration of the f -Mxene increased. Accelerated degradation tests demonstrated that increasing filler concentration in the reinforced scaffolds progressively delayed degradation compared to the control. The in vitro characterization showed the adherence of MC3T3-E1 preosteoblast cells on MX/PCL scaffolds and their enhanced osteogenic differentiation. The findings indicate that 3D printed MX/PCL nanocomposite scaffolds have significant potential as mechanically robust scaffolds with controlled degradation rate and cytocompatibility for tissue regeneration, with properties tunable for specific applications.

Acknowledgment:
Note: in case this passes to be an invited talk, the abstract will change to cover the broad applications we are persuing.

ORCID:
Mina Namvari: https://orcid.org/0000-0003-2457-1484

Keyword: *MXene, tissue engineering*

Molecularly Imprinted Polymer Based Surface Acoustic Wave Gas Sensor for Indoor Air Quality

Alp Kılıç [*1], Onur Alev[2], Michael Cheffena[2], Serkan Büyükköse[3]

[1] *Gebze Technical University Department of Physics*
[2] *Norwegian University of Science and Tehnology (NTNU) Department of Civil Engineering*
[3] *Gebze Technical University Department of Physics and The Central Research Laboratory Application and Research Center (GTUMAR)*

Indoor air quality plays a crucial role in enhancing quality of life and preventing long-term health problems due to individuals spend a substantial portion of their daily lives in various public indoor environments. Poor indoor air quality is strongly associated with a wide range of health issues, particularly respiratory diseases. Therefore, the regular monitoring of indoor air quality is of critical importance, especially for the protection of vulnerable populations. Indoor air pollutants are generally classified into three categories: chemical, biological, and particulate contaminants. Among these, volatile organic compounds (VOCs) widely used in everyday life for diverse purposes are of particular concern. Accordingly, systematic monitoring of indoor air and development of reliable sensing systems is of key issue.

Conventional methods such as gas chromatography, mass spectrometry, Raman spectroscopy, and infrared spectroscopy are well-established and reliable for indoor air monitoring. However, their practical use in daily life is limited due to requirement of complex instrumentation, lengthy analysis times, lack of user-friendliness, and high costs [1].

Surface acoustic wave (SAW) devices offer several distinct advantages, including wide operating frequency ranges, high sensitivity, low power consumption, miniaturized fabrication, ease of integration into various systems, and suitability for remote sensing applications [2]. SAW sensors have gained considerable attention in the field of gas sensing due to these advantages.

Compared to widely used sensing materials such as semiconductor metal oxides, conducting polymers, and carbon-based nanomaterials, molecularly imprinted polymers have recently emerged as promising candidates owing to their exceptional selectivity, chemical stability, and the presence of synthetic recognition elements tailored for specific analytes [3]. These polymers can be designed as recognition sites and cavities for the target analytes by incorporating functional monomers and cross-linkers.

In this study, a molecularly imprinted polymer based SAW gas sensor was fabricated to detect various volatile organic compound pollutants. The fabricated sensor was tested against ethanol, ammonia, HCN (hydrogen cyanide), and H_2S (hydrogen sulfide) gases at room temperature within a very low concentration regime from a few ppm (parts per million) to ppb (parts per billion). It was also tested against various relative humidity concentrations to assess its usability in real-world applications. The sensor tests revealed that the polymer-based sensor exhibited a selective detection performance against ethanol at target gas concentrations around 1 ppm and below. Furthermore, a long-term stability test against ethanol was also conducted as part of this study.

Acknowledgment:
This work was supported by The Scientific and Technological Research Council of Turkey (TUBITAK), Project Number: 125E928.

ORCID:
Alp Kılıç: 0000-0003-2065-2965
Onur Alev: 0000-0002-2882-2802
Michael Cheffena: 0000-0003-2086-8627
Serkan Büyükköse: 0000-0001-9456-682X

References:
[1] Schütze, A., & Sauerwald, T. (2020). Indoor air quality monitoring. In Advanced Nanomaterials for Inexpensive Gas Microsensors (pp. 209-234). Elsevier.
[2] Kılıç, A., Alev, O., Öztürk, Z. Z., & Büyükköse, S. (2025). Fabrication and Room Temperature Volatile Organic Compounds Sensing Performance of ZnO-Based Surface Acoustic Wave Gas Sensor. IEEE Sensors Journal, 25(23), 42629-42637.
[3] Alev, O., & Cheffena, M. (2025). Molecularly imprinted polymers in chemical sensing: Functional polymer strategies for selective gas analyte detection. Microchemical Journal, 116419.

Keyword: *Indoor Air Quality, Molecularly Imprinted Polymers (MIPs), Surface Acoustic Wave (SAW)*

Synthesis of Dendritic Nickel Nanoparticles And Development of QTC-Based Flexible Pressure and Temperature Sensors

Ethem Ünal Saçlı[1], Batuhan Parlak[1], Taylan Irmak Kılıç[1], Doğan Sarper Ataman[1], Yunus Emre Sarkmaz[1], Faruk Oğuzhan Karman[1], Furkan Sarıboğa[1], Arif Altan Selçuk[2], Şeyma Özkan[3,4], Barış Oğuz Gürses [* 1]

[1] Ege University, Faculty of Engineering, Mechanical Engineering
[2] Ege University, Faculty of Science, Biology
[3] Ege University, Central Research Test and Analysis Laboratory Application and Research Center
[4] Dokuz Eylül University, Faculty of Science, Chemistry

The rapid advancement of flexible electronics, wearable technologies, and smart systems has created growing demand for highly sensitive, low-cost pressure and temperature sensors. Quantum tunneling composites (QTCs), which consist of conductive particles dispersed within an insulating elastomer matrix, are promising candidates for such applications owing to their nonlinear electrical response to mechanical and thermal stimuli. In this study, flexible dual-mode sensors were developed by incorporating hydrothermally synthesized dendritic nickel nanoparticles into an Ecoflex 00-30 silicone elastomer matrix. The nanoparticle morphology was controlled by systematically varying the synthesis pH and temperature, and the resulting microstructures were characterized by scanning electron microscopy (SEM). The electromechanical performance of the fabricated composites was evaluated using impedance spectroscopy under incremental mechanical loading and controlled temperature variation. The sensors exhibited a pronounced nonlinear (exponential) decrease in impedance with increasing applied pressure and decreasing temperature, consistent with a quantum tunneling conduction mechanism activated by reduced interparticle separation. Hydrazine was employed as a reducing agent during nanoparticle synthesis, enabling the formation of high-surface-area dendritic architectures that facilitate tunneling-favorable particle networks within the elastomer. The pressure sensitivity was determined to be −0.075 Ω/Pa (R^2 = 0.99) and the temperature sensitivity was 0.242 Ω/°C (R^2 = 0.85) across their respective measurement ranges, demonstrating the potential of these QTC composites as flexible, dual-parameter sensing elements for wearable and soft robotic applications.

ORCID:
Şeyma Özkan: 0000-0002-0255-3763
Barış Oğuz Gürses: 0000-0002-2755-3452

Keyword: *Quantum tunneling composites, sensors, nickel nanoparticles*

Using an Interferometric Imaging Sensor to Characterize Receptor Binding Affinity for Vascular Endothelial Growth Factor

Nese Lortlar Unlu [*] [1,2], Monireh Bakhshpour-Yücel[3], M Selim Ünlü[4]

[1] *Atlas University, Faculty of Medicine, Department of Histology and Embryology*
[2] *Boston University, Department of Biomedical Engineering*
[3] *Uludag University, Faculty of Art and Science, Department of Chemistry*
[4] *Boston University, Department of Electrical and Computer Engineering*

Wet age-related macular degeneration (AMD) is a leading cause of irreversible vision loss worldwide and is primarily driven by pathological angiogenesis mediated by vascular endothelial growth factor (VEGF). Anti-VEGF biologics such as aflibercept and bevacizumab have become the standard of care; however, quantitative characterization of their binding affinity remains essential for evaluating therapeutic efficacy and comparing treatment options [1]. In this study, an Interferometric Reflectance Imaging Sensor (IRIS) platform was employed to evaluate the in vitro binding affinity of two clinically relevant anti-VEGF therapeutics, aflibercept and bevacizumab. Therapeutic molecules were immobilized on MCP-2 polymer-functionalized silicon chips in a microarray format. Recombinant human VEGF (rhVEGF) was introduced through a microfluidic system, and binding interactions were monitored continuously. Differential signal analysis and adsorption isotherm modeling were used to characterize binding behavior. The IRIS platform enabled real-time, label-free detection of VEGF interactions with both anti-VEGF therapeutics. Binding curves demonstrated specific molecular recognition, while control spots showed negligible signal responses. The results demonstrate that IRIS is a robust, cost-effective, and highly sensitive platform for the characterization of therapeutic biomolecular interactions. The ability to perform real-time, label-free, and multiplexed measurements makes IRIS a promising technology for drug development, biologic characterization, and translational biomedical research. Beyond anti-VEGF therapeutics, the platform has significant potential for broader applications in biomarker detection and precision medicine [2].

ORCID:
Nese Lortlar Unlu: 0000-0003-4578-6089
Monireh Bakhshpour-Yücel: 0000-00025737-720X
M Selim Ünlü: 0000-0002-8594-892X

References:

MacDonald, D.A.; Martin, J.; Muthusamy, K.K.; Luo, J.K.; Pyles, E.; Rafique, A.; Huang, T.; Potocky, T.; Liu, Y.; Cao, J.; et al. Aflibercept exhibits VEGF binding stoichiometry distinct from bevacizumab and does not support formation of immune-like complexes. Angiogenesis 2016, 19, 389–406.

Keyword: *IRIS; VEGF; aflibercept; bevacizumab; biosensor; label-free detection; therapeutic biologics; binding affinity.*

Organ-On-Chip and Microwave Biosensor Integrated Membrane Model for Drug Screening

Gurkan Yesiloz [*1,2], **Faruk Aksoy**[1], **Servin Bagheralmoosavi**[1], **Fayiti Fuerkaiti**[1]

[1] *1. Yesiloz Research Laboratory, National Nanotechnology Research Center (UNAM) - Bilkent University, 06800, Cankaya-Ankara, Türkiye.*
[2] *2. Institute of Materials Science and Nanotechnology, Bilkent University, 06800, Cankaya-Ankara, Türkiye.*

Understanding and monitoring molecular transport across physiological barriers are essential for drug discovery, pharmacological screening, and organ-on-chip technologies. Current approaches predominantly rely on fluorescence-based assays and endpoint measurements, which provide limited temporal information and often require labeling strategies that may interfere with biological processes [1,2]. To address these limitations, we present a double-layer organ-on-chip membrane platform integrated with a label-free microwave biosensor capable of continuously monitoring transport processes across porous membranes and endothelial barriers while simultaneously providing optical visualization.

The platform consists of vertically aligned upper and lower PDMS microchannels separated by an 8 μm porous PET membrane positioned above an integrated microwave sensing region. Reservoirs connected to both channels enable controlled sample loading and real-time transport measurements. Fluorescein isothiocyanate (FITC) and doxorubicin (Dox) were introduced into the upper channel while fluorescence microscopy and microwave measurements were recorded simultaneously. Human umbilical vein endothelial cells (HUVECs) were cultured on the membrane to establish a physiologically relevant endothelial barrier. Cellular morphology and barrier integrity were confirmed through F-actin/DAPI staining. In addition, verapamil-mediated P-glycoprotein (P-gp) inhibition was employed to investigate the influence of transporter activity on intracellular doxorubicin transport. Spheroid-based toxicity assays, live/dead staining, and conventional 96-well plate experiments were performed to evaluate biological functionality and drug response.

FITC diffusion experiments revealed rapid fluorescence increases near the upper reservoir and membrane interface, whereas delayed responses were observed in distal lower-channel regions due to transport distance. These changes were accompanied by time-dependent resonance shifts measured by the microwave biosensor, demonstrating successful label-free monitoring of molecular transport. Doxorubicin experiments exhibited similar trends, although transport occurred more gradually because of the larger molecular size and distinct transport characteristics of Dox. The microwave sensor consistently detected measurable resonance variations associated with Dox diffusion across the membrane.

HUVECs formed a confluent endothelial layer, enabling investigation of P-gp-mediated transport. Untreated samples displayed progressively increasing intracellular Dox accumulation, whereas verapamil-treated samples exhibited reduced fluorescence intensity and smaller microwave signal variations, indicating inhibited intracellular transport activity. Furthermore, spheroid morphology after four days suggested reduced Dox-associated toxicity in the presence of verapamil [3].

Overall, the proposed microwave biosensor-integrated organ-on-chip platform enables continuous, non-invasive, and label-free monitoring of barrier function and drug transport. This versatile approach provides a promising tool for next-generation pharmacological screening and physiologically relevant transport studies. Future work will focus on quantitative permeability measurements, tight-junction characterization, long-term barrier stability, and disease-specific endothelial models.

Acknowledgment:
G.Y. gratefully acknowledge the support from the Scientific and Technological Research Council of Türkiye (TUBITAK) under 118C263 & 123E157 grants, and the Health Institutes of Türkiye (TUSEB) (Grant No: 34150 and 35722).

References:
1. Yesiloz G., Boybay M.S. and Ren C.L., “Label-Free High-Throughput Detection and Content Sensing of Individual Droplets in Microfluidic Systems”, Lab on a Chip, 15, 4008-4019, 2015.
2. Koziolek et al., Pharmaceutics, 2023, 15(10), 2397.
3. Cai et al., Xenobiotica, 2022, 52(7), 742–750.

Keyword: *Microwave biosensors, Organ-on-Chips, Label-free sensing; endothelial barrier*

Broadband Photoresponse of Electrodeposited Al:NiO/Porous Silicon Photodetectors: Bias-Dependent Spectral Uniformity

Mohammed Sulaiman Mustafa Mustafa * **, Alper Çetinel**

Ege University

This study examines the photoresponse characteristics of 3 mM aluminum-doped nickel oxide (Al:NiO) thin films electrochemically deposited onto porous silicon (PSi) substrates. Current–time (I–t) measurements were performed under three illumination wavelengths (365, 650, and 850 nm) at bias voltages of 1, 3, 5, 7, and 9 V. Rise and decay times were extracted from the switching cycles to assess device speed and stability. The results showed that spectral uniformity of the photoresponse varied with the applied bias. At 5 V, the device showed a more balanced response across the measured range, with responsivity values of 36.31 mA/W at 365 nm, 35.37 mA/W at 650 nm, and 37.21 mA/W at 850 nm, corresponding to a variation of about 5%. A detectivity of 1.76×10^{13} Jones was recorded at 850 nm, and the quantum efficiency at 365 nm was calculated as 123%, which is attributed to trap-assisted carrier processes at the Al:NiO/PSi interface. The device showed repeatable on/off switching at all tested conditions. These findings suggest that 5 V may be a suitable operating point for broadband operation, and that the Al:NiO/PSi structure could be considered for applications such as environmental monitoring, optical sensing, and biomedical imaging.

ORCID:
Mohammed Sulaiman Mustafa Mustafa: 0009-0002-7165-5365
Alper Çetinel: 0000-0003-0626-8721

References:
Raj, I. Loyola Poul, Valanarasu, S., Asuntha, A., Rimal Isaac, R. S., Shkir, M., Algarni, H., & AlFaify, S. (2022). Development of a highly sensitive UV sensor using Al, Ga, and In-doped NiO thin films via nebulizer spray pyrolysis method for photodetector applications. Journal of Materials Science: Materials in Electronics, 33(15), 11753–11767. https://doi.org/10.1007/s10854-022-08140-w
Caglar, M., Sever, K., Aktas, S., & Demiroglu, A. (2023). Improving the electrical performance of NiO based photodiode fabricated by sol-gel process with Al doping. Sensors and Actuators A: Physical, 350, 114099. https://doi.org/10.1016/j.sna.2022.114099
Althobaiti, M. G., Alosaimi, M. A., Alharthi, S. S., Alotaibi, A. A., & Badawi, A. (2024). Tailoring the optical performance of sprayed NiO nanostructured films through cobalt doping for optoelectronic device applications. Optical Materials, 151. https://doi.org/10.1016/j.optmat.2024.115341
Ahmed, A. A., Devarajan, M., & Afzal, N. (2017). Fabrication and characterization of high performance MSM UV photodetector based on NiO film. Sensors and Actuators, A: Physical, 262, 78–86. https://doi.org/10.1016/j.sna.2017.05.028

Keyword: *Broadband photodetector, Aluminum-doped NiO, Porous silicon, Spectral uniformity, Transient photoresponse, Electrochemical deposition*

Investigation of the Wound Healing Properties of the Bioactive Regenerative Peptide BPC-157 Via a Nanocarrier System

Alper Filiz [*] [1], Bilge Ölçeroğlu[1], Şima Mertol[1], Kartal Çetintürk[1], Şahika Sena Bayazıt[2], Ahmet Katı[3], Fırat Barış Barlas[1]

[1] Department of Biotechnology, Institute of Nanotechnology and Biotechnology, Istanbul University-Cerrahpasa
[2] Department of Nanotechnology, Institute of Nanotechnology and Biotechnology, Istanbul University-Cerrahpasa
[3] Department of Biotechnology, Institute of Health Sciences, University of Health Sciences

Metal–organic frameworks (MOFs) have emerged as promising biomedical carriers due to their tunable porosity, biocompatible compositions, and capacity for controlled loading and release of therapeutic agents [1]. In this study, a synergistic therapeutic platform for wound healing by immobilizing a bioactive–regenerative peptide onto a bioavailable metal–organic framework (bioMOF) structure developed. To this end, a zinc(Zn)–glutamic acid(GA)–based bioavailable–MOF (Zn-GA-bioMOF) was synthesized [2], comprehensively characterized, and covalently conjugated with the regenerative peptide BPC-157 [3]. The obtained findings demonstrate that the designed system represents a promising nanocarrier platform from both structural and biological perspectives.

The hydrothermal synthesis of Zn-GA-bioMOF in an aqueous environment eliminated the need for toxic organic solvents, providing a significant advantage for biomedical applications. FT-IR and XRD analyses confirmed the successful formation of the crystalline structure and metal–ligand coordination, while SEM and DLS analyses revealed particle sizes in the nanometer range suitable for biomedical use. Covalent attachment of the BPC-157 peptide to the MOF surface via EDC/NHS chemistry resulted in a conjugation efficiency of 58% and conjugation rate of 4.39%, which was reliably validated through LC-MS/MS analysis.

In vitro cell studies demonstrated that the Zn-GA-bioMOF-BPC-157 complex exerted a more pronounced regenerative effect on cell proliferation and migration compared with its individual components. In particular, the results obtained in the HDF (human dermal fibroblast, PCS 201-012) cell line supported a synergistic biological response arising from the simultaneous and controlled action of zinc, glutamic acid, and BPC-157. Minimum inhibitory concentration testing showed that S. aureus growth was suppressed by approximately 1 log at 80 µg/mL, while significant bacteriostatic effect against both S. aureus and E. coli was achieved at 320 µg/mL. Furthermore, in vivo intradermal irritation and acute systemic toxicity studies indicated that the developed platform is biocompatible and safe within the therapeutic dose range. Overall, these findings suggest that MOF-based peptide carrier systems offer a controlled, targeted, and effective therapeutic approach for wound healing applications.

References:

Filiz, A., Bayazit, S. S., Baris Barlas, F. 2025. "Metal–Organic Frameworks (MOFs) in Drug Delivery: Emerging Trends, Functional Enhancements, and Biocompatibility Challenges". Journal of Drug Delivery Science and Technology, 107284.
Long, P., Zhao, Q., Dong, J., Li, J. 2009. "Synthesis of metal-organic frameworks from the system metal/ L -glutamic acid/TEA/H 2 O". Journal of Coordination Chemistry, 62(12), 1959-1963.
Seiwerth, S., Sikiric, P., Grabarevic, Z., Zoricic, I., Hanzevacki, M., Ljubanovic, D., … Kolega, Z. 1997. "BPC 157's effect on healing". Journal of Physiology-Paris, 91(3-5), 173-178.

Keyword: *Bioactive regenerative peptide, BPC-157, Metal-organic framework (MOF)*

Synthesis, Characterization, and Biomedical Application of Europium, Samarium Single and Co-Doped Calcium Tetraborate Nanoparticles

Huseynagha Abasov * **, Ayşen Yılmaz**

Middle East Technical University

Attention to inorganic nanoparticles has spanned various but not limited to disciplines, including photodynamic therapy, antibacterial coatings, drug delivery systems in pharmacology and toxicology, and optics and electromagnetism. This study aims to explore the application of synthesized polydopamine-coated calcium tetraborate nanoparticles doped with lanthanides, Eu^{3+} and Sm^{3+}.

Calcium tetraborate particles (CTB), which have been proven to be potent drug-delivering nanoparticles with Eu^{3+} dopant, will be synthesized and doped with Eu^{3+}, Sm^{3+}, and co-doped with Eu^{3+}/Sm^{3+} with varying proportions. Optimum molar conditions have been set for the dopant-to-host ratio with optimization studies utilizing photoluminescence spectroscopy to obtain the highest intensity. In this work, Eu^{3+}/Sm^{3+} doped and Sm^{3+} co-doped CTB will be investigated as drug delivery systems for the first time.

The single-doped and co-doped nanoparticles are supposed to be coated with some functional groups, such as polymers, in order to aid them in carrying the drug particles. The functional group in this study will be polydopamine (PDA), which is a biocompatible material with surface functionality. This feature of the PDA makes it a potential host to attract drug particles for constant, slow, and controlled delivery to the cancer cell lines. Moreover, the further modifiability characteristic of PDA provides alternative routes from the coating perspective.

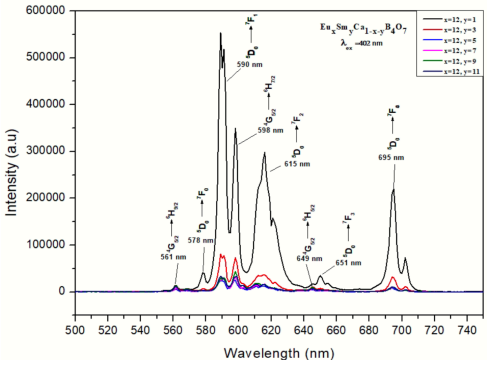


Figure 1. Photoluminescence emission spectrum of Eu^{3+}/Sm^{3+} co-doped calcium tetraborate nanoparticles at 402 nm

Acknowledgment:
I would like to thank my supervisor, Prof.Dr. Ayşen Yılmaz for providing me the opportunity to work in her lab. I would also like to appreciate İpek Yıldırım and Akif Şafaklı, along with all Ayşen Yılmaz Research Group members, for their endless support in this project. This project is supported by the Middle East Technical University Scientific Research Coordination Unit, namely project Genel-103-2025-11701.

ORCID:
Huseynagha Abasov: https://orcid.org/0009-0003-2412-0701

References:
Yang, XM., Yin, GZ., Amorós, O.Z. et al. Polydopamine surface functionalized submicron ZnO for broadening the processing window of 3D printable PLA composites. J Polym Res 30, 165 (2023). https://doi.org/10.1007/s10965-023-03540-w
Binnemans, K. (2015). Interpretation of europium(III) spectra. Coordination Chemistry Reviews, 295, 1–45. https://doi.org/10.1016/j.ccr.2015.02.015
Jiang, S., Win, K. Y ., Liu, S., Teng, C. P ., Zheng, Y ., & Han, M. -Y .(2013). Surface-functionalized nanoparticles for biosensing andimaging-guided therapeutics. Nanoscale, 5(8), 3127–3148.https://doi.org/10.1039/C3NR34005H
Kang, J. -S., Jeong, Y . -K., Kang, J. -G., Zhao, L., Sohn, Y ., Pradhan, D.,& Leung, K. T . (2015). Observation of Mediated Cascade EnergyTransfer in Europium- Doped ZnO Nanowalls by 1,10-Phenanthroline. The Journal of Physical Chemistry C, 119(4), 2142–2147. https://doi.org/10.1021/jp5090795
Yıldırım, İ., Altındal, D. Ç., & Yılmaz, A. (2025). Eu3+ doped MB4O7 (M= Ca and Sr) nanoparticles for cancer treatment. Journal of Drug Delivery Science and Technology, 105, 106611. https://doi.org/10.1016/j.jddst.2025.106611

Keyword: *Calcium tetraborate, rare-earth metal doping, drug delivery systems*

Engineering Rice Husk-Derived Mesoporous Silica Nanocarriers for Enhanced Blood–Brain Barrier Penetration and Glioblastoma Therapy

Sahar Porrang [*] [1], Turkan Doga Gizer[1], Birsen Beril Bildirici[1], Gulin Baran[1], Ahmet Baki Sahin[1], Nur Mustafaoglu[1,2,3]

[1] *Molecular Biology, Genetics and Bioengineering Program, Faculty of Engineering and Natural Sciences, Sabanci University, Tuzla – 34956, Istanbul, Turkiye*

[2] *Sabanci University Nanotechnology Research and Application Center (SUNUM), Tuzla – 34956, Istanbul, Turkiye*

[3] *Center of Excellence for Functional Surfaces and Interfaces for Nano Diagnostics (EFSUN), Sabanci University, Tuzla – 34956, Istanbul, Turkiye*

Glioblastoma is one of the most aggressive and lethal primary brain tumors, with a median survival of approximately 15 months despite current treatment strategies [1, 2]. The blood–brain barrier (BBB) remains a major obstacle to the effective delivery of therapeutics to the brain, significantly limiting treatment options for central nervous system disorders, including glioblastoma. The limited efficacy of current glioblastoma treatments highlights the urgent need for innovative therapeutic strategies capable of overcoming the BBB and delivering therapeutic agents selectively to tumor tissues without disrupting BBB integrity. In this context, functionalized nanocarriers have emerged as attractive platforms for enhancing drug transport to the brain.

In this study, we developed a sustainable and biocompatible nanocarrier platform based on rice husk-derived mesoporous silica nanoparticles (RPMSNs) for enhanced BBB penetration and targeted GBM therapy. RPMSNs were synthesized via a green sol-gel route eliminating acid pretreatment and energy-intensive calcination and subsequently functionalized with amine (-NH_2), carboxyl (-COOH), or polyethylene glycol (PEG) to tailor surface chemistry and biological performance. Comprehensive physicochemical characterization by FTIR, XRD, BET, TGA, Zeta potential, SEM and TEM confirmed the formation of highly porous, amorphous mesoporous silica with large surface area and successful surface modification.

Doxorubicin (DOX) was employed as model anticancer drugs to investigate loading and release efficiency. All formulations demonstrated pH-dependent release, with enhanced drug liberation under acidic tumor-mimicking conditions. In vitro cytotoxicity studies confirmed excellent biocompatibility of blank nanoparticles in endothelial, fibroblast, and glioblastoma cells, while DOX-loaded PEG-modified RPMSNs exhibited pronounced and selective cytotoxicity toward GBM cells with minimal toxicity to brain endothelial cells.

Nanoparticle uptake studies revealed significantly higher internalization in GBM cells compared with iPSC-derived brain microvascular endothelial cells (iBMECs) [3], with surface functionalization governing uptake efficiency. Using a human derived BBB and GBM-BBB Transwell model, PEGylated RPMSNs demonstrated the highest BBB translocation among blank nanoparticles, while DOX loading markedly enhanced transport efficiency across the BBB without compromising barrier integrity which approved by both permeability assay and fluorescent imaging. Notably, DOX-loaded PEG-modified RPMSNs achieved up to ~20% BBB translocation in the GBM-BBB model and induced substantial cytotoxic effects in GBM cells.

Overall, this work presents an eco-friendly, surface-engineered mesoporous silica nanoplatform that combines sustainable synthesis, controlled drug delivery, effective BBB penetration, and selective GBM cytotoxicity, highlighting its strong potential for next-generation brain cancer nanotherapeutics.

Acknowledgment:
The authors gratefully acknowledge financial support from the Marie Skłodowska-Curie Actions (MSCA) Postdoctoral Fellowship (Enhanced-DDS, Grant No. 101110722), TÜBİTAK 3501 Career Development Program (Grant No. 225S785), TÜBİTAK 1001 Scientific and Technological Research Projects Program (Grant No. 325S484), and the European Research Council (ERC) Starting Grant Meta-Brain (Grant No. 101116521).

ORCID:
Sahar Porrang: 0000-0001-8284-7931

References:
Singh, S., Dey, D., Barik, D., Mohapatra, I., Kim, S., Sharma, M., Prasad, S., Wang, P., Singh, A. and Singh, G., 2025. Glioblastoma at the crossroads: current understanding and future therapeutic horizons. Signal transduction and targeted therapy, 10(1), p.213.
Tamimi, A.F. and Juweid, M., 2017. Epidemiology and outcome of glioblastoma. Exon Publications, pp.143-153.
Park, T.E., Mustafaoglu, N., Herland, A., Hasselkus, R., Mannix, R., FitzGerald, E.A., Prantil-Baun, R., Watters, A., Henry, O., Benz, M. and Sanchez, H., 2019. Hypoxia-enhanced Blood-Brain Barrier Chip recapitulates human barrier function and shuttling of drugs and antibodies. Nature communications, 10(1), p.2621.

Keyword: *Mesoporous Silica Nanoparticles, Blood Brain Barrier, Glioblastoma*

Ternary Active Layer Design Utilizing BDT-Based Novel Donor for Semitransparent Organic Photovoltaics

Elif Pınar Yılmaz [*1], **Sevgi Aydın**[1], **Gönül Hızalan Özsoy**[2], **Ali Çırpan**[1,2,3,4]

[1] *Department of Chemistry, Middle East Technical University (METU), 06800, Ankara, Turkiye*
[2] *ODTU- GUNAM, Middle East Technical University, 06800, Ankara, Turkiye*
[3] *Department of Polymer Science and Technology, Middle East Technical University, 06800, Ankara, Turkiye*
[4] *Department of Micro and Nanotechnology, Middle East Technical University, 06800, Ankara, Turkiye*

Solar cells are photovoltaic devices designed to convert sunlight into electrical energy. They have emerged as one of the most promising solutions to the global energy crisis. Organic solar cells (OSCs) have attracted significant attention as a promising class of photovoltaic technologies due to their flexibility, lightweight nature, tunable optical properties, and compatibility with low-cost solution processing. OSCs offer unique advantages such as tunable light absorption and semitransparency through molecular design and device engineering, enabling the development of semitransparent organic solar cell (ST-OSC) architectures. Benzodithiophene (BDT) based donor polymers are widely used in OSCs due to their strong light absorption, efficient charge transport, and structural tunability. In this study, binary and ternary blends were fabricated with a novel BDT based donor and nonfullerene acceptors in the active layer with the device architecture of ITO/PEDOT:PSS/Active Layer/PNDIT-F3N/Ag. Introduction of a ternary component optimized the blend morphology and broadened the absorption spectrum. The optimized ternary OSC achieved a power conversion efficiency (PCE) of 10.24%, a short-circuit current density (J_{SC}) of 21.82 mA.cm^{-2}, an open-circuit voltage (V_{OC}) of 0.76 V and a fill factor (FF) of 62.42%. Best performing device was fabricated as a semitransparent organic solar cell, achieving power conversion efficiency (PCE) of 7.31%, a short-circuit current density (J_{SC}) of 16.15 mA.cm^{-2}, an open-circuit voltage (V_{OC}) of 0.80 V, fill factor (FF) of 56.64% and a AVT of 18.58%.

Acknowledgment:
This study was supported by Scientific and Technological Research Council of Turkey (TUBITAK) under the Grant Number 222Z151. The authors thank to TUBITAK for their supports.

ORCID:
Elif Pınar Yılmaz: 0009-0007-3376-1542
Sevgi Aydın: 0009-0007-8570-9447
Gönül Hızalan Özsoy: 0000-0002-3308-404X
Ali Çırpan: 0000-0003-3051-8380
Ali Çırpan: 0000-0003-3051-8380
Ali Çırpan: 0000-0003-3051-8380
Ali Çırpan: 0000-0003-3051-8380

Keyword: *Organic photovoltaics, Benzodithiophene, Ternary semitransparent OSCs*

Lateral metal-semiconductor homojunctions in Janus Sc2CClBr MXene: Electron transport and thermoelectric properties

Gözde Özbal Sargın *

Department of Fundamental Sciences, Air NCO Vocational HE School, Turkish National Defence University, İzmir, 35415 Türkiye

Tuning the electronic phases of two-dimensional MXenes provides a practical route for designing nanoscale junctions. In this work, we study the quantum transport and finite-bias thermoelectric properties of Sc_2CClBr using density functional theory combined with the non-equilibrium Green's function (DFT-NEGF) approach. We find that a 10% uniaxial compressive strain induces a semiconductor-to-metal transition in the pristine monolayer. By laterally interfacing the strained and unstrained phases, we construct a phase-engineered metal-semiconductor homojunction. The simulated device exhibits highly nonlinear current-voltage characteristics with a sharp current enhancement under high reverse bias voltages. Spatially resolved projected local density of states (PLDOS) analysis reveals that this transport mechanism is driven by direct band-to-band tunneling. Furthermore, evaluating the finite-bias thermoelectric performance demonstrates that the broadened bias window in the deep reverse-bias regime induces severe energy smearing. This effect suppresses the peak electronic figure of merit (ZT_e) to approximately one-third as the reverse bias increases from 0.5 V to 1.5 V. Along with this suppression, the thermoelectric peaks shift toward positive chemical potentials, indicating that electrostatic gate-tuning is strictly required for optimal energy harvesting under high operational biases. These findings highlight the potential of Sc_2CClBr homojunctions for voltage-tunable quantum switching and nanoscale thermoelectric applications.

ORCID:
Gözde Özbal Sargın: 0000-0002-6265-964X

Keyword: *MXenes, Quantum Transport, Thermoelectrics*

Bridging Research and Application in Printable Electrochromics: A Start-Up Perspective

Elif Begüm Elçioğlu [*1,2], **Ömür Şaylıgil**[1]

[1] *Nanoplexia Teknoloji A.Ş., 75. Yıl OSB Mah. Bilim Cad. Yazılım Kule 5/510, 26110 Odunpazari, Eskişehir, Türkiye*
[2] *Eskişehir Technical University, Faculty of Engineering, Department of Mechanical Engineering, 26555 Eskişehir, Türkiye*

Nanoplexia Technology A.Ş. was established in 2023 in Eskisehir Technology Development Zone through financial support and investment received under the TÜBİTAK BiGG Fund (1812 - Investment Based Entrepreneurship Support Program (BiGG Investment) - Phase 2) [1]. The founding team consists of two women executives with complementary expertise in nanofluids, nanoscale energy harvesting systems, and research and technology ethics. This multi-disciplinary background enabled the company to approach current energy efficiency and thermal comfort challenges by combining engineering and regulatory-ethical perspectives.

Driven by increasing demands for energy efficiency, the company has focused on the development of printable electrochromic systems for thermal comfort applications. This work builds upon prior research on nanoparticle-based printable formulations and printability characterization [2]. As an independent example from the literature, Zhou et al. [3] recently demonstrated the potential role of electrochromic technologies in intelligent thermal management systems for electric vehicle cabin climate control. During the BiGG Investment Phase 2 [1], we developed a minimum viable product (MVP) through a series of technology verification and validation activities. Through iterative formulation development, targeted compositional design, electrochemical performance optimization and validation studies, the electrochromic system progressed from TRL3 to TRL5.

The following are among the key insights gained throughout this particular transition from laboratory research to application-oriented development. In case the application scale and implementation conditions vary, the laboratory-scale performance alone is not sufficient to define technology readiness. Translating functional materials into applicable systems required simultaneous consideration of manufacturability, process compatibility, safety, cost, and intellectual property strategies alongside primary performance. This experience demonstrated that the primary challenge in research-to-application transition is not merely developing high-performance materials, but treating the material-process-application chain as an integrated framework from the early stages of development. Our future efforts will focus on validating the system under actual manufacturing conditions and advancing the technology toward larger-scale implementation. The experience gained during this process continues to shape the company's approach to bridging the gap between scientific research and real-world deployment.

ORCID:
Elif Begüm Elçioğlu: 0000-0002-1005-4294
Ömür Şaylıgil: 0000-0001-7517-7503

References:
https://tubitak.gov.tr/tr/destekler/sanayi/ulusal-destek-programlari/1812-yatirim-tabanli-girisimcilik-destek-programi-bigg-yatirim, Date accessed: July 6, 2026
E.B. Elcioglu, S.M.S. Murshed, Drop-on-demand assessment of microdrops of dilute ZnO–water nanofluids, Phys. Fluids 33, 012013 (2021).
R. Zhou, B. Yang, S. Dong, Y. Zhang, G. Wang, Z. Zhang, Research on the regulation of electrochromic vehicle windows balancing thermal comfort and energy consumption, Applied Thermal Engineering 302, 4, 131971 (2026).

Keyword: *deep-tech, entrepreneurship, functional nanomaterials*

Advanced Nanomaterial-Based NFC-Enabled Battery-Free Electrochemical Biosensors for Point-of-Care Diagnostics

Saniye Soylemez [*] [1,2], **Dilek Soyler**[1,2], **Dilara Yeniterzi**[1,2]

[1] *Department of Biomedical Engineering, Faculty of Engineering, Necmettin Erbakan University, Konya, 42090, Türkiye*
[2] *Science Technology Research and Application Center (BITAM), Necmettin Erbakan University, Konya, 42090, Türkiye*

The growing demand for decentralized healthcare has accelerated the development of smart point-ofcare (POC) diagnostic technologies. Among these, near-field communication (NFC)-enabled electrochemical biosensors integrated with functional nanomaterials have emerged as a promising platform owing to their battery-free operation, wireless data transmission, smartphone compatibility, and enhanced analytical performance [1-3].

Herein, we present two nanomaterial-engineered NFC-enabled electrochemical biosensing platforms for the sensitive detection of clinically relevant biomarkers associated with chronic kidney disease (CKD) and cardiovascular disorders. To demonstrate the versatility of the proposed approach, two distinct nanostructured sensing interfaces were developed. For CKD biomarker detection, mesoporous hollow carbon nanospheres (MHCNSs) integrated with a spiro polymer-based immunosensing interface were employed. The highly porous architecture provides a large electroactive surface area, accelerates electron-transfer kinetics, and promotes efficient immobilization of biorecognition elements, resulting in enhanced analytical sensitivity [2]. For cardiac troponin T (cTnT) detection, a liquid metal Bi–Sn/Au hybrid nanostructured interface was utilized. The synergistic combination of liquid-metal characteristics and Au nanostructures improves electrical conductivity, interfacial charge transfer, and electrocatalytic activity, enabling amplified electrochemical signal transduction for myocardial injury diagnosis [3].

Both sensing platforms were integrated with battery-free NFC modules, allowing real-time wireless electrochemical signal acquisition using portable smart devices without the need for external power sources. Overall, the synergistic integration of engineered nanomaterials, advanced electrochemical sensing interfaces, and NFC technology demonstrates a versatile and scalable strategy for nextgeneration POC diagnostics, offering highly sensitive, portable, battery-free, and user-friendly solutions for real-time disease monitoring.

Acknowledgment:
S. Söylemez gratefully acknowledges the Science Academy, Türkiye, for the Young Scientist Award Program (BAGEP), and TÜBİTAK for financial support through the 2224-B Domestic Scientific Events Participation Support Program for conference participation.

ORCID:
Saniye Soylemez: 0000-0002-8955-133X

References:
[1] Ait Lahcen, A., Rajendran, J., & Slaughter, G. (2025). Advances and challenges in digitally connected point-of-care biosensing. Biosensors and Bioelectronics: X, 100728.
[2] Soyler, D., Tugay, S., Oz, S., Ucar, A.D., Kaya, S., Cevher, S.C., Ozufuklar, O., Celik, E.G., Bulut, U., Unalan, H.E., Timur, S., Soylemez, S. (2026). Mesoporous Hollow Carbon Nanospheres/Spiro Polymer-Based Immunosensors for Near-Field Communication (NFC)-Enabled Detection of Chronic Kidney Disease. ACS Applied Nano Materials, 9, 23, 10963–10974.
[3] Yeniterzi, D., Soyler, D., İnce, D., Çeyirdekçi, V., Çelik, E.G., Unalan, H.E., Timur, S., Aygün, S.Ç., & Soylemez, S. (2026). Smart NFC-enabled point-of-care biosensor utilizing liquid metal Bi–Sn/Au nanostructures for cardiac troponin T detection. Chemical Engineering Journal, 529, 172751.

Keyword: *NFC-enabled biosensors, Nanomaterial-based-electrochemical biosensors, Point-of-care diagnostics*

ID: 499

Metrohm Hyphenated EC-Raman solution

Selin Altınapa *

Metrohm Turkey

Performing **Raman spectroscopy** at the surface of an electrode during electrochemical measurements (e.g., cyclic or linear sweep voltammetry and chronoamperometry) can provide additional molecular or structural information about the redox process. Hyphenation of the analytical techniques synchronizes both Raman spectra acquisition and electrochemical measurement, allowing researchers to correlate electrochemical (EC) processes to changes in the Raman spectra. This **EC-Raman** hyphenation thus helps identify electron transfer-induced molecular changes.

Raman spectroscopy is used for in-situ, real-time monitoring of chemical reactions, among other things. When combined with electrochemical techniques this allows researchers to monitor physicochemical changes occurring in electrolytes at different depths, at electrode surfaces, and more. This powerful combination of techniques (otherwise known as spectroelectrochemistry or SEC) provides further insight into the progress of electrochemical reactions.

Keyword: *EC-raman, Raman, Electrochemistry*

AFM Investigation of Strain Relaxation Mechanisms in Epitaxial Graphene Ridges

Özhan Ünverdi *

Yaşar University

Epitaxial graphene grown on silicon carbide (SiC) is one of the most promising material platforms for future nanoelectronic and nanomechanical applications due to its exceptional electrical, thermal, and mechanical properties [1,2]. However, the mismatch between the thermal expansion coefficients of graphene and the SiC substrate generates residual compressive stress during the post-growth cooling process, leading to the formation of characteristic ridge-like structures that serve as stress-relief features within the graphene layer [3–5]. Understanding the role of these morphological structures in stress relaxation is essential for strain engineering and the optimization of graphene-based devices.

In this study, the strain relaxation behavior of ridge structures formed in epitaxial graphene grown on the C-face of 6H-SiC was investigated using high-resolution Atomic Force Microscopy (AFM). Graphene growth was achieved by thermal decomposition under ultra-high vacuum conditions using a capping-assisted growth approach to control the growth rate and promote the formation of homogeneous single-layer graphene. Raman spectroscopy measurements confirmed the high crystalline quality and single-layer nature of the graphene film while also revealing the presence of residual compressive strain induced during cooling.

AFM topographical imaging revealed the widespread presence of ridge structures across the graphene surface. Detailed height-profile analyses were performed on multiple ridges, and local strain values were calculated using a curvature-based mechanical model. The results demonstrate that ridge formation serves as an efficient stress-relief mechanism within the graphene layer. The strain magnitude decreases significantly at ridge crests, approaching nearly relaxed conditions, whereas elevated strain values are observed near ridge boundaries where stress accumulates prior to relaxation. Furthermore, a distinct strain gradient extending from planar graphene regions toward the ridge structures was identified, indicating progressive stress concentration and redistribution around the relaxation sites.

A clear correlation between ridge morphology and local strain was also observed. Increasing ridge height was associated with larger local strain values, demonstrating that the nanomechanical response of the graphene film is strongly linked to surface morphology. These findings provide direct experimental evidence for the role of ridge formation in thermal stress dissipation and offer valuable insight into the nanoscale strain-management mechanisms of epitaxial graphene. The results highlight the importance of morphological control for the development of graphene-based nanoelectronic, nanomechanical, and strain-engineered device architectures.

This work is supported within the scope of the scientific research project as a part of the Project No. BAP155, which was accepted by the Yaşar University Project Evaluation Commission (PEC).

Acknowledgment:
This work is supported within the scope of the scientific research project as a part of the Project No. BAP155, which was accepted by the Yaşar University Project Evaluation Commission (PEC).

ORCID:
Özhan Ünverdi: 0000-0001-9994-3487

References:
[1] K.S. Novoselov et al., Electric field effect in atomically thin carbon films, Science 306, 666–669 (2004).
[2] C. Berger et al., Electronic confinement and coherence in patterned epitaxial graphene, Science 312, 1191–1196 (2006).
[3] N. Ferralis, J. Kawasaki, R. Maboudian, C. Carraro, Evolution in surface morphology of epitaxial graphene layers on SiC induced by controlled structural strain, Applied Physics Letters 93, 191916 (2008).
[4] W. Bao et al., Controlled ripple texturing of suspended graphene and ultrathin graphite membranes, Nature Nanotechnology 4, 562–566 (2009).
[5] G. Prakash et al., Nanomanipulation of ridges in few-layer epitaxial graphene grown on the carbon face of 4H-SiC, New Journal of Physics 12, 125009 (2010).

Keyword: *Graphene, Atomic Force Microscopy, Nanomechanics*

Interfacial Nano-Frictional Behavior of Para-Aramid Fibers Modified with nano-Hexagonal Boron Carbide (nh-B_4C)

Erman Bilisik [*1], Havva Esra Bakbak[2], Mahmut Korkmaz[3], Gulhan Erdogan[1], Kadir Bilişik[1]

[1] *Erciyes University*
[2] *Ege University*
[3] *Kayseri University*

Nano-scale friction plays a decisive role in the load transfer, energy dissipation, and damage tolerance of high-performance fibrous materials. In this study, the dry and wet nano-frictional behavior of nano-coated para-aramid fibers is systematically investigated with a particular focus on the distinction between nano-static and nano-kinetic friction regimes. By integrating controlled nano-scale surface modification with frictional measurements, the transition from static fiber to fiber interfacial locking to kinetic sliding is quantitatively captured.

The results reveal that nano-coating induces a pronounced increase in nano-static friction, attributed to enhanced interfacial adhesion and surface energy interactions at the fiber–fiber interface. In contrast, nano-kinetic friction exhibits a stabilized and controllable response, governed by friction-induced nano-ploughing and progressive interfacial smoothing during sliding. This frictional duality directly governs pull-out resistance and energy absorption, highlighting the critical role of nano-friction in fracture toughness evolution.

The findings demonstrate that friction-controlled pull-out behavior at the nano-scale is not merely a consequence of surface roughness, but an engineered outcome of interfacial nano-mechanics. The presented insights establish nano-friction engineering as a key design strategy for next-generation para-aramid-based systems, particularly for applications requiring superior damage tolerance and controlled failure mechanisms.

Acknowledgment:
This research was financially supported by a grant awarded by the Erciyes University Scientific Research Unit (EUBAP) under contract number FDK-2023-13113. The authors express their sincere gratitude for this crucial support.

ORCID:
Erman Bilisik: 0000-0002-8172-6318
Havva Esra Bakbak: 0000-0001-5432-6944
Mahmut Korkmaz: 0000-0001-6755-8461
Gulhan Erdogan: 0000-0001-6269-3314
Kadir Bilişik: 0000-0002-0592-980X

References:
[1] Y. Zhou, M. Ali, X. Gong, D. Yang, An overview of yarn pull-out behavior of woven fabrics, Text. Res. J. 89 (2019) 223–234, https://doi.org/10.1177/0040517517741156.
[2] K. Bilisik, Two dimensional (2D) fabrics and three dimensional (3D) preforms for ballistic and stabbing protection: A review, Text. Res. J. 87 (2017) 2275–2304, https://doi.org/10.1177/0040517516669075.
[3] P.M. Gore, B. Kandasubramanian, Functionalized aramid fibers and composites for protective applications: A review, Ind. Eng. Chem. Res. 57 (2018) 16537–16563, https://doi.org/10.1021/acs.iecr.8b04903.
[4] W. Chen, X. Qian, X. He, Z. Liu, J. Liu, Surface modification of Kevlar by grafting carbon nanotubes, J. Appl. Polym. Sci. 123 (2011) 1983–1990, https://doi.org/10.1002/app.34576.
[5] J. Chen, Y. Zhu, Q. Ni, Y. Fu, X. Fu, Surface modification and characterization of aramid fibers with hybrid coating, Appl. Surf. Sci. 321 (2014) 103–108, https://doi.org/10.1016/j.apsusc.2014.09.203.

Keyword: *Aramid fiber; Nano pull-out; Friction; Nano boron carbide (n-B_4C); MWCNTs; GNPs*

Bridging Atomic-Scale to Hierarchical Architecture: Neutron Techniques for Advanced Hybrid Nanomaterials

Selay Sert Çok [*1], Zoltán Dudás[2]

[1] *Ege University, Chemical Engineering Department*
[2] *HUN-REN Centre for Energy Research, Budapest Neutron Center*

Understanding how structural features across multiple length scales govern material performance is essential for the rational design of advanced hybrid nanomaterials. However, establishing reliable structure–property relationships remains challenging, as conventional characterization techniques often fail to capture the full complexity of hierarchical porous architectures. Neutron-based characterization methods offer unique opportunities to bridge this gap by providing complementary insights into the structure and dynamics of complex materials across multiple length scales, owing to their sensitivity to light elements and exceptional penetration depth.

In this work, complementary neutron techniques were employed to investigate functional hybrid nanomaterials prepared through sustainable sol–gel approaches. Neutron diffraction (ND) was utilized to investigate the structural evolution of rare-earth-element-doped silica nanocomposites for catalytic applications, providing insight into phase evolution, crystallinity, and structural development. In parallel, Small-Angle Neutron Scattering (SANS) was employed to probe the hierarchical architecture of functionalized silica-based hybrid porous networks developed for rare-earth-element removal and recovery by adsorption. SANS revealed hierarchical structural features and nanoscale heterogeneities that could not be resolved using conventional characterization methods alone.

The results of these studies demonstrate that material performance cannot be explained solely by composition or surface area but is instead strongly governed by structural features spanning multiple length scales. Neutron-based characterization revealed how crystallinity, nanoscale heterogeneity, and hierarchical structural organization collectively govern functional behavior in hybrid porous materials, establishing mechanistic links between structural organization and performance in adsorption, separation, catalytic, and energy-related applications.

Acknowledgment:
S.S.Ç. acknowledges financial support from the Scientific and Technological Research Council of Türkiye (TÜBİTAK) through the 2219 – International Postdoctoral Research Fellowship Program for Turkish Citizens. The authors also acknowledge the Budapest Neutron Centre (BNC), HUN-REN Centre for Energy Research, for providing the research environment and neutron characterization facilities utilized in this work.

ORCID:
Selay Sert Çok: https://orcid.org/0000-0001-7595-2151
Zoltán Dudás: https://orcid.org/0000-0001-7839-8934

Keyword: *neutron-based characterization techniques, hybrid porous nanomaterials, small angle neutron scattering*

Strain Engineering at the Nanoscale: Computational Insights into Catalytic Materials

Mehya Mansoor [*1], Mubashir Mansoor[1], Maryam Mansoor[2], Sina Rouhi[3], Onur Ergen[4], Kamil Czelej[5], Servet Timur[1], Mustafa Ürgen[1], Sebahattin Gürmen[1]

[1] Istanbul Technical University, Metallurgical and materials engineering department Istanbul 34469, Türkiye
[2] Istanbul Technical University, Energy Institute, Ayazaga Campus, Maslak, Sarıyer, Istanbul 34469, Türkiye
[3] Department of Nanotechnology Engineering, ÖSTİM Technical University, Ankara 06374, Türkiye
[4] Department of Communications and Electrical Engineering, Istanbul Technical University, 34469 Istanbul,Türkiye
[5] Faculty of Chemical and Process Engineering, Warsaw University of Technology, Waryńskiego 1, 00-645, Warsaw, Poland

Catalytic materials are traditionally evaluated through composition, surface area, crystallinity, and active-site availability. However, at the nanoscale, catalytic behavior is also shaped by more subtle atomic-level features, including defects, local lattice distortions, interfacial mismatch, and strain fields. These structural factors can modify electronic states, redistribute charge, alter adsorption behavior, and change reaction pathways. Therefore, strain and defect engineering should not be viewed only as secondary modifications, but as fundamental design dimensions for next-generation catalytic materials.

This study presents a computational materials science perspective on how nanoscale strain and defect structures can be used to rethink catalyst design. By connecting existing knowledge from atomistic modeling, surface chemistry, and materials engineering, the work emphasizes that catalytic performance may be intentionally tuned through controlled atomic displacement and non-ideal local environments. Rather than treating strain and defects as isolated phenomena, the study considers them as coupled structural tools that can influence active-site formation, adsorption strength, electronic structure, and catalytic stability.

The research focuses on nanoscale catalytic systems such as two-dimensional materials, defect-rich surfaces, heterostructures, and nanostructured compounds, where strain effects are often amplified by reduced dimensionality and complex interfaces. Computational approaches, particularly density functional theory-based modeling, provide a powerful route to interpret these relationships by linking atomic configuration with catalytic descriptors such as adsorption energies, charge transfer, electronic-state redistribution, and reaction barriers. The broader significance of this work lies in opening a more integrated way of thinking about catalytic material development. Instead of searching only for new compositions, future catalyst design may increasingly rely on controlling atomic environments, defect landscapes, and strain distributions. This perspective can guide more rational selection of material systems, support experimentally testable predictions, and contribute to the development of efficient, stable, and tunable catalysts for sustainable energy and environmental technologies

ORCID:
Mehya Mansoor: 0000-0002-3848-5838
Mubashir Mansoor: 0000-0001-8097-8823
Maryam Mansoor: 0000-0001-8482-8726
Sina Rouhi: 0000-0003-4430-7568

Keyword: *Catalysis, Strain engineering, DFT*

Characterization of Silver Nanoparticles Synthesized from Astragalus membranaceus Extract via Green Synthesis Method: Assessment of Their Antioxidant Activity, and Antimicrobial Effects

Emir Kermen [*1], Kader Kelle[1], Yagmur Kose[1], Emre Erden Kopar[1], Serife Tozan Ruzgar[2]

[1] *Ege University, Faculty of Science, Department of Biochemistry, Izmir, Türkiye*

[2] *Ege University, Central Research, Testing, and Analysis Laboratory Application and Research Center (MATAL), Bornova-Izmir/Türkiye*

Nanoparticles (NPs) are materials with dimensions ranging from 1 to 100 nm that possess unique physicochemical properties, including a high surface-to-volume ratio, size-dependent optical and electronic characteristics, and enhanced biocompatibility. These properties have led to their widespread application in industrial and biomedical fields such as agriculture, pharmaceuticals, cosmetics, sensor technologies, and textiles, making them an important focus of scientific research (Altammar, 2023).

Since the physical and chemical methods used in nanoparticle synthesis require toxic and expensive chemicals, pose environmental risks, and exhibit relatively low efficiency, interest in green synthesis methods—which offer eco-friendly, sustainable, and economic benefits—has increased significantly in recent years. These methods enable nanoparticle synthesis by utilizing natural sources such as plants and microorganisms (Osman et al., 2024). In green synthesis, phytochemicals and enzymes act as reducing agents and coating materials; thus, nanoparticle synthesis can be carried out without toxic substances, and well-defined nanoparticles can be produced on a large scale while minimizing environmental impacts (Bao et al., 2021).

Astragalus membranaceus is a medicinal plant rich in phytochemicals, particularly astragalosides (ASTs), calicosin, and calicosin-7-O-β-D-glucoside (CG); all of these possess potent reducing and antioxidant properties (Dong et al., 2018). It has been reported that these phytometabolites effectively promote the reduction of metal ions due to their high flavonoid and terpenoid content, while also acting as coating/stabilizing agents on the nanoparticle surface (Villagrán et al., 2024).

Silver nanoparticles (AgNPs) were successfully synthesized via a green method using an aqueous root extract of Astragalus membranaceus. Synthesis conditions were optimized to obtain the highest nanoparticle yield at 60 °C, pH 9, a 12 h reaction time, and 10 mM $AgNO_3$. UV–Vis spectroscopy confirmed the formation of AgNPs with a characteristic peak at 433 nm. SEM analysis revealed predominantly spherical nanoparticles ranging from 40 to 60 nm, while ATR-FTIR and XRD analyses showed that plant-derived biomolecules were involved in nanoparticle reduction and stabilization and confirmed the face-centered cubic crystalline structure of the AgNPs. The synthesized AgNPs also exhibited notable antioxidant activity, with a DPPH radical scavenging inhibition of 57.52 ± 0.38%. As well as, strong antibacterial activity against Escherichia coli, Staphylococcus aureus, and Klebsiella pneumoniae, and significant antifungal activity against Candida albicans. These findings demonstrate that A. membranaceus-mediated AgNPs possess promising antioxidant and antimicrobial properties, highlighting their potential for biomedical applications and the development of next-generation therapeutic agents.

ORCID:
Emir Kermen: 0009-0007-9582-2531
Kader Kelle: 0009-0000-0437-039X
Yagmur Kose: 0009-0009-3184-6109
Emre Erden Kopar: 0000-0002-6641-4367
Serife Tozan Ruzgar: 0000-0002-9550-2868

References:

Altammar, K. A. (2023). A review on nanoparticles: characteristics, synthesis, applications, and challenges. Frontiers in microbiology, 14, 1155622.

Bao, Y., He, J., Song, K., Guo, J., Zhou, X., & Liu, S. (2021). Plant-extract-mediated synthesis of metal nanoparticles. Journal of Chemistry, 2021(1), 6562687.

Dong, M., Li, J., Yang, D., Li, M., & Wei, J. (2023). Biosynthesis and pharmacological activities of flavonoids, triterpene saponins and polysaccharides derived from Astragalus membranaceus. Molecules, 28(13), 5018.

Osman, A. I., Zhang, Y., Farghali, M., Rashwan, A. K., Eltaweil, A. S., Abd El-Monaem, E. M., and Yap, P. S. (2024). Synthesis of green nanoparticles for energy, biomedical, environmental, agricultural, and food applications: A review. Environmental Chemistry Letters, 22(2), 841-887.

Villagrán, Z., Anaya-Esparza, L. M., Velázquez-Carriles, C. A., Silva-Jara, J. M., Ruvalcaba-Gómez, J. M., Aurora-Vigo, E. F., and Martínez-Esquivias, F. (2024). Plant-based extracts as reducing, capping, and stabilizing agents for the green synthesis of inorganic nanoparticles. Resources, 13(6), 70.

Keyword: *Silver nanoparticles (AgNPs), Astragalus membranaceus, Green synthesis*

Green Synthesis and Antibacterial Potential of N,S-Doped Carbon Dots Derived from Nettle (Urtica dioica)

Özlem Gümrah [*] [1], Pınar Acar Bozkurt[2], Mahdi Marzi[3], Şeniz Özalp Yaman[4]

[1] *Department of Pharmacy, Faculty of Pharmacy, Fenerbahçe University, İstanbul, Türkiye*
[2] *Department of Chemistry, Ankara University, Ankara, Türkiye*
[3] *Department of Pharmaceutical Microbiology, Faculty of Pharmacy, Fenerbahçe University, İstanbul, Türkiye*
[4] *Department of Chemical Engineering, Atılım University, Ankara, Türkiye*

Carbon dots (CDs) are nanomaterials with a wide range of applications owing to their low toxicity, high biocompatibility, tunable optical properties, and the possibility of being produced through green synthesis approaches using renewable biomass resources [1-3]. In recent years, heteroatom doping has emerged as an effective strategy to improve the surface characteristics and electron transfer capabilities of CDs. In particular, nitrogen and sulfur doping can promote the formation of active surface sites, contributing to the development of enzyme-like catalytic behavior [4]. In this study, N,S-doped CDs were synthesized from the leaves of nettle (Urtica dioica), a renewable biomass resource, using hydrothermal and sonochemical methods, and their peroxidase-like nanozyme activity and antibacterial potential were investigated.

The structural and optical properties of the obtained CDs were characterized by UV–Vis spectroscopy, fluorescence spectroscopy, FT-IR, Raman spectroscopy, XRD, XPS, TEM, SEM, DLS, and zeta potential analyses. Samples produced via hydrothermal and sonochemical routes were compared, and the effects of the synthesis method on the properties of the resulting CDs were evaluated.

The peroxidase-like nanozyme activity of the CDs was evaluated through the oxidation of ABTS (2,2′-azino-bis(3-ethylbenzothiazoline-6-sulfonic acid)) in the presence of hydrogen peroxide. In addition, the behavior of the nanozyme activity under different pH conditions was investigated.

The antibacterial activity of the N,S-doped CDs was investigated against representative Gram-negative pathogens (Escherichia coli and Acinetobacter baumannii) and Gram-positive pathogens (Staphylococcus aureus and Enterococcus faecalis). The antibacterial effects of CDs alone and in combination with hydrogen peroxide were compared to elucidate potential nanozyme-mediated mechanisms of action.

In conclusion, the results indicate that N,S-doped CDs derived from nettle can be obtained through a green synthesis approach and exhibit potential for nanozyme and antibacterial applications. The study may contribute to the development of biomass-derived functional nanomaterials for future biotechnological, environmental, and biomedical applications.

ORCID:
Özlem Gümrah: 0000-0002-6327-7758
Pınar Acar Bozkurt: 0000-0001-8743-9734
Mahdi Marzi: 0000-0002-8518-0818
Şeniz Özalp Yaman: 0000-0002-4166-0529

References:

1. Wang, Y., & Hu, A. (2014). Carbon quantum dots: synthesis, properties and applications. Journal of Materials Chemistry C, 2(40), 6921–6939. https://doi.org/10.1039/C4TC00988F
2. Kang, C., Huang, Y., Yang H., Yan, X. F., Chen, Z. P., Chen, Z. P. (2020). A Review of Carbon Dots Produced from Biomass Wastes. Nanomaterials, 10(11), 2316. https://doi.org/10.3390/nano10112316
3. Kuang, T., Jin, M., Lu, X., Liu, T., Vahabi, H., Gu, Z., & Gong, X. (2023). Functional carbon dots derived from biomass and plastic wastes. Green Chemistry, 25, 6581–6602. https://doi.org/10.1039/D3GC01763J
4. K.M. Tripathi, H.T. Ahn, M. Chung, X.A. Le, D. Saini, A. Bhati, S.K. Sonkar, M.I. Kim, T. Kim, N, S, and P-Co-doped Carbon Quantum Dots: Intrinsic Peroxidase Activity in a Wide pH Range and Its Antibacterial Applications, ACS Biomater. Sci. Eng. 6 (2020) 5527–5537. https://doi.org/10.1021/acsbiomaterials.0c00831

Keyword: *N,S-doped carbon dots, antibacterial activity, biomass-derived nanomaterials*

Green Synthesis, Characterization, and Antibacterial Activity of Silver Nanoparticles Derived From Centaurea Kirmacii Aqueous Extract

Zehra Sinem Yılmaz [*1], **Hüsniye Kayalar**[2], **Tuğçe Fafal**[2]

[1] *Center for Materials Research, Izmir Institute of Technology, İzmir, Türkiye*
[2] *Department of Pharmacognosy, Faculty of Pharmacy, Ege University, İzmir, Türkiye*

The green synthesis of metallic nanoparticles using plant extracts has emerged as an environmentally benign and cost-efficient alternative to conventional chemical and physical methods, with endemic species attracting particular interest owing to their distinctive phytochemical profiles that serve as natural reducing and stabilizing agents. In light of this, the present study aimed to develop a green synthesis route for silver nanoparticles (AgNPs) utilizing Centaurea kirmacii as a biological reducing agent, offering a sustainable and economical alternative to traditional chemical fabrication techniques.

AgNPs were prepared by reducing silver nitrate with C. kirmacii aqueous extract. Nanoparticle formation was verified by UV-Vis spectroscopy, and colloidal stability was confirmed over the evaluated storage period. Fourier Transform Infrared Spectroscopy (FTIR) was employed to identify functional groups involved in reduction and stabilization, while Scanning Electron Microscopy (SEM) was used to examine nanoparticle morphology. In vitro antibacterial activities of the AgNPs and the plant extract were assessed against common pathogenic bacteria using the Minimum Inhibitory Concentration (MIC) assay.

UV-Vis spectroscopy revealed a characteristic surface plasmon resonance (SPR) absorption band at 440 nm, confirming monodisperse AgNP formation. FTIR analysis identified key absorption bands at 3259 cm^{-1} (O-H/N-H stretching), 2932 cm^{-1} (C-H stretching), 1583 cm^{-1} (C=C/amide I), 1394 cm^{-1} (C-H bending/carboxylate), 1259 cm^{-1} (C-O stretching), and 1031 cm^{-1} (C-O-C/glycosidic linkages), confirming the involvement of C. kirmacii biomolecules in bioreduction and surface capping. SEM analysis revealed spherical nanoparticles with an approximate size of 15 nm. The strong silver peak seen in EDX confirmed particle formation. MIC assay results demonstrated that AgNPs achieved complete eradication of S. aureus and E. coli (100% reduction) and near-complete inhibition of S. epidermidis (99.99% reduction), while the aqueous extract alone showed excellent activity against S. aureus (99.99%), moderate activity against E. coli (78.00%), and limited activity against S. epidermidis (69.58%).

Centaurea kirmacii-mediated green synthesis yielded stable, spherical AgNPs (~15 nm) whose formation and surface functionalization were confirmed by UV-Vis, FTIR, SEM, and SEM-EDX analyses. The synthesized AgNPs displayed superior broad-spectrum antibacterial activity, markedly outperforming the plant extract alone, and established C. kirmacii as a valuable biogenic platform for the eco-friendly production of AgNPs with strong potential in combating antimicrobial resistance.

Acknowledgment:
The authors acknowledge the Center for Materials Research (CMR) at IZTECH and the Pharmaceutical Sciences Research Center at Ege University.

ORCID:
Zehra Sinem Yılmaz: 0000-0002-7105-8117
Hüsniye Kayalar: 0000-0001-7882-0517
Tuğçe Fafal: 0000-0002-7445-5855

References:
Karamenderes, C., Khan, S., Tekwani, B. L., Jacob, M. R., & Khan, I. A. (2006). Antiprotozoal and Antimicrobial Activities of Centaurea. Species Growing in Turkey. Pharmaceutical Biology, 44(7), 534-539. https://doi.org/10.1080/13880200600883080
Karunakaran, G., Sudha, K. G., Ali, S., & Cho, E.-B. (2023). Biosynthesis of Nanoparticles from Various Biological Sources and Its Biomedical Applications. Molecules, 28(11), 4527. https://doi.org/10.3390/molecules28114527
Tuzun, B. S., Fafal, T., Ozguney, I., & Kivcak, B. (2024). Green Synthesis of Silver Nanoparticles by Using Anthemis Tricolor Boiss., Factorial Design for Parameter Optimization, Characterization and In-Vitro Biological Activities. Journal of Pharmaceutical Innovation, 19(3), 32. https://doi.org/10.1007/s12247-024-09842-w
Tuzun, B. S., Hohmann, J., & Kivcak, B. (2018). Green bio-inspired synthesis, characterization and activity of silver nanoparticle forms of Centaurea virgata Lam. And the isolated flavonoid eupatorin. Green Processing and Synthesis, 7(4), 372-379. https://doi.org/10.1515/gps-2017-0027
E35 Committee. (t.y.). Test Method for Determining the Antimicrobial Activity of Antimicrobial Agents Under Dynamic Contact Conditions. ASTM International. https://doi.org/10.1520/E2149-20

Keyword: *Centaurea kirmacii, Biogenic silver nanoparticles, Antimicrobial activity*

One-Step Green Fabrication of AgNP-Embedded Electrospun PVA Nanofibers for Dual Antibacterial and Photocatalytic Performance

Seda Şen [*1,2], **Nalan Oya San Keskin**[2]

[1] *Institute of Graduate Programs and Department of Biology, Polatlı Science and Literature Faculty, Ankara Hacı Bayram Veli University, Ankara 06900, Türkiye*

[2] *Polatlı Science and Literature Faculty, Biology Department, Nanosan Laboratory, Ankara Hacı Bayram Veli University, Ankara 6900, Türkiye*

Electrospinning is an effective method for the production of functional materials, enabling the easy and controlled production of nanofibers. While interest in developing nanofibers focused on specific properties such as antibacterial and photocatalytic activity has increased in recent years, research into multifunctional materials that combine these functions on a single platform and are obtained through a green synthesis approach is needed. In this study, silver nanoparticles (AgNP) produced using bacterial supernatant via a green synthesis approach and polyvinyl alcohol (PVA) based nanofibers (AgNP/PVA NF) were produced in a one-step using the electrospinning method, and the material was evaluated in terms of its antibacterial and photocatalytic activity. To improve the structural stability of the produced AgNP/PVA nanofibers, they were cross-linked using a glutaraldehyde immersion technique. Subsequently, the material was characterized using scanning electron microscopy (SEM), transmission electron microscopy (TEM), energy dispersive X-ray spectroscopy (EDX), Fourier transform infrared spectroscopy (FTIR), X-ray diffraction (XRD), thermogravimetric analysis (TGA), water solubility test, and water contact angle measurements. According to SEM micrographs, AgNP/PVA NFs with a diameter of 304 ± 6 nm were produced, while TEM micrographs showed that very small AgNPs with an average size of 4.9 ± 0.1 nm were successfully formed within the PVA nanofiber. In antibacterial activity tests performed using the colony count assay method against Escherichia coli (E. coli) and Staphylococcus aureus (S. aureus), 99.9% inhibition was observed for E. coli and 100% for S. aureus, indicating that AgNP/PVA NF completely inhibited bacterial growth in both gram-positive and gram-negative bacteria. Photocatalytic degradation studies of methylene blue dye, performed under UV light and visible light, were evaluated separately against an initial dye concentration of approximately 10 mg/L. Degradation capacity was investigated by taking samples at specific minutes (5, 10, 15, 30, 45, and 60 minutes). After a 30-minute dark phase under UV light, 21.1% removal was obtained, and after turning on the UV light, 33.9% removal was observed at 60 min. Under visible light, 16.24% removal was achieved after 30 minutes of dark phase, and 19.9% photodegradation efficiency was obtained at 60 minutes. Therefore, AgNP/PVA nanofibers can be used as an effective multifunctional material offering structural stability, eco-friendly production, and one-step synthesis advantages, in addition to their antibacterial and photocatalytic properties. We would like to thank the Scientific and Technological Research Council of Türkiye (TÜBİTAK and the TÜBİTAK-BİDEB 2211-A Domestic Doctoral Scholarship Program) for their support.

Acknowledgment:
We would like to thank the Scientific and Technological Research Council of Türkiye (TÜBİTAK and the TÜBİTAK-BİDEB 2211-A Domestic Doctoral Scholarship Program) for their support.

ORCID:
Seda Şen: 0000-0002-1187-2811
Nalan Oya San Keskin: 0000-0001-6645-3561

Keyword: *Green synthesis, antibacterial and photocatalytic activity, one-step fabrication AgNP/PVA nanofibers*

Development of Antibacterial Coatings on Micro-Arc Oxidized Titanium Surfaces via Chitosan-Silver Hybrid Functionalization

Sıla Özay * **, Tuğçe Aybüke Arıca Güvenç, Ezgi Oğur, Fatih Toptan**

Department of Materials Science and Engineering, Izmir Institute of Technology, Izmir, Urla 35430, Turkey

Titanium and its alloys are most commonly used materials for load-bearing implants due to their favorable mechanical properties, corrosion resistance, and biocompatibility. However, implant-associated infections remain a significant clinical problem, frequently leading to implant failure, revision surgery, prolonged antibiotic treatment, and increased healthcare costs [1]. Therefore, developing multifunctional surface coatings that inhibit bacterial growth while preserving biocompatibility is essential for improving long-term implant performance. This study presents a novel multifunctional surface engineering approach for load-bearing titanium implants, addressing both osseointegration and bacterial infection through a stepwise surface modification strategy.

Micro-arc oxidation (MAO) was applied to titanium substrates to generate a porous, calcium and potassium incorporated TiO_2 layer with strong adhesion to the underlying metal, high hardness, and improved protection against wear and corrosion [2]. The MAO-treated surface served as a reservoir for the subsequent chitosan-silver nanoparticle (AgNP) hydrogel coating. To promote strong and durable covalent anchoring of the chitosan hydrogel onto the MAO layer, the surface was sequentially functionalized with (3-aminopropyl) triethoxysilane (APTES) and glutaraldehyde (GA), with stepwise bonding confirmed by Raman spectroscopy [3]. Silver nanoparticles, selected as the antimicrobial agent due to their broad-spectrum antibacterial activity, were synthesized by chemical reduction of $AgNO_3$ within a chitosan solution, where chitosan served as stabilizer to prevent agglomeration; synthesis parameters were optimized to yield monodisperse particles below 30 nm, confirmed by DLS and SEM [4]. The resulting chitosan-coated AgNPs were subsequently integrated into the chitosan hydrogel matrix to achieve homogeneous nanoparticle distribution throughout the coating. Chitosan was selected as the coating matrix not only for its natural biocompatibility, biodegradability, and intrinsic antibacterial properties, but also for its pH-sensitive swelling behavior. Since bacterial metabolism and local inflammatory reactions can decrease the pH around infected implant sites, the coating was designed to enhance Ag^+ release under acidic conditions [5]. The AgNP-loaded chitosan hydrogel was crosslinked with GA at optimized ratios and evaluated by swelling tests in phosphate-buffered saline (PBS) at pH 7.0 and pH 5.5, representing healthy and infected tissue environments. Silver ion release was quantified by ICP-OES, while coating integrity, silver distribution, and coating thickness were examined by FIB-SEM.

Electrochemical performance was assessed under static conditions through OCP monitoring, potentiodynamic polarization, and electrochemical impedance spectroscopy (EIS), while tribocorrosion behavior was evaluated in a simulated physiological environment; open-circuit potential was monitored, and post-test wear track morphology was characterized by SEM to elucidate coating performance under the synergistic action of mechanical wear and electrochemical corrosion. This integrated approach yields a coating that combines enhanced osseointegration potential, mechanical durability, and antimicrobial release triggered by the acidic microenvironment of bacterial infection.

Acknowledgment:
This research was financially supported by the Scientific and Technological Research Council of Türkiye (TÜBİTAK) under the 2210-C National Scholarship Programme for MSc Students (Project No: 1919B012321366). The authors would like to express gratitude to the Integrated Research Center (TAM) at Izmir Institute of Technology (IZTECH) for providing the necessary infrastructure and facilities. Special thanks are extended to the Materials Research Center (MAM), BIYOMER, and Environmental R&D Department for their technical support and contributions during the characterization studies, and to Lecturer Adem Yavuz for his expertise and guidance throughout the Raman spectroscopy analyses.

ORCID:
Sıla Özay: 0009-0001-8881-7669
Tuğçe Aybüke Arıca Güvenç: 0000-0001-8018-0520
Ezgi Oğur: 0000-0001-9999-7063
Fatih Toptan: 0000-0001-9138-9119

References:
Chen, X., Zhou, J., Qian, Y. & Zhao, L. Antibacterial coatings on orthopedic implants. Materials Today Bio 19, 100586 (2023).
Ogur, E., Alves, A. C. & Toptan, F. Advancing titanium-based surfaces via micro-arc oxidation with solid substance incorporation: A systematic review. Materials Today Communications 41, 110343 (2024).
Hiraoui, M. et al. Spectroscopy studies of functionalized oxidized porous silicon surface for biosensing applications. Materials Chemistry and Physics 128, 151–156 (2011).
Akshaya, S., Rowlo, P. K., Dukle, A. & Nathanael, A. J. Antibacterial Coatings for Titanium Implants: Recent Trends and Future Perspectives. Antibiotics 11, 1719 (2022).
Tan, G. et al. Antibacterial and Anti-Inflammatory Coating Materials for Orthopedic Implants: A Review. Coatings 11, 1401 (2021).

Keyword: *Chitosan based nanocomposite, Titanium, Degradation*

Development of Collagen Hydrolysate-Based Gel Electrolytes Derived from Leather Industry Wastes for Sustainable Supercapacitors

Halil Utku Peker [*1], Damla Sahin[2], Gulsah Yılmaz[2], Sirin Siyahjani-Gultekin[2], Batikan Kavukcu[3], Bugra Ocak[4], Bahri Basaran[4], Burak Gultekin[2], Gulsah Türkmen[4]

[1] Ege University Material Science and Engineering Department
[2] Ege University, Solar Energy Institute
[3] Ege University, Department of Chemistry
[4] Ege University, Leather Engineering Department

In this study, in line with green technology and sustainability principles, collagen hydrolysate (CH) was obtained via enzymatic hydrolysis of significant industrial waste, aiming to evaluate eco-friendly biopolymers from leather industry waste. This biopolymer has been successfully modified as an alternative matrix gel polymer electrolyte (GPE), which minimize leakage and safety risks in supercapacitors, stand out for offering both ionic conductivity and mechanical property.

Collagen hydrolysate polymer matrices were modified under optimized conditions using pectin as a secondary polymer support and tannic acid as a crosslinking agent. Films prepared with pectin exhibited superior ionic conductivity. The structural, thermal, and morphological properties of CH based electrolytes were verified through XRD, FTIR, and DSC and TGA analyses. Collagen hydrolysate based electrolytes showed high ionic conductivity, flexibility and mechanical properties.

Thanks to the high ionic conductivity and optimized amorphous matrix structure achieved, the electrochemical stability and electrolyte/electrode interface compatibility of the developed bio-based gel electrolytes were successfully tested for green-design supercapacitor cells, This study provides a fully sustainable, high-performance route for the utilization of industrial by-products of leather industry wastes, as functional components in value-added energy storage devices.

Acknowledgment:
This work was supported by the Scientific and Technological Research Council of Türkiye (TÜBİTAK) under Project Number 124M968 (1001 Program).

ORCID:
Halil Utku Peker: 000900043547844X

References:
1. S. Dalwadi et al., "The Integration of Biopolymer-Based Materials for Energy Storage Applications: A Review," Int. J. Mol. Sci., vol. 24, no. 4, p. 3975, Feb. 2023, doi: 10.3390/ijms24043975.
2. A. Aguzin et al., "Gelatin and Tannic Acid Based Iongels for Muscle Activity Recording and Stimulation Electrodes," ACS Biomater. Sci. Eng., vol. 8, no. 6, pp. 2598–2609, Jun. 2022, doi: 10.1021/acsbiomaterials.2c00129.
3. E. C. Fluker et al., "Polyvinylidene Fluoride-Based Gel Polymer Electrolytes for Calcium Ion Conduction: A Study of the Influence of Salt Concentration and Drying Temperature on Coordination Environment and Ionic Conductivity," J. Phys. Chem. C, vol. 127, no. 33, pp. 16231–16242, Aug. 2023, doi: 10.1021/acs.jpcc.3c02342.
4. H. Yang et al., "Lignocellulose-Mediated Gel Polymer Electrolytes Toward Next-Generation Energy Storage," Nano-Micro Lett., vol. 18, no. 1, p. 84, Nov. 2025, doi: 10.1007/s40820-025-01927-

Keyword: *Collagen Hydrolysate, Gel Polymer Electrolyte, Leather Waste*

Multifunctional Electrospun Cellulose Acetate Nanofibrous Mat with Molecular Release, Biocompatibility, pH-Responsiveness and Sensor Properties

Osman Arslan * **, Merve Esra Üngör**

İstanbul Sabahattin Zaim University, Food Engineering Department

As a representative example of multifunctional smart materials, this study reports the fabrication of electrospun cellulose acetate nanofibers engineered to exhibit visible light emission, pH responsiveness and molecular encapsulation capabilities. These properties were achieved through a sequential loading strategy combining encapsulation and surface functionalization via controlled dipping techniques. During electrospinning, nanofibers were functionalized with citral, a pH-responsive indicator dye and silicon quantum dots as fluorescent emitters. The incorporated functionalities were characterized by FT-IR spectroscopy, photoluminescence analysis (PL) and thermal profiling (TG-DTA), confirming programmable molecular encapsulation and release, pH responsiveness and stable visible fluorescence from silicon quantum dots.In TGA, there is a little mass loss before 100 °C and after that till 300 C a small degradation possible removal of physically adsorbed molecules are seen. Nanofiber degradation started at 300 °C and was completed at 550 °C with a sample loss of 85%, which is mostly consistent with that described in the literature. Si QDs display visible light emission between 520 and 590 nm with varying excitation wavelengths between 300 and 410 nm, respectively. Obtained results showed that emission maxima corresponding to the λmax = 596 nm are changing. Scanning electron microscopy (SEM), energy-dispersive X-ray spectroscopy (EDX) and X-ray photoelectron spectroscopy (XPS) analyses validated surface uniformity, elemental distribution and the successful integration of multiple active components. SEM investigation of the latest multifunctional nanofibers yielded a morphologically integrated and functionally synergistic system. There is no any bead is observed but as expectedly average diameter was increased when compared to previous forms of the nanofiber. SEM clearly revealed mildly more tangled and coherent fibers (~300-320 nm). Survey XPS spectrum of final multifunctional nanofiber confirms the availibility of silicon 2s peak at 101.3 eV, carbon 2s peak at 237.1 eV and oxygen 2 s peaks at 537 .4 eV. Nitrogen peak is slightly low in intensity in the survey spectrum but in high resolution investigation 2 s peak of the nitrogen appears at 402.2 eV. Silicon peak appears at 103.3 eV and carbon and oxygen deconvolutions basically replicate the corresponding peaks with slight shifts due to the electron density variation. Multifunctional (CA) nanofibers exhibited distinct, rapid, and visibly detectable color transitions upon exposure to 0.1 M ammonia (NH_3), 0.1 M aqueous sodium hydroxide (NaOH), and traditionally available hypochloride solution, the nanofibers shifted from colorless to bright pink due to phenolphthalein's well-known pH-responsive structural transformation: under basic conditions (pH > 8.5). Quenching efficiencies of the Si QD solutions by different concentrations of the dinitrobenzene (DNB) and results revelaed that it was possible to detect the Stern-Volmer plot and the fitting result showed that quenching relationship was y= 1.71 [DNB]+ 2.3 and there is a direct relationship between the quenching constant and the concentration of dinitro benzene group.

Acknowledgment:
We would like to acknowledge Asst. Prof. Dr. Yasemin Yılmazer, M.Sc. Ferhat Bostancı for the cytotoxicity and other biological tests. We would like to thank to the partial support of the Istanbul Sabahattin Zaim University-IZU 500-Nanomagnetic Plastics-1 project.

ORCID:
Osman Arslan: 0000-0002-3011-1663
Merve Esra Üngör: 0009-0002-9720-2161

References:
1-Multifunctional electrospun polymeric nanofibrous mats for catalytic reduction, photocatalysis and sensing, O Arslan, T Uyar, Nanoscale 9 (27), 9606-9614
2-Superhydrophobic, hybrid, electrospun cellulose acetate nanofibrous mats for oil/water separation by tailored surface modification, O Arslan, Z Aytac, T Uyar, ACS Applied Materials & Interfaces 8 (30), 19747-19754

Keyword: *electrospinning, multifunctional nanomaterial, nanotechnology*

Haptic In-Sensor Computing Device Based on CNT/PDMS Nanocomposite Physical Reservoir

Kouki Kimizuka [*1], Ahmet Karacali[2], Saman Azhari[3], Yuki Usami[1,2], Shuhei Ikemoto[1,2], Hakaru Tamukoh[1,2], Hirofumi Tanaka[1,2]

[1] Research Center for Neuromorphic AI Hardware, Kyushu Institute of Technology, Kitakyushu, Japan.
[2] Graduate School of Life Science and Systems Engineering, Kyushu Institute of Technology, Kitakyushu,Japan.
[3] Graduate School of Information, Production and Systems (IPS), Waseda University, Kitakyushu, Japan.

The rapid expansion of intelligent robotic systems has increased the demand for tactile sensors capable of processing information directly at the sensing node. In-sensor computing offers a promising solution by reducing the latency and power consumption associated with conventional sensor–processor architectures.
In this work, we present a porous carbon nanotube/polydimethylsiloxane (CNT/PDMS) nanocomposite that functions simultaneously as a tactile sensor and a physical reservoir computing (RC) device for neuromorphic information processing.
The porous CNT/PDMS structure was fabricated using a sacrificial sugar-template method, forming an interconnected conductive network within an elastic polymer matrix. Mechanical deformation dynamically modifies conductive pathways between CNTs, producing nonlinear and history-dependent electrical responses suitable for reservoir computing. These material dynamics enable information processing without complex digital computation.
The device was integrated into a robotic gripper, and tactile signals generated during grasping were directly used as reservoir states for object classification. Analysis of transient tactile responses revealed that rich computational features emerge immediately after contact, allowing accurate object discrimination using only a small fraction of the acquired data. Real-time recognition experiments demonstrated classification accuracies exceeding 90% for multiple objects with different mechanical and geometrical characteristics.
The results demonstrate that porous CNT/PDMS nanocomposites can simultaneously perform sensing and computation, offering a compact and energy-efficient platform for robotic perception. This approach provides a promising pathway toward next-generation tactile intelligence for edge-AI robotics and autonomous systems.

ORCID:
Kouki Kimizuka: 0009-0008-0462-0967
Ahmet Karacali: 0009-0000-4695-2814
Saman Azhari: 0000-0002-7043-0909
Yuki Usami: 0000-0002-8583-325X
Shuhei Ikemoto: 0000-0003-4885-8746
Hakaru Tamukoh: 0000-0002-3669-1371
Hirofumi Tanaka: 0000-0002-4378-5747

References:
Kimizuka, K., Azhari, S., Tokuno, S., Karacali, A., Usami, Y., Ikemoto, S., Tamukoh, H. and Tanaka, H. (2025), Haptic In-Sensor Computing Device Based on CNT/PDMS Nanocomposite Physical Reservoir. Adv. Intell. Syst., 7: 2400640. https://doi.org/10.1002/aisy.202400640

Keyword: *In-Sensor Computing, Soft Robotics, Tactile Intelligence*

Highly Uniform Microfabricated 3D Ring-Shaped Electrode Arrays: From Thin Films to Mesoscale Structures

Patricia Pereira Silva[1], Inês S. Garcia[1], Filipe S. Alves[1], Rosana A. Dias [* 1], Mehmet Selim Hanay[1,2]

[1] INL - International Iberial Nanotechnology Laboratory
[2] Bilkent University

We report the development of ring-shaped electrodes (ringlets) arrays, implemented using a high-uniformity, high-throughput and high scalability thin-film microfabrication process. This 3D mesoscale electrode arrays approach is based on self-assembly driven by engineered residual stress of multilayer thin films. It can deliver high geometrical uniformity and relies on wafer-level processes with clear scalability advantages over 2PP (feature size control up to 100 nm) or post-fabrication assembly techniques (positioning accuracy typically limited to 250 nm).

The self-rolled metal-clad microcantilevers, comprised by SiO_2/SiN_x/Cr/Au multilayers (total thickness of 430nm) are patterned on 200 mm silicon substrates. Release by XeF_2 yields reproducible ringlets with diameters 140–185 µm for designs covering ~57–75% of the perimeter, with low in-wafer non-uniformity (up to ~3.7%). At the individual array level, we demonstrate standard deviations better than 0.05% (70 nm) within 65 metalized electrode array groups with 144 µm diameter, which represents more than a 20-fold improvement in the uniformity of the ringlets compared to the state of the art.

The ringlets exhibit robust roll-up driven by the through-thickness stress gradient without widespread stiction between ringlets. These electrode arrays present high geometrical precision with inherently aligned electrodes that can be used to create electrostatic fields with high uniformity. Since microfabrication is inherently a parallel process, this approach enables the construction and operation of large numbers of on-chip arrays.

Acknowledgment:
The authors acknowledge the support of the project with the reference n.º 1313551786, funded by FCT – Fundação para a Ciência e a Tecnologia, I.P. under the Portuguese Resilience and Recovery Plan, through the NextGenerationEU Fund.

ORCID:
Patricia Pereira Silva: 0000-0001-5867-9085
Inês S. Garcia: 0000-0002-4605-6961
Filipe S. Alves: 0000-0002-3439-8235
Rosana A. Dias: 0000-0002-3877-0946
Mehmet Selim Hanay: 0000-0002-1928-044X

References:
O. G. Schmidt and K. Eberl, “Nanotechnology. Thin solid films roll up into nanotubes,” Nature, vol. 410, no. 6825, p. 168, 2001.
S. Gu et al., “3D nanolithography with metalens arrays and spatially adaptive illumination,” Nat. 2025 6488094, vol. 648, no. 8094, pp. 591–599, 2025.
M. Saha et al., “Nanophotonic waveguide chip-to-world beam scanning,” Nat. 2026 6518105, vol. 651, no. 8105, pp. 356–363, 2026.

Keyword: *Stress engineered thin-films, Self-rolled microstructures, 3D self-assembly*

Towards HSV Management with Minimal Invasiveness: Mechanical Integrity, Skin Penetration and Ex Vivo Deposition of Bilayer Berberine-Loaded Dissolving Microneedles

Zakaria Ouzaid [*1], Ebru Altuntaş[2], Ceren Koca[1,2], Hasan Sercan Palancı[3]

[1] *Pharmaceutical Technology, Graduate School of Health Sciences, İstanbul University, İstanbul, Türkiye*
[2] *Pharmaceutical Technology, Faculty of Pharmacy, İstanbul University, İstanbul, Türkiye*
[3] *Virology, Faculty of Veterinary Medicine, Dokuz Eylül University, İzmir, Türkiye*

Herpes simplex virus (HSV) causes recurrent mucocutaneous infections and lifelong latency. Although nucleoside analogues such as acyclovir inhibit viral DNA polymerase, resistance may develop with prolonged use [1]. Berberine (BER), an isoquinoline alkaloid from Coptidis rhizoma, has demonstrated inhibitory activity against HSV replication [2]. We sought to create BER-loaded dissolving microneedles (DMNs) that could penetrate the stratum corneum and deliver the drug intradermally with minimal invasiveness. A master mold comprising a 11 × 11 array of pyramidal microneedles (MNs) (base width 300 μm; height 900 μm) was 3D-printed at a 45° tilt [3]. Bilayer BER-DMNs were produced by two-step casting and centrifugation [4]. DSC confirmed drug–polymer compatibility, and FTIR revealed no chemical changes in the BER structure. Under a 32 N axial load, MN height reduction remained below 10%, and Parafilm M® analysis confirmed effective multilayer skin insertion [5]. Before the application, Confocal laser scanning microscopy showed intact, fluorescent tips. After that, the tips dissolved in less than an hour, and the signal was strong throughout the epidermis and upper dermis. The system successfully penetrated the skin barrier and enabled effective intradermal deposition of berberine, delivering 267.1 ± 6.8 μg within one hour while maintaining adequate drug loading (1.07 ± 0.09 mg per patch). After three months of physicochemical stability testing at 25 °C and 60% RH, no statistically significant decrease was observed in the mechanical strength, and the active ingredient content of the DMNs. Bilayer DMNs represent a promising minimally invasive platform for intradermal delivery of antiviral phytochemicals for localized HSV management, while SLA 3D printing enables rapid, cost-effective, and industrially scalable fabrication.

Acknowledgment:
This research was financially supported by the Scientific Research Projects Coordination Unit of Istanbul University BAP No. 40671 and TUSEB No. 12201.

References:
1. van de Sand, L., et al., Antiviral active compounds derived from natural sources against herpes simplex viruses. Viruses, 2021. 13(7): p. 1386.
2. Chin, L.W., et al., Anti-herpes simplex virus effects of berberine from Coptidis rhizoma, a major component of a Chinese herbal medicine, Ching-Wei-San. Archives of virology, 2010. 155(12): p. 1933-1941.
3. Razzaghi, M. and M. Akbari, The effect of 3D printing tilt angle on the penetration of 3D-printed microneedle arrays. Micromachines, 2023. 14(6): p. 1157.
4. Nasiri, M.I., et al., Nanoemulsion-based dissolving microneedle arrays for enhanced intradermal and transdermal delivery. Drug Delivery and Translational Research, 2022. 12(4): p. 881-896.
5. Larrañeta, E., et al., Microneedle arrays as transdermal and intradermal drug delivery systems: Materials science, manufacture and commercial development. Materials Science and Engineering: R: Reports, 2016. 104: p. 1-32.

Keyword: *Advanced drug delivery system, Dissolving microneedles, Stereolithography 3D printing*

Microfluidically Synthesized Aprotinin Nanoconjugates for Enhanced Therapeutic Response in 3D Tumor Spheroid Model

Iqra Munir[1], Faiqa Nazir[1], Gurkan Yesiloz[1,2], Faruk Aksoy [* 2]

[1] Yesiloz Research Lab, National Nanotechnology Research Center (UNAM)- Bilkent University, 06800, Cankaya-Ankara, Türkiye.
[2] Institute of Material Science and Nanotechnology, Bilkent University, 06800, Cankaya-Ankara, Türkiye.

Nanomedicine strategies leveraging bio-derived nano-carriers offer promising avenues for precision chemotherapy. Here, we introduce a microfluidics-assisted nanoconjugate platform that repurposes Aprotinin (Apr); a naturally occurring protein, as an enhanced anti-cancer nano-carrier for Valproic Acid (VPA), a histone deacetylase inhibitor with anticancer properties. The resulting Aprotinin-Valproic Acid (Apr-VPA) nanoconjugates synthesized via a flow-controlled microfluidic process were characterized by various physioco-chemical methods confirming the stable binding. When tested on in vitro studies in 2D cell culture followed by custom designed 3D tumor spheroid models, the Apr-VPA nanoconjugates demonstrated dose-dependent inhibition of spheroid growth and viability, supporting the nanoconjugate's therapeutic potential. Preliminary in vitro comparisons with healthy endothelial cells suggest selective cytotoxicity, warranting further investigation. Interestingly, the designed nanoconjugates also exhibited pH-responsive release behavior under acidic conditions, indicating potential for envirnment-triggered drug release.

Thus, it was expected that a novel high technology-controlled synthesis and stimuli sensitive release system, increasing the bioavailability of drug when conjugated (Apr-VPA) as compared to free VPA may perhaps be tranlated to the clinics when validated in vivo. Therefore, plasma profile of VPA and Apr-VPA nanoconjugates by LC-MS/MS and serum enzymatic markers were assessed in wildtype balb/c mice, depicting significantly enhanced availability of drug when conjugated with a carrier.

These analysis highlight the feasibility of using aprotinin as a scalable protein-based nanocarrier for tumor-preferential therapeutic response in tested cancer models and support its future development in advanced nanomedicine applications. Moreover, the findings support the concept of chemically engineered protein-drug hybrid carriers as next-generation nano-therapeutics. By offering (a) the use of aprotinin as a functionally active carrier rather than an inert protein scaffold, (b) the formation of a pH-responsive supramolecular drug–protein nanoconjugate, and (c) the integration of physicochemical, biological (2D and 3D), pharmacokinetic, and hemocompatibility evaluations within a unified platform, such nanoconjugate platforms have the potential to bridge the gap between preclinical drug screening and clinical translation, offering new avenues for precision-targeted therapies in oncology and beyond.

Acknowledgment:
We gratefully acknowledge the support from the Türkiye Sağlık Enstitüleri Başkanlığı (TÜSEB) and Scientific and Technological Research Council of Türkiye (TUBITAK).

References:
1. Munir, I., Ajmal, S., Shah, M. R., Ahmad, A., Hameed, A., & Ali, S. A. (2017). International Journal of Biological Macromolecules, 101, 131-145.
2. Nazir, F., Munir, I., & Yesiloz, G. A. (2024). ACS Applied Materials & Interfaces. 16(15), 18311-18326.
3. Munir, I., Nazir, F., & Yesiloz, G. (2024). ACS Applied Materials & Interfaces, 16(51), 70187-70204.

Keyword: *microfluidics, protein-drug nanoconjugates, spheroids*

Albumin Polyelectrolyte Complex Nanoparticles as a Novel Platform for Therapeutic mRNA Delivery

Aytul Gul-Mete [*] [1,2], **Sümeyra Cigdem Sözer-Demirdas**[3], **Merve Basol**[1,2], **Ozlem Erez**[1], **Yasar Akdogan**[3], **Gulcin Cakan-Akdogan**[1,2]

[1] *Izmir Biomedicine and Genome Center, Izmir, Türkiye*
[2] *Izmir International Biomedicine and Genome Institute, Dokuz Eylul University, Izmir, Türkiye*
[3] *Department of Materials Science and Engineering, Izmir Institute of Technology, Izmir, Türkiye*

Background: Messenger RNA (mRNA)-based therapeutics have emerged as a promising strategy for the treatment of genetic diseases. However, efficient and biocompatible delivery systems remain a major challenge. Our group previously developed albumin-based polyelectrolyte complex nanoparticles as a solvent-free drug delivery platform and demonstrated their high loading capacity and anticancer efficacy with small-molecule therapeutics. In the present study, we extend this platform to therapeutic mRNA delivery for gene therapy applications.

Methods: Albumin was chemically modified with ethylenediamine to generate cationic albumin. Albumin-based polyelectrolyte complex nanoparticles (PEC-NPs) were produced through the self-assembly of native albumin and cationic albumin in aqueous media without the use of organic solvents or chemical crosslinkers. Fluorescent reporter and therapeutic mRNAs were synthesized by in vitro transcription and used to evaluate mRNA production and loading efficiency. Nanoparticles were characterized by dynamic light scattering (DLS), zeta potential analysis, and scanning electron microscopy (SEM). Encapsulation efficiency was determined by spectrophotometric analysis and gel retardation assays. Cytotoxicity studies were performed in HEK293T. Protein expression studies were evaluated in the mutant zebrafish model.

Results: Ethylenediamine conjugation successfully converted albumin from an anionic protein (−28 mV) to a cationic form (+27 mV). Optimized albumin PEC-NPs exhibited a spherical morphology with an average hydrodynamic diameter of approximately 140 nm, low polydispersity (PDI = 0.08), and a zeta potential of +34.5 mV, indicating high colloidal stability. The nanoparticles achieved efficient mRNA encapsulation, reaching up to 100% loading efficiency at a 1:100 mRNA-to-nanoparticle ratio and approximately 97.5% at a 1:20 ratio. Proteinase K digestion and gel analyses confirmed successful mRNA encapsulation. Cytotoxicity assays demonstrated acceptable biocompatibility at concentrations ≤12.5 µg/mL, while PEG coating further improved cell viability. Furthermore, albumin PEC-NPs loaded with therapeutic mRNA successfully produced protein expression in the mutant zebrafish model. These findings provide conceptual proof for the therapeutic use of albumin-based mRNA.

Conclusion: We have developed a biocompatible, solvent-free, virus-free albumin nanoparticle platform that is capable of effective mRNA delivery and successful protein expression in the in vivo model.

Acknowledgment:
This project was supported by Health Institutes of Turkiye (TUSEB) via 2024-B-01-40001. Aytul Gul and Ozlem Erez were funded by the European Union RareBoost Project #952346.

ORCID:
Aytul Gul-Mete: 0000-0002-0594-5295
Aytul Gul-Mete: 0000-0002-0594-5295
Sümeyra Cigdem Sözer-Demirdas: 0000-0001-9950-9525
Merve Basol: 0000-0003-0142-3964
Merve Basol: 0000-0003-0142-3964
Ozlem Erez: 0009-0004-2020-4008
Yasar Akdogan: 0000-0002-2465-8873
Gulcin Cakan-Akdogan: 0000-0002-6356-5979
Gulcin Cakan-Akdogan: 0000-0002-6356-5979

Keyword: *mRNA Delivery, Albumin Nanoparticles, Polyelectrolyte Complexes*

Routine operando studies with Near Ambient Pressure (NAP) - XPS

Liana Socaciu-Siebert *

SPECS Surface Nano Analysis GmbH, Voltastr. 5, 13355 Berlin, Germany

Over the last decades it has been possible to develop XPS systems that can work far beyond the standard conditions of high or ultrahigh vacuum. Thus, Near Ambient Pressure (NAP) - XPS has become a rapidly growing field and has demonstrated its capability in a wide variety of applications. Starting from operando studies of surface reactions in catalysis, the applications soon have been extended towards studies of processes at liquid surfaces. Since more than 15 years, the need for basic studies of the fundamental chemistry at solid-liquid interfaces has attracted growing interest. Dip-and-pull experiments at synchrotrons finally demonstrated, that in-situ and operando XPS in electrochemical experiments can be realized, significantly contributing to the basic understanding of modern energy converting or storing devices, like batteries, fuel cells, etc.

The development of pure laboratory NAP-XPS systems by using small spot and high photon flux density monochromatic X-ray sources together with the development of optimized sample environments, like Peltier coolers and operando electrochemical cells open the possibility for the preparation and analysis of a multitude of liquid samples or solid-liquid interfaces on a reliable daily base. Furthermore, the combination of various analysis methods (NAP-SPM, IRRAS, NAP-HAXPES etc.) allows for gaining insights into the fundamental processes that take place during a chemical reaction.

Existing solutions for NAP-XPS will be presented, with an emphasis on latest developments of instruments and material analysis methods. Examples and results will be shown as well as future perspective of applications and scientific contributions of routine operando NAP-XPS.

Keyword: .

Vertically Aligned Carbon Nanostructures: From Electrode Architecture to Functional Performance in Electrochemistry and Sensing

Eser Metin Akinoglu * **, Zijie Luo**

South China Normal University, South China Academy of Advanced Optoelectronics, Guangdong Provincial Key Laboratory of Optical Information Materials and Technology, Institute of Electronic Paper Displays, Guangzhou 510006, P. R. China

Vertically aligned multi-walled carbon nanotubes (VA-MWCNTs) are a versatile platform for nanoscale electrochemistry, electrocatalysis, and surface-enhanced spectroscopy. VA-MWCNTs directly grown on carbon substrates are nanoscopic carbon electrode systems based on free-standing VA-MWCNTs. This architecture enables Ohmic contact at the individual nanotube level and leads to significantly enhanced double-layer capacitance and altered mass transport characteristics. Surface-enhanced Raman spectroscopy (SERS) revealed that the MWCNTs remain vertically aligned when immersed into liquid, but undergo irreversible structural deformations into MWCNT bundles when dried. Building upon this structure, a conformal coating of the VA-MWCNT scaffold with copper yields nano-forested Cu/CNT composite catalysts that markedly improve CO_2 electroreduction performance. Morphological confinement within the Cu forest is shown to enhance methane selectivity, current density, and reaction onset potential via synergistic electron–proton transfer.

Acknowledgment:
This work has been funded by the Research Fund for International Scientists of the National Natural Science Foundation of China (No.22350410388), the Guangdong Provincial Key Laboratory of Optical Information Materials and Technology (No. 2023B1212060065), the National Center for International Research on Green Optoelectronics (No. 2016B01018), the MOE International Laboratory for Optical Information Technologies, and the 111 Project (No. D16009). Furthermore, we acknowledge contributions by Liwei Ding, Ruiting Chen, and Michael Giersig.

ORCID:
Eser Metin Akinoglu: 0000-0002-0463-5543

References:
Akinoglu, E. M.; Kätelhön, E.; Pampel, J.; Ban, Z.; Antonietti, M.; Compton, R. G.; Giersig, M. Nanoscopic Carbon Electrodes: Structure, Electrical Properties and Application for Electrochemistry. Carbon 2018, 130, 768–774.
Chen, R.; Xue, Y.; Xu, X.; Yang, H.; Qiu, T.; Shui, L.; Wang, X.; Zhou, G.; Giersig, M.; Pidot, S.; Hutchison, J. A.; Akinoglu, E. M. Lithography-Free Synthesis of Periodic, Vertically-Aligned, Multi-Walled Carbon Nanotube Arrays. Nanotechnology 2022, 33, 065304.
Ding, L.; Lu, H.; Luo, Z.; He, G.; Jin, M.; Wang, X.; Zhou, G.; Shui, L.; Akinoglu, E. M. Deciphering the Alignment of Vertically Aligned Multi-Walled Carbon Nanotubes in Wet State Using Surface Enhanced Raman Spectroscopy. Surfaces and Interfaces 2025, 63, 106307.
Akinoglu, E. M.; Ren, B.; Xu, J.; Su, D.; Qiu, T.; Giersig, M.; Wen, G. Vertically Aligned Multiwalled Carbon Nanotube/Cu Catalysts for CO_2 Electroreduction. ACS Applied Nano Materials 2022, 5 (8), 10399–10408.

Keyword: *Vertically Alligned MWCNT Nanoelectrodes, CO2 Electroreduction, Raman Spectroscopy for Electrochemical Mechanism Monitoring*

EPR-Guided Defect and Particle-Size Engineering of Fe-Doped ZnO Nanostructures for Energy-Storage Applications

İpek Deniz Yıldırım [*1,2], **Ahmet Güngör**[1,2,3], **Oluwatosin Johnson Ajala**[1], **Emre Erdem**[1,2]

[1] *Faculty of Engineering and Natural Sciences, Sabancı University, Tuzla 34956, İstanbul, Turkiye*

[2] *Center of Excellence for Functional Surfaces and Interfaces for Nano-Diagnostics (EFSUN), Sabancı University, Tuzla 34956, İstanbul, Turkiye*

[3] *Kocaeli University, Department of Chemical Engineering, 41001, İzmit, Kocaeli, Turkiye*

Fe-doped ZnO is a promising transition-metal-doped oxide system for electrochemical energy storage applications due to its tunable defect chemistry, structural stability, and pseudocapacstorage behavior. Supercapacitors are attractive energy-storage devices because of their high power capability, rapid charge–discharge response, and long cycling stability; however, further improvement of electrode materials is required to enhance their energy density [1,2]. In this context, transition-metal doping and defect engineering are effective strategies for tuning electronic conductivity, ion-diffusion pathways, and surface redox activity in metal-oxide-based electrodes [3].In this study, Fe-doped ZnO nanostructures were synthesized via a facile solid-state reaction route, and the effects of Fe concentration, calcination temperature, and post-synthetic ball milling on defect formation and electrochemical performance were investigated. X-ray diffraction and Raman spectroscopy were used to evaluate phase formation and lattice disorder, while photoluminescence spectroscopy provided insight into defect-related optical emissions. Electron paramagnetic resonance spectroscopy was employed as a sensitive probe to identify Fe-related paramagnetic centers and intrinsic defect states in ZnO, since EPR is particularly effective for detecting unpaired electrons and transition-metal-related paramagnetic centers such as Fe^{3+} [4,5].

The results show that Fe doping strongly modifies the local defect environment of ZnO, with EPR spectra revealing Fe^{3+}-related centers and defect-associated resonance features. At higher Fe contents, increased spin–spin interactions resulted in spectral broadening, indicating stronger magnetic interactions between Fe centers. To further tune the morphology and electrochemical response, the 1 mol% Fe-doped ZnO sample was subjected to high-energy ball milling. This treatment reduced the effective particle size and modified the defect environment, as evidenced by the emergence of a broad Gaussian EPR signal. The reduced particle size is expected to increase the accessible surface area and improve electrode–electrolyte contact, thereby enhancing charge-storage kinetics.The electrochemical behavior of the Fe-doped ZnO electrodes was evaluated in two-electrode supercapacitor configurations using aqueous electrolyte. Among the symmetric Fe-doped ZnO devices, the 3 mol% Fe-doped ZnO sample delivered the highest performance, reaching a specific capacitance of 323 F g^{-1}, an energy density of 58 Wh kg^{-1}, and a power density of 1049 W kg^{-1}. In addition, the ball-milled Fe-doped ZnO electrode exhibited enhanced charge-storage behavior compared with its non-milled counterpart, demonstrating the importance of particle-size control in improving electrochemical performance. These findings highlight that both defect engineering and particle-size modulation are effective strategies for optimizing transition-metal-doped ZnO nanostructures for next-generation energy-storage devices.

ORCID:
İpek Deniz Yıldırım: 0000-0002-5559-8447

References:

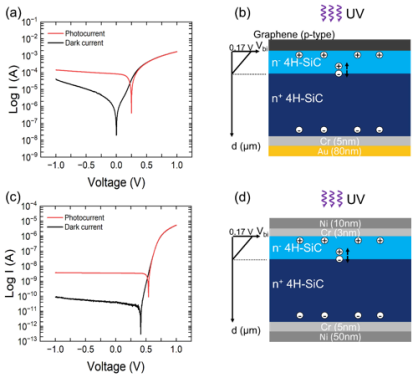
P. Simon, Y. Gogotsi, and B. Dunn, “Where do batteries end and supercapacitors begin?”, Science, 343, 1210–1211, 2014.
Y. Wu and C. Cao, “The way to improve the energy density of supercapacitors: Progress and perspective”, Science China Materials, 61, 1517–1526, 2018.
S. Najib and E. Erdem, “Current progress achieved in novel materials for supercapacitor electrodes: mini review”, Nanoscale Advances, 1, 2817–2827, 2019.
H. Kaftelen et al., “EPR and photoluminescence spectroscopy studies on the defect structure of ZnO nanocrystals”, Physical Review B, 86, 014113, 2012.
R. Heitz, A. Hoffmann, and I. Broser, “Fe^{3+} center in ZnO”, Physical Review B, 45, 8977, 1992.

Keyword: *Fe-doped ZnO, EPR spectroscopy, Supercapacitors*

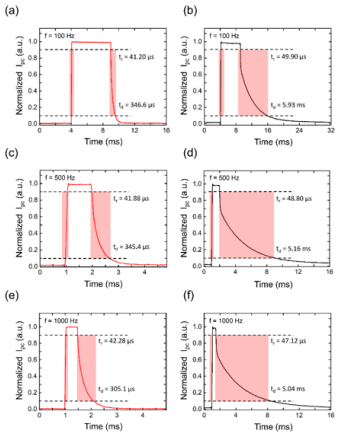
Comparison of the photoresponse characteristics for 4H–SiC Schottky barrier UV photodetector with graphene and Ni/Cr electrode

Atilla Mert Dülcel * [1], **Melike Gözek**[1], **Özhan Ünverdi**[2], **Cem Çelebi**[1]

[1] *Department of Physics, Izmir Institute of Technology, Izmir, 35430, Türkiye*
[2] *Department of Electrical and Electronics Engineering, Yaşar University, Izmir, 35100, Türkiye*



Gr/4H–SiC and Ni/Cr/4H–SiC Schottky junction UV photodetectors were fabricated and investigated to reveal the effect of electrode materials on the device performance such as spectral response and response speed. I–V characterization, spectral response, and response speed (on-off) measurements were conducted for the UV wavelength range between 220 and 400 nm. The maximum photo-responsivity was obtained as 0.081 A/W for Gr/4H–SiC and 0.041 A/W for Ni/Cr/4H–SiC at a wavelength of 260 nm as can be seen on figure 1. This result was attributed to the higher optical transmittance of the graphene electrode compared to the semitransparent Ni/Cr electrode. Zero bias response speed measurements were done under 280 nm wavelength UV light pulsed at different frequencies such as 100 Hz, 500 Hz, and 1000 Hz. The Gr/4H–SiC and Ni/Cr/4H–SiC photodetectors show distinctly different decay times of 5.04 ms and 305.1 μs which can be seen on figure 2, respectively, while their rise times were found to be similar. This observation has been explained by the inclination of graphene to act as a trap site for photogenerated holes.



Acknowledgment:
The authors thank Tuana Karakoyun Barandır for AFM measurements and analysis. This work is supported by the Turkish Council of Higher Education Research Universities Support Program (ADEP) as a part of the Project No. 2023IYTE-2-0008 which was accepted by the Scientific Research Projects Commission of Izmir Institute of Technology.

References:
Dülcel, A.M.; Gözek, M.; Ünverdi, Ö.; Çelebi, C. Comparison of the Photoresponse Characteristics for 4H–SiC Schottky Barrier UV Photodetector with Graphene and Ni/Cr Electrode. Opt. Mater. 2026, 173, 117854

Keyword: *Graphene, Silicon carbide, UV photodetector*

Advanced Metrology based on analytical SEM for Nanofabrication Applications

Muhammed Bekin [*] [1], **Nezih Ünal**[1], **Sven Bauerdick**[2], **Dmitri Titko**[2]

[1] *GenISys Bilgi Teknolojileri A.Ş.*
[2] *GenISys GmbH*

Monitoring and optimization of nano structures and devices require SEM investigation (scanning electron microscope) for imaging, metrology, and inspection. In particular, electron beam or laser beam lithography processes include careful calibration and modeling using sophisticated test patterns for different materials, doses, densities, thicknesses, or dimensions (CD). Therefore, acquiring and analyzing numerous scans is involved both with large image sets for routine calibration and inspection at critical positions of patterns or structures.

In R&D prototyping and small batch production, analytical SEMs are used instead of the CD-SEMs in high-volume production. While the versatility and flexibility of a conventional SEM is important for covering various applications, there is a growing demand for analyzing large areas and large numbers of structures requiring more advanced and automated SEM metrology capabilities.

With offline image analysis software (ProSEM), a first approach is available for supporting versatile SEMs with metrology functionality. Moreover, this allows for automated SEM image acquisition interfacing with the tool software.

Here, we will also present a novel upgrade kit (InSPEC) which provides a more sophisticated software workflow of metrology capabilities and is more integrated with the SEM tool by hardware connections (Fig. 1). This includes stage control and other SEM settings via a data connection and most importantly, direct access to column scanning and detector signals. The package includes a hardware unit and extensive software suite enabling improved scanning integrated with automation, metrology, and data processing. Overall, this provides a comprehensive workflow of a SEM for metrology and inspection, while the integrated control also enables compensation of effects like limited stage accuracy or focus/ topography changes.

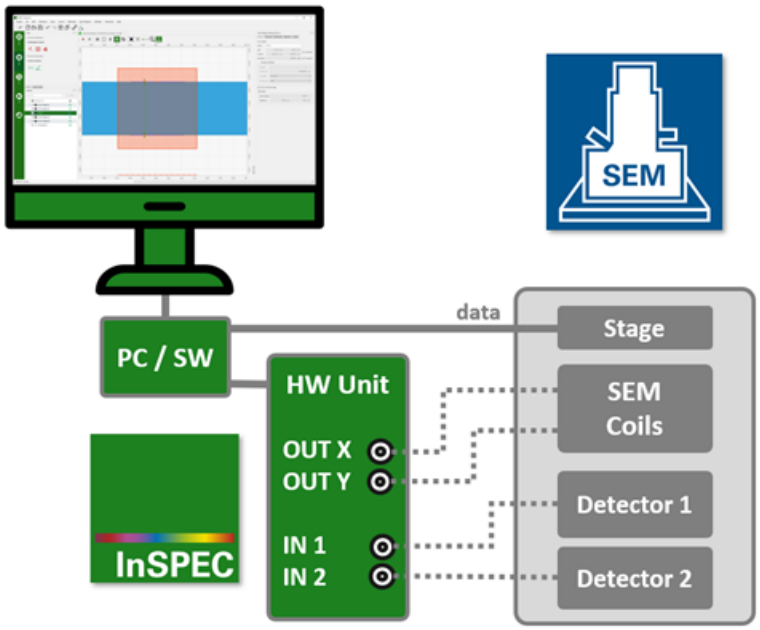


Figure 1: Schematic showing the general setup of the upgrade kit for metrology (InSPEC) as connected to a scanning electron microscope.

Keyword: *Electron Microscopy, Inspection, SEM*

From Cell to Module: Scaling-Up Effects on PM6:Y6-Based Organic Photovoltaic Performance

Bilgenur Kazancıoğlu [*1], Gönül Hızalan Özsoy[2], Bahri Eren Uzuner[2], Selçuk Yerci[1,2,3], Ali Çırpan[1,2,4,5]

[1] Department of Micro and Nano Technology, Middle East Technical University, 06800, Ankara, Turkiye
[2] ODTU-GUNAM, Middle East Technical University, 06800, Ankara, Turkiye
[3] Department of Electrical and Electronics Engineering, Middle East Technical University, 06800, Ankara, Turkiye
[4] Department of Chemistry, Middle East Technical University, 06800, Ankara, Turkiye
[5] Department of Polymer Science and Technology, Middle East Technical University, 06800, Ankara, Turkiye

The rapid depletion of fossil fuel reserves and growing environmental concerns necessitate a shift toward sustainable energy alternatives. Solar energy offers a powerful solution to reduce greenhouse gas emissions and meet global electricity demands. In this regard, organic photovoltaic (OPV) modules have emerged as a highly promising technology. By scaling up individual cells into large-area modules, OPVs can provide lightweight, flexible, and cost-effective energy solutions for real-world applications such as building-integrated photovoltaics (BIPV) and wearable electronics. In this work, we report the fabrication of OPV modules based on an ITO/2PACZ/PM6:Y6/PDINN/Ag device architecture. To investigate the effects of scaling up, module fabrication was systematically performed on three different substrate sizes: 3cm x 3cm, 5cm x 5cm, 10cm x 10cm. The small area organic solar cell achieved power conversion efficiency (PCE) of 15.24%, short circuit current density (J_{sc}) of 25.34 mA/cm^2, open circuit voltage (V_{oc}) of 0.84 V, fill factor of 72.02%. The fabricated modules achieved power conversion efficiencies (PCE) of 12.64%, 11.16%, and 10.88%, respectively. These results demonstrate a scalable and efficient pathway for transitioning from laboratory-scale cells to large-area OPV applications.

ORCID:
Bilgenur Kazancıoğlu: 0009-0002-3109-9130
Gönül Hızalan Özsoy: 0000-0002-3308-404X
Bahri Eren Uzuner: 0000-0002-7363-0084
Selçuk Yerci: 0000-0003-0599-588X
Selçuk Yerci: 0000-0003-0599-588X
Selçuk Yerci: 0000-0003-0599-588X
Ali Çırpan: 0000-0003-3051-8380
Ali Çırpan: 0000-0003-3051-8380
Ali Çırpan: 0000-0003-3051-8380
Ali Çırpan: 0000-0003-3051-8380

References:
1. Basu R, Gumpert F, Lohbreier J .Large-area organic photovoltaic modules with 14.5% certified world record efficiency, Joule, 2024; 8, 970-978

Keyword: *Organic photovoltaics (OPVs), Module fabrication, Scaling up*

Investigation of the Photoanode Properties of Pulsed Voltage Electrodeposited WO_3 Thin Films

Ece Değirmenci * **, Gamze Atak**

Department of Physics Engineering, Hacettepe University, Türkiye

Hydrogen production by solar water splitting is considered one of the most promising methods for obtaining clean and renewable energy [1,2]. The efficiency of photoelectrodes used in this process depends on critical parameters such as corrosion resistance, light absorption capacity, and suitable band edge positions [3]. Tungsten oxide (WO_3), an n-type semiconductor, is an important photoanode candidate for PEC water splitting due to its sensitivity to visible light and high stability against photocorrosion [3,4]. Although there are many different methods for preparing photoelectrodes, electrodeposition—being low-cost and suitable for large-area coating—is a promising technique for producing WO_3 thin films. [2,3,5].

In this study, WO_3 thin films were prepared at different deposition potentials using the single-step pulsed voltage electrodeposition (PVE) method. The films were deposited for 1000 cycles at potentials of -0.6 V and -0.7 V against an Ag/AgCl reference electrode, using an electrolyte solution containing $Na_2WO_4 \cdot 2H_2O$, H_2O_2, and $HClO_4$. The structural (XRD), morphological (SEM), optical (UV-Vis), electronic (Mott-Schottky), and PEC (LSV) properties of the samples were analyzed in detail.

XRD results showed that the synthesized WO_3 films were in the amorphous phase. SEM analysis revealed that the films have a porous and interconnected structure that provides a large surface area and facilitates charge transport. According to Tauc plot, the band gap decreased from 3.17 eV to 3.13 eV when the deposition potential changed from -0.7 V to -0.6 V. In PEC measurements performed in 0.5 M H_2SO_4 electrolyte, the sample deposited at -0.6 V showed a photocurrent density of 0.0038 mA cm^{-2} at 1.23 V vs. RHE and an onset potential of 0.450 V. Mott–Schottky measurements showed donor densities of 7.79×10^{18} cm^{-3} and 9.67×10^{18} cm^{-3} for -0.6 V and -0.7 V, respectively. The low photocurrent efficiencies were attributed to charge carrier recombination occurring within lattice defects in the amorphous structure. Thus, it was observed that the applied potential directly affects the structural, optical, and photoelectrochemical properties of WO_3 films. These findings suggest that PEC performance can be further improved by optimizing electrodeposition parameters.

Acknowledgment:
The authors want to thank the Scientific and Technological Research Council of Turkey (TÜBİTAK) for financial support with Project ID 223M337 and Hacettepe University Scientific Research Projects Coordination Unit with Project ID FHD-2024-21270, FYL-2026-22

References:
[1] Chatterjee, P., Piecha, D., Szczerba, M., Marzec, M. M., Pisarek, M., Uchacz, T., Sulka, G. D. (2025). Enhanced photoelectrochemical water splitting activity of porous anodic WO_3 photoelectrodes decorated with $FeWO_4$ nanoparticles. Materials & Design, 260, 115018.
[2] Kwong, W.L., Qiu, H., Nakaruk, A., Koshy, P., Sorrell, C.C. (2013). Photoelectrochemical Properties of WO_3 Thin Films Prepared by Electrodeposition. Energy Procedia, 34, 617–626.
[3] Kwong, W.L., Savvides, N., Sorrell, C.C. (2012). Electrodeposited nanostructured WO_3 thin films for photoelectrochemical applications. Electrochimica Acta, 75, 371–380.
[4] Arslan, M., Fırat, Y.E., Tokgöz, S.R., Peksoz, A. (2021). Fast electrochromic response and high coloration efficiency of Al-doped WO_3 thin films for smart window applications. Ceramics International, 47, 32570–325
[5] Gu, H., Tan, M., Wang, T., Sun, J., Du, J., Ma, R., Wang, W., Hu, D. (2024). Boosting the electrochromic performance of P-doped WO_3 films via electrodeposition for smart window applications. RSC Advances, 14(15), 10298–10303. https://doi.org/10.1039/d4ra00979q

Keyword: *electrodeposition, photoanode, thin film*

Exploiting Metal Mobility in Liquid Metals for Ammonia Production

Karma Zuraiqi *

Riga Technical University

The outlook for sustainable economic and ecological growth projects an ammonia economy as a key enabler to the energy transition landscape. Proponents of ammonia utilization, however, are subdued by the technical infeasibility and cost of advancing ammonia synthesis beyond the Haber-Bosch process. Liquid metals are rapidly emerging as a new frontier in chemistry and have recently gained traction as an emerging class of catalysts, utilized both in their bulk liquid form and as supported nanodroplets.

This talk is primarily focused on developing new liqud metals alloys as catalysts for ammonia production by utilizing supported liquid metal nanodroplets. We use a Cu-Ga alloy, capitalizing on the inherent atomic structure of the liquid metal, and the ability to modulate the electronic and geometric structures of liquid metal catalysts to drive the thermocatalytic synthesis of ammonia. The liquid metal alloy offers a dynamic metal complex with synergistic advantages that lift the activity of the individual metals. Detailed analysis revealed that the developed catalyst exploits a novel reaction pathway that is different from the conventional Haber-Bosch process, exhibiting high activity at low pressures. Gallium is found to activate the N-N bond, while the dissolved copper plays an important role in activating H_2, and ultimately releasing the gallium-bound nitrogen in the form of NH_3. The liquid state of the alloy also minimizes catalyst deactivation due to the highly mobile and self-restructuring nature of the liquid metal surface. This allows us to demonstrate high turnover numbers and high stability.

The developed approach facilitates exemplary alignment between high catalytic efficiency, robustness, and sustainable ammonia production that is predicated on the use of naturally abundant metals.

ORCID:
Karma Zuraiqi: 0000-0002-9214-6992

References:
[1] K. Zuraiqi, Y. Jin, C. J. Parker, J. Meilak, N. Meftahi, A. J. Christofferson, S. P. Russo, M. J. S. Spencer, H. Yon Zhu, L. Wang, J. Huang, R. K. Hocking, K. Chiang, S. Sarina, and T. Daeneke, " Unveiling metal mobility in a liquid Cu-Ga catalyst for ammonia synthesis," in Nature Catalysis, 2024.
[2] S. S. Fatima, K. Zuraiqi, A. Zavabeti, V. Krishnamurthi, K. Kalantar-Zadeh, K. Chiang, and T. Daeneke, “Current state and future prospects of liquid metal catalysis,” in Nature Catalysis, vol. 6. no. 12, pp. 1131-1139, 2023.
[3] C. J. Parker, K. Zuraiqi, V. Krishnamurthi, E. L. Mayes, P. H. A. Vaillant, S. S. Fatima, K. Matuszek, J. Tang, K. Kalantar-Zadeh, N. Meftahi, C. F. McConville, A. Elbourne, S. P. Russo, A. J. Christofferson, K. Chiang, and T. Daeneke, “Spontaneous Liquefaction of Solid Metal–Liquid Metal Interfaces in Colloidal Binary Alloys,” in Advanced Science, pp. 2400147, 2024.
[4] K. Zuraiqi, A. Zavabeti, F.M. Allioux, J. Tang, C.K. Nguyen, P. Tafazolymotie, M. Mayyas, A.V. Ramarao, M. Spencer, K. Shah, C. F McConville, K. Kalantar-Zadeh, K. Chiang, and T. Daeneke, "Liquid metals in catalysis for energy applications," Joule, vol. 4, no. 11, pp. 2290-2321, 2020.

Keyword: *liquid metals, ammonia synthesis, nanodroplets*

Superconducting diode effect and topological superconductivity in microwave-cQED embedded planar Josephson junctions

Barış Pekerten *

University at Bufffalo, SUNY

Planar Josephson junctions provide a platform to host topological superconductivity which, through manipulating Majorana bound states, could enable fault-tolerant quantum computing. A standard model of these Josephson junctions, which can be fabricated to have a nearly perfect interfacial transparency, predicts a simple universal behavior. In contrast, we find a much richer and nonuniversal behavior for a finite-sized system with possible anisotropies, where the topological phase diagram is shifted and distorted and the expected superconducting phase jump is not absolute. We demonstrate that the magneto–current–phase relation (magneto-CPR) provides a powerful and unified probe of their microscopic and topological properties. Furthermore, these Josephson junctions show a striking example of a nonreciprocal transport and superconducting diode effect. We develop a phenomenological model showing that the diode efficiency depends on the relative alignment between spin–orbit and magnetic fields, and corroborate this behavior in the narrow-junction, low-field regime using an analytical approach that links the anisotropy of the diode response to SOC-induced Fermi surface distortions and anisotropic Cooper pair momentum. Guided by the advances in microwave spectroscopy, we show that even in a wide planar Josephson junction with many Andreev bound states, a topological signature is distinguishable in the resonance frequency shift of a microwave drive. Our findings provide guidance for future superconducting spintronics and an important step towards experimental detection of non-Abelian statistics and implementing scalable topological quantum computing.

Acknowledgment:
This work was supported by DARPA Grant No. DP18AP900007, MURI ONR Award No. N00014-22-1-2764, N00014-17-1-2793, and NSF ECCS-2130845. Computational resources were provided by the University at Buffalo Center for Computational Research and Wayne State University.

ORCID:
Barış Pekerten: 0000-0002-5794-9706

References:
B. Pekerten, J. D. Pakizer, B. Hawn, and A. Matos-Abiague, Anisotropic topological superconductivity in Josephson junctions, Phys. Rev. B 105, 054504 (2022).
N. Lotfizadeh, W. Schiela, B. Pekerten, P. Yu, W. Strickland,A. Matos-Abiague, and J. Shabani, Superconducting diode effect sign change in epitaxial Al-InAs Josepshon junctions, Commun. Phys. 7, 120 (2024).
B. Pekerten, D. Brandão, B. Bussiere, D. Monroe, T. Zhou, J. E. Han, J. Shabani, A.-M. Abiague, and I. Žutić, Beyond the standard model of topological Josephson junctions: From crystalline anisotropy to finite-size and diode effects, Appl. Phys. Lett. 124, 252602 (2024).
B. Pekerten, D. Brandão, B. H. Elfeky, T. Zhou, J. E. Han, J. Shabani, and I. Žutíc, Microwave signatures of topological superconductivity in planar Josephson junctions, Phys. Rev. B 110, 6 (2024).
B. H. Elfeky, K. Dindial, D. S. Brandão, B. Pekerten, J. Lee, W. M. Strickland, P. J. Strohbeen, A. Danilenko, L. Baker, M. Mikalsen, W. Schiela, Z. Liang, J. Issokson, I. Levy, I. Žutić, and J. Shabani, Microwave Andreev bound state spectroscopy in a semiconductor-based planar Josephson junction, Phys. Rev. Research 7, 013248 (2025).

Keyword: *Superconducting diode effect, Topological superconductivity, Topological quantum computing*

Exploring Topological Properties of Two-Dimensional Materials Through Berry Curvature Analysis

Sümeyye Cörüt [*] [1], **Semran İpek**[2]

[1] *Department of Nanoscience and Nanoengineering, Faculty of Engineering and Natural Sciences, Istanbul Medeniyet University, Istanbul, Türkiye*

[2] *Department of Physics Engineering, Faculty of Engineering and Natural Sciences, Istanbul Medeniyet University, Istanbul, Türkiye*

The emergence of topological quantum materials has opened new directions in condensed matter physics and nanotechnology by revealing the fundamental role of geometric and topological properties in determining electronic behavior. Among these systems, two-dimensional (2D) materials have attracted significant attention due to their potential to host non-trivial quantum states and novel transport phenomena. In this context, Berry curvature has emerged as a key quantity for characterizing topological phases and understanding the electronic properties of low-dimensional materials.

The primary objective of this work is to investigate Berry-curvature distributions in two-dimensional quantum materials and to identify topological signatures associated with non-trivial electronic states. Particular attention will be given to the interplay between topology and electronic correlations, with the aim of elucidating the mechanisms underlying emergent quantum phenomena in low-dimensional systems. Understanding this relationship is essential for the characterization and design of next-generation quantum materials with tailored electronic properties.

To achieve these goals, a computational framework integrating Density Functional Theory (DFT), Wannier-function techniques, and Dynamical Mean-Field Theory (DMFT) is being developed. The computational workflow is implemented using Quantum ESPRESSO, Wannier90, and the TRIQS library, enabling the construction of effective low-energy Hamiltonians and the investigation of electronic properties beyond conventional band-theory descriptions. Benchmark calculations on correlated electron systems are employed to validate the methodology prior to its application to topological 2D materials.

The developed framework is expected to provide a versatile platform for studying Berry-curvature-related phenomena and correlation-driven effects in emerging quantum materials, contributing to a deeper understanding of topology in condensed matter systems and supporting future developments in nanoelectronic and quantum technologies.

ORCID:
Sümeyye Cörüt: 0009-0007-0139-3482
Semran İpek: 0000-0003-4103-9510

References:

Berry, M. V. (1984). Quantal phase factors accompanying adiabatic changes. Proceedings of the Royal Society A: Mathematical, Physical and Engineering Sciences, 392(1802), 45–57.
Vanderbilt, D. (2018). Berry Phases in Electronic Structure Theory: Electric Polarization, Orbital Magnetization and Topological Insulators. Cambridge University Press.
Marzari, N., Mostofi, A. A., Yates, J. R., Souza, I., & Vanderbilt, D. (2012). Maximally localized Wannier functions: Theory and applications. Reviews of Modern Physics, 84(4), 1419–1475.
Georges, A., Kotliar, G., Krauth, W., & Rozenberg, M. J. (1996). Dynamical mean-field theory of strongly correlated fermion systems and the limit of infinite dimensions. Reviews of Modern Physics, 68(1), 13–125.
Parcollet, O., Ferrero, M., Ayral, T., Hafermann, H., Krivenko, I., Messio, L., & Seth, P. (2015). TRIQS: A toolbox for research on interacting quantum systems. Computer Physics Communications, 196, 398–415.

Keyword: *Two-Dimensional Materials, Berry Curvature, Topological Quantum Materials*

Geometry-Controlled Exciton Selectivity In Monolayer Mos2 Using Plasmonic Hollow Nanocavities

Abdullah Efe Yıldız * **, Emre Ozan Polat**

Department of Physics and National Nanotechnology Research Center, Bilkent University, Ankara, Türkiye, 06800

Selective control of closely spaced excitonic transitions in atomically thin semiconductors is an important challenge for nanoscale photonics, wavelength-selective light emission, and exciton-based optoelectronic devices. Monolayer molybdenum disulfide (MoS_2) is particularly attractive in this context because its A and B excitons originate from spin-orbit-split valence bands and are separated by only a small energy difference. Therefore, selectively enhancing one excitonic channel over the other requires precise control of the local optical environment.

Here, we numerically investigate geometry-controlled excitonic emission from monolayer MoS_2 coupled to vertically oriented hollow gold nanocylindrical cavities. The hybrid system is designed using two dielectric spacer materials, Al_2O_3 and PMMA, with varying spacer thicknesses to regulate the near-field coupling strength between the plasmonic cavity and the MoS_2 monolayer. By tuning the inner radius of the hollow nanocavity, the localized surface plasmon resonance can be spectrally aligned preferentially with either the A- or B-exciton transition. This enables structural control of excitonic emission without requiring external fields, chemical doping, or active tuning schemes.

Using finite-difference time-domain simulations combined with a photoluminescence-rate model, we separate the contributions of excitation-rate enhancement, radiative decay modification, nonradiative loss, and excitonic generation. The optimized cavity-spacer configurations provide excitation-rate enhancements up to 4.34 and radiative decay-rate enhancements exceeding 40. These combined effects lead to calculated photoluminescence enhancement factors of 143.85 for the A exciton and 87.27 for the B exciton. In addition to increasing the overall emission intensity, the hollow nanocavity geometry redistributes the relative A- and B-exciton emission strengths, yielding normalized excitonic peak ratios up to 2.4 times larger than bare monolayer MoS_2.

Overall, these results show that plasmonic hollow nanocavities provide a compact and scalable route for exciton-selective emission control in two-dimensional semiconductors. The proposed platform offers a purely geometrical and dielectric design strategy for engineering excitonic light emission in integrated 2D-material-based nanophotonic devices.

Acknowledgment:
E.O.P. acknowledges financial support from the Scientific and Technological Research Council of Türkiye (TÜBİTAK) through Grant No. 222N308 within the CHIST-ERA program. Additional support was provided by the Turkish Academy of Sciences Outstanding Young Scientists Awards (GEBİP) 2025.

ORCID:
Abdullah Efe Yıldız: https://orcid.org/0009-0001-9818-632X
Emre Ozan Polat: https://orcid.org/0000-0002-6652-059X

References:
Yildiz, A. E. & Polat, E. O. Geometry-Controlled Exciton Selectivity in Monolayer MoS_2 Using Plasmonic Hollow Nanocavities. arXiv:2603.07732
Wang, G. et al. Colloquium: Excitons in atomically thin transition metal dichalcogenides. Reviews of Modern Physics vol. 90 (2018).
Bharadwaj, P., Deutsch, B. & Novotny, L. Optical Antennas. Advances in Optics and Photonics vol. 1 438–483 (2009).

Keyword: *Monolayer MoS2; Exciton-plasmon coupling; Purcell enhancement; Exciton selectivity; Charge Generation Rate*

Investigation of Magnetotransport Effects in Ferromagnet/Normal-Metal (FM/NM) Multilayer Thin Films

Murat Kol [*1], Perihan Aksu[2,3], Erdem Demirci[1], Mustafa Öztürk[1]

[1] *Department of Physics, Gebze Technical University, 41400 Gebze, Kocaeli, Turkey*
[2] *Nanotechnology Institute, Gebze Technical University, 41400 Gebze, Kocaeli, Turkey*
[3] *Nanotechnology Research and Application Center, Gebze Technical University, 41400 Gebze, Kocaeli, Turkey*

Magnetotransport effects, such as anisotropic magnetoresistance (AMR) and the planar Hall effect (PHE), are useful electrical techniques for studying magnetic anisotropy and magnetization direction in ferromagnet/normal-metal (FM/NM) structures and play an important role in the operation of spintronic devices [1]. In this work, we investigate the structural, magnetic and magnetotransport properties of CuIr/NiFe (Permalloy) multilayer thin films, in which the dilute Cu–Ir alloy serves as a normal-metal layer incorporating heavy Ir atoms with strong spin–orbit coupling. Thin films were grown on thermally oxidized Si substrates by magnetron sputtering, and Hall-bar devices were defined by optical lithography. Layer thickness, density, composition and surface morphology were characterized by XRR, XRD, XPS, EDS and AFM, while the magnetic response was studied by MOKE and VSM. Magnetotransport was probed through angle- and field-dependent AMR, PHE and first-harmonic Hall-voltage measurements. The films exhibit well-defined layer structures and in-plane square hysteresis, with an easy-axis orientation that depends on the layer-stacking sequence. The angular AMR and PHE responses follow the expected $\cos^2\varphi$ and $\sin\varphi\cdot\cos\varphi$ dependences and are mutually consistent [2,3], and the first-harmonic Hall signal reproduces the PHE behaviour, establishing a reliable magnetotransport baseline for these CuIr-based FM/NM multilayers. These results clarify how the stacking order and capping layer govern the magnetic anisotropy and magnetotransport response of the system.

This study is supported by TÜBİTAK under project number 125F020.

Acknowledgment:
This study is supported by TÜBİTAK under project number 125F020.

References:
T. R. McGuire, R. I. Potter, IEEE Trans. Magn. 11, 1018 (1975
M. Öztürk and E. Demirci, Journal of Physics D: Applied Physics, 55, 445002 (2022)
E. Demirci and M. Öztürk, Appl. Phys. A 129, 179 (2023)

Keyword: *magnetotransport, anisotropic magnetoresistance, Planar Hall effect*

Theoretical Investigation of pH-Responsive Lenvatinib Release from Halloysite Nanotubes via Steered Molecular Dynamics

Celal Yıldıray Köylü * **, Harun Nalçakan, Müşerref Önal**

Ankara University

Halloysite nanotubes (HNTs) offer a distinct lumen structure for the targeted delivery of hydrophobic oncological agents, such as the tyrosine kinase inhibitor Lenvatinib. In this study, the release mechanism and structural dissociation pathways of the protonated Lenvatinib species, which are significantly populated in acidic endosomal and tumor microenvironments (pH 5.0–5.5), were theoretically investigated using an idealized, ultra-confined HNT lumen model via the CLAYFF and OPLS-AA force fields. Simulations were performed utilizing the LAMMPS package. Following structural equilibration at physiological temperature (310 K), non-equilibrium steered molecular dynamics (SMD) simulations (k=5 kcal.mol^{-1}.Å^{-2}, v=5 Å.ns^{-1}) were executed to map the continuous dissociation pathway. The resulting profiles revealed a pronounced stick-slip mechanism characteristic of highly confined transport, with the non-equilibrium pulling force peaking at ∼70 kcal.mol^{-1}.Å^{-1}. This resistance indicates that the drug overcomes sequential steric barriers and localized hydrogen-bonding networks, while electrostatic repulsion between the alumina lumen and the cationic drug partially offsets this steric hindrance. Overall, this study provides a structural roadmap for the dissociation process. The extracted trajectories lay the groundwork for future umbrella sampling (US) simulations to calculate the binding free energy (ΔG), fully elucidating the thermodynamic landscape governing pH-responsive, targeted drug release.

Acknowledgment:
This work was supported by the Ankara University Scientific Research Projects (BAP) Coordination Office under Project No: FBG-2025-4390.

ORCID:
Celal Yıldıray Köylü: 0009-0006-0755-7671
Harun Nalçakan: 0000-0003-3821-8681
Müşerref Önal: 0000-0002-1540-8389

Keyword: *Halloysite Nanotube, Lenvatinib, Steered Molecular Dynamics*

Simulation of coupled fluid–ion transport through a biological nanopore

Maxim Solovchuk [*] [1,2], **Kumar Saurabh**[3]

[1] *National Health Research Institutes, Institute of Biomedical Engineering and Nanomedicine*
[2] *National Taiwan University*
[3] *National Health Research Institutes*

Nanoscale fluid–ion transport plays a critical role in biophysical chemistry, drug delivery, protein sequencing, and related applications. However, efficient three-dimensional simulation frameworks for transport through biological nanopores remain limited. This study presents a parallel multi-GPU framework for simulating nanoscale fluid–ion transport in complex biological nanopores. The transport process is described using the fourth-order Poisson–Nernst–Planck–Bikerman model coupled with the Navier–Stokes equations, accounting for ionic and non-ionic interactions, ion solvation, nonlocal electrostatics, and finite particle size effects. The proposed framework is applied to simulate electro-osmotic flow through a large biological nanopore using the complete three-dimensional channel geometry. The simulations show good agreement with published results and capture detailed axial and radial variations in ion concentration and fluid velocity, as well as flow recirculation around the channel. The effects of applied electric potential and finite particle size on transport behavior are also investigated. The proposed methodology provides an accurate and computationally efficient approach for characterizing both symmetric and asymmetric biological nanopores, offering valuable insights into nanoscale transport phenomena and supporting the design and analysis of nanofluidic systems.

ORCID:
Maxim Solovchuk: 0000-0002-5800-9951

References:
https://doi.org/10.1063/5.0274994

Keyword: *nanopore, fluid-ion transport, GPU computing*

Molecular Dynamics Simulations of the Self-Assembly Mechanisms of Antimicrobial Peptides and Their Interactions with Lipid Membranes

Emine Deniz Tekin *

Department of Computer Engineering, University of Turkish Aeronautical Association, Ankara, Türkiye

The global rise of antibiotic resistance poses a major challenge to the effectiveness of conventional antibiotics, particularly in biofilm-associated infections, and motivates the search for alternative antimicrobial strategies. Antimicrobial peptides (AMPs) have attracted increasing attention due to their broad biological activity and membrane-targeting mechanisms. Positively charged AMPs can interact electrostatically with negatively charged bacterial membranes, potentially leading to membrane disruption. However, the molecular details of how AMPs interact with and penetrate membranes are still not fully understood.

PTP-7 (FLGALFKALSKLL) and CL-1 (FLGALFRALSRLL) represent two short peptides that provide a useful model system for investigating these processes. Experimental studies have shown that PTP-7 exhibits antimicrobial activity but does not display clear self-assembly behavior in aqueous solution. In contrast, CL-1, which differs from PTP-7 by only two amino acid substitutions (K→R), has been reported to form fibril-like nanostructures through self-assembly. The molecular basis of these different behaviors remains unclear.

In this study, the self-assembly tendencies of PTP-7 and CL-1 and their interactions with negatively charged model membranes representing Gram-positive bacterial membranes are examined at the atomistic level. Molecular dynamics (MD) simulations are performed using the GROMACS software package, and peptide accumulation, orientation, and membrane interaction behaviors are analyzed on a DPPC:DPPG (1:3) model membrane. The results may contribute to a better understanding of the relationship between AMP self-assembly and membrane interactions.

Acknowledgment:
This work was supported by the Scientific Research Projects Unit of University of Turkish Aeronautical Association (THKÜ BAP). The numerical calculations reported in this paper were fully/partially performed at TUBITAK ULAKBIM, High Performance and Grid Computing Center (TRUBA resources).

Keyword: *Antimicrobial peptides, antibiotic resistance, self-assembly, molecular dynamics*

Computational Studies on the electronic, structural, and optoelectronic properties of pristine graphene, holey graphene, and their doped derivatives

Erol Yıldırım * **, Berrin Ayyıldız, Benan Nakipoğlu**

Middle East Technical University, Department of Chemistry, 06800, Çankaya, Ankara

The fundamental electronic, structural, and optoelectronic properties of pristine graphene, holey graphene, and their doped derivatives were comprehensively investigated using Density Functional Theory (DFT). A total of 30 different model structures were prepared, representing different hole sizes and doping ratios, to systematically explore the influence of these parameters on the electronic and structural characteristics. Since the systems contained a large number of atoms, geometry optimizations were performed using the Jaguar software, which provided significantly shorter computation times compared to Gaussian for such large-scale models. After the optimizations will be completed, the effects of dopant concentration and pore size on key properties such as band structure, density of states (DOS), charge distribution, and structural stability were analysed. The results obtained in this study established a theoretical foundation for selecting the most suitable dopant types and structural configurations for the application-oriented studies presented in the experimental studies. In addition, lithium ion adsorption, intercalation, and diffusion behaviour on doped graphene, holey graphene, and doped holey graphene surfaces using a combined DFT and molecular dynamics (MD) framework. The aim is to assess their potential as anode materials for lithium-ion batteries by evaluating adsorption energies, diffusion barriers, charge transfer characteristics, and open-circuit voltage profiles. Structural dynamics under lithium insertion and extraction processes will be examined through MD simulations to determine the mechanical and thermal stabilities of each configuration. The comparative analysis reveals how doping and porosity synergistically enhance lithium storage capacity and ion mobility relative to pristine graphene.

Acknowledgment:
We gratefully acknowledge support from the ADEP-103-2024-11510.

ORCID:
Erol Yıldırım: 0000-0002-9989-9882

Keyword: *Density Functional Theory, graphene, holey graphene*

Advanced Hydrogel Matrix Supporting Oxygenation and Probiotic-Derived Metabolite Release

Nermin Seda Kehr * **, Ulvi Süleymanzade, Tuğba Ezgi Şahin, Yağmur Damla Demir**

Department of Chemistry, Faculty of Science, Izmir Institute of Technology

Cancer is a global health problem affecting countries all over the world. Both traditional and modern methods or combinational strategies do not consider the impact of hypoxia and subsequent chronic inflammation on cancer tissue development and metastasis, despite the fact that hypoxia, cancer and inflammation share an interdependent relationship. Inadequate and heterogeneous oxygen (O_2) distribution in tissues leads to hypoxic conditions and consequently to cell apoptosis, tissue necrosis, and failures in tissue healing. Hypoxia is a common feature of solid tumors, as tumor tissue tends to have a leaky and abnormal vascular structure and rapidly proliferating cancer cells, which leads to low oxygen concentrations. Low oxygen levels affect cancer cell signaling and biological activity and can prevent anticancer drugs from destroying the tumor, thereby allowing cancer cells to migrate and tumors to metastasize. Therefore, oxygen O_2 generating and transporting systems have been developed to ensure adequate and controlled O_2 delivery to tissues. [1] However, there are few studies using O_2 and drug-releasing nanoparticles for cancer therapy under hypoxic conditions. [2,3]

In this context, we developed a novel injectable living biomaterial called BioHybrid Hydrogel, composed of oxygen (O_2)- and anticancer drug-loaded nanomaterials together with probiotics encapsulated within a three-dimensional hydrogel network. This multifunctional platform enables sustained O_2 release and the co-delivery of an acidic pH (pH 6.0)-responsive anticancer agent, doxorubicin (DOX), alongside bioactive probiotic metabolites with anticancer and anti-inflammatory properties. In vitro studies conducted under hypoxic conditions demonstrated that healthy cell viability was higher than that of cancer cells after 1 and 7 days of incubation with BioHybrid Hydrogel, indicating a selective therapeutic effect attributed to the synergistic co-administration of O_2, DOX, and probiotic-derived metabolites. To our knowledge, this system represents the first biomaterial platform that integrates a stimuli-responsive non-viable drug delivery component (nanocarrier-based drug delivery) with a stimuli-responsive viable drug delivery component (probiotic-mediated metabolite production) within a single injectable construct for cancer therapy, highlighting its strong potential for minimally invasive multidrug treatment of hypoxic tumor microenvironments.

Acknowledgment:
We would like to thank the Scientific and Technological Research Council of Turkey (TÜBİTAK) ARDEB 1001 Grant No. 223Z039 for funding. We would like to thank Izmir Institute of Technology MAM and BIOMER Center for analytical measurements (SEM, DLS, and zeta potential) and cell culture laboratory use.

ORCID:
Nermin Seda Kehr: 0000-0003-2275-1254

References:
[1] Bayraktar et al., Macromol. Biosci. 24 (2024) e2300363.
[2] Kehr et al., Macromol. Biosci. (2024) 2400181.
[3] Kehr et al., Biomed Mater. 20 (2025) 015035.

Keyword: *Oxygen, anticancer drug, probiotic metabolites*

Investigation of Antioxidant and In Vitro Wound Healing Potential of Electrospun Chitosan/Peo Nanofibers Containing Aronia Melanocarpa Fruit Extract

Ümran Ünüvar [*1,2], **Fuat Aslan**[2]

[1] *Department of Molecular Biology and Genetics, Faculty of Science, Necmettin Erbakan University, Konya, Turkey*
[2] *Science and Technology Research and Application Center (BITAM), Necmettin Erbakan University, Konya, Turkey*

Polymeric biocompatible biomaterials with a nanofiber structure obtained by electrospinning mimic the natural extracellular matrix owing to their high surface area, tunable porosity, and ability to support biological interactions; thereby offering suitable environments for cell adhesion, proliferation, and tissue regeneration (1). In this study, Aronia melanocarpa fruit extract which contributes to wound healing and tissue regrowth, with its strong antioxidant property thanks to its high anthocyanin and polyphenol content, was loaded into polyethylene oxide (PEO)-blended chitosan solution and nanofiber structures were obtained using electrospinning technique (2). PEO is a water-soluble, non-toxic and non-immunogenic polymer (3). Chitosan is a natural polysaccharide with excellent biocompatibility, biodegradability, and low toxicity (4). Its antibacterial property makes it highly a beneficial material in wound-healing applications while offering a proper microenvironment for cell proliferation and tissue regeneration thanks to their high surface area and porosity. The obtained nanofibers were characterized using FESEM, XRD, and FTIR methods. During the wound healing process, oxidative stres levels increase in time, thereby causing elevated cellular damage and slowing down tissue regeneration. Antioxidant compunds are known to contribute to the suppression of reactive oxygen species, these provide controlling inflammation and accelerating wound healing. Here in, antioxidant capacity of nanofibers was assessed using DPPH (2,2-diphenyl-1-picrylhydrazyl) radical scavenging test. The nanofibers exhibited significant free radical scavenging activity, like that of BHT (2,6-bis(1,1-dimethylethyl)-4-methylphenol), as a positive control, within the concentration range studied. To evaluate the biocompatibility of the nanofibers, MTT [3-(4,5-dimethylthiazol-2-yl)-2,5-diphenyltetrazolium bromide] cytotoxicity test was performed on L929 fibroblast cell lines. The IC_{50} dose of the nanofibers was determined from MTT assay results. The effect of the nanofibers, with the low-toxic dose ($<IC_{50}$), on cell migration and wound closure was evaluated using a scratch assay. The in vitro scratch assay results demonstrated that the nanofibers promote cell migration and proliferation while maintaining cell viability, resulting in a wound closure within 72 hours.

ORCID:
Ümran Ünüvar: 0000-0002-1071-6059
Fuat Aslan: 0000-0002-6830-6490

References:
Wang, Q., Ji, P., Bu, T., Mao, Y., He, H., & Ge, N. (2025). Recent progress in the application of electrospinning technology in the biomedical field. Journal of Functional Biomaterials, 16(7), 266.
Woo, H. W., & Lee, J. S. Characterization of electrospun Aronia melanocarpa fruit extracts loaded polyurethane nanoweb. Fash Text 8, 12 (2021).
Shah, J., Patel, D., Rananavare, D., Hudson, D., Tran, M., Schloss, R., ... & Kumar, S. (2025). Recent advancements in chitosan-based biomaterials for wound healing. Journal of functional biomaterials, 16(2), 45.
Nikfarjam, Z., & Biglari, N. (2025). Innovative applications of poloxamers in tissue engineering and drug delivery vehicles: An up-to-date review. Nano Micro Biosystems, 4(2), 45-51.

Keyword: *Aronia melanocarpa, Electrospinning, Wound Healing*

Design and Fabrication of Nanostructured TiNbTaZr-Hf Alloy for Biomedical Applications

Yaşar Kemal Erdoğan [*] [1,2], **Gökhan Polat**[3], **Batur Ercan**[2,4,5]

[1] *Dept.of Biomedical Engineering, Isparta University of Applied Sciences, Isparta, Turkey*
[2] *Program of Biomedical Engineering, METU, 06800 Ankara, Turkey*
[3] *Department of Metallurgical and Materials Engineering, IKCU, İzmir, Turkey*
[4] *Department of Metallurgical and Materials Engineering, METU, 06800 Ankara, Turkey*
[5] *BIOMATEN, METU Center of Excellence in Biomaterials and Tissue Engineering, 06800 Ankara, Türkiye*

Ti–Nb–Ta–Zr–Hf (TNTZ-Hf) is a biomedical high-entropy alloy that has attracted attention for orthopedic and dental implants because it combines several properties that are difficult to achieve simultaneously in conventional implant materials. This high-entropy alloy was produced using a copper-hearth vacuum arc melting furnace. The melting process was carried out in an argon atmosphere with a pressure of 5-8 mbar. Each charge was melted to produce a single alloy ingot. XRD analysis confirmed that adding Hf does not result in a discernible secondary phase. These findings are consistent with HEA systems, in which significant configurational entropy stabilizes simple solid-solution structures. We observed that the Hf content in the alloy significantly affects mechanical properties. That said, increasing the Hf atomic ratio from 20% to 35% reduces compressive strength by approximately 45%. Mechanical analysis showed that including Hf content results in a decrease in the slope of the stress-strain curve, which causes a reduction in the elastic modulus.

After design of alloys, the anodization process was applied in NH_4F electrolyte solution to fabricate nanostructured on surfaces. SEM images confirmed that we fabricated 21±1 nm and 42±2 nm feature sizes on TNTZ-Hf surfaces. Moreover, AFM analysis confirmed that uniform nanoroughness was created, being about 3 times rougher than the bare surface. The hydrophilicity of the surface was observed as 71° and 21° for bare and nanostructured surfaces, respectively. XPS analysis confirmed that nanostructured surfaces consisted of oxide-based layers, which include titanium oxide, zirconium oxide, tantalum oxide, niobium oxide and hafnium oxide peaks. Mesenchymal Stem Cell (hMSC) experiments showed that nanotopography provides a supportive environment that cell viability. The observed cell spreading and focal adhesion formation suggest that nanostructured surface provide a favorable microenvironment for cell attachment and cytoskeletal organization.

In conclusion, nanostructured TiNbTaZr-Hf alloys for medical applications combine high biocompatibility, low elastic modulus, and high strength, making them a promising next-generation implant material that may outperform conventional titanium alloys in reducing stress shielding while maintaining mechanical reliability.

Acknowledgment:
The authors would like to thank Oğulcan Demirağ for help during the anodization process.

ORCID:
Yaşar Kemal Erdoğan: 0000-0002-5662-5398
Batur Ercan: 0000-0003-1657-1142

Keyword: *High Entropy Alloy, Nanostructures, Characterization*

Synthesis of Cyclodextrin Modified Cellulose Nanocrystal Nanofibers

Kazım Köse [*1], Yirou Wang[2], Akshat Verma[2], Jeffrey P. Youngblood[2]

[1] *Hitit University, Medical Laboratory Techniques, Çorum 19040, Turkey, Purdue University, School of Materials Engineering, West Lafayette, IN 47906, USA*

[2] *Purdue University, School of Materials Engineering, West Lafayette, IN 47906, USA*

The chemicals utilized in the synthesis of plastics, which have become indispensable and increasingly central to our daily lives, and the chemical byproducts released after their use, have been cited as the cause of numerous diseases. The number of these diseases has been steadily increasing for almost the last fifty years [1]. This study was conducted with the objective of addressing the necessity to eliminate these chemicals from wastewater or environmental sources. The study's primary focus is the development of a novel generation of cyclodextrin-modified cellulosic nanocrystalline nanofiber materials for the removal of lipophilic pollutants such as phthalate, dioxane, and paraben compounds, which are among the most prevalent pollutants [2]. From the standpoint of "green chemistry," the use of hydrophobic cellulose nanocrystals is advantageous not only over carcinogenic monomers but also enables the ability to target accessibility. The exploitation of the host-guest relationship, attributable to the hydrophobic internal surface, was achieved by the use of cyclodextrin in the modification of the cellulose backbone. The resulting synergy was subsequently transferred to a nanofiber structure, which was obtained through an electrospinning process. Nanofibers with a diameter of approximately 200 nanometers effectively retained micropollutants within the cyclodextrin cavity, achieving removal rates of 167, 6, and 73 milligrams per gram for dioxane, paraben, and phthalate compounds, respectively. The dimensional selectivity intrinsic to β-cyclodextrin, attributable to its distinct cavity size, has rendered dioxane adsorption more conducive in both competitive and non-competitive adsorption environments. Moreover, the electrospun nanofibers containing 90% CNC that were successfully produced in this study have not yet been obtained by the electrospinning method described in the literature; only 50% has been achieved [3].

Acknowledgment:
We were hugely indebted to TUBITAK for the support with a 2219-International Postdoctoral Research Fellowship Program with a Grant Number: 1059B192400015.

ORCID:
Kazım Köse: https://orcid.org/0000-0003-1467-2898

References:
Landrigan, P.J., et al., The Lancet, Countdown on health and plastics. The Lancet, 2025. 406(10507): p. 1044-1062.
Bilal, M. and H.M.N. Iqbal, An insight into toxicity and human-health-related adverse consequences of cosmeceuticals — A review. Science of The Total Environment, 2019. 670: p. 555-568.
Sanders, J.E., et al. Electrospinning of Cellulose Nanocrystal-Filled Poly (Vinyl Alcohol) Solutions: Material Property Assessment. Nanomaterials, 2019. 9, 805 DOI: 10.3390/nano9050805.

Keyword: *Electrospinning, Cellulose Nanomaterials, β-Cyclodextrin*

Ultrafast Eco-Friendly Synthesis of Functional Nanoparticles for Biomedical Applications

Güneş Kibar *

Micro Nano Particles (MNP) Research Group, Dpt of Materials Science and Engineering, Adana Alparslan Turkes Science and Technology University, 01250, Adana, Türkiye

The development of environmentally friendly and rapid synthesis methods for functional nanomaterials has become a critical focus in nanotechnology and biomedical engineering. In this study, we present an ultrafast green synthesis strategy for the fabrication of fluorescent hybrid nanoparticles with tunable physicochemical and optical properties. The proposed approach eliminates the need for toxic reducing agents and harsh organic solvents, relying instead on biocompatible components and mild reaction conditions.

The synthesized nanoparticles are engineered through a hybrid organic–inorganic platform, enabling precise control over particle size, surface chemistry, and fluorescence intensity. The incorporation of functional coatings and metal/metal-oxide nanostructures enhances both stability and optical performance. Depending on the design, the resulting systems exhibit strong and stable fluorescence suitable for bioimaging applications.

Beyond synthesis, the biomedical potential of these nanoparticles is evaluated in terms of cellular compatibility, imaging efficiency, and potential biomedical applications. Preliminary results indicate efficient low cytotoxicity, and strong imaging contrast, suggesting their suitability for real-time biological tracking and diagnostic applications.

The developed fluorescent hybrid nanoparticles exhibited an average particle size of approximately 120 nm and demonstrated tunable gradient fluorescence emission, enabling multicolor luminescence ranging from green to red depending on the synthesis conditions. The nanoparticles, possessing both organic and inorganic characteristics, were synthesized within 5 min using both batch and microfluidic platforms. Surface functionalization was readily achieved through co-monomer incorporation, allowing further conjugation with recognition elements such as aptamers and oligonucleotides for biosensing applications. Using an aptamer-functionalized platform, sensitive pathogen detection was successfully achieved with a detection limit of 10^2 CFU mL^{-1}. In addition, the particles were successfully decorated with ~10 nm superparamagnetic iron oxide nanoparticles (SPIONs) via a co-precipitation approach, resulting in a saturation magnetization of approximately 10 emu g^{-1} and enabling magnetic manipulation. Cytocompatibility studies using HepG2 cells demonstrated >80% cell viability even at a nanoparticle concentration of 200 μg mL^{-1}. These findings validate a versatile and scalable synthesis platform that can be extended to different monomer systems for the development of multifunctional nanomaterials for bioimaging, biosensing, targeted delivery, and theranostic applications.
Overall, this work demonstrates a scalable, rapid, and environmentally sustainable route for producing multifunctional fluorescent nanoparticles, bridging green chemistry principles with advanced biomedical technologies. The platform offers promising opportunities for future applications in bioimaging, targeted drug delivery, and diagnostic nanomedicine.

Acknowledgment:
The authors gratefully acknowledge financial support from the Scientific and Technological Research Council of Türkiye (TÜBİTAK) through Projects 122C228 and 123M943.

ORCID:
Güneş Kibar: 0000-0002-2586-6770

References:
Microfluidic vs. batch synthesis of fluorescent poly (GMA-co-EGDMA) micro/nanoparticles for biomedical applications B Kılınçlı, AD Çınar, B Çetin, G Kibar Emergent Materials 8 (2), 1101-1110
Ultrafast green synthesis of superparamagnetic hybrid nanoparticle for advanced applications G Kibar Polymers for Advanced Technologies 36 (9), e70343
Magneto-electrochemical biosensing for pathogen detection using nuclease-responsive nanohybrids G Kibar, M Kavruk, FJ Hernandez, BA Borsa, AD Dursun, VC Ozalp Microchimica Acta 193 (5), 366

Keyword: *Organic–inorganic hybrids, Emulsion Polymerization, UV-polymerization*

Synthesis of 2-inch Free-Standing Polycrystalline Diamond Wafers with Controlled {110} Texture and Surface Properties to Enhance Thermal Conductivity by MPCVD

Neslihan Şişman * **, Yiğit Can Urlu**

Appsilon İleri Malzemeler Danışmanlık Sanayi ve Ticaret A.Ş., İstanbul, Türkiye

Polycrystalline diamond (PCD) is an exceptional material for extreme thermal, optical , and mechanical applications, combining ultrahigh thermal conductivity (1000-1800 $W m^{-1} K^{-1}$) [1], outstanding hardness (9000-10000 HV) [2], chemical inertness, and broadband optical transparency (0.225-15 μm) [3]. These properties make wafer-scale PCD highly suitable for high-power electronics, advanced heat spreaders, optical windows, semiconductor processing components, and wear-resistant surfaces. However, realizing diamond's intrinsic properties in large-area free-standing wafers requires precise control over phase purity, crystallographic texture, grain coalescence, residual stress, thickness uniformity, and surface finish.

In this study, 2-inch free-standing PCD wafers were developed on tungsten substrates using a custom-built 2.45 GHz microwave plasma chemical vapor deposition system. To enhance thermal conductivity through microstructural control; chamber pressure (60-300 Torr), substrate temperature (800-1200 °C), CH_4/H_2 (1-7%) ratio, and N_2/H_2 (0-0.012%) addition were systematically refined to regulate plasma chemistry, carbon supersaturation, hydrogen etching activity, nitrogen-assisted growth kinetics, and stress evolution. Preferential {110} texture formation was achieved by balancing these parameters to promote compact lateral grain coalescence while suppressing competing {100}/{111}-type morphologies [3]. In-situ optical emission spectroscopy (OES) was used to link reactive plasma chemistry with growth regimes governing phase purity, texture development, and wafer-scale uniformity.

The optimized process yielded crack-free 2-inch PCD wafers with homogeneous color and strain distribution, high diamond phase purity, dense coalescence, and excellent surface quality. OES showed Hα emission at 656.9 nm and a C_2 Swan-band feature at 517.0 nm with $I(C_2)/I(H\alpha) \approx 0.85$, while CH emission at 431.5 nm remained weak, $I(CH)/I(H\alpha) \approx 0.03$, indicating stable hydrogen-rich plasma chemistry with controlled carbon precursor formation. X-ray diffraction (XRD) confirmed a highly dominant {110} texture through the diamond (220) peak at $2\theta \approx 75.3°$. Raman spectroscopy showed a sharp diamond peak at 1332 cm^{-1} with FWHM <10 cm^{-1} and no detectable graphitic G-band at 1550-1580 cm^{-1}. Scanning electron microscopy (SEM) revealed compact {110}-type morphology with twinning-related re-entrant corner features promoting lateral grain interlocking. Dark-field polarized light imaging confirmed uniform strain without macroscopic cracking, while optical profilometry showed 8.5% as-deposited thickness homogeneity, polished roughness below Ra <10 nm, and 0.1° flatness deviation. Laser Flash Analyzer (LFA) and dilatometer further confirmed an enhanced thermal conductivity of ~1800 $W \cdot m^{-1} \cdot K^{-1}$ and a low coefficient of thermal expansion of ~1.0×10^{-6} K^{-1}, respectively.

These results establish a reproducible domestic MPCVD route for 2-inch free-standing PCD wafer production in Türkiye and provide a scalable baseline for 3 to 4-inch PCD wafer showing homogeneous thermal conductivity.

Acknowledgment:
The authors gratefully acknowledge Dr. Nuri Solak from Istanbul Technical University for his support in laser flash analysis (LFA) and dilatometry measurements.

ORCID:
Neslihan Şişman: 0000-0003-0408-7644

References:
1. Wort, C. J. H., Sweeney, C. G., Cooper, M. A., Scarsbrook, G. A., and Sussmann, R. S., "Thermal properties of bulk polycrystalline CVD diamond," Diamond and Related Materials, vol. 3, pp. 1158–1167, 1994. https://doi.org/10.1016/0925-9635(94)90162-7
2. Lammer, A. (1988). Mechanical properties of polycrystalline diamonds. Materials Science and Technology, 4(11), 949–955. https://doi.org/10.1179/026708388790329909
3. Yang, G., Sun, P., Zhu, T., Wang, Y., Li, S., Liu, C., Yang, G., Yang, K., Yang, X., Lian, W., Peng, Z., Lu, Y., Liu, H., & Jiang, N. (2024). Fabrication, microstructure and optical properties of 〈110〉 textured CVD polycrystalline diamond infrared materials. Diamond and Related Materials, 141, 110600. https://doi.org/10.1016/j.diamond.2023.110600

Keyword: *polycrystalline diamond, thermal conductivity, crystallographic texture*

Tuning the Structural, Optical, and Electronic Properties of WS2 Thin Films via Controlled Potassium Doping

Ali Altuntepe[1], Güldöne Toplu [* 2], Mehmet Ali Olğar[2], Recep Zan[2]

[1] Optical Excellence Application and Research Center, Sivas University of Science and Technology, Sivas 58000, Türkiye
[2] Department of Physics, Niğde Ömer Halisdemir University,Niğde 51000, Türkiye

Two-dimensional transition metal dichalcogenides (TMDs) have attracted significant attention for next-generation optoelectronic and photovoltaic applications due to their tunable electronic properties, strong optical absorption, and compatibility with flexible devices[1]. Among these materials, tungsten disulfide (WS_2) stands out because of its favorable electronic structure, high thermal stability, and tunable bandgap [2,3]. However, efficient control of its carrier concentration and electronic properties remains essential for device optimization. In this study, the effects of potassium (K) doping on the structural, optical, and electronic properties of large-area WS_2 thin films were systematically investigated.

Prior to the post-treatment, the initial RF magnetron sputtered WS_2 thin films possessed a high crystalline quality and a distinct optical bandgap of 2.20 eV. Potassium doping was introduced through a chemical vapor deposition (CVD)-assisted post-treatment process using KOH solutions with concentrations of 0.1 M, 0.3 M, and 0.5 M. The influence of post-deposition annealing temperatures (100 °C, 200 °C, and 300 °C) on doping efficiency was also examined. The films were characterized by Raman spectroscopy, UV–Vis spectroscopy, AFM, and Hall effect measurements.

Raman spectra confirmed the preservation of the WS_2 layered crystal structure after potassium incorporation through the characteristic E_{2g}^1 and A_{1g} vibrational modes. A red shift in the A_{1g} peak indicated increased electron concentration, confirming successful n-type doping. Among the investigated concentrations, the 0.3 M KOH-treated sample exhibited the highest Raman intensity and the most favorable crystalline characteristics, suggesting optimal dopant distribution without significant lattice distortion.

Optical analysis revealed that the bandgap could be tuned from 2.20 eV to 2.10 eV depending on KOH concentration and annealing conditions. This reduction was attributed to dopant-induced electronic states and bandgap renormalization effects. Annealing temperature strongly influenced dopant activation and diffusion. While lower temperatures were insufficient for effective incorporation, annealing at 300 °C provided the optimum conditions for potassium diffusion into the van der Waals gaps, resulting in improved crystallinity and structural stability.

Hall effect measurements verified successful n-type doping through increased carrier concentration and reduced sheet resistance, accompanied by a slight decrease in carrier mobility due to ionized impurity scattering. AFM results showed increased surface roughness and morphological changes following doping, reflecting modifications in crystal growth behavior. Overall, the results demonstrate that KOH-assisted potassium doping is an effective and scalable approach for tailoring the electronic and optical properties of PVD-grown WS_2 thin films, making them promising candidates for photodetectors, optoelectronic devices, and photovoltaic applications.

References:

[1] B. Luo, G. Liu, and L. J. N. Wang, "Recent advances in 2D materials for photocatalysis," vol. 8, no. 13, pp. 6904-6920, 2016.
[2] M. Donarelli and L. J. S. Ottaviano, "2D materials for gas sensing applications: a review on graphene oxide, MoS2, WS2 and phosphorene," vol. 18, no. 11, p. 3638, 2018.
[3] C. Cong, J. Shang, Y. Wang, and T. J. A. O. M. Yu, "Optical properties of 2D semiconductor WS2," vol. 6, no. 1, p. 1700767, 2018.

Keyword: *Thin films, TMDs, doping*

Fabrication of High-Purity V_2O_5 Thin Films by Pulsed Electron Deposition Technique

Sefer Haşim Burgaz [*1], **Cem Çelebi**[2], **Gökhan Utlu**[1]

[1] *Ege University*
[2] *Izmir Institute of Technology*

For the first time, vanadium pentoxide (V_2O_5) thin films were grown by pulsed electron deposition (PED), a technique not previously reported for this functional oxide. Depositions were carried out on n-type Si(100) at a fixed accelerating voltage of 18 kV, an O_2 working pressure of 5 mTorr, and a 6 Hz pulse repetition rate, while the deposition pulse count was varied from 5000 to 20000 to control film build-up. The surface morphology, topography, and chemical state were then examined.

SEM revealed a granular surface of spherical and hemispherical nanoparticles (≈80–500 nm) lying on a continuous base layer. AFM was used to follow the surface evolution with pulse number: the RMS roughness increased from ~33 nm (5000 pulses) to ~48 nm (10000 pulses) before stabilizing near 45 nm, while the surface-area ratio grew from ~17% to ~28%, indicating increasingly three-dimensional texture. The persistently positive skewness (≈1.1–3.5) and elevated kurtosis at low pulse counts point to peak-dominated surfaces studded with tall, isolated asperities, consistent with the SEM images. XPS of the V $2p_{3/2}$ region was dominated by V^{5+} with only a minor V^{4+} component ($V^{5+}/V^{4+} \approx 13$), confirming V_2O_5 as the main phase, together with a thin hydrated near-surface layer arising from brief ambient exposure.

These results establish PED as a practical and tunable route to high-purity V_2O_5 thin films, offering a baseline for future studies on crystallization, doping, and device integration in energy-storage, sensing, and optoelectronic applications.

Acknowledgment:
Characterizations of samples were conducted in the Ege University Central Research Test & Analysis Laboratory Application & Research Center (EGE-MATAL) and Surface Physics Laboratory, Yaşar University.

ORCID:
Sefer Haşim Burgaz: 0009-0009-9334-1739
Cem Çelebi: 0000-0003-1070-1129
Gökhan Utlu: 0000-0003-0105-7562

References:
Ratke, L., & Voorhees, P. W. (2002). Growth and coarsening: Ostwald ripening in material processing. Springer.
Mjejri, I., Rougier, A., & Gaudon, M. (2018). Low-cost and facile synthesis of the vanadium oxides V_2O_3, VO_2, and V_2O_5 and their magnetic, thermochromic and electrochromic properties. Solar Energy Materials and Solar Cells, 198, 19-29 pp.
Demeter, M., Neumann, M., & Reichelt, W. (2000). Mixed-valence vanadium oxides studied by XPS. Surface Science, 454-456, 41-44 pp.
Silversmit, G., Depla, D., Poelman, H., Marin, G. B., & De Gryse, R. (2004). Determination of the V2p XPS binding energies for different vanadium oxidation states (V^{5+} to V^{0+}). Surface Science, 560(1-3), 341-354 pp.
Biesinger, M. C., Lau, L. W., Gerson, A. R., & Smart, R. S. C. (2010). Resolving surface chemical states in XPS analysis of first row transition metals, oxides and hydroxides: Sc, Ti, V, Cu and Zn. Applied Surface Science, 257(3), 887 898 pp.
Mendialdua, J., Casanova, R., & Barbaux, Y. (1995). XPS studies of V_2O_5, V_6O_{13}, VO_2 and V_2O_3. Journal of Electron Spectroscopy and Related Phenomena, 71(3), 249-261 pp.

Keyword: *Vanadium pentoxide, Pulsed electron deposition, Surface morphology*

The Role of Sodium Metavanadate Concentration in the Green Synthesis of Vanadium Oxides Using Fumaria officinalis Extract

Kübra Özlen [*1], Tuğba Soğancı Aras[2], Elif Begüm Elçioğlu[3]

[1] *Eskisehir Technical University, Institute of Graduate Programs, Department of Mechanical Engineering, 26555 Eskisehir, Türkiye*
[2] *Eskisehir Technical University, Institute of Graduate Programs, Department of Advanced Technologies, 26555 Eskisehir, Türkiye*
[3] *Eskisehir Technical University, Faculty of Engineering, Department of Mechanical Engineering, 26555 Eskisehir, Türkiye*

Vanadium oxides are technologically important transition metal oxides owing to their thermochromic, electrochromic, and optoelectronic properties. [1] In recent years, plant-mediated green synthesis approaches have attracted increasing attention as sustainable alternatives to conventional production routes. However, the reproducibility of these processes remains a major challenge, since variations in the phytochemical composition of plant extracts and synthesis conditions can significantly affect phase formation and crystal growth. [2]

In this study, the effect of sodium metavanadate concentration on vanadium oxide formation was systematically investigated using Fumaria officinalis extract as a green synthesis medium. Synthesis reactions were carried out using precursor concentrations of 0.75 M, 0.70 M, and 0.14 M, and the obtained products were characterized by FT-IR analyses.

FT-IR results confirmed the formation of vanadium oxide-related structures in all samples; however, significant differences in band intensities and characteristic peak positions were observed, indicating that precursor concentration strongly influences crystallization behavior and phase evolution. Notably, samples synthesized at high sodium metavanadate concentrations (0.7 M, 0.75 M and 1.0 M) yielded whitish products even after calcination. Considering the characteristic yellow-orange color of V_2O_5, these findings suggest the formation of phases different from the targeted vanadium pentoxide structure.

According to the literature, elevated vanadate and Na^+ concentrations promote the polymerization of vanadate species and favor the formation of sodium vanadate and polyvanadate phases. [3] Therefore, it is proposed that at high precursor concentrations, vanadium preferentially crystallizes as sodium-containing vanadate structures rather than forming pure V_2O_5. In contrast, lower precursor concentrations enabled a more controlled nucleation and crystal growth process, resulting in products closer to the desired vanadium pentoxide phase.

The FT-IR results demonstrate that vanadium oxide formation is influenced not only by precursor concentration but also by the ionic equilibrium of the reaction medium. The findings indicate that sodium metavanadate concentrations of approximately 0.1 M yielded products exhibiting characteristics closer to the targeted V_2O_5 structure, whereas increasing precursor concentration resulted in significant changes in the spectral features and promoted the formation of alternative vanadate structures.

Acknowledgment:
The authors would like to thank TÜBİTAK for its support under Project No. 224M656 within the scope of the 1002-A program.

References:
[1] T. K. Le et al., “Recent advances in vanadium pentoxide (V2O5) towards related applications in chromogenics and beyond: fundamentals{,} progress{,} and perspectives,” J. Mater. Chem. C, vol. 10, no. 11, pp. 4019–4071, 2022, doi: 10.1039/D1TC04872D
[2] M. Javed et al., “Potential and Challenges in Green Synthesis of Nanoparticles: A Review,” Xi’an Shiyou Daxue Xuebao (Ziran Kexue Ban)/Journal Xi’an Shiyou Univ., vol. 19, no. February, pp. 1155–1165, 2023.
[3] Rehder, D. (2008). Inorganic and Coordination Compounds of Vanadium. In Bioinorganic Vanadium Chemistry, D. Rehder (Ed.). https://doi.org/10.1002/9780470994429.ch2

Keyword: *Vanadium Oxide, Green Synthesis, Precursor Consentration Effect*

From PET Waste to Upcycled Conductive Graphene Sheets for Reinforcement of Semi-Crystalline Thermoplastics

Nihan Birgun [*1,2], Havva Baskan-Bayrak[2], Semih Doğan[2], Israr Ahmed[3], Ebrahim Al Hajri[4], Yarjan Abdul Samad[3,5], Burcu Saner Okan[1,2]

[1] *Faculty of Engineering and Natural Sciences, Sabanci University, Tuzla, Istanbul, 34956, Turkiye*

[2] *Sabanci University Integrated Manufacturing Technologies Research and Application Center & Composite Technologies Center of Excellence, Manufacturing Technologies, Istanbul, 34906, Turkiye*

[3] *Department of Aerospace Engineering, Khalifa University, 127788, Abu Dhabi, United Arab Emirates*

[4] *Department of Mechanical Engineering, Khalifa University, 127788, Abu Dhabi, United Arab Emirates*

[5] *The Research & Innovation Center for Graphene and 2D Materials (RIC2D), Khalifa University, 127788, Abu Dhabi, United Arab Emirates*

Post-consumer polyethylene terephthalate (PET) bottles are typically downcycled into low-value products, limiting their contribution to a circular plastics economy. Here, we present a closed-loop upcycling strategy that converts waste PET bottles into graphene sheet additives for semi-crystalline thermoplastics. PET was upcycled into multilayer graphene through talc-assisted catalytic pyrolysis using two distinct routes, namely Fe-assisted chemical activation and Zn-assisted physical blending. This approach enabled control over the structure, electrical conductivity, and reinforcement potential of the resulting graphene materials. Structural characterization revealed distinct differences between the Fe- and Zn-derived graphene in terms of crystallinity, layer structure, purity, and conductivity. Fe-derived graphene exhibited sharper XRD reflections, an approximately four-layered stacked structure, and a crystallinity index of 83%, whereas Zn-derived graphene displayed a thinner 1–2 layer morphology with 80% crystallinity. TEM observations supported this trend, showing interlayer spacings of 0.34 nm for Fe-derived graphene and 0.23 nm for Zn-derived graphene. While XPS analysis indicated higher carbon purity for Zn-derived graphene (86.2 at.%) than for Fe-derived graphene (82.2 at.%), conductivity measurements showed that Fe-derived graphene achieved a markedly higher electrical conductivity of 0.44 S/cm, compared with 0.14 S/cm for Zn-derived graphene. To highlight its multifunctional role across the thermoplastic pyramid, the upcycled graphene was incorporated at 0.5 wt.% into polypropylene (PP), polyamide 66 (PA66), and PET matrices, spanning commodity, engineering, and closed-loop recyclable thermoplastics. In all cases, the additive acted as both a nucleating and reinforcing agent, demonstrating how waste PET can be circularly revalorized into a high-value graphene additive for diverse semi-crystalline polymer systems. Mechanical testing showed 21–28% increases in PP flexural strength and modulus, a 31% increase in PA66 tensile modulus, and a 26% increase in PET tensile strength, confirming effective reinforcement alongside circular materials design. Life-cycle assessment further revealed that the proposed upcycling route can lower carbon dioxide (CO_2) emissions by nearly 98% relative to conventional graphene production. Collectively, these findings demonstrate that PET-derived graphene is a sustainable multifunctional additive that combines electrical conductivity, mechanical reinforcement, and circular value creation, offering a promising route for plastic valorization across the thermoplastic pyramid.

Acknowledgment:
This material is based on work supported by the Research and Innovation Center for Graphene and 2D Materials (RIC2D) at Khalifa University, UAE. The support was provided through the project “Lightweight, Sustainable, and Energy-Efficient Designs and Production Methods for Upcycled Graphene-Reinforced Hybrid Composites (Light-G-Comp),” project reference no. OC060.

ORCID:
Nihan Birgun: 0000-0002-4364-6325

Keyword: *post-consumer PET waste; thermo-catalytic upcycling; multilayer graphene; electrical properties; mechanical reinforcement; life-cycle assessment*

Investigation of the Use of Phosphate Modified rGO and rGO-Alginate Microspheres in Lanthanum and Cerium Adsorption

Nursu Aydın * **, Şenol Sert**

Institute of Nuclear Sciences

Abstract

Rare earth elements are strategically important materials that are widely used in electronic systems, energy technologies, catalytic applications, and defense industries. In particular, the expanding industrial utilization of lanthanum and cerium has increased the need for efficient and environmentally friendly recovery methods for these elements [1]. Adsorption, which is a low-cost, practical, and highly efficient technique, has been employed for the removal of La and Ce from aqueous solutions. In this study, reduced graphene oxide (rGO) was synthesized in a single step by applying thermal treatment to the ethylene glycol solution obtained from the H_2SO_4 hydrolysis of waste PET bottles. This approach aims not only to valorize plastic waste but also to develop an economical and environmentally friendly synthesis route [2]. Due to its high surface area, chemical stability, and suitability for surface functionalization, rGO was selected as the adsorbent material and modified with phosphate functional groups to enrich its active binding sites for adsorption. In addition, the use of phosphate-modified rGO in the form of sodium alginate-based microbeads was investigated, and the biocompatible structure of alginate, rich in carboxyl groups, was found to contribute positively to adsorption performance [3]. In this study, the adsorption performance of phosphate-modified reduced graphene oxide (rGO) for the removal of La (III) and Ce (III) ions was evaluated. The results demonstrated that the optimum pH value for both metal ions was 4, while the optimum contact time was 90 min. The maximum adsorption capacities were determined as 29.31 mg g^{-1} for Ce (III) and 37.90 mg g^{-1} for La (III). Isotherm analyses revealed that the Langmuir model provided the best fit to the experimental data, indicating that adsorption predominantly occurred through monolayer coverage. Kinetic studies showed a better agreement with the Pseudo-Second-Order (PSO) kinetic model, suggesting that chemical interactions played a significant role in the adsorption mechanism. For alginate-rGO micro beads prepared in different weight ratios, pH optimization experiments indicated that the adsorbent containing 40 wt.% rGO achieved adsorption capacities of 25.34 mg g^{-1} for Ce (III) and 24.86 mg g^{-1} for La (III) at pH 5. Structural and surface characteristics of the adsorbents were comprehensively investigated using SEM, FTIR, and XPS analyses.

Acknowledgment:
This study is supported by Ege University Scientific Research Projects Coordination Unit. Project Number: 33495

ORCID:
Nursu Aydın: 0009-0005-2271-8819
Şenol Sert: 0000-0003-1967-7858

References:
[1] Balaram, V. (2019). Rare earth elements: A review of applications, occurrence, exploration, analysis, recycling, and environmental impact. Geoscience Frontiers, 10(4), 1285–1303.
[2] Milig, O., & Sert, Ş. (2025). Efficient thermal approach for producing reduced graphene oxide from ethylene glycol derived from PET waste. Materials and Manufacturing Processes, 40(15), 1996–2003.

Keyword: *rGO, Alginate, PET, Rare earth elements, adsorption*

Formation and Field Emission Behavior of Graphitic Nanosheet Networks on SiC

Erhan Gurpinar [*1], Jose Navarrete[2], Marc Cahay[2,3], Goknur Cambaz Buke[1,4,5]

[1] *Micro and Nanotechnology, Graduate School of Engineering and Science, TOBB University of Economics and Technology, Ankara 06560, Turkey*

[2] *Spintronics and Vacuum Nanoelectronics Laboratory, University of Cincinnati, Cincinnati, OH, USA*

[3] *BlueHalo, 4401 Dayton-Xenia Rd., Dayton, Ohio 45432, USA*

[4] *A.J. Drexel Nanomaterials Institute, Drexel University, Philadelphia, Pennsylvania 19104, United States*

[5] *UNAM — National Nanotechnology Research Center and Institute of Materials Science and Nanotechnology, Bilkent University, Ankara, Turkey*

Graphitic nanostructures directly integrated with semiconductor substrates are promising candidates for vacuum electronic applications. In this study, porous graphitic nanosheet networks (GNSs) were synthesized on the C-face of 4H-SiC by high-temperature vacuum decomposition at 1700 °C. The resulting carbon architecture was investigated using SEM, TEM, Raman spectroscopy, AFM, Kelvin probe force microscopy, and field-emission measurements.

Microscopy analyses revealed a porous graphitic coating composed of interconnected nanosheets with thicknesses of approximately 5–20 nm, conformally attached to the underlying SiC substrate. Raman spectroscopy confirmed the graphitic nature of the coating, while AFM and Kelvin probe measurements demonstrated pronounced nanoscale topographical and surface-potential variations, indicating local electronic heterogeneity. Field-emission measurements exhibited stable electron emission with a turn-on field of 10.9 V μm^{-1} and a field-enhancement factor of approximately 680. Post-emission characterization revealed localized rupture of surface graphitic regions, exposing graphene edges and the underlying nanosheet network which result in the decrease of turn-on field. These observations suggest that electron emission is primarily governed by surface-accessible graphitic regions rather than the buried nanosheet framework itself.

The results establish a direct correlation between graphitization-induced surface morphology, local electronic heterogeneity, and electron-emission behavior. Vacuum decomposition of SiC therefore provides a versatile route for producing a variety of graphitic architectures with potential applications in vacuum microelectronics and electron-emission devices.

(This study was supported by the Air Force Office of Scientific Research, grant numbers FA9550-23-1-0593, FA9550-21-1-0202 and FA9550-26-1-B062.)

References:

Cambaz Z G, Yushin G, Osswald S, Mochalin V and Gogotsi Y 2008 Noncatalytic synthesis of carbon nanotubes, graphene and graphite on SiC Carbon 46 841–9

Gogotsi Y and Presser V 2013 Carbon Nanomaterials (Boca Raton: CRC Press)

Keyword: *Graphitic nanostructures, Field emission*

Growth of Ultrathin TaC Crystals on Copper via CVD

Eren Atlı [*] [1], **Göknur Cambaz Büke**[1,2,3]

[1] *Materials Science and Nanotechnology Engineering, Micro and Nanotechnology Program, TOBB University of Economics and Technology, Ankara, Turkey*

[2] *A.J. Drexel Nanomaterials Institute, Materials Science and Engineering Department, Drexel University, Philadelphia, PA, USA*

[3] *UNAM — National Nanotechnology Research Center and Institute of Materials Science and Nanotechnology, Bilkent University, Ankara, Turkey*

Two-dimensional transition metal carbides [1-3] (2D TMCs) have recently emerged as a promising class of quantum and electronic materials. Recent studies on ultrathin Mo_2C [2] and WC [3] have revealed thickness-dependent physical properties, including superconducting behavior, highlighting the importance of synthesizing high-quality TMC crystals with controlled dimensions. Here, we report the chemical vapor deposition growth of ultrathin TaC crystals through a graphene-driven growth mechanism on liquid copper. Unlike conventional carbide CVD processes, no gaseous carbon precursor was introduced during growth. Instead, a pre-grown graphene layer served as the sole carbon source. Upon annealing a Ta/Cu/graphene structure at 1130 °C, graphene progressively decomposed and supplied carbon atoms that reacted with Ta species transported through molten Cu. This process resulted in the direct formation of well-faceted TaC crystals without residual graphene coverage. The growth mechanism promotes lateral crystal expansion and yields ultrathin TaC domains approximately 30 nm thick with lateral dimensions reaching 20 μm. The complete consumption of graphene during growth eliminates the need for post-growth graphene removal and provides direct access to the intrinsic properties of TaC. (This study was supported by the Air Force Office of Scientific Research, grant numbers FA9550-22-1-0358 and FA9550-21-1-0202.)

Acknowledgment:
(This study was supported by the Air Force Office of Scientific Research, grant numbers FA9550-22-1-0358 and FA9550-21-1-0202.)

ORCID:
Göknur Cambaz Büke: https://orcid.org/0000-0001-9587-519X

References:
Zhang, C., Guo, H., Zhu, T., Xu, Q., Li, B. W., Tu, R., ... & Zhang, S. (2022). Growth of self-aligned nonlayered TaC nanosheets on liquid copper by a solid phase diffusion strategy. Materials Today Nano, 19, 100237.
Xu, C., Wang, L., Liu, Z., Chen, L., Guo, J., Kang, N., ... & Ren, W. (2015). Large-area high-quality 2D ultrathin Mo2C superconducting crystals. Nature materials, 14(11), 1135-1141.
Sredenschek, A. J., Sanchez, D., Wang, J., Zhou, D., Yi, L., Yu, Z., ... & Terrones, M. (2026). Phase-controlled synthesis and two-dimensional electronic transport of ultrathin tungsten carbide platelets. npj 2D Materials and Applications, 10(1), 38.

Keyword: *2D Materials, CVD, Tantalum Carbide*

Probing CVD Graphene on Cu Foil by Simultaneous UHV AFM/STM: From Atomic Defects to Folded Nanoribbons

Feyza Nur Yıldırım * **, Hakan Özgür Özer**

Istanbul Technical University, Department of Physics Engineering, 34469 Maslak, Istanbul, Turkey

Two-dimensional materials are a compelling platform for next-generation electronic and sensor devices. Understanding graphene at the atomic scale, however, requires techniques capable of simultaneously resolving structural and electronic degrees of freedom. In this work, we employ a room-temperature ultra-high vacuum (UHV) simultaneous Atomic Force / Scanning Tunneling Microscopy (AFM/STM) system with a heavily boron-doped diamond (BDD) cantilever to characterize CVD-grown graphene on Cu foil. Simultaneous AFM/STM imaging of this system was previously established in our group using a metallic tip [1]; here we extend it to a diamond probe, whose chemical inertness and stiffness prove critical both for stable atomic-resolution imaging [2] and for tip-induced manipulation. The cantilever is operated in off-resonance, small-amplitude mode, so that the tunneling current and force/force-gradient channels are acquired simultaneously at the same point. This lets us investigate, within a single instrument, both the mechanical and electronic properties of graphene and the formation of graphene nanostructures by tip manipulation. We first resolve an intrinsic vacancy at which the apparent barrier height rises sharply from ~2.4 eV over pristine lattice sites to values exceeding 7 eV, accompanied by a modified local density of states around the defect [3]. The force channel resolves the atomic stiffness corrugation of the surrounding pristine lattice, with a local interaction stiffness of ~35.2 N/m at on-top sites and ~32.3 N/m at hollow sites, while the vacancy produces no resolvable change in force, demonstrating the selective contrast between the force and current channels. We further present tip-induced folding of bilayer and multilayer graphene regions by mechanical manipulation of the diamond probe, a form of graphene origami previously realized with metal STM tips [4]. Folding events were produced repeatedly, and a subset could be reversibly switched between folded and unfolded configurations with different twist angles. Among the folds resolved at atomic scale, one produced a twisted stacking whose moiré superlattice corresponds to a twist angle of ~3.9° (Figure b). In the folded regions the apparent barrier height varies spatially, ~3.8 eV over the folded area rising to ~5.5 eV at the fold edge, while force-distance spectroscopy measures diamond-graphene interaction forces across folded and planar regions, revealing mechanical differences. As two carbon allotropes, the diamond-graphene interface is of interest for fundamental carbon-carbon interactions and carbon-based device applications. By combining atomic-scale imaging, spectroscopy, and tip manipulation in one platform, this work contributes insight into this interface.

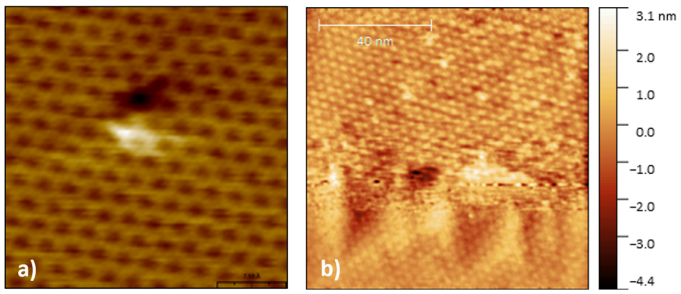


Figure: a) Tunnel current modulation amplitude map of an atomic-scale defect on CVD-grown graphene. The image size is 30×30 Å², I_t = 0.25 nA, and V_{bias} = 2.5 V. b) STM Topography image: Moiré patterns on a folded graphene sheet, with a twist angle of 3.9°. It = 0.3nA, V_{bias} = 630mV.

Acknowledgment:
The measurements were performed using an SPM control unit and software provided by NanoMagnetics Instruments.

ORCID:
Feyza Nur Yıldırım: 0009-0002-5976-1990
Hakan Özgür Özer: 0000-0002-2279-8098

References:
[1] M. F. Jadidi, U. Kamber, O. Gürlü, H. Ö. Özer, Beilstein J. Nanotechnol. 9, 2953–2959 (2018).
[2] V. Grushko, O. Lübben, A. N. Chaika, N. Novikov, E. Mitskevich, A. Chepugov, O. Lysenko, B. E. Murphy, S. A. Krasnikov, I. V. Shvets, Nanotechnology 25, 025706 (2014).
[3] M. M. Ugeda, I. Brihuega, F. Guinea, J. M. Gómez-Rodríguez, Phys. Rev. Lett. 104, 096804 (2010).
[4] H. Chen, X. J. Zhang, Y. L. Zhang, D. Wang, D. L. Bao, Y. Que, W. Xiao, S. Du, M. Ouyang, S. T. Pantelides, H.-J. Gao, Science 365, 1036–1040 (2019).

Keyword: *graphene, Atomic Force Microscopy, Scanning Tunneling Microscopy*

Quartic Energy Band Engineering in Artificial Semiconductor Honeycomb Lattices

Emre Okcu [*1], Emre Mesudiyeli[1], Haldun Sevinçli[2], A. Devrim Güçlü[1]

[1] *İzmir Institute of Technology*
[2] *Bilkent University*

Recent advances in semiconductor-based superlattices have opened new avenues for developing tunable quantum simulators. Artificial graphene nanostructures, realized by imposing a periodic potential on a two-dimensional electron gas, provide a controllable platform for engineering graphene-like Dirac cones and for exploring correlated electronic phases through adjustable lattice parameters such as lattice constant, dot radius, and potential depth [1–3]. Beyond massless Dirac dispersion, hexagonal lattices can also host unconventional band structures, including Mexican-hat-shaped (MHS), purely quartic, and non-MHS quartic dispersions. These quartic bands form around the center of the Brillouin zone and exhibit strong Van Hove singularities, which are associated with enhanced interaction effects and correlated many-body phenomena [4–6].

In this work, we demonstrate the emergence of quartic energy dispersion in artificial semiconductor honeycomb lattices through analytical tight-binding modeling and numerical Bloch-wave calculations under realistic system parameters. We determine the conditions under which the three distinct quartic band types arise and identify sublattice staggering as the decisive structural mechanism that unlocks the full diversity of quartic dispersion. Our results show that a staggered honeycomb lattice supports MHS, purely quartic, and non-MHS quartic bands, whereas its planar counterpart yields only purely quartic and non-MHS forms. These findings demonstrate the feasibility of engineering quartic band edges in artificial semiconductor lattices and clarify how lattice geometry can be used to tailor their electronic characteristics.

Acknowledgment:
This work was supported by the Izmir Institute of Technology Scientific Research Projects under the program of ADEP (Project No: 2022IYTE-3-0031). HS acknowledges support from Air Force Office of Scientific Research (AFOSR, FA9550-21-1-0261)

References:
M. Gibertini, A. Singha, V. Pellegrini, M. Polini, G. Vignale, A. Pinczuk, L. N. Pfeiffer, and K.W.West, “Engineering artificial graphene in a two-dimensional electron gas,” Physical Review B 79, 241406(R) (2009).
A. Singha, M. Gibertini, B. Karmakar, S. Yuan, M. Polini, G. Vignale, M. I. Katsnelson, A. Pinczuk, L. N. Pfeiffer, K. W. West, and V. Pellegrini, “Two-dimensional Mott-Hubbard electrons in an artificial honeycomb lattice,” Science 332, 1176– 1179 (2011).
S. Wang, D. Scarabelli, L. Du, Y. Y. Kuznetsova, L. N. Pfeiffer, K. W. West, G. C. Gardner, M. J. Manfra, V. Pellegrini, S. J. Wind, and A. Pinczuk, “Observation of Dirac bands in artificial graphene in small-period nanopatterned GaAs quantum wells,” Nature Nanotechnology 13, 29–33 (2018).
H. Sevinçli, “Quartic dispersion, strong singularity, magnetic instability, and unique thermoelectric properties in twodimensional hexagonal lattices of group-VA elements,” Nano Letters 17, 2589–2595 (2017).
A. D. Güçlü, “Wigner crystallization at graphene edges,” Physical Review B 93, 045114 (2016).
A. U. Canbolat, H. Sevinçli, and Ö. Çakır, “Indirect exchange interaction in two-dimensional materials with quartic dispersion,” Physical Review B 106, 104409 (2022).

Keyword: *Quartic dispersion, Mexican-hat shaped band structure, van Hove singularity, semiconductor heterostructures, artificial graphene, quantum simulators, two-dimensional electron systems.*

Development of Recycled Graphene-Based Polypropylene and PEEK Compounds Derived from Waste Tires for Automotive and Aerospace Applications

Tülin Erdal Erikli [*1], **Selin Arıcan**[1], **Burcu Saner Okan**[2], **Murat Cansever**[1]

[1] *Eurotec Engineering Plastics*

[2] *Sabanci University Integrated Manufacturing Technologies Research and Application Center & Composite Technologies Center of Excellence*

The increasing demand for lightweight, sustainable, and multifunctional materials in the automotive and aerospace industries has accelerated the development of advanced polymer nanocomposites. This study focuses on the development of recycled graphene-reinforced polypropylene (PP) and polyether ether ketone (PEEK) compounds for engineering applications that require enhanced mechanical and functional performance. PP was chosen for its low density, cost-effectiveness, and broad applicability in automotive components. In contrast, PEEK was selected for its superior thermal resistance, chemical durability, and high-performance capability in demanding aerospace applications. Waste tire driven recycled graphene served as a sustainable nanoplatelet material, enhancing stiffness, conductivity, thermal stability, and structural performance while supporting life cycle assessment studies. The PP and PEEK samples were produced in granule form using a twin-screw extruder during the extrusion process, making them suitable for various manufacturing methods, such as film extrusion, 3D printing, and injection molding. Target applications include lightweight structural parts, conductive components, interior automotive and aerospace parts, and high-temperature engineering components. To investigate the effects of incorporating waste tire-derived recycled graphene into PP and PEEK matrices, physical, mechanical, impact, and thermal characterizations were conducted. Density values were measured to assess lightweight performance, while tensile and impact tests evaluated mechanical performance. Additionally, the heat deformation temperature (HDT) test was conducted to examine the thermal behavior of the developed samples under mechanical load. Preliminary findings indicate that recycled graphene-reinforced PP and PEEK systems hold promising potential for sustainable lightweight engineering applications where improved functionality is required.

This project is funded by the Research & Innovation Center for Graphene and 2D Materials (RIC-2D) under the Light-G-Comp project

ORCID:
Selin Arıcan: 0000-0003-0855-8765
Burcu Saner Okan: 0000-0002-5940-7345

Keyword: *Waste tire driven recycled graphene, automotive, aerospace*

Engineering Bifunctional Conjugated Polymers: Triphenylamine-Based Systems for Electrochromic Energy Storage in Asymmetric Hybrid Supercapacitor Devices

Arya Zelal Keserci [*1], **Ali Çırpan**[1,2,3,4]

[1] *Department of Polymer Science and Technology, Middle East Technical University, Ankara, 06800, Turkey*
[2] *Department of Chemistry, Middle East Technical University, Ankara, 06800, Turkey*
[3] *ODTU GUNAM, Middle East Technical University, Ankara, 06800, Turkey*
[4] *Department of Micro and Nanotechnology, Middle East Technical University, Ankara, 06800, Turkey*

Current energy storage research increasingly targets devices that combine high capacitive performance with additional functionalities such as electrochromism. Supercapacitors have emerged as promising energy storage devices bridging conventional capacitors and batteries, offering high power density, fast charge-discharge rates, and long cycle life. Conjugated polymers have emerged as attractive multifunctional electrode materials owing to their π-delocalized backbones, tunable redox properties, and optical switching capabilities.

This study reports the synthesis and characterization of five triphenylamine (TPA)-based conjugated polymers (P1-P5) designed for asymmetric hybrid electrochromic supercapacitor devices (AESDs). The polymer series was systematically engineered by varying the π-bridge unit: P1, P2, and P3 incorporate furan, selenophene, and thiophene as π-bridges in a D-π architecture. P4 and P5 adopt a D-π-A architecture in which EDOT serves as a donor unit and thiophene and 3,4-dicyanothiophene act as the π-bridge, respectively, with the electron-withdrawing cyano substituent in P6 promoting extended charge delocalization. Monomers were synthesized via Stille and Suzuki cross-coupling reactions and polymerized electrochemically onto ITO-coated glass substrates. Polymers were characterized by CV, GCD, EIS, SEM, and spectroelectrochemistry.

The D-π-A polymers exhibited significantly enhanced capacitive performance, with P6 reaching 43 mF/cm^2. AESDs were fabricated using the conjugated polymer films as anodes, PEDOT as the cathode, and PMMA-based gel electrolytes. All devices demonstrated dual electrochromic-energy storage functionality with high coloration efficiencies and stable cycling performance. This work establishes the π-bridge identity as a key structural parameter governing both capacitive behavior and optical properties in multifunctional polymer-based energy storage devices.

Acknowledgment:
This study was supported by Scientific and Technological Research Council of Turkey (TUBITAK) under the Grant Number 124Z087. The authors thank TUBITAK for their supports.

ORCID:
Arya Zelal Keserci: 0009-0005-6468-5920
Ali Çırpan: 0000-0003-3051-8380

References:
Cevher, D., & Cirpan, A. (2025). Design, strategies and recent advances in conjugated polymers for supercapacitors. Journal of Energy Storage, 109, 115246. https://doi.org/10.1016/j.est.2024.115246
Béguin, F., & Frąckowiak, E. (2013). Supercapacitors : materials, systems, and applications. Wiley-VCH.
Abofoul, A., Görgün, K., & Hür, E. (2026). From molecular design to electroactive polymer: Synthesis, electropolymerization, and DFT analysis of a carbazole EDOT-based compound. Synthetic Metals, 319, 118141. https://doi.org/10.1016/j.synthmet.2026.118141

Keyword: *Electrochromism, Asymmetric Electrochromic Supercapacitor Devices (AESDs), Triphenylamine (TPA)*

Controllable porosity and conductivity in graphene-polymer nanocomposite fiber as multimodal wearable sensors

Arooj Fatima [*1], **Mustafa Ordu**[2]

[1] *Material Science and Nanotechnology UNAM, Bilkent University (PhD student)*
[2] *Material Science and Nanotechnology UNAM, Bilkent University (Assistant Professor)*

The evolution of wearable technology is increasingly driven by demand for flexible, breathable materials capable of continuous, real-time health monitoring. To address this need, fiber-based devices offer a promising pathway for seamless textile integration. This study presents a high-throughput fabrication method for conductive porous nanocomposite fibers utilizing thermally induced phase separation within the thermal fiber drawing process. Graphene (Gr) with varying ratios was homogenously integrated into the porous polyvinylidene fluoride (PVDF) matrix, and then encapsulated by a styrene-ethylene-butylene-styrene (SEBS) cladding. The addition of Gr serves a dual purpose as (i) establishing electrical conductivity and (ii) modulating the fiber's morphological, structural, and mechanical characteristics. Notably, increasing the graphene content reduced the size of spherulites within the PVDF matrix, and the spherulites reached the sub-micron range at a Gr:PVDF ratio of 45:55 (labeled as Gr_{45} fibers). Furthermore, electrical characterization revealed conductivity scales with graphene loading, achieving a percolation threshold with Gr_{25} fibers and a maximum conductivity of $1.35x10^{-3}$ S/m in the Gr_{45} samples. These fibers exhibit high sensitivity and rapid response times, making them well-suited for temperature sensing, pressure monitoring, and physiological data tracking.

Keyword: *Thermal induce phase separation (TIPS), Temperature sensor, Pressure sensor*

Design Parameters of PbSe Nanorod–Quantum Dot Bulk Nano-Heterojunction Platforms for Multiple Exciton Generation-Based Solar Cells

Demet Asil * [1,2,3], İrem Kolay[1], Tuğba Hacıefendioğlu[1]

[1] *Middle East Technical University (METU), Department of Chemistry, Ankara 06800, Turkey*
[2] *Department of Micro and Nanotechnology, METU, Ankara 06800, Turkey*
[3] *METU-MEMS Center, Ankara 06800, Turkey*

Overcoming the Shockley–Queisser efficiency limit remains one of the central challenges in photovoltaics. Multiple exciton generation (MEG), a process by which a single high-energy photon produces more than one electron-hole pair, offers a thermodynamically viable route to push photoconversion efficiencies beyond this fundamental boundary. Among the materials explored for MEG-based devices, PbSe nanostructures stand out due to their exceptionally high MEG yields, size-tunable bandgaps, and anisotropic carrier transport properties. However, translating these optical advantages into functional solar cells has remained elusive, primarily due to challenges in film morphology, charge extraction, and the unresolved role of nanorod (NR) geometry in device performance.

In this work, we present a systematic investigation of PbSe nanorods and quantum dots (QDs) as active components in bulk nano-heterojunction (BNHJ) solar cell architectures designed to harness MEG. Our approach begins with the controlled synthesis of PbSe NRs with tunable aspect ratios and bandgaps, followed by a detailed theoretical and experimental study of ligand-directed NR assembly. We demonstrate that ligand chemistry critically governs interparticle spacing, film microstructure, and ultimately photovoltaic performance, providing design rules for optimizing NR-based layers.

Building on these insights, we engineer BNHJ active layers by blending covalently coupled PbSe NR-donors with PbSe QD-acceptors. Transmission electron microscopy confirms that QD-acceptors surround NR-donors, forming an intimate donor-acceptor network with interfacial band offsets of 0.20–0.25 eV that facilitate efficient exciton dissociation and charge separation. Insertion of an electron-blocking QD interlayer at the NR/metal interface further suppresses back injection losses. The resulting devices exhibit photocurrent enhancements at photon energies ≥ 2Eg — the spectral signature of MEG — with a peak internal quantum efficiency of 100% and a MEG threshold of 2.9 Eg. Progressive improvements to the BNHJ architecture yield record photoconversion efficiencies among MEG-active cells incorporating PbSe NRs, while simultaneously revealing the essential role of NR bandgap engineering and donor concentration in lowering MEG thresholds.

Collectively, this body of work establishes the BNHJ platform as a robust and scalable strategy for exploiting MEG in working photovoltaic cells, offering a practical pathway toward third-generation solar energy conversion.

Acknowledgment:
This research was funded by The Scientific and Technological Research Council of Turkey (TÜBİTAK) (Grant No. 117E787, 123N542) and Middle East Technical University (Grant Nos. TEZ-YL-103-2019-10154, BAP-08-11-2017-012, TEZ-YL-103-2022-10860).

ORCID:
Demet Asil: https://orcid.org/0000-0001-6368-7151
İrem Kolay: https://orcid.org/0000-0001-9950-517X
Tuğba Hacıefendioğlu: https://orcid.org/0000-0001-5231-5416

References:
İ. Kolay, T. Hacıefendioğlu, F. Aydın, E. Yıldırım, D. Asil, Theoretical and Experimental Investigation of the Ligand-Directed Assembly and Photovoltaic Performance of PbSe Nanorods. Adv. Mater. Interfaces2025, 12, 2500127. https://doi.org/10.1002/admi.202500127
İrem Kolay, Demet Asil, PbSe nanorod-quantum dot bulk nano-heterojunction solar cells generating multiple excitons with record photo conversion efficiencies, Materials Today Communications, Volume 35, 2023, 106064. https://doi.org/10.1016/j.mtcomm.2023.106064.
Hacıefendioğlu, T., Balıkoğlu, B., Aydın, F. et al. Enhanced photocurrent in PbSe nanorod-quantum dot bulk nano-heterojunction solar cells. J Mater Sci: Mater Electron 33, 714–724 (2022). https://doi.org/10.1007/s10854-021-07342-y

Keyword: *PbSe nanorods, quantum dots, multiple exciton generation*

Homoepitaxial Quantum Diamond Growth by MP-CVD: Effect of O_2 Pre-Treatment on Crystal Quality, Substitutional Nitrogen, and NV^- Center Activation

Vildan Aker * **, Neslihan Şişman**

Appsilon Advanced Materials Consulting Industry and Trade Inc., Gebze, Kocaeli, Türkiye

Diamond is among the most compelling solid-state platforms for quantum sensing, with nitrogen-vacancy (NV) centers enabling room-temperature magnetometry, spin-based quantum information processing, and nanoscale field detection. Achieving the required material purity demands homoepitaxial films with sub-ppm substitutional nitrogen ([Ns]) and minimal lattice defects — parameters directly tied to long spin coherence times (T_2). Surface pre-treatment prior to MP-CVD growth governs seed chemistry, nucleation quality, and defect propagation, yet systematic comparisons of O_2-based protocols remain scarce.

To identify the optimal preparation route for quantum-grade diamond, homoepitaxial growths were carried out on single-crystal seeds in a 2.45 GHz MP-CVD reactor under four O_2 pre-treatment conditions: no pre-treatment (control), O_2 plasma etching, O_2 annealing, and their combination. Birefringence imaging evaluated crystal quality, in-situ OES monitored plasma chemistry over 96 hours, UV-VIS transmittance spectroscopy (220–800 nm) assessed optical purity, and XRD rocking curve analysis on control samples established the crystallographic baseline. NV^- activation was assessed by ODMR (100 mW, 300 mA) after electron irradiation and thermal annealing. [Ns] was calculated from the 270 nm absorption feature via Beer-Lambert law using Collins & Williams (1971) calibration and growth-rate-corrected thicknesses (24.3, 21.1, 18.6, and 15.3 µm/h for control, O_2 plasma etching, O_2 annealing, and combination). Control samples underwent electron irradiation (10^{18} e^-/cm^2, 10 mA, 150 min) and annealing at 900°C for 1 hour.

Among the four conditions, O_2 annealing stood out across every metric: the most stable plasma chemistry with a progressively increasing normalized Hα emission ratio (0.79), the lowest lattice strain in birefringence imaging, and the highest UV transmittance at 270 nm (40.83%). O_2 plasma etching returned a lower C_2/Hα ratio (1.72), suggesting more favorable sp^3 growth chemistry, yet fell short on all other parameters. The combined pre-treatment showed the highest defect density and anomalous broad-band OES emission between 800–1100 nm, warranting photoluminescence investigation. All [Ns] values (0.06–0.09 ppm) fell well below both the <1 ppm high-T_2 and <5 ppm NV-sensor thresholds. XRD on control samples as crystallographic baseline gave FWHM values of 44.4 and 46.4 arcsec with dislocation densities of ~8.1×10^{10} and ~8.9×10^{10} cm^{-2}, consistent with quantum-grade standards. ODMR confirmed NV^- activation at 2.870 GHz with Zeeman splitting of ~28 MHz under 1 mT and contrasts of ~4–9.5%, consistent with ensemble NV^- densities reported for CVD diamond.

These findings establish O_2 annealing as the preferred surface preparation protocol for quantum-grade MP-CVD diamond and offer a reproducible multi-parameter characterization approach for NV-center quantum sensor development.

ORCID:
Vildan Aker: 0000-0002-1216-9941
Neslihan Şişman: 0000-0003-0408-7644

Keyword: *quantum diamond, MP-CVD, NV center*

Investigation Of The Effect Of Nanoclay Incorporation On Structural, Mechanical, And Biological Properties Of Yttria-Stabilized Zirconia Bone Grafts

Doğa Memioğlu [* 1], Yiğithan Tufan[1], Jae-Hyung Park[2,3], Abdullah Öztürk[1], Jongee Park[4], Young-Hag Koh[2,3], Batur Ercan[1,5]

[1] Department of Metallurgical and Materials Engineering, Middle East Technical University, 06800 Ankara, Turkey
[2] School of Biomedical Engineering, Korea University, Seoul 02841, Republic of Korea
[3] Interdisciplinary Program in Precision Public Health, Korea University, Seoul 02841, Republic of Korea
[4] Department of Metallurgical and Materials Engineering, ATILIM University, Ankara, 06830, Turkey
[5] BIOMATEN, METU Center of Excellence in Biomaterials and Tissue Engineering, 06800 Ankara, Turkey

Bone tissue engineering is an important field of study due to its need to meet the mechanical properties matching those of the bone tissue itself, and to elicit an appropriate biological response for proliferation and bone regeneration. Yttria-stabilized zirconia (YSZ) is a widely used material for this purpose due to its superior mechanical properties, such as fracture toughness and flexural strength. However, its low-temperature degradation (LTD) behavior affects its structural and mechanical properties negatively. Its LTD behavior, biological response in the body, and the effect of pore structure on those phenomena are still research topics.

In this study, the effect of further nanoclay incorporation up to 8% on pore structure, structural, mechanical, and biological properties of porous YSZ/nanoclay nanocomposite is researched. These nanocomposite scaffolds are produced by Digital Light Processing (DLP), and nanoclay is used as a multifunctional additive to limit LTD of the tetragonal zirconia phase of the YSZ ceramic, modify the pore size, morphology, and interconnectivity, and increase the cell-material interactions.

From the preliminary data, it was seen that the time needed for LTD behavior of YSZ/nanoclay nanocomposites is longer than that of those that do not have nanoclay in their structure, and the LTD resistance increased significantly. Although surface roughness remained comparable, nanoclay incorporation changed the surface chemistry of the material. As nanoclay incorporation into YSZ increased, the water contact angle decreased from 54° to 40° by 4% nanoclay incorporation, so the hydrophilicity increased as well. Moreover, it was seen that the nanoclay amount affected the cell proliferation positively; the most significant increase in cellular viability was observed at 4% nanoclay incorporation. Also, the cell spreading was greater at 4% nanoclay content than in the groups of lower nanoclay-containing YSZ. Increasing hydrophilicity pointed out this result as well. Lastly, the enhanced calcium mineral deposition was observed in the group that 4% nanoclay, which was an indicator for increased osteogenic behavior of osteoblasts.

Acknowledgment:
This work was supported by the Scientific and Technological Research Council of Türkiye (TÜBİTAK) under Project No: 123R056.

Keyword: *Yttria-stabilized zirconia, Nanoclay, Low-temperature degradation (LTD)*

Surface Characteristics and Antibacterial Performance of Medium-Entropy Alloys Functionalized with Dual-Functional Chimeric Peptides

Turgut Güven Tarım [*1], Ayşe Öykü Ova[2], Sevgi Berfin Kıran[3], Ferda Soyer[2], Esra Şahin[2], Deniz Yücesoy[3], Benay Uzer[1]

[1] *Izmir Institute of Technology, Department of Mechanical Engineering*
[2] *Izmir Institute of Technology, Department of Molecular Biology and Genetics*
[3] *Izmir Institute of Technology, Department of Bioengineering*

Implant-associated infections remain one of the leading causes of implant failure due to bacterial adhesion and biofilm formation on implant surfaces. Opportunistic pathogens such as methicillin-resistant Staphylococcus aureus (MRSA), Staphylococcus epidermidis, and Pseudomonas aeruginosa readily colonize implant surfaces, leading to persistent infections and unsuccessful treatments. To address this challenge, this study aims to improve the antibacterial performance of Ti6Al4V and newly developed medium-entropy alloys (MEAs). Initially, bacterial attachment on Ti6Al4V and the developed MEAs was evaluated using implant-associated bacterial strains. Adherent bacterial colonies on each surface were quantified following incubation. The results demonstrated species-dependent differences in bacterial adhesion between Ti6Al4V and the developed MEAs, indicating that the antibacterial performance of the developed MEAs depended on both bacterial species and alloy composition, with no single MEA composition consistently exhibiting superior performance against all tested bacterial strains. To further prevent bacterial colonization on these surfaces, dual-functional chimeric peptides were designed by combining broad-spectrum antimicrobial peptide (AMP) sequences (LKLLKKLLKLLKKL and KWKRWWWWR) with titanium-binding peptides (TiBPs) (HAYKQPVLSTPF and RPREQRGERPRP) using a flexible GGG linker. The AMP domains were selected for their cationic and amphipathic structures that disrupt negatively charged bacterial membranes, whereas the TiBP domains provide specific affinity toward titanium surfaces and stable surface immobilization. Furthermore, the in vitro antimicrobial activity and the effect of chimeric peptides on bacterial adhesion were evaluated. Antimicrobial activity was first investigated in solution against MRSA and E. coli over 24 h to determine the minimum inhibitory concentration (MIC). Preliminary findings demonstrated antibacterial activity against E. coli at 256 µg/mL, while promising antimicrobial activity against MRSA was also observed, although the MIC value remains to be fully determined. Bacterial adhesion assays were performed on peptide-coated titanium surfaces using MRSA. Overall, Chimeric-2 demonstrated lower bacterial adhesion on Ti6Al4V and the developed MEAs, whereas Chimeric-1 exhibited lower bacterial adhesion on a subset of the developed MEAs, indicating that peptide performance depended on the alloy composition. Ongoing studies focus on MIC determination and quantification of bacterial adhesion against the remaining bacterial species, S. epidermidis and P. aeruginosa. SEM analyses revealed composition-dependent variations in phase morphology and phase contrast between Ti6Al4V and the developed MEAs. Contact angle measurements showed average contact angles of approximately 63° for the developed MEAs and 73° for Ti6Al4V. Although the developed MEAs exhibited lower contact angles, the differences in wettability were not statistically significant. Since surface wettability is known to influence the initial adsorption of proteins and subsequent bacterial attachment, the comparable wettability suggests that bacterial adhesion behavior cannot be explained solely by contact angle. Therefore, the observed differences in bacterial adhesion are more likely associated with composition-dependent microstructural features, including variations in phase morphology and phase contrast, rather than wettability alone.

Acknowledgment:
This study is supported by TÜBİTAK (Project No: 22AG053) and IYTE Scientific Research Projects (Project No: 2022İYTE-3-0014).

Keyword: *Medium-entropy alloys (MEAs), Bacterial adhesion, Chimeric peptides*

Thin Film Metallic Glass Coatings for Magnesium Implants

Kaan Yetiş [*] [1], Iulian Pana[2], Senem Büyüksungur[3], Anca Constantina Parau[2], Mihaela Dinu[2], Catalin Vitelaru[2], Alina Vladescu Dragomir[2], Nesrin Hasırcı[3,4,5,6], Batur Ercan[1,3,6]

[1] *Department of Metallurgical and Materials Engineering, Middle East Technical University (METU), 06800 Ankara, Türkiye*
[2] *National Institute of Research and Development for Optoelectronics—INOE 2000, 077125 Magurele, Romania*
[3] *BIOMATEN, METU CoE in Biomaterials and Tissue Engineering, 06800 Ankara, Türkiye*
[4] *Department of Bioengineering, Near East University, Lefkoşa TRNC, Mersin 10, Türkiye*
[5] *Department of Chemistry, METU, 06800 Ankara, Türkiye*
[6] *Biomedical Engineering Program, METU, 06800 Ankara, Türkiye*

Biodegradable metallic implants are designed to degrade after fulfilling their mechanical and biological functions, eliminating the need for secondary removal surgeries associated with permanent implants such as titanium alloys. Among biodegradable metallic implant materials, magnesium (Mg) alloys are considered the most promising candidates due to their favorable mechanical properties and biocompatibility. However, their rapid degradation may lead to premature loss of mechanical integrity before the healing process is complete. Another important limitation of Mg alloys is the rapid release of hydrogen gas during degradation, which can cause cavity formation. For these reasons, researchers are seeking strategies to improve the performance of Mg-based implants for orthopedic applications.

In this study, thin-film metallic glass (TFMG) coatings were deposited on Mg alloy (AZ31B) substrates by cathodic arc evaporation to reduce the degradation rate, enhance biocompatibility, and provide antibacterial activity. Both amorphous Zr- and Cu-based coatings and crystalline Ti- and Zr-based coatings were deposited on AZ31B substrates. Calcium (Ca), strontium (Sr), copper (Cu), and niobium (Nb) were incorporated as dopant elements to stimulate bone cell functions, enhance bioactivity, and impart antibacterial properties. Scanning Electron Microscopy (SEM) analysis showed that while the amorphous TFMG coatings exhibited island-like morphologies, the crystalline coatings created designs that mimicked the surface of the Mg substrate. The amorphous and crystalline structure of the coatings was confirmed by grazing-incidence X-ray diffraction (GIXRD). The presence and concentration of the dopant elements were confirmed by energy-dispersive X-ray spectroscopy (EDS) and X-ray photoelectron spectroscopy (XPS). The amorphous TFMG coatings showed an increase in average surface roughness from 4.49 ± 0.46 to 12.29 ± 5.30 nm at the nanoscale and from 0.23 ± 0.01 to 1.09 ± 0.25 μm at the microscale, whereas the crystalline coatings increased the corresponding values to 9.10 ± 4.48 nm and 0.95 ± 0.55 μm, respectively. Corrosion and degradation tests showed that the coatings reduced the degradation rate of AZ31B. Antibacterial and biological assays will be completed to assess the biological performance of these coatings for orthopedic applications.

Acknowledgment:
This project is funded by the TÜBİTAK, project no 124N777.

Keyword: *Thin Film Metallic Glasses, Temporary Implants, Biodegradable Materials*

Valorization of Discarded Cigarette Butts into High-Performance Carbon Electrodes for Supercapacitors

Oluwatosin Johnson Ajala [* 1], Ipek Deniz Yıldırım[1], Ahmet Güngör[1,2], Feray Bakan Misirlioglu[3], Emre Erdem[1,3]

[1] Faculty of Engineering and Natural Sciences, Sabanci University, Tuzla, Istanbul, 34956, Turkey
[2] Department of Chemical Engineering, Faculty of Engineering, Kocaeli University, Izmit, 41001, Kocaeli, Turkey
[3] Nanotechnology Research and Application Center (SUNUM), Sabanci University, Tuzla, Istanbul, 34956, Turkey

Discarded cigarette butt (CB) waste was transformed into porous activated carbon (AC) through controlled pyrolysis and KOH activation for supercapacitor applications. The influence of pyrolysis temperature on the electrochemical and structural characteristics of the produced carbons was extensively investigated. The carbon structure's pore development, defect density, and graphitic ordering are all significantly influenced by temperature, according to morphological and structural investigations. Owing to enhanced electrolyte accessibility and a BET surface area of 426.29 $m^2 g^{-1}$, AC-500 demonstrated the most optimal ordered porous structure among the samples. Due to better ion transport and charge-transfer behavior, AC-500 produced the highest specific capacitance of 840 F g^{-1}, energy density of 116 Wh kg^{-1}, and power density of 44.54 kW kg^{-1}, according to electrochemical measurement. On the contrary, excessive pyrolysis temperature at 600 °C caused structural degradation and pore coalescence, which decreased electrochemical performance. The findings show that CB waste is efficiently converted into high-performance porous carbon electrodes for sustainable supercapacitor energy storage applications via optimal pyrolysis and activation.

ORCID:
Oluwatosin Johnson Ajala: https://orcid.org/0009-0001-4478-3567

References:
Guo, Y., Sun, K., Kong, L., Li, C., Fan, M., Zhang, L., ... & Hu, X. (2025). Pyro-reforming of cigarette butts for co-productions of hydrogen and organics over nickel catalyst supporting on biochar from cigarette. International Journal of Hydrogen Energy, 109, 150-163.
Herrera-Puerta, C. F., Suspes-García, S., Galindres-Jiménez, D. M., Cifuentes-Galindres, D., Tinoco, L. E., Moreno-Piraján, J. C., & Murillo-Acevedo, Y. S. (2023). Thermogravimetric Kinetic Analysis of the Pyrolysis of Cigarette Butts and Its Application in Chromium Adsorption Processes.
Wu, F. C., Tseng, R. L., Hu, C. C., & Wang, C. C. (2005). Effects of pore structure and electrolyte on the capacitive characteristics of steam- and KOH-activated carbons for supercapacitors. Journal of Power Sources, 144(1), 302-309.

Keyword: *Cigarette butt, Activated carbon, Supercapacitor*

Investigation of the Durability and Insulation Properties of Polyurethane-Silica Nanocomposite Coatings Produced by One-Step Spray Method

Semih Pehlivan * **, Fatih Büyükserin**

TOBB University of Technology and Economics

Electrical transmission lines face multi-faceted technical challenges, including power theft, arc formation, fire risks, and insulation deficiencies. Particularly in medium-voltage lines, illegal electricity usage causes an annual energy loss of over 20,000 GWh in Turkey, posing severe economic and infrastructural burdens. Conventional insulation systems relying on silicone, rubber, or ceramics are heavy, costly, and prone to mechanical deformation, failing to fully eliminate fire hazards due to insufficient electrical insulation. While silicone rubber and silica-based coatings offer environmental durability and hydrophobicity, their dielectric performance remains limited under high-voltage conditions; silicone degrades under UV exposure, and heavy rubber coatings introduce mechanical strain that leads to line sagging.

Polyurethane (PU)-based nanocomposite coatings have emerged as a promising alternative owing to their tunable mechanical durability, chemical resistance, and long-term environmental stability. However, their potential in high-voltage applications remains under-explored. Existing literature predominantly focuses on the superhydrophobic surface properties of PU coatings, typically synthesized through high-temperature, multi-step processes that neglect detailed electrical insulation performance [1,2,3]. Furthermore, rare single-step spray formulations rely on expensive solvents like absolute ethanol and are limited to mechanical assessments [1]. While common polymers like PDMS and silicone rubber-silica nanocomposites exhibit low dielectric constants (around 2.8 and 4.2, respectively) [3,4], hexamethylene diisocyanate (HDI)-crosslinked polyurethane structures can achieve dielectric constants up to 13.64, demonstrating superior potential for high-voltage insulation [5]. Nevertheless, systematic research is still required regarding their long-term water resistance, surface energy stability, and interfacial interactions.

In this study, sprayability optimization was initially conducted by dispersing a commercial polyurethane dispersion, Alberdingk Boley U9150, in various solvents. Trials with THF, IPA, and DMSO resulted in precipitation, whereas acetone yielded a stable, sprayable polyurethane formulation. Subsequently, the solution was coated onto a 1.5-meter electrical wire positioned between two medium-voltage lines to investigate the breakdown voltage causing short circuits. The experimental results revealed that the pure PU coating failed at 8 kV, the PU-commercial silica nanocomposite with 2 wt% loading at 14.2 kV, and the PU-hollow silica nanocomposite with 2 wt% loading at 15.4 kV. Ongoing efforts focus on dielectric constant characterization using Electrochemical Impedance Spectroscopy (EIS) alongside ongoing mechanical durability assessments.

This study aims to develop a comprehensive solution to these challenges by investigating the thermal, electrical, and mechanical properties of polyurethane-silica nanocomposite coatings fabricated via a cost-effective, one-step spray method. The developed coatings are designed to prevent expansion-induced line sagging and spark formation. By systematically analyzing the durability, surface stability, and dielectric performance of these nanocomposites, this research addresses a critical gap in the literature and proposes a scalable, high-performance coating alternative for the optimization and safety of modern power distribution grids.

Acknowledgment:
The author wishes to thank the Scientific and Technological Research Council of Turkey (TÜBİTAK) for the financial support provided under the 2210-C National MSc Scholarship Program for Priority Areas.

ORCID:
Semih Pehlivan: https://orcid.org/https://orcid.org/0009-0000-0395-6145

References:
Miao J, Shen Y, Tao J, et al (2023) Design and spraying-preparation of the gradient coatings with various diameters and contents of SiO2 nano-particles for the enhanced anti-impact and thermal insulation performance. Progress in Organic Coatings 179:107491. doi: 10.1016/j.porgcoat.2023.107491
Przybyszewski B, Boczkowska A, Kozera R, et al (2019) Hydrophobic and icephobic behaviour of polyurethane-based nanocomposite coatings. Coatings 9:811. doi: 10.3390/coatings9120811
Zolriasatein A, Rajabi Mashhadi Z, Navazani S, et al (2021) Investigation of electrical properties of silica-reinforced RTV nanocomposite coatings. Journal of Materials Science: Materials in Electronics 32:12265–12274. doi: 10.1007/s10854-021-05855-0
In: PDMS. https://www.mit.edu/~6.777/matprops/pdms.htm. Accessed 25 May 2026
Yan Z, Yang H, Zheng S, Tan Z (2025) Preparation and characterization of high-dielectric-performance polyurethane based on various diisocyanates. Journal of Applied Polymer Science. doi: 10.1002/app.57027

Keyword: *Polyurethane-silica nanocomposites, One-step spray method, High-voltage insulation*

Development of Carbon-Based Supercapacitor Electrode Materials from Waste Wet Wipes via Hydrothermal Carbonization

Ezgi Nur Belek [*1], Burak Dalkılıç[1], Anas Abofoul[2], Selva Bilge[1]

[1] *Ankara University, Faculty of Science, Department of Chemistry, Türkiye*
[2] *Ankara University, Graduate School of Natural and Applied Sciences, Department of Chemistry, Türkiye*

Single-use wet wipes have become a significant component of domestic waste owing to their cellulosic and/or synthetic fiber content, together with surfactants, preservatives, and other additives that hinder their degradation. Converting this waste into value-added carbon materials offers a sustainable route that addresses both waste management and the growing demand for energy-storage materials. In this study, waste wet wipes were converted into carbon-based electrode materials by hydrothermal carbonization (HTC), and the resulting hydrochars were evaluated for supercapacitor applications.

HTC was performed at 220, 250, and 280 °C for reaction periods of 1, 3, and 6 h to examine how temperature and duration influence the physicochemical and electrochemical properties of the carbons. The hydrochars were characterized by scanning electron microscopy (SEM), X-ray diffraction (XRD), Raman spectroscopy, Fourier-transform infrared spectroscopy (FTIR), and X-ray photoelectron spectroscopy (XPS). Hydrothermal treatment yielded carbon materials with a heterogeneous surface morphology and oxygen-containing functional groups, while variations in temperature and reaction time altered their structural organization, surface chemistry, and degree of carbonization.

Selected hydrochars were then used to modify electrode surfaces, and their electrochemical behavior was assessed by cyclic voltammetry (CV), galvanostatic charge–discharge (GCD), and electrochemical impedance spectroscopy (EIS). The modified electrodes showed promising capacitive behavior and favorable charge-transfer characteristics. These findings indicate that waste wet wipes can serve as a low-cost, sustainable precursor for carbon-based supercapacitor electrode materials.

Acknowledgment:
This work was financially supported by the Scientific and Technological Research Council of Türkiye (TÜBİTAK) through the 2209-A Undergraduate Research Projects Grant Program (Project No. 1919B012538626).

Keyword: *Waste wet wipes, hydrothermal carbonization, supercapacitor*

A Shallow Plasma Nanotexturing Regime For Passivation-Compatible Silicon Surfaces

Ozan Aydın * [1], **Milad Ghasemi**[2], **Hisham Nasser**[2], **Raşit Turan**[1]

[1] *ODTÜ-GÜNAM, Middle East Technical University (METU)*
[2] *ODTÜ-GÜNAM*

Conventional silicon surface texturing in photovoltaic manufacturing relies heavily on wet chemical processes, which require substantial amounts of chemicals and ultrapure water and generate chemical waste streams. As increasing pressure is placed on reducing resource consumption in semiconductor and photovoltaic manufacturing, alternative surface engineering approaches are becoming increasingly important. Plasma-based nanotexturing has emerged as a promising dry-processing route; however, most reported processes produce highly porous, high-aspect-ratio structures that often suffer from limited passivation compatibility despite their excellent optical performance.

In this study, a controllable shallow nanotexturing regime is demonstrated on crystalline silicon using SF_6/O_2 inductively coupled plasma reactive ion etching (ICP-RIE). By systematically varying chamber pressure and ICP power, distinct transitions between smooth, controlled nanotextured, and non-uniform etching regimes were identified. Within a narrow process window, shallow (~100–250 nm), rounded and shallow nanostructures were reproducibly formed under simplified process conditions, including room-temperature (~18 °C) processing, zero bias power, and short etching durations (~60 seconds). The nanotextured surfaces exhibited weighted average reflectance values as low as ~5%, outperforming conventional saw-damage-etched and alkaline pyramid-textured silicon surfaces. Morphological analysis by FE-SEM revealed shallow surface nanofeatures with substantially lower structural complexity than conventional black silicon morphologies.

To evaluate passivation compatibility, 5 and 10 nm Al_2O_3 layers were deposited by atomic layer deposition (ALD), followed by minority carrier lifetime and implied open-circuit voltage (iVoc) measurements. The nanotextured surfaces exhibited iVoc values between 660 and 710 mV, indicating promising passivation.

The results demonstrate a controllable dry plasma nanotexturing approach that provides a balance between optical performance and passivation compatibility while offering a potential pathway toward reducing the chemical and water consumption associated with conventional wet texturing processes. Future work will focus on full device integration and quantitative life-cycle assessment of the proposed approach.

Acknowledgment:
This work was supported by the Scientific and Technological Research Council of Türkiye (TÜBİTAK) under the TANDEM project (Grant No. 224N162). The authors acknowledge the facilities and technical support provided by the Center for Solar Energy Research and Applications (ODTÜ-GÜNAM).

ORCID:
Ozan Aydın: https://orcid.org/0000-0002-7116-9669

References:
Jiang, H., Zhang, X., et al., “Black silicon nanostructures for solar energy conversion and photonic applications: a review,” Advanced Photonics, 7 (2025) 034004.
Huo, C., Zhang, J., Wang, Y., et al., “Surface texturing of silicon wafers for solar cells: a review,” Applied Surface Science, 360 (2016), 803–815

Keyword: *silicon, nanotexturing, ICP-RIE*

Recycling of $Ca_2NaNb_4O_{13}^-$ Perovskite Nanosheets: Structural Reintegration and Life Cycle Assessment

Atahan Orhon [*1], **Mine Güngörmüşler**[2], **Özge Sağlam**[1,3]

[1] *Mechanical Engineering Graduate Program, Graduate School, İzmir University of Economics, İzmir, Türkiye*
[2] *Department of Genetics and Bioengineering, Faculty of Engineering, İzmir University of Economics, İzmir, Türkiye.*
[3] *Department of Mechanical Engineering, Faculty of Engineering, İzmir University of Economics, İzmir, Türkiye*

Two-dimensional $Ca_2NaNb_4O_{13}^-$ perovskite nanosheets are promising functional materials for solar cells, dielectrics, sensors, and photocatalysis, yet their conventional synthesis relies on energy-intensive solid-state processing and the use of niobium, a critical raw material with a constrained supply chain. This study investigates whether the residual powders remaining after liquid exfoliation can be recovered and reintegrated into the production cycle, and quantifies the environmental benefit of doing so. Spent exfoliation powders were re-protonated with 5M HNO_3 and re-exfoliated with tetrabutylammonium hydroxide, and nanosheets produced via the conventional and recycled-precursor routes were compared using X-ray diffraction (XRD), scanning electron microscopy (SEM), atomic force microscopy (AFM), and UV–Vis spectroscopy. XRD and SEM confirmed that the orthorhombic crystal structure and layered morphology were preserved after re-protonation, respectively. UV–Vis spectra retained the characteristic absorption maximum at ~272 nm across all cycles, indicating preserved structural and electronic integrity; however, area-under-the-curve analysis revealed reductions in suspended nanosheet concentration of 53% and 61% for the first and second recycling cycles, respectively, attributable to material loss and partial layer restacking. AFM statistical analysis (n = 96 per group) showed a small decrease in average lateral size, from 938.07 ± 180.73 nm for conventional nanosheets to 879.57 ± 222.63 nm for recycled nanosheets (Welch's t-test, $p = 0.0483$), along with a more heterogeneous size distribution. A comparative cradle-to-gate life cycle assessment (LCA), conducted in accordance with ISO 14040/44 using primary laboratory inventory data and the ReCiPe 2016 Midpoint (H) method, showed that the recycled route outperformed the conventional route across all 18 impact categories, with a mean reduction of 32.3%. By eliminating the high-temperature solid-state sintering step (1200 °C) and its associated upstream precursor burdens, the climate change impact was reduced by 35.0% (from 47.38 to 30.78 kg CO_2-eq per batch), while marine eutrophication potential decreased by 93.4%. To the best of our knowledge, this is the first LCA to characterize the environmental profile of perovskite nanosheets and to substantiate the benefits of precursor recycling, demonstrating a sustainable production pathway aligned with the objectives of the EU Green Deal. This work was supported by The Scientific and Technological Research Council of Turkey [Grant number 125M751].

ORCID:
Atahan Orhon: 0009-0009-6469-0702
Mine Güngörmüşler: 0000-0002-0207-405X
Özge Sağlam: 0000-0002-5583-3662

Keyword: *2D perovskite nanosheets, Chemical exfoliation, Life cycle assessment*

Ultra-Thin Mo_2C/W_2C Heterostructures for Tunable Electromagnetic Interference Shielding

Sina Rouhi [*1], **Mehya Mansoor**[2], **Mubashir Mansoor**[2], **Maryam Mansoor**[3]

[1] *Department of Nanotechnology Engineering, Faculty of Engineering, OSTİM Technical University, 06374 Ankara, Turkey*
[2] *Istanbul Technical University, Metallurgical and materials engineering department Istanbul 34469, Türkiye*
[3] *Istanbul Technical University, Energy Institute, Ayazaga Campus, Maslak, Sarıyer, Istanbul 34469, Türkiye*

Title:

Ultra-Thin Mo_2C/W_2C Heterostructures for Tunable Electromagnetic Interference Shielding

Abstract

The increasing demand for compact and high-frequency electronic systems requires lightweight and efficient electromagnetic interference (EMI) shielding materials. Transition metal carbides such as Mo_2C and W_2C offer promising properties including high conductivity and strong electromagnetic wave interaction. In this study, ultra-thin carbide-based layered structures are investigated for their EMI shielding performance [1,2].

A key challenge in current research is the limited understanding of how nanoscale thickness, hybrid configurations, and double-sided coatings influence shielding efficiency. In particular, the optimization of absorption behavior across frequencies remains unclear, restricting the design of high-performance thin-film materials [3,4,5].

Mo_2C and W_2C thin films with thicknesses between 10–30 nm were systematically analyzed, including single-layer, hybrid, and double-sided configurations. Results show that double-sided coatings significantly enhance shielding performance, with a maximum absorption of 17.9% observed for a 10 nm W / 10 nm W structure. Hybrid configurations provide a balance between absorption and functional properties, while excessive thickness does not necessarily improve performance. These findings highlight the importance of nanoscale design and interface engineering for next-generation EMI shielding applications.

ORCID:
Sina Rouhi: 0000-0003-4430-7568

References:
Smith, J. et al., Journal of Materials Science, 2018
Lee, K. et al., Applied Physics Letters, 2019
Wang, Y. et al., Carbon, 2020
Zhang, H. et al., Advanced Functional Materials, 2021
Kumar, R. et al., Surface and Coatings Technology, 2022

Keyword: *electromagnetic interference-Mo_2C/W_2C Heterostructures, Thin films*

Fluorine-Free Synthesis of Two-Dimensional Mo2AlB2 MBene for OLED Applications

Hilal Doğan [* 1], Aseel Zaid[1], Selin Piravadili[2], Müslüm Demir[1]

[1] Department of Chemical Engineering, Bogazici University, Istanbul, 34342, Türkiye
[2] Materials Institute, The Scientific and Technological Research Council of Turkey (TUBITAK) – Marmara Research Center (MAM), Gebze, Türkiye

Two-dimensional transition-metal borides, known as MBenes, have recently attracted considerable attention as MAB-derived layered materials due to their metallic conductivity, structural stability, tunable surface chemistry, and potential for electrochemical and optoelectronic applications. Compared with the extensively studied MXenes, experimental reports on MBenes remain limited, and fluorine-free synthesis routes are particularly important for developing safer and more sustainable processing strategies. In this context, the present study focuses on the synthesis of an Al-deficient Mo_2AlB_2 MBene-like structure from a MoAlB precursor by using an alkaline hydrothermal deintercalation approach.

The synthesis strategy was optimized to selectively remove Al-containing layers from the parent MoAlB phase while preserving the Mo-B framework. For this purpose, MoAlB powder was treated in a 10 wt% aqueous NaOH solution under hydrothermal conditions at 150 °C for 24 h. NaOH-based etching was selected because alkaline treatment can induce stepwise Al deintercalation from MoAlB and generate layered Mo-Al-B or MBene-like structures without the use of hazardous HF-based etchants. After the reaction, the product was repeatedly washed and centrifuged until a near-neutral pH was reached, then dried under controlled conditions.

The obtained results confirmed that the alkaline treatment successfully altered the parent MoAlB structure. X-ray diffraction (XRD) analysis revealed that the characteristic reflections of the precursor changed significantly after etching. Specifically, the characteristic (0 2 0) peak of pristine MoAlB, originally located at $2\theta \approx 12.8°$, shifted to a higher angle ($2\theta \approx 14.5°–15.0°$) following the 10 wt% NaOH treatment. This rightward shift indicates a decrease in interlayer spacing, consistent with the successful deintercalation of Al atoms and structural rearrangement. Furthermore, the experimental diffraction pattern of the etched sample closely matches the reference patterns for Mo_2AlB_2 and MoB, confirming the formation of an Al-deficient Mo_2AlB_2 MBene-like structure. Morphological observations revealed a more open and layered structure compared with the compact precursor morphology. Additionally, XPS demonstrated a clear decrease in the Al atomic ratio.

Overall, this work demonstrates a fluorine-free, more environmentally compatible route for producing MoAlB-derived Mo_2AlB_2 MBene-like materials. Ongoing studies focus on integrating these structures into organic light-emitting diode (OLED) devices as anodes or interfacial materials and evaluating their impact on device performance.

Acknowledgment:
This work was supported by the Boğaziçi University Scientific Research Projects Coordination Unit (BAP) under Project No. -50140, titled 'Synthesis of 2D Metal Borides (MBenes) for OLED Applications'

ORCID:
Hilal Doğan: 0000-0002-7522-6288
Selin Piravadili: 0000-0001-5030-6698
Müslüm Demir: 0000-0001-6842-8124

References:
1. Zhang, B., Zhou, J., & Sun, Z. (2022). MBenes: progress, challenges and future. Journal of Materials Chemistry A, 10(30), 15865-15880.
2. Xu, T., Wang, Y., Xiong, Z., Wang, Y., Zhou, Y., & Li, X. (2023). A rising 2D star: novel MBenes with excellent performance in energy conversion and storage. Nano-Micro Letters, 15(1), 6.
3. Chandel, M., Purbayanto, M. A. K., Kowal, D., Moszczyńska, D., Wójcik, A., Birowosuto, M. D., ... & Jastrzębska, A. M. (2025). Multilayered MoAlB@ MBene structures using mild microwave-assisted etching and their optical properties. Materials Horizons, 12(10), 3473-3484.
4. Alameda, L. T., Moradifar, P., Metzger, Z. P., Alem, N., & Schaak, R. E. (2018). Topochemical deintercalation of Al from MoAlB: stepwise etching pathway, layered intergrowth structures, and two-dimensional MBene. Journal of the American Chemical Society, 140(28), 8833-8840.
6. Wei, S., Kale, G., & Lai, X. (2024). Unlocking Enhanced Electrochemical Performance of MBene-MoB Through Controlled Aluminum Dissipation from MoAlB. Small, 20(38), 2401573.
Xiong, W., Feng, X., Xiao, Y., Huang, T., Li, X., Huang, Z., ... & Liu, J. (2022). Fluorine-free prepared two-dimensional molybdenum boride (MBene) as a promising anode for lithium-ion batteries with superior electrochemical performance. Chemical Engineering Journal, 446, 137466.

Keyword: *Mo_2AlB_2, Mbene, 2D Materials*

Investigation of the Removal of Sr(II) and Pb(II) Ions from Aqueous Media Using Green-Synthesized Quantum Dots and Polyoxometalate-Based Biohydrogels

Zehra Sisman [*1], **Sabriye Yusan**[2], **Taha Furkan Gül**[3], **Eduardo Alberto Lopez Maldonado**[4]

[1] *Department of Nuclear Sciences, Graduate School of Natural and Applied Sciences, Ege University, Bornova-Izmir, Türkiye*
[2] *Institute of Nuclear Sciences, Ege University, 35100, Bornova-Izmir, Türkiye*
[3] *Faculty of Engineering, Chemical Engineering Department, Ege University, Bornova-Izmir, Türkiye*
[4] *Faculty of Chemical Sciences and Engineering, Autonomous University of Baja California, 22424, Tijuana, Mexico*

The increasing global energy demand is one of the major challenges worldwide. The environmental impacts associated with fossil fuel-based energy sources have made nuclear energy an alternative and sustainable energy option [1]. Although nuclear energy provides high energy density, low carbon emissions, and continuous energy production, radioactive pollutants released as a result of nuclear activities pose significant risks to water resources. Among these pollutants, strontium and lead can cause severe toxic effects on human health [2]. Adsorption is widely preferred for the removal of Sr^{+2} and Pb^{+2} from aqueous media due to its economic, rapid, and practical nature. Polyoxometalates (POMs), which are metal-oxo clusters, have attracted considerable attention in adsorption applications because of their high surface activity, strong electrostatic interactions with cations, and abundance of active binding sites [3]. In addition, CQDs, a class of carbon-based nanomaterials, possess unique physicochemical properties, including rich surface functionalities and high surface area. Their excellent ion-binding performance further supports the introduction of functional groups into the adsorbent structure, enhancing adsorption efficiency [4].

In this study, POM (Mo_{74}) and CQDs were first synthesized using the hydrothermal method, and biohydrogels were subsequently prepared by encapsulating these materials within alginate biopolymer (Figure 1). The adsorbents were characterized using SEM, XRD, XPS, and FT-IR techniques. The adsorption performance of the synthesized adsorbents (POM-Alg and CQD-Alg) toward Sr^{+2} and Pb^{+2} ions was then evaluated by examining the effects of operational parameters, including solution pH, temperature, initial ion concentration, and contact time. The equilibrium adsorption data were fitted using the Langmuir, Freundlich and Dubinin-Radushkevich isotherm models to elucidate the adsorption mechanism. Thermodynamic parameters were also determined to assess the feasibility, spontaneity, and nature of the adsorption process. The higher adsorption performance obtained by POM-Alg and the maximum adsorption capacities (q_{max}) for Pb^{+2} and Sr^{+2} ions were determined to be 103.092 mg/g and 33.89 mg/g, respectively. This study presents novel adsorbent based on POM- and CQD-functionalized alginate biohydrogels, combining green nanomaterial synthesis with biopolymer immobilization for the efficient removal of radionuclide-related Sr(II) and Pb(II) ions from water.

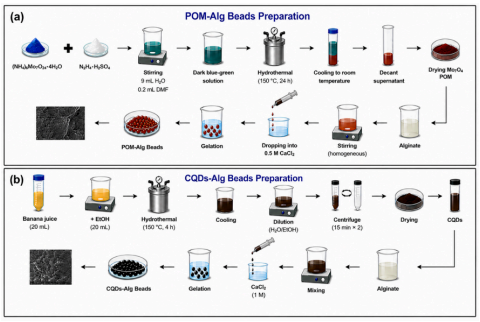


Figure 1. Preparation procedure of **(a)** POM-Alg, **(b)** CQD-Alg.

Acknowledgment:
This study is supported by Ege University Scientific Research Projects Coordination Unit. (Project No: 33431). The authors would like to thank Prof. Dr. Şule AYTAŞ for her valuable contributions and guidance.

ORCID:
Zehra Sisman: 0009-0001-6811-6945
Sabriye Yusan: 0000-0001-8058-2335
Taha Furkan Gül: 0009-0007-6607-8870

References:
Pravalie, R., Bandoc, G. (2018). Nuclear energy: Between global electricity demand, worldwide decarbonisation imperativeness, and planetary environmental implications. Journal of Environmental Management, 209, 81-92.
Aliyu, A., Evangeliou, N., Mousseau, T., Wu, J., Ramli, A. (2015). An overview of current knowledge concerning the health and environmental consequences of the Fukushima Daiichi Nuclear Power Plant (FDNPP) accident. Environment International, 85, 213-228.
Dong, A., Dong, Z., Zhang, Z., Liu, Y., Cheng, W., Miao, H., He, X., Xu, Y. (2017). POM Constructed from Super-Sodalite Cage with Extra-

Large 24 Membered Channels: Effective Sorbent for Uranium Adsorption. Applied Materials Interfaces.
Singh, P., Singh, L. (2025). Carbon quantum dots as a promising tool for heavy metal sensing and removal in wastewater. Desalination and Water Treatment, 324, 101435.

Keyword: *Adsorption, polyoxometalate (POM), carbon quantum dots (CQD)*

Optimization of Electrospun PAN/Amino-MWCNT Nanocomposite Fibers for SPME: Tuning Carbon Nanotube Content for Enhanced Fire Debris Analysis

Rukiye Aslan [*1], Mihriban Dilan Kılıç[2], Merve Kuloğlu Genç[2], Tuğçe Töngüç Yalçinkaya[3], Selda Mercan[2], Ahmet Çay[3], Serap Annette Akgür[1], Fatma Nil Ertaş[4]

[1] Ege University, Institute on Drug Abuse, Toxicology and Pharmaceutical Science, İzmir, Türkiye
[2] Istanbul-University-Cerrahpaşa, Institute of Forensic Sciences and Legal Medicine, Department of Science, Büyükçekmece, Istanbul, Türkiye
[3] Ege University, Faculty of Engineering Department of Textile Engineering, İzmir, Türkiye
[4] Ege University, Faculty of Science Department of Chemistry, İzmir, Türkiye

Advanced nanomaterials with high surface-area-to-volume ratios offer new horizons for analytical sample preparation. Although SPME–GC/MS is the gold standard for identifying ignitable liquid residues in forensic arson investigations, routine use depends on expensive commercial fibers. This study focuses on the fabrication, optimization, and forensic application of eco-friendly, electrospun polyacrylonitrile (PAN)/amino-functionalized multi-walled carbon nanotube(MWCNT) nanocomposite fibers for gasoline analysis.

To incorporate sustainable practices, waste-derived PAN was electrospun with varying nanotube concentrations (0.5%, 1.0%, and 1.5% w/w) onto stainless-steel supports to form porous networks, benchmarked in the light of preliminary study (1). The fibers' performance was evaluated using carpet samples burnt with 500 µL of gasoline. Results were compared against a commercial 100 µm PDMS fiber using a validated SPME–GC/MS protocol under identical conditions (70°C, 6 min extraction; 20 s desorption) (2). Extraction efficiency was assessed per ASTM E1618-19 by monitoring four mandatory gasoline markers and fourteen supplementary aromatic indicators.

All formulations successfully detected all target indicators, revealing a clear material optimization trend. The 0.5% fiber exhibited the highest sensitivity among the fabricated nanofibers, yielding chromatographic responses in the 10^7 range, matching the intensity of the commercial PDMS fiber ($10^{7\text{-}8}$ range). For the four mandatory markers (m-ethyltoluene,1,3,5-trimethylbenzene, o-ethyltoluene, and 1,2,4-trimethylbenzene), the commercial PDMS fiber yielded RSD% values of 16%–22%, while the 0.5% amino-MWCNT/PAN fibers demonstrated a highly competitive, stable repeatability range between 36% and 38%. Increasing the nanotube loading systematically suppressed efficiency; the 1.0% loading dropped to the 10^6 range with elevated RSD% values (50%–61%), while the 1.5% loading fell to the 10^5 range despite a uniform RSD% of 27%. 0.5% fibers maintained structural integrity over 70 analytical cycles.

The optimization trend highlights a critical balance between nanomaterial loading and extraction performance. The competitive sensitivity and robust reproducibility of the 0.5% amino-MWCNT/PAN fiber stem from homogeneous nanotube dispersion within the waste-derived PAN matrix, maximizing active surface area and porosity to match the commercial standard. Conversely, higher loadings trigger a systematic decline due to nanotube agglomeration, which blocks nanofiber pores and restricts analyte adsorption. In conclusion, precisely tuning the amino-MWCNT content to 0.5% on a recycled polymer backbone delivers a highly viable, robust, and cost-effective alternative performing comparably to commercial PDMS fibers, offering immense potential for sustainable forensic trace fire debris analysis.

References:

ASLAN R., KILIÇ MD, KULOĞLU GENÇ M., TÖNGÜÇ YALÇINKAYA T. , MERCAN S., ÇAY A., ERTAŞ FN., AKGÜR SA., Multi-Purpose Electrospun PAN/MWCNT Nanocomposite Fibers for SPME: From Drug Testing to Fire Debris Analysis, ExTech 2026.
Kilic, M. D., Yayla, M., & Mercan, S. (2024). Detection of gasoline residues on household materials up to 60 days: Comparison of two extinguishing methods. Forensic Science International, 364, 112222.

Keyword: *Fire debris analysis, nanomaterials, SPME-GC/MS*

A Naturally Fluorescent Micellar Platform for Imaging-Guided Delivery

Esmanur Akdoğan, Zeliha Soran Erdem *

Abdullah Gül Üniversitesi

The polymeric micelles have received a significant amount of attention lately as a versatile nanocarrier for biomedical applications, as they can be used for controlled delivery and for optical tracking [1,2]. This study aimed at preparing a simple and naturally fluorescent carrier system with pumpkin seed extract by using Pluronic F108 micelles. This system is based on natural fluorescence from the extract without the need for additional synthetic dyes, and could be useful in imaging-guided delivery application.

Before evaluating the delivery performance, the extract was analyzed by GC–MS to identify its chemical composition, while absorbance and photoluminescence (PL) measurements were carried out to examine its optical properties. The prepared micelles were then characterized by dynamic light scattering (DLS), confirming their nanoscale size and colloidal stability. Finally, release studies were performed to assess the drug delivery potential of the micellar system.

The results showed that the natural fluorescent properties of the extract were preserved after encapsulation, while the release profile demonstrated the controlled delivery capability of the system. Overall, this study presents a practical micelle-based platform primarily designed for controlled drug delivery, with natural fluorescence offering an additional advantage for future theranostic applications.

Acknowledgment:
This study was supported by TÜBİTAK 2209-A University Students Research Project Program and TÜBİTAK 1001 Project No: 123M876.

ORCID:
Zeliha Soran Erdem: Zeliha Soran Erdem: https://orcid.org/0000-0001-7607-9286

References:
1. Kotta, S.; Aldawsari, H. M.; Badr-Eldin, S. M.; Nair, A. B.; Kamal, K. Y. T. Progress in Polymeric Micelles for Drug Delivery Applications. Pharmaceutics 2022, 14(8), 1636. DOI: 10.3390/pharmaceutics14081636.
2. Li, S.; Liang, N.; Liu, J.; Shi, Y.; et al. Fabrication of AIE-Featured Probe-Incorporated Multifunctional Polymeric Micelles for Cellular Imaging and Intelligent Delivery of Paclitaxel. ACS Applied Polymer Materials 2024, 6 (1), 484–495. DOI: 10.1021/acsapm.3c02171.

Keyword: *Fluorescent micelles, polymeric nanocarriers, plant extract*

Effect of Plasmonic Shell in Photothermal Heating in Core-Shell Nanoparticles

Seda Aygül Akyüz * **, Zeliha Cansu Canbek Ozdil**

Department of Materials Science and Nanotechnology Engineering, Yeditepe University, İstanbul, Türkiye

Core-shell nanoparticles are effective agents for multimodal therapies, where the core can serve functions such as drug delivery or magnetic tracing, while the plasmonic shell is widely assumed to enhance the optical absorption and improve photothermal therapy (PTT) performance. Whether this assumption holds across a broad range of material combinations, remains largely unexplored. Building on our recent Gaussian process regression study of Fe_3O_4@Au core-shell nanoparticles, which established geometric design rules for a single system and highlighted the need for broader material explorations, in this work, we develop a high-throughput Mie-theory engine to screen core-shell nanoparticles spanning seven core families (metals, semiconductors, carbides, oxides, sulfides, polymers, and glasses) combined with 22 metallic shells [1]. The engine is based on the open-source PyMieLab platform but extends it by incorporating a wavelength-dependent medium rather than assuming a constant refractive index [2]. This enhancement captures a secondary resonance, pronounced for large cores, and produces spectra that are in closer agreement with finite-element (COMSOL) simulations. The resulting database of ~3.8-million spectra, spanning 300-900 nm, enables a physically constrained screening strategy based on a purity metric ($C_{abs}/C_{ext} \leq 1$) and a balanced performance score ($C_{abs} \times$ purity) that removes the inflation artifacts of conventional absorption-fraction ranking.

Across the explored materials space, the shell emerges not as a universal enhancer but as a material dependent regulator for optical absorption. Namely, for transparent dielectric cores, the shell function as a plasmonic antenna that enhances absorption, whereas for intrinsically absorbing cores, it increasingly screens the incident electromagnetic field causing shell material to suppress rather than amplify absorption. Consequently, dielectric cores (glasses, oxides) retain nearly all candidate geometries, whereas absorbing cores (carbides, metals) lose more than half to this screening effect, indicating a bare strong absorber can often outperform its coated counterpart. The optimal choice further depends on the target figure of merit, bulk absorbers such as Zr shells maximize absolute absorption power but are less favorable for localized PTT heating, whereas plasmonic shells (Au, Ag, Pd) achieve the highest absorption efficiencies and volumetric heating densities, particularly when paired with oxide, glass, and polymer cores. Beyond ranking candidates, the framework provides transferable, physically grounded design rules and places previously reported dispersion shifted Fe_3O_4@Au optimum within a unified materials landscape.

Acknowledgment:
Financial support for this study was provided by the Scientific and Technological Research Council of Turkey (TÜBİTAK) under contract numbers 23AG002 and 224M049.

ORCID:
Seda Aygül Akyüz: https://orcid.org/0009-0003-6464-3347
Zeliha Cansu Canbek Ozdil: https://orcid.org/0000-0001-9420-567X

References:
[1] S. A. Akyuz and Z. C. Canbek Ozdil, “Predictive Modeling of Core–Shell Magnetoplasmonic Nanoparticles: GPR-Based Optimization for Enhanced Photothermal Heating,” ACS Omega, Dec. 2025, doi: 10.1021/acsomega.5c09634.
[2] D. Ma, P. Tuersun, L. Cheng, Y. Zheng, and R. Abulaiti, “PyMieLab_V1.0: A software for calculating the light scattering and absorption of spherical particles,” Heliyon, vol. 8, no. 11, p. e11469, Nov. 2022, doi: 10.1016/j.heliyon.2022.e11469.

Keyword: *photothermal therapy, core-shell nanoparticles, Mie theory, plasmonic antenna effect, optical shielding*

Ge-Based Thin-Film Photodiodes for Near-Infrared Detection: Structural and Optoelectronic Investigation

Koray Soydaner [*1], **Abdulsalam Aji Suleiman**[1], **Timuçin Emre Tabaru**[2]

[1] *Sivas University of Science and Technology, Faculty of Engineering and Natural Sciences, Sivas, Türkiye*
[2] *Sivas University of Science and Technology, Faculty of Engineering and Natural Sciences, Department of Electrical and Electronics Engineering, Sivas, Türkiye*

Germanium is an attractive semiconductor for near-infrared (NIR) photodetection due to its strong optical absorption in the NIR spectral region, narrow bandgap, and compatibility with thin-film device architectures. These properties make Ge-based structures promising candidates for compact, scalable, and cost-effective photodetectors, particularly in spectral ranges where conventional Si-based detection becomes limited. Ge-based thin-film photodiode heterostructures were fabricated using a sputtering-based deposition process. The device architecture was designed by integrating metallic contacts, TiO_2 carrier-selective interlayers, Ge active layers, and B-assisted Ge multilayers within a sputter-compatible structure. This approach was employed to support interface-related charge control while preserving the near-infrared absorption capability of Ge.

Optoelectronic measurements were carried out under 515, 730, and 950 nm illumination. The devices exhibited rectifying behavior and measurable photoresponse under different optical excitation wavelengths. For the 950 nm measurement at a bias voltage of +8 V, the current increased from 582.639 nA in the dark condition to 1.3126 µA under illumination, corresponding to a photocurrent of approximately 729.961 nA. Considering an active device area of 0.325 cm^2 and an incident optical power density of 100 mW/cm^2 at 100% illumination, the total optical power reaching the photodiode was calculated as 32.5 mW. The photoresponsivity, calculated from the extracted photocurrent and incident optical power, was found to be (2.25×10^{-5}) A/W. The specific detectivity, calculated using a shot-noise-limited approach, was found to be (2.96×10^{7}) Jones. Under periodic 950 nm illumination, the device exhibited a reproducible transient photoresponse, with an illumination-to-dark current contrast of approximately 2.25, a current enhancement of about 125.3% relative to the dark state, and a rise time of nearly 1.1 s. Although the response speed is moderate compared with optimized Ge-based photodiodes, it is reasonable for a sputter-fabricated thin-film heterostructure where interface states, carrier trapping, and contact-related effects can influence the transient dynamics.

Power-dependent measurements under 950 nm illumination confirmed the reproducible NIR photoresponse of the sputtered Ge/TiO_2-based heterostructure, with photocurrent, responsivity, and shot-noise-limited specific detectivity varying consistently with the incident optical power density. Overall, the integration of Ge thin-film absorption, TiO_2-based carrier selectivity, and B-assisted multilayer engineering within a sputter-compatible process provides a promising preliminary route toward scalable Ge-based thin-film photodetectors, although further optimization of interface quality, dark current, optical coupling, and transient response is still required.

Acknowledgment:
The authors would like to thank Sivas University of Science and Technology for the laboratory facilities and technical support provided during the fabrication and characterization processes.

ORCID:
Koray Soydaner: 0000-0001-6979-9058

References:
J. Michel, J. Liu, and L. C. Kimerling, “High-performance Ge-on-Si photodetectors,” Nature Photonics, vol. 4, pp. 527–534, 2010.
A. Rogalski, “Infrared detectors: status and trends,” Progress in Quantum Electronics, vol. 27, no. 2–3, pp. 59–210, 2003.

Keyword: *Germanium, Magnetron sputtering, Thin-film photodiode*

In Silico Design of Peptide-dsDNA Molecular Constructs for Bioelectronic Glucose Sensing

Ravza Nur Ceran * **, Ersin Emre Ören**

Bionanodesign Laboratory, Department of Biomedical Engineering, TOBB University of Economics and Technology, Ankara, Türkiye

With global diabetes cases exceeding 500 million, modern bioelectronics urgently require highly reliable, continuous glucose monitoring systems [1]. Although traditional enzyme-based glucose biosensors offer high sensitivity, enzymatic instabilities caused by environmental factors and long-term degradation issues limit the operational lifespan of these systems [2]. To overcome these limitations, the development of stable biomimetic sensing elements with enzyme-free detection mechanisms is of great importance. In particular, the unique charge-carrying capability exhibited by double-stranded DNA (dsDNA) molecules through base stacking (π-π stacking) in their core region [3] makes the use of these nanostructures as efficient “molecular wires” in bioelectronic devices highly attractive [4]. At the same time, the integration of cyclic peptides that specifically bind to glucose into sensor interfaces offers critical advantages in non-enzymatic systems, such as high structural stability, ease of miniaturization, and superior target-specific affinity [5].

This study introduces a novel in silico design of a peptide-dsDNA hybrid structure engineered to act as a molecular conductor for ultra-sensitive glucose detection. The system’s fundamental sensing mechanism is based on the principle that conformational changes in the dsDNA structure caused by the binding of the target molecule are reflected in the electrical conductivity profile between the electrodes. A glucose-binding peptide has been rationally integrated into a specially designed, highly conductive (GC-rich) dsDNA sequence to optimize electron transfer. This integration is achieved through a five-membered 1,2,3-tetrazole ring formed between the deoxyuridine (dU) modification in the DNA sequence and the phenylalanine residue in the peptide chain, thereby preserving structural integrity.

The system's structural stability and sensing viability were evaluated using a multiscale computational workflow. After generating customized force field parameters (frcmod) for the modified residues, Molecular Dynamics (MD) simulations were used to sample the conformational space, followed by clustering analysis to isolate representative structures. These structures were then analyzed using molecular docking, Density Functional Theory (DFT), and charge transport calculations to assess the electronic band structure and conductivity profiles. Ultimately, this comprehensive computational framework offers an innovative and robust strategy for the rational design of target-specific bioelectronic interfaces.

Acknowledgment:
We thank TÜBİTAK ULAKBİM High Performance and Grid Computing Center (TRUBA resources) for providing the computing infrastructure used for the MD calculations.

ORCID:
Ersin Emre Ören: 0000-0001-5902-083X

References:
[1] Zhou, B., Rayner, A. W., Gregg, E. W., Sheffer, K. E., Carrillo-Larco, R. M., Bennett, J. E., ... & Can, G. (2024). Worldwide trends in diabetes prevalence and treatment from 1990 to 2022: a pooled analysis of 1108 population-representative studies with 141 million participants. The Lancet, 404(10467), 2077-2093.
[2] Teymourian, H., Barfidokht, A., & Wang, J. (2020). Electrochemical glucose sensors in diabetes management: an updated review (2010–2020). Chemical Society Reviews, 49(21), 7671-7709.
[3] Arnold, A. R., Grodick, M. A., & Barton, J. K. (2016). DNA charge transport: From chemical principles to the cell. Cell Chemical Biology, 23(1), 183-197.
[4] Guo, X., Gorodetsky, A. A., Hone, J., Barton, J. K., & Nuckolls, C. (2008). Conductivity of a single DNA duplex bridging a carbon nanotube gap. Nature Nanotechnology, 3(3), 163-167.
[5] Sfragano, P. S., Moro, G., Polo, F., & Palchetti, I. (2021). The role of peptides in the design of electrochemical biosensors for clinical diagnostics. Biosensors, 11(8), 246.

Keyword: *In Silico Design, Peptide-dsDNA Hybrids, Bioelectronic Sensors*

Novel Altermagnetic Monolayer of Vanadium Oxide with a Buckled Lieb Structure

Tamer Taşkıran [*1], Soheil Ershadrad[2], Biplab Sanyal[3], Cüneyt Şahin[1]

[1] *UNAM - National Nanotechnology Research Center and Institute of Materials Science and Nanotechnology, Bilkent University, Ankara 06800, Turkey*

[2] *Materials Design Division, Department of Physics, Chemistry, and Biology (IFM), Linköping University, SE-58183 Linköping, Sweden*

[3] *Department of Physics and Astronomy, Uppsala University, Box 516, 751 20 Uppsala, Sweden*

As a novel magnetic phase combining the core benefits of conventional ferromagnets and antiferromagnets, altermagnetism has attracted significant interest for next-generation spintronic applications. In this work, we employ density functional theory (DFT) to identify a 2D altermagnetic platform: a monolayer V_2O crystal arranged in a buckled Lieb lattice. We verify its structural, mechanical, and thermal stability via formation energies, phonon dispersion relations, stiffness matrix calculations, and room-temperature ab initio molecular dynamics simulations, noting that the lattice displays a negative Poisson's ratio. The system stabilizes in an antiferromagnetic phase with a local vanadium magnetic moment of 2.79 μB and a clear preference for out-of-plane magnetization due to magnetocrystalline anisotropy. Notably, the electronic structure exhibits a substantial 1.2 eV momentum-dependent spin splitting. Incorporating spin-orbit coupling lifts the degeneracy at the quadratic band crossing near the Fermi level by breaking its symmetry, which induces a strong Berry curvature and a high intrinsic spin Hall conductivity of about 40 (hbar/e) S cm^{-1}. Ultimately, our study highlights monolayer V_2O as a resilient room-temperature material for exploring altermagnetic physics and spin-dependent transport.

Acknowledgment:
This work was supported by the Scientific and Technological Research Council of Turkey (TÜBİTAK) under the 1001--Scientific and Technological Research Projects Funding Program (Project No. 124F108). The numerical calculations were carried out on the MareNostrum 5 supercomputer of Barcelona Supercomputing Center (BSC) and the TUBITAK ULAKBIM High Performance and Grid Computing Center (TRUBA). This work was supported by the BAGEP Award of the Science Academy. B.S. acknowledges financial support from Swedish Research Council (grant no. 2022-04309) and STINT Mobility Grant for Internationalization (grant no. MG2022-9386). The computational resources provided by the National Academic Infrastructure for Supercomputing in Sweden (NAISS) at NSC(NAISS 2025/3-68) and PDC (NAISS 2025/3-68 and NAISS 2026/1-46) partially funded by the Swedish Research Council through grant agreement no. 2022-06725 are gratefully acknowledged.

ORCID:
Tamer Taşkıran: 0000-0003-1838-0753

Keyword: *altermagnetism, two-dimensional materials, first-principles calculations*

A Novel PEGylated Cationic Liposomal Platform for Sorafenib Delivery in Triple-Negative Breast Cancer: Design, Optimization, and In Vitro Evaluation

Esra Merve Zanbak Çotaoğlu [*1], Kubra Kılıc[2], Gizem Ruya Topal[2]

[1] *Department of Pharmaceutical Technology, Gulhane Faculty of Pharmacy, University of Health Sciences, Ankara, Türkiye*
[2] *Department of Pharmaceutical Biotechnology, Gulhane Faculty of Pharmacy, University of Health Sciences, Ankara, Türkiye*

Breast cancer (TNBC) is one of the most aggressive breast cancer subtypes, accounting for approximately 20% of all breast cancer cases and exhibiting poor prognosis, early metastasis, and limited therapeutic options (1). Sorafenib, a multikinase inhibitor with anti-proliferative and anti-angiogenic properties, has shown promise in breast cancer treatment; however, its poor aqueous solubility and limited tumor-specific accumulation restrict its therapeutic efficacy. PEGylated cationic liposomes have emerged as attractive nanocarriers capable of improving drug stability, prolonging circulation time, and enhancing interactions with negatively charged tumor cells and angiogenic vasculature. To the best of our knowledge, sorafenib-loaded PEGylated cationic liposomes have not previously been investigated as a therapeutic strategy for TNBC. Therefore, this study aimed to develop and optimize DSPE-PEG2000-modified, sorafenib-loaded cationic liposomes for the treatment of TNBC (2,3).

Sorafenib-loaded liposomes were prepared using the thin-film hydration method. Briefly, lecithin, cholesterol, DOTAP, and DSPE-PEG2000 were dissolved in chloroform, and a thin lipid film was formed by rotary evaporation. The film was hydrated with phosphate-buffered saline (PBS, pH 7.4), followed by probe sonication and centrifugation. A total of 20 formulations were generated according to a Design-Expert®-based experimental design to optimize the percentage of DOTAP, percentage of cholesterol, and drug-to-total lipid ratio. The optimized formulation was characterized in terms of particle size (PS), polydispersity index (PDI), zeta potential (ZP), and encapsulation efficiency (EE%). Furthermore, in vitro release studies, Fourier-transform infrared spectroscopy (FTIR), and MTT cytotoxicity assays using MDA-MB-231 TNBC cells were performed.

The optimized formulation exhibited a particle size of 123.8 ± 0.92 nm with a narrow size distribution (PDI: 0.20 ± 0.01), indicating the formation of a homogeneous nanosized system. A slightly positive zeta potential (+22.7 ± 0.76 mV) confirmed the preservation of the cationic character following PEGylation, while a high encapsulation efficiency (84.8%) demonstrated efficient sorafenib incorporation. In vitro release studies revealed that liposomal encapsulation provided a sustained release profile compared with free sorafenib. FTIR analyses further confirmed the successful incorporation of sorafenib within the liposomal matrix. Moreover, MTT assays demonstrated concentration-dependent cytotoxic effects against MDA-MB-231 cells and indicated that liposomal delivery reduced the effective concentration of sorafenib required to induce cancer cell death compared with the free drug.

In conclusion, the developed DSPE-PEG2000-modified cationic liposomes exhibited favorable physicochemical characteristics, high drug encapsulation efficiency, and sustained drug release while enhancing the in vitro anticancer activity of sorafenib against TNBC cells. Given the apparent lack of previous reports investigating this nanoplatform for TNBC, these findings introduce a potentially novel therapeutic approach and support further preclinical evaluation of sorafenib-loaded PEGylated cationic liposomes for triple-negative breast cancer treatment.

ORCID:
Esra Merve Zanbak Çotaoğlu: https://orcid.org/0000-0002-6607-8973
Kubra Kılıc: https://orcid.org/0009-0007-0699-5976
Gizem Ruya Topal: https://orcid.org/0000-0002-7715-6383

References:
1.Zafrakas, M., P. Papasozomenou, and C. Emmanouilides, Sorafenib in breast cancer treatment: A systematic review and overview of clinical trials. World J Clin Oncol, 2016. 7(4): p. 331-6.
2.Hajimolaali, M., F.A. Dorkoosh, and S.G. Antimisiaris, Review of recent preclinical and clinical research on ligand-targeted liposomes as delivery systems in triple negative breast cancer therapy. Journal of Liposome Research, 2024. 34(4): p. 671-696.
3.Chowdhury, N., et al., Targeted Delivery of Doxorubicin Liposomes for Her-2+ Breast Cancer Treatment. AAPS PharmSciTech, 2020. 21(6): p. 202.

Keyword: *sorafenib, TNBC, cationic Pegylated liposomes*

Monobee: Micro-Dispensing Based Flexible Electronics Platform for Printed Functional Materials

Kaan Yapıcı *

Beespenser Teknoloji Anonim Şirketi

Beespenser presents Monobee, a micro-dispensing device developed for the direct deposition of conductive and functional inks in printed and flexible electronics applications. The system is designed to pattern materials onto rigid, flexible, and wearable substrates without the need for photolithography, etching, or cleanroom-based fabrication steps. By enabling controlled material deposition in standard laboratory environments, Monobee supports rapid prototyping of printed circuits, flexible interconnects, sensor structures, electrodes, and functional material patterns.

The device combines precision motion control, adjustable dispensing parameters, and substrate heating capabilities to support different ink-substrate combinations. Its micro-dispensing architecture allows users to work with silver nanoparticle inks, carbon-based conductive inks, dielectric materials, adhesives, and other functional formulations. Process parameters such as nozzle size, dispensing speed, material flow, layer thickness, and curing conditions can be adjusted according to the rheological behavior of the ink and the target pattern geometry.

Monobee is positioned as a laboratory-scale fabrication tool that connects material development with device-level prototyping. By allowing researchers and R&D teams to test ink formulations, optimize printing conditions, and produce functional patterns on different substrates, the device provides an accessible route for experimental printed electronics development. This approach is particularly relevant for applications involving flexible sensors, IoT devices, wearable electronics, printed electrodes, and early-stage energy storage components.

Keyword: *micro-dispensing, printed electronics, flexible electronics, conductive ink, functional ink, prototyping*

CNC-machined Alumina Doughs as Robust Ceramic Platforms for Prototyping of Microchannels and Micromixers

Ceren Özsaltık [*] [1], **Öykü Yanaz**[1], **Omid Moradi**[2], **Özge Akbulut**[1]

[1] *Faculty of Engineering and Natural Sciences, Sabanci University, Tuzla, Istanbul, 34956, Turkiye*

[2] *Faculty of Engineering and Natural Sciences, Sabanci University, Tuzla, Istanbul, 34956, Turkiye, Center of Excellence for Functional Surfaces and Interfaces for Nano-Diagnostics (EFSUN), Sabanci University, Tuzla, Istanbul, 34956, Turkiye*

Microfluidic devices are commonly fabricated from polymers or glass; however, chemically and mechanically robust ceramic platforms are attractive for applications involving harsh solvents, high shear, or repeated operations. Here, we demonstrate a rapid route for fabricating microchannels by CNC machining of self-standing, malleable alumina doughs. The doughs are consolidated through polymer-bridging-induced homogeneous coagulation of alumina particles in the presence of an ionic copolymer. Then, they were molded into 5-mm-thick, substrates and, after a short period of drying, surface-patterned in the green state using 1.0 and 0.5 mm cutting tools to obtain standard and fine channel geometries. A design library consisting of straight, angled, Y-shaped, and T-shaped channel layouts was produced to evaluate the effects of channel angle, tool diameter, and sintering profile on dimensional fidelity, surface quality, and mechanical integrity. After sintering, the open-channel ceramic substrates were sealed with a transparent cover to enable flow visualization. Ink-based solvent and gel formulations were pumped through the channels, and high-speed imaging was used to quantify flow-front velocity, residence behavior, and mixing patterns as a function of pumping speed and channel geometry. The resulting velocity fields were used to estimate wall shear stress and relate local hydrodynamic forces to surface damage, crack initiation, and crack propagation in the ceramic channels. Preliminary comparisons indicated that finer channels increased fluid–wall interaction and improved visualization of localized shear-driven effects, whereas angled and T/Y-junction designs promoted stronger transverse flow components and more effective mixing than straight channels. This study establishes CNC-machined alumina doughs as a simple, reusable, and mechanically robust prototyping platform for ceramic microfluidics. The first-generation results will guide the design of an optimized passive ceramic micromixer for solvent-, gel-, and particle-containing formulations.

ORCID:
Ceren Özsaltık: 0009-0006-9879-1067
Öykü Yanaz: 0009-0006-1847-6893
Omid Moradi: 0000-0001-8126-4531
Özge Akbulut: 0000-0002-8273-7772

Keyword: *alumina dough, CNC machining, ceramic microfluidics*

Mold-Free, Dough-Based Processing of Highly Loaded Strontium Hexaferrite Ceramics for Conformal X-Band EMI Absorbers

İleyna Uvak [*1], Batuhan Özkaya[1], Ozan Akdogan[2,3], Özge Akbulut[1]

[1] *Faculty of Engineering and Natural Sciences, Sabanci University, 34956 Istanbul, Turkiye*
[2] *Faculty of Engineering, Bahcesehir University, 34353 Istanbul, Turkiye*
[3] *NANOTerial Technology Corporation, 34077 Istanbul, Turkiye*

Conventional processing routes for strontium hexaferrite ($SrFe_{12}O_{19}$, SrM) ceramics constrain components to simple geometries defined by rigid tooling, whereas polymer-based EMI shielding systems trade magnetic loading and mechanical robustness for geometric freedom. Many EMI absorber applications, however, such as antenna radomes, curved enclosures, and coatings on non-planar surfaces, require parts that conform to complex geometries, which flat sintered ferrite tiles cannot cover without segmentation or air gaps. In this work, we present a dough-based processing strategy that decouples formability from magnetic content by formulating a highly loaded SrM dough (80 wt%) with only 0.20 wt% poly(vinyl alcohol) (PVA, Mw ≈ 9–10 kDa) as a temporary binder. The resulting viscoplastic dough exhibits clay-like workability, enabling free-form, benchtop shaping of curved and conformal green bodies without molds, casting infrastructure, or specialized equipment. The formulation was optimized across PVA molecular weights and solid loadings in the 78–82 wt% range, with macroscopic handling, shape retention under self-weight, and crack-free drying, rather than steady-shear rheology alone, serving as the primary selection criteria at these high solid contents.

Following pressureless sintering at 1150 °C, the optimized doughs yield dense (∼91% of theoretical density), phase-pure $SrFe_{12}O_{19}$ ceramics with a flexural strength of 45 ± 4.6 MPa, demonstrating that the minimal PVA content does not compromise final mechanical performance. Electromagnetic characterization in the X-band (8–12 GHz), performed on 1 mm thick as-sintered specimens fitted to a WR-90 waveguide sample holder, reveals absorption-dominated shielding behavior, with S_{11},min = −8.83 dB and S_{21},min = −10.87 dB, corresponding to a power absorption coefficient of 0.3–0.4 across the upper X-band. These attenuation levels are achieved without conductive fillers, metallic coatings, or multilayer architectures, highlighting the intrinsic absorbing capability of the dense SrM ceramics produced via this route. As a proof of concept for geometric versatility, we manually wrap the dough around a hemispherical template (e.g., a pingpong ball) and sinter it to obtain a conformal ferrite shell. This demonstration underscores the potential of dough-based processing as a simple, scalable, and mold-free method for prototyping geometrically complex, shape-specific EMI absorbers based on highly loaded ferrite ceramics.

ORCID:
İleyna Uvak: 0000-0002-2647-8796
Batuhan Özkaya: 0009-0008-9398-3865
Ozan Akdogan: 0000-0002-0775-066X
Özge Akbulut: 0000-0002-8273-7772

Keyword: *EMI shielding, strontium hexaferrite, advanced ceramics*

Theoretical Understanding of Stability in Atomically Precise Nanoclusters

Fahri Alkan *

Bilkent University, Department of Chemistry, Ankara, Türkiye

Atomically precise metal nanoclusters represent a unique class of nanomaterials that bridge the gap between molecular compounds and bulk metals. Their well-defined atomic structures provide an opportunity to establish direct relationships between composition, geometric structure, electronic properties, and thermodynamic stability. Understanding the factors governing nanocluster stability is of fundamental importance for the rational design of functional materials for catalysis, optics, sensing, and energy-related applications.

In this presentation, recent theoretical studies on the stability of atomically precise gold and silver nanoclusters will be discussed with a particular emphasis on the role of heteroatom doping and electronic structure. Using density functional theory and electronic structure analysis, we investigate how the local coordination environment, dopant identity, and electronic shell structure influence the preferred location and stability of foreign atoms within metal nanoclusters. Comparisons between transition-metal and coinage-metal dopants reveal distinct stabilization mechanisms associated with dopant–framework interactions and the redistribution of electronic states. The interplay between geometric factors, superatomic shell effects, and dopant-induced electronic perturbations will be highlighted through representative examples from ligand-protected gold and silver nanoclusters.

The results provide a unified perspective on the origin of stability in atomically precise nanoclusters and demonstrate how principles of electronic structure can guide the design of nanoclusters with tailored structural, optical, and catalytic properties.

Acknowledgment:
This work is funded by TÜBİTAK. (122N449)

ORCID:
Fahri Alkan: 0000-0002-4046-9044

Keyword: *Nanoclusters, Doping, Thermodynamic Stability, Electronic Structure, DFT*

First-Principles Investigation of Electronic Structure and Magnetic Properties of Fe-Intercalated 2H-NbSe2

Mustafa İnanç [*1], Abdulsalam Aji Suleiman[2], Aydan Yeltik[3]

[1] Micro and Nanotechnology Graduate Program, TOBB University of Economics and Technology, 06560, Ankara, Turkey
[2] Department of Engineering Fundamental Sciences, Sivas University of Science and Technology, 58000, Sivas, Turkey
[3] Micro and Nanotechnology Graduate Program, TOBB University of Economics and Technology, 06560, Ankara, Turkey, Department of Materials Science and Nanotechnology Engineering, TOBB University of Economics and Technology, 06560 Ankara, Turkey

Transition metal dichalcogenides (TMDs) are layered materials that exhibit a wide range of electronic and structural properties. Especially after the isolation of 2D monolayer structures from their bulk phase via simple methods such as mechanical exfoliation, TMDs have gained considerable attention. 2H-$NbSe_2$ is one of these TMDs, hosting two competing quantum phases at low temperatures. Bulk 2H-$NbSe_2$ undergoes a charge density wave (CDW) transition at 33 K and becomes superconducting at 7.2 K. The competition between CDW order, driven by periodic charge density modulations, and superconductivity, arising from Cooper pair formation, makes 2H-NbSe₂ a pivotal material for understanding the electronic mechanisms underlying exotic quantum phases at low temperatures. To systematically investigate the interplay between these competing phases and varying electronic structure, we perform a first-principles study of Fe intercalation with different concentrations and configurations into van der Waals gap of 2H-$NbSe_2$. Since Fe intercalation introduces both charge transfer and local magnetic moments into the system, it serves as a powerful tool for tuning the competing phases. For the systems of Fe_xNbSe_2 with x = 0.125, 0.250, and 0.375, spin-polarized DFT calculations reveal the energetically competing magnetic phases with corresponding numerical results. Meanwhile, density of states (DOS/PDOS) and unfolded band structure calculations reveal that varying Fe concentration and magnetic configuration result in orbital hybridizations and varying electronic structures near the Fermi level. Further phonon-based calculations for CDW and superconducting transition temperatures will also be presented. This work will contribute to the fundamental understanding of intercalation-based modifications in TMDs.

Acknowledgment:
This work was supported by the Scientific and Technological Research Council of Turkey (TUBITAK) under Grant No. 124F315. All numerical calculations were performed at the TUBITAK ULAKBIM High Performance and Grid Computing Center (TRUBA).

ORCID:
Abdulsalam Aji Suleiman: https://orcid.org/0000-0002-7087-2715
Aydan Yeltik: https://orcid.org/0000-0001-6976-4680

Keyword: *Density functional theory, transition metal dichalcogenides (TMDs), Fe intercalation*

Theoretical Investigation of Perovskite/Polymer Heterostructures for Improved Interfacial Charge Transfer

Somayyeh Alidoust * **, V. Ongun Özçelik**

Materials Science and Nano Engineering Program, Sabanci University, Istanbul, 34956, Turkey.

Perovskite solar cells based on methylammonium lead iodide ($MAPbI_3$) demonstrate outstanding photovoltaic performance, where interface engineering with hole transport layers plays a key role in optimizing charge transfer and tailoring interfacial electronic properties. In this work, we perform a density functional theory investigation of the $MAPbI_3$/poly(3-hexylthiophene) (P3HT) hybrid interface, with particular emphasis on how perovskite surface termination influences interfacial stability and electronic behavior. MAI- and PbI-terminated $MAPbI_3$ surfaces interfaced with P3HT are modeled and systematically compared in terms of their electronic characteristics.

Electronic structure analysis reveals notable differences in orbital interactions and band alignment between the two interfaces: the MAI/m-P3HT interface exhibits relatively weak electronic coupling, whereas the PbI/m-P3HT interface shows stronger orbital hybridization and enhanced charge transfer. Band alignment calculations indicate type-II, hole-selective behavior for both interfaces, with a more significant valence band maximum shift observed for PbI termination. Charge density difference analysis, Bader charge calculations, and local density of states consistently support increased charge transfer and stronger interfacial electronic coupling in the PbI-terminated system. In addition, electrostatic potential offsets and transport-related parameters reveal termination-dependent variations, with lower effective masses obtained for PbI/m-P3HT than for MAI/m-P3HT. These results provide theoretical insight into interfacial charge transport mechanisms and offer guidance for understanding and tuning the electronic properties of perovskite–organic hybrid interfaces.

Acknowledgment:
We acknowledge funding from the Scientific and Technological Research Council of Turkey (TUBITAK) under project No 123F264. Computational resources have been provided by TUBITAK ULAKBIM, High Performance and Grid Computing Center, and by the National Center for High Performance Computing of Turkey (UHeM) under grant number 1013432022.

ORCID:
Somayyeh Alidoust: https://orcid.org/0000-0002-9071-9371
V. Ongun Özçelik: http://orcid.org/0000-0003-0645-7231

References:
Alidoust, S., & Özçelik, V. O. (2026). Interface Modeling of Perovskite/Polymer Heterostructures for Enhanced Charge-Transfer Efficiency in Hybrid Photovoltaic Materials. ACS Applied Energy Materials, 9(8), 4722–4730. doi:10.1021/acsaem.5c04025

Keyword: *Perovskite solar cells; $MAPbI_3$; P3HT; Interface engineering; Density functional theory (DFT); Charge transfer; Band alignment; Surface termination*

Effects of Calcination Process on Crystallization of Aluminum Oxide Nanoparticles

Alp Bigalı * **, Elif Begüm Elçioğlu**

Eskisehir Technical University, Faculty of Engineering, Department of Mechanical Engineering, 26555 Eskişehir, Turkiye

Nanomaterials live up to their names as they have at least one dimension having less than 100 nanometers. Dimensionally, they are classified as four different classes from 0 D to 3 D according to number of axis or axes larger than nanoscale. One of the examples for 0 D nanomaterials are nanoparticles. They can be in the form of amorphous or crystalline (single or poly). Aluminum oxide (Al_2O_3) nanoparticles have a vast application potential covering industrial coatings, energy, and medicine fields. Al_2O_3 nanoparticles synthesis methods range from precipitation and sol-gel to combustion methods [1]. Apart from chemical synthesis, green synthesis routes have been emerging due to improved eco-friendliness and large-scale production potential at lower cost [2], highlighting the sustainability aspect by exploiting outstanding properties of Al_2O_3 nanoparticles and omitting the risk of an environmental footprint at the same time. Typically, green synthesis of Al_2O_3 nanoparticles is followed by a calcination procedure to remove organic residuals coming from the bio-source used. Calcination is also important to obtain repeatability in structures after each synthesis run, since the bio-sources (e.g., plants) characteristics are prone to variations, which is a parameter that is difficult to isolate and affects the synthesis product. The calcination temperature influences the internal structure, and setting an optimum temperature level facilitates the necessary types of crystals to emerge ([3][4][5]). This poster presentation aims at providing a critical review of literature focusing on obtaining specific crystal forms including alpha, gamma, and theta, in terms of the necessary calcination conditions (environment, temperature ramp-up/down rates, temperature, and duration). Deductions from the literature will be discussed using custom-synthesized Aluminum oxide nanoparticles as a benchmark case, with the light of systematic FTIR spectroscopy and XRD measurements.

ORCID:
Alp Bigalı: https://orcid.org/0009-0007-5840-3186
Elif Begüm Elçioğlu: https://orcid.org/0000-0002-1005-4294

References:
“Recent Progress on the Production of Aluminum Oxide (Al2O3) Nanoparticles: A Review,” Mech. Eng. Soc. Ind., vol. 1, no. 2 SE-Articles, pp. 54–77, doi: 10.31603/mesi.5493.
R. C. Congreve, C. P. Quezada, and V. Kokkarachedu, “Aluminum Oxide Nanoparticles: Properties and Applications Overview,” Nanotechnol. Life Sci., vol. Part F2344, pp. 265–288, 2024, doi: 10.1007/978-3-031-50093-0_12.
A. H. Tavakoli et al., “Amorphous alumina nanoparticles: Structure, surface energy, and thermodynamic phase stability,” J. Phys. Chem. C, vol. 117, no. 33, pp. 17123–17130, 2013, doi: 10.1021/jp405820g.
B. Sathyaseelan, I. Baskaran, and K. Sivakumar, “Phase Transition Behavior of Nanocrystalline Al₂O₃ Powders,” Soft Nanosci. Lett., vol. 03, no. 04, pp. 69–74, 2013, doi: 10.4236/snl.2013.34012.
D. G. Syarif, D. H. Prajitno, and J. S. Pane, “Effect of calcination temperature during synthesis of Al2O3 from local bauxite on stability and CHF of water-Al2O3 nanofluids,” J. Aust. Ceram. Soc., vol. 54, no. 1, pp. 47–53, 2018, doi: 10.1007/s41779-017-0125-8.

Keyword: *Nanomaterials, Al2O3 Nanoparticles, Calcination process*

Unraveling CeO_2- and FeO_x-Induced Surface Restructuring in Rh/HAP Catalysts: A Spectroscopic Mechanistic Study of Dry Reforming of Methane

Aybala Büşra Topcu [*1], **Ayse Dilay Erdali**[2], **Erdem Deniz**[1], **Yusuf Kocak**[2], **Zafer Say**[1,3]

[1] *Micro and Nanotechnology Department, TOBB University of Economics and Technology, Ankara, Turkey*
[2] *Department of Chemistry, Bilkent University, Ankara, Turkey*
[3] *Material Science and Nanotechnology Engineering, TOBB University of Economics and Technology, Ankara, Turkey*

Dry reforming of methane (DRM) is an attractive and promising reaction that simultaneously utilizes two major greenhouse gases, CH_4 and CO_2, to produce synthesis gas. Ni-based DRM catalysts have been extensively studied in the literature due to their high activity and low cost. However, they suffer from severe coking and sintering. Therefore, alternative formulations and cost-effective synthesis strategies remain a major challenge for the commercialization of DRM catalysts.

Herein, we demonstrate a 0.2RhCeHAP catalyst with superior activity and excellent resistance to deactivation compared to its Fe-containing counterpart. This catalyst not only exhibited the highest conversion performance at 700^{o}C but, more importantly, showed negligible deactivation over 100 hours on stream. Above a critical reaction temperature, the strength of metal–support interactions delicately determines the surface electronic properties of Rh nanoclusters/particles and leads to the formation of bridging oxygen species between Rh and Ce (i.e., $Rh^{\delta+}$-O-Ce_{2-x}), which were not observed for the 0.2RhFeHAP catalyst. This metal-support interaction and interfacial oxygen not only provide higher activity but also enhance the stability of metallic Rh(0) through dynamic oxygen replenishment from the reducible ceria lattice, resulting in excellent high-temperature time-on-stream stability. This unique metal–support interface is considered an intrinsic active site that facilitates CO_2 dissociation.

These results were confirmed by in situ FTIR and XPS analyses, which revealed that, unlike the Rh-Ce interface, the Fe-containing catalyst formed surface $FePO_4$ domains that blocked Rh sites and inhibited their reduction, ultimately leading to rapid deactivation. The formation of metallic Rh species under reaction conditions was clearly evidenced by in situ CO adsorption FTIR and XPS. These analyses confirmed the reduction of RhO_x domains to metallic Rh sites during operation, highlighting the dynamic restructuring of the catalyst surface in response to the reaction environment.

These findings provide valuable insights into the role of promoter elements in modulating the surface structure and electronic states of active metals. Such understanding is critical for the rational design of stable and efficient catalysts for environmental applications, particularly under dynamic reaction conditions.

Keyword: *Dry Reforming of Methane (DRM), Hydroxyapatite (HAP), Metal-support interactions*

Ultrasound-Assisted Synthesis of Morphology-Controlled Copper Hydroxy Sulfate Micro/Nanoparticles

Sibel Şentürk[1], Chenyang Liu[1], Halide Sezi Hasin[1], Abdurahman Aghamaliyev[1], Sıla Boyacıgil[1], Cansu Yıldırım [*] [1,2], Hüseyin Enis Karahan[1,3]

[1] Department of Chemical Engineering, Istanbul Technical University, Maslak 34469, Istanbul, Türkiye
[2] Polymer Science and Technology Graduate Program, Istanbul Technical University, Maslak 34469, Istanbul, Türkiye
[3] Synthetic Fuels & Chemicals Technology Center (SENTEK), Istanbul Technical University, Maslak 34469, Istanbul, Türkiye

Naturally available secondary copper hydroxy sulfate minerals, such as brochantite ($Cu_4(SO_4)(OH)_6$), antlerite ($Cu_3(SO_4)(OH)_4$), posnjakite ($Cu_4(SO_4)(OH)_6 \cdot H_2O$), and langite ($Cu_4(SO_4)(OH)_6 \cdot 2H_2O$), can be synthesized via several synthetic routes, such as precipitation in alkaline solutions [1] and hydrothermal reactions [2]. The resulting products have several potential uses such as enzyme immobilization [3], pesticide production [4], and dye degradation [1]. On the other hand, it is established that the morphology of copper hydroxy sulfates, namely brochantite, can be sonochemically controlled [5]. Nevertheless, it is unclear if such shape-control has a major impact on the application potential of copper hydroxy sulfate minerals. To address this gap, we have explored the effect of various synthesis conditions on the ultrasound-assisted morphological control of copper hydroxy sulfates. Using copper acetate and potassium peroxysulfate, we have successfully controlled the shape and size of brochantite by manipulating the pH in the range 5.5 and 7.5 (at 25 °C). We have characterized the products by X-ray diffraction (XRD), Fourier-Transform Infrared Spectrometry (FT-IR), and Scanning Electron Microscopy (SEM). In alignment with previous observations [5], we obtained brochantite in different shapes and sizes in all conditions. However, interestingly, at pH 6, we obtained a mixture of brochantite and posnjakite (nanobricks and micro/nanobelts), a less stable phase. We also found that the product yield increased with an increasing pH, from almost negligible (at pH 5.5) to ~23% (at pH 7.5). We anticipate that these materials will show promising performance in different applications such as dye removal.

ORCID:
Sibel Şentürk: 0009-0007-8116-673X
Cansu Yıldırım: 0000-0003-1023-4030
Hüseyin Enis Karahan: 0000-0002-7753-1024

References:
[1]X.Z. Xiao, T.T. Dai, J. Guo, J.H. Wu, Flowerlike Brochantite Nanoplate Superstructures for Catalytic Wet Peroxide Oxidation of Congo Red, ACS Appl. Nano Mater. 2 (2019) 4159–4168.
[2]K. Huang, J. Wang, D. Wu, S. Lin, Copper hydroxyl sulfate as a heterogeneous catalyst for the catalytic wet peroxide oxidation of phenol, RSC Adv. 5 (2015) 8455–8462.
[3]Z. Li, Y. Ding, S. Li, Y. Jiang, Z. Liu, J. Ge, Highly active, stable and self-antimicrobial enzyme catalysts prepared by biomimetic mineralization of copper hydroxysulfate, Nanoscale. 8 (2016) 17440–17445.
[4]C. Gazzurelli, A. Migliori, P.P. Mazzeo, M. Carcelli, S. Pietarinen, G. Leonardi, A. Pandolfi, D. Rogolino, P. Pelagatti, Making Agriculture More Sustainable: An Environmentally Friendly Approach to the Synthesis of Lignin@Cu Pesticides, ACS Sustain. Chem. Eng. 8 (2020) 14886–14895.
[5]R. Kaş, Ö. Birer, Sonochemical shape control of copper hydroxysulfates, Ultrason. Sonochem. 19 (2012) 692–700.

Keyword: *Ultrasonication, Brochantite, Size Control*

Green Synthesis of Silver Nanoparticles Using Turkish White Tea (Camellia sinensis) Extract: Optimization of Synthesis Parameters and Physicochemical Characterization

Danya Anbar [*] [1,2], **Berkcan Zulfikar**[1,2], **Osman Eksik**[1,2], **Nihan Aydemir**[1,2]

[1] *Institute of Nanotechnology, Gebze Technical University, Kocaeli, 41400, Turkey*
[2] *Nanotechnology Research and Application Center, Gebze Technical University, Kocaeli, 41400, Turkey*

Silver nanoparticles (AgNPs) have emerged as one of the most utilized antimicrobial agents in biology and medicine, owing to their potent biocidal activity against a broad spectrum of microorganisms. Beyond antimicrobial efficacy, AgNPs exhibit a diverse range of bioactive properties, including anti-fungal, anti-inflammatory, anti-viral, anti-angiogenic, and anti-platelet effects, underpinning their widespread incorporation into medical textiles, food packaging, wound dressings and implant surface coatings (1). Plant-based green synthesis has gained considerable attention as a rapid, cost-effective, and environmentally benign route to producing highly stable AgNPs, whereby the rich diversity of phytochemicals present in plant extracts enables fine control over nanoparticle physicochemical properties, positioning it as a scalable platform for commercial manufacturing (2).

In the present study, AgNPs were synthesized using an aqueous extract of Turkish white tea (Camellia sinensis), selected for its rich phytochemical composition, including alkaloids, terpenoids, polyphenols, and flavonoids. The most abundant and bioactive among these are catechins, particularly epigallocatechin gallate (EGCG), renowned for its antioxidant, anti-inflammatory and anticancer properties. These biomolecules facilitate the reduction of silver ions (Ag^+) to metallic AgNPs while simultaneously stabilizing nanoparticle surfaces, enhancing their biological functionality (3). White tea represents a largely underexplored biosource for AgNP synthesis, potentially offering superior and more reproducible reducing activity compared to previously reported systems. The influence of three key synthesis parameters was systematically investigated: (i) tea mass used for extraction (1–10 g), (ii) reaction duration (30–60 min), and (iii) solution pH (3–9).

The synthesized AgNPs were characterized using a complementary suite of analytical techniques: scanning electron microscopy (SEM) for morphological evaluation and size distribution; X-ray diffraction (XRD) for confirmation of crystalline structure and phase purity; and dynamic light scattering (DLS) coupled with zeta potential measurements for hydrodynamic size determination and colloidal stability assessment. Through systematic correlation of synthesis parameters with nanoparticle characteristics, this work establishes rational parameter–property relationships enabling targeted tuning of AgNP size, morphology, aggregation behavior, and stability, with direct implications for antimicrobial, catalytic, and environmental remediation applications.

References:

1. Nishibuchi M, Loo YY. Synthesis of silver nanoparticles by using tea leaf extract from Camellia sinensis. Int J Nanomedicine. 2012;7:4263–4267. https://doi.org/10.2147/IJN.S33344
2. Eker F, Akdaşçi E, Duman H, Bechelany M, Karav S. Green synthesis of silver nanoparticles using plant extracts: A comprehensive review of physicochemical properties and multifunctional applications. Int J Mol Sci.2025;26(13):6222. https://doi.org/10.3390/ijms26136222
3. Demir A. Green-synthesized silver nanoparticles from Camellia sinensis: mechanistic insights into phenolic-mediated multifunctional biological activities. BMC Plant Biol. 2025;25(1):1734. https://doi.org/10.1186/s12870-025-07881-0

Keyword: *silver nanoparticles; green synthesis; Camellia sinensis; white tea; synthesis parameters; characterization; polyphenols*

Sulfur-Assisted Growth and Phase Evolution of Mo-Based Carbide Crystals via Chemical Vapor Deposition

Deniz Cakir [*] [1], **Goknur Buke**[1], **Michael Naguib**[2], **Yury Gogotsi**[1]

[1] *A.J. Drexel Nanomaterials Institute, and Materials Science and Engineering Department, Drexel University, Philadelphia, PA, USA*
[2] *Department of Physics and Engineering Physics, Tulane University, New Orleans, Louisiana 70118, USA*

Transition metal carbides are promising materials for catalysis, electronics, and energy storage due to their tunable structural and chemical properties. Introducing sulfur into carbide growth environments may significantly alter crystal growth pathways and promote the formation of complex sulfur-containing carbide/sulfide architectures with potentially MXene-relevant layered characteristics.

In this work, sulfur-assisted chemical vapor deposition (CVD) growth experiments were performed in Ta-C and Mo-C systems using Cu-mediated high-temperature synthesis environments. The study explores the influence of sulfur on crystal morphology, interfacial growth behavior, and possible phase evolution toward sulfur-containing carbide/sulfide structures. Preliminary SEM, EDS, Raman spectroscopy, and XRD analyses revealed distinct morphological and structural differences compared to sulfur-free growth conditions. These early results provide insight into sulfur-mediated growth processes in transition metal carbide systems and suggest a potential pathway toward the controlled synthesis of novel carbide/sulfide materials with layered characteristics.

Acknowledgment:
The authors acknowledge the A.J. Drexel Nanomaterials Institute at Drexel University for providing research facilities and instrumentation support for this work.

Keyword: *Chemical vapor deposition (CVD), Sulfur-assisted growth, MXene-relevant layered structures*

Characterization and Evaluation of Bioactivities of Green Synthesized Silver Nanoparticles Through Tarragon (Artemisia dracunculus) Extract[

Deniz Nur Erbey * [1], **Ayşegül Öztürk**[1], **Zalike Keskin Erdoğan**[2], **Yılmaz Yürekli**[3], **Aylin Şendemir**[2,4]

[1] *Ege University, Institute of Natural and Applied Sciences, Department of Bioengineering, Izmir, Türkiye*
[2] *Department of Bioengineering, Engineering Faculty, Ege University, Izmir Turkiye.*
[3] *Department of Bioengineering, Engineering an Natural Sciences Faculty, Manisa Celal Bayar University, Manisa, Turkiye.*
[4] *Depatment of Biomedical Technologies, Institute of Natural and Applied Sciences,Ege University, Izmir, Türkiye*

Introduction

Silver nanoparticles (AgNPs) are widely researched in biomedical applications such as wound healing, drug delivery, and tissue engineering thanks to their high surface area, strong antimicrobial activity, and ability to interact with biological systems. Driven by the growing interest in environmentally friendly sustainable production, green synthesis approaches using plant extracts has emerged as a prominent alternative for nanoparticle fabrication. Tarragon (Artemisia dracunculus), rich in phenolic compounds, flavonoids, and antioxidant metabolites, offers great potential to be used as both a reducing and stabilizing agent. This study aims to green synthesis silver nanoparticles using tarragon extract, characterize their physicochemical properties, evaluate the antimicrobial, antioxidant, and wound healing potentials.

Method

Silver nanoparticles (AgNPs) were green-synthesized using tarragon extract. Nanoparticle formation was confirmed via UV-Vis spectrophotometry, while particle size distribution and colloidal stability were determined by dynamic light scattering (DLS) and zeta potential analyses. Antimicrobial efficacy was evaluated against Gram-positive (Staphylococcus aureus) and Gram-negative (Escherichia coli) bacteria and yeast (Candida sp) species. Additionally antioxidant activities will be assessed using radical scavenging assays. Finally, biocompatibility and wound healing potential will be investigated using cell viability in HaCaT cells and in vitro diabetic wound model.

Expected Findings and Contribution

It is anticipated that the phenolic and flavonoid compounds within the tarragon extract will effectively reduce silver ions yielding stable nanoparticles with homogeneous size distribution. The synthesized AgNPs are projected to exhibit potent antimicrobial activity against the tested microorganisms, demonstrate strong antioxidant properties through free radical scavenging and maintain biocompatible profile on HaCaT cells at optimal concentrations. Furthermore, these AgNPs are expected to accelerate the wound healing process by promoting cell migration within the in vitro diabetic wound model. Ultimately study will contribute valuable insights to the existing literature regarding the integration of plant-based green synthesis approaches in biomedical applications.

Conclusion

This study successfully demonstrates that tarragon extract mediated silver nanoparticles can be fabricated through an environmentally friendly sustainable method. Given their robust antimicrobial activity, antioxidant capacity, and wound healing-supporting properties, these green-synthesized AgNPs represent a highly promising nanomaterial candidate in biomedical applications. The findings are expected to establish a foundational framework for future innovations in wound care products, biomaterial development, and tissue engineering.

Acknowledgment:
Part of this study was carried out at Manisa Celal Bayar University. The authors would like to thank Dr. Zalike Keskin Erdoğan for her valuable contributions to the antimicrobial activity studies and Prof. Dr. Özlem Yeşil Çeliktaş for her valuable contributions to the zeta potential measurements.

References:
Valeria De Matteis, M. C. (2023). Aloe vera silver nanoparticles addition in chitosan films: improvement of physicochemical properties for eco-friendly food packaging material. Journal of Materials Research and Technology, 1015-1033.
Mădălina Țicolea, R. M.-O. (2024). Phytochemical Composition Antioxidant and Anti-Inflammatory Activity of Artemisia dracunculus and Artemisia abrotanum. Antioxidants.
Osorio-Tobón, J. F. (2020). Recent advances and comparisons of conventional and alternative extraction techniques of phenolic compounds. Journal of Food Science and Technology, 4299–4315.
Michael Ayodele Odeniyi, V. C.-T. (2020). Green synthesis and cream formulations of silver nanoparticles of Nauclea latifolia (African peach) fruit extracts and evaluation of antimicrobial and antioxidant activities. Sustainable Chemistry and Pharmacy, 100-197.

Keyword: *Tarragon, silver nanoparticle (AgNPs), green synthesis, antimicrobial activity, diabetic wound model*

Synthesis and Characterization of BODIPY-Modified Mesoporous Silica Nanoparticles

Eda Erdemir Tavukçu [*1], **Nisa Demirbilek**[2], **Erman Karakuş**[2]

[1] *Department of Chemistry, Faculty of Science, Istanbul University, 34134, Istanbul, Türkiye*

[2] *Organic Chemistry Laboratory, Chemistry Group, The Scientific & Technological Research Council of Türkiye, National Metrology Institute, (TUBITAK UME), 41470 Gebze, Kocaeli, Türkiye*

Mesoporous silica nanoparticles (MSNPs) are solid inorganic nanomaterials composed of porous structures containing empty channels that enable the encapsulation and retention of relatively large amounts of molecules. The mesoporous architecture provides the presence of ordered pores within the silica nanoparticles. These pores possess a regular nanometer-scale structure and typically exhibit diameters ranging from 2 to 50 nm [1]. Owing to their high surface area and pore volume, unique physicochemical and biochemical stability, uniform and tunable pore size, and ease of surface functionalization, MSNPs have attracted considerable attention in nanotechnology and nanomaterials research. They have been widely employed in applications such as encapsulation, drug delivery, catalysis, and sensor technologies [2]. Among the various fluorophores used for the functionalization of nanomaterials, BODIPY dyes have emerged as promising candidates owing to their overall neutral character, sharp absorption and emission bands, high fluorescence quantum yields, and excellent photostability. These advantageous photophysical properties make BODIPY derivatives attractive building blocks for fluorescence-based biological imaging applications [3].

In the present study, mesoporous silica nanoparticles with an average size of approximately 150 nm were synthesized via the sol-gel method using tetraethyl orthosilicate as the silica precursor in the presence of alcohol, water, and ammonia as a catalyst. To enable surface functionalization of the MSNPs, a BODIPY derivative bearing a long alkyl chain terminated with a carboxylic acid functional group was designed and synthesized. The synthesized BODIPY derivative was covalently attached to the surface of the silica nanoparticles, yielding an organic-inorganic hybrid nanoplatform. The resulting hybrid nanoplatform was developed for potential biological applications, including cell toxicity and fluorescence imaging studies. Characterization of both bare and modified MSNPs was performed using dynamic light scattering (DLS), zeta potential analysis, and transmission electron microscopy (TEM) to determine particle size, surface charge, and morphological properties. Furthermore, surface modification and the successful attachment of the BODIPY derivative onto the MSNP surface were confirmed by FTIR spectroscopy. The optical properties of the nanoplatform were investigated using UV-Vis absorption and fluorescence spectroscopy.

Acknowledgment:
This research was also partially funded by the 22HLT04 MetrINo project. The project (22HLT04 MetrINo) has received funding from the European Partnership on Metrology, co-financed from the European Union's Horizon Europe Research and Innovation Programme and by the Participating States (Funder name: European Partnership on Metrology; Funder ID: 10.13039/100019599; Grant no: 22HLT04 MetrINo).

ORCID:
Eda Erdemir Tavukçu: 0000-0002-8709-8340

References:
[1] Pal, N., Lee, J.-H. and Cho, E.-B. (2020) 'Recent Trends in Morphology-Controlled Synthesis and Application of Mesoporous Silica Nanoparticles.', Nanomaterials (Basel, Switzerland), 10(11).
[2] Tallury, P., Payton, K. and Santra, S. (2008) 'Silica-based multimodal/multifunctional nanoparticles for bioimaging and biosensing applications.', Nanomedicine (London, England), 3(4), pp. 579–592.
[3] Ulrich, G., Ziessel, R., Harriman, A., 2008, The chemistry of fluorescent BODIPY dyes: Versatility unsurpassed, Angewandte Chemie – International Edition, 47, 1184–1201.

Keyword: *Mesoporous silica nanoparticles (MSNPs), BODIPY, Surface functionalization, Hybrid nanoplatform*

Effect of Fluoride Concentration on the Morphology and Corrosion Behavior of Anodized Pure Iron

İlkim Dila Kaya * **, İlkim Tuana Gümüşkaya, Batur Ercan**

Middle East Technical University

Pure iron has attracted considerable attention as a biodegradable metal for temporary biomedical implants due to its favorable mechanical properties, biocompatibility, and gradual degradation characteristics. However, its relatively slow corrosion rate remains a major challenge for clinical applications. [1] Anodization is a promising surface modification technique for tailoring the morphology and corrosion behavior of pure iron. Among various anodization parameters, electrolyte composition plays a critical role in determining oxide layer growth and nanotube formation. [2]

In this study, pure iron samples were anodized at 40 V in ethylene glycol-based electrolytes containing NH_4F. NH_4F concentrations ranging from 0.025 to 0.40 M were investigated. The results demonstrated that increasing NH_4F concentration modifies the balance between oxide growth and fluoride-assisted dissolution, thereby influencing pore development and overall surface structure. In this study, 0.1 , 0.15 , and 0.2 M NH_4F containing electrolytes were selected for further investigation. Additionally, the influence of anodization time, ranging from 1 to 9 min, was examined for the selected electrolyte compositions. Time-dependent evaluations revealed that anodization duration plays a critical role in nanotube evolution, with an optimal anodization time of 5 min yielding homogeneous and well-defined nanotubular structures. SEM analysis showed that nanotubular diameter remained nearly constant (44–47 nm), whereas oxide layer thickness increased significantly from 200 ± 11 nm to 433 ± 44 nm with increasing NH_4F concentration. The pore size diameters were kept similar to investigate the effect of oxide layer thickness, surface chemistry, and nanotubular arrangement on corrosion behavior, wettability, and roughness. Increasing fluoride content resulted in a more homogeneous nanotubular arrangement across the anodized surface. To investigate the degradation behavior of the anodized samples, potentiodynamic polarization and electrochemical impedance spectroscopy analyses were conducted in 1× PBS at 37 °C. The measured corrosion rates ranged between 0.02 and 0.05 mm $year^{-1}$. Surface wettability was evaluated by contact angle measurements, which revealed that anodization enhanced the hydrophilicity of pure iron surfaces.

These findings demonstrate that controlling the fluoride concentration in the anodization electrolyte is an effective strategy for tailoring the morphology, oxide layer characteristics, surface wettability, and corrosion behavior of pure iron, thereby enhancing its potential for biodegradable implant applications.

Acknowledgment:
This study is supported by Middle East Technical University Scientific Research Coordination Unit (ODTÜ BAP) (Project ID: 11276).

References:
[1] Ang, H. Y., et al. "Fundamentals of bioresorbable stents." Functionalised cardiovascular stents. Woodhead Publishing, 2018. 75-97.
[2] Xie, Keyu, et al. "Fabrication of iron oxide nanotube arrays by electrochemical anodization." Corrosion science 88 (2014): 66-75.

Keyword: *pure iron, anodization, nanotube, fluoride concentration*

Eco-Friendly synthesis of ZnO Nanoparticles Using Endemic Flora from Türkiye: Morphological, Optical and Photoelectrochemical Insights

Eylül Sude Tırpan * **, Betül Bibin, İrem Beyza Dolu, Serra Ersoy, Cengiz Kaya**

Yildiz Technical University, Department of Metallurgy and Materials Engineering, 34210 Istanbul, Türkiye

Transition metal oxide nanoparticles play a significant role in photocatalysis and photoelectrochemical energy conversion due to their controllable morphology, wide band gap, and high surface area. Among them, zinc oxide (ZnO) is a semiconductor with a band gap of 3.37 eV and high binding energy, enabling efficient charge carrier generation under UV illumination. In recent years, increasing interest in environmentally friendly and sustainable synthesis methods has highlighted green synthesis using endemic plant extracts, as it avoids toxic chemicals and requires lower energy input.

In this study, ZnO nanoparticles were synthesized using extracts from endemic Turkish plant species: Datça almond (Prunus dulcis), mountain tea (Sideritis stricta), and hawthorn fruit (Crataegus spp.). Eight different samples were produced by varying extract pH values and zinc acetate concentrations between 0.1 M and 1 M. The samples were calcined at 450–550°C. The effects of plant type, pH, and molarity on the crystal structure and morphology of ZnO were systematically investigated.

The synthesized nanoparticles were characterized by X-ray diffraction (XRD) for phase analysis and scanning electron microscopy (SEM) for morphological evaluation. XRD results confirmed the formation of a high-purity hexagonal wurtzite phase in all samples. SEM images revealed that lower pH conditions produced smaller and more porous particles, while higher molarity led to noticeable agglomeration and more compact morphologies. Additionally, ZnO nanoparticles were deposited onto indium tin oxide (ITO) and fluorine-doped tin oxide (FTO) conductive glass substrates via electrospray and spin coating. The samples were prepared with one and six layers. Also, these coated glasses were tested photoelectrochemically in a three-electrode system using 1 M KOH electrolyte. Chronoamperometry measurements were performed at 0.1 V, 0.2 V, and 0.3 V under 20 s light/20 s dark cycles, showing a clear photocurrent increase under illumination. The results demonstrate that morphological variations directly influence photocurrent response.

Overall, these findings indicate that green synthesis using endemic plant extracts enables controlled modification of ZnO nanoparticles' structural and functional properties, offering a sustainable approach for hydrogen production and environmentally friendly energy technologies.

Acknowledgment:
This study was supported under the TÜBİTAK 2209-A project (project number 1919B012422519) and the Yıldız Technical University BAP LİKAP FLO-2025-7159 project.

Keyword: *Green synthesis, Photocatalysis, Hydrogen production*

Characterization, Rheological Behavior and Physical Stability Evaluation of Plant-Based Wax Nanoemulsions Produced by Ultrasonic Emulsification

Ezgi Zekiye Aktürk [*1], **Çağla Ural Aytuna**[2], **Beril Atmaca**[2], **Tolga Duran**[2]

[1] *Mercan Kimya, Izmir Institute of Technology*
[2] *Mercan Kimya*

Plant-based waxes have attracted increasing attention in food, cosmetic, coating, and advanced material applications due to their renewable origin, biodegradability, and environmentally friendly characteristics. In particular, natural waxes such as soy wax and carnauba wax offer sustainable alternatives to synthetic and petroleum-derived waxes. However, their limited dispersibility and stability in aqueous media restrict their broader utilization. Nanoemulsion technology provides an effective approach to overcome these limitations by reducing wax particle size to the nanometer scale, thereby enhancing dispersion stability, increasing surface area, and improving functional performance.

In this study, soy wax- and carnauba wax-based nanoemulsions were prepared using an ultrasonic emulsification method. Different wax concentrations and emulsifier ratios were evaluated to determine the optimum formulation and processing conditions. Particle size distributions and average particle sizes of the nanoemulsions were determined by Particle Size Analysis (PSA). To assess the time-dependent physical stability of the systems, pH, viscosity, and density measurements were performed. Furthermore, the flow behavior, viscosity profiles, and structural properties of the nanoemulsions were investigated through rheological analyses using a rheometer. Physical stability was evaluated by accelerated centrifugation tests and temperature cycling studies. The chemical compositions and characteristic constituents of the waxes were analyzed by Gas Chromatography–Mass Spectrometry (GC–MS), while their chemical structures were characterized using Fourier Transform Infrared Spectroscopy (FTIR).

The results demonstrated that ultrasonic emulsification significantly reduced wax particle size, leading to the formation of nanoemulsions with narrower particle size distributions. Rheological analyses indicated that the nanoemulsions exhibited favorable flow properties suitable for practical applications. Accelerated stability and temperature cycling tests revealed that the formulations maintained high physical stability without phase separation during storage. Characterization results confirmed that no significant chemical changes occurred in the wax structure during the emulsification process. Moreover, the reduction in particle size contributed to improved dispersion stability and enhanced system homogeneity.

The findings suggest that plant-based wax nanoemulsions have considerable potential as sustainable, environmentally friendly, and high-performance dispersion systems for various industrial applications. This study presents a comprehensive approach for optimizing formulation parameters, determining physicochemical properties, and evaluating the stability behavior of natural wax-based nanoemulsions, thereby providing a scientific foundation for future applications in functional coatings, agricultural protective systems, and advanced materials.

Acknowledgment:
The authors would like to express their sincere gratitude to Mercan Kimya Sanayi ve Ticaret A.Ş. for providing financial support, technical resources, and laboratory facilities that made this study possible.

ORCID:
Ezgi Zekiye Aktürk: 0000-0003-1538-2008

References:
Samyn, P., & Rastogi, V. K. (2022). Stabilization of an aqueous bio-based wax nano-emulsion through encapsulation. Nanomaterials, 12(23), 4329.
Cheng, Z., Wang, W., Tai, X., & Geng, T. (2024). Study on the formation and stabilization of natural wax emulsions. Journal of Dispersion Science and Technology, 1-9.
Xie, B., Zhang, X., Luo, X., Wang, Y., Li, Y., Li, B., & Liu, S. (2020). Edible coating based on beeswax-in-water Pickering emulsion stabilized by cellulose nanofibrils and carboxymethyl chitosan. Food Chemistry, 331, 127108.

Keyword: *Nanoemulsion, Plant-based waxes, Ultrasonic emulsification Method*

In situ Chlorophyll Decoration of ZIF-8 for Structural Modulation of Porous Frameworks

Fatma Yelda Ünlü * **, Özge İbiş, Caner Ünlü**

İstanbul Teknik Üniversitesi

ZIF-8 is a widely studied porous framework whose crystallization, morphology, and surface properties can be influenced by molecular additives introduced during synthesis. In this work, chlorophyll molecules were incorporated into the ZIF-8 formation medium to prepare chlorophyll-decorated ZIF-8 through an in situ synthesis approach. The aim was to examine whether chlorophyll can act not only as a bio-derived functional component, but also as a molecular modulator during ZIF-8 growth. Pristine ZIF-8 and chlorophyll-containing ZIF-8 samples will be compared in terms of crystallinity, particle morphology, surface area, porosity, and optical response. Powder X-ray diffraction, electron microscopy, BET surface-area analysis, solid-state UV–Vis absorption, and fluorescence spectroscopy will be used to evaluate the structural and photophysical effects of chlorophyll incorporation. Particular attention will be given to changes in ZIF-8 crystallization behavior and to the retention of chlorophyll-related optical features in the final solid. This study provides a direct route to chlorophyll-decorated ZIF-8 materials and explores how natural pigment molecules can be used to tune the structural properties of metal–organic frameworks during synthesis.

Keyword: *Metal Organic frameworks, Chlorophyll, Porous Materials*

Bio-Derived SiO_2-Based Hybrid Sols for Transparent Anti-Reflective Coatings on Glass Surfaces

Fatoş Koç * **, Nazire Türköz, Murat Özkan, Merve Deniz Köse, Berrin İkizler, Şerife Şeref Helvacı**

Ege University, Chemical Engineering Department

Transparent anti-reflective coatings require controlled surface morphology, high optical clarity, and stable sol formulations [1,2]. In this study, bio-derived silica gels were used as precursors for SiO_2-based and SiO_2–TiO_2 hybrid coating sols designed for transparent anti-reflective glass surfaces. The use of rice husk ash-derived silica provides a sustainable silica source, while TiO_2 incorporation enables the development of hybrid oxide coating systems [3-5]. The use of plant extract was introduced as a bio-mediated strategy to influence silica gel formation and provide an additional sustainable control parameter for the coating precursor design [6]. The work focuses on the relationship between silica gel preparation conditions, sol stability, thermal treatment, and final optical response.

Silica gels were prepared using a systematic experimental design based on three main variables: plant extract addition, pH, and solvent exchange. Eight silica gel formulations were obtained and further converted into coating sols using co-poly (acrylic acid), ammonium hydroxide, and ethanol. Each sol was prepared with and without titanium(IV) isopropoxide addition, leading to sixteen coating sol formulations. The sols were deposited onto glass substrates as single-layer coatings using a dip-coating method [1,2]. Two post-treatment conditions were compared: drying at 80 °C for 1 h and calcination at 500 °C. The gel and sol systems were evaluated by particle size distribution, zeta potential, and dry solid content measurements. The optical behavior of the coated glass substrates was assessed by transmittance and reflectance measurements. In addition, coating add-on values were calculated gravimetrically to correlate optical performance with coating mass per unit area.

This work presents a sustainable and systematic approach for designing transparent anti-reflective coatings from bio-derived silica gel precursors. The combination of plant extract-assisted gel formation, solvent exchange, TiO_2 incorporation, and thermal treatment provides a versatile route for tuning sol stability and optical coating performance. In this context, the study extends previous work on rice husk ash-derived silica, SiO_2–TiO_2 hybrid systems, surface-modified silica-based clearcoats, and plant-extract-assisted biosilica nanoparticle synthesis toward transparent optical coating applications [3,6].

ORCID:
Fatoş Koç: 0000-0002-2996-110X
Berrin İkizler: 0000-0001-8889-0754
Şerife Şeref Helvacı: 0000-0002-0272-1106

References:
Öz, P. (2021). Anti-reflective SiO_2, TiO_2, SiO_2/TiO_2 thin film coatings: Synthesis, characterization and applications (Thesis No: 699276) Master's Thesis, Ege University, Graduate School of Natural and Applied Sciences, Department of Chemical Engineering, İzmir. Supervisor: Prof. Dr. Şerife Şeref Helvacı.
İkizler, B. (2020). Preparation of single- and double-layer antireflective coatings by sol-gel method. Research on Engineering Structures and Materials, 6(1), 1–21. https://doi.org/10.17515/resm2019.105ma0130
Yener, H. B., &Helvacı, Ş. Ş. (2015). Effect of synthesis temperature on the structural properties and photocatalytic activity of TiO_2/SiO_2 composites synthesized using rice husk ash as a SiO_2 source. Separation and Purification Technology, 140, 84–93. https://doi.org/10.1016/j.seppur.2014.11.013
Tufaner, G., Çalışkan, A., Yener, H. B., &Helvacı, Ş. Ş. (2019). Preparation of amorphous silica from a renewable agricultural waste of rice husk ash by calcination method combined with chemical activation. Research on Engineering Structures and Materials, 5(3), 299–310. https://doi.org/10.17515/resm2019.79ma1205
Yılmaz, M., Yener, H. B., &Helvacı, Ş. Ş. (2026). Rice husk ash-derived silica particles for the adsorptive removal of acetylsalicylic acid from water: synthesis, characterization, isotherm, kinetic, and thermodynamic studies. ChemistrySelect, 11, e202505802. https://doi.org/10.1002/slct.202505802
Köse, M. D. (2025). Extraction of natural compounds from ficus carica leaves and their usage in the green synthesis of biosilica nanoparticles (Tez No. 940003) PhD Thesis, Ege University, Graduate School of Applied and Natural Science, Chemical Engineering Department, İzmir. Supervisor: Prof. Dr. Şerife Şeref Helvacı.

Keyword: *Bio-derived SiO_2–TiO_2 hybrid sol, anti-reflective transparent coating, Plant extract*

Green Synthesis of Nitrogen-Doped Carbon Dots by Hydrothermal and Sonochemical Methods

Fethi Emre Bayat [*] [1], **Sinemis Met Turhan**[1], **Ayşe Elif Yılmaz**[1], **Özlem Gümrah**[2], **Pınar Acar Bozkurt**[1]

[1] *Department of Chemistry, Ankara University, Ankara, Türkiye*
[2] *Department of Pharmacy, Faculty of Pharmacy, Fenerbahçe University, İstanbul, Türkiye*

Carbon dots (CDs) have attracted significant attention due to their low toxicity, high biocompatibility, tunable optical properties, strong photoluminescence, and chemical stability. These characteristics make them promising nanomaterials for a wide range of applications, including bioimaging, sensor technologies, energy storage, and environmental remediation. In addition, their production from renewable biomass resources through environmentally friendly methods has further increased interest in these materials. Although various approaches have been employed for nanoparticle synthesis, green synthesis strategies have emerged as sustainable alternatives that minimize environmental impact and support eco-friendly production processes.

In this study, undoped carbon dots (CDs) and nitrogen-doped carbon dots (N-CDs) were synthesized from nettle (Urtica dioica), a naturally abundant biomass resource, using hydrothermal and sonochemical methods employing a probe-type sonicator. Nettle is rich in proteins, amino acids, chlorophyll, and phenolic compounds, making it a suitable precursor for CD synthesis due to its natural nitrogen and oxygen content. Nitrogen doping was employed to enhance the surface functional groups and improve the optical properties of the resulting CDs.

The structural, morphological, surface, and optical properties of the synthesized N-CDs were characterized using FT-IR, XRD, SEM, TEM, XPS, DLS, zeta potential, UV–Vis absorption, and fluorescence spectroscopy techniques. Samples obtained through hydrothermal and sonochemical routes were comparatively evaluated to investigate the influence of the synthesis method on particle formation and optical behavior.

The results demonstrated that CDs could be successfully produced from nettle using environmentally friendly synthesis approaches, and that the synthesis method played a significant role in determining the structural and optical characteristics of the obtained materials. This study provides a sustainable and low-cost strategy for the development of biomass-derived carbon-based nanomaterials.

ORCID:
Özlem Gümrah: 0000-0002-6327-7758
Pınar Acar Bozkurt: 0000-0001-8743-9734

References:
1. Namakka, M., Rahman, M.R., Said, K., Mannan, M.A., Patwary, A.M. 2023. “A review of nanoparticle synthesis methods, classifications, applications, and characterization”, Environmental Nanotechnology Monitoring & Management, 20, 100900.
2. Manikandan, V. ve Lee, N. 2022. “Green synthesis of carbon quantum dots and their environmental applications”, Environmental Research, 212 (B), 113283.
3. Quaid, T., Ghalandari, V., Reza, T. 2022. “Effect of synthesis process, synthesis temperature, and reaction time on chemical, morphological, and quantum properties of carbon dots derived from loblolly pine”, Biomass, 2(4), 250–263.
4. Elkun, S., Ghali, M., Sharshar, T., Mosaad, M.M. 2023 “Green synthesis of fluorescent N-doped carbon quantum dots from castor seeds and their applications in cell imaging and pH sensing”, Sci Rep 14, 27927.

Keyword: *Carbon Dots, Green Synthesis, Hidrothermal and Sonochemical Methods*

Controlled Synthesis and Surface Modification of Magnetite Nanoparticles as Optimized Tracers for Magnetic Particle Imaging

Firdevs Aydın [*1], **Damla Alptekin Soydan**[2], **Sefa Karaca**[2], **Can Barış Top**[2], **Gökçen Birlik Demirel**[1]

[1] *Department of Chemistry, Ankara Hacı Bayram Veli University, Ankara, Türkiye*
[2] *ASELSAN A.Ş, Ankara, Türkiye*

Significant advances have been made in medical imaging techniques with methods such as magnetic resonance imaging, positron emission tomography, and ultrasound. However, the sensitivity, resolution, and toxicity of these imaging techniques remain significant challenges. Therefore, magnetic particle imaging (MPI) is a newly emerging non-invasive imaging technique that has garnered significant interest due to its high sensitivity, high resolution, and strong signal densities without background signals. In this context, superparamagnetic magnetic nanoparticles (SPIONs) are particularly used as tracers[1]. SPIONs are characterized by superparamagnetism, ease of preparation, and low toxicity, making it the most widely used core material for MPI[2]. For biomedical use, the magnetite core is typically coated with a biocompatible shell, which prevents agglomeration and improves its stability under applied magnetic fields[3]. In this study, we focused on the controlled synthesis, surface modification, and magnetic characterization of iron oxide nanoparticles optimized specifically for high-performance MPI applications.

ORCID:
Firdevs Aydın: 0000-0003-2706-500X

References:
(1) Duong, H. T. K.; Abdibastami, A.; Gloag, L.; Barrera, L.; Gooding, J. J.; Tilley, R. D. A Guide to the Design of Magnetic Particle Imaging Tracers for Biomedical Applications. Nanoscale 2022, 14 (38), 13890–13914. https://doi.org/10.1039/D2NR01897G.
(2) Karouta, N.; Simos, Y. V.; Basina, G.; Spyrou, K.; Subrati, M.; Chatzikonstantinou, A. V.; Hammami, M. A.; Tzitzios, V.; Alhassan, S. M.; Al Wahedi, Y.; Douvalis, A. P.; Hadjipanayis, G. C.; Tsamis, K.; Dounousi, E.; Markopoulos, G. S.; Bellou, S.; Georgakilas, V.; Peschos, D.; Sideratou, Z.; Stamatis, H.; Gournis, D. P.; Giannelis, E. P. Highly Hydrophilic Oleylamine-Modified Superparamagnetic Iron Oxide Nanoparticles for Biomedical Applications. ACS Appl. Nano Mater. 2023, 6 (4),
(3) Chen, R.; Christiansen, M. G.; Sourakov, A.; Mohr, A.; Matsumoto, Y.; Okada, S.; Jasanoff, A.; Anikeeva, P. High-Performance Ferrite Nanoparticles through Nonaqueous Redox Phase Tuning. Nano Lett. 2016, 16 (2), 1345–1351. https://doi.org/10.1021/acs.nanolett.5b04761.

Keyword: *Magnetic Nanoparticles, Magnetic Particle Imaging, Surface Modification*

Synthesis and Characterization of PEI Coated Iron Sulfide Nanostructures

Mine Yiğit * **, Gülce Özkan, Selin Şen, Ayben Top**

Department of Chemical Engineering, Izmir Institute of Technology, Urla 35430, Izmir, Türkiye

Photothermal materials convert photon energy directly into heat. An ideal material should exhibit strong absorption over a wide wavelength range, high photothermal conversion efficiency, chemical stability, and low cytotoxicity for biomedical applications. Near-infrared (NIR) light can scatter less and penetrate deeper into biological tissues. Because of this, photothermal materials are designed to selectively absorb in the NIR region.[1-3] In recent years, iron sulfide nanoparticles have become a promising alternative to traditional gold and metal oxide nanostructures. They offer narrow band gaps, rich phase diversity, low cost, and abundance. These sulfide-based nanostructures exhibit better NIR optical absorption and photothermal conversion performance compared with iron oxides. However, their use has been limited because they tend to aggregate due to high surface energy and low stability in water and oxidative environments. To address this, polymeric coatings are commonly used to improve stability and provide functional surface groups.[4-5] In this study, polyethyleneimine (PEI) was used as a capping agent during the hydrothermal synthesis of iron sulfide (Fe_xS_y) nanoparticles. This aimed to improve their stability and evaluate their suitability for photothermal biomedical applications. PEI-coated Fe_xS_y nanoparticles were synthesized using a hydrothermal method with an Fe:S molar ratio of 1:6 followed by purification and characterization. Structural, optical, and colloidal properties were investigated by ATR-FTIR, XRD, UV–Vis spectroscopy, dynamic light scattering (DLS), and zeta potential analysis. Photothermal performance was evaluated under 808 nm laser irradiation with different power densities, while cytotoxicity was assessed on A549 human lung cancer cells using the Alamar Blue assay. The results confirmed the successful formation of PEI-coated iron sulfide nanoparticles. DLS measurements revealed an average hydrodynamic diameter of 68.1 ± 5.8 nm with a relatively narrow size distribution. The nanoparticles exhibited a positive zeta potential of 32.82 ± 2.81 mV, suggesting enhanced colloidal stability provided by the PEI coating. UV–Vis analysis showed broad absorption extending into the NIR region. Under 808 nm laser irradiation, the nanoparticle dispersion showed a significant temperature increase, confirming effective photothermal conversion. Cytotoxicity studies showed concentration-dependent effects on A549 cells, with a noticeable decrease in cell viability observed above 250 µg/mL. These findings demonstrate that PEI-capped Fe_xS_y nanoparticles provide good colloidal stability, NIR-responsive photothermal performance, and biological activity. This highlights their potential as promising nanoplatforms for future photothermal therapy applications.

Acknowledgment:
This study was supported by the Scientific and Technological Research Council of Turkey (TUBITAK) with number 1919B012507943.

ORCID:
Selin Şen: https://orcid.org/0000-0001-9449-0896
Ayben Top: https://orcid.org/0000-0003-0554-2506

References:
Pham, T.-T. D.; Phan, L. M. T.; Cho, S.; Park, J., Enhancement Approaches for Photothermal Conversion of Donor–Acceptor Conjugated Polymer for Photothermal Therapy: A review. Science and Technology of Advanced Materials 2022, 23 (1), 707-734.
Estelrich, J.; Busquets, M. A., Iron Oxide Nanoparticles in Photothermal Therapy. Molecules 2018, 23 (7), 1567.
Han, H. S.; Choi, K. Y., Advances in Nanomaterial-Mediated Photothermal Cancer Therapies: Toward Clinical Applications. Biomedicines 2021, 9 (3), 305.
Hernández-Hernández, A. A.; Aguirre-Álvarez, G.; Cariño-Cortés, R.; Mendoza-Huizar, L. H.; Jiménez-Alvarado, R., Iron Oxide Nanoparticles: Synthesis, Functionalization, and Applications in Diagnosis and Treatment of Cancer. Chemical Papers 2020, 74 (11), 3809-3824.
Faraji, M.; Yamini, Y.; Rezaee, M., Magnetic Nanoparticles: Synthesis, Stabilization, Functionalization, Characterization, and Applications. Journal of the Iranian Chemical Society 2010, 7 (1), 1-37.

Keyword: *iron sulfide, polyethyleneimine, photothermal*

Effect of Morphological and Structural Features of Silica Nanoparticles on Functional Coating Properties

Miray Kaya [*1], Merve Çevik Eren[1], Hürriyet Polat[2], Mehmet Polat[1]

[1] *Department of Chemical Engineering, Izmir Institute of Technology, Urla-Izmir Türkiye.*
[2] *Department of Chemistry, Izmir Institute of Technology, Urla-Izmir Türkiye*

Silica nanoparticles are widely used inorganic fillers in coating technologies due to their chemical stability, high hardness, surface reactivity, and tunable morphology. These characteristics make silica-based fillers important for designing hydrophobic, scratch-resistant, and durable coating systems. However, coating performance is not determined only by the presence of silica, but also by particle-related parameters such as size, shape, internal structure, and compositional modification. Therefore, the size effect, shape effect including spherical and rod-like morphologies, structural effect including porous and hollow architectures, and compositional effect particularly boron content should be evaluated to understand their influence on coating applications[1-4].

Particle size is one of the main parameters controlling the micro- and nano-scale roughness generated on the coating surface. Smaller silica nanoparticles can provide higher surface area and stronger interaction with the coating matrix, while broader or bimodal particle size distributions may promote hierarchical surface topography. Such topography changes the contact area between water droplets and the coated surface and therefore influences hydrophobic behavior. In addition, particle size and size distribution affect filler dispersion, agglomeration tendency, film uniformity, and the mechanical contribution of nanoparticles within the coating layer[1,4].

Particle shape is another important factor in coating design. Spherical silica nanoparticles are generally preferred because they are easy to synthesize, disperse more uniformly, and show good compatibility with polymeric coating matrices. In contrast, rod-like silica particles introduce anisotropic geometry into the coating film. Their elongated structure may create different contact areas, orientation behavior, and mechanical interlocking with the surrounding matrix. As a result, particle morphology can influence how the coating responds to deformation, abrasion, and scratching[1,2].

The internal structure of silica nanoparticles also affects surface and mechanical properties. Porous silica structures offer high surface area and tunable surface functionality, which may improve matrix interaction and support controlled surface roughness. Hollow silica particles are attractive due to their low density, controllable shell thickness, and surface architecture. These structural features may contribute to hydrophobicity, barrier properties, and mechanical performance[2,5].

Compositional modification provides an additional route for adjusting silica performance in coatings. Boron-containing silica composites can be considered hybrid filler systems designed to improve the surface and mechanical properties of silica. Boron incorporation may affect hardness, wear resistance, and scratch resistance; however, this effect depends on boron amount, its distribution within the silica matrix, and the synthesis route. Overall, controlled design of silica nanoparticles provides an approach for improving hydrophobicity and scratch resistance in applications[3].

ORCID:
Miray Kaya: 0009-0008-9435-1552
Merve Çevik Eren: 0000-0002-2473-2025
Hürriyet Polat: 0000-0002-1573-0351
Mehmet Polat: 0000-0002-1546-0013

References:
Sulubaş, Ş. (2023). Use of SNPs with controlled size & shape for enhanced surface hydrophobicity & hardness for coil coating applications [Master's thesis, İzmir Institute of Technology].
Siretli, Ç. (2012). Synthesis of silica nano particles with custom-made morphology for controlled drug delivery [Master's thesis, İzmir Institute of Technology].
Paker, H. (2024). Synthesis of composite filling materials for non-scratch paints and coatings [Master's thesis, İzmir Institute of Technology].
Nguyen-Tri, P., Tran, H. N., Plamondon, C. O., Tuduri, L., Vo, D.-V. N., Nanda, S., Mishra, A., Chao, H.-P., & Bajpai, A. K. (2019). Recent progress in the preparation, properties and applications of superhydrophobic nano-based coatings and surfaces: A review. Progress in Organic Coatings, 132, 235–256. https://doi.org/10.1016/j.porgcoat.2019.03.042
Teng, Z., Han, Y., Li, J., Yan, F., & Yang, W. (2010). Preparation of hollow mesoporous silica spheres by a sol–gel/emulsion approach. Microporous and Mesoporous Materials, 127(1–2), 67–72. https://doi.org/10.1016/j.micromeso.2009.06.028

Keyword: *Silica-based nanofillers, Functional coatings, nanoparticle morphology*

Morphology-Dependent Triboelectric Performance of Ce-Doped ZnO Nanoparticles Synthesized by Thermal Decomposition and Hydrothermal Routes

Melisa Atay[1], Metin Yurddaskal[2,3], Neslihan Sakar [* 4]

[1] *Dokuz Eylul University, The Graduate School of Natural and Applied Sciences, Izmir, Turkey*
[2] *Dokuz Eylul University, Department of Metallurgical and Materials Engineering, Izmir, Turkey*
[3] *Dokuz Eylul University, Department of Nanoscience and Nanoengineering, Izmir, Turkey*
[4] *Dokuz Eylul University, Center for Fabrication and Application of Electronic Materials, Izmir, Turkey*

Cerium-doped zinc oxide (Ce:ZnO) nanoparticles were synthesized by two different methods, thermal decomposition and hydrothermal processing, to investigate the effect of synthesis route on morphology and triboelectric performance. Since cerium can influence the defect chemistry, crystal growth behavior, and phase evolution of ZnO, controlling the synthesis pathway is critical for obtaining suitable nanostructures for triboelectric nanogenerators. In this study, Ce:ZnO nanocomposites with 3 and 6 at.% The obtained particles were comparatively evaluated in terms of morphology, agglomeration behavior, and structural characteristics by SEM and XRD analyses. The synthesized Ce-doped ZnO nanoparticles were incorporated into a PDMS matrix as active fillers to fabricate nanocomposite negative tribo-layers, while electrospun polyvinyl alcohol (PVA) structures were considered as positive tribo-layers for flexible triboelectric nanogenerator design. The main objective was to determine how morphology differences induced by the synthesis method affect charge generation and energy harvesting behavior. The triboelectric nanogenerator systems performed open-circut voltage between 3-10 volt to obtain renewable and sustainable energy for sensor applications.

References:

[1] M.B. Durukan, M.O. Cicek, D. Doganay, M.C. Gorur, S. Çınar, H.E. Unalan, Multifunctional and Physically Transient Supercapacitors, Triboelectric Nanogenerators, and Capacitive Sensors, Adv. Funct. Mater. 32 (2022). https://doi.org/10.1002/adfm.202106066
[2] K. Lee, J.H. Ryu, H.S. Han, B. Kim, K. Jung, I.Y. Moon, O. Kwon, C.Y. Chung, S. Mhin, K.M. Kim, Boosting triboelectric performance of PDMS-based nanogenerators through dual-filler embedded triboelectric layers, J. Alloys Compd. 1010 (2025). https://doi.org/10.1016/j.jallcom.2024.177114
[3] Khan, Rajwali, et al. "Carrier-mediated ferromagnetism and dielectric tailoring in dual-doped ZnO semiconductor nanoparticles for spintronics." Materials Science in Semiconductor Processing 193 (2025): 109487. https://doi.org/10.1016/j.mssp.2025.109487

Keyword: *Triboelectric Nanogenerator, Energy Harvesting, Renewable Energy*

Defect-Engineered ZnO-Gd2O3 composites for energy storage applications

Oluwatosin Johnson Ajala [*1], **Emre Erdem**[2]

[1] *Faculty of Engineering and Natural Sciences, Sabanci University*
[2] *Faculty of Engineering and Natural Sciences Sabanci University, Center of Excellence for Functional Surfaces and Interfaces (EFSUN)*

Defect-engineered ZnO-Gd_2O_3 composites were synthesized using a wet chemical precipitation technique and employed as electrode materials for supercapacitor applications. The influence of controlled incorporation of Gd_2O_3 on the defect structure and electrochemical behavior of ZnO was systematically investigated. Electron paramagnetic resonance, Raman, and photoluminescence spectroscopy were used to characterize paramagnetic and optically active defect centers within the ZnO host lattice. The electrochemical performance of the prepared electrodes was evaluated by assembling symmetric supercapacitor devices. Incorporation of Gd_2O_3 significantly enhanced the electrochemical behavior of ZnO. The optimal ZnO-Gd_2O_3 (0.5%) electrode delivered a maximum specific capacitance of 72 F/g, an energy density of 9.7 Wh/kg, a power density of 7.5 kW/kg, and cycling stability with 90% capacitance retention after 10000 cycles. These results demonstrate that controlled defect engineering via Gd_2O_3 incorporation effectively enhances ionic and electronic transport and charge-storage efficiency, establishing ZnO-Gd_2O_3 composites as promising electrode materials for high-performance supercapacitors

Acknowledgment:
This work was also supported by a grant from the Ministry of Research, Innovation, and Digitization, CNCS/CCCDI-UEFISCDI, project number ERANET-PECZIB, within PNCDI IV. Emre Erdem thanks the Scientific and Technological Research Council of Türkiye (TUBITAK) for financial support within grant no. 124M115

ORCID:
Oluwatosin Johnson Ajala: 0009-0001-4478-3567
Emre Erdem: 0000-0002-8395-0364

References:
A. U. Ammar, I. D. Yildirim, M. H. Aleinawi, M. Buldu-Akturk, N. S. Turhan, S. Nadupalli, A. M. Rostas, E. Erdem, Multifrequency EPR spectroscopy study of mn, fe, and cu doped nanocrystalline ZnO, Materials Research Bulletin 160 (2023) 112117.
M. Stefan, A. M. Rostas, A. U. Ammar, A. Gungor, E. Saritas, D. Toloman, A. Varadi, S. Macavei, L. Barbu-Tudoran, C. Leostean, et al., Cerium enhanced supercapacitive properties of zinc oxide nanoflowers, Energy & Fuels 38 (2024) 19088–19099
M. H. Aleinawi, A. U. Ammar, D. Şentürk, L. Barbu-Tudoran, O. J. Ajala, D. Eşkin, F. B. Misirlioglu, A. M. Rostas, E. Erdem, Microwave-tuned mn-doped ZnO for all-in-one supercapacitors: Cor- relating defect chemistry with electrochemical behavior, Journal of Colloid and Interface Science 698 (2025) 138012
M. Carofiglio, S. Barui, V. Cauda, M. Laurenti, Doped zinc ox- ide nanoparticles: synthesis, characterization and potential use in nanomedicine, Applied Sciences (Basel, Switzerland) 10 (2020) 5194.
I. Ardelean, L. Griguta, EPR and magnetic susceptibility studies of B2O3–Bi2O3–Gd2O3 glasses, Journal of non-crystalline solids 353 (2007) 2363–2366.

Keyword: *Supercapacitors, ZnO–Gd2O3 composites, Defect engineering*

Effect of 355 nm Pulsed Laser Ablation Parameters on the Synthesis and EPR Characterization of NiO and Ni Nanoparticles

Omid Moradi * **, Ipek Deniz Yıldırım, Emre Erdem, Ali Koşar**

Sabanci University, Center of Excellence for Functional Surfaces and Interfaces for Nano-Diagnostics (EFSUN)

Nickel oxide nanoparticles have attracted considerable attention in recent years owing to their unique physicochemical properties and wide range of potential applications in photocatalysis, sensing, energy storage, and biomedicine. In this study, NiO and Ni nanoparticles were synthesized via pulsed laser ablation in liquid (PLAL) using a 355 nm UV laser operating on a nickel target immersed in an aqueous medium. The influence of key laser parameters, including pulse energy, repetition rate, and ablation duration on the structural, morphological, and physicochemical properties of the resulting nanoparticles was systematically investigated.

The phase composition and oxidation state of the synthesized nanoparticles were confirmed through X-ray diffraction (XRD) and selected complementary techniques, revealing the successful formation of both NiO (bunsenite) and metallic Ni phases with tunable phase ratios depending on the applied laser conditions. Electron Paramagnetic Resonance (EPR) spectroscopy was employed as the primary characterization tool to probe the electronic and structural properties of the nanoparticles at the atomic scale. Power-dependent, and room-temperature sweep EPR analyses provides detailed insight into lattice defects, nickel oxidation states (such as Ni3+), the presence and concentration of oxygen vacancies, and the relationship between particle size, morphology, and EPR spectral parameters such as g-factor anisotropy and linewidth.

The results demonstrate that PLAL at 355 nm offers a clean, surfactant-free and highly controllable route for producing nickel oxide nanoparticles with distinct phase compositions. EPR characterization proved particularly sensitive to subtle changes in defect density and Ni^{2+} spin dynamics as a function of laser parameters, highlighting its value as a diagnostic tool in nanoparticle synthesis optimization. The correlation established between laser processing conditions and EPR-derived structural signatures contributes to a deeper understanding of the formation mechanisms governing nickel oxide nanophases produced by laser ablation.

References:

Rahman, A.; Guisbiers, G. Synthesis of Nickel-Based Nanoparticles by Pulsed Laser Ablation in Liquids: Correlations between Laser Beam Power, Size Distribution and Cavitation Bubble Lifetime. Metals 2024, 14, 224. https://doi.org/10.3390/met14020224

Catalina G. Mihalcea, Mariana Stefan, Corneliu Ghica, Ovidiu G. Florea, Adelina Stanoiu, Cristian E. Simion, Simona Somacescu, Daniela Ghica, In-depth insight into the structural properties of nanoparticulate NiO for CO sensing, Applied Surface Science, Volume 651, 2024, 159252, ISSN 0169-4332, https://doi.org/10.1016/j.apsusc.2023.159252.

Surajit Das, Ashok Kumar, Jitendra Singh, Mahesh Kumar, Fabrication and modeling of laser ablated NiO nanoparticles decorated SnO2 based formaldehyde sensor, Sensors and Actuators B: Chemical, Volume 387, 2023, 133824, ISSN 0925-4005, https://doi.org/10.1016/j.snb.2023.133824.

Wang, Fulin, Zhenzhen Yu, Kaiyang Shi, Xiangwei Li, Kangqiang Lu, Weiya Huang, Changlin Yu, and Kai Yang. 2023. One-Pot Synthesis of N-Doped NiO for Enhanced Photocatalytic CO2 Reduction with Efficient Charge Transfer, Molecules 28, no. 6: 2435. https://doi.org/10.3390/molecules28062435

Keyword: *NiO and Ni nanoparticles, Pulsed laser ablation in liquid (PLAL), Electron Paramagnetic Resonance (EPR) spectroscopy*

Investigation of the Thermoelectric Synergistic Mechanism in Self-Powered Systems Employing MOF-Derived Carbon/MXene Heterojunctions Synthesized through Large-Scale Solar Furnace Thermal Shock

Saidov Kamoladdin[1], Sattorov Khurshid [*] [1], Pecherskaya Mariya[2], Ahmedova Dilbar[2], Abdullaev Abdubakir[1], Butanov Khakimjan[2], Razzokov Jamoliddin[3], Mamatkulov Shavkat[2], Ruzimuradov Olim[4]

[1] Department of Electronics and Radio Engineering, Tashkent University of Information Technologies
[2] Institute of Materials Science, Uzbekistan Academy of Sciences
[3] Institute of Fundamental and Applied Research, National Research University TIIAME, Tashkent, Uzbekistan
[4] Turin Polytechnic University in Tashkent

Efficient self-powered systems are critical for next-generation Internet of Things (IoT) sensors, wearable electronics, and autonomous devices. However, triboelectric nanogenerator (TENG)-supercapacitor systems are limited by poor charge transport, weak interfacial coupling, and energy mismatch between harvesting and storage units. To overcome these challenges, this project develops MOF-derived carbon/MXene heterojunctions using ultrafast thermal shock processing in a large-scale solar furnace. The millisecond thermal shock enables simultaneous carbon framework reconstruction, defect engineering, and confined MXene growth, forming strongly coupled three-dimensional heterostructures. This non-equilibrium synthesis improves electrical conductivity, increases active sites, and enhances ion/electron transport, leading to improved charge capture and storage performance. The thermal shock conditions on heterostructure evolution, interfacial charge transport, and ion adsorption/intercalation mechanisms. By establishing thermal–electric–chemical coupling relationships and optimizing material composition and interfaces, this research aims to improve the efficiency of hybrid self-powered systems. The expected outcomes will provide new design strategies for advanced energy harvesting and storage technologies in smart sensing and wearable electronics.

ORCID:
Saidov Kamoladdin: https://orcid.org/https://orcid.org/0000-0001-6797-502X

Keyword: *TENG-supercapacitor, MOF-derived carbon/MXene, self-powered systems, Solar Furnace*

Synthesis and Characterization of Carbon Quantum Dots from Organometallic Complexes

Serhat Demirci [*1], Taha Yasin Bayram[1], Aslı Yılmaz[1,2], Özlem Gündoğdu Aytaç[3,4], Sertan Aytaç[3,4], Yunus Kara[4], Mehmet Yılmaz[2,5]

[1] Atatürk University, Department of Molecular Biology and Genetics, Erzurum, Turkiye.
[2] East Anatolia High Technology Application and Research Center (DAYTAM), Atatürk University, 25240 Erzurum, Türkiye
[3] Kırşehir Ahi Evran University, Kaman Vocational School, Department of Food Processing, Food Technology Program, Kırşehir, Türkiye
[4] Department of Chemistry, Sciences Faculty, Atatürk University, Erzurum 25240, Turkiye
[5] Atatürk University, Department of Chemical Engineering, Erzurum, Turkiye.

Carbon quantum dots (CQDs) have emerged as promising carbon-based nanomaterials due to their broad emission range, high optical stability, facile synthesis, excellent electron transfer capability, and environmentally friendly nature. The chemical composition and, consequently, the optical properties of CQDs are strongly influenced by the precursor materials employed during synthesis. Organometallic complexes, characterized by metal–carbon bonds, have been widely utilized in photocatalysis, photovoltaic systems, and nanoparticle synthesis owing to their controllable synthesis, ease of characterization, efficient light absorption, and electron transfer properties. However, their application as precursors for CQD synthesis remains largely unexplored. In this study, CQDs were synthesized via a hydrothermal method using organometallic complexes containing the same central metal atom but different functional groups as carbon precursors. The morphological, chemical, and optical properties of the synthesized nanomaterials were systematically investigated using UV–Vis absorption spectroscopy, fluorescence spectroscopy, and complementary characterization techniques. Furthermore, the influence of the molecular structure of the precursor complexes on the physicochemical and optical properties of the resulting CQDs was evaluated. This study aims to demonstrate the potential of organometallic complexes as versatile precursors for CQD synthesis and to provide insights into how different functional groups affect the optical and surface characteristics of CQDs, thereby contributing to the rational design of next-generation photocatalytic materials.

Acknowledgment:
This study was supported by the Scientific Research Projects Coordination Unit (BAP) of Atatürk University under Project No. FBA-2026-16557. The authors sincerely acknowledge this financial support.

ORCID:
Serhat Demirci: 0009-0000-7975-1998
Taha Yasin Bayram: 0000-0003-4625-7429
Aslı Yılmaz: 0000-0001-7874-5641
Özlem Gündoğdu Aytaç: 0000-0002-6943-9674
Yunus Kara: 0000-0001-7552-9425
Mehmet Yılmaz: 0000-0003-2687-9167

Keyword: *Carbon Quantum Dots (CQDs), Organometallic Complexes, Hydrothermal Synthesis*

Low-Concentration Citric Acid Catalyzed Sol-Gel Synthesis Of Mesoporous 45S5 Bioactive Glass For Dental Applications

Sevgi Berfin Kıran * **, Eyüp Bilgi, Ceyda Öksel Karakuş**

Izmir Institute of Technology, Department of Bioengineering

Bioactive glass (BAG) is an amorphous biomaterial capable of bonding to hard tissues through hydroxyapatite ($Ca_{10}(PO_4)_6(OH)_2$) layer formation. Among various BAG compositions, 45S5 BAG has attracted considerable attention in dental applications for its ion-release behavior, remineralization potential, and high bioactivity. Conventional melt-quenching methods used for 45S5 BAG synthesis require high processing temperatures, which may reduce porosity and bioactivity. In contrast, sol-gel methods require relatively low temperatures and enable the production of highly porous and homogeneous 45S5 BAG structures with enhanced surface area and improved biological performance. Previous studies have highlighted that the acids employed to catalyze hydrolysis reactions during sol-gel synthesis play a crucial role in determining the properties of 45S5 BAG. Citric acid has been shown to function effectively as a catalyst, resulting in 45S5 BAG with superior purity, finer particle size, greater porosity, higher specific surface area, and enhanced bioactivity.

In this study, 45S5 mesoporous BAG was synthesized via a sol-gel route using low-concentration citric acid as an organic acid catalyst. The synthesis procedure was based on a previously reported protocol, with two modifications: nitric acid was replaced by citric acid, and the calcination temperature was increased to 800 °C. The synthesized 45S5 BAG was characterized using SEM-EDS, FTIR, XRD, and BET. EDS results demonstrated that the elemental composition of the synthesized 45S5 BAG was highly consistent with the nominal 45S5 BAG composition, with a Ca/P ratio of approximately 5.05, close to the theoretical value of 5.28. SEM and BET analyses demonstrated the formation of a mesoporous structure, as evidenced by the porous and heterogeneous surface morphology, high specific surface area, and pore size distribution within the mesoporous range, with pore widths of approximately 3-5 nm. FTIR and XRD analyses confirmed the amorphous silicate glass structure of the synthesized 45S5 BAG, with characteristic Si-O-Si vibrational bands and a predominantly amorphous XRD pattern, both associated with enhanced BAG bioactivity.

These findings suggest that low-concentration citric acid catalysis provides an effective and environmentally favorable approach for the synthesis of mesoporous 45S5 BAG. Ongoing mineralization kinetics studies in artificial saliva and simulated body fluid are being conducted to assess the bioactivity of the synthesized 45S5 BAG. These studies will provide additional insight into its suitability for dental applications.

Acknowledgment:
This study is supported by the Turkish Health Institutes (TÜSEB) through the A2 Project Support Program under Project No: 52943, titled "Development of Peptide-Mediated Controlled Zn^{2+} Release 45S5 Bioactive Glasses for Dental Remineralization and Antimicrobial Effect".

References:
Thomas NG, Junior FGS, Ninan N, Anil S, Raju RS, Varghese N, Chopra A, Thomas S. Bioglass in dentistry: A comprehensive review of current applications and innovative frontiers. Journal of Dentistry. 2025;162:106017. https://doi.org/10.1016/j.jdent.2025.106017
Skallevold HE, Rokaya D, Khurshid Z, Zafar MS. Bioactive glass applications in dentistry. International Journal of Molecular Sciences. 2019;20(23):5960. https://doi.org/10.3390/ijms20235960
Kaou MH, Furkó M, Balázsi K, Balázsi C. Advanced bioactive glasses: the newest achievements and breakthroughs in the area. Nanomaterials (Basel). 2023;13(16):2287. https://doi.org/10.3390/nano13162287
Tüncer M, Yücesoy DT, Öksel Karakuş C. Investigating early-stage mineralization behavior and bioactivity of acid-free bioactive glass 45S5 with enhanced dissolution kinetics. JOM. 2025;77:5064–5075. https://doi.org/10.1007/s11837-025-07167-8

Keyword: *45S5 Bioactive Glass, Sol-Gel Synthesis, Dental Applications*

Development of High-Performance Gel Electrolyte Reinforced with Waste Textile-Derived Cellulose and h-BN for Wearable Supercapacitors

Mehmet Can Göreli, Yiğit Efe Yılmaz, Eren Doğukan Kala, Tolga Bakırsoy * , Serra Ersoy, Suna Avcıoğlu

Yıldız Technical University, Department of Metallurgy and Materials Engineering, 34210 Istanbul, Türkiye

Wearable electronics have enormous potential in the future because of their flexible architectures that allow for smart systems, ongoing health monitoring, and body movement adaptation. Bendable supercapacitors with immediate high power are necessary for these systems to run continuously. At this point, the use of gel electrolytes, which directly affect the device's performance and safety, is crucial. Solid electrolytes cause low ionic conductivity, while traditional liquid electrolytes present safety risks like leakage and flammability; gel electrolytes, on the other hand, provide high ionic conductivity in the form of a flexible skeleton, striking an ideal balance between these two extremes. However, because of their high water content, conventional hydrogels that are commonly utilized in the literature continue to be mechanically weak, show significant swelling anomalies, and readily lose their structural integrity during extreme deformations (bending, folding), which leads to the device collapsing.z

In this study, a high-performance hybrid gel electrolyte was created to address the mechanical and thermal drawbacks of gel-electrolyte systems. To achieve the best viscosity and ionic mobility, the system's ionic carrier matrix was calculated to comprise 10% polyvinyl alcohol (PVA) and 2% sodium sulfate (Na_2SO_4) by weight.The environmentally friendly deep eutectic solvent (DES) approach which contains choline chloride and urea was used to synthesis and purify cellulose from waste cotton textiles, which was then included into this matrix. The construction also included hexagonal boron nitride (h-BN) nanoplatelets, which provide exceptional mechanical and thermal strength. h-BN was synthesized by sol-gel method using boric acid, glycerin and modifying agents in a nitrogen atmosphere.

Gel electrolytes were produced for characterization: PVA/Na2SO4, PVA/Na2SO4/Cellulose, PVA/Na2SO4/h-BN, and PVA/Na2SO4/cellulose/h-BN. Mechanical analyses of the four different gel electrolytes were performed. Their thermal, morphological, and electrical performances were also investigated. The mechanical network formed by cellulose nanofibrils within the gel provided the developed gel electrolyte with extreme tensile and flexural strength, in contrast to the brittle structure of standard hydrogels. Simultaneously, homogeneously dispersed h-BN layers formed low-resistance ionic superhighways within the gel, effectively solving the problem of balancing increased flexibility with decreased conductivity. Unlike conventional hydrogels, this cellulose/h-BN reinforced 10% PVA - 2% Na_2SO_4 based gel electrolyte simultaneously increases both mechanical strength and ionic conductivity, offering a reliable and sustainable alternative for wearable energy storage systems.

Acknowledgment:
This study was supported under the TÜBİTAK 2209-A project.

Keyword: *gel electrolyte, wearable supercapacitor, waste cellulose extraction*

Design and Fabrication Of Non-Toxic Bi2O3 Nanoparticles With Finite Element Method and Pulsed-Laser Ablation in Liquid Phase

Yasemin Arslan [*1], Timuçin Emre Tabaru[1], Hamd Alhaj Qasem[2], Bülend Ortaç[2], Ali Karatutlu[1,2]

[1] Sivas University Of Science and Technology
[2] Bilkent University UNAM

Bismuth oxide (Bi_2O_3), which is among the functional sensor materials of critical importance in the defense, environment, and health industries, stands out with its wide bandgap, high refractive index, and super-ionic conductivity properties. One of the most significant advantages of Bi2O3 is that it is a non-toxic, biocompatible material with high environmental compliance compared to traditional semiconductors containing heavy metals such as lead or cadmium. This study aims to produce these safe nanostructures with high purity using the Pulsed Laser Ablation in Liquids (PLAL) method, in accordance with "green synthesis" principles, without requiring any chemical precursors or surfactants. In order to minimize trial-and-error costs in the experimental process, we have utilized Finite Element Method (FEM) using Comsol MultiPhysics software. Critical parameters such as frequency, pulse duration, and laser power are optimized during the simulations. These numerical models allow us to predict the temperature distrubutioon and the thermal stresses on the target surface. In the PLAL phase, atoms ablated from the bulk target by focused 1064 nm wavelength Nd:YAG laser pulses rapidly cool in the liquid medium to form stable and homogeneous colloidal solutions. The produced nanoparticles were characterized by TEM and SEM imaging, UV-Vis absorption spectroscopy and Raman spectroscopy. The combined numerical and experimental strategy serves as strong evidence for innovative and safe production processes in a wide R&D spectrum, ranging from biomedical diagnostic kits to defense industry applications, due to its non-toxic structure.

Acknowledgment:
We would like to thank the infrastructural support provided by Bilkent University UNAM and Photonic Innovation and Technology Research Center at Sivas University of Science and Technology.

References:
Amendola, V., & Meneghetti, M. (2013). Laser ablation in liquids: applications in structural and functional nanomaterials. Physical Chemistry Chemical Physics, 15(9), 3027-3046.
Gondal, M. A., Chang, X. F., & Yamani, Z. H. (2015). Synthesis of Bismuth Oxide (Bi2O3) nanoparticles via pulsed laser ablation in liquids and their optical properties. Applied Physics A, 121(1), 223-231.
Rehbock, C., & Barcikowski, S. (2021). Laser ablation in liquids: a versatile tool. Handbook of Laser Micro-and Nano-Engineering. Springer.
Selahuddin, M., et al. (2024). A Comprehensive Review of Nanoparticles. MDPI, 14(3), 290.
Zhang, D., Gökce, B., & Barcikowski, S. (2017). Laser synthesis and processing of colloids: fundamentals and applications. Chemical Reviews, 117(5), 3990-4103.

Keyword: *Nanomaterials, Laser ablation, Finite Element Method*

Boron-Based 2D Materials for Hydrogen Storage: Synthesis and Characterization

Yıldıray Yılmaz [*1], **Mehmet Ali Gülgün**[1], **Ahmet Eymen Akşener**[2]

[1] *Sabancı University, Istanbul, Türkiye*
[2] *Sabancı University Nanotechnology Research and Application Center*

Two-dimensional boron-sulfur (BxSy) phases represent lightweight, structurally diverse host frameworks for reversible solid-state hydrogen storage. In their pristine state, these monolayers are limited by weak molecular hydrogen (H2) physisorption [1][2]. Pristine hexagonal B2S3 undergoes weak physisorption over its vacant triangular sites, with a saturation limit of 18 H2 molecules at an internuclear distance of 4 Å (dH-S=3.26 Å), yielding an average adsorption energy of −0.07 eV/H2 and a gravimetric density of 2.30 wt% [2]. To optimize adsorption thermodynamics into the ideal reversible window (0.1–0.6 eV), lightweight alkali-metal functionalization (principally Li) is employed to modify surface binding sites [2]. For Li-decorated B2S (B8S4Li4), each protruding Li cation coordinates up to three H2 molecules (dLi-H2≈2.0 Å), achieving a theoretical gravimetric storage capacity of 9.1 wt% and an average binding energy of 0.14 eV/H2, with zero kinetic barrier during desorption [1]. On Li-decorated hexagonal B2S3 (Li18B2S3), the fully saturated phase adsorbs up to 54 H2 molecules on vacant triangular sites, achieving a gravimetric capacity of 6.35 wt%, an average adsorption energy of −0.15 to −0.16 eV/H2, and a practical desorption temperature (TD) of 209.84 K [2].

Motivated by these predictions, we report the synthesis of boron-sulfide powders as a route toward experimentally realized BxSy hydrogen-storage hosts. B2S3-targeted products have been obtained by sulfurization of a boron precursor with elemental sulfur in a horizontal quartz-tube furnace under sealed static vacuum following argon purging. The sulfur reservoir temperature was controlled independently of the reaction zone to sustain sulfur vapor pressure, and co-condensed excess sulfur was removed by mild post-synthesis vacuum heating.

Phase identification is performed by powder XRD with search-match and Rietveld analysis against rhombohedral and monoclinic B2S3, trigonal B12S, and BS2 reference structures, accounting for α-sulfur and calcium borate byproducts. Experimental Raman spectra have been compared with first-principles (DFT/DFPT, VASP) phonon and Raman calculations of the candidate phases to support phase assignment. SEM and EDS probed particle morphology and B/S stoichiometry, while FTIR monitored B–S vibrational signatures and residual borate species. Together, these results establish a combined synthesis–characterization–simulation workflow for boron-sulfide hydrogen-storage materials.

ORCID:
Yıldıray Yılmaz: https://orcid.org/0009-0006-7534-9911
Mehmet Ali Gülgün: https://orcid.org/0000-0002-7096-6252
Ahmet Eymen Akşener: https://orcid.org/0009-0002-7373-1974

References:
[1] F. Zhang, R. Chen, W. Zhang, and W. Zhang, "A Ti-decorated boron monolayer: a promising material for hydrogen storage," RSC Advances, vol. 6, pp. 12925, 2016, doi: 10.1039/C5RA25926G.
[2] A. Seif and K. Azizi, "A new strategy for hydrogen storage using BNNS: simultaneous effects of doping and charge modulation," RSC Advances, vol. 6, pp. 58458, 2016, doi: 10.1039/c6ra06634h.

Keyword: *Boron sulfide (B_2S_3), CVD synthesis, Hydrogen storage*

Synthesis and Characterization of Bioactive Carbon Dots Derived from Citric Acid and Hydroquinone

İdil Savru * **, Selin Şen, Ayben Top**

Department of Chemical Engineering, Izmir Institute of Technology, Urla 35430, Izmir, Türkiye

Chronic wounds represent a significant global health burden, demanding advanced therapeutic materials that simultaneously address bacterial infection, oxidative stress, and impaired tissue regeneration. Carbon dots (CDs), a rapidly emerging class of zero-dimensional carbon-based nanomaterials, have attracted considerable attention in biomedical research owing to their tuneable surface chemistry, high surface-to-volume ratio, low cytotoxicity, and ease of functionalization.[1] Their multifunctional character makes them particularly attractive for smart wound care platforms.[2] In this study, citric acid–hydroquinone-derived carbon dots were developed for incorporation into multifunctional hydrogels targeting wound healing applications. CDs were synthesised via a hydrothermal method with varying precursor molar ratios to investigate the effect of composition on structural and biological properties. Crystalline structure and functional groups were characterised using XRD and ATR-FTIR spectroscopy. Biological performance was evaluated through antioxidant activity, cytotoxicity, minimum inhibitory concentration (MIC) against Escherichia coli and Staphylococcus aureus, and in vitro wound closure capacity via scratch assay. All CD formulations at concentrations above 0.05 mg/mL demonstrated radical scavenging activity exceeding 50%, underscoring their antioxidant potential in oxidative-stress-rich wound microenvironments. Among the synthesised formulations, the CD with the highest citric acid content (C2H1) demonstrated the most favourable biocompatibility profile, with cell viability exceeding 90% at concentrations below 0.1 mg/mL. C2H1 exhibited notable antibacterial activity. Scratch assay results further demonstrated enhanced wound closure rates in CD-treated cells, supporting the potential of these nanomaterials to actively promote tissue regeneration.[1] Collectively, these results highlight C2H1 as a dual-function nanomaterial integrating antioxidant and antimicrobial properties within a single nanoplatform. Thus, the incorporation of these CDs into hydrogel matrices can be promising therapeutic molecules in wound dressings applications.

Acknowledgment:
This study was supported by Izmir Institute of Technology Research Foundation for the BAP project with a grant number of 2024İYTE-1-0060.

ORCID:
İdil Savru: https://orcid.org/0009-0005-0448-6815
Selin Şen: https://orcid.org/0000-0001-9449-0896
Ayben Top: https://orcid.org/0000-0003-0554-2506

References:
Li, X.; Yu, L.; He, M.; Chen, C.; Yu, Z.; Jiang, S.; Wang, Y.; Li, L.; Li, B.; Wang, G. Review on carbon dots: Synthesis and application in biology field. BMEMat 2023, 1 (4), e12045.
Wang, H.; Sun, S.; Zhao, Y.; Wang, P.; Zhou, Y.; Sun, H.; Lin, H. Carbon Dots with Integrated Photothermal Antibacterial and Heat-Enhanced Antioxidant Properties for Diabetic Wound Healing. Small 2024, 20 (45), 2403160.

Keyword: *carbon dots*, *wound healing*, *antioxidant*

Novel Nanocomposite Triboelectric Nanogenerators (TENG) Through Combining Thermal Drawing and Electrospinning Techniques

Ali Eren Yüksel [*] [1], Vishwa Pratap Singh[1], Maliha Rahman[1], Enes Dirican[1], Savaş Sönmezoğlu[2], Tudor Braniste[3], Mustafa Ordu[1]

[1] UNAM--Institute of Materials Science and Nanotechnology, Bilkent University
[2] Department of Metallurgical and Materials Engineering, Karamanoglu Mehmetbey University
[3] National Center for Materials Study and Testing, Technical University of Moldova

Triboelectric nanogenerators (TENGs) are highly attracted alternative energy harvesting systems for several reasons such as high voltage outputs, low cost, simple structure, lightweight nature, and broad material selection. However, current TENG systems suffer from low charge density and total electrical output. The electrospinning method, which has recently attracted great interest, allows for the production of nanofibers with high surface area. Polyvinylidene fluoride (PVDF) is a ferroelectric fluoropolymer, which is highly flexible, electronegative and polarizable. Integration of PVDF nanofibers into TENG systems, offering a solution to those problems. In this work, a novel, cost-effective, and highly efficient TENG fiber system is presented by the combination of thermal drawing and electrospinning production methods with two different structural approaches. In the first approach electrospun-PVDF nanofibers, having diameters around 100-200 nm, employed on conductive polyethylene (cPE) core electrode as a negative triboelectric layer in order to construct single-filament TENG structures that was produced in meter-scale lengths with overall diameter of 0.7 mm through thermal fiber drawing. The second approach includes coating of electrospun fibers onto thermally drawn cPE directly. Maximum open circuit voltage of the first approach was 6 V, whereas the second approach lead to 17 V, approximately 3 times higher output by consuming 10 times less material. Additionally, integration of 2wt% ZnO, SiO_2 and ZTO nanoparticles into PVDF nanofibers improves the electrical outcome up to 21 V by increasing the the β-phase crystallinity of PVDF nanofibers by 1.3%, 3%, and 5%, respectively. By combining electrospinning and thermal drawing, the novel TENG fiber system has improved interfacial polarization and electron trapping, thereby has advanced triboelectric performance beyond the current state of the art.

Acknowledgment:
This work was supported by the Contemporary Fibers Laboratory. The authors thank the National Nanotechnology Research Center (UNAM) for providing the equipment and facilities used in this study.

References:
Hasan, M. M., Sadeque, M. S. B., Albasar, I., Pecenek, H., Dokan, F. K., Onses, M. S., & Ordu, M. (2023). Scalable fabrication of MXene-PVDF nanocomposite triboelectric fibers via thermal drawing. Small, 19(6), 2206107.
Hussain, S. Z., Singh, V. P., Sadeque, M. S. B., Yavari, S., Kalimuldina, G., & Ordu, M. (2025). Piezoelectric-Triboelectric Hybrid Nanogenerator for Energy Harvesting and Self-Powered Sensing Applications. Small, 21(43), 2504626.

Keyword: *energy harvesting, scalable fibers, triboelectric nanogenerators*

Microwave-Assisted Synthesis of Co3O4/rGO Nanocomposites toward Promising Supercapacitor Electrodes

Anas Abofoul [*] [1,2], **Amira Gaber**[1,2], **Soliman I. El-Hout**[3], **Selva Bilge**[1]

[1] *Department of Chemistry, Faculty of Science, Ankara University, Ankara, Türkiye*
[2] *Department of Chemistry, Graduate School of Natural and Applied Sciences, Ankara University, Ankara, Türkiye*
[3] *Nanomaterials and Nanotechnology Department, Advanced Materials Division, Central Metallurgical Research and Development Institute CMRDI, Helwan, Egypt*

Cobalt oxide/carbon-based nanocomposites are promising supercapacitor electrode materials because their composition and film preparation strongly influence accessible charge storage. In this study, spinel Co_3O_4 and Co_3O_4 composites modified with carbon-based materials were prepared by a microwave-assisted route and drop-cast onto a boron-doped diamond electrode, which exhibited negligible background current and therefore provided robust, wide-window support. X-ray diffraction, Raman spectroscopy, FT-IR, and electron microscopy confirmed the cubic spinel Co_3O_4 phase, incorporation of the carbon-based phases, and structural modification of the oxide framework; the average crystallite size decreased from 44.2 nm for pristine Co_3O_4 to 28.1 nm after graphene-based modification, while Raman analysis indicated defect-rich carbon domains. Electrochemical performance was evaluated by cyclic voltammetry, galvanostatic charge–discharge, and impedance spectroscopy in an aqueous ferricyanide/ferrocyanide ($[Fe(CN)_6]^{3-/4-}$) redox electrolyte. At 10 µL loading and 1 mA cm^{-2}, pristine Co_3O_4 delivered an areal capacitance of 56.8 mF cm^{-2}, whereas modification with activated carbon (Co_3O_4/AC) and reduced graphene oxide (Co_3O_4/rGO) increased it to 289.5 and 315.0 mF cm^{-2}, respectively. Further optimization of the modification ratio identified a Co_3O_4/rGO:CB:PVDF ratio of 7:2:1 as the optimum composition at 10 µL, reaching 383.2 mF cm^{-2} at 1 mA cm^{-2}. Film loading was equally decisive: increasing the 7:2:1 coating volume to 12 µL raised the capacitance to 571.5 mF cm^{-2} at 1 mA cm^{-2} and 742.1 mF cm^{-2} at 0.6 mA cm^{-2}, whereas 14 µL caused film cracking. The optimally modified electrode retained measurable capacitance across 0.6–2.0 mA cm^{-2}. These results show that coupled control of carbon composition and film loading substantially enhances the areal charge-storage performance of Co_3O_4-modified electrodes.

ORCID:
Anas Abofoul: 0000-0002-1816-2476
Amira Gaber: 0000-0003-3051-5569
Soliman I. El-Hout: 0000-0002-1076-4237
Selva Bilge: 0000-0001-5514-208X

Keyword: *Supercapacitor · Co3O4 · Reduced graphene oxide (rGO) · Boron-doped diamond electrode · Areal capacitance · Microwave synthesis*

Electric-Field-Assisted Facile Growth of Aligned ZnO Nanowires on Flexible Substrates for High-Performance Piezoelectric Nanogenerators

Ayşegül Demircioğlu [* 1], Eminenur Sarıtaş[2], Murathan Kabak[1], Kuzey Kaya[3], Mohamad Hasan Aleinawi[1], Omid Moradi[1], Emre Erdem[1]

[1] *Faculty of Engineering and Natural Sciences, Sabancı University, 34956, Tuzla, Istanbul, Turkey*
[2] *Department of Electrical and Electronics Engineering, Middle East Technical University, 06800, Çankaya, Ankara, Turkey*
[3] *Francis College of Engineering, University of Massachusetts Lowell, Lowell, Massachusetts, United States of America.*

Zinc oxide (ZnO) nanowires (NWs) have emerged as promising building blocks for next-generation energy harvesting devices due to their semiconducting and piezoelectric properties (Wang & Song, 2006). The alignment and aspect ratio of ZnO NWs are critical factors in determining their efficiency in piezoelectric nanogenerators (PENGs) (Xu et al., 2010). Conventional synthesis techniques like chemical vapor deposition (CVD) or hydrothermal growth often face trade-offs between crystallinity, scalability, and compatibility with flexible substrates (Vayssieres, 2003) . In particular, scalable, low-voltage approaches enabling simultaneous vertical alignment and high aspect ratio growth on flexible, non-crystalline substrates remain underexplored.

Here, we demonstrate a facile electric-field-assisted synthesis method that enables the direct growth of highly aligned ZnO NWs on polyethylene terephthalate (PET) substrates at a comparably low electric field (10 V/cm). The approach integrates a sol–gel-derived ZnO seed layer deposited on Au–Pd-coated flexible substrates, followed by hydrothermal growth in an equimolar zinc nitrate hexahydrate ($Zn(NO_3)_2 \cdot 6H_2O$) and hexamethylenetetramine (HMTA) precursor solution under mild conditions (80 °C). The application of a modest electric field across parallel substrates effectively guided nanowire orientation, eliminating the need for templating or high-temperature processing.

We systematically investigated the effect of growth duration on nanowire alignment and morphology. Our findings revealed that the synthesis carried out for 4 hours resulted in the most uniform and highly aligned nanowire arrays, demonstrating the effectiveness of the electric field in promoting ordered growth over a longer period.

Morphological analyses using scanning electron microscopy (SEM) revealed vertically aligned ZnO NW arrays with uniform diameters and enhanced aspect ratios. Complementary photoluminescence and electron paramagnetic resonance (EPR) studies provided insights into defect structures and crystallographic order, confirming the role of the applied electric field in reducing structural disorder. The technique offers significant advantages in terms of simplicity, low cost, and compatibility with flexible electronics, opening new opportunities for scalable integration into wearable energy systems and roll-to-roll manufacturing platforms.

Our findings establish a novel, energy-efficient pathway to synthesize aligned ZnO NW arrays while elucidating the interplay between electric fields and nanowire orientation. This work contributes to the rational design of advanced piezoelectric materials and expands the potential of ZnO nanostructures for energy harvesting, sensing, and flexible optoelectronic applications.

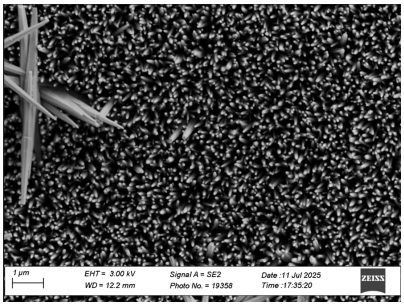


Figure 1: SEM image of ZnO nanowires with 4 hours synthesis duration.

Acknowledgment:
The authors would like to express their sincere gratitude to Sabancı University and the EFSUN (Center of Excellence for Functional Surfaces and Interfaces for Nano-diagnostics) Laboratories for granting access to their advanced research facilities, which were essential for the completion of this work.

ORCID:
Emre Erdem: 0000-0002-8395-0364

References:
Vayssieres, L. (2003). Growth of Arrayed Nanorods and Nanowires of ZnO from Aqueous Solutions. Advanced Materials, 15(5), 464–466. https://doi.org/10.1002/adma.200390108

Wang, Z. L., & Song, J. (2006). Piezoelectric nanogenerators based on Zinc oxide nanowire arrays. Science, 312(5771), 242–246. https://doi.org/10.1126/science.1124005
Xu, S., Hansen, B. J., & Wang, Z. L. (2010). Piezoelectric-nanowire-enabled power source for driving wireless microelectronics. Nature Communications, 1(1). https://doi.org/10.1038/ncomms1098 .

Keyword: *ZnO nanowires, electric-field-assisted growth, piezoelectric nanogenerators*

A New Quinone-Based Molecule as Cathode Material for Long-Life Aqueous Zinc-Ion Batteries

Batu Sercan Cantürk * **, Yasmin Geçalp, Mustafa Erdoğmuş, Onur Büyükçakır**

Department of Chemistry, Izmir Institute of Technology, İzmir, Türkiye

Redox-active organic molecules have long been investigated as cathode materials for aqueous zinc-ion batteries (AZIBs) due to their design flexibility, environmental friendliness, and resistance to structural deformation. Despite these advantages, organic small molecules, particularly their discharged products, exhibit high solubility in aqueous electrolytes [1,2]. To address this issue, herein we have synthesized and tested a new quinone-based redox active molecule (QBRAM), which is insoluble in the commonly employed aqueous 1 M $ZnSO_4$ electrolyte solution due to its structure and relatively large molecular weight. We have investigated QBRAM's electrochemical performance and charge-storage mechanism as a cathode material for rechargeable zinc-ion batteries. QBRAM delivers an extraordinarily long 10000 cycle life as a cathode material at a high current rate of 5 A g^{-1}, while providing an astonishing discharge capacity of 158 mAh g^{-1}.

References:

[1] Xu, Y.; Tang, X.-Z.; Xie, X.; Wang, N.; Komarneni, S., Zinc-ion storage mechanisms in poly(o-phenylenediamine): insights into structural advantages and electrochemical performance. Journal of Materials Chemistry A 2025, 13 (33), 27599-27606.
[2] Canakci, U. C.; Gecalp, Y.; Canturk, B. S.; Erdogmus, M.; Erozen, Y. N.; Buyukcakir, O., Monomer-Engineered Quinone-Based Conjugated Polymers for High-Rate Aqueous Zinc-Ion Batteries. ACS Applied Energy Materials 2025, 8 (12), 8399-8408.

Keyword: *Zinc-ion batteries, Organic cathodes, Small Molecule*

Experimental and Machine Learning Investigation of the Annealing Temperature-Dependent Structural Evolution of N-Type Window Layers Used in Solar Cells

Caner İldeş * **, Tarık Akan**

Yozgat Bozok Üniversity

High-efficiency thin-film solar cells require high-quality n-type window layers that play a critical role in the effective transmission of incident light to the absorber layer. In this study, CdS thin films were deposited on FTO substrates by the Chemical Bath Deposition (CBD) technique and employed as n-type window layers. The effects of annealing temperatures of 200, 250, and 300 °C on the structural and morphological properties of the films were experimentally investigated. GI-XRD analyses confirmed the formation of the hexagonal CdS phase in all samples and revealed that the crystalline characteristics of the films changed with increasing annealing temperature. FE-SEM observations demonstrated improved surface homogeneity and a significant reduction in uncovered regions after the annealing process. Machine learning models were developed using the experimental data to predict the structural behavior of the films at intermediate and higher temperatures where experimental measurements were not available. The results indicate that machine learning can serve as a powerful complementary tool to experimental studies and can be effectively utilized to determine the optimum annealing conditions for CdS window layers. This approach offers significant potential for enhancing material performance and optimizing fabrication processes in CdS/CIGS and CdS/CdTe thin-film solar cells.

Acknowledgment:
This work was supported by the Scientific Research Projects Coordination Unit of Yozgat Bozok University under Project No. FKA-2025-1502. The authors would like to thank Yozgat Bozok University for its financial support and research infrastructure.

ORCID:
Caner İldeş: 0000-0003-3168-935X
Tarık Akan: 0000-0002-9751-3405

Keyword: *Chemical Bath Deposition (CBD), Annealing Temperature, Machine Learning*

Ni-MOF-Based Platforms for Advanced Electrochemical Energy Storage Applications

Damla Tezcan [*1], Umut Güzel[2], Ulku Anik[1,2]

[1] *1 Faculty of Science, Chemistry Department, Mugla Sitki Kocman University, Mugla 48000, Turkey*

[2] *2 Sensors, Biosensors and Nano-diagnostic Systems Laboratory, Research Laboratory Center, Mugla Sitki Kocman University, Mugla 48000, Turkey*

The global energy crisis and the growing demand for sustainable energy have increased the need for high-performance energy storage systems. In this context, supercapacitors have attracted considerable attention due to their high power density, rapid charge–discharge capability, and long cycle life [1]. Metal–organic frameworks (MOFs) are regarded as important materials for energy storage applications owing to their high surface area, tunable pore structure, and chemical stability [1]. In particular, nickel-based MOFs (Ni-MOFs) are considered promising electrode materials because of their redox-active centers and high porosity [1]..In this study, the development of a high-performance electrochemical supercapacitor based on the interaction between Ni-MOF and carbon felt (CF) was aimed. Within this scope, the Ni-MOF structure was integrated onto CF using two different methods, and the capacitive properties of the obtained electrodes in were comparatively evaluated. In the first method, the Ni-MOF structure was directly grown on the CF surface, whereas in the second method, the synthesized and dried Ni-MOF was dispersed in N,N-dimethylformamide and coated onto CF via the drop-casting technique. The synthesized structures were characterized using X-ray diffraction, Fourier transform infrared spectroscopy and scanning electron microscopy analyses. Electrochemical performance evaluations were carried out using cyclic voltammetry, and electrochemical impedance spectroscopy techniques. The performances of the electrodes were investigated in 1 M H_2SO_4, 6 M KOH, and 1 M Na_2SO_4 electrolyte media, and the electrode exhibiting the highest capaciance value and optimal performance was identified. The obtained results are expected to contribute to the literature by providing insight into the development of next-generation Ni-MOF-based supercapacitor electrodes through synthesis approaches.

Derived from the author’s Master’s thesis.

References:

[1] Ebenezer, T., Johnson, I., Galeb, W., & Arockiasamy, J. S. K. (2024). Synthesis and investigation of charge storage characteristics in Ni-MOF/PANI composite as an active electrode material for supercapacitor. Electrochimica Acta, 507, 145130.

Keyword: *Ni-MOF, Supercapacitor electrodes, Capacitive properties, Electrochemistry.*

Multiphase Displacement Application of Green Nanofluid In Reservoir-on-Chip

Robab Jahangir[1,2], Faruk Aksoy [* 1,2], Gurkan Yesiloz[1,2]

[1] Yesiloz Research Laboratory, National Nanotechnology Research Center (UNAM) - Bilkent University, 06800, Cankaya-Ankara, Türkiye
[2] Institute of Materials Science and Nanotechnology, Bilkent University, 06800, Cankaya-Ankara, Türkiye

Residual oil trapping, caused by capillary forces and unfavorable wettability, remains a major challenge that limits the efficiency of conventional waterflooding processes. Nanofluids have recently emerged as promising enhanced oil recovery (EOR) agents due to their ability to modify interfacial properties and mobilize trapped oil [1,2]. In this study, a reservoir-on-a-chip (RoC) microfluidic platform is employed to investigate the pore-scale displacement performance of environmentally friendly silver nanoparticle (AgNP)-based nanofluids synthesized using glycerol as both solvent and reducing agent. AgNPs were produced through a simple room-temperature synthesis route and subsequently diluted to concentrations of 1, 3, 5, 7, 10, 20, and 20 vol.% for flooding experiments.

The interconnected porous network of the micromodel was initially saturated with green fluorescent oil and then subjected to waterflooding and nanofluid flooding under identical operating conditions. Real-time microscopic imaging combined with image processing and binary masking enabled quantitative evaluation of oil displacement and recovery efficiency. Conventional waterflooding resulted in an oil recovery of ~41%, leaving a considerable amount of residual oil trapped within dead-end pores and high-resistance regions. In contrast, the introduction of AgNP-based nanofluids progressively enhanced sweep efficiency with increasing nanoparticle concentration. The improved recovery is attributed to the combined effects of wettability alteration and structural disjoining pressure generated by nanoparticle accumulation near the oil-solid interface. The nanoparticle-induced thin film promotes detachment and mobilization of oil ganglia, facilitating displacement of oil trapped by capillary forces. Time-resolved pore-scale observations revealed a more efficient invasion front and reduced residual oil saturation in the presence of nanofluids compared with water alone. Higher AgNP concentrations exhibited superior displacement performance, demonstrating the concentration-dependent influence of nanoparticles on fluid-rock interactions.

Overall, this work demonstrates the potential of green AgNP-based nanofluids as effective EOR agents and highlights the advantages of reservoir-on-a-chip platforms for direct visualization and quantitative analysis of multiphase displacement phenomena. Future studies will focus on coupling nanofluid flooding with acoustic stimulation and extending the approach to more heterogeneous micromodels to further improve oil recovery.

Acknowledgment:
Authors gratefully acknowledge the support from the Scientific and Technological Research Council of Türkiye (TUBITAK) under 118C263 and 123E157 grants. The financial support received from TUBITAK does not mean that the content of the submission is approved in a scientific sense by TUBITAK.

References:
Jahangir et al., Anal. Chem., 2023, 95(47), 17177-17186.
Munir et al., ACS Omega, 2023, 8(31), 28456-28466.

Keyword: *Reservoir-on-Chip, Pore-Scale Displacement, Silver Nanoparticles (AgNPs)*

Sol-Gel Based High-Durability Nano Coating Technology for Solar Panel Glass Surfaces to Enhance Energy Efficiency

Orhan Alal, Duygu Kaya * , Mihriban Demir

Kocaeli University Faculty of Science Physics Department

1. Introduction

The rapid expansion of photovoltaic (PV) technologies has intensified the demand for advanced surface engineering strategies to mitigate efficiency losses caused by environmental soiling and optical limitations. Dust deposition, condensed water films, bird droppings, and organic contaminants diminish solar transmittance and elevate maintenance costs, thereby constraining the long-term sustainability of PV systems. [1] [2]

Hydrophobic/Superhydrophobic coatings, typically fabricated via sol-gel processing and nanoparticle modification, generate hierarchical nano-scale morphologies that simultaneously enhance water repellency and optical transparency. Optimized formulations exhibit water contact angles of $115 \pm 5°$, sliding angles near $4 \pm 1°$, and transmittance exceeding 96%. These physicochemical properties yield exceptional self-cleaning performance against particulate and dye contaminants, while mechanical and chemical stability under abrasion, alkaline/acidic exposure, and outdoor weathering confirm their durability. [3]

2. Experimental Section 2.1. Materials

Tetraethyl orthosilicate (TEOS), (3-glycidyloxypropyl)trimethoxysilane (GPTMS), and nonafluorohexyltriethoxysilane were purchased from [Sigma-Aldrich] and used as received. Polydimethylsiloxane (PDMS, viscosity 200 cSt) was obtained from [Gelest]. Acetone, absolute ethanol (EtOH), and hydrochloric acid (HCl, used as an acid catalyst) were of analytical grade and procured from [Sigma-Aldrich]. Deionized (DI) water was used throughout the experiments. Solar-grade glass substrates were utilized as the deposition templates.

2.2. Synthesis of the Hydrophobic Nanocomposite Sol

The hybrid sol was prepared via a modified sol-gel route:

Matrix Hydrolysis: TEOS was dissolved in absolute ethanol and hydrolyzed by the dropwise addition of DI water(pH=3-4) (catalyzed by HCl (37%)) under vigorous stirring to initiate the formation of the silica inorganic matrix. [2] **Coupling & Flexibility Modification:** GPTMS was introduced into the hydrolyzed TEOS solution as a coupling agent to prevent subsequent drying cracks and enhance interfacial adhesion. PDMS (200 cSt) was then incorporated into the mixture to impart structural flexibility and thermal shock resistance.Next, nonafluorohexyltriethoxysilane was added systematically to the solution. 2.3. Characterization

The optical and wetting properties of the finalized hybrid nanocoating were evaluated. The coating exhibited an optical transmittance of approximately 96%, alongside anti-reflective characteristics and autonomous self-cleaning functionality under simulated outdoor conditions.

Acknowledgment:
This study was supported by TÜBİTAK under the 1507 SME R&D Start-Up Support Program, within the scope of the project entitled “Sol-Gel Based High-Durability Nano Coating Technology for Solar Panel Glass Surfaces to Enhance Energy Efficiency.” We also extend our sincere thanks to Nasiol/Artekya Technology for their valuable contributions, including participation support and comprehensive assistance in R&D and analytical studies.

References:
M. Sakhuja, J. Son, H. Yang, C.S. Bhatia, A.J. Danner Outdoor performance and durability testing of antireflecting and self-cleaning glass for photovoltaic applications Sol. Energy, 110 (2014), pp. 231-238
X. Wu, R. S. Sutar, E. He, S.S. Latthe, S. Pitchaimuthu, B. Shi, R. Xing, S. Liu, Sol-gel preparation of transparent and superhydrophobic silica coatings for self-cleaning solar panels,Colloids and Surfaces A: Physicochemical and Engineering Aspects, Colloids and Surfaces A: Physicochemical and Engineering Aspects 737 (2026), art. 139910
I. Nayshevsky, Q.F. Xu, G. Barahman, A.M. Lyons Fluoropolymer coatings for solar cover glass: Anti-soiling mechanisms in the presence of dew Sol. Energy Mater. Sol. Cells, 206 (2020), Article 110281

Keyword: *Solar panel, Self-cleaning, sol-gel*

Synchrotron-Based X-Ray Raman Spectroscopy of a Ni-Decorated Nitrogen-Doped Graphene Quantum Dot Anode for Lithium-Ion Batteries

Kayra Ümekkan [*1], Didem Ketenoğlu[1], Erdinç Öz[2], Georg Spiekermann[3], Manuel Harder[4], Bahadir Boyacioglu[5], Mustafa Yıldız[6]

[1] *Department of Physics Engineering, Faculty of Engineering, Ankara University, 06100-Ankara, Türkiye*
[2] *Department of Physics, Atatürk University, 25400-Erzurum, Türkiye*
[3] *University of Münster, Institute of Mineralogie, Corrensstraße 24, 48149-Münster, Germany*
[4] *European XFEL GmbH, Holzkoppel 4, 22869-Schenefeld, Germany*
[5] *Vocational School of Health Services, Ankara University, 06290-Ankara, Türkiye*
[6] *Department of Chemistry, Faculty of Sciences, Çanakkale Onsekiz Mart University, 17100-Canakkale, Türkiye*

Advanced characterization of the local electronic structure is essential for understanding the electrochemical behavior of emerging graphene-based anode materials. In this study, nitrogen-doped graphene quantum dots decorated with Ni nanoparticles (PEI-HCl N-GQDs/Ni) were investigated as anodes for lithium-ion batteries. The nanocomposite was synthesized using a green approach based on PEI-HCl functionalization and nitrogen doping. The Ni-containing composite exhibited an initial discharge capacity of 144.6 mAh g^{-1}, approximately 32 times higher than that of pristine PEI-HCl N-GQDs.

To elucidate the electronic and chemical structure underlying this enhanced performance, ex-situ synchrotron-based X-ray Raman scattering (XRS) measurements were performed at the P01 beamline of PETRA III, DESY (Hamburg, Germany). Electrodes were analyzed in the pristine state and after 50, 100, and 250 charge-discharge cycles. Measurements at the C, N, and O K-edges together with the Ni L-edge enabled the evolution of the carbon framework, nitrogen and oxygen functionalities, and Ni-centered electronic states to be examined as a function of cycling. This multi-edge approach provides bulk-sensitive insight into cycle-dependent changes in the local chemical and electronic structure that cannot be obtained from surface-sensitive techniques alone.

The XRS measurements provide a direct spectroscopic framework for correlating cycle-dependent changes in local chemical and electronic structure with electrochemical behavior. The results indicate that Ni incorporation substantially modifies the electronic structure of the N-GQD framework, consistent with the experimentally observed enhancement in lithium-storage performance. This work demonstrates the potential of synchrotron XRS as a powerful bulk-sensitive probe for elucidating structure–electrochemistry relationships in graphene quantum dot-based battery electrodes.

Acknowledgment:
This work was supported by the Ankara University Scientific Research Projects Coordination Unit (BAP) under Grant No. FBA-2024-3174

References:
Ansari, S. A. (2022). Graphene quantum dots: novel properties and their applications for energy storage devices. Nanomaterials, 12(21), 3814
Im, M. J., Kim, J. I., Hyeong, S. K., Moon, B. J., & Bae, S. (2023). From pristine to heteroatom-doped graphene quantum dots: an essential review and prospects for future research. Small, 19(47), 2304497
Kaur, M., Kaur, M., & Sharma, V. K. (2018). Nitrogen-doped graphene and graphene quantum dots: A review on synthesis and applications in energy, sensors and environment. Advances in colloid and interface science, 259, 44-64.

Keyword: *Nitrogen-Doped Graphene Quantum Dots, Lithium-Ion Batteries, X-ray Raman scattering*

Cu Nanoparticle-Decorated Nitrogen-Doped Graphene Quantum Dots as High-Performance Anodes for Lithium-Ion Batteries

Mustafa Sezgin Tekkalmaz [* 1], Didem Ketenoğlu[1], Erdinç Öz[2], Yunus Emre Uyanık[3], Georg Spiekermann[4], Manuel Harder[5], Bahadır Boyacıoğlu[6], Hüseyin Ünver[7], Ashok Chatterjee[8], Mustafa Yıldız[9]

[1] Department of Physics Engineering, Faculty of Engineering, Ankara University, 06100-Ankara, Türkiye
[2] Department of Physics, Ataturk University, 25400-Erzurum, Türkiye
[3] Department of Physics, Institute of Science, Ataturk University, 25400-Erzurum, Türkiye
[4] University of Münster, Institute of Mineralogie, Corrensstraße 24, 48149-Münster, Germany
[5] European XFEL GmbH, Holzkoppel 4, 22869-Schenefeld, Germany
[6] Vocational School of Health Services, Ankara University, 06290-Ankara, Türkiye
[7] Department of Physics, Faculty of Science, Ankara University, 06100-Ankara, Türkiye
[8] Department of Physics, Anurag University, 500088-Hyderabad, India
[9] Department of Chemistry, Faculty of Sciences, Canakkale Onsekiz Mart University, 17100-Canakkale, Türkiye

The limited theoretical capacity and slow reaction kinetics of conventional graphite anodes motivate the development of advanced electrode materials for next-generation lithium-ion batteries. Nitrogen-doped graphene quantum dots (N-GQDs) have attracted considerable attention owing to their high surface area, tunable electronic structure, abundant surface functional groups, and excellent electrical conductivity. In this study, Cu nanoparticle-decorated nitrogen-doped graphene quantum dots (PEI-HCl N-GQDs/Cu) were synthesized via a green synthesis approach using PEI-HCl functionalization and urea-assisted nitrogen doping, and their potential as anode materials for lithium-ion batteries was investigated.

The structural, morphological, and chemical properties of the synthesized nanocomposite were characterized by scanning electron microscopy (SEM), X-ray diffraction (XRD), X-ray photoelectron spectroscopy (XPS), and Fourier transform infrared spectroscopy (FTIR). The results confirmed the successful formation of PEI-HCl N-GQDs, homogeneous incorporation of Cu nanoparticles, and effective nitrogen doping with pyridinic and pyrrolic nitrogen species, providing abundant lithiophilic active sites for lithium storage. The electrochemical performance of the synthesized material was evaluated in Li half-cells using cyclic voltammetry and galvanostatic charge-discharge measurements. The PEI-HCl N-GQDs/Cu electrode exhibited significantly improved reversible capacity, rate capability, and cycling stability compared with pristine PEI-HCl N-GQDs, demonstrating that Cu incorporation effectively enhances charge transport, reaction kinetics, and structural stability.

To gain further insight into the electronic structure evolution during electrochemical cycling, ex-situ synchrotron-based X-ray Raman scattering (XRS) spectroscopy was performed at the P01 beamline of PETRA III synchrotron, DESY (Hamburg, Germany). Pristine and electrochemically cycled electrodes were analyzed at the C, N, and O K-edges together with the Cu L-edge, enabling direct correlation of local electronic structure changes upon cycling. The combined electrochemical and synchrotron spectroscopic results demonstrate that the synergistic interaction between nitrogen functionalities and Cu nanoparticles enhances lithium storage behavior and provides valuable insights for the rational design of high-performance graphene quantum dot-based anode materials.

Acknowledgment:
This work was supported by the Ankara University Scientific Research Projects Coordination Unit under the general research project No: FBA-2024-3174, titled 'Azot-Katkılı Grafen Kuantum Nokta/Metal Nanokompozitlerinin Sentezi ve Lityum-iyon Pillerinde Ano

Keyword: *Nitrogen-doped graphene quantum dots, copper nanoparticles, lithium-ion batteries*

Semitransparent Organic Solar Cell Applications of Thienothiophene Π-Bridge based Novel Conjugated Polymer

Mürüvvet Ganız [*1], **Gizem Arslan**[2], **Gönül Hızalan Özsoy**[3], **Ali Çırpan**[1,2,3,4]

[1] *Department of Polymer Science and Technology, Middle East Technical University (METU), 06800, Ankara, Turkiye*
[2] *Department of Chemistry, Middle East Technical University (METU), 06800, Ankara, Turkiye*
[3] *ODTU-GUNAM, Middle East Technical University, 06800, Ankara, Turkiye*
[4] *Department of Micro and Nanotechnology, Middle East Technical University (METU), 06800, Ankara, Turkiye*

Organic solar cells (OSCs) offer a significant opportunity due to their light weight, flexibility, and compatibility with cost-effective, solution-based manufacturing methods. Recently, semitransparent organic solar cells (ST-OSCs) have attracted considerable attention due to their functionality in both energy generation and light transmission. Therefore, ST-OSCs are becoming promising candidates for the design of building-integrated photovoltaic (BIPV) systems by combining solar energy harvesting with various building materials. In addition to the PCE, FF, Jsc, and Voc parameters, the Average Visible Light Transmission (AVT) value is also an important parameter for the characterization of ST-OSCs. Quinoxaline-based conjugated polymer modified with a thienothiophene π-bridge has emerged as a promising donor material for organic solar cells (OSCs) due to its favorable optoelectronic properties, tunable energy levels, and strong absorption in the visible region. Additionally, the fabrication parameters of the optimized opaque device were investigated in semi-transparent OSC architecture. Device fabrication and characterization were carried out in a glovebox system filled with N_2. Current-voltage (I-V) characteristics were measured under solar simulator (AM1.5G). The best performing opaque device exhibited power conversion efficiency (PCE) of 7.55%, short circuit current density (Jsc) of 17.35 mA/cm², open circuit voltage (Voc) of 0.84 V, and fill factor of 52.10%. The best performance semitransparent OSC exhibits power conversion efficiency (PCE) of 5.22 %, short circuit current density (Jsc) of 13.37 mA/cm^2, open circuit voltage (Voc) of 0.82 V, fill factor of 47.77% and AVT of 20.51%.

This study was supported by the Scientific and Technological Research Council of TURKEY (TUBITAK) under the Grant Number 222Z151. The authors thank to TÜBİTAK for their supports.

Acknowledgment:
This study was supported by the Scientific and Technological Research Council of TURKEY (TUBITAK) under the Grant Number 222Z151. The authors thank to TÜBİTAK for their supports.

ORCID:
Mürüvvet Ganız: 0009-0009-6304-6245
Gönül Hızalan Özsoy: 0000-0002-3308-404X
Ali Çırpan: 0000-0003-3051-8380
Ali Çırpan: 0000-0003-3051-8380
Ali Çırpan: 0000-0003-3051-8380
Ali Çırpan: 0000-0003-3051-8380

References:
1. Liu, H., Geng, Y., Xiao, Z., Ding, L., Du, J., Tang, A., & Zhou, E. (2024). The Development of Quinoxaline-Based Electron Acceptors for High Performance Organic Solar Cells. Advanced Materials, 36(33), 2404660.
2. Xie, Y., Huo, L., Fan, B., Fu, H., Cai, Y., Zhang, L., ... & Sun, Y. (2018). High-performance semitransparent ternary organic solar cells. Advanced Functional Materials, 28(49), 1800627.
3. Zhu, C., Meng, L., Zhang, J., Qin, S., Lai, W., Qiu, B., ... & Li, Y. (2021). A quinoxaline-based D–A copolymer donor achieving 17.62% efficiency of organic solar cells. Advanced Materials, 33(23), 2100474.

Keyword: *semitransparent, organic solar cell, thienothiophene π-bridge*

Surface and Thickness Effects in Nanostructured Copper Films for CO2 Electroreduction on Gas Diffusion Electrodes

Patrycja Kolbusz * **, Sebastian Jarczewski, Krzysztof Mech**

Academic Centre for Materials and Nanotechnology, AGH University of Krakow, al. Mickiewicza 30, 30-059 Krakow, Poland

Electrochemical CO_2 reduction offers a promising route for converting carbon dioxide into value-added chemicals using renewable electricity. Copper is one of the most widely studied catalyst materials for this process because it can produce hydrocarbons and multicarbon products. However, its catalytic behavior strongly depends on the architecture of the active layer, particularly when copper is used on gas diffusion electrodes under high-current-density conditions.

In this work, copper thin films with nominal thicknesses of 100, 150, and 200 nm were deposited on gas diffusion electrodes by magnetron sputtering and investigated as nanostructured catalytic layers for CO_2 electroreduction. The electrodes were tested in a CO_2-fed flow cell with 1 M $KHCO_3$ electrolyte at current densities from -140 to -200 mA cm^{-2}. Gaseous products, including carbon monoxide, methane, ethylene, and hydrogen, were quantified by gas chromatography. The morphology, structure, surface chemistry, and roughness of the sputtered layers were examined using scanning electron microscopy, X-ray diffraction, Fourier-transform infrared spectroscopy, and contact profilometry.

The comparison of different film thicknesses showed that the catalytic response of copper gas diffusion electrodes is strongly affected by the amount and architecture of the deposited material. The formation of methane, ethylene, carbon monoxide, and hydrogen varied with both copper layer thickness and applied current density, indicating changes in the balance between CO_2 reduction pathways and the competing hydrogen evolution reaction. Post-reaction characterization revealed surface and structural changes of the sputtered films, suggesting that catalyst reconstruction contributes to the observed product distribution.

These results indicate that the thickness of magnetron-sputtered copper films is a key design parameter that affects surface reconstruction, product distribution, and the balance between CO_2 reduction and hydrogen evolution on gas diffusion electrodes.

Acknowledgment:
This work was supported by the Polish National Science Centre under grant 2023/49/B/ST8/01887

ORCID:
Patrycja Kolbusz: 0009-0004-7411-2774
Sebastian Jarczewski: 0000-0002-6423-3220
Krzysztof Mech: 0000-0002-0119-8456

References:
[1] D. Takamatsu, N. Fukatani, A. Yoneyama, T. Hirano, K. Hirai, S. Yabuuchi, K. Watanabe, K. Kamiya, S. Nakanishi, Dynamic Relocation of Copper Catalysts in Gas Diffusion Electrodes during CO2 Electroreduction, Journal of the American Chemical Society, 2025, 147, 24103-24112. DOI: 10.1021/jacs.5c07944.
[2] L. R. Manpatilan, S. Bianco, G. Cicero, J. Zeng, E. M. Tresso, Vapor Deposition Strategies for Copper-Based Electrocatalysts in CO2 Reduction Applications, ChemSusChem, 2025, 18, e202500813. DOI: 10.1002/cssc.202500813.
[3] S. Nitopi, E. Bertheussen, S. B. Scott, et al., Progress and Perspectives of Electrochemical CO2 Reduction on Copper in Aqueous Electrolyte, Chemical Reviews, 2019, 119, 7610-7672. DOI: 10.1021/acs.chemrev.8b00705.

Keyword: *CO2 electroreduction, magnetron sputtering, gas diffusion electrode*

Transesterification-Based Biodiesel Production Using Micro-Nano-Sized Spinel Zinc Ferrite Particles

Yasemin Fatih Aghdaei * [1,2], Gökçe Zeynep Yılmaz[1,2], Cansu Yıldırım[1,3], Hüseyin Enis Karahan[1,2]

[1] *Department of Chemical Engineering, Istanbul Technical University, Istanbul, 34469, Istanbul, Türkiye*
[2] *Synthetic Fuels & Chemicals Technology Center (SENTEK), Istanbul Technical University, 34469, Istanbul, Türkiye*
[3] *Polymer Science and Technology Graduate Program, Istanbul Technical University, Maslak, Istanbul, 34469, Turkey*

Ever increasing global energy demand and intensifying supply chain issues have reignited sustainable energy research lately. Among various alternatives, biodiesel has gained considerable attention as a renewable fuel. Nevertheless, there are major hurdles in widespread production of biodiesel at high quality. Particularly, the conventional choice, homogeneous catalysts, complicates the purification needs, making heterogeneous catalysts attractive. In this regard, mixed metal oxides come with notable advantages such as high reusability, low waste generation, facile separation, good thermal stability, and affordability. Among these materials, particularly spinel zinc ferrite ($ZnFe_2O_4$) has emerged as a promising catalyst for transesterification reaction owing to its favorable catalytic properties. Here, we report the synthesis and magnetic separability of $ZnFe_2O_4$ for biodiesel production. For the synthesis of $ZnFe_2O_4$, we employ a standard co-precipitation routine using Fe and Zn nitrate salts and sodium carbonate as a precipitation agent. We have characterized the as-produced particles with X-Ray Diffraction (XRD), Scanning Electron Microscopy (SEM), and Dynamic Light Scattering (DLS). XRD confirmed the successful formation of crystalline $ZnFe_2O_4$, with characteristic diffraction peaks corresponding to the spinel phase of $ZnFe_2O_4$. When prepared directly from the calcined samples without sonication, $ZnFe_2O_4$ particles were in agglomerated state under SEM. DLS observations, however, revealed that those micron-sized agglomerates can be broken down into nano-sized particles, suggesting that the catalysts include nano-to-submicron-scale primary particles. We later evaluated the performance of the synthesized catalysts in biodiesel production from sunflower oil. The transesterification reaction was carried out using 2 wt.% $ZnFe_2O_4$ (with respect to oil) at a typical condition (65 °C, 180 min) with excess methanol (methanol:oil molar ratio: 9:1). We could separate the majority of the catalysts from the product by a simple magnet. With the aid of additional centrifugation, we obtained a single phase. To break the emulsion and wash the product, we added water to the crude product. Eventually, we obtained two separate phases, which are rich in glycerol and biodiesel. Fourier-Transform Infrared spectroscopy (FTIR) analyses further confirmed that biodiesel was rich in characteristic methyl ester and ester absorption bands. Accordingly, we identified fatty acid methyl esters (FAMEs) and several other ester compounds by Gas Chromatography-Mass Spectrometry (GC-MS). We are currently in the process of making the hybrids of these catalysts with more affordable co-catalysts and support materials to further reduce its cost.

ORCID:
Yasemin Fatih Aghdaei: 0000-0003-0453-212X
Cansu Yıldırım: 0000-0003-1023-4030
Hüseyin Enis Karahan: 0000-0002-7753-1024

Keyword: *magnetic nanoparticles, biofuel, sustainability*

Synergistic Enhancement of Uranium Adsorption Kinetics and Selectivity through In Situ Growth of ZIF-8 on Amidoxime-Functionalized Polyacrylonitrile Membranes

Taha Furkan Gül[1], Zehra Sisman [* 1], Sabriye Yusan[1], Sule Aytas[1], Nalan Kabay[2]

[1] Institute of Nuclear Sciences, Ege University, 35100, Bornova-Izmir, Türkiye
[2] Faculty of Engineering, Chemical Engineering Department, Ege University, Bornova-Izmir, Türkiye

Selective uranium recovery and removal have become important research topics owing to the growing demand for efficient remediation and resource utilization technologies. Due to their strong and selective binding affinity toward uranyl (UO_2^{2+}) ions, amidoxime-functionalized adsorbents have been thoroughly studied for uranium sequestration and recovery [1,2]. However, despite the high selectivity of these materials, mass-transfer limitations and restricted access to active sites frequently lower their adsorption rates [3]. In this study, in order to overcome these limitations, ZIF-8@AO-PAN composite membranes were subsequently prepared by amidoxime functionalization of polyacrylonitrile membranes followed by in situ growth of ZIF-8 crystals on the membrane surface through sequential Zn^{2+} adsorption and ligand coordination (Figure 1). FTIR, SEM-EDS, and XPS characterization confirmed that ZIF-8 was successfully integrated into the membrane while preserving its structural integrity. The prepared composite membranes improved both the adsorption kinetics and selectivity toward UO_2^{2+} ions by combining the rapid mass-transfer characteristics offered by the porous ZIF-8 with the high uranyl-chelating capacity of amidoxime groups. As a result, the pseudo-second-order rate constant increased from 5.0×10^{-5} g/mg.min for AO-PAN to 2.26×10^{-4} g/mg.min for ZIF-8@AO-PAN, representing an approximately 4.5-fold enhancement in adsorption kinetics. The findings indicate a synergistic effect, where the highly porous structure of ZIF-8 enhances adsorption kinetics, while amidoxime groups are primarily responsible for the selective binding of UO_2^{2+}.

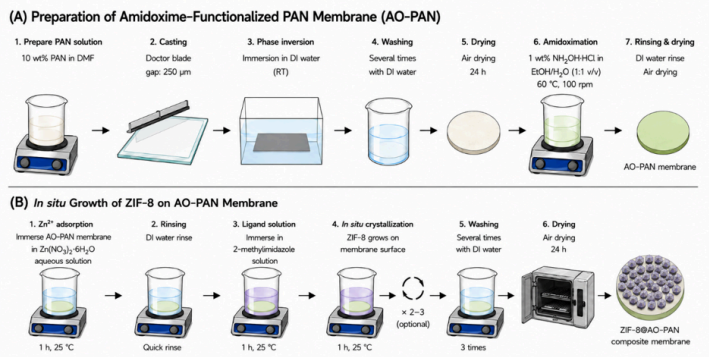


Figure 1. Preparation procedure of **(a)** AO-PAN, **(b)** ZIF-8@AO-PAN.

Acknowledgment:
This study was supported by the Scientific and Technological Research Council of Türkiye (TÜBİTAK) under the 1002-A Program (Project No: 225M166).

References:

[1] Abney, C.W.; Mayes, R.T.; Saito, T.; Dai, S. Materials for the Recovery of Uranium from Seawater. Chem. Rev. 2017, 117, 13935–14013.https://doi.org/10.1021/acs.chemrev.7b00355
[2] Xie, Y.; Liu, Z.; Geng, Y.; Li, H.; Wang, N.; Song, Y.; Wang, X.; Chen, J.; Wang, J.; Ma, S.; Ye, G. Uranium Extraction from Seawater: Material Design, Emerging Technologies and Marine Engineering. Chem. Soc. Rev. 2023, 52, 97–162.https://doi.org/10.1039/D2CS00595F
[3] Wang, H.; Yao, W.; Yuan, Y.; Shi, S.; Liu, T.; Wang, N. Yeast-Raised Polyamidoxime Hydrogel Prepared by Ice Crystal Dispersion for Efficient Uranium Extraction from Seawater. Adv. Sci. 2024, 11, e2306534. https://doi.org/10.1002/advs.202306534

Keyword: *Uranium adsorption, Amidoxime-functionalized membrane, ZIF-8*

Co-Doped TiO_2 Nanorods for Triple-Cation Perovskite Solar Cells: From Synthesis to Device Application

Şeydanur Kaya [*1,2], **Andrés-Felipe Castro-Méndez**[2], **Felix Lang**[2]

[1] *Central Research Laboratory, Kastamonu University, 37100, Kastamonu, Turkiye*
[2] *Institute of Physics and Astronomy, University of Potsdam, 14476 Potsdam, Germany*

Perovskite solar cells (PSCs) have emerged as one of the most promising photovoltaic technologies owing to their high power conversion efficiencies and low fabrication costs. Among the various device components, the electron transport layer (ETL) plays a critical role in facilitating charge extraction and minimizing carrier recombination. In this context, the development of well-defined one-dimensional TiO_2 nanostructures with enhanced electronic and interfacial properties is of significant interest. In this study, undoped and cobalt (Co) doped TiO_2 nanorods were synthesized via a hydrothermal method and employed as electron transport layers in triple-cation perovskite solar cells. The incorporation of cobalt resulted in notable improvements in the morphological and optical properties of the TiO_2 nanorods, leading to more uniform and vertically aligned nanorod arrays. Triple-cation perovskite, $Cs_{0.05}(FA_{0.83}MA_{0.17})Pb(I_{0.83}Br_{0.17})_3$, was used as the absorber layer. Structural characterization revealed the formation of a high-quality interface between the perovskite layer and the TiO_2 nanorods without detectable secondary PbI_2 phases, indicating efficient crystal growth and phase purity. Photovoltaic measurements showed that devices incorporating undoped TiO_2 nanorods exhibited relatively modest performance. In contrast, Co-doped TiO_2 nanorods promoted more efficient charge transport and suppressed recombination processes, resulting in enhanced photovoltaic characteristics. The best-performing device, based on 5% Co-doped TiO_2 nanorods, achieved a power conversion efficiency (PCE) of 15% and an open-circuit voltage (Voc) of 1.19 V. These findings demonstrate that cobalt incorporation effectively enhances the functionality of TiO_2 nanorod-based electron transport layers, representing a promising strategy for improving the performance of triple-cation perovskite solar cells.

Acknowledgment:
S.K. acknowledges TÜBİTAK under the 2219 International Postdoctoral Research Fellowship Program. F.L. acknowledges funding from the Volkswagen Foundation via the Freigeist Programme.

ORCID:
Şeydanur Kaya: 0000-0002-6894-9082
Andrés-Felipe Castro-Méndez: 0000-0001-8320-353X
Felix Lang: 0000-0001-9711-380X

Keyword: *Perovskite Solar Cells, Cobalt-Doped TiO_2 Nanorods, Electron Transport Layer*

A Conjugated Polymer-Based Asymmetric Supercapacitor With Integrated Electrochromic Functionality

Asude Gürsoy [*] [1], Eminenur Baran[1], Elif Demir Arabacı[1], Ali Çırpan[1,2,3,4]

[1] Middle East Technical University, Department of Chemistry, 06800, Ankara, Turkey
[2] Middle East Technical University, Department of Polymer Science and Technology, 06800, Ankara, Turkey
[3] Middle East Technical University, ODTU GUNAM, 06800 Ankara, Turkey
[4] Middle East Technical University, Department of Micro and Nanotechnology, 06800, Ankara, Turkey

Supercapacitors have emerged as promising energy storage devices owing to their high-power density, rapid charge-discharge rates, and long cycle life. To further enhance performance and functional diversity, conjugated polymers are increasingly employed due to their tunable properties. This project aims to develop a high-performance, multifunctional asymmetric hybrid electrochromic supercapacitor device (AESD) utilizing a TPA-core monomer, TPA-TT (triphenylamine functionalized with thienothiophene), as the anode material paired with a PEDOT cathode. TPA-TT is synthesized via n-BuLi-mediated stannylation of thienothiophene followed by palladium-catalyzed Stille cross-coupling with a brominated triphenylamine derivative. The methodology follows a three-stage approach: electropolymerization of the monomer onto ITO-coated glass to yield a polymer film, device assembly using a PMMA-based gel electrolyte ensuring ionic conductivity between electrodes, and comprehensive characterization via CV, GCD, and EIS techniques. A defining feature of this device is its dual functionality-serving simultaneously as an energy storage unit and an electrochromic display. The distinct color changes of the TPA-TT and PEDOT layers during redox cycling provide a visual indicator of the state-of-charge, enabling monitoring without external instrumentation. The asymmetric configuration expands the operating voltage window through complementary redox-active polymer electrodes, thereby enhancing energy storage performance. Furthermore, the fully organic, metal-free composition offers advantages in environmental sustainability, processability, and mechanical flexibility.

Overall, this work demonstrates the potential of conjugated polymer-based AESDs as multifunctional systems integrating energy storage with optical functionality, offering a promising framework for next-generation smart devices in wearable electronics and flexible optoelectronics.

Acknowledgment:
This study was supported by the Scientific and Technological Research Council of Turkey (TUBITAK) under Grant Number 124Z087, and by AdımODTÜ within the scope of the Undergraduate Research Program. The authors gratefully thank both organizations for their support.

References:
Cevher, D., & Cirpan, A. (2025). Design, strategies and recent advances in conjugated polymers for supercapacitors. Journal of Energy Storage, 109, 115246. https://doi.org/10.1016/j.est.2024.115246
Xie, Y., Zhang, Y., Zhu, M., Huang, R., & Chao, D. (2023). High-performance electrochromic supercapacitor based on a new EDOT–triphenylamine conjugated polymer. Dyes and Pigments, 208, 110889. https://doi.org/10.1016/j.dyepig.2022.110889
Choudhary, N., Li, C., Moore, J., Nagaiah, N., Zhai, L., Jung, Y., & Thomas, J. (2017). Asymmetric supercapacitor electrodes and devices. Advanced Materials, 29(21), 1605336. https://doi.org/10.1002/adma.201605336
Pholauyphon, W., Charoen-amornkitt, P., Suzuki, T., & Tsushima, S. (2024). Guidelines for supercapacitor electrochemical analysis: A comprehensive review of methodologies for finding charge storage mechanisms. Journal of Energy Storage, 98(Part A), 112833. https://doi.org/10.1016/j.est.2024.112833

Keyword: *Asymmetric supercapacitors, Conjugated polymers, Electrochromism*

Injectable MXene-Based Composite Hydrogels for Photothermal Cancer Therapy

Berivan Polat * **, Gökçen Birlik Demirel**

Ankara Hacı Bayram Veli University

Breast cancer remains one of the most common types of cancer among women worldwide[1]. Traditional treatments such as surgery, chemotherapy, and radiotherapy have limitations including systemic toxicity, damage to healthy tissues, high recurrence rates, and treatment resistance. To overcome these challenges, photothermal therapy (PTT) has emerged as a promising approach for localized and minimally invasive cancer treatment. In this method, near-infrared (NIR) absorbing nanomaterials convert light into heat, selectively destroying tumor cells while protecting surrounding healthy tissue[2-4]. In this study, an injectable hydrogel platform was developed for the localized delivery of photothermal nanomaterials. Two naturally derived polymers, oxidized alginate (AlgOX) and N-succinyl chitosan (NS-CS), were synthesized via a dynamic Schiff base reaction and cross-linked to obtain a biocompatible three-dimensional hydrogel network that rapidly hydrogels under physiological conditions. Two-dimensional MXene nanomaterials, characterized by strong NIR absorption and high photothermal conversion efficiency, were incorporated into a hydrogel matrix to function as a photothermal agent. The photothermal therapeutic efficacy of the prepared nanocomposite hydrogel system was systematically evaluated through in vitro studies.

References:

[1] Cao, W., Qin, K., Li, F., & Chen, W. (2024). Comparative study of cancer profiles between 2020 and 2022 using global cancer statistics (GLOBOCAN). Journal of the National Cancer Center, 4(2), 128-134.

[2] Oudjedi, F., & Kirk, A. G. (2025). Near-infrared nanoparticle-mediated photothermal cancer therapy: a comprehensive review of advances in monitoring and controlling thermal effects for effective cancer treatment. Nano Select, 6(3), e202400107.

[3] Shi, Y., Zhu, H., Li, C., Hou, Y., Su, Y., Zhao, J., ... & Xue, J. (2025). Multifunctional injectable hydrogel incorporated with CuS nanoparticles for concurrent photothermal-chemotherapy, breast cancer recurrence prevention and wound healing. Colloids and Surfaces A: Physicochemical and Engineering Aspects, 725, 137612.

[4]S. M. Yang vd., “MXene/Doxorubicin Complex-Loaded Supramolecular Hydrogels for Near Infrared-Triggered Synergistic Cancer Therapy”, Biomater. Res., c. 29, s. 0163, Oca

Keyword: *injectable hydrogel, photothermal therapy, Mxene*

MXene-Based Nanocomposite Ionogels for Flexible Wearable Strain Sensors

Büşra Çevik * **, Gökçen Birlik Demirel**

Ankara Hacı Bayram Veli University

Flexible electronic devices are rapidly evolving in applications such as wearable sensors, human motion detection[1], electronic skin,[2] and soft robotics[3]. In these systems, strain sensors are crucial because they convert mechanical deformations into electrical signals for real-time monitoring of physiological movements. Compared to traditional rigid and metallic sensors, hydrogel-based sensors are attractive due to their soft, skin-like structure and natural flexibility, allowing them to conform closely to the body. However, their high water content makes them susceptible to dehydration upon prolonged exposure to air and freezing at low temperatures, leading to reduced flexibility and impaired sensing performance, thus weakening their long-term reliability. While ionic liquid-based systems have been developed to overcome these challenges, the increasing demand for more environmentally friendly and cost-effective alternatives has positioned deep eutectic solvents (DESs) as particularly promising substitutes[4]. In this study, MXene-enhanced ionogels were developed using acrylamide (AAm) and 2-acrylamido-2-methyl-1-propanesulfonic acid (AMPS) monomers in a choline chloride/urea-based DES. The addition of MXene increased both the electrical conductivity and mechanical strength of the resulting ionogel system. The performance of the developed MXene-based ionogel was systematically investigated for wearable sensor applications.

References:

1. Wen, X., Deng, Z., Wang, H., Shi, J., Wang, S., Wang, H., ... & Cheng, X. (2023). High strength, self-healing sensitive ionogel sensor based on MXene/ionic liquid synergistic conductive network for human-motion detection. Journal of Materials Chemistry B, 11(47), 11251-11264.
2. Sun, J., Li, R., Lu, G., Yuan, Y., Zhu, X., & Nie, J. (2020). A facile strategy for fabricating multifunctional ionogel based electronic skin. Journal of Materials Chemistry C, 8(25), 8368-8373.
3. Zhang, M., Yu, R., Tao, X., He, Y., Li, X., Tian, F., ... & Huang, W. (2023). Mechanically robust and highly conductive ionogels for soft ionotronics. Advanced Functional Materials, 33(10), 2208083.
4. Abbott, A. P., Boothby, D., Capper, G., Davies, D. L., & Rasheed, R. K. (2004). Deep eutectic solvents formed between choline chloride and carboxylic acids: versatile alternatives to ionic liquids. Journal of the American Chemical Society, 126(29), 9142-9147.

Keyword: *Ionogel, Strain sensor, Mxene*

Design and Synthesis of A Dual-Function Phenyl-Linked Carbazole-Based Polymer for Supercapacitors

Dilan Akdeniz [*] [1], **Elif Demir Arabacı**[1], **Ali Çırpan**[1,2,3,4]

[1] *Middle East Technical University, Department of Chemistry, 06800, Ankara, Turkey*
[2] *Middle East Technical University, Department of Polymer Science and Technology, 06800, Ankara, Turkey*
[3] *Middle East Technical University, ODTU GUNAM, Ankara, 06800, Turkey*
[4] *Middle East Technical University, Department of Micro and Nanotechnology, Ankara, 06800, Turkey*

Supercapacitors bridge the gap between conventional capacitors and batteries owing to their rapid charge-discharge capability, long cycle life, and environmentally friendly nature. As increasing global energy demand and the transition toward sustainable energy systems drive the need for advanced energy-storage technologies, supercapacitors have emerged as promising candidates.

Among various electrode materials, conjugated polymers have attracted considerable attention because their delocalized π-electron networks provide electrical conductivity and high charge-storage capability while maintaining low cost, light weight, facile synthesis, and excellent processability.

This study aims to develop a multifunctional conjugated polymer based on a phenyl-linked carbazole-thiophene-3,4 ethylenedioxythiophene (EDOT) framework for supercapacitor applications. The molecular architecture was designed to enhance pseudocapacitive energy storage through multicenter redox processes and efficient charge transport while simultaneously providing reversible electrochromic properties for real-time state-of-charge monitoring. The target monomer was synthesized through Stille cross-coupling and Buchwald–Hartwig coupling reactions, in which thiophene and EDOT units were introduced onto the carbazole core and the carbazole moieties were linked via a phenyl bridge. Electropolymerization was subsequently carried out on indium tin oxide (ITO)-coated glass electrodes using cyclic voltammetry. The optical, and electrochemical performance of the resulting polymer film was evaluated by UV-Vis spectrometry, cyclic voltammetry (CV).

ORCID:
Elif Demir Arabacı: https://orcid.org/0000-0002-3406-135X
Ali Çırpan: https://orcid.org/0000-0003-3051-8380
Ali Çırpan: https://orcid.org/0000-0003-3051-8380
Ali Çırpan: https://orcid.org/0000-0003-3051-8380
Ali Çırpan: https://orcid.org/0000-0003-3051-8380

References:
Ates, M., & Uludag, N. (2016). Carbazole derivative synthesis and their electropolymerization. Journal of Solid-State Electrochemistry, 20(9), 2599–2612. https://doi.org/10.1007/s10008-016-3269-0
Beaujuge, P. M., & Reynolds, J. R. (2010). Color control in π-conjugated organic polymers for use in electrochromic devices. Chemical reviews, 110(1), 268-320.
Liu, J., Hou, W., Xu, R., Gao, Y., Xu, L., Jiang, L., & Zhang, C. (2022). Synthesis and electrochemical properties of donor–acceptor-conjugated polymers based on carbazole-EDOT derivatives with different electron-withdrawing groups. ACS Applied Polymer Materials, 4(3), 2132–2139. https://doi.org/10.1021/acsapm.2c00087

Keyword: *Supercapacitors, Conjugated polymers, Carbazole-based polymer, Energy storage*

Design and Synthesis Cyano-Functionalized Triphenylamine-Based Monomer for Supercapacitor Application

Gülten Yıldırım [*1], Sedanur Şahinaslan[2], Oğuzhan Karakurt[2], Ali Çırpan[2,3,4,5]

[1] *Middle East Technical University, Department of Chemistry Education, 06800, Ankara, Turkey*
[2] *Middle East Technical University, Department of Chemistry, 06800, Ankara, Turkey*
[3] *Middle East Technical University, Department of Polymer Science and Technology, 06800, Ankara, Turkey*
[4] *Middle East Technical University, ODTU GUNAM, Ankara, 06800, Turkey*
[5] *Middle East Technical University, Department of Micro and Nanotechnology, Ankara, 06800, Turkey*

As portable electronics, electric vehicles, and renewable energy systems continue to grow, the demand for efficient energy storage technologies is increasing. Supercapacitors bridge the gap between conventional capacitors and batteries by combining high power density, fast charge–discharge rates, and long cycle life. Among them, asymmetric supercapacitors offer improved energy and power performance through the combination of different electrode materials. This project aims to develop an asymmetric supercapacitor using a conjugated polymer incorporating triphenylamine (TPA) as an acceptor unit, 3-cyanothiophene as a π-bridge to enhance conjugation and charge distribution, and EDOT as donor unit. The incorporation of a cyano (-CN) group lowers the LUMO level of the resulting polymer, increasing redox reversibility and electrochemical stability. The device consists of a P1/ITO anode, a V_2O_5/ITO cathode, and a gel electrolyte, combining the polymer's fast charge-discharge capability with the high capacitance of V_2O_5 to achieve balanced energy and power density. The target monomer (M1) was synthesized through a multistep route introducing EDOT and cyanothiophene units onto a TPA core via successive Buchwald-Hartwig coupling, bromination, and Stille cross-coupling reactions. Structural confirmation was carried out using NMR spectroscopy and HRMS. The optoelectronic properties of the monomer were investigated by UV-Vis absorption spectroscopy, while its electrochemical behavior was examined by CV. Overall, the results suggest that the synthesized conjugated polymer is a promising candidate for asymmetric supercapacitor applications owing to its favorable optoelectronic and electrochemical properties.

Acknowledgment:
This study was supported by Scientific and Technological Research Council of Turkey (TUBITAK) under the Grant Number 124Z087. The authors thank TUBITAK for their supports.

References:
Cevher, D., Cevher, S. C., Toppare, L., & Cirpan, A. (2023). Enhancing electrochromic supercapacitor electrode performance through different donor compartments in DAD type conjugated polymers. Journal of Energy Storage, 74, 109501.
Rajagopal, R., Lee, Y. S., Ryu, K. S. 2017. “Synthesis and electrochemical analysis of Nb2O5-TiO2/H-rGO sandwich type layered architecture electrode for supercapacitor application”. Chemical Engineering Journal, 325, 611-623.
Lee, J. H., Yang, G., Kim, C. H., Mahajan, R. L., Lee, S. Y., & Park, S. J. (2022). Flexible solid-state hybrid supercapacitors for the internet of everything (IoE). Energy & Environmental Science, 15(6), 2233-2258.

Keyword: *Conjugated polymers, Electrochromism, Supercapacitors*

Nanoadhesive Polymer Coating Development for Enhanced Grip on Complex 3D Surfaces

Melike Nur Öz * **, Göksu Yağız, Merve Karabıyık, Özgenç Ebil**

Departmentof Chemical Engineering, Izmir Institute of Technology, Izmir, Türkiye

This study focuses on the development of iCVD-based nano-adhesive polymer coatings for enhanced adhesion on complex three-dimensional surfaces under mild processing conditions. Functional polymer thin films based on poly(glycidyl methacrylate) (pGMA), poly(glycidyl methacrylate-co-diethylaminoethyl acrylate) [p(GMA-co-DEAEA)], and poly(glycidyl methacrylate-co-diethylaminoethyl methacrylate) [p(GMA-co-DEAEMA)] were deposited using initiated Chemical Vapor Deposition (iCVD). This solvent-free technique enabled conformal polymer coating formation while preserving reactive epoxy and amine-related functional groups required for interfacial bonding. Epoxy ring-opening modification was performed using ethylenediamine (EDA) to introduce amine functionalities onto the polymer surfaces. The deposited coatings were characterized by thickness measurements, FTIR, TGA, EDX, optical microscopy, and SEM. FTIR results confirmed the successful deposition of the targeted polymer coatings, while EDX analysis indicated successful amine functionalization after EDA treatment. TGA results showed that the coatings had sufficient thermal stability for the bonding and durability tests. Adhesion performance was evaluated by manual separation ranking, microscopic failure analysis, weight-based load-bearing tests, solvent resistance, hydrolytic stability, and thermal stability tests. Among the investigated systems, pGMA-pGMA and pGDM-pGDM showed promising adhesion behavior; however, pGDM-pGDM failed during solvent and water immersion tests. In contrast, pGMA-pGMA demonstrated superior chemical, hydrolytic, and thermal durability. After thermal treatment at 200 °C for 3 h, the pGMA-pGMA bonded sample supported 7.7 kg, corresponding to 377.7 kPa for a 2 cm^2 bonded area. The selected pGMA-based strategy was also applied to PDMS integration on three dimensional nickel foam, demonstrating its potential for complex surface bonding. Overall, this study presents a solvent-free, low-temperature, and conformal nano-adhesive coating approach for advanced surface engineering applications.

Acknowledgment:
This studywas supported by TÜBİTAK 2209-A(ProjectNo:1919B012505754)

References:
Moni,P.,Al-Obeidi,A.,&Gleason,K.K. (2017).Vapordepositionroutestoconformalpolymer thinfilms.Beilstein JournalofNanotechnology,8,723-735.
PryceLewis,H.G.,Lau,K.K.S.,Mao,Y.,&Gleason,K.K. (2005). Initiatedchemicalvapordeposition(iCVD)of polymerthinfilms.In48thAnnualTechnicalConferenceProceedingsoftheSocietyofVacuumCoaters(pp.90-94).
Bakker,R.,Verlaan,V., vanderWerf,C.H.M.,Rath, J.K.,Gleason,K.K.,&Schropp,R.E. I. (2007). Initiated chemicalvapourdeposition(iCVD)ofthermallystablepoly(glycidylmethacrylate).SurfaceandCoatingsTechnology, 201(22-23),9422-9425.
Muzammil, E. M., Khan, A., Stuparu, M. C. Post-polymerization modification reactions of poly(glycidyl methacrylate)s. RSC Adv, 2017, 7(88):55874–55884

Keyword: *Initiated Chemical Vapor Deposition (iCVD), Poly(glycidyl methacrylate) (pGMA), Nano-adhesive polymer coatings*

Quinoline-Based Porous Organic Polymers for Enhanced CO_2 Uptake and Catalytic Conversion

Mustafa Erdogmus * **, Mehmet Anil Arapoglu, Batu Sercan Canturk, Yasmin Gecalp, Onur Büyükcakir**

Izmir Institute of Technology, Department of Chemistry, Izmir, Türkiye

The increase in atmospheric CO_2 levels, caused by fossil fuel consumption and industrial activities, is one of the main contributors to global warming and climate change. For this reason, the development of efficient materials for CO_2 capture has become an important research area.[1] Furthermore, the conversion of CO_2 into valuable chemicals is also highly important and offers a more sustainable route for carbon utilization.[2] In this work, quinoline-based porous organic polymers were prepared to obtain nitrogen-rich frameworks, which were then further modified by post-synthetic ionic functionalization to generate charged frameworks. The incorporation of ionic sites was aimed at improving the polymer's affinity for CO_2 while introducing active sites for catalytic reactions.

The charged polymers were tested as a heterogeneous catalyst for the cycloaddition of CO_2 with epoxides to form cyclic carbonates.[3] Compared with the neutral porous organic polymers, the charged frameworks exhibited better catalytic activity under relatively mild reaction conditions. Overall, the results show that post-synthetic ionic functionalization is a practical strategy for developing porous polymers that combine CO_2 adsorption with catalytic conversion.

Acknowledgment:
The authors gratefully acknowledge the Scientific and Technological Research Council of Türkiye (TÜBİTAK) for supporting this work under Project No. 123Z550 and through the 2211/A National PhD Scholarship Program.

ORCID:
Mustafa Erdogmus: 0000-0001-6586-1846

References:
[1] Wang, C.; Wang, M.; Lin, R. B.; Wang, B.; Chen, B. Sorption of Carbon Dioxide in Porous Metal–Organic Frameworks and Porous Organic Polymers. Coord. Chem. Rev. 2021, 426, 213479.
[2] Song, K. S.; Fritz, P. W.; Coskun, A. Porous Organic Polymers for CO_2 Capture, Separation and Conversion. Chem. Soc. Rev. 2022, 51, 9831–9852
[3] Büyükçakır, O.; Je, S. H.; Talapaneni, S. N.; Kim, D.; Coskun, A. Charged Covalent Triazine Frameworks for CO_2 Capture and Conversion. ACS Appl. Mater. Interfaces 2017, 9, 7209–7216.

Keyword: *porous organic polymers, CO2 capture and conversion, environmental remediation*

Fabrication And Characterization Of PVDF-HFP Nanofiber-Reinforced Composite Sponges For Biomedical Applications

Ozlem Ceren Aktas [* 1], Aylin Ziylan Albayrak[1], Oylum Colpankan Gunes[1], Taner Goktas[2], Neslihan Sakar[3]

[1] Dokuz Eylul University, Department of Metallurgical and Materials Engineering, Buca, Izmir / Turkiye
[2] Dokuz Eylul University, Department of Electrical and Electronics Engineering, Buca, Izmir / Turkiye
[3] Dokuz Eylul University, Center for Fabrication and Application of Electronic Materials, Buca, Izmir / Turkiye

Natural polymer-based hydrogels are widely used in biomedical applications such as wound dressings, tissue engineering, and drug delivery systems due to their high water retention capacity, three-dimensional porous structure, and biocompatibility [1]. However, their poor mechanical strength poses a major limitation for applications requiring long-term structural stability [2]. In this study, a three-dimensional nanofiber-reinforced composite structure was designed to enhance the mechanical performance of hydrogel systems while simultaneously introducing functional properties. For this purpose, composite sponges were fabricated by incorporating wet-electrospun poly(vinylidene fluoride-co-hexafluoropropylene) (PVDF-HFP) nanofibers into a hydrogel matrix composed of highly biocompatible silk fibroin and water-soluble O-carboxymethyl chitosan [3], [4]. PVDF-HFP was selected as the reinforcing phase due to its flexibility, biocompatibility, and inherent piezoelectric properties [5] . Three-dimensional nanofibers were produced via wet electrospinning, a technique that has not previously been reported for PVDF-HFP. This approach enabled the formation of three-dimensional cotton-wool-like nanofibrous structures. The obtained nanofibers were incorporated into the hydrogel matrix solution and homogeneously distributed throughout the matrix, followed by chemical crosslinking using poly(ethylene glycol) diglycidyl ether (PEGDE) [4]. The resulting composite hydrogels were subsequently converted into sponge-like structures through lyophilization. The chemical properties of the wet-electrospun PVDF-HFP nanofibers and PVDF-HFP nanofiber reinforced composite sponges were investigated by attenuated total reflectance-Fourier transform infrared (ATR-FTIR) spectroscopy, their morphological characteristics were examined by scanning electron microscopy (SEM), and mechanical behavior was determined by texture profile analysis (TPA). Also, the piezoelectric performance of the composite sponges under mechanical loading was evaluated using an oscilloscope, while their swelling characteristics were investigated in PBS. The results demonstrated the effective integration of the three-dimensional nanofiber network into the hydrogel matrix and its homogeneous distribution throughout the structure. Furthermore, compared to the neat hydrogel matrix, the PVDF-HFP nanofiber-reinforced composite sponges exhibited enhanced mechanical properties and piezoelectric activity. In conclusion, fabricated PVDF-HFP nanofiber-reinforced composite sponges exhibit features that make them promising candidates for tissue engineering and smart wound-dressing applications.

Acknowledgment:
This study was supported by TUBITAK under the 1002-A Short-Term Support Module (Project No: 225M255).

ORCID:
Aylin Ziylan Albayrak: 0000-0003-4137-5696
Oylum Colpankan Gunes: 0000-0002-2440-3256
Taner Goktas: 0000-0002-8218-3239

References:
[1] Kamoun, E. A., Kenawy, E. R. S., Chen, X. 2017. “A review on polymeric hydrogel membranes for wound dressing applications: PVA-based hydrogel dressings,” Journal of Advanced Research, 8(3), 217–233.
[2] Wang, W., Ummartyotin, S., Narain, R. 2023. “Advances and challenges on hydrogels for wound dressing,” Current Opinion in Biomedical Engineering, 26, 100443.
[3] Veronica, A., Hsing, I. M. 2021. “An insight into tunable innate piezoelectricity of silk for green bioelectronics,” ChemPhysChem, 22(22), 2266–2280.
[4] Gunes, O. C., Albayrak, A. Z., Tasdemir, S., Sendemir, A. 2020. “Wet-electrospun PHBV nanofiber reinforced carboxymethyl chitosan-silk hydrogel composite scaffolds for articular cartilage repair,” Journal of Biomaterials Applications, 35(4–5), 515–531.
[5] Zhang, Z., Liu, L., Wang, H., Xie, W., Zhai, W., Wen, L., Zhang, B., Liu, K., Zhang, X., Liu, S., Huang, L., Li, D., Zhou, Y. “LIPUS Responsive Dopamine-Modified PVDF Piezoelectric Nanofiber Membrane for Full-Thickness Skin Wound Healing,” Int J Nanomedicine, 20:5693-5707.

Keyword: *PVDF-HFP Nanofiber, Hydrogel, Wet Electrospinning*

Injectable Hydrogels for Controlled Delivery of Allocryptopine in Alzheimer's Disease

Simge Koç * [1], Gökçen Birlik Demirel[1], Belma Aslım[2], Mine Türktaş[2], Büşra Aktaş Mansuroğlu[2], Filiz Kardiyen[2], Serap Niğdelioğlu Dolanbay[2], Zehra Kübra Yılmaz[2]

[1] Ankara Hacı Bayram Veli University
[2] Gazi University

Treatment of Alzheimer's disease (AD) is severely limited by the blood-brain barrier (BBB), which restricts the access of most therapeutic agents to the brain, along with the low bioavailability, poor pharmacokinetic profiles, and undesirable side effects of conventional drugs[1]. These limitations have spurred the development of localized, controlled-release delivery systems. In this context, hydrogels have emerged as particularly promising carriers, owing to the high water-holding capacity of their three-dimensional network structures and, depending on the polymers used, their biocompatibility, biodegradability, and low toxicity. Injectable hydrogels are especially advantageous for local applications. Applied in liquid form, these hydrogels create a hydrogel in situ at the target site, enabling a minimally invasive procedure. They can provide a continuous and controlled release of the loaded therapeutic agent[2,3].

Based on this motivation, an injectable hydrogel system was designed using N-succinyl chitosan (NS-CS) polymer and polyethylene glycol dibenzaldehyde (diBA-PEG) polymer as gel precursor components. Nanoencapsulated allocryptopine therapeutic molecules were integrated into this biocompatible injectable hydrogel system. The resulting nanocomposite injectable hydrogel system was subsequently subjected to comprehensive chemical and mechanical characterization. In addition, the potential for localized and controlled drug delivery of this nanocomposite injectable hydrogel system has been evaluated.

Acknowledgment:
This work is supported by Gazi University (Grant Number: FGA-2025-9961)

References:
Nunes, D., Loureiro, J. A., & Pereira, M. C. (2022). Drug delivery systems as a strategy to improve the efficacy of FDA-approved Alzheimer's drugs. Pharmaceutics, 14(11), 2296.
Xie, B., & Xie, H. (2024). Application of stimuli-responsive hydrogel in brain disease treatment. Frontiers in Bioengineering and Biotechnology, 12, 1450267.
Kang, N. W., Yoon, S. Y., Kim, S., Yu, N. Y., Park, J. H., Lee, J. Y., ... & Kim, D. D. (2021). Subcutaneously injectable hyaluronic acid hydrogel for sustained release of donepezil with reduced initial burst release: Effect of hybridization of microstructured lipid carriers and albumin. Pharmaceutics, 13(6), 864.

Keyword: *Alzheimer's Disease, Injectable Hydrogel, Controlled Drug Delivery*

Mechanical Performance and Degradation Behavior of 3D-Printed Biodegradable Graded Gyroid Bone Scaffolds with Hierarchical Porosities

Duygu Üçüncü, Miray Dereli, Nehir Heppekcan, Sinem Gülseroğlu * , Fatih Büyükserin, Mervenaz Şahin

TOBB ETU, Biomedical Engineering

3D-printed nanostructures are increasingly utilized to understand and advance the mechanical behavior of biomedical implants. To provide insight into this, this study evaluates the mechanical performance and in vitro degradation behavior of 3D-printed polylactic acid (PLA)-based gyroid scaffolds with hierarchical porosity from nano to macro, with both uniform and porosity gradient architectures. Bone tissue engineering necessitates scaffolds that offer high surface-area-to-volume ratios and interconnected porosity while maintaining structural integrity. Utilizing nTop software for gyroid scaffold design and fused filament fabrication (FFF) for fabrication, scaffolds were developed at porosity levels of 20%, 45%, and 70% of uniform (GUS) and graded gyroid (GGS) structures. The GGS groups featured a linear porosity gradient along the z-axis (20% to 70%) to mimic the transition from cortical to trabecular bone. The specimens underwent a 6-week degradation in phosphate-buffered saline (PBS) at 37˚C. Results indicated high chemical stability, characterized by minimal mass loss (<3%) and stable pH values (7.40–7.90), suggesting the early induction phase of hydrolytic degradation. Mechanical characterization demonstrated that while high-porosity scaffolds aligned with human trabecular bone (50–500 MPa modulus) , scaffolds with 70% porosity exhibited peak stress values of 5.43–5.56 MPa, falling precisely within the reported range for natural trabecular bone (2–8 MPa). Simultaneously, scaffolds with lower porosity achieved higher stiffness (up to 776 ± 10 MPa), approaching cortical bone values. Notably, degraded samples exhibited higher peak stress values (e.g., for GGS with 20% porosity increasing from 21.12 MPa to 24.92 MPa). This phenomenon is attributed to the preferential hydrolytic cleavage of amorphous regions in PLA, which increases overall crystallinity—effectively acting as an in-situ annealing process. Furthermore, functionally graded scaffolds demonstrated superior mechanical stability over uniform designs. At a 45% porosity level, uniform scaffolds exhibited a significantly higher compressive modulus compared to graded structures ($p < 0.001$), whereas this difference was non-significant at the 70% porosity level ($p = 0.154$). Their spatial gradients allowed for more even distribution of hydrolytic stresses. These findings confirm that 3D-printed PLA-based gyroid scaffolds, particularly graded architectures, possess the necessary mechanical and degradation characteristics to successfully mimic the functional properties of natural bone.

ORCID:
Fatih Büyükserin: 0000-0001-6365-3808
Mervenaz Şahin: 0000-0002-2627-8970

Keyword: *Graded gyroid bone scaffold, 3D printing, Degradation-related mechanical properties*

Cargo Transportation via Magnetically Responsive Soft Robotic Platforms

Sudenaz Ergen * **, Kubra Ozkan Hukum, Gorkem Liman, Gokhan Demirel**

Bio-inspired Materials Research Laboratory (BIMREL), Department of Chemistry, Gazi University, 06500 Ankara, Turkey

Soft robots adopt more flexible designs compared to conventional rigid structures. Unlike their rigid counterparts, they can be fabricated from flexible materials such as polymers, shape-memory alloys, hydrogels, and liquid metals. Owing to these properties, soft robots exhibit enhanced adaptability and mobility, enabling them to perform complex tasks effectively. Although these systems have been widely utilized in fields such as personalized medicine, smart electronics, and sensing, challenges remain in integrating functional components with diverse material compositions into soft robotic systems. In this study, paper-based magnetic films were fabricated, and the cargo-carrying capacities of robotic structures designed using these films were systematically analyzed. Furthermore, the influence of structural design parameters on cargo-carrying performance was investigated to reveal their potential for practical real-world applications.

Acknowledgment:
This work was supported by the Scientific and Technological Research Council of Türkiye (TUBITAK), 2209-A Research Project Support Program for Undergraduate Students (grant no: 1919B012404297)

ORCID:
Sudenaz Ergen: https://orcid.org/0009-0000-3985-8133
Kubra Ozkan Hukum: https://orcid.org/0000-0003-4520-1917
Gorkem Liman: https://orcid.org/0000-0002-0778-9783
Gokhan Demirel: https://orcid.org/0000-0002-9778-917X

Keyword: *Cargo Transportation, Paper-Based Platforms, Soft Actuator*

Fluorine-Rich Porous Organic Polymers for Electrochemical CO_2 Conversion

Yasmin Gecalp * **, Mustafa Erdogmus, Batu Sercan Canturk, Onur Buyukcakir**

Department of Chemistry, Izmir Institute of Technology, Izmir, Türkiye

Elevated levels of anthropogenic carbon dioxide (CO_2) emissions disrupt the carbon cycle and lead to global warming.[1] This serious predicament has intensified the need to develop effective strategies towards decreasing the concentration of CO_2 in the atmosphere. Among the methods, electrochemical CO_2 conversion has been proposed as a promising way to afford value-added products from the recycling of CO_2 through reduction.[2] Although noble- or transition-metal-derived electrocatalysts have been predominantly studied, their limited abundance and high cost have led to the pursuit of metal-free materials with tunable structures, such as porous organic polymers (POPs).[3] These materials, which possess interconnected pore networks and high surface areas that facilitate rapid transport of CO_2, can be furnished with highly CO_2-philic groups containing fluorine atoms to promote enhanced CO_2 capture and regulated electrocatalytic selectivity.[4] In this regard, novel fluorine-rich porous organic polymers were synthesized for electrochemical CO_2 conversion. The CO_2 adsorption capacity and faradaic efficiencies (FEs) of these polymers toward the production of various target products were evaluated to determine the selectivity of the POPs as an electrocatalyst.

Acknowledgment:
This work is supported by the Scientific and Technological Research Council of Türkiye (TÜBİTAK) under Project No. 123Z550.

References:
[1] a) H. Chen, Z. Yang, C.-L. Do-Thanh, S. Dai, ChemSusChem 2020, 13, 6182; b) S. N. Talapaneni, O. Buyukcakir, S. H. Je, S. Srinivasan, Y. Seo, K. Polychronopoulou, A. Coskun, Chemistry of Materials 2015, 27, 6818.
[2] Y. Wang, J. Chen, G. Wang, Y. Li, Z. Wen, Angewandte Chemie International Edition 2018, 57, 13120.
[3] H. Wang, G. Wang, L. Hu, B. Ge, X. Yu, J. Deng, Materials 2023, 16, 1630.
[4] X. Suo, F. Zhang, Z. Yang, L. Wang, M. Lei, J. A. Gaugler, M. Li, J. Fan, B. P. Thapaliya, I. Popovs, A. S. Ivanov, L. C. Gallington, D.-e. Jiang, Z. Liu, S. Dai, Chem Catalysis 2023, 3.

Keyword: *porous organic polymers, environmental remediation, electrochemical CO₂ conversion*

Data-Driven Optimization of Experimental Design Using Machine Learning and Active Learning

Ata Gazi Kuş * **, Gamze Atak**

Department of Physics Engineering, Hacettepe University, Ankara, Turkey

This project aims to optimize the electrochromic performance of tungsten oxide thin films used in smart glass technologies. The limited data problems encountered due to the costly and time-consuming nature of laboratory experiments were overcome using machine learning and artificial intelligence algorithms.

As a method, the RF magnetron sputtering production parameters of the films (RF power, total pressure, oxygen partial pressure) were used as input and a Random Forest algorithm was developed for training the model [1]. A Leave-One-Out validation method was applied to test the model's efficiency. Then instead of testing features uncontrollably, an Active Learning cycle incorporating Goal-Directed (UCB) algorithm and Grid-Based scanning strategies was integrated into the system to reach specific targets with minimal error [2].

The generalization of the model was also targeted. To this end, studies were conducted with numerous random data points found on the internet. As a result of these studies, it was proven that the model can be used not only for a specific experiment but also in a more general sense. The obtained outputs showed that the algorithm successfully resolved complex relationships between parameters, generated heat maps, and steadily reduced the error margin with simulations. Instead of scanning infinite space, the model successfully identified the experimental points that yielded the highest information gain. As a result, thin-film optimization was transformed from a passive data analysis process into an autonomous assistant framework.

References:

[1] Faceira, B., Teule-Gay, L., Rignanese, G.-M., & Rougier, A. (2022). Toward the Prediction of Electrochromic Properties of WO3 Films: Combination of Experimental and Machine Learning Approaches. The Journal of Physical Chemistry Letters, 13, 8111-8115.
[2] Johnson, N. S., et al. (2024). Active Learning for Rapid Targeted Synthesis of Compositionally Complex Alloys. Materials, 17(16), 4038.

Keyword: *Machine Learning, Active Learning, Materials Optimization*

A Drift-Aware Framework for Reliability Assessment and Spatiotemporal Interpretation of Atomic Force Microscopy Measurements

Batuhan Yenen [*1], Seda N. Sönmez[1], Derya Gemici Deveci[2], Özhan Ünverdi[3], H. Özgür Özer[1]

[1] *Department of Physics Engineering, Istanbul Technical University, Istanbul, 34467, Türkiye*
[2] *Institute of Graduate Studies, Department of Electrical and Computer Engineering, Altınbaş University, Istanbul, 34217, Türkiye*
[3] *Yaşar University, Department of Electrical and Electronics Engineering, Bornova, 35100, İzmir, Türkiye*

Nanoscale characterization by atomic force microscopy (AFM) is fundamentally affected by positional drift arising from piezoelectric creep, thermal fluctuations, hysteresis, and environmental vibrations [1]. To address this nonstationary behavior, a hybrid framework integrating numerical analysis, computer vision (CV), and machine learning (ML) was developed for drift characterization and prediction under ambient conditions.

This study presents a hybrid physics-informed and data-driven framework for assessing the effects of drift on the reliability and comparability of consecutive AFM topography measurements. Fifteen sequential AFM images acquired from the same surface region were analyzed, and reliable inter-frame correspondences were identified using a SuperPoint–LightGlue-based deep-learning (DL) approach. These correspondences were associated with physical coordinates, acquisition time, ambient temperature, lateral displacement, relative height difference, and drift-velocity magnitude.

The results show that drift evolves over time in both magnitude and direction. While the early frame pairs exhibited a more dispersed directional distribution, the later measurements were predominantly characterized by upward and rightward drift. A LightGBM regression model was evaluated using an expanding-window walk-forward validation strategy, and the inclusion of temperature as an input feature yielded more stable predictions, particularly in the final validation windows.

The proposed approach demonstrates that AFM drift should not be interpreted solely as a two-dimensional positional displacement, but rather within a combined spatial, temporal, and experimental context. The framework therefore provides a systematic basis for drift-aware AFM metrology and the reliability assessment of repeated scans.

References:
Henriksen, K., Stipp, S.L.S., 2002. Image distortion in scanning probe microscopy. Am. Mineral. 87, 5–16.

Keyword: *Drift, Atomic Force Microscope (AFM), Computer Vision (CV)*

The Shape of Color: 3D Machine Learning Meets Electrochromic Nanomaterial Discovery

Derya Hazal Yıldırım * **, Erol Yıldırım, Levent Toppare**

Middle East Technical University

Rational design of electrochromic polymer nanomaterials remains largely empirical despite the fact that their optical contrast, switching speed and coloration efficiency are physically dictated by molecular geometry: inter-ring dihedral angles govern π-orbital overlap, backbone planarity controls charge delocalization and side-chain architecture shapes ion transport at the polymer-electrolyte interface. Yet conventional 2D fingerprint-based machine learning has largely failed to capture these geometry-property relationships. We introduce an integrated platform pairing a large curated electrochromic polymer dataset with quantum-chemically optimized 3D conformer workflows and geometry-aware descriptors, enabling machine learning models that learn directly from the structural features that actually drive electrochromic behavior. The trained models are then deployed to screen tens of thousands of donor–acceptor copolymer candidates, identifying high-performing structures that would be prohibitively resource-intensive for traditional experimental campaigns and establishing a computational foundation for autonomous electrochromic nanomaterial discovery.

Acknowledgment:
I would like to thank Prof. Dr. Levent Toppare and Asst. Prof. Dr. Erol Yıldırım at Middle East Technical University for their invaluable guidance and supervision, and Dr. Özlem Özcan at Bundesanstalt für Materialforschung und -prüfung for her mentorship and support.

Keyword: *electrochromic nanomaterials, 3D machine learning, geometry-aware descriptors*

Integration of Digital Colorimetry and Machine Learning for the Evaluation of CdZnSeS Quantum Dots

Ezgi Tan * [1], Preston T. Snee[2], Abdurrahim Akgündoğdu[3]

[1] *Istanbul University-Cerrahpaşa, Department of Chemistry, Istanbul, Türkiye*
[2] *University of Illinois at Chicago, Department of Chemistry, Chicago, USA*
[3] *Istanbul University-Cerrahpaşa, Department of Electrical and Electronics Engineering, Istanbul, Türkiye*

Quantum dots (QDs) are semiconductor nanocrystals with sizes typically ranging from 2 to 10 nm [1]. Owing to their pronounced size-dependent optical and chemical properties, their tunable color variations have attracted significant attention in colorimetric sensing applications. However, the quantitative interpretation of colorimetric responses remains challenging and often requires complementary spectroscopic analyses. In this study, CdZnSeS quantum dots were synthesized via the hot-injection method under systematically varied precursor ratios and reaction temperatures. Their structural and optical properties were investigated using X-ray diffraction (XRD), UV–Vis spectroscopy, and photoluminescence (PL) spectroscopy. The results showed that the quantum yield (%) of the QDs varied up to 85%, depending on their composition. Digital colorimetric data were extracted from UV-illuminated images of the synthesized QDs, and Euclidean color difference (ΔE) values were calculated to quantify perceptual color variations via RGB analysis. To evaluate the predictive potential of image-derived color features, a hybrid Adaptive Neuro-Fuzzy Inference System (ANFIS) was developed to estimate PL intensity using RGB values and ΔE as input parameters [2,3]. To improve model robustness and generalization performance, Gaussian noise-based data augmentation was applied to the original dataset consisting of 30 samples, expanding it to a total of 150 samples.

Correlation analysis revealed that the green channel exhibited the highest positive correlation with PL intensity ($r = 0.51$). Furthermore, ΔE displayed strong correlations with both the red and green channels, indicating its effectiveness in representing combined color variations and overall optical behavior. The proposed ANFIS model demonstrated strong predictive capability for estimating PL intensity from image-derived color features. The model achieved a Pearson correlation coefficient of $R = 0.917$ and a coefficient of determination (R^2) of 0.749 on unseen test samples. The incorporation of output constraints enabled the generation of physically meaningful predictions while effectively capturing dynamic variations in PL intensity. These findings demonstrate that image-derived colorimetric descriptors can serve as rapid and low-cost proxies for optical measurements, highlighting the potential of integrating digital colorimetry, machine learning, and fuzzy intelligence into next-generation quantum dot sensing platforms.

References:

[1] Ezgi Tan, Preston T. Snee, & F. Danışman Kalındemirtaş (2024). An investigation of quantum dot theranostic probes for prostate and leukemia cancer cells using a CdZnSeS QD-based nanoformulation. Journal of Colloid and Interface Science, 675, 1032–1039.
[2] Jyh-Shing Roger Jang (1993). ANFIS: Adaptive-network-based fuzzy inference system. IEEE Transactions on Systems, Man, and Cybernetics, 665–685.
[3] F. Pedregosa, G. Varoquaux, et al. (2011). Scikit-learn: Machine Learning in Python. Journal of Machine Learning Research, 2825–2830.

Keyword: *CdZnSeS QDs, Colorimetric Analysis, Machine Learning*

A Modular CNN-Attention Framework for SEM Microstructure Classification of Nanofibrous Materials

Miray Esma Yalçın * **, Ahmet Emrehan Emre, Burak Alakent**

Department of Chemical Engineering, Boğaziçi University, İstanbul

This study explores how scanning electron microscopy (SEM) images can reveal detailed morphological features essential for understanding and classifying the microstructures of nanofibrous materials. We have developed a specialized deep learning framework tailored for SEM-based microstructure analysis. The main component is a multi-scale convolutional neural network that captures various features, from individual fiber details and pore-like structures to dense regions and overall network shapes, by analyzing intermediate representations. To enhance the model's ability to identify complex spatial patterns, we are also incorporating attention mechanisms, including Vision Transformer-inspired modules and lightweight options like CBAM, to improve accuracy and interpretability. The model framework is carefully tested through multiple rounds of data splits and training repetitions to ensure reliability across different scenarios. Besides evaluating how accurately it classifies data, the interpretability of the model is also explored by using a multi-layer Grad-CAM technique. This approach highlights which microstructural regions, such as fiber intersections, dense bundles, pore boundaries, and network junctions, play the most significant roles in the model's decisions. These preliminary insights show that intermediate layers of the CNN can effectively locate these important features. Overall, this work provides a versatile platform for comparing CNN-based and attention-augmented architectures in microstructure analysis, ultimately aiming to advance data-driven methods for characterizing and designing innovative nanofibrous materials.

Keyword: *Microstructure Classification, Nanofibrous Materials, Data-Driven Materials Characterization*

Neural Score Models for Control of Active Dynamical Systems

Rosha Razmarafar [*1], **Francesco Cagnetta**[2], **Alessio Ansuini**[3], **Giuseppe Negro**[4], **Livio Nicola Carenza**[5]

[1] *Computational Science and Engineering, Koç University*
[2] *Scuola Internazionale Superiore di Studi Avanzati (SISSA)*
[3] *Area Science Park, SISSA*
[4] *SUPA, School of Physics and Astronomy, University of Edinburgh*
[5] *Physics Department, College of Sciences, Koç University*

Steering a stochastic dynamical system toward a prescribed terminal state requires a guidance drift that continuously corrects its evolution. Deriving this field analytically is possible only for a limited class of stochastic differential equations, while many systems of interest have coupled, high-dimensional, or non-equilibrium dynamics. This difficulty is particularly important in active matter, where internal active variables generate persistent motion and must be included explicitly in the state description.

We develop a score-based control framework for the Active Ornstein–Uhlenbeck Process (AOUP), introducing a controlled formulation, C-AOUP, in terms of both position and active velocity. Endpoint conditioning is formulated through a Doob h-transform, yielding a time-dependent guidance field defined on the full augmented state and acting through both dynamical equations. We train a time-conditioned neural score model directly from uncontrolled reference trajectories using an importance-weighted transition-score regression objective based on the Z-variable identity. The model therefore learns the state-, target-, and time-dependent guidance field without requiring the analytic score as a supervision signal.

The linear-Gaussian AOUP provides an exact reference solution against which the learned guidance field can be evaluated. This allows us to validate the Z-variable learning formulation in a controlled setting while retaining a training procedure that does not require a closed-form guidance field. The resulting framework connects stochastic control, active-matter physics, and neural score modeling for trajectory conditioning under persistent, non-equilibrium dynamics.

ORCID:
Rosha Razmarafar: 0009-0002-1736-5789
Francesco Cagnetta: 0000-0002-8302-431X
Alessio Ansuini: 0000-0002-3117-3532
Giuseppe Negro: 0000-0003-1755-7051
Livio Nicola Carenza: 0000-0001-5996-331X

References:
Jakiw Pidstrigach, Elizabeth Baker, Carles Domingo-Enrich, George Deligiannidis, and Nikolas Nüsken. Conditioning Diffusions Using Malliavin Calculus. arXiv:2504.03461, 2025
Luke K. Davis. Optimal Multi-Parameter Control of Trapped Active Matter. arXiv:2603.16778, 2026
Song, Y., Sohl-Dickstein, J., Kingma, D. P., Kumar, A., Ermon, S., and Poole, B. Score-Based Generative Modeling through Stochastic Differential Equations. arXiv:2011.13456 (2021)

Keyword: *score-based learning, neural stochastic control, trajectory conditioning*

Comprehensive Drift Analysis and Machine Learning-Based Predictions in Atomic Force Microscopy

Derya Gemici Deveci[1], Tuana Karakoyun Barandır [* 2], Özhan Ünverdi[3], Cem Çelebi[2], Lütviye Özge Temur[4], Doğu Çağdaş Atilla[4]

[1] Institute of Graduate Studies, Department of Electrical and Computer Engineering, Altınbaş University, Istanbul, 34217, Turkey
[2] İzmir Institute of Technology, Faculty of Science, Department of Physics, Urla, 35430, İzmir, Turkey
[3] Yaşar University, Department of Electrical and Electronics Engineering, Bornova, 35100, İzmir, Turkey
[4] Institute of Graduate Studies, Department of Data Analytics, Altınbaş University, Istanbul, 34217, Turkey

Nanoscale characterization with Atomic Force Microscopy (AFM) is fundamentally limited by positional drift, a spatial displacement arising from sources such as piezoelectric creep, thermal effect, hysteresis, and environmental vibrations [1]. To address this nonstationary behavior, a data-driven predictive framework that integrates numerical computations, computer vision (CV), and machine learning (ML) models to characterize and predict drift behavior under ambient conditions.

In this study, we present an ML-driven methodology to characterize and predict these dynamic drift variations in AFM imaging. We utilized an experimental dataset acquired from an epitaxial graphene sample grown on Silicon Carbide (SiC) under different pixel resolutions and scan speeds. CV algorithms extracted spatial displacement and drift velocity (v_d) from consecutive AFM images. LSTM predicted the temporal evolution of v_d, while LightGBM classified drift directions and performed velocity regression. The LSTM model achieved $R^2 > 90\%$ with fewer training pairs when target-related features were included, reaching this threshold after 13–14 pairs instead of 16–17. LightGBM achieved 97.53% and 92.22% directional accuracy along the x- and y-axes, respectively, with $R^2 = 0.9398$ for velocity regression. [2].

Overall, this framework demonstrates the potential of integrating numerical computation, CV, and ML approaches to predict and analyze drift behavior in high-resolution AFM imaging under ambient conditions. The results also suggest that such models may support future real-time drift correction strategies.

ORCID:
Derya Gemici Deveci: 0000-0003-3998-1910
Tuana Karakoyun Barandır: 0009-0003-2137-7341
Özhan Ünverdi: 0000-0001-9994-3487
Cem Çelebi: 0000-0003-1070-1129
Lütviye Özge Temur: 0000-0001-7118-5370
Doğu Çağdaş Atilla: 0000-0002-4249-6951

References:
Henriksen, K., Stipp, S.L.S., 2002. Image distortion in scanning probe microscopy. Am. Mineral. 87, 5–16.
Gemici Deveci, D., Karakoyun Barandır, T., Ünverdi, Ö., Çelebi, C., Temur, L.Ö., & Atilla, D. Ç. (2025). Comprehensive analysis and machine learning-based solutions for drift behavior in ambient Atomic Force Microscope conditions. Engineering Applications of Artificial Intelligence, 159, 111678.

Keyword: *Atomic Force Microscope (AFM), Machine Learning (ML), Artificial Intelligence (AI)*

Superlattice Formation of PBI_2 Passivated PBS Quantum Dots via Langmuir-Schaefer Method

Ecem Efe [*1], **İrem Kolay**[1], **Demet Asil Alptekin**[1,2,3]

[1] *Department of Chemistry, Middle East Technical University (METU), Ankara, 06800, Türkiye*
[2] *Department of Micro and Nanotechnology, METU, Ankara, 06800, Türkiye*
[3] *METU-MEMS Center, Ankara, 06800, Türkiye*

Lead sulfide (PbS) colloidal quantum dots (CQDs) are excellent materials for Short-Wavelength Infrared (SWIR) technologies due to their size-tunable bandgap. Nevertheless, as-synthesised PbS CQDs are capped with long-chain, insulating oleic acid (OA) ligands, which obstruct charge transmission. In order to overcome this, shorter, conductive inorganic lead (II) iodide (PbI_2) was substituted for OA using an improved solution-phase ligand exchange (SPLE) technique. This work proposes a specific Langmuir-Schaefer (LS) assembly technique combined with a unique 16-hour precursor maturation strategy, whereas traditional LS techniques and spin-coating deposition frequently result in uncontrolled fusion of quantum dots, or necking, which results in a disordered thin layer of PbS CQDs, decreasing the open-circuit voltage (V_{oc}) of the devices. This study shows how LS deposition parameters affect the thin film morphology and excited state dynamics of the PbS QDs. It is hoped that the LS method developed in this study will enable the assembly of the CQDs into highly ordered, neck-free superlattice thin films by using an ethylene glycol subphase to precisely manage inter-particle spacing. This integrated strategy provides a reliable, scalable route to ultra-sensitive, next-generation SWIR optoelectronics with high energy homogeneity.

Acknowledgment:
I would like to thank my supervisor, Assoc. Prof. Demet Asil Alptekin, for her guidance and for giving me the opportunity to work on her TÜBİTAK ADEP project. I also want to thank Ph.D. students İrem Kolay and Firdevs Aydın for their patience and technical help during the experiments. Finally, thanks to my lab partners—Sezin Şevval Acar, Furkan Arda Koca, Mert Eray, and Yiğit Emre Karakaş—for their great teamwork and daily support in the lab.

ORCID:
İrem Kolay: 0000-0001-9950-517X
Demet Asil Alptekin: 0000-0001-6368-7151

References:
F. Pelayo García de Arquer et al., Semiconductor quantum dots: Technological progress and future challenges.Science373,eaaz8541(2021).DOI:10.1126/science.aaz8541
Mengfan , G., & Yongjie , W. (2019). Stable PbS quantum dot ink for efficient solar cells by solution-phase ligand engineering. Journal of Materials Chemistry A. https://doi.org/DOI https://doi.org/10.1039/C9TA02393C
Jacopo Pinna, Elisa Pili, Razieh Mehrabi Koushki, Dnyaneshwar S. Gavhane, Francesco Carlà, Bart J. Kooi, Giuseppe Portale, and Maria Antonietta Loi ACS Nano 2024 18 (29), 19124-19136 DOI: 10.1021/acsnano.4c04076
Wang, Chuanglei & Chen, Zhenjun & Liu, Zheng & Ma, Tianchan & Chen, Xiya & Zhang, Menglong & Luo, Dongxiang & Hyun, Byung-Ryool & Liu, Xiao. (2023). Adjusting Microscale to Atomic-Scale Structural Order in PbS Nanocrystal Superlattice for Enhanced Photodetector Performance. Small. 19. e2300975. 10.1002/smll.202300975

Keyword: *PbS QD, Superlattice, Langmuir-Schaefer Deposition*

Effect of Ligand Length on PbSe Quantum Dot Films for SWIR Photodetectors: Solution-Phase and Layer-by-Layer Ligand Exchange

Furkan Arda Koca [*1], **Demet Asil Alptekin**[1,2,3], **İrem Kolay**[1]

[1] *Department of Chemistry, Middle East Technical University (METU), Ankara, 06800, Türkiye*
[2] *Department of Micro and Nanotechnology, METU, Ankara, 06800, Türkiye*
[3] *METU-MEMS Center, Ankara, 06800, Türkiye*

Colloidal PbSe quantum dots (QDs) are size-tunable, solution-processable absorbers that are well suited to short-wave infrared (SWIR) photodetection. As-synthesised dots, however, are capped with long, insulating oleic acid (OA) ligands that hold neighbouring dots apart and obstruct charge transport. Replacing OA with shorter ligands shrinks the inter-dot spacing and enhances electronic coupling, which makes the length of the exchange ligand a key parameter. Most work in this area has focused on a single ligand or a single exchange route; a systematic comparison of ligand length together with the exchange method has remained limited. In this work, OA-capped PbSe QDs were exchanged with three diiodoalkane ligands of increasing chain length (diiodomethane (DIM), 1,2-diiodoethane (DIE) and 1,8-diiodooctane (DIO)) using two routes, solution-phase (SPLE) and layer-by-layer (LbL) exchange.

This study examines how the length of the diiodoalkane ligand and the choice of exchange route affect the physical, optical and excited-state dynamics of PbSe QD films. To investigate the effect of ligand length on morphological properties, AFM imaging techniques were used. Additionally, the solution-phase exchange kinetics were followed as a function of chain length, and the LbL films were characterised by UV-Vis absorption together with steady-state and time-resolved photoluminescence to track the exciton position, emission and carrier lifetimes. The effect of ligand exposure time in the LbL route and the air stability of the resulting films were also investigated.To explore the effect of ligand length on photovoltaic performance parameters, cells with varying ligands were fabricated and tested.

Acknowledgment:
This work was supported by the Scientific and Technological Research Council of Turkey (TÜBİTAK) under Project Number 124F413.

ORCID:
Demet Asil Alptekin: 0000-0001-6368-7151
İrem Kolay: 0000-0001-9950-517X

References:
Kolay, İ. (2022). Donor–Acceptor Type Bulk Nano-Heterojunction Solar Cell Designs Based on Electronically Coupled Lead Selenide Nanorods and Lead Selenide Quantum Dots (Master's thesis, Middle East Technical University, Türkiye).
Liu, M., Tang, G., Liu, Y., & Jiang, F.-L. (2024). Ligand exchange of quantum dots: a thermodynamic perspective. The Journal of Physical Chemistry Letters, 15(7), 1975–1984.
Gao, Y., Aerts, M., Sandeep, C. S., Talgorn, E., Savenije, T. J., Kinge, S., Siebbeles, L. D. A., & Houtepen, A. J. (2012). Photoconductivity of PbSe quantum-dot solids: dependence on ligand anchor group and length. ACS Nano, 6(11), 9606–9614.

Keyword: *PbSe quantum dots, ligand exchange, SWIR photodetector*

Joint Estimation of Phase-Shift And Losses in SU(2) and SU(1,1) Interferometers

Hasan Mermer *

Koç Üniversitesi

Optical interferometry is a cornerstone of precision measurement, with applications spanning gravitational-wave detection, quantum sensing, and fundamental tests of quantum mechanics. In realistic interferometric settings, optical loss and detector inefficiency are unavoidable, degrading the quantum enhancement that nonclassical states provide. While loss is typically calibrated independently using classical methods, such approaches may not faithfully characterize device behavior in the quantum regime. This thesis investigates the joint estimation of an interferometric phase shift and optical loss in two-mode Gaussian interferometers, evaluating the ultimate precision limits imposed by quantum mechanics and identifying optimal measurement strategies.

The analysis is carried out within the continuous-variable Gaussian framework, wherein the full quantum state is encoded in a displacement vector and a covariance matrix evolving under symplectic transformations. Two interferometric architectures are compared: passive Mach–Zehnder-type interferometers based on beam splitters, implementing SU(2) transformations, and active SU(1,1) interferometers based on parametric amplification, which generate internal squeezing without requiring nonclassical input states. The quantum Fisher information matrix (QFIM) is computed analytically for the two-parameter problem of jointly estimating phase and a common loss parameter, and numerically for the three-parameter extension to asymmetric losses. Scalar precision bounds are derived from the QFIM and optimized over input Gaussian states at fixed mean photon number, enabling a fair energetic comparison between the two architectures. Where optimal measurements for the two parameters are mutually incompatible, the Holevo Cramér–Rao bound is evaluated via semidefinite programming, providing an operationally tight limit on simultaneously attainable precision. The achievability of these quantum bounds is further assessed for experimentally realistic detection schemes including homodyne and heterodyne measurement.

The central question addressed is whether active SU(1,1) interferometry offers a genuine metrological advantage over passive SU(2) configurations when phase and loss must be estimated simultaneously under equivalent resource constraints. The results are expected to clarify the interplay between phase sensitivity, loss robustness, and measurement incompatibility in realistic quantum-enhanced interferometry, providing guidance for the design of practical joint estimation schemes.

Acknowledgment:
This project is co-supervised by Prof. Özgür E. Müstecaplıoğlu of Koç University and Prof. Matteo Paris of Milan.

ORCID:
Hasan Mermer: 0009-0009-6723-4876

Keyword: *Quantum Estimation, Multi-parameter Estimation, Gaussian Interferometry*

Development of an In-Situ Bromoplumbate Surface Passivation Protocol for Directly Synthesized PbS Quantum Dots

Mert Eray [*] [1], **İrem Kolay**[1], **Demet Asil Alptekin**[1,2,3]

[1] *Department of Chemistry, Middle East Technical University (METU), Ankara, 06800, Türkiye*
[2] *Department of Micro and Nanotechnology, METU, Ankara, 06800, Türkiye*
[3] *METU-MEMS Center, Ankara, 06530, Türkiye*

Colloidal lead sulfide (PbS) quantum dots (QDs) are promising materials for next-generation short-wavelength infrared (SWIR) optoelectronic devices, owing to their size tunable bandgaps and solution processability. Conventional hot injection synthesis relies on insulating long alkyl chain ligands that must later be removed through multi-step ligand exchange method, whereas the Direct Synthesis (DS) approach delivers semiconductive, halide passivated quantum dots in a single step, making it far more scalable. Despite this advantage, the large surface-to-volume ratio of these nanocrystals leaves undercoordinated lead (Pb) atoms with dangling bonds that introduce non-radiative trap states and limit device performance. The surface needs to be passivated at the end of the colloidal growth where traps are formed.

In this work, we develop an in-situ bromoplumbate surface passivation strategy to eliminate these trap states. Existing strategies typically rely on pre- or post-synthesis treatments; instead, we passivate the surface during synthesis, before traps can form, by injecting a bromoplumbate solution at the critical time of colloidal growth [4]. Unlike traditional approaches that use $PbBr_2$ alone, we combine $PbBr_2$ with NH_4Br to form reactive bromoplumbate complexes. We systematically investigate how the $PbBr_2$:NH_4Br molar ratio, and the mixing time of the two precursors affect bromoplumbate formation and the resulting passivation efficiency. Our findings show that controlling the precursor molar ratio together with the mixing time provides a simple yet powerful route to more stable, high quality PbS QD inks.

Acknowledgment:
This work is financially supported by ADEP-103-2025-11660.

ORCID:
İrem Kolay: https://orcid.org/0000-0001-9950-517X
Demet Asil Alptekin: https://orcid.org/0000-0001-6368-7151

References:
Moreels, I., Lambert, K., Smeets, D., De Muynck, D., Nollet, T., Martins, J. C., Vanhaecke, F., Vantomme, A., Delerue, C., Allan, G., & Hens, Z. (2009). Size-dependent optical properties of colloidal PbS quantum dots. ACS Nano, 3(10), 3023–3030.
Wang, H., Pinna, J., Garcia Romero, D., et al. (2024). PbS quantum dots ink with months-long shelf-lifetime enabling scalable and efficient short-wavelength infrared photodetectors. Advanced Materials, 36(13), 2311526.
Liu, Y., Gao, Y., Yang, Q., et al. (2023). Breaking the size limitation of directly-synthesized PbS quantum dot inks toward efficient short-wavelength infrared optoelectronic applications. Angewandte Chemie International Edition, 62(17), e202300396.
Crisp, R. W., Kroupa, D. M., Marshall, A. R., Miller, E. M., Zhang, J., Beard, M. C., & Luther, J. M. (2015). Metal halide solid-state surface treatment for high efficiency PbS and PbSe QD solar cells. Scientific Reports, 5, 9945.

Keyword: *Directly Synthesized PbS Quantum Dots, Bromoplumbate, In-Situ Surface Passivation*

Doping of ZNO Electron Transport Layers for PBS Quantum Dot Solar Cells

Sezin Şevval Acar [*1], **İrem Kolay**[1], **Demet Asil Alptekin**[1,2,3]

[1] *Department of Chemistry, Middle East Technical University (METU), Ankara, 06800, Türkiye*
[2] *Department of Micro and Nanotechnology, METU, Ankara, 06800, Türkiye*
[3] *METU-MEMS Center, Ankara, 06530, Türkiye*

Zinc oxide (ZnO) is one of the most widely used electron transport layer (ETL) in colloidal QDs and perovskite photovoltaics. It crystallises in the wurtzite structure, an n-type, direct gap semiconductor with a wide band gap and a large exciton binding energy. Its high intrinsic electron mobility, optical transparency across the visible spectrum, and energetically favourable conduction band position make ZnO well suited to accept electrons from active layer while blocking holes. However, due to trap states arising from oxygen vacancies (V_O) in the ZnO, device performances of solar cells could not reach the theoretical limit. Most studies in the literature to date have focused on active layer optimization, but optimization of the ZnO layer has been insufficient. In this work, we screened a periodically organized library of Group 1A/2A cations and Group 7A anions by applying the dip-coating protocol to thin films prepared from the same sol–gel ZnO batch. This study shows how electronegativity, size, and identity of the various anions and cations affect the optical and excited state dynamics of the ZnO thin films. Additionally, the effect of doping on ZnO crystal structure and thin film morphology is investigated. Finally, the effect of structural doping on photovoltaic performance for PbS colloidal quantum dot solar cells was evaluated. The results show that cells with doped ZnO ETLs exhibit approximately eightfold increases in power conversion efficiency, while also providing improvements in short-circuit current density and fill factor.

Acknowledgment:
This work was financially supported by the Scientific and Technological Research Council of Turkey (TÜBİTAK) under Project Number 124F413.

ORCID:
İrem Kolay: 0000-0001-9950-517X
Demet Asil Alptekin: 0000-0001-6368-7151

References:

He, J., Ge, Y., Wang, Y., Yuan, M., Xia, H., Zhang, X., Chen, X., Wang, X., Zhou, X., Li, K., Chen, C., & Tang, J. (2023). Fluoride passivation of ZnO electron transport layers for efficient PbSe colloidal quantum dot photovoltaics. Frontiers of Optoelectronics, 16(1), Article 28. https://doi.org/10.1007/s12200-023-00082-3

Nozik, A. J. (2012). Photovoltaics: Separating multiple excitons. Nature Photonics, 6(5), 277–278. https://doi.org/10.1038/nphoton.2012.78

Beard, M. C., Luther, J. M., & Nozik, A. J. (2013). Multiple exciton generation in semiconductor quantum dots and electronically coupled quantum dot arrays for application to third-generation photovoltaic solar cells. In G. Konstantatos & E. H. Sargent (Eds.), Colloidal Quantum Dot Optoelectronics and Photovoltaics (pp. 112-147). Cambridge University Press.

Zhang, J., Shankar, A. G., & Wang, X. (2024). On-chip lasers for silicon photonics. Photonics, 11(3), Article 212. https://doi.org/10.3390/photonics11030212

Tseng, Z.-L., Chiang, C.-H., Chang, S.-H., & Wu, C.-G. (2016). Surface engineering of ZnO electron transporting layer via Al doping for high efficiency planar perovskite solar cells. Nano Energy, 28, 311–318. https://doi.org/10.1016/j.nanoen.2016.08.035

Tyona, M. D. (2019). Doped zinc oxide nanostructures for photovoltaic solar cells application. In A. M. Nahhas (Ed.), Zinc Oxide Based Nano Materials and Devices. IntechOpen. https://doi.org/10.5772/intechopen.86254

Keyword: *oxygen-vacancy passivation, ZnO electron transport layer, PbS QD solar cell*

Direct Conversion of Highly Monodisperse CdS Quantum Dots into Halide-Passivated PbS INKS via In-Situ Cation Exchange

Yiğit Emre Karakaş [* 1], İrem Kolay[1], Demet Asil Alptekin[1,2,3]

[1] *Department of Chemistry, Middle East Technical University (METU), Ankara, 06800, Türkiye*
[2] *Department of Micro and Nanotechnology, METU, Ankara, 06800, Türkiye*
[3] *METU-MEMS Center, Ankara, 06530, Türkiye*

Lead sulfide (PbS) colloidal quantum dots (CQDs) are one of the best candidate materials for optoelectronic applications owing to their unique properties. Their exceptionally large Bohr exciton radius enables strong quantum confinement effects, allowing their band gap to be precisely tuned across the near-infrared region simply by adjusting particle size. Combined with high NIR absorption coefficients and solution processability, PbS CQDs offer a compelling platform for scalable, low cost device fabrication, making them particularly promising candidates for infrared photodetectors and solar cells. However, conventional PbS CQD synthesis via the hot-injection method can result in broader FWHM values, indicating a broader size distribution. In addition, subsequent ligand exchange steps can introduce surface defects. These surface defects create trap states and promote charge carrier recombination, which can significantly reduce device performance. In this study, we developed one step in situ cation exchange strategy for the direct conversion of Cadmium Sulfide (CdS) QDs into halide passivated PbS QDs ink. CdS QDs can be prepared by hot injection with a narrow size distribution. Since the particles are uniform in size and shape, they provide a well-defined starting point for converting CdS QDS into PbS ink by cation exchange. The temperature and time parameters for in situ cation exchange reaction were optimized. Thanks to this optimization, potential surface defects that might occur during conversion have been minimized, resulting in high quality, low defect density PbS ink.

Optical properties of CdS QDs and resulting PbS inks were characterized by the following measurements; UV–Vis absorption measurements were used to assess the monodispersity of the CdS QDs and the optical band gaps of the resulting PbS QD inks. PL and TRPL measurements were performed to investigate emission behavior, carrier lifetimes, and trap assisted recombination pathways. FTIR spectroscopy was used to confirm ligand exchange. AFM was used to evaluate thinfilm surface morphology and roughness, while TEM was used to examine QD size, morphology, size distribution, and crystallinity.

This method provides a simplified and scalable pathway for the production of high quality, single step synthesized ink formulations of PbS quantum dots, with significant implications for next generation infrared photodetectors and solar cells.

ORCID:
İrem Kolay: https://orcid.org/0000-0001-9950-517X
Demet Asil Alptekin: https://orcid.org/0000-0001-6368-7151

References:
Liu, J., Liu, P., Shi, T., Ke, M., Xiong, K., Liu, Y., ... & Tang, J. (2023). Flexible and broadband colloidal quantum dot photodiode array for pixel-level X-ray-to-near-infrared image fusion. Nature Communications, 14(1), 5352.
Patidar, K., Shieh, H. Y., & Chen, H. S. (2026). Temperature-optimized liquid-phase iodide ligand exchange enables low-trap solution-processed PbS quantum dot photodetection at 940 nm. Nanomaterials, 16(6), 380.
Yu, D., Yu, Z., Zhang, Y., Chang, Y., & Yu, D. (2020). Cation-exchange synthesis and measurement of PbS quantum dots with high nonlinear optical properties. Optik, 210, 164509.
Yuan, M., Hu, H., Wang, Y., Xia, H., Zhang, X., Wang, B., & Tang, J. (2022). Cation exchange enables in situ preparation of PbSe quantum dot ink for high-performance solar cells. Small, 18(48), 2205356.
Zhang, C., Xia, Y., Zhang, Z., Huang, Z., Lian, L., Miao, X., ... & Zhang, J. (2017). Combination of cation exchange and quantitative Ostwald ripening for controlling the size distribution of lead chalcogenide quantum dots. Chemistry of Materials, 29(8), 3615-3622.

Keyword: *PbS colloidal quantum dots, in-situ cation exchange, halide passivation*

Tuning Energy Transfer Efficiency in PBSE Quantum Dot – Nanorod Heterojunctions for Enhanced Exciton Harvesting

İrem Kolay [*1], **Demet Asil Alptekin**[1,2,3]

[1] *Department of Chemistry, Middle East Technical University (METU), Ankara, 06800, Türkiye*
[2] *Department of Micro and Nanotechnology, METU, Ankara, 06800, Türkiye*
[3] *METU-MEMS Center, Ankara, 06530, Türkiye*

Colloidal lead selenide (PbSe) quantum dots (QDs) are emerging as exceptional optoelectronic materials owing to their size-tunable band gaps, broad absorption spectrum, large exciton Bohr radius (46 nm), and high multiple exciton generation (MEG) yields. When coupled with PbSe nanorods (NRs), which offer anisotropic electronic properties and strong absorption cross sections, these materials form promising donor–acceptor (D–A) heterojunction architectures for next generation solar energy harvesting.

Despite their potential, critical challenges remain in understanding how interparticle distance, structural disorder, and energetic alignment govern D-A interactions in QD-NR systems. In densely packed NR solids, exciton transport is significantly limited, and strong Coulombic confinement within PbSe NRs prevents spontaneous exciton dissociation, necessitating a heterojunction design to drive efficient charge separation.

In this work, we systematically investigate energy transfer mechanisms in bulk-nano heterojunctions (BNHJs) composed of oleic acid-capped PbSe QDs of varying sizes blended with PbSe NRs at different (v/v) ratios. By tuning QD size, we engineer band alignments between donor QDs and acceptor NRs, enabling controlled modulation of spectral overlap for efficient energy transfer.

Steady-state and time-dependent photoluminescence (PL) spectroscopy serve as fundamental tools for investigating energy transfer dynamics. The dependence of transfer efficiency on QD size, and consequently on the degree of spectral overlap and band shift, has been carefully examined. These PL measurements provide a detailed insight into how exciton dynamics, charge localization, and MEG processes evolve in different heterojunction types. The fabricated solar cells further confirm which BNHJ design provides superior photovoltaic performance and relate fundamental photophysics to device results.

Our results reveal how the dimensional mismatch between QDs and NRs affects exciton transport and energy transfer efficiency. These findings provide fundamental guidelines for rationally designing inter-nanocrystalline coupling and offer a clear path towards high efficiency MEG based photovoltaic devices.

Acknowledgment:
This work was supported by the Scientific and Technological Research Council of Turkey (TÜBİTAK) under Project Number 123N542.

ORCID:
İrem Kolay: 0000-0001-9950-517X
Demet Asil Alptekin: 0000-0001-6368-7151

References:
O.E. Semonin, J.M. Luther, S. Choi, H.-Y. Chen, J. Gao, A.J. Nozik, M.C. Beard, Peak External Photocurrent Quantum Efficiency Exceeding 100% via MEG in a Quantum Dot Solar Cell, n.d. https://www.science.org.
N.J.L.K. Davis, M.L. Böhm, M. Tabachnyk, F. Wisnivesky-Rocca-Rivarola, T.C. Jellicoe, C. Ducati, B. Ehrler, N.C. Greenham, Multiple-Exciton Generation in Lead Selenide Nanorod Solar Cells with External Quantum Efficiencies Exceeding 120%, Nat Commun 6 (2015) 1–7. https://doi.org/10.1038/ncomms9259.
Y. Gao, M. Aerts, C.S.S. Sandeep, E. Talgorn, T.J. Savenije, S. Kinge, L.D.A. Siebbeles, A.J. Houtepen, Photoconductivity of PbSe quantum-dot solids: Dependence on ligand anchor group and length, ACS Nano 6 (2012) 9606–9614. https://doi.org/10.1021/nn3029716.
İ. Kolay, D. Asil, PbSe nanorod-quantum dot bulk nano-heterojunction solar cells generating multiple excitons with record photo conversion efficiencies, Mater Today Commun 35 (2023). https://doi.org/10.1016/j.mtcomm.2023.106064.

Keyword: *multiple exciton generation, energy transfer, PbSe bulk nano heterojunction*

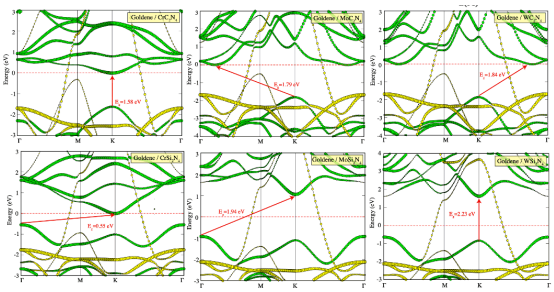
Goldene/MX2N4 Metal-Semiconductor Heterostructures As Promising Platforms For High-Performance Gas Sensing

Mehmet Özcan[1], Berna Akgenc Hanedar [* 2]

[1] Department of Physics, Kırklareli University, Kırklareli 39100, Turkey
[2] Department of Physics, Kırklareli University, Kırklareli 39100, Türkiye

The recent synthesis of atomically thin goldene has opened new opportunities for the development of advanced two-dimensional (2D) gas-sensing materials. Combining metallic goldene with semiconducting MX_2N_4 monolayers (M = Cr, Mo, W; X = C, Si) offers a promising strategy to simultaneously achieve efficient carrier transport and enhanced surface sensitivity.

In this work, were performed to investigate the structural stability, electronic properties, interfacial charge transfer, and gas-sensing potential of Goldene/MX_2N_4 van der Waals heterostructures within density functional calculations. The pristine MX_2N_4 monolayers exhibit semiconducting behavior with band gaps ranging from 0.48 to 2.11 eV, whereas goldene retains its intrinsic metallic character. After identifying the most stable stacking configurations, the electronic and interfacial properties of the heterostructures were systematically analyzed. Projected band structure calculations reveal that metallic states originating from goldene dominate near the Fermi level, while the semiconducting characteristics of MX_2N_4 are largely preserved.



Work-function calculations, electrostatic potential profiles, and band alignment analyses indicate favorable carrier transport across the interface and the formation of p-type Ohmic contacts in several heterostructures. Charge-density-difference calculations further demonstrate pronounced interfacial charge redistribution and electron transfer within the van der Waals gap region. To evaluate their sensing capability, thermally stable heterostructures were investigated toward toxic target gases (NO_2, NH_3, and H_2S), interfering gases (NO, SO_2, and CO), and common atmospheric species (H_2O, O_2, and CO_2). Adsorption energies, preferred binding configurations, charge transfer, charge-density differences, and work-function variations were analyzed to identify the key mechanisms governing sensor response and selectivity.

Ab initio molecular dynamics simulations at 300 K reveal that carbon-based heterostructures undergo structural degradation, whereas silicon-based counterparts remain thermally stable under ambient conditions. The combination of room-temperature stability, strong interfacial coupling, efficient charge-transfer pathways, and favorable gas adsorption characteristics identifies Goldene/MSi_2N_4 heterostructures as promising candidates for highly sensitive and selective gas sensors. These findings provide valuable design guidelines for the development of next-generation 2D gas-sensing devices.

Acknowledgment:
This work was performed at the MareNostrum 5 (MN5) at the Barcelona Supercomputing Center (BSC) and the the High Performance Grid Computing Center (TR-Grid eInfrastructure), TÜBİTAK-ULAKBİM. This study was funded by the Scientific and Technological Research Council of Turkey (TÜBİTAK) under Project No 125F626.

ORCID:
Berna Akgenc Hanedar: 0000-0002-8998-0257

References:
Picello, S., Inico, E., Saetta, C., Di Liberto, G., & Pacchioni, G. (2025). Single-Atom Catalysts on Goldene. ACS catalysis, 15(13), 11232-11242.
Kashiwaya, S., Shi, Y., Lu, J., Sangiovanni, D. G., Greczynski, G., Magnuson, M., ... & Hultman, L. (2024). Synthesis of goldene comprising single-atom layer gold. Nature Synthesis, 3(6), 744-751.
Sang, N. X., & Cuong, N. Q. (2026). Intrinsic Ohmic contact and electric-field tunable interface in a 2D NbS 2/As 2 C 3 metal–semiconductor heterostructure. Nanoscale Advances, 8(3), 1005-1013

Keyword: *DFT, Metal-Semiconductor Heterostuctures, Gas Sensing*

Strain-Dependent Evolution of Crystallographic Texture and Microstructure in Laser Powder Bed Fusion-Processed 316L Stainless Steel

Büşra İrem Türkpençesi [*1], **Kemal Davut**[2], **Mustafa Güden**[1], **Benay Uzer**[1], **Kay-Peter Hoyer**[3]

[1] *Department of Mechanical Engineering, Izmir Institute of Technology*
[2] *Department of Materials Science and Engineering, İzmir Institute of Technology*
[3] *Faculty of Mechanical Engineering, Chair of Materials Science, Paderborn University*

The ability of laser powder bed fusion (L-PBF) to tailor crystallographic texture offers new opportunities for controlling the mechanical behavior of metallic materials. In particular, preferred <110> orientations in austenitic stainless steels have been associated with enhanced deformation twinning, resulting in improved ductility (Güden et al., 2021). Despite these advances, relatively few studies have investigated the evolution of crystallographic texture and microstructure during plastic deformation. In this study, 316L stainless steel specimens were fabricated by selective laser melting (SLM) using a laser power of 195 W, a scanning speed of 1000 mm s^{-1}, a hatch spacing of 90 µm, and a layer thickness of 20 µm. The tensile behavior of the material was first characterized by uniaxial tensile testing. The material exhibited an ultimate tensile strength of 546 MPa and an elongation to failure of 56%. Subsequently, specimens were subjected to interrupted tensile deformation up to 30% strain. The strain-dependent evolution of crystallographic texture and microstructure was investigated using scanning electron microscopy (SEM), electron backscatter diffraction (EBSD), and Vickers hardness measurements. SEM observations revealed a progressive increase in the density and complexity of deformation bands with increasing strain. EBSD analysis showed that the kernel average misorientation (KAM) increased from 0.78° in the as-built condition to 1.99° after 30% tensile deformation, indicating progressive local lattice misorientation and deformation heterogeneity (Kale et al., 2020). Furthermore, the average geometrically necessary dislocation (GND) density increased from $(1.9 \pm 1.4) \times 10^{14}$ to $(5.3 \pm 2.4) \times 10^{14}$ m^{-2}, indicating progressive dislocation accumulation during plastic deformation (Barkia et al., 2025). In addition, the preferred crystallographic texture gradually shifted from <110> to <001> with increasing tensile strain, while the maximum texture intensity decreased from 8.72 to 5.09. The Vickers hardness increased from 221.8 ±1.2 HV in the as-built condition to 311.8 ± 9.8 HV after 30% tensile deformation. These findings improve the understanding of strain-dependent microstructural evolution and provide a basis for future TEM investigations of deformation mechanisms.

Acknowledgment:
This work was supported by the Scientific and Technological Research Council of Türkiye (TÜBİTAK) under Project No. 122M991. The authors also acknowledge the Materials Research Center of İzmir Institute of Technology (İYTE-MAM) for SEM analysis.

References:
Barkia, B., Vallet, M., Tanguy, A., Auger, T., & Héripré, E. (2025). New insights into microstructure evolution and deformation mechanisms in additively manufactured 316L stainless steel. Materials Science and Engineering: A, 934, 148327. https://doi.org/10.1016/j.msea.2025.148327
Güden, M., Yavaş, H., Tanrıkulu, A. A., Taşdemirci, A., Akın, B., Enser, S., Karakuş, A., & Hamat, B. A. (2021). Orientation dependent tensile properties of a selective-laser-melt 316L stainless steel. Materials Science and Engineering: A, 824, 141808. https://doi.org/10.1016/j.msea.2021.141808
Kale, A. B., Singh, J., Kim, B.-K., Kim, D.-I., & Choi, S.-H. (2020). Effect of initial microstructure on the deformation heterogeneities of 316L stainless steels fabricated by selective laser melting processing. Journal of Materials Research and Technology, 9(4), 8867–8883. https://doi.org/10.1016/j.jmrt.2020.06.015

Keyword: *Laser powder bed fusion (L-PBF), plastic deformation, electron backscatter diffraction (EBSD)*

Development of a Flexible Carbon Fiber Supercapacitor and Integration with a Triboelectric Nanogenerator for Self-Charging Energy Systems

Kaan Yapıcı * **, Serap Hayat Soytaş**

Sabanci University

The growing demand for wearable electronics has highlighted the need for lightweight, flexible, and autonomous energy systems. Although conventional energy storage devices can provide reliable power, they often require external charging and may lack the mechanical adaptability needed for next-generation wearable platforms. To address these challenges, this study proposes the development of a self-charging energy platform that integrates a flexible carbon fiber supercapacitor with a triboelectric nanogenerator (TENG) into a unified, flexible architecture. While TENGs and flexible supercapacitors have been widely investigated as individual systems, their integration remains a promising route toward autonomous wearable power units. The proposed system aims to combine mechanical energy harvesting, rapid charge–discharge capability, cycling stability, and practical usability in wearable electronics.

The flexible supercapacitor is fabricated using carbon fiber-based electrodes derived from polyacrylonitrile (PAN), providing mechanical flexibility, electrical conductivity, and durability under motion. Nanostructured conductive pathways are introduced to enhance charge transport while preserving flexibility. A gel polymer electrolyte is used instead of conventional liquid electrolytes, offering improved safety, leakage resistance, and mechanical compatibility with flexible form factors. The electrolyte provides ionic conductivity and interfacial adhesion to the electrode layers, supporting stable electrochemical performance under deformation. The supercapacitor design is optimized for operation under bending and repetitive mechanical stress conditions typical of wearable applications.

Simultaneously, the TENG is fabricated using electrospun nanofiber layers with high triboelectric polarity. These high-surface-area membranes harvest biomechanical energy from movements like walking or fabric deformation. The system includes custom energy conditioning circuits to convert the pulsed AC output of the TENG into a regulated form suitable for real-time supercapacitor charging.

Keyword: *Triboelectric nanogenerator, self-charging energy system, wearable electronics*

Nanoscale Friction Mechanisms of SnSe and SnSe2 Nanoflakes as Solid Lubricants

Mehmet Ozdogan * **, Thomas Iken, Deniz Cakir, Nuri Oncel**

University of North Dakota

Solid lubrication at small length scales is essential for micro- and nanoelectromechanical systems, precision components, and mechanisms operating in environments where liquid lubricants are unsuitable. Layered van der Waals materials are attractive for this purpose because their atomic planes can shear with relatively low energy dissipation. In this study, we examine the nanotribological behavior of exfoliated SnSe and $SnSe_2$, two layered tin chalcogenides with emerging relevance beyond their established thermoelectric and optoelectronic properties.

Nanoscale friction measurements were carried out using atomic force microscopy-based lateral-force microscopy on mechanically exfoliated SnSe and $SnSe_2$ flakes deposited on SiO_2. To provide a direct benchmark, graphene flakes with similar thickness were measured under identical ambient conditions. The friction force was extracted from forward and backward lateral signals, and friction coefficients were obtained from load-dependent measurements. Both tin chalcogenides exhibited excellent lubricating behavior, with friction coefficients of 0.023 ± 0.004 for SnSe and 0.027 ± 0.019 for $SnSe_2$, which are lower than the value measured for graphene under the same experimental conditions. Among the two Sn-based materials, SnSe exhibited the lowest measured friction and adhesion, suggesting particularly favorable surface-sliding behavior in ambient air.

The apparent difference between experimental friction and the intrinsic theoretical expectation was investigated using X-ray photoelectron spectroscopy and density functional theory. Calculations for pristine layers predict lower sliding barriers for $SnSe_2$ than for SnSe, implying that $SnSe_2$ should have the stronger intrinsic potential for ultralow friction. However, XPS measurements show that both surfaces develop native oxide layers after exposure to air, with SnSe forming a SnO-like surface and $SnSe_2$ forming a SnO_2-like surface. Atomistic calculations on oxygen-modified monolayers reveal that oxidation distorts the surface lattice and substantially increases the sliding barrier, especially for $SnSe_2$. This oxidation-induced change explains why $SnSe_2$ displays higher friction than SnSe in ambient lateral-force measurements despite its lower intrinsic interlayer shear strength.

Overall, the results demonstrate that SnSe and $SnSe_2$ nanoflakes are promising layered solid lubricants, with experimentally measured friction coefficients in the 0.02–0.03 range under ambient conditions. The discrepancy between experiment and pristine-surface calculations is explained by native oxide formation, which increases the sliding barrier more strongly for $SnSe_2$. Importantly, the calculated interlayer potential-energy surfaces indicate that pristine $SnSe_2$ has lower intrinsic shear resistance than SnSe, suggesting that minimizing oxidation may unlock even lower-friction behavior, particularly in vacuum or space environments [1].

Acknowledgment:
The material contained in this work is based upon work supported by a National Aeronautics and Space Administration (NASA) grant, the North Dakota Space Grant Consortium (NDSGC) research fellowship program, and the National Science Foundation (NSF) through S-STEM award no. 1742269 and (MRI-2117014).

ORCID:
Mehmet Ozdogan: 0000-0002-2874-4787

References:
[1]. ACS Appl. Nano Mater. 2025, 8, 14713−14719.

Keyword: *SnSe*, *friction*, *solid lubrication*

Micro Structured Surface Creation for Leidenfrost Enhancement in Low Temperatures

Monika Maziukiene * **, Raminta Skvorcinskiene, Lina Vorotinskiene, Ainė Antanavičė**

Lithuanian Energy Institute

Leidenfrost effect onset on hot surfaces is highly dependent on the material temperature, its nature, samples geometrical parameters, surface properties. A lack of scientific studies was provided how Leidenfrost occurred in relatively low temperature range to make it practically applicable phenomena. One of the most important parameters for Leidenfrost occurrence is superhydrophobic surface creation. Surface that has larger water contact angle significantly enhance vapor layer formation. In this study we investigate how LE forms on steel surface, which is modified by two stage chemical etching and in the last stage covered with PMHS. The aim is to lower Leidenfrost effect occurrence temperature on hot surfaces when samples are cooling in deionized and saline water under natural convection (20ºC). Steel is widely applicable material in industry sector and many experiments were performed to investigate LE at high temperatures. Surface chemically was etched by applying two stage chemical etching. In the first stage samples were immersed in HCl (10%) solution and kept approximately 30 minutes. In second stage samples were put in aqueous $FeCl_3 \cdot 6H_2O$ (40%) solution at 40–50 °C and kept for about 30 minutes to obtain a deeper surface texture. Such surface creation allowed to create WCA from 90º for polished steel (St) to 159 º for St-HCl+$FeCl_3$+PMHS. In the last step textured surfaces were covered with polymethylhydrosiloxane (PMHS) coating to have higher values water contact angle on the surface. The conducted experiments and received results indicate that LE can form on chemically etched steel surfaces when surface temperature is 120 ºC. This work presents a novel investigation of vapor film dynamics in not-ionized and saline water on steel surfaces heated within the temperature range of 120–340°C, focusing on the mechanisms governing vapor film formation and stable persistence.

Acknowledgment:
This work has received funding from the Research Council of Lithuania (LMT LT), agreement No. S-PD-25-8.

ORCID:
Monika Maziukiene: https://orcid.org/0000-0003-0080-188X
Raminta Skvorcinskiene: https://orcid.org/0000-0002-6281-2720
Lina Vorotinskiene: https://orcid.org/0009-0000-2379-557X
Ainė Antanavičė: https://orcid.org/0009-0003-8087-4938

Keyword: *Two phase flow, Vapour film, Leidenfrost effect*

Wafer-Scale Characterization of Orientation- and Doping-Density-Dependent β-Ga_2O_3 Single Crystals for Optoelectronic and Electrooptic Applications

Selen Nur Yılmaz [*1], **Ümit Doğan**[2], **Muratcan Aydoğdu**[1], **Mustafa Aydın**[1], **Şahin Yakut**[1], **Deniz Bozoğlu Parto**[1], **Hüseyin Furkan Eminoğlu**[1], **Ayşe Erol**[1], **Ömer Dönmez**[1]

[1] *Istanbul University, Faculty of Science, Department of Physics*
[2] *Istanbul University, Institute of Graduate Studies in Sciences,*

Gallium oxide (β-Ga_2O_3) has emerged as a premier ultra-wide-bandgap semiconductor for next-generation high-power electronics and deep-ultraviolet optoelectronics because of its high breakdown field and scalable bulk growth. Due to its low monoclinic symmetry, the macroscopic properties of β-Ga_2O_3 are highly anisotropic, making orientation-aware substrate selection and process monitoring critical for advanced device engineering. This study systematically investigates the orientation-dependent structural and optical evolution of unintentionally doped (UID) and tin (Sn)-doped bulk β-Ga_2O_3 single crystals grown by the edge-defined film-fed growth (EFG) method. To resolve the coupled effects of structural anisotropy and heavy donor incorporation, 2-inch wafers with (001) and ($\bar{2}$01) surface orientations were comprehensively evaluated across a wide range of donor concentrations using angle-resolved high-resolution X-ray diffraction (HRXRD) and room-temperature optical absorption spectroscopy.

Angle-resolved HRXRD measurements confirm that all samples maintain a phase-pure monoclinic structure (space group C2/m) with no detectable secondary phases, such as SnO or SnO_2, at any azimuthal rotation angle. This demonstrates that both orientations successfully accommodate heavy n-type doping without phase degradation. However, structural quality shows a strong orientation dependence, indicating that the structural perfection of these substrates is fundamentally governed by their crystallographic plane. The (001)-oriented wafers display significantly narrower full-width at half-maximum (FWHM) values than the ($\bar{2}$01) counterparts, indicating superior crystalline perfection and a minimized mosaic spread along the c-axis. Furthermore, Sn incorporation in the (001) series modestly narrows the FWHM values, suggesting that donor doping may mitigate native point defects or relax local strains during EFG melt growth while preserving the superior structural framework of the (001) plane.

Optical absorption analysis shows that both the crystallographic orientation and Sn-doping profiles strongly govern the fundamental band-edge response and the near-edge optical landscape. Under unpolarized conditions, the Tauc-derived effective optical bandgap of the UID samples is resolved at 4.65 eV for the (001) orientation and 4.63 eV for the ($\bar{2}$01) orientation, directly reflecting the intrinsic optical anisotropy of the monoclinic lattice. With increasing Sn incorporation, both orientation series exhibit a significant, concentration-dependent blue shift of the absorption edge by up to 53 meV, demonstrating that the effective bandgap can be controllably expanded via the Burstein-Moss shift. This substantial blue shift is consistent with the filling of the lowest conduction-band states as the Fermi level moves upward. Logarithmic absorption-tail (ln(α)-E) analyses reveal distinct sub-bandgap disorder characteristics between the two orientations; the ($\bar{2}$01) series shows a robust baseline, with the broad near-edge tail of the undoped crystal notably narrowing and stabilizing upon Sn introduction.

ORCID:
Selen Nur Yılmaz: 0009-0000-8185-2413

Keyword: *β-Ga_2O_3, Single crystal, HRXRD*

A Safety-by-Design Framework for Silver Nanoparticles in Biomedical Applications

Melis Kaya * **, Furkan Eker, Sercan Karav**

Department of Molecular Biology and Genetics, Çanakkale Onsekiz Mart University

Silver nanoparticles are an important research topic in nanotechnology due to their strong antimicrobial activity, functionalizable surface properties and capacity to be integrated into different biomedical systems. These nanoparticles are widely evaluated in areas including wound healing, drug delivery systems, antimicrobial coatings, implant surface modification, biosensors and infection-control biomaterials. However, their biological effects cannot be explained only by their therapeutic potential. Key parameters such as synthesis method, particle size and shape, surface charge, coating material, agglomeration tendency, silver ion release profile, dose, exposure time and route of administration can directly affect cellular responses and biological safety outcomes. In addition, the protein corona formed on the nanoparticle surface in biological environments can alter particle stability, cellular interactions, biodistribution and toxicity profiles. Therefore, for the translation of silver nanoparticles into biomedical applications, safety evaluation should not be considered only as a final-stage test but should be included as a fundamental criterion from the beginning of the design process. This study proposes a conceptual safety-by-design framework and decision matrix for silver nanoparticles in biomedical applications. In this approach, physicochemical properties, nano–bio interactions, therapeutic efficacy and toxicity risks are evaluated together to establish a design strategy that balances efficacy and safety. Rather than focusing on a single parameter, this framework emphasizes the combined optimization of synthesis-related factors, particle properties, surface chemistry, silver ion release behavior, exposure conditions and route of administration. This optimization can be supported by biocompatible surface coatings, controlled ion release, stability evaluation under biological conditions, determination of an appropriate dose range and early integration of application-specific safety tests into the design process. In conclusion, the future success of silver nanoparticle-based biomedical systems depends not only on high therapeutic efficacy but also on application-specific, controlled and safety-oriented design approaches.

ORCID:
Melis Kaya: 0009-0006-0763-6812
Furkan Eker: 0009-0002-5260-6111

References:
https://doi.org/10.3389/fbioe.2022.836742
https://doi.org/10.3390/nano14181527
https://doi.org/10.3389/fbioe.2022.987650

Keyword: *Silver nanoparticles, Safety-by-design, Biological safety*

Human Intestinal Organoid-Derived Monolayers Recapitulate Epithelial Features Relevant to Oral Nanomedicine Evaluation

Merve Ceylan [*] [1,2,3], **Zekai Serhan Derici**[4], **Nilay Danış**[5], **Anıl Aysal Ağalar**[6], **Sinan Güven**[1]

[1] *İzmir Biomedicine and Genome Center, İzmir, Türkiye*
[2] *Department of Pharmacy, Uppsala Biomedical Centre, Uppsala University, Uppsala, Sweden*
[3] *Department of Biomedical Equipment Technology, İzmir Democracy University, İzmir, Türkiye*
[4] *Department of General Surgery, Faculty of Medicine, Dokuz Eylül University, İzmir, Türkiye*
[5] *Department of Internal Medicine, Faculty of Medicine, Dokuz Eylül University, İzmir, Türkiye*
[6] *Department of Pathology, Faculty of Medicine, Dokuz Eylül University, İzmir, Türkiye*

Human intestinal organoids have emerged as powerful human-relevant in vitro models for investigating tissue biology and disease mechanisms, addressing important limitations of conventional cell cultures and animal models. Adult stem cell-derived intestinal organoids are self-organizing three-dimensional structures that reproduce key architectural, cellular and functional features of their tissue of origin. Their capacity to preserve donor-associated biological features has positioned these models as valuable tools in personalized medicine. In parallel, nanotechnology has enabled the development of diagnostic and therapeutic systems with controllable size, surface chemistry, and biological behavior. Integrating organoid and nanomedicine technologies may therefore enable more physiologically relevant and predictive platforms for drug discovery and development.

This need is particularly relevant for orally administered nanomedicines, whose therapeutic performance is influenced not only by formulation properties but also by the biological characteristics of the intestinal barrier. To establish a more physiologically representative model of the human intestinal barrier, van Rijn et al. (Cell Reports, 2025) generated human intestinal organoids from adult intestinal stem cells and differentiated them into polarized epithelial monolayers. Electron and confocal microscopy, together with omics-based characterization, demonstrated progressive epithelial maturation, including the formation of microvilli, an apical glycocalyx, and the intermicrovillar adhesion complex. Here, the corresponding global proteomics dataset was reanalysed to identify molecular machinery relevant to nanomedicine–epithelium interactions. Differentiated monolayers expressed proteins associated with epithelial barrier integrity, cell-surface recognition, endocytic pathways, endo-lysosomal compartments and intestinal drug disposition. These pathways collectively define the epithelial machinery relevant to the recognition, internalization, trafficking, and intracellular fate of nanomedicines.

Together, these findings support human intestinal organoid-derived monolayers as a biologically characterized and experimentally accessible platform for evaluating oral nanomedicine formulations.

Acknowledgment:
We acknowledge all authors of van Rijn et al. (Cell Reports, 2025), led by Prof. Mikael E. Sellin, for their contributions to the development and characterization of the human organoid-derived epithelial monolayer models. M.C. acknowledges the Ph.D. scholarship from the Ministry of National Education of the Turkish Republic.

ORCID:
Merve Ceylan: 0000-0003-4252-6329
Zekai Serhan Derici: 0000-0002-2828-1452
Nilay Danış: 0000-0002-3939-3089
Anıl Aysal Ağalar: 0009-0003-6183-6848
Sinan Güven: 0000-0001-5212-5516

References:
van Rijn JM, Lopes ACC, Dienhart FSV, Ceylan M, Trinks N, Eriksson J, Bergholtz A, Ntokaki A, Hammar R, Sundbom M, Skogar M, Graf W, Webb DL, Hellström PM, Artursson P, Pelaseyed T, Di Martino ML, Sellin ME. Maturation of human intestinal epithelial cell layers fortifies the apical surface against Salmonella attack. Cell Rep. 2025 Dec 23;44(12):116579. doi: 10.1016/j.celrep.2025.116579.

Keyword: *Adult intestinal stem cell, human intestinal organoids, epithelial monolayers, differentiation, global proteomics, organoid−nanoparticle interaction*

Fabrication and Characterization of PANI-DMF Based Thin Film Sensor for NH3 Gas Detection

Erdi Ağrı * **, Ümit Doğan, Ahmet Ünverdi, Alican Ökçün, Şule Özdilek**

Department of Advanced R&D, Nero Industry Inc., 06909, Ankara, Türkiye

In this study, an NH_3 gas sensor was fabricated using a PANI-DMF solution prepared by dissolving polyaniline (PANI) in dimethylformamide (DMF). The sensor was investigated in terms of its structural, morphological, electrical, and gas-sensing properties. The prepared PANI-DMF solution was deposited onto an Au/Cr/SiO_2/Si substrate by spin coating, and the structural and morphological properties of the resulting thin films were characterized using scanning electron microscopy (SEM), energy-dispersive X-ray spectroscopy (EDS), and X-ray diffraction (XRD). Cross-sectional SEM analysis revealed a PANI thin-film thickness of approximately 250 nm ±10 nm. EDS analysis showed a high carbon content distributed across the surface, indicating the homogeneous formation of the PANI layer on the substrate. XRD analysis exhibited a diffraction peak at approximately 2θ =16.6° and 19.6°, attributed to the characteristic structure of PANI, thereby confirming the formation of the PANI thin film.

To evaluate the electrical and gas-sensing performance of the sensor, interdigitated transducer (IDT) structures were fabricated on Si/SiO_2 substrates using conventional photolithography, followed by direct deposition of the PANI-DMF solution onto the electrodes by spin coating. The electrical properties of the fabricated sensors were investigated through current-voltage (I-V) and time-dependent current (I-t) measurements. The I-V measurements indicated an electrical resistance of approximately 645 Ω for the PANI thin film. Time-dependent current measurements conducted under an NH_3 (100 ppm) atmosphere at room temperature and 53% relative humidity revealed a response and recovery times of approximately 50 s and 60 s, respectively. In addition, the sensor response toward NH_3 gas was calculated to be 43.17 ($(R_{gas}/R_{air})/R_{air}$). These results demonstrate that solution-processable PANI-DMF thin films are an effective active material for NH_3 detection and represent a promising candidate for the development of low-cost and easily fabricated gas sensors.

ORCID:
Erdi Ağrı: 0009-0007-6694-3182
Ümit Doğan: 0000-0002-7317-8497
Ahmet Ünverdi: 0000-0001-6144-1158
Alican Ökçün: 0009-0004-8599-7002
Şule Özdilek: 0000-0002-2859-1645

Keyword: *Pani, DMF, NH3 Sensor*

Protein A-Engineered SPR Biosensor for Real-Time IgG Capture and Purification

Ayşegül Bülbül [*] [1,2], Fatma Yılmaz[3], Ateş Kara[2,4], Adil Denizli[1]

[1] *Hacettepe University, Department of Chemistry, Ankara, Türkiye*
[2] *Health Institutes of Türkiye,Türkiye Vaccine Institute, Ankara, Türkiye*
[3] *Bolu Abant Izzet Baysal University, Department of Chemistry Technology, Bolu, Turkey*
[4] *Hacettepe University, Department of Pediatrics, Faculty of Medicine, Ankara, Türkiye*

Immunoglobulin G (IgG) plays a crucial role in therapeutic antibody production, diagnostic applications, and biomedical research. Conventional IgG purification techniques often involve multiple processing steps, lengthy procedures, and high operational costs, which makes advanced affinity systems highly desirable **[1]**. To address these challenges, we developed a Surface Plasmon Resonance (SPR)-based biosensor platform utilizing a Sepharose-supported Protein A affinity layer for the selective capture and purification of human IgG, building upon established high-precision SPR strategies for IgG sensing **[2]**.

This study focuses on the fabrication of a selective recognition surface by immobilizing Protein A onto a Sepharose-modified SPR sensor chip. The resulting affinity platform enables specific interaction with the Fc region of IgG molecules, facilitating selective antibody recognition. Characterization studies, including Fourier Transform Infrared Spectroscopy (FTIR), Scanning Electron Microscopy (SEM), Atomic Force Microscopy (AFM), and contact angle measurements, confirmed the successful formation of the Sepharose-based affinity layer, Protein A immobilization, and modifications in the surface morphology and wettability of the sensing platform. Preliminary binding studies demonstrated the effective interaction of IgG molecules with the Protein A-functionalized sensor surface under physiological conditions. The developed SPR platform exhibited rapid response characteristics and high selectivity toward IgG, highlighting its potential for real-time monitoring of antibody interactions. Furthermore, the integration of Sepharose and Protein A provides an affinity-based approach that may contribute to antibody purification and bioseparation applications. The proposed biosensor represents a promising platform for selective IgG recognition and purification, offering potential advantages in bioprocess monitoring, antibody production, and biomedical applications **[3]**. Moreover, the developed strategy may be extended to other biomolecular targets through the incorporation of alternative affinity ligands.

ORCID:
Ayşegül Bülbül: 0009-0000-7445-3086
Fatma Yılmaz: 0000-0003-4837-5066
Ateş Kara: 000-0002-1654-3232
Adil Denizli: 0000-0001-7548-5741

References:

Uzun, L., Türkmen, D., Karakoç, V., Yavuz, H., & Denizli, A. (2011). Performance of protein-A-based affinity membranes for antibody purification. Journal of Biomaterials Science, Polymer Edition, 22(17), 2325–2341.
Türkoğlu, E. A., Yavuz, H., Uzun, L., Akgöl, S., & Denizli, A. (2013). The fabrication of nanosensor-based surface plasmon resonance for IgG detection. Artificial Cells, Nanomedicine, and Biotechnology, 41(3), 213-221.
Parkkila, P., Härkönen, K., Ilvonen, P., Laitinen, S., & Viitala, T. (2022). Protein A/G-based surface plasmon resonance biosensor for regenerable antibody-mediated capture and analysis of nanoparticles. Biosensors and Bioelectronics, 207, 114175.

Keyword: *Surface Plasmon Resonance, Immunoglobulin G, Protein A*

Design of Biomaterial-Film-Modified Screen-Printed Platforms for Glucose Biosensing

Azra Kolukısa [*] [1], Eren Polat[1], Zeynep Elçim Koru[1], Selin Yavuzhan[1], Gözde Duman[2], Büşra Başol[2], Buğra Gizlenci[2], Suna Timur[1]

[1] *Ege University Faculty of Science, Department of Biochemistry*
[2] *Ege University Faculty of Science, Department of Chemistry*

The development of sensitive, low-cost, and portable glucose biosensors remains a major focus in electrochemical sensing due to their widespread applications in clinical diagnostics, food analysis, and point-of-care testing. In this study, a novel enzymatic glucose biosensor was fabricated using a screen-printed carbon electrode (SPCE) modified with a biochar/chitosan–tripolyphosphate (BC-CS–TPP) crosslinked film for the immobilization of glucose oxidase (GOx).

Electrochemical measurements were carried out by chronoamperometry in phosphate-buffered saline (PBS). The sensing mechanism was based on the enzymatic oxidation of glucose by GOx, producing hydrogen peroxide as a reaction product. The generated hydrogen peroxide was electrochemically oxidized at the electrode surface, and the resulting current response was monitored as the analytical signal. The BC-CS–TPP matrix not only served as an efficient enzyme immobilization platform but also enhanced biointerface stability and promoted effective mass transport at the electrode surface.

The proposed biosensor combines the advantages of disposable screen-printed electrodes with a biopolymer-based immobilization strategy, offering a simple, economical, and promising platform for electrochemical glucose monitoring. This approach may contribute to the development of next-generation biosensing systems employing biocompatible and environmentally friendly surface engineering strategies.

References:

Electrochemical and biosensing applications of biochar and biochar-based composites. Front. Sens. 6:1552969. doi: 10.3389/fsens.2025.1552969

Gupta, S., & Tai, N.-H. (2024). Carbon nanomaterials and their composites for electrochemical glucose biosensors: A review on fabrication and sensing properties. Journal of the Taiwan Institute of Chemical Engineers, 154, Article 104957. https://doi.org/10.1016/j.jtice.2023.104957

Kalinke, C., de Oliveira, P. R., Marcolino-Júnior, L. H., & Bergamini, M. F. (2024). Nanostructures of Prussian blue supported on activated biochar for the development of a glucose biosensor. Talanta, 274, Article 126042. https://doi.org/10.1016/j.talanta.2024.126042

Keyword: *Glucose biosensor, Biochar, Electrochemical sensing*

Development of a Mushroom-Derived Ce–N Co-Doped Carbon Quantum Dot/Alginate Biosensor for Glyphosate Detection in Water

Berkant Senturk [*1], Burak Tas[2], Ozge Tuzun Ozmen[3], Sabriye Yusan[1]

[1] *Ege University, Institute of Nuclear Sciences, İzmir, Türkiye*
[2] *İzmir Bakırcay University, Department of Electrical and Electronics Engineering, İzmir, Türkiye*
[3] *İzmir Bakırcay University, Department of Basic Sciences, İzmir, Türkiye*

Glyphosate is one of the most extensively used herbicides in modern agriculture, valued for its effectiveness in weed control and crop productivity enhancement. Nevertheless, its widespread application has raised growing concerns over environmental contamination and potential adverse effects on human health, particularly through its accumulation in water resources. Consequently, the development of sensitive, reliable, and cost-effective detection platforms for glyphosate monitoring in water has emerged as a significant research priority. Carbon quantum dot (CQD)-based sensing platforms have recently attracted considerable attention owing to their excellent optical and electrochemical properties, large surface area, and facile surface functionalization capabilities, making them highly promising materials for biosensing applications [1].

In this study, a novel biosensor for glyphosate detection in water was developed using carbon quantum dots (CQDs) synthesized from Agaricus bisporus biomass and co-doped with 0.5% Ce and 1% N. The synthesized CQDs were incorporated into a 2% alginate matrix to construct the sensing platform. Three identical biosensors were fabricated and designated as S1, S2, and S3 for systematic performance evaluation. Current–voltage (I–V) characterization was conducted using a Keithley 2450 Sourcemeter to assess the sensitivity and electrical stability of the developed sensors. S1 was measured without any analyte as a reference, while S2 and S3 were tested with clean water and glyphosate-contaminated water, respectively.

Comparison of the electrical responses revealed that S2 exhibited a 28% response toward clean water, whereas S3 demonstrated a markedly higher response of 72% toward glyphosate-contaminated water. The substantial difference in electrical output between the two conditions demonstrates the biosensor's capability to effectively discriminate between uncontaminated and herbicide-containing water samples with high sensitivity and reproducibility.

These results demonstrate that mushroom-derived Ce–N co-doped CQD/alginate biosensors hold significant potential for sensitive and stable glyphosate detection in aqueous environments. The proposed platform provides an environmentally friendly and analytically robust approach for water quality monitoring, offering a viable contribution to environmental protection and public health safety.

ORCID:
Berkant Senturk: 0000-0002-9127-583X
Burak Tas: 0000-0002-9928-5004
Ozge Tuzun Ozmen: 0000-0002-5204-3737
Sabriye Yusan: 0000-0002-1843-8591

References:
Ji, H., Zhou, F., Gu, J., Shu, C., Xi, K., & Jia, X. (2016). Nitrogen-doped carbon dots as a new substrate for sensitive glucose determination. Sensors, 16(5), 630.

Keyword: *Carbon quantum dots, Biosensor, Detection of Glyphosate*

A Complete Low-Volume Electrochemical System Employing SPE for Biosensing

Damla Aydogan [*1], Seda Nur Topkaya[2], Arif E. Cetin[3]

[1] *Izmir Biomedicine and Genome Center, Balcova, Izmir, Turkey; Department of Biomedical Engineering, Faculty of Engineering and Architecture, Izmir Bakircay University, Menemen, Izmir, Turkey*

[2] *Izmir Biomedicine and Genome Center, Balcova, Izmir, Turkey; Izmir International Biomedicine and Genome Institute, Dokuz Eylul University, Balcova, Izmir, Turkey*

[3] *Izmir Biomedicine and Genome Center, Balcova, Izmir, Turkey; Department of Biophysics, Faculty of Medicine, Dokuz Eylul University, Balcova, Izmir, Turkey*

Screen-printed electrodes (SPEs) are central to portable electrochemical biosensing, yet conventional pipette-based workflows suffer from uneven sample distribution, operator-dependent variability, and high consumable use, while reported SPE flow cells typically lack an integrated pumping mechanism (Kurul et al., 2025; Madadelahi et al., 2025). To address these limitations, we present a fully integrated, low-cost electrochemical sensing platform that unifies a custom 3D-printed flow cell, an embedded microfluidic pumping and valve module, an electrochemical regeneration unit, and a dedicated C# graphical user interface (GUI) for synchronized control, acquisition, and on-board analysis. The SLA-printed flow cell (clear resin) defines an effective contact volume of ~15 µL (per-run sample load ~45 µL) and aligns precisely with the full three-electrode SPE area. A piezoelectric micropump operating in suction mode, four solenoid valves, and an upstream flow sensor enable scripted delivery–measure–rinse sequences under PID-regulated closed-loop flow, while computational fluid dynamics (COMSOL) confirmed laminar transport (Reynolds number 2.4–7.2) with uniform velocity and low pressure drop across the sensing chamber.

Using double-stranded DNA (dsDNA) as a label-free model analyte, chronoamperometry under continuous flow yielded a linear calibration across 100–1000 µg/mL ($R^2 = 0.965$). Under matched conditions, closed-loop flow delivered comparable signal to pipetting while markedly improving reproducibility (CV ~3% vs ~8%), reducing baseline drift and carryover (<1%), and shortening hands-on time. A single electrochemical regeneration step (+1.8 V, 60 s) preserved ~90% of the initial signal, defining a realistic limited-reuse window for SPEs. Critically, the integrated GUI consolidates instrument control, automated dilution calculators, regression analysis, and real-time visualization, minimizing operator variability without external software. With a ~$6 flow-cell fabrication cost and off-the-shelf components, this compact, programmable chassis advances reproducible low-volume SPE assays and is readily adaptable to point-of-care and field diagnostics.

Acknowledgment:
This work was supported by the Scientific and Technological Research Council of Türkiye (TÜBİTAK) under Project No. 123Z570.

ORCID:
Damla Aydogan: https://orcid.org/0009-0007-5095-790X
Seda Nur Topkaya: https://orcid.org/0000-0002-7816-3155
Arif E. Cetin: https://orcid.org/0000-0002-0788-8108

References:

Kurul, F., Avci, M. B., Bertan Acar, H., Topkaya, S. N., & Cetin, A. E. (2025). Incubator-integrated electrochemical analysis platform for cell-based studies. npj Biosensing, 2, 6. https://doi.org/10.1038/s44328-025-00018-2

Madadelahi, M., Romero-Soto, F. O., Kumar, R., Tlaxcala, U. B., & Madou, M. J. (2025). Electrochemical sensors: Types, applications, and the novel impacts of vibration and fluid flow for microfluidic integration. Biosensors and Bioelectronics, 272, 117099. https://doi.org/10.1016/j.bios.2024.117099

Keyword: *Electrochemical biosensing, Screen-printed electrodes (SPEs), Microfluidics*

Au/Co3O4 Nanoparticle-Modified Platform for Multiplex Sensing of Galantamine, Dopamine, and Uric Acid

Dilara Yeniterzi [*] [1,2], Umut Bulut[3,4], Serdar Akbayrak[5], Saniye Soylemez[1,2]

[1] *Faculty of Engineering, Department of Biomedical Engineering, Necmettin Erbakan University, 42100, Konya, Türkiye*
[2] *Science Technology Research and Application Center (BITAM), Necmettin Erbakan University, 42100, Konya, Türkiye*
[3] *Faculty of Pharmacy, Department of Analytical Chemistry, Acıbadem Mehmet Ali Aydınlar University, Istanbul 34752, Türkiye*
[4] *Graduate School of Natural and Applied Sciences, Department of Chemistry, Acıbadem Mehmet Ali Aydınlar University, Istanbul 34752, Türkiye*
[5] *Faculty of Engineering, Department of Basic Sciences, Necmettin Erbakan University, 42140, Konya, Türkiye*

Simultaneous monitoring of galantamine (Gal), dopamine (DA), and uric acid (UA) is clinically important, as DA is associated with neurological disorders [1], UA is a key biomarker of oxidative stress and metabolic dysfunction [2], and Gal monitoring is essential for therapeutic drug control and pharmacokinetic studies [3]. In this study, an Au/Co₃O₄ nanoparticle-modified electrochemical platform was developed for the multiplex detection of these analytes using screen-printed electrodes (SPEs). The electrode surface was modified through a simple drop-casting strategy, and electrochemical measurements were performed using differential pulse voltammetry (DPV).

In this study, the synergistic combination of Au nanoparticles and Co_3O_4 significantly enhanced the electroactive surface area and facilitated electron transfer, resulting in wellresolved oxidation signals for Gal, DA, and UA despite their closely spaced oxidation potentials. Under optimized conditions, the platform exhibited linear response ranges of 2.0– 100.0 μM for Gal, 0.01–33.0 μM for DA, and 0.5–75.0 μM for UA, with corresponding detection limits of 3.97 μM, 0.51 μM, and 1.51 μM. Interference studies confirmed excellent selectivity toward the target analytes in the presence of common electroactive species. Furthermore, the proposed platform showed h gh analyt cal sens t v ty toward dopam ne (DA), ur c ac d (UA), and galantam ne (Gal), h ghl ght ng ts potent al for cl n cal appl cat ons. The platform also exhibited good reproducibility, with an RSD value of 1.97%, indicating excellent repeatability, along with rapid response characteristics and a simple, costeffective fabrication process. Its practical applicability was successfully validated using spiked artificial human serum samples, providing satisfactory analytical performance.

Overall, the developed Au/Co_3O_4 nanoparticle-modified platform represents a promising strategy for multiplex electrochemical sensing and simultaneous monitoring of clinically relevant biomarkers in complex biological matrices.

Acknowledgment:
S. Soylemez acknowledges financial support from the NEU-BAP (ULAP-24UA19001) project. S.Soylemez also gratefully acknowledges the Science Academy, Türkiye, for the Young Scientist Award Program (BAGEP). D.Yeniterzi gratefully acknowledges the financial support provided by the TÜBİTAK 2224-B Domestic Scientific Events Participation Support Program for conference participation.

References:
[1] Tóth, A. D.; Prokop, S.; Gyombolai, P.; Várnai, P.; Balla, A.; Gurevich, V. V.; Hunyady, X. L.; Turu, X. G. Heterologous Phosphorylation–Induced Formation of a Stability Lock Permits Regulation of Inactive Receptors by β-Arrestins. Journal of Biological Chemistry 2018, 293 (3), 876–892.
[2] Gherghina, M. E.; Peride, I.; Tiglis, M.; Neagu, T. P.; Niculae, A.; Checherita, I. A. Uric Acid and Oxidative Stress-Relationship with Cardiovascular, Metabolic, and Renal Impairment. Int. J. Mol. Sci. 2022, 23 (6).
[3] Huang, F.; Fu, Y. A Review of Clinical Pharmacokinetics and Pharmacodynamics of Galantamine, a Reversible Acetylcholinesterase Inhibitor for the Treatment of Alzheimer's Disease, in Healthy Subjects and Patients. Curr. Clin. Pharmacol. 2010, 5 (2), 115–124.

Keyword: *Gold Nanoparticles, Multiplex electrochemical detection, Galantamine, Dopamine, Uric acid.*

Smartphone-Assisted PAN Nanofiber-Based Fluorescent Biosensing Platform for Epidermal Growth Factor Receptor Detection

Dilek Soyler * [1,2], **Semih Can Çakmaktepe**[3], **Oguzhan Karakurt**[3], **Ali Cirpan**[3,4,5,6], **Serdar Akbayrak**[7], **Saniye Soylemez**[1,2]

[1] *Department of Biomedical Engineering, Necmettin Erbakan University, Konya, Türkiye*
[2] *Science Technology Research and Application Center (BITAM), Necmettin Erbakan University, Konya, Türkiye*
[3] *Department of Chemistry, Middle East Technical University, Ankara, Türkiye*
[4] *The Center for Solar Energy Research and Application (GUNAM), Middle East Technical University, Ankara, Türkiye*
[5] *Department of Polymer Science and Technology, Middle East Technical University, Ankara, Türkiye*
[6] *Department of Micro and Nanotechnology, Middle East Technical University, Ankara, Türkiye*
[7] *Department of Basic Sciences, Necmettin Erbakan University, Konya, Türkiye*

Fluorescent 3,3'-((5,6-bis(octyloxy)benzo[c][1,2,5]thiadiazole-4,7-diyl)bis(thieno[3,2b]thiophene-5,2-diyl))dianiline (BThTt-NH_2)-embedded PAN nanofibers have attracted considerable attention in biosensing applications due to their high fluorescence efficiency, tunable optical properties, and large surface area for biomolecule immobilization [1]. Their nanofibrous architecture enables enhanced interaction with target analytes and provides a promising platform for the development of sensitive and portable diagnostic systems. Epidermal Growth Factor Receptor (EGFR) is a clinically important biomarker associated with the diagnosis and progression of lung cancer. Rapid and accurate detection of EGFR is essential for early diagnosis and personalized treatment strategies [2]. In this study, a fluorescence-based biosensor platform utilizing small-molecule fluorescent nanofibers was developed for the sensitive detection of EGFR, aiming to provide a simple, portable, and point-of-care diagnostic approach [3]. This fluorescence-based biosensor system was designed for the detection of a critical lung cancer biomarker, EGFR. For the fabrication process, small-molecule fluorescent nanofibers were first prepared by dissolving the fluorescent BThTt-NH_2 precursor in an appropriate solvent system, followed by nanofiber formation through an electrospinning approach. The resulting fluorescent nanofibers were then deposited onto paper support materials to obtain uniform sensing surfaces. Anti-EGFR antibodies were immobilized onto these designated spots through physical adsorption, enabling specific antigen–antibody recognition. After incubation with EGFR-containing samples, the fluorescence intensity of the nanofiber layer changed depending on the biomolecular interaction occurring at the sensing interface. The fluorescent responses were visualized under UV illumination and recorded using a smartphone camera. The captured images were analyzed in RGB channels using ImageJ software to obtain quantitative fluorescence data. This approach enables the development of a portable, smartphone-assisted point-of-care (POC) biosensing platform based on smallmolecule fluorescent nanofibers. The combination of fluorescent BThTt-NH_2-embedded PAN nanofibers-based sensing, and smartphone-assisted analysis offers a simple, low-cost, and portable approach for point-of-care diagnostics. The results obtained so far demonstrate the promising performance of the developed nanofiber-based biosensor platform. Further studies are currently underway to perform comprehensive analytical validation, including sensitivity, selectivity, reproducibility, stability, and real-sample analyses.

Acknowledgment:
S.Soylemez acknowledges the Science Academy, Türkiye for the Young Scientist Award Program (BAGEP). D.Soyler gratefully acknowledges the financial support provided by the TÜBİTAK 2224-B Domestic Scientific Events Participation Support Program for conference participation.

ORCID:
Dilek Soyler: 0000-0003-3937-5830

References:
[1] Tian, X., Murfin, L. C., Wu, L., Lewis, S. E., & James, T. D. (2021). Fluorescent small organic probes for biosensing. Chem. Sci., 12(10), 3406-3426.
[2] Chen, S., Li, M., Weng, T., Wang, D., & Geng, J. (2023). Recent progress of biosensors for the detection of lung cancer markers. J. Mat. Chem. B, 11(25), 5715-5747.
[3] Halicka, K., & Cabaj, J. (2021). Electrospun nanofibers for sensing and biosensing applications—a review. Int. J. Mol. Sci., 22(12), 6357.

Keyword: *Fluorescent Nanofiber, Free-Standing Platforms, Point-of-Care Test System*

Development of a Fluorescence-Based Sensor with Fe_3O_4@SiO_2 Magnetic Nanoparticles; Application in Environmental Water Samples

Zeynep Azra Demir, Doğa Yücesoy * , Reyhan Selin Uysal Afacan

Department of Genetics and Bioengineering, Istanbul Bilgi University, Istanbul, 34060, Türkiye

Increased industrial activity, wastewater, and managementchemicals today are causing widespread heavy metal ion (lead, cadmium, etc.) in aqueous environments, leading to significanthealth and stress problems [3]. Long-term exposure to these ionscan cause permanent effects such as kidney, heart, and nervedamage. Therefore, rapid, sensitive, low-growth, andenvironmentally friendly detection of heavy metals in aqueousenvironments is becoming increasingly important in focusanalyses. This planning objective is to develop a non-toxic sensor system based on Fe_3O_4@SiO_2 magnetic nanoparticles (MNPs) exhibiting fluorescent properties and to define its applicability forheavy metal allocation from water samples. The sensor is constructed by combining the magnetic properties of Fe_3O_4 elements, the solubility of the SiO_2 coating, and the bonding of a fluorescent dye onto functional surfaces obtained via APTES (3-aminopropyltriethoxysilane) [1,2]. Thanks to this structure, thesystem will be able to provide both magnetic and fluorescent-based optical signal generation. The characterization of thesynthesized nanocomposite will be validated by FT-IR and ICP-MS [1,2] analyses, and fluorescence spectroscopy and UV-Vis willbe used as measurement methods. The resulting sensor will be determined as a component with improved detection range andlimit of detection (LOD) against Pb and Cd ions [4]. The change in optical response and distribution will be examined by monitoringthe fluorescence peak change after interaction with ion solutions at different temperatures. In addition, the selectivity and stability of the sensor will be evaluated by assessing the accuracy rate in thesamples during the testing period. For these evaluations, 3 samplestaken at different times of the day and 3 copies taken on differentdays will be compared. The sensor system within the scope of theproject can be produced from non-deformable, economical anddurable materials, unlike the quantum dot systematic details andelectrochemical sensors commonly used in the literature. Thesensor system that will emerge as a result of this study is a fast, low-cost and portable detection system that can be grown in bothlaboratory and field environments. In this way, the projectcontributes to the development of an environmentally friendly andadvanced sensor used in areas such as water quality monitoring, environmental health protection, and wastewater analysis [3].

References:

[1] Bilgic, A., & Cimen, A. (2020). A highly sensitive and selective ON-OFF fluorescent sensor based on functionalized magnetite nanoparticles for detection of Cr(VI) metal ions in the aqueous medium. Journal of Molecular Liquids, 312, 113398. https://doi.org/10.1016/j.molliq.2020.113398 [2] Karakelle, Saliha Büşra Avşar. (2019, October 18). Fonksiyonelleştirilmiş manyetik nanopartiküllerin sentezi ve boyar madde adsorpsiyonunda kullanılması. Uludag.edu.tr; Bursa Uludağ Üniversitesi

Keyword: *Keywords: Heavy metal, Magnetic nanoparticle, Aqueous medium, Fluorescence*

Beyond Spherical Gold Nanoparticles: Comparative Evaluation of Gold Nanolabels for Enhanced Lateral Flow Assays

Egemen Aydin [*1], Ozge Ozufuklar[2], Veysel Ceyirdekci[3], Suna Timur[4], Emine Guler Celik[1]

[1] *Department of Bioengineering, Faculty of Engineering, Ege University*

[2] *Department of Biotechnology, Institute of Natural Sciences, Ege University, Izmir 35100, Türkiye*

[3] *Department of Bioengineering, Institute of Natural Sciences, Ege University, Izmir 35100, Türkiye, Ege Science Pro Scientific Research Inc., Izmir 35100, Türkiye*

[4] *Department of Biochemistry, Faculty of Science, Ege University, Izmir 35100, Türkiye*

Lateral flow assays (LFAs) have emerged as promising point-of-care testing (POCT) platforms due to their ease of use, rapid results, and low cost. However, their analytical performance is often influenced by the properties of gold nanoparticles (AuNPs) used as signal labels. In this study, different AuNP morphologies were compared in terms of their effects on LFA performance[1]. For this purpose, gold nanospheres, nanoflowers, nanostars, nanorods, and nanocubes were synthesized, as each morphology offers different surface area and optical properties, including antibody-binding capacity, plasmonic behavior, and signal-enhancing features such as sharp edges or branched structures. The synthesized AuNPs were characterized and then conjugated with the same detection antibody to allow a fair comparison using the same target analyte[2]. The influence of stabilization and antibody conjugation conditions was also evaluated to better understand morphology-dependent assay behavior.

Assay performance was assessed through visual observation and quantitative analysis by considering colloidal stability, dispersibility, signal intensity, and limit of detection (LOD). In addition, shelf-life performance was compared through aging tests to evaluate the long-term stability of the prepared LFA strips. Overall, the results indicated that AuNP morphology, together with stabilization and conjugation strategies, strongly affects the sensitivity, reproducibility, reliability, and storage stability of LFAs. This improvement can be mainly associated with morphology-dependent differences in surface area, antibody loading behavior, plasmonic properties, and visual signal formation[3]. These findings suggest that selecting the appropriate AuNP morphology is an important step in designing more effective and stable next-generation POCT platforms.

This research was also supported by TUBITAK 2209-B - Industry Oriented Research Project Support Program for Undergraduate Students and Republic of Turkey─Ministry of Development via the 2016K121190 grant.

Acknowledgment:
This research was also supported by TUBITAK 2209-B - Industry Oriented Research Project Support Program for Undergraduate Students and Republic of Turkey─Ministry of Development via the 2016K121190 grant.

References:

Li, M., Wei, J., Song, Y., & Chen, F. (2022). Gold nanocrystals: Optical properties, fine-tuning of the shape, and biomedical applications. RSC Advances, 12(36), 23057–23073.

Zhang, L., Mazouzi, Y., Salmain, M., Liedberg, B., & Boujday, S. (2020). Antibody-Gold Nanoparticle Bioconjugates for Biosensors: Synthesis, Characterization and Selected Applications. Biosensors and Bioelectronics, 165, 112370.

Liang, R., Wang, F., Li, S., Niu, Y., Sun, Y., Hong, S., & Fan, A. (2024). A sensitive gold nanoflower-based lateral flow assay coupled with gold staining technique for the detection of SARS-CoV-2 antigen. Mikrochimica acta, 191(7), 434.

Keyword: *Lateral flow assay, Point-of-care, Gold nanoparticles*

Developing a QCM-based Biosignature Detection Concept Using Molecularly Imprinted Polymeric Adsorbents Embedded in Multilayered Nanofilms

Egemen Sönmez [* 1], Yaren Özkaynak[1], Selin Baş[2], Kaan Arıduman[2], Cansu Yıldırım[3,4], Tuğrul Cem Bıçak[4,5], Hüseyin Enis Karahan[4,5]

[1] Department of Geological Engineering, Istanbul Technical University, Maslak 34469, Istanbul, Türkiye
[2] Department of Molecular Biology and Genetics, Istanbul Technical University, Maslak 34469, Istanbul, Türkiye
[3] Polymer Science and Technology Graduate Program, Istanbul Technical University , Maslak 34469, Istanbul, Türkiye
[4] Synthetic Fuels & Chemicals Technology Center (ITU-SENTEK), Istanbul Technical University , Maslak 34469, Istanbul, Türkiye
[5] Department of Chemical Engineering, Istanbul Technical University , Maslak 34469, Istanbul, Türkiye

The detection of molecular biosignatures is a primary objective in planetary exploration and astrobiology, as these complex chemical structures provide evidence of past or present life that cannot be replicated by abiotic processes. Targeting hopanoids (a type of membrane lipid) is particularly valuable as they can be preserved over the geological record from the Precambrian to the present. Their resistance to thermal and biological degradation makes them robust targets for potential life detection. To identify such biomarkers, planetary rovers must perform autonomous onboard analyses directly on the planet's surface. Conventionally, analytical techniques such as Gas Chromatography-Mass Spectrometry (GC-MS) are used for their detection [1]. However, such techniques are highly destructive for samples containing organic materials. To overcome these limitations, this study proposes a non-destructive detection method employing a quartz crystal microbalance (QCM) coated with a molecularly imprinted polymer (MIP) using cholesterol as a template molecule. Cholesterol was chosen as an analogue molecule of hopanoids based on their molecular similarity, suitability for molecular imprinting, and commercial availability [2]. The MIP is synthesized by thermally initiated solution polymerisation, using methacrylic acid as the functional monomer, divinylbenzene as the crosslinker, and cholesterol as the template [3]. Once the polymerisation was completed, the template was extracted from the polymer matrix, yielding cavities specific for cholesterol recognition. In the designed concept device, the adsorbed mass shifts the crystal's resonant frequency, enabling precise quantification. A major limitation, however, is the stabilization of MIP particles on the QCM surface. For surface adhesion, a layer-by-layer (LbL) assembly approach was employed to embed the particles within a stable polymeric film as the matrix. To this end, spray-assisted poly(N-vinylpyrrolidone) and tannic acid (PVPON/TA) films [4] were tested for the first time to embed these particles. Using such a thin and permeable film, we aimed to circumvent potential mass transfer limitations. Optical microscopy analyses ensured a fairly uniform dispersion of MIP particles in view of their particle size distribution. Yet still, the existing onboard sensor, initially developed for the ITU Rover Science Team's rover vehicle, is expectedly instrumental for extraterrestrial life search purposes and beyond. Given that the synthesized MIPs were irregular in shape, we are currently focused on MIP particles having a narrow size distribution. Overall, this project introduces an autonomous sensor design by combining molecular imprinting with quartz crystals and offers an alternative to conventional onboard rover systems designed for biosignature detection.

Acknowledgment:
We thank all the past and present members and advisors of the ITU Rover Team.

ORCID:
Egemen Sönmez: 0009-0007-4117-1083
Yaren Özkaynak: 0009-0005-2430-0977
Selin Baş: 0009-0003-6376-8578
Kaan Arıduman: 0009-0002-7234-0744
Cansu Yıldırım: 0000-0003-1023-4030
Tuğrul Cem Bıçak: 0000-0002-8761-0121
Hüseyin Enis Karahan: 0000-0002-7753-1024

References:
[1] Summons, R. E., Welander, P. V., & Gold, D. A. (2022). Lipid biomarkers: molecular tools for illuminating the history of microbial life. Nature Reviews Microbiology, 20(3), 174-185.
[2] Sáenz, J. P., Sezgin, E., Schwille, P., & Simons, K. (2012). Functional convergence of hopanoids and sterols in membrane ordering. Proceedings of the National Academy of Sciences of the United States of America, 109(35), 14236–14240.
[3] Hwang, C. C., & Lee, W. C. (2002). Chromatographic characteristics of cholesterol-imprinted polymers prepared by covalent and non-covalent imprinting methods. Journal of Chromatography A, 962(1–2), 69–78.
[4] Karahan, H. E., Eyüboğlu, L., Kıyılar, D., & Demirel, A. L. (2014). pH-stability and pH-annealing of H-bonded multilayer films prepared by layer-by-layer spin-assembly. European Polymer Journal, 56, 159-167.

Keyword: *Biosensor, Cholesterol, Layer-by-Layer*

ITO-Based Dual-Mode Lateral Flow Biosensor Integrating Smartphone Imaging and Electrochemical Quantification

Ela Koçhan [* 1], Ozge Ozufuklar[2], Sena Yanasık[3], Veysel Ceyirdekci[3], Suna Timur[4], Emine Guler Celik[5]

[1] *Department of Bioengineering, Institute of Natural Sciences, Ege University, Izmir 35100, Türkiye*
[2] *Department of Biotechnology, Institute of Natural Sciences, Ege University, Izmir 35100, Türkiye*
[3] *Department of Bioengineering, Institute of Natural Sciences, Ege University, Izmir 35100, Türkiye , Ege Science Pro Scientific Research Inc., Izmir 35100, Türkiye*
[4] *Department of Biochemistry, Faculty of Science, Ege University, Izmir 35100, Türkiye*
[5] *Department of Bioengineering, Faculty of Engineering, Ege University, Izmir 35100, Türkiye*

Optical and electrochemical detection channels integrated within a single platform offer analytical advantages including signal cross-validation, extended dynamic range, and enhanced specificity against biological matrix interference, representing an increasingly prominent strategy in biosensor design[1]. Here, we present a novel integrated opto-electrochemical (O-EC) lateral flow assay (LFA) platform for the rapid, wash-free detection of salivary morphine levels. In LFA-based systems, the capillary flow principle enables an intrinsic self-washing mechanism whereby the sample is driven across the membrane by absorbent pad-generated forces, simultaneously carrying unbound reagents along the flow path and thereby systematically eliminating the discrete washing steps required in spot-based tests. In the platform described herein, the conventional nitrocellulose membrane was replaced by an indium tin oxide (ITO)-coated glass substrate which simultaneously functions as a microfluidic channel, immunoreactive surface, and dual-mode transducer. The ITO surface was silanized with (3-aminopropyl)triethoxysilane (APTES) and subsequently activated with glutaraldehyde as a crosslinker, a chemistry that provides stable and reproducible biomolecule immobilization on oxide surfaces[2]. Gold nanoparticle–antibody conjugates deposited at the conjugate zone served as colorimetric reporters, while Tollens reagent-based silver enhancement amplified both the visual contrast and the electrochemical signal[3]. Optical readout was achieved via smartphone-based RGB imaging, while electrochemical quantification was performed by differential pulse voltammetry (DPV) the mutual cross-validation of the two channels extends the effective dynamic range of the assay and functionally distinguishes this platform from single-mode approaches[1]. These findings demonstrate that the integrated O-EC LFA platform is capable of simultaneously delivering quantitative accuracy and operational simplicity within a single biosensor architecture, constituting a viable approach for practical point-of-care drug screening.

This research was also supported by TUBITAK 2209-B - Industry Oriented Research Project Support Program for Undergraduate Students.

Acknowledgment:
This research was also supported by TUBITAK 2209-B - Industry Oriented Research Project Support Program for Undergraduate Students.

References:
Blackshare, J., Corman, B., Rajwa, B., Robinson, J. P. & Bae, E. Portable Dual-Mode Biosensor for Quantitative Determination of Salmonella in Lateral Flow Assays Using Machine Learning and Smartphone-Assisted Operation. Biosensors (Basel) 16, 57 (2026).
Sypabekova, M., Hagemann, A., Rho, D. & Kim, S. Review: 3-Aminopropyltriethoxysilane (APTES) Deposition Methods on Oxide Surfaces in Solution and Vapor Phases for Biosensing Applications. Biosensors (Basel) 13, 36 (2022).
Beck, F., Loessl, M. & Baeumner, A. J. Signaling strategies of silver nanoparticles in optical and electrochemical biosensors: considering their potential for the point-of-care. Microchim Acta 190, 91 (2023).

Keyword: *ITO Glass, Silver Enhancement, Wash-free assay*

Dual Electrodes, Triple Detection: A Flexible MXene-Based Platform for Simultaneous Electrochemical Detection of Dopamine, Uric Acid, and Glucose

Esra Nur Elmas [*] [1,2], Dilara Yeniterzi[1,2], Serdar Akbayrak[3], Saniye Soylemez[1,2]

[1] Faculty of Engineering, Department of Biomedical Engineering, Necmettin Erbakan University, 42100, Konya, Türkiye
[2] Science Technology Research and Application Center (BITAM), Necmettin Erbakan University, 42100, Konya, Türkiye
[3] Necmettin Erbakan University, Faculty of Engineering, Department of Basic Sciences, 42140, Konya, Türkiye

MXenes, a class of two-dimensional transition metal carbides and nitrides, are promising materials for electrochemical biosensing due to their high electrical conductivity, large surface area, and efficient charge-transfer properties. Their performance can be further enhanced by coupling with catalytically active nanostructures and metallic nanoparticles, leading to improved electron transfer kinetics, increased active site density, and enhanced electrocatalytic activity [1,2]. Prussian Blue (PB) is widely used as an artificial peroxidase in electrochemical biosensors, enabling efficient hydrogen peroxide reduction at low potentials and signal amplification, particularly for glucose detection [3]. Simultaneous detection of dopamine (DA), uric acid (UA), and glucose is clinically important due to their association with neurological and metabolic disorders such as Parkinson's disease, gout, renal dysfunction, and diabetes [4]. Flexible electrochemical sensors offer significant advantages for real-time and multiplexed wearable biosensing applications [5].

In this study, a flexible dual-electrode MXene-based electrochemical biosensing platform was developed for the simultaneous and selective detection of dopamine (DA), uric acid (UA), and glucose. The first working electrode was engineered with Ni–MXene nanocomposites to enable sensitive detection of DA and UA, while the second electrode was modified with a GOximmobilized PB/Ni–MXene composite to achieve selective glucose sensing with enhanced electrocatalytic performance. The proposed dual-electrode architecture provides efficient signal separation and improved analytical reliability, demonstrating strong potential for real-time, wearable, and multiplexed biosensing applications in personalized health monitoring.

Acknowledgment:
S. Soylemez acknowledges financial support from the NEU-BAP (ULAP-24UA19001) project. S.Soylemez also gratefully acknowledges the Science Academy, Türkiye, for the Young Scientist Award Program (BAGEP).

References:
[1] Ali, M.; Barman, S. C.; Steer, I.; Alshareef, A. H.; Alsulaiman, D. Unlocking the Potential of MXene-Based Electrochemical Biosensors: A Review of Biofunctionalization Strategies and Biosensing Principles. Adv. Mater. Technol. 2026, e02120.
[2] Riazi, H.; Taghizadeh, G.; Soroush, M. MXene-Based Nanocomposite Sensors. ACS Omega 2021, 6 (17), 11103–11112.
[3] Cinti, S.; Cusenza, R.; Moscone, D.; Arduini, F. Paper-Based Synthesis of Prussian Blue Nanoparticles for the Development of Whole Blood Glucose Electrochemical Biosensor. Talanta 2018, 187, 59–64.
[4] Sun, Y.; Ma, J.; Wang, Y.; Qiao, S.; Feng, Y.; Li, Z.; Wang, Z.; Han, Y.; Zhu, Z. A Wearable Patch Sensor for Simultaneous Detection of Dopamine and Glucose in Sweat. Analytica 2023, Vol. 4, Pages 170-181 2023, 4 (2), 170–181.
[5] Bariya, M.; Yin, H.; Nyein, Y.; Javey, A. Wearable Sweat Sensors. 1928.

Keyword: *Ni-MXene, Prussian Blue, Electrochemical Sensor, Multiplexed Detection*

Development of Antibody-Antigen-Based Plasmonic Sensors for the Rapid, Simple, and Inexpensive Detection of the Mutant Huntington Protein (mHTT), a Biomarker of Huntington's Disease

Fatma Dalkilic [*1], Nimet Temur[2], Seyma Dadi[3], Cemile Yilmaz[1], Aslihan Kiraz[4], Begum Unveroglu[5], Ismail Ocsoy[1]

[1] *Department of Analytical Chemistry, Faculty of Pharmacy, Erciyes University, Kayseri 38039, Turkey*
[2] *Erciyes University, Graduate School of Natural and Applied Sciences, Department of Nanoscience and Nanotechnology, Kayseri, Turkey*
[3] *Department of Engineering Fundamental Sciences, Faculty of Engineering and Natural Sciences, Sivas University of Science and Technology, Sivas, Türkiye*
[4] *Department of Medical Genetics, Erciyes University Medicine Faculty Kayseri, 38039, Kayseri, Turkey*
[5] *Metallurgical and Materials Engineering Department, Ankara Yildirim Beyazit University, Ankara, Turkey*

Huntington’s disease (HTT) is a rare genetic disorder that affects the central nervous system and leads to severe neurological impairments. At the core of the disease lies the mutant Huntington protein (mHTT), which results from a mutation in the HTT gene. The mHTT protein disrupts cellular functions, leading to neuronal damage, neurotransmitter imbalances, and disruptions in DNA repair mechanisms, thereby playing a significant role in the progression of the disease. Therefore, the sensitive and reliable detection of mHTT is of great importance for the early diagnosis of Huntington’s disease and the monitoring of its progression.

In this study, an innovative plasmonic and colorimetric-based immunosensor platform for the detection of the mHTT protein was developed. First, the synthesized magnetic nanoparticles were conjugated with antibodies. Subsequently, glucose oxidase (GOx) constructs functionalized with polyclonal antibodies were prepared. In the presence of the target molecule (mHTT), a sandwich assay was formed as a result of the specific binding of the antibodies to their binding sites. When glucose is added to the system in the presence of the target, it reacts with GOx to produce hydrogen peroxide (H_2O_2). The resulting H_2O_2 causes structural changes by inducing the oxidation of gold nanostars added to the solution. This change was detected both through a colorimetric signal and via a wavelength shift observed in the spectrum.

This newly developed method offers a significant diagnostic advantage for the early and reliable detection of Huntington’s disease by enabling the monitoring of the analyte’s presence through visual and spectroscopic changes.

Keyword: *Mutant Huntington protein (mHTT), Plasmonic sensor, Altın nanostar*

Amplification-Free Detection of HBV cccDNA Using CRISPR-Cas12 and Photonic Resonator Absorption Microscopy

Fatma Uysal Ciloglu [*1,2], **My Nguyen**[3], **Lucas D. Akin**[3], **Sneha Mittal**[3], **Weinan Liu**[4], **Saurabh Umrao**[3], **Seemesh Bhaskar**[1], **Xing Wang**[3], **Daryl T. Lau**[5], **Brian T. Cunningham**[1]

[1] *Nick Holonyak Jr. Micro and Nanotechnology Laboratory, University of Illinois at Urbana-Champaign, Urbana, Illinois 61801, USA*
[2] *Department of Biomedical Engineering, Erciyes University, Kayseri 38039, Türkiye*
[3] *Departments of Bioengineering, Grainger College of Engineering, University of Illinois at Urbana-Champaign, IL 61801, USA*
[4] *Electrical and Computer Engineering, Grainger College of Engineering, University of Illinois at Urbana-Champaign, IL 61801, USA*
[5] *Liver Center, Division of Gastroenterology and Hepatology, Beth Israel Deaconess Medical Center, Boston, Massachusetts, USA*

Covalently closed circular DNA (cccDNA) is the persistent viral reservoir responsible for the chronic nature of Hepatitis B virus (HBV) infection and remains a major barrier to achieving a functional cure [1]. Consequently, sensitive and specific detection of cccDNA is critical for monitoring disease progression and evaluating therapeutic efficacy. However, current detection methods often rely on labor-intensive workflows and nucleic acid amplification, limiting their practicality for routine analysis.

In this study, we developed an amplification-free detection platform that integrates CRISPR-Cas12 molecular recognition with Photonic Resonator Absorption Microscopy (PRAM) [2] for sensitive detection of HBV cccDNA . The designed gRNAs were initially evaluated by gel electrophoresis and fluorescence spectroscopy, confirming efficient and target-specific Cas12 activation. Following validation, the assay was implemented using an Activate, Cleave, Capture, and Count (AC3) strategy. Target recognition activates Cas12-mediated collateral cleavage, releasing gold nanoparticles (AuNPs) attached to a surface through DNA linkers. The released AuNPs are then captured on a photonic crystal biosensor and digitally counted using PRAM. Using this approach, HBV cccDNA was detected down to 1 pM without nucleic acid amplification. These results demonstrate the potential of combining CRISPR-Cas12 and PRAM for rapid, highly specific, and amplification-free detection of HBV cccDNA and highlight its promise for future viral diagnostics and treatment monitoring applications.

Acknowledgment:
F.U.C. acknowledges support from the Scientific and Technological Research Council of Türkiye (TUBITAK), 2219 - International Postdoctoral Research Fellowship Program, Grant Agreement No: 1059B192302020.

ORCID:
Fatma Uysal Ciloglu: 0000-0001-8827-3668

References:
[1] Yuen, M. F., Chen, D. S., Dusheiko, G. M., Janssen, H. L., Lau, D. T., Locarnini, S. A., ... & Lai, C. L. (2018). Hepatitis B virus infection. Nature reviews Disease primers, 4(1), 18035.
[2] Canady, T. D., Li, N., Smith, L. D., Lu, Y., Kohli, M., Smith, A. M., & Cunningham, B. T. (2019). Digital-resolution detection of microRNA with single-base selectivity by photonic resonator absorption microscopy. Proceedings of the National Academy of Sciences, 116(39), 19362-19367.

Keyword: *HBV cccDNA, CRISPR-Cas12, Photonic Crystal Biosensor*

High-Sensitivity Biothiol Detection Utilizing Gold Nanoparticle-Functionalized Fluorescent Turn-On Probe

Garen Suna * [1], Eda Erdemir[1], Erman Karakuş[2], Songül Eğlence Bakır[1], Musa Şahin[1]

[1] *Istanbul University*
[2] *Tubitak*

The sensitive detection of low molecular weight biothiols such as cysteine, homocysteine and glutathione is vital for clinical diagnostics. Abnormal physiological levels are strongly linked to cancer and neurodegenerative disorders. In this work, we design a highly sensitive and selective fluorescent sensor system based on a novel fluorophore functionalized with gold nanoparticles (AuNPs).

Exploiting the exceptionally strong, thiophilic affinity of gold, the introduction of target biothiols induces a competitive displacement reaction at the nanoparticle interface. This disrupts the quenching pathway and releases the fluorescent moiety, triggering a robust "turn-on" fluorescence response that is directly proportional to biothiol concentration. The developed hybrid nanoprobe demonstrates an ultra-low detection limit, a wide linear dynamic range, and rapid kinetic performance under physiological conditions. Furthermore, the probe exhibits outstanding selectivity against a comprehensive panel of interfering amino acids, ions, and cellular reductants. This AuNP-functionalized platform presents a promising strategy for tracking intracellular thiol dynamics and holds significant potential for integration into advanced diagnostic biosensors.

ORCID:
Garen Suna: 0000-0002-8347-4134

References:
[1] W. Zhou, X. Gao, D. Liu, X. Chen, Gold Nanoparticles for In Vitro Diagnostics, Chem. Rev. 115 (2015) 10575–10636.
[2] S.J. Chen, Nile Red-Adsorbed Gold Nanoparticles for Selective Determination of Thiols Based on Energy Transfer and Aggregation, Anal. Chem. 77 (2005) 4166–4172.
[3] X. Su, H. Jiang, X. Wang, Thiols-Induced Rapid Photoluminescent Enhancement of Glutathione-Capped Gold Nanoparticles for Intracellular Thiols Imaging Applications, Anal. Chem. 87 (2015) 10230–10236.
[4] F. Li, Y. Liu, M. Zhuang, H. Zhang, X. Liu, H. Cui, Biothiols as Chelators for Preparation of N-(aminobutyl)-N-(ethylisoluminol)/Cu2+ Complexes Bifunctionalized Gold Nanoparticles and Sensitive Sensing of Pyrophosphate Ion, ACS Appl. Mater. Interfaces 6 (2014) 18104–18111.
[5] P.P.P. Kumar, A Multimode Detection Platform for Biothiols Using BODIPY Dye-Conjugated Gold Nanoparticles, Colorants 3 (2024) 214–228.

Keyword: *Fluorescent Sensors, Gold Nanoparticles, Biothiols, Turn-On Detection.*

CHIKV Lateral Flow Diagnostic Platform Enabled by Aptamer–Nanogold Conjugates

Gunes Ertemcoz [*] [1], Ozge Ozufuklar[2], Veysel Ceyirdekci[3], Jagriti Narang[4], Suna Timur[5], Emine Guler Celik[1]

[1] *Department of Bioengineering, Faculty of Engineering, Ege University, Izmir 35100, Türkiye*
[2] *Department of Biotechnology, Institute of Natural Sciences, Ege University, Izmir 35100, Türkiye*
[3] *Department of Bioengineering, Institute of Natural Sciences, Ege University, Izmir 35100, Türkiye, Ege Science Pro Scientific Research Inc., Izmir 35100, Türkiye*
[4] *Department of Biotechnology, School of Chemical and Life Science, Jamia Hamdard University, New Delhi 110062, India*
[5] *Department of Biochemistry, Faculty of Science, Ege University, Izmir 35100, Türkiye*

Recently, the rapid spread of viral diseases and their potential to cause outbreaks to have increased the need for fast, reliable, and easily applicable diagnostic systems for early detection. In this context, point-of-care testing (POCT), which enables diagnosis at or near the patient site, has become an important approach for early infection detection, faster clinical decision-making, and effective control of transmission[1].

Among POCT systems, lateral flow assays (LFA) are widely used because of their low-cost, rapid, portable, and user-friendly properties. In addition, their ability to work with small sample volumes, maintain stability under environmental conditions, and provide a long shelf life makes LFA systems advantages for rapid diagnostic applications[2].

In conventional LFA systems, antibodies are commonly used as target recognition element. However, their high production cost, long production process, and sensitivity to changes in temperature and pH have increased interest in alternative recognition elements. Therefore, interest in nucleic acid-based diagnostic approaches has gained increasing attention, and aptamers have started to provide an attractive alternative to antibodies. Aptamers are short single-stranded nucleic acid molecules capable of producing specifically target molecules. Compared with antibodies, aptamers offer several advantages, including cost effective, target-specific synthesis, easy chemical modification, and higher stability under different environmental conditions[3].

Integrating aptamers into LFA systems can improve the stability and specificity of rapid diagnostic platforms. In this study, a competitive aptamer-based LFA system was developed for CHIKV protein detection. CHIKV aptamers were conjugated with gold nanoparticles (AuNPs), which are widely used in commercial LFAs due to their strong optical properties and characteristic red color[2]. In the presence of CHIKV protein, the aptamer–AuNP conjugate binds to the target, preventing interaction with T DNA-long at the test line and producing no or weak T-line signal. In the absence of the target, the free conjugate binds to T DNA-long and generates a visible T-line signal. The control line is produced by the interaction between the biotinylated aptamer and streptavidin. Thus, a single C line indicates a positive result, whereas both T and C lines indicate a negative result. The system showed high specificity toward CHIKV protein and a linear response from 10 to 1000 ng/mL, with an R^2 value of 0.96. Overall, this study presents a rapid, accessible, user-friendly, and cost-effective aptamer-based LFA platform for CHIKV detection.

This research was also supported by TUBITAK 2209-B - Industry Oriented Research Project Support Program for Undergraduate Students and TUBITAK 2221 Program for Visiting Scientists and Scientists on Sabbatical Leave under the project titled “Development of a Multiplexed Lateral Flow Assay for the Colorimetric Detection of Dengue and Chikungunya”.

Acknowledgment:
This research was also supported by TUBITAK 2209-B - Industry Oriented Research Project Support Program for Undergraduate Students and TUBITAK 2221 Program for Visiting Scientists and Scientists on Sabbatical Leave under the project titled “Development of a Multiplexed Lateral Flow Assay for the Colorimetric Detection of Dengue and Chikungunya”.

References:
Naseri, M., Ziora, Z. M., Simon, G. P., & Batchelor, W. (2022). ASSURED-compliant point-of-care diagnostics for the detection of human viral infections. Reviews in Medical Virology, 32(2), e2263.
Wang, C., Liu, M., Wang, Z., Li, S., Deng, Y., & He, N. (2021). Point-of-care diagnostics for infectious diseases: From methods to devices. Nano Today, 37, 101092.
Huang, L., Tian, S., Zhao, W., Liu, K., Ma, X., & Guo, J. (2021). Aptamer-based lateral flow assay on-site biosensors. Biosensors and Bioelectronics, 186, 113279.

Keyword: *Lateral flow assay, Aptamer, Chikungunya virus*

Mo-MOF@GNR Nanohybrid-Based Electrochemical Sensors for the Detection of Bisphenol A

Havva Nur Gürbüz * **, Özlem Şahin, Yasemin Öztekin, Mustafa Şahin**

Selcuk University, Faculty of Science, Department of Chemistry, Konya, Turkey

Nanomaterial science is a multidisciplinary field that enables the tailored improvement of electronic, catalytic, and interfacial properties of materials through the quantum size effect. In this study, an efficient and sustainable electrochemical sensor based on a novel Metal Organic Frameworks (MOF) and Graphene Nanoribbon (GNR) hybrid structure was developed for the highly sensitive and selective detection of Bisphenol A (BPA), which stands as one of recently most critical health concerns. While the vast majority of existing MOF-based sensor studies in the literature focus on graphene and its derivatives (GO, rGO), a direct GNR integration for BPA determination represents a prime novelty in the literature. Characterization studies of the synthesized Mo-MOF@GNR nanohybrid material via different techniques confirmed that the controlled longitudinal unzipping process of carbon nanotubes was successfully completed, and the restacking problem frequently encountered in graphene sheets was completely prevented. Within this nanohybrid architecture, Mo-MOF enhances the analyte adsorption capacity and selectivity through its high porosity and specific coordination sites, while GNR accelerates the electron transfer rate owing to its superior electrical conductivity.The presence of structural defects and homogeneous nano-perforations created a high density of electroactive sites on the electrode surface, thereby significantly accelerating electron transfer. The analytical performance of the prepared nanohybrid material, modified onto a glassy carbon electrode (GCE) surface, was investigated in the presence of the target analyte via electrochemical techniques (cyclic voltammetry (CV) and chronoamperometry (CA)). Under optimized chronoamperometric conditions, where precise current-time responses were monitored, the sensor exhibited a remarkably wide linear range of 10-150 µM, reaching a highly successful limit of detection (LOD) of 0.75 µM along with a successful limit of quantification (LOQ: 2.50 µM). The real sample applicability of the developed nanobiosensor was tested on plastic bottle samples, demonstrating excellent accuracy with a relative standard deviation (RSD) below 5% and recoveries exceeding 95%. These novel findings demonstrate the synergistic potential of both MOF and GNR in electrochemical sensor architectures and offer a highly stable, innovative analytical tool for monitoring studies in clinical and environmental analytics.

Acknowledgment:
This study was financially supported by the Scientific and Technological Research Council of Türkiye (TÜBİTAK) under the 1002-Quick Support Program (Project No: 225M179).

ORCID:
Havva Nur Gürbüz: 0009-0007-4424-0662

References:

Zaman, N., Iqbal, N., Noor, T., Shahzad, N., & Gao, J. (2024). Sulfide-based Mo-MOF derived bifunctional electrocatalysts for direct methanol fuel cells. Fuel, 362, 130813. https://doi.org/https://doi.org/10.1016/j.fuel.2023.130813

Sahu, V., Shekhar, S., Sharma, R. K., & Singh, G. (2015). Ultrahigh performance supercapacitor from lacey reduced graphene oxide nanoribbons. ACS applied materials & interfaces, 7(5), 3110-3116

Kanarya, D., Gürbüz, H. N., & Tirgil, N. Y. (2026). Electrochemical SARS-CoV-2 IgG immunosensor with a high-surface-area PThi/MXene/SPE. Applied Surface Science, 741, 167221. https://doi.org/https://doi.org/10.1016/j.apsusc.2026.167221

Guo, S., Han, H., Gao, X., Zhai, Y., Wang, J., Zhang, Z., Liu, X., Yuan, R., Yang, L., & Wang, X. (2025). Functionalized β-cyclodextrin MOF with carbon nanotube conductive veins for highly sensitive and wide-concentration-range bisphenol A sensing. Microchemical Journal, 213, 113845. https://doi.org/https://doi.org/10.1016/j.microc.2025.113845

Han, X., Ai, Y., Wang, L., Liu, T., Badshah, A., Hu, X., Huang, Z., Mansoor, A. and Sun, W. (2025), Flexible Electrochemical Sensing: Compact and Efficient Detection of Bisphenol A Using Copper Nanoparticle Decorated Laser-Induced Graphene-Based Electrode. Electroanalysis, 37: e12025. https://doi.org/10.1002/elan.12025

Keyword: *Mo-MOF, Graphene Nanoribbon (GNR), Bisphenol A (BPA)*

Fabrication Of Laser-Induced Graphene And Screen-Printed Hybrid Electrodes For Electrochemical Sensing

Hikmet Batuhan Balki * **, Ezgi Kivrak, Eren Kucuk, Levent Beker**

Koç University, Mechanical engineering

Laser-induced graphene (LIG) has emerged as a promising electrode material for flexible electrochemical sensing platforms due to its porous morphology, good electrical conductivity, mechanical compliance, and direct patterning on polymeric substrates [1,2]. Wearable electrochemical biosensors have also shown strong potential for continuous and non-invasive monitoring of biochemical markers, further motivating the development of flexible electrode platforms [3]. However, practical sensor fabrication also requires reliable electrical interconnections and reference electrode integration, which can be challenging to achieve using laser processing alone. In this study, we present a hybrid fabrication approach combining LIG formation and screen printing for the development of flexible electrochemical electrodes.

LIG regions were patterned on 135 µm thick polyimide substrates using an LPKF R4 infrared laser system to form the carbon-based working and counter electrode areas. Screen printing was then used to define silver-based conductive paths and reference electrode regions through a stencil-based process. This hybrid strategy combines the mask-free, localized graphitization capability of laser processing with the simplicity and scalability of screen printing, enabling rapid fabrication of flexible electrode platforms.

The fabricated electrodes were characterized structurally and electrochemically to evaluate their suitability for sensing applications. Raman spectroscopy confirmed the formation of graphene-like carbon structures through the presence of characteristic D, G, and 2D bands. Scanning electron microscopy revealed a porous and flake-like LIG surface morphology, which is advantageous for increasing the active electrochemical surface area. Cyclic voltammetry measurements demonstrated the electrochemical functionality of the hybrid electrodes and confirmed their ability to support redox reactions.

Overall, we demonstrate a simple, low-cost, and adaptable fabrication route for LIG and screen-printed hybrid electrodes. As a next step, we plan to functionalize this platform with different recognition layers and adapt it for point-of-care and wearable electrochemical sensing applications, particularly for non-invasive biomarker monitoring and on-site biosensing.

Acknowledgment:
This work was supported by The Scientific and Technological Research Council of Türkiye (TÜBİTAK), project number 125E626.

ORCID:
Hikmet Batuhan Balki: 0009-0006-3263-232X
Ezgi Kivrak: 0000-0001-8552-3473
Levent Beker: 0000-0002-9777-6619

References:
[1] Lin, J., Peng, Z., Liu, Y., Ruiz-Zepeda, F., Ye, R., Samuel, E. L. G., Yacaman, M. J., Yakobson, B. I., and Tour, J. M. “Laser-Induced Porous Graphene Films From Commercial Polymers.” Nature Communications, 5, 5714, 2014. https://doi.org/10.1038/ncomms6714
[2] Wan, Z., Nguyen, N. T., Gao, Y., and Li, Q. “Laser Induced Graphene For Biosensors.” Sustainable Materials and Technologies, 25, e00205, 2020. https://doi.org/10.1016/j.susmat.2020.e00205
[3] Wang, M., Yang, Y., Min, J., Song, Y., Tu, J., Mukasa, D., Ye, C., Xu, C., Heflin, N., McCune, J. S., Hsiai, T. K., Li, Z., and Gao, W. “A Wearable Electrochemical Biosensor For The Monitoring Of Metabolites And Nutrients.” Nature Biomedical Engineering, 6, 1225–1235, 2022. https://doi.org/10.1038/s41551-022-00916-z

Keyword: *Laser-Induced Graphene, Electrochemical Sensing, Wearable Sensors*

Fabricating Metal-Organic-Framework-Based Paper Biosensor for Colorimetric Detection of Glucose as a Vitality Biosignature

Kaan Arıduman [*1], Selin Baş[1], Nil Ürküt[1], Cansu Yıldırım[2,3], Hüseyin Enis Karahan[2,4]

[1] *Department of Molecular Biology and Genetics, Istanbul Technical University, Maslak 34469, Istanbul, Türkiye*
[2] *Department of Chemical Engineering, Istanbul Technical University , Maslak 34469, Istanbul, Türkiye*
[3] *Polymer Science and Technology Graduate Program, Istanbul Technical University , Maslak 34469, Istanbul, Türkiye*
[4] *Synthetic Fuels & Chemicals Technology Center (ITU-SENTEK), Istanbul Technical University , Maslak 34469, Istanbul, Türkiye*

Glucose, a fundamental molecular precursor for glycolysis, is the primary carbon source for known life observed in the earliest and most conserved metabolic pathways. This picture makes glucose a potential biosignature for vitality analyses essential for rover missions. Moreover, glucose sensing can be performed with low-cost and compact platforms at an acceptable sensitivity, which is advantageous for rover vehicles as they should ideally be equipped with such biosensors. Among the available glucose sensing platforms, paper-based colorimetric biosensors are particularly appealing candidates as they have been successfully used for detecting glucose concentration in soil. Such biosensors are typically based on the enzymatic oxidation of glucose, primarily collected from the dissolved soil, yielding gluconolactone and hydrogen peroxide (H_2O_2) as in the case of by glucose oxidase (GOx). In this reaction, H_2O_2 subsequently reacts with o-phenylenediamine (OPD) in the presence of peroxidase (POx), producing a yellow-colored product [1]. Inconveniently, such biosensors come with certain application bottlenecks inherent to bio-based enzymes, including expensive production, storage, and poor stability under temperature fluctuations [2]. Therefore, as the ITU Rover Science subteam, we have replaced peroxidase with a metal-organic framework (MOF) particles as an enzyme mimic as the first step of our efforts aimed at developing bio-based-enzyme-free glucose biosensors for rover missions. As the MOF system, we have focused on Mn-based MOF (Mn-MOF, also known as Mn-BDC MOF), which stands out from other MOFs exhibiting high oxidative stability, optical white feature and native to 3,3’,5,5’-tetramethylbenzidine (TMB) substrate [3]. In this regard, Mn-MOF is synthesized in aqueous conditions with slight modifications on a reported protocol. Based on X-ray diffraction (XRD) measurements, we have confirmed the successful synthesis of Mn-MOF particles. Scanning electron microscopy (SEM) and dynamic light scattering (DLS) studies revealed the synthesis of 2D particles with uniform particle size distribution. Similar to the function of peroxidase, Mn-MOF nanomaterials, catalyses the oxidation of the selected substrate, TMB, in the presence of H_2O_2, leading to significant color change to blue. Notably, we have employed chitosan as a binder and stability enhancer for immobilizing GOx and Mn-MOF onto paper surface. For the detection purposes, we have relied on an in-house RGB analysis system fully developed by ITU Rover Team. Overall, this nanozyme-based system demonstrates the potential for smart material design as a versatile tool for diagnostics in medicine and portable systems.

Acknowledgment:
We thank all the past and present members and advisors of ITU Rover Team.

ORCID:
Kaan Arıduman: 0009-0002-7234-0744
Selin Baş: 0009-0003-6376-8578
Nil Ürküt: 0009-0000-5219-2356
Cansu Yıldırım: 0000-0003-1023-4030
Hüseyin Enis Karahan: 0000-0002-7753-1024

References:
[1] Martinkova, P., Brtnicky, M., Kynicky, J., & Pohanka, M. (2018). Fast and simple glucose assay based on filter paper as enzymes carrier using phone camera detection. Chemical Papers, 72(11), 2719-2728.
[2] Ren, Y., Zuo, X., Liu, Z., Yu, M., Zhou, B., Xue, Y., ... & Yang, R. (2024). Paper chip-based colorimetric biosensor for glucose by using CuFe2O4@ GO as nanozyme. Microchemical Journal, 206, 111504.
[3] Han, L., Tan, J., & Zhang, Y. (2025). White Mn-MOF nanozymes with peroxidase-activity specificity overcome color and O2 effects on colorimetric test strips. Communications Chemistry, 8(1), 389.

Keyword: *Nanozyme, Peroxidase mimicking, Chitosan*

Mip-Based Electrochemical Analytical Method for Alpha-Hederin Quantification in Complex Plant-Based Systems

M.Mesud Hürkul [*] [1], Seyda Yayla[1], Asmin Kurt[2,3], Ahmet Cetinkaya[4], Sonja Jovanović[5], Marija Milićević[5], Sibel A. Ozkan[2]

[1] Ankara University, Faculty of Pharmacy, Department of Pharmaceutical Botany, Ankara, Türkiye
[2] Ankara University, Faculty of Pharmacy, Department of Analytical Chemistry, Ankara, Türkiye
[3] Ankara University, Graduate School of Health Sciences, Ankara, Türkiye
[4] University of Health Sciences, Gülhane Faculty of Pharmacy, Department of Analytical Chemistry, 06018, Ankara, Türkiye
[5] University of Belgrade, Vinča Institute of Nuclear Sciences – National Institute of the Republic of Serbia Laboratory of Physics, Belgrade, Serbia

Hedera helix L., commonly known as ivy, is widely used worldwide, particularly as a complementary therapy for upper respiratory tract infections. The plant's leaves are rich in saponins, which have mucolytic, antispasmodic, bronchodilating, and antibacterial properties. Dried ivy leaves, known as 'Hederae helicis folium', are used as an expectorant to relieve coughs. Key bioactive constituents found in the leaves include alpha-hederin, hederacoside C, and hederagenin. This study introduces a novel electrochemical sensor based on a molecularly imprinted polymer (MIP) for highly sensitive and selective detection of alpha-hederin (AHD)[1,2].

This surface modification substantially enhanced the electroactive surface area and porous structure of the glassy carbon electrode (GCE), promoting more efficient electron transport and providing a greater number of accessible recognition sites. For MIP fabrication, 2-thienylboronic acid (2-TBA) was selected as the functional monomer due to its strong affinity for the target analyte through specific molecular interactions. The imprinted polymer network was generated using ethylene glycol dimethacrylate (EGDMA) as the crosslinker, 2-hydroxyethyl methacrylate (HEMA) as the basic monomer, and 2-methylpropiophenone as the photoinitiator, yielding a robust, structurally uniform polymeric matrix. The morphological and electrochemical properties of the fabricated AHD/CFO_DHCA/2-TBA@MIP-GCE sensor were evaluated by scanning electron microscopy (SEM), cyclic voltammetry (CV), and electrochemical impedance spectroscopy (EIS). Under optimized experimental conditions, the sensor exhibited a linear response toward AHD over the concentration range of 1.0×10^{-13}–1.0×10^{-12} M using the indirect detection approach based on 5.0 mM $[Fe(CN)_6]^{3-/4-}$. The limits of detection (LOD) and quantification (LOQ) were determined to be 3.12×10^{-14} M and 9.36×10^{-14} M, respectively. The excellent analytical performance demonstrated that the MIP-based sensor provides highly selective, specific, and sensitive detection of AHD. Furthermore, satisfactory recovery values from real-sample analyses confirmed the practical applicability and reliability of the proposed sensing platform. These findings indicate that the developed sensor is a promising analytical tool for the accurate determination of the AHD in complex matrices.

References:

Holzinger, F., & Chenot, J. F. (2011). Systematic review of clinical trials assessing the effectiveness of ivy leaf (hedera helix) for acute upper respiratory tract infections. Evidence-Based Complementary and Alternative Medicine, 2011(1), 382789.
Gepdiremen, A., Mshvildadze, V., Süleyman, H., & Elias, R. (2005). Acute anti-inflammatory activity of four saponins isolated from ivy: alpha-hederin, hederasaponin-C, hederacolchiside-E and hederacolchiside-F in carrageenan-induced rat paw edema. Phytomedicine, 12(6-7), 440-444.

Keyword: *Electrochemical sensor, Molecularly imprinted polymer, alpha-hederin*

Polylysine-Fullerenol Nanoarchitectonics: A High-Performance Platform for PoC Biosensor Application

Mehmet Hakan Yorgancılar [*] [1,2], **Dilek Soyler**[1,2], **Yasin Sozer**[3], **Salih Ozcubukcu**[4], **Saniye Soylemez**[1,2]

[1] *Department of Biomedical Engineering, Necmettin Erbakan University, Konya, Türkiye*
[2] *Science Technology Research and Application Center (BITAM), Necmettin Erbakan University, Konya, Türkiye*
[3] *Department of Biomedical Engineering, Middle East Technical University, Ankara, Türkiye*
[4] *Department of Chemistry, Middle East Technical University, Ankara, Türkiye*

Alzheimer's disease is a prevalent neurodegenerative disorder associated with progressive cognitive decline. Since acetylcholinesterase (AChE) inhibition is a widely used therapeutic strategy for its treatment, the development of sensitive and practical platforms for monitoring AChE activity and inhibition has attracted considerable attention [1].

Fullerenes are promising nanomaterials with unique electronic and chemical properties that make them attractive for biosensing applications. Their spherical structure facilitates electron transfer, enables operation at lower potentials, and improves the selective detection of electroactive analytes while minimizing interference effects. Furthermore, functionalized fullerene derivatives have attracted considerable attention in electrochemical biosensors due to their high surface area, excellent electron-transfer properties, and ability to facilitate biomolecule immobilization [2-4].

In this study, a novel AChE-based electrochemical biosensor was developed using a Fullerenol–Polylysine–AChE bioconjugate to facilitate the covalent immobilization of AChE. The biosensor was fabricated by directly depositing the synthesized Fullerenol–Polylysine–AChE material onto the surface of a screen-printed electrode (SPE). This modification strategy ensures a straightforward and robust covalent attachment of enzymes, preventing leaching and maintaining catalytic activity. The electrochemical response of the biosensor was investigated using acetylthiocholine chloride (AThCl) as the enzymatic substrate, while inhibition studies were carried out using galantamine as a model AChE inhibitor. Measurements were performed by chronoamperometry using a portable electrochemical potentiostat integrated with a smartphone

The developed biosensor exhibited a linear range of 0.1-4.0 mM, a detection limit of 0.097 mM, and a sensitivity of 3.083 μA mM^{-1} cm^{-2}, demonstrating excellent analytical performance. The inhibition response toward galantamine was observed within the concentration range of 1-25 μM, with a maximum inhibition efficiency of 1.33-54.22%.

The results demonstrate that the proposed Fullerenol–Polylysine–AChE-based biosensor provides a practical and effective platform for AChE inhibition analysis. The proposed sensor fabrication and smartphone-assisted portable electrochemical measurements highlights its potential for rapid on-site pharmaceutical analysis and Alzheimer's disease-related inhibitor screening applications.

ORCID:
Mehmet Hakan Yorgancılar: 0000-0003-0907-0956
Dilek Soyler: 0000-0003-3937-5830

References:
[1] Altay, D. N., Yagar, H., & Ozcan, H. M. (2023). A new ITO-based Aβ42 biosensor for early detection of Alzheimer's disease. Bioelectrochemistry, 153, 108501.
[2] Yáñez-Sedeño, P., Campuzano, S., & Pingarrón, J. M. (2017). Fullerenes in electrochemical catalytic and affinity biosensing: a review. C, 3(3), 21.
[3] Singh, A., Sharma, A., Ahmed, A., Sundramoorthy, A. K., Furukawa, H., Arya, S., & Khosla, A. (2021). Recent advances in electrochemical biosensors: Applications, challenges, and future scope. Biosensors, 11(9), 336.
[4] Soyler, D., Dolgun, V., Kurbanoglu, S., Ozcubukcu, S., & Soylemez, S. (2025). Synthesis and design of functional fullerenol-based electrochemical nanobiosensor to examine the inhibition effects of anti-Alzheimer drug active pyridostigmine on acetylcholinesterase. Measurement, 253, 117494.

Keyword: *Alzheimer's disease, Functionalized Fullerene, Electrochemical biosensor*

Real-time Capture and Visualization of Whole Cell E. coli for Rapid Detection and Antimicrobial Susceptibility Testing via IRIS

Neşe Lortlar Ünlü [*] [1,2], **Monireh Bakhshpour-Yücel**[3], **Sinem Diken Gür**[4], **Neval Elgörmüş**[5,6], **Negin Zaraee**[5], **M Selim Unlu**[5]

[1] *Atlas University, Faculty of Medicine, Department of Histology and Embryology*
[2] *Boston University, Department of Biomedical Engineering*
[3] *Uludag University, Faculty of Art and Science, Department of Chemistry*
[4] *Faculty of Science, Department of Biology, Hacettepe University*
[5] *Boston University, Department of Electrical and Computer Engineering*
[6] *Atlas University, Faculty of Medicine, Department of Microbiology*

Rapid identification of bacterial pathogens and timely determination of antimicrobial susceptibility remain major challenges in clinical diagnostics. Conventional culture-based approaches often require several days to generate results, delaying appropriate treatment and contributing to the emergence of antimicrobial resistance [1]. Optical biosensing technologies offer an attractive alternative by enabling rapid, sensitive, and label-free detection of bacterial pathogens. In this study, we developed a real-time interferometric reflectance imaging sensor (IRIS) [2] platform integrated with a disposable microfluidic cartridge for whole-cell bacterial detection and rapid antimicrobial susceptibility testing (AST). The sensing platform employs DNA-directed immobilization (DDI) to enhance bacterial capture efficiency and assay reproducibility. Universal DNA microarrays were fabricated on polymer-coated Si/SiO_2 substrates and converted into pathogen-specific capture surfaces through antibody–DNA conjugates. Both heterogeneous and homogeneous assay formats were investigated using Escherichia coli (E. coli) as a model organism. Real-time imaging was performed within a microfluidic flow chamber, enabling direct visualization and tracking of individual bacterial cells without fluorescent labels. In addition, image analysis algorithms were developed to monitor bacterial growth dynamics and estimate single-cell growth rates for AST applications. The IRIS platform enabled sensitive and real-time detection of intact E. coli cells over a concentration range of 10^3–10^7 CFU/mL. Homogeneous DDI assays demonstrated highly efficient bacterial capture, approaching complete recovery at low bacterial concentrations. Compared with direct antibody immobilization, DDI significantly enhanced capture efficiency, particularly at low target concentrations, resulting in an approximately 100-fold improvement in dynamic range.

ORCID:
Neşe Lortlar Ünlü: 0000-0003-4578-6089
Monireh Bakhshpour-Yücel: 0000-0002-5737-720X
Sinem Diken Gür: 0000-0001-6105-4609
Neval Elgörmüş: 0000-0002-8594-892X
Negin Zaraee: 0000-0003-4578-6089.
M Selim Unlu: 0000-0002-8594-892X

References:

Yamin, D.; Uskoković, V.; Wakil, A.M.; Goni, M.D.; Shamsuddin, S.H.; Mustafa, F.H.; Alfouzan, W.A.; Alissa, M.; Alshengeti, A.; Almaghrabi, R.H.; et al. Current and Future Technologies for the Detection of Antibiotic-Resistant Bacteria. Diagnostics 2023, 13, 3246. https://doi.org/10.3390/diagnostics13203246
Aslan, M., Snekvik, S., Seymour, E. et al. Multi-parametric interferometric reflectance imaging sensor. Sci Rep 16, 10780 (2026). https://doi.org/10.1038/s41598-026-45282-x

Keyword: *E. coli, Detection, Antimicrobial Susceptibility Testing, IRIS, DNA-directed immobilization*

Early Detection of HIV Using Infection Mechanism-Based Gold Nanoparticle Spectrophotometric Biosensor

Burak Ekrem Çitil[1], Nil Su Çaylayık [* 2], Ülkü Anık[2,3]

[1] *Faculty of Medicine, Department of Biostatistic, Mugla Sitki Kocman University, Kotekli, Mugla, Türkiye*
[2] *Faculty of Science, Chemistry Department, Mugla Sitki Kocman University, 48000 Kotekli, Mugla, Türkiye*
[3] *Research Laboratory Center, Mugla Sitki Kocman University, Sensors, Biosensors and Nano-Diagnostic Systems Laboratory, Kotekli-Mugla, Türkiye*

Human Immunodeficiency Virus (HIV) remains one of the major global public health threats, increasing the demand for rapid, sensitive, and cost-effective diagnostic approaches [1,2]. The HIV infection mechanism is initiated through the specific binding of the viral envelope glycoprotein gp120 to the CD4 receptor located on the surface of host cells. This critical biomolecular interaction constitutes the fundamental infection mechanism that enables viral attachment and subsequent entry into target cells [3,4]. Therefore, the highly specific CD4–gp120 interaction was selected as the biorecognition mechanism for the developed biosensor platform. In this study, a novel gold nanoparticle (AuNP)-based spectrophotometric biosensor was developed for the detection of HIV. AuNPs were preferred due to their localized surface plasmon resonance (LSPR) properties, high surface-area-to-volume ratio, strong optical responses, excellent biocompatibility, and their ability to generate distinct spectrophotometric changes following biomolecular interactions [5]. Optical changes occurring in AuNPs as a result of the specific interaction between CD4 molecules used as the biorecognition element and the HIV surface gp120 glycoprotein were monitored using UV–Vis spectrophotometric analysis. In addition, the structural morphology of the developed spectrophotometric HIV biosensor was characterized using Scanning Electron Microscopy (SEM), Atomic Force Microscopy (AFM), and Fourier Transform Infrared Spectroscopy (FTIR). To enhance biosensor performance, experimental parameters including CD4 concentration, CD4 incubation time, CD4 incubation temperature, as well as the incubation time and temperature of the CD4–gp120 interaction were systematically optimized. The developed biosensor exhibited two linear detection ranges between 0.1–2 ng/mL and 5–100 ng/mL. Significant absorbance changes observed in the presence of gp120 confirmed successful biomolecular recognition. Consequently, the proposed AuNP-based spectrophotometric biosensor provides a rapid, simple, and reliable platform for HIV detection and demonstrates considerable potential for future point-of-care diagnostic applications.

Acknowledgment:
The authors would like to thank Nukleus Sağlık Hizmetleri A.Ş. for kindly providing the reagents used in this study.

References:
(1) World Health Organization. HIV and AIDS. World Health Organization; 2025.
(2) Deeks, S. G., Overbaugh, J., Phillips, A., & Buchbinder, S. HIV infection. Nature Reviews Disease Primers, 2015, 1, 15035.
(3) Kwong, P. D., Wyatt, R., Robinson, J., Sweet, R. W., Sodroski, J., & Hendrickson, W. A. Structure of an HIV gp120 envelope glycoprotein in complex with the CD4 receptor and a neutralizing human antibody. Nature, 1998, 393, 648–659.
(4) Wilen, C. B., Tilton, J. C., & Doms, R. W. HIV: cell binding and entry. Cold Spring Harbor Perspectives in Medicine, 2012, 2(8), a006866.
(5) Dykman, L., & Khlebtsov, N. Gold nanoparticles in biomedical applications: recent advances and perspectives. Chemical Society Reviews, 2012, 41, 2256–2282.

Keyword: *HIV, Gold Nanoparticles, Biosensors*

Self-Organized Nanostructure Formation through Solid-State Thermal Dewetting for Label-Free Biosensing Platforms

Sena Simsek [*1], Meryem Beyza Avci[2], Tossaporn Lertvanithphol[3], Mati Horprathum[3], Khwanchai Tantiwanichapan[3], Chanunthorn Chananonnawathorn[3], Wantanee Hincheeranan[3], Hande Nur Yılmaz[4], Arif E. Cetin[5]

[1] Izmir Biomedicine and Genome Center, Balçova, Izmir 35340, Turkey; Izmir International Biomedicine and Genome Institute, Dokuz Eylül University, Balçova, Izmir 35340, Turkey

[2] Izmir Biomedicine and Genome Center, Balcova, Izmir 35340, Turkey; Izmir International Biomedicine and Genome Institute, Dokuz Eylul University, Balcova, Izmir 35340, Turkey

[3] Opto-Electrochemical Sensing Research Team, National Electronics and Computer Technology Center, Pathum Thani 12120, Thailand

[4] Department of Computer Engineering, Yeditepe University, Istanbul 34755, Turkey

[5] Izmir Biomedicine and Genome Center, Balcova, Izmir 35340, Turkey; Department of Biophysics, Faculty of Medicine, Dokuz Eylul University, Balcova, Izmir 35340, Turkey;

Plasmonic biosensors based on localized surface plasmon resonance (LSPR) in metallic nanostructures offer a powerful platform for label-free, real-time, and highly sensitive molecular detection (Altug et al., 2022). In this work, we present a tunable fabrication strategy for LSPR-based biosensing substrates using solid-state thermal dewetting (SSTD) of ultrathin gold films sputtered onto glass substrates. By systematically varying the sputtering duration (9 and 12 s) and applying up to five sequential thermal dewetting cycles, building on recent multicycle SSTD approaches (Hincheeranan et al., 2024; Lamtha et al., 2025), we investigated the morphological and optical evolution of the resulting gold nanoantenna arrays. Scanning electron microscopy (SEM) combined with quantitative image analysis revealed precise control over nanoparticle size, density, and spatial distribution, while broadband spectroscopy and finite-difference time-domain (FDTD) simulations were used to assess resonance behavior and nearfield enhancement. A spectral integral (SI)-based quantification method was employed to evaluate refractive index sensitivity and determine the theoretical limit of detection (LOD), consistent with recent plasmonic biosensor platforms developed for clinical pre-diagnostic applications (Karaca Acari et al., 2024). The optimal structure, fabricated with a 9 s sputtering time and two dewetting cycles, exhibited the narrowest resonance line width, the highest figure of merit (FOM), and the strongest simulated field enhancement. This configuration was selected for proof-of-concept label-free detection of human immunoglobulin G (IgG) using a protein A/G-functionalized surface, achieving a theoretical LOD of approximately 80 pg/mL. These results confirm that this lithography-free, scalable, and cost-effective approach provides a practical and reproducible plasmonic biosensing platform suitable for point-of-care diagnostic applications.

Acknowledgment:
This work was supported by the Development of International Cooperation Network on Science Technology and Innovation, Program Management Unit for Human Resources & Institutional Development, Research and Innovation (PMUB) of Thailand (which is under the Program 16: Partnership Initiative Fund: S&T) Grant B16F640194, National Higher Education Science Research and Innovation Policy Council.

References:
Altug, H., Oh, S. H., Maier, S. A., & Homola, J. (2022). Advances and applications of nanophotonic biosensors. Nature Nanotechnology, 17(1), 5–16.
Hincheeranan, W., Chananonnawathorn, C., Duangkanya, K., Waiwijit, U., Wongpanya, K., Amarit, R., Sathukarn, A., Bamrungsap, S., Lertvanithphol, T., & Horprathum, M. (2024). A study of multiple solid-state dewetting of sputtered Au ultra-thin films for chip-based LSPR sensor applications. Optical Materials, 157, Article 116137.
Karaca Acari, I., Kurul, F., Avci, M. B., Yasar, S. D., Topkaya, S. N., Açarı, C., Ünsal, E., Makay, B., Köytepe, S., Ateş, B., Yilmaz, İ., Seçkin, T., & Cetin, A. E. (2024). A plasmonic biosensor pre-diagnostic tool for familial Mediterranean fever. Nature Communications, 15(1), Article 8515.
Lamtha, T., Waiwijit, U., Duangkanya, K., Lertvanithphol, T., Amarit, R., Tantiwanichapan, K., Sathukarn, A., Chananonnawathorn, C., Hincheeranan, W., Dhanasiwawong, K., Choowongkomon, K., Sritrakul, T., Boodde, O., Sukmak, M., & Horprathum, M. (2025). Solid-state dewetting sputtered ultra-thin Au films for LSPR sensing chip toward African swine fever virus detection. Sensors and Actuators A: Physical, 382, Article 116165.

Keyword: *Label-Free Biosensing, Solid-State Thermal Dewetting, Localized Surface Plasmon Resonance (LSPR)*

A Computational Modeling Approach for ITO-Based Competitive Lateral Flow Assay

Sena Yanasik [*] [1,2], Ela Kochan[1], Emine Guler Celik[1,2]

[1] Department of Bioengineering, Faculty of Engineering, Ege University, Izmir 35100, Turkey
[2] Ege Science Pro Scientific Research Inc., Izmir 35100, Turkey

Point-of-care testing (POCT) refers to diagnostic testing performed at or near the patient site, independent of centralized laboratory[1]. Lateral flow assays (LFAs) are among the most widely used approaches in POCT, due to their rapid response, cost-effectiveness, and user-friendliness[2]. Recently, numerical simulations have become increasingly important for understanding LFA mechanisms and supporting assay development. These models help reduce the time and resources required for optimization processes and provide important information for evaluating how different materials influence binding efficiency and detection sensitivity [3,4].

Here, we report a finite element-based numerical simulation model developed to characterize flow behavior, mass transport, and reaction kinetics in an ITO-based lateral flow assay designed for a competitive assay format. The model combines Richards equation with the solute transport in porous media interface to investigate fluid flow, mass transport, and surface reactions across the sample pad, conjugate pad, sensing region and absorbent pad. By numerically representing the flow, transport, and binding dynamics of a competitive LFA system on a material platform distinct from conventional membrane structures, this model provides a useful approach for developing alternative platform designs and predicting assay performance.

ORCID:
Sena Yanasik: 0000-0002-5685-3737
Ela Kochan: 0009-0008-1827-3150
Emine Guler Celik: 0000-0003-2381-9775

References:
Elrobaa IH, Khan K, Mohamed E. (2024) “The Role of Point-of-Care Testing to Improve Acute Care and Health Care Services”, Cureus, 16(3):e55315.
Sadeghi P., Sohrabi H., Hejazi M., Jahanban-Esfahlan A., Baradaran B., Tohidast M., Majidi M.R., Mokhtarzadeh A., Tavangar S.M., de la Guardia M.,(2021) “Lateral flow assays (LFA) as an alternative medical diagnosis method for detection of virus species: The intertwine of nanotechnology with sensing strategies”, Trends Analyt Chem., 145:116460.
Nalumachu R., Anandita A. and Rath D. (2023) “Computational modelling of a competitive immunoassay in lateral flow diagnostic devices”, Sensors & Diagnostics, 2, 687–698.
Zhao X, Zhang Y, Niu Q, Wang L, Xing C, Wang Q, Bao H. (2024) “Research on the Flow Characteristics and Reaction Mechanisms of Lateral Flow Immunoassay under Non-Uniform Flow”,Sensors, 24(6):1989.

Keyword: *Competitive Lateral Flow Assay, Computational Modelling, Point-of-Care Testing*

Magnetic Nanoparticle-Based Reusable Electrode Surfaces: Psychostimulant Aptasensor

Veysel Ceyirdekci [*1,2], Ezgi Man[3], Ozge Ozufuklar[4], Aysenur Yardim[1], Jagriti Narang[5], Serap Evran[3], Suna Timur[2,3], Emine Guler Celik[2,6]

[1] *Department of Bioengineering, Institute of Natural Sciences, Ege University, Izmir 35100, Türkiye*
[2] *Ege Science Pro Scientific Research Inc., Izmir 35100, Türkiye*
[3] *Department of Biochemistry, Faculty of Science, Ege University, Bornova, Izmir 35100, Turkey*
[4] *Department of Biotechnology, Institute of Natural Sciences, Ege University, Izmir 35100, Türkiye*
[5] *Department of Biotechnology, School of Chemical and Life Science, Jamia Hamdard University, New Delhi 110062, India*
[6] *Department of Bioengineering, Faculty of Engineering, Ege University, 35040 Izmir, Türkiye*

Drug overdose-related mortality remains a critical public health concern worldwide [UNODC, 2024]. This problem is mainly driven by the simultaneous use of multiple psychoactive substances. Conventional detection techniques are often slow, costly, and dependent on centralized laboratories. These limitations restrict their use for on-site forensic and clinical settings. The aim of this study was to develop a low-cost, disposable, paper-based electrochemical aptasensor [Anzar, N., et al, 2023]. The proposed platform enables the simultaneous detection of cocaine (COC) and methamphetamine (METH) psychostimulants. To achieve multiplex sensing on a single device, two key strategies were combined [Mao, K., et al 2019]. Streptavidin-coated magnetic beads (MBs) were used for efficient aptamer immobilization via biotin–avidin interaction. In addition, two independent working electrodes were integrated on a paper substrate to allow dual-target recognition.

In the experimental setup, biotinylated COC and METH specific aptamers were conjugated to streptavidin MBs. The aptamer MB complexes were then immobilized on the paper-based electrodes. Electrochemical measurements were performed by cyclic voltammetry (CV). The surface morphology of the modified electrodes was characterized by scanning electron microscopy (SEM). The aptasensor showed linear responses in the ranges of 5.0–100 ng/mL for COC (R^2 = 0.965) and 5.0–50 ng/mL for METH (R^2 = 0.992). The limits of detection (LOD) values were calculated as 56.95 ng/mL for COC and 13.62 ng/mL for METH. Selectivity was tested against structurally related interferents, including morphine, codeine, and benzodiazepine. These tests confirmed the specificity of the platform. Reproducibility was assessed on five independent electrodes. The relative standard deviations were 5.59% for COC and 6.06% for METH. The results demonstrated satisfactory analytical performance for the simultaneous detection of two major substances of abuse. Furthermore, this design has strong potential for simple adaptation to other aptamer-based targets. Therefore, the platform offers a versatile tool for point-of-care (POC) forensic and clinical diagnostics.

This study is supported by the TÜBİTAK 2209-B Industry-Oriented Research Project Support Program for Undergraduate Students.

ORCID:
Veysel Ceyirdekci: 0009-0009-3070-6294

References:
United Nations Office on Drugs and Crime. (2024). World Drug Report 2024. UNODC. https://www.unodc.org/unodc/en/data-and-analysis/world-drug-report-2024.html
Anzar, N., Suleman, S., Bano, H., Parvez, S., Khanuja, M., Pilloton, R., & Narang, J. (2023). Paper-Based Electrodes Decorated with Silver and Zinc Oxide Nanocomposite for Electro-Chemical Sensing of Methamphetamine. Sensors (Basel, Switzerland), 23(12), 5519. https://doi.org/10.3390/s23125519
Mao, K., Ma, J., Li, X., & Yang, Z. (2019). Rapid duplexed detection of illicit drugs in wastewater using gold nanoparticle conjugated aptamer sensors. Science of the Total Environment, 688, 771-779.

Keyword: *Aptasensor, Electrochemical Biosensor, Psychostimulant*

Comparative Analysis of Faradaic and Non-Faradaic Impedimetric Sensing Methods for Immunosensors Using PCB Interdigitated Electrodes

Alper Demirhan[1,2], Yagmur Ozdemir [*] [1,2]

[1] *Ankara University*
[2] *Sensitify*

The development of sensitive and stable immunosensors is essential for scalable point of care diagnostics. Signal amplification in these platforms often relies on nanoparticles. However, conventional quantification methods have limitations such as signal saturation, baseline drift, and poor repeatability. In this study, a printed-circuit board interdigitated electrode was developed to comparatively evaluate two distinct impedance measurement strategies for nanoparticle amplified biosensing: Faradaic electrochemical impedance spectroscopy with a redox probe and high frequency non-Faradaic impedance sensing without any redox probe. Custom interdigitated electrodes were fabricated on an FR4 substrate with a 150 micrometer finger width and spacing with a 5 mm by 5 mm active area. Hemoglobin immunosensor was used as model. Latex nanoparticles were used for signal amplification. In the Faradaic method, measurements were performed in a potassium fero/ferricyanide redox probe over 1 Hz to 100 kHz with a 10 mV AC perturbation. Charge transfer resistance was extracted to evaluate interfacial electron transfer kinetics. Alternatively, the non-Faradaic method was used for direct impedance measurement in a dry environment. Following target binding and nanoparticle accumulation, the electrode surface was washed and dried. Impedance was measured from 1 kHz to 1 MHz using an impedance analyser with a 50 mV AC signal. It exploits the frequency dependent reduction in capacitive reactance to quantify surface coverage accurately.

The two methodologies were assessed based on signal stability, complexity, and baseline drift. While Faradaic measurements provide kinetic insights, it can yield unstable results over time. The high frequency non-Faradaic measurements simplifies the assay development, eliminates chemical probes, and demonstrates improved signal robustness with reduced drift. This comparative study provides a methodology for developing highly repeatable and sensitive sensing into low-cost biosensors.

Keyword: *biosensor, PCB electrode*

Development and In Vitro Evaluation of Lipid Nanoparticle-Mediated CRISPR/Cas9 Ribonucleoprotein Delivery Targeting VEGFR, p65 and Survivin in Non-Small Cell Lung Cancer

Deniz Onan * **, Hasan Akbaba**

Department of Pharmaceutical Biotechnology, Faculty of Pharmacy, Ege University, Izmir, Turkiye

Accounting for nearly 85% of all lung cancer cases, non-small cell lung cancer (NSCLC) remains a leading cause of cancer-related deaths worldwide despite recent advances in targeted therapies and immunotherapy. Since the abnormal activation of angiogenesis, inflammatory signaling, and apoptosis resistance pathways plays a critical role in tumor progression and treatment resistance, vascular endothelial growth factor receptor (VEGFR), nuclear factor-kappa B subunit p65 (RELA), and survivin (BIRC5) have emerged as priority therapeutic targets. In this study, lipid nanoparticle (LNP)-based ribonucleoprotein (RNP) delivery system was developed to enable CRISPR-Cas9-mediated knockout of target genes. Target-specific single-stranded DNA (ssDNA) templates were designed, and sgRNAs were synthesized using in vitro transcription. Cas9 nuclease was isolated and purified from transformed E. coli BL21, with its activity successfully verified against commercial Cas9. Subsequently, RNP complexes were prepared using Cas9 and target-specific sgRNAs and their efficacy was demonstrated via in vitro cleavage assays. The resulting RNPs were encapsulated into LNPs produced by microfluidic technique and the nanoparticles were evaluated by mean of particle size (269.7 ± 31.6), polydispersity index (0.377 ± 0.281), zeta potential (-9.4 ± 1.6), encapsulation efficiency (% 87.9 ± 4.2) , and in vitro release characteristics. The results demonstrated that the developed LNP formulations exhibited high encapsulation efficiency and controlled release profile. The gene-editing efficacy of RNP-loaded LNPs was evaluated in A549 cells using a T7 endonuclease I (T7E1)-based mutation detection assay, while the success of GFP gene knockout in A549-GFP cells was determined by the reduction in fluorescent signal. Notably, the GFP expression level in A549-GFP cells significantly decreased to 26%. This study demonstrates that critical molecular pathways involved in NSCLC treatment can be safely and effectively delivered via targeted RNP-loaded LNPs, and holds the potential to contribute to the development of next-generation nanotechnology-based gene regulation strategies by modulating relevant diseases and molecular pathways.

Acknowledgment:
The authors gratefully acknowledge the financial support provided by TÜBİTAK COST-2515, 125S401 and TÜSEB-2025-A3-01- 48356.

ORCID:
Deniz Onan: 0000-0002-4451-2687
Hasan Akbaba: 0000-0001-9273-6346

References:
Jin Y, Yu W, Zhang W, Wang C, Liu Y, Yuan WE, Feng Y. A novel fluorinated polyethyleneimine with microRNA-942-5p-sponges polyplex gene delivery system for non-small-cell lung cancer therapy. J Colloid Interface Sci. 2023 Oct 15;648:287-298. doi: 10.1016/j.jcis.2023.05.153. Epub 2023 May 29. PMID: 37301153.
Li YL, Zhao H, Ren XB, Relationship of VEGF/VEGFR with immune and cancer cells: staggering or forward?, Cancer Biol Med 2015. doi: 10.20892/j.issn.2095-3941.2015.0070
Bialas N, Müller EK, Epple M, Hilger I, Silica-coated calcium phosphate nanoparticles for gene silencing of NF-κB p65 by siRNA and their impact on cellular players of inflammation, Biomaterials Vol 276, 2021, 121013
Ma S, Li X, Ran M, Ji M, Gou J, Yin T, He H, Wang Y, Zhang Y, Tang X, Fabricating nanoparticles co-loaded with survivin siRNA and Pt(IV) prodrug for the treatment of platinum-resistant lung cancer, International Journal of Pharmaceutics Vol 601, 2021, 120577
Ryann A. Joseph, Rebecca M. Haley, Marshall S. Padilla, Adele S. Ricciardi, Hannah M. Yamagata, and Michael J. Mitchell Nano Letters 2025 25 (39), 14348-14355 DOI: 10.1021/acs.nanolett.5c03548

Keyword: *NSCLC, lipid nanoparticle, CRISPR/Cas9*

Functional Antibody-Modified Gold Biointerface for Electrochemical Recognition of Lung Cancer Cell-Derived Extracellular Vesicles

Eren Polat [*] [1], Zeynep Elcim Koru[1], Selin Yavuzhan[1], Sude Yılmaz[2], Didem Aksu[3], Kerem Tok[2], Figen Zihnioglu[1], Suna Timur[1]

[1] Department of Biochemistry, Institute of Natural and Applied Sciences, Ege University, İzmir, Turkey
[2] Ege University, Faculty of Science, Department of Biochemistry
[3] Ege University,Central Research Test and Analysis Laboratory Application and Research Center (MATAL)

The design of functional biointerfaces on electrode surfaces plays a critical role in the selective recognition of extracellular vesicles (EVs) for diagnostic sensing applications [1,4]. EVs carry molecular information from their cells of origin and have attracted increasing attention as potential biomarkers for cancer diagnosis [2,3]. In this study, an antibody-modified gold biointerface was developed on screen-printed gold electrodes (SPGEs) for the electrochemical recognition of lung cancer cell-derived EVs.

The gold surface was functionalized through thiol-based self-assembled monolayer chemistry to enable stable antibody immobilization and controlled bio-recognition at the electrode interface. Anti-CD9 was used as the capture antibody to interact with EV-associated tetraspanins, while anti-Napsin A was employed as the detection antibody to provide lung adenocarcinoma-related selectivity. This sandwich-type surface architecture allowed selective signal generation through specific antibody–EV interactions on the gold interface.

Stepwise surface modification and immunorecognition events were characterized using Electrochemical Impedance Spectroscopy (EIS), Cyclic Voltammetry (CV), and Differential Pulse Voltammetry (DPV). EVs isolated from the conditioned culture media of A549 human lung adenocarcinoma cells and BEAS-2B non-malignant bronchial epithelial cells were used to evaluate the sensing performance. The developed biointerface successfully differentiated EV populations derived from malignant and non-malignant cell lines. A calibration study performed with standard EV preparations demonstrated a linear response in the 10–200 ng range ($R^2 = 0.990$).

These findings indicate that the antibody-modified gold biointerface provides a selective and functional electrochemical sensing platform for EV analysis. The proposed surface design highlights the importance of engineered biointerfaces for future EV-based lung cancer diagnostic applications [1,4].

ORCID:
Eren Polat: 0009-0005-7343-965X
Selin Yavuzhan: 0009-0008-8724-4150

References:
[1] Chen, J., Zhao, Z., Zhu, H., & Li, X. (2025). Advances in electrochemical biosensors for the detection of tumor-derived exosomes. Frontiers in Chemistry, 13, 1556595. https://doi.org/10.3389/fchem.2025.1556595
[2] Čeri, V., et al. (2024). Extracellular vesicle proteins for early cancer diagnosis. Biochimica et Biophysica Acta (BBA) - Reviews on Cancer, 1879(2), 188196. https://doi.org/10.1016/j.bbcan.2024.188196
[3] Delshad, M., Sanaei, M.-J., Mohammadi, M. H., Sadeghi, A., & Bashash, D. (2025). Exosomal biomarkers: A comprehensive overview of diagnostic and prognostic applications in malignant and non-malignant disorders. Biomolecules, 15(4), 587. https://doi.org/10.3390/biom15040587
[4] Cao, B., Wang, Y., Zhang, X., Shi, W., Jiang, Z., & Zhao, Z. (2024). Recent progress of electrochemical biosensors for liquid biopsy in cancer early diagnosis. TrAC Trends in Analytical Chemistry. https://doi.org/10.1016/j.trac.2024.11776

Keyword: *Extracellular Vesicles, Gold Biointerface, Surface Functionalization*

Transcriptomic and Proteomic Expression Level of IL-6/JAK/STAT3 Pathway Inhibition by Tocilizumab-Conjugated 5-Fluorouracil-Loaded Lipid–Polymer Hybrid Nanoparticles in Oral Squamous Cell Carcinoma

Ezgi Özdemir * **, Demet Cansaran Duman, Pelin Mutlu**

Ankara University, Institute of Biotechnology, Ankara, Türkiye

Aberrant activation of the IL-6/JAK/STAT3 signaling pathway plays a pivotal role in the progression of oral squamous cell carcinoma (OSCC), promoting tumor proliferation, metastasis, immune evasion, and resistance to chemotherapy (1, 2). Although targeted nanocarrier systems have emerged as promising approaches for improving anticancer drug delivery, their molecular mechanisms of action remain insufficiently understood (3). Therefore, this study aimed to investigate the transcriptomic and proteomic alterations induced by a tocilizumab-conjugated 5-fluorouracil (5-FU)-loaded lipid–polymer hybrid nanoparticle (LPHN) system in OSCC cells. Human OSC-19 oral squamous cell carcinoma cells and normal gingival fibroblasts (HGF-1) were treated with free 5-FU, free tocilizumab, 5-FU-loaded nanoparticles, and the dual-functional tocilizumab-conjugated 5-FU-loaded LPHNs. Treatment-induced molecular responses were evaluated by quantitative real-time PCR (qRT-PCR), while protein expression was assessed by western blot analysis. qRT-PCR analysis demonstrated that the dual-targeted nanoparticle formulation markedly downregulated the expression of **STAT3, JAK1, JAK2, IL6R, IL-6, CD274, and PD-L1** compared with the control and free-drug treatment groups, with **STAT3 exhibiting the most pronounced suppression**. Consistent with these transcriptomic findings, western blot analysis revealed a **significant reduction in JAK1 and STAT3 protein expression relative to the housekeeping protein β-Actin**, confirming effective inhibition of the IL-6/JAK/STAT3 signaling pathway at both the transcriptional and protein levels. These findings demonstrate that the therapeutic effect of the developed targeted nanocarrier extends beyond enhanced drug delivery by directly modulating key oncogenic signaling pathways involved in OSCC progression. The lipid–polymer hybrid nanoparticle platform therefore represents a promising precision nanomedicine strategy for molecularly targeted therapy of oral squamous cell carcinoma.

Acknowledgment:
This research was funded by the TUBİTAK Project no 124S815.

ORCID:
Ezgi Özdemir: 0009-0006-3888-6347
Demet Cansaran Duman: 0000-0001-5662-2333
Pelin Mutlu: 0000-0001-7970-880X

References:

1. Liu C, Zhou J, Zhang S, Fu J, Li Y, Hao Y, et al. Mesenchymal stem cells-derived IL-6 promotes invasion and metastasis of oral squamous cell carcinoma via JAK-STAT3 signalling. Oral Dis. 2024. 30(4):2097–109. doi:10.1111/ODI.14617
2. Wang SW, Sun YM. The IL-6/JAK/STAT3 pathway: potential therapeutic strategies in treating colorectal cancer (Review). Int J Oncol. 2014. 44(4):1032–40. doi:10.3892/IJO.2014.2259
3. Batool S, Sohail S, ud Din F, Alamri AH, Alqahtani AS, Alshahrani MA, et al. A detailed insight of the tumor targeting using nanocarrier drug delivery system. Drug Deliv. 2023. 30(1):2183815. doi:10.1080/10717544.2023.2183815

Keyword: *Oral squamous cell carcinoma; Lipid–polymer hybrid nanoparticles; IL-6/JAK/STAT3 signaling; qRT-PCR; Western blot*

Graphene-Reinforced Polyimide-Modified Electrodes for the Voltammetric Determination of Sorbic Acid

Esra Yetişkin[1], Fatma Bilge Emre [* 2], Süleyman Köytepe[1], Turgay Seçkin[1], Ergun Ekinci[1]

[1] Inönü University, Faculty of Arts and Sciences, Department of Chemistry, 44280, Battalgazi, Malatya
[2] Inönü University, Faculty of Education, Department of Mathematics and Science Education, 44280, Battalgazi, Malatya

Sorbic acid (2,4-hexadienoic acid, E200) is an important food additive widely used in the food industry to inhibit the growth of molds and fungi [1]. Because of its antimicrobial activity, it is incorporated into various food products to prevent spoilage and extend shelf life. Although sorbic acid occurs naturally in some plants as an unsaturated fatty acid, manufacturers predominantly produce it synthetically for industrial applications. Previous studies have demonstrated that sorbic acid is an indispensable functional component for ensuring a sustainable food supply, optimizing food logistics, and eliminating biological risks caused by pathogenic microorganisms. Therefore, maintaining sorbic acid at appropriate concentrations in food products is of critical importance for both regulatory compliance and product quality. Although sorbic acid is commonly determined by high-performance liquid chromatography (HPLC) and UV spectrophotometry, these techniques require expensive instrumentation and relatively long analysis times [2]. Compared with conventional methods, electrochemical sensors offer several advantages, including rapid analysis, the absence of sample pretreatment, low instrumentation cost, and minimal requirement for skilled personnel [3]. Consequently, electrochemical sensors have attracted considerable attention for food quality control, pharmaceutical analysis, and the determination of bioactive compounds.

In this study, graphene (GR)-based pyridine-containing polyimide-modified electrodes were developed for the voltammetric determination of sorbic acid. Polyimide was synthesized from 2,5-diaminopyridine and 3,3′,4,4′-benzophenonetetracarboxylic dianhydride (BTDA); to enhance electrode sensitivity, graphene was integrated into the polymer matrix at 3%, 5%, and 10 wt% concentrations. The resulting graphene-reinforced polyimide composites were used to modify the electrode surface and subsequently applied to the voltammetric determination of sorbic acid. The results demonstrated that the graphene-containing polyimide-modified electrodes provide a selective, rapid, and sensitive platform for the determination of sorbic acid in different food samples.

References:

[1] Plumridge A, Hesse SJ, Watson AJ, Lowe KC, Stratford M, Archer DB. (2004) The weak acid preservative sorbic acid inhibits conidial germination and mycelial growth of Aspergillus niger through intracellular acidification. Appl Environ Microbiol. 70(6):3506-11. doi: 10.1128/AEM.70.6.3506-3511.2004
[2] Özdemir A, Şanlı S, Sardoğan B, Sardoğan S. (2020) Determination of Sorbic Acid in Cheese Samples by Rapid HPLC-DAD Method. Int J Anal Chem. 6049028, 1-4. doi: 10.1155/2020/6049028
[3] Zheng Y, Fu L, Yang J, Gao S, Sun H, Zhang F. (2026) Electrochemical Biosensing Platforms for Rapid and Early Diagnosis of Crop Fungal and Viral Diseases. Sensors (Basel). 26(6):2004. doi: 10.3390/s26062004.

Keyword: *Sorbic acid, Polyimide, Voltammetric sensor*

ID: 98

Magnetic Micropatterned Platform for High-Throughput 3D Liver Spheroid Engineering and Toxicity Screening

Merve Oztas [*] [1], Mehmet Ali Onur[1], Gunes Kibar[2]

[1] *Department of Biology, Hacettepe University, Ankara, Türkiye*

[2] *Micro Nano Particles (MNP) Research Group, Department of Materials Science and Engineering, Adana Alparslan Türkeş Science and Technology University, Adana, Türkiye*

Conventional two-dimensional (2D) hepatocyte culture systems fail to recapitulate the structural and functional complexity of the native liver microenvironment, limiting their predictive accuracy in drug screening and toxicity assessment. To address these limitations, we developed a micropatterned high-throughput magnetic platform for the controlled assembly and manipulation of 3D HepG2 liver spheroids.

Magnetically decorated microbeads were engineered to facilitate cell aggregation and enable external magnetic control, allowing rapid, reproducible, and uniform spheroid formation. The micropatterned design of the platform ensured spatially controlled cell organization and improved consistency across experiments, while maintaining compatibility with standard multi-well culture workflows for scalable and parallel analysis.

A systematic optimization of magnetic bead concentration was performed to evaluate its effects on spheroid formation efficiency, structural integrity, and cellular viability. Cytotoxicity assays demonstrated that optimized bead loading supported stable spheroid formation with high viability, whereas excessive concentrations induced measurable cytotoxic effects. Importantly, the magnetic responsiveness of the system enabled non-invasive manipulation and positioning of spheroids without compromising cellular integrity.

This platform provides a cost-effective, scalable, and high-throughput approach for engineering 3D liver spheroids, with strong potential for applications in drug screening, nanotoxicology, and liver disease modeling. The integration of magnetic control with micropatterned design offers a versatile and robust tool for next-generation in vitro liver models.

Acknowledgment:
The authors gratefully acknowledge the financial support provided by TÜBİTAK 123M943 project, which significantly contributed to the execution of this study and experimental procedures. We also sincerely thank Mahmut Garip for his valuable technical support in 3D printing processes.

Keyword: *Micropatterned platform, SPION, 3D cell culture*

Ferroptosis-Driven Macrophage Polarization Assessed by Flow Cytometric Profiling of THP-1 Derived M1/M2 Cells

Kübra Solak [*] [1,2,3], **Adem Kara**[3], **Ahmet Mavi**[2,4,5]

[1] *Department of Molecular Biology and Genetics, Faculty of Science, Atatürk University, Erzurum, Türkiye.*
[2] *East Anatolia High Technology Application and Research Center (DAYTAM), Atatürk University, 25240 Erzurum, Türkiye.*
[3] *Department of Molecular Biology and Genetics, Faculty of Science, Erzurum Technical University, Erzurum, Türkiye.*
[4] *Department of Mathematics and Science Education, Education Faculty of Kazim Karabekir, Atatürk University, Erzurum, Türkiye.*
[5] *Department of Nanoscience and Nanoengineering, Institute of Science and Technology, Atatürk University, Erzurum, Türkiye.*

In recent years, researchers have shown that ferroptosis, a form of programmed cell death characterized by iron-dependent lipid peroxidation, plays an important role in both cancer biology and immune regulation. Macrophages are plastic cells that can functionally differentiate in response to microenvironmental cues and exhibit a dynamic balance between conventional (M1) and alternative (M2) activation phenotypes. This study aims to evaluate the impact of ferroptosis on macrophage polarization and quantify it using flow cytometry. In this regard, human monocyte-derived THP-1 cells were differentiated into sticky M0 macrophages by phorbol myristate acetate (PMA). M0 macrophages were polarized to the M1 phenotype with lipopolysaccharide (LPS) and interferon-γ (IFN-γ) and to the M2 phenotype with interleukin-4 (IL-4) by standard techniques. To investigate the role of ferroptosis in macrophage polarization, cells were treated with ferroptosis inducers/inhibitors or iron-oxide nanoparticles. Flow cytometry was employed to analyze macrophage phenotypes, and subpopulations were identified by surface markers. THP-1-derived M0 macrophages were characterized with CD14, CCR7, CD80, and CD86 for the M1 phenotype and CD206 and CD163 for the M2 phenotype. At least 15000 cell events were assessed, and the percentages of macrophage polarization were compared in different settings. Results indicate that ferroptosis may affect the functional reprogramming of macrophages and may be involved, particularly in the balance between pro-inflammatory (M1) and anti-inflammatory (M2) states. This study demonstrates the association between ferroptosis and immune cell polarization and provides an experimental framework for developing new therapeutic approaches for cancer microenvironments and inflammatory diseases.

Acknowledgment:
This study was supported by Scientific and Technological Research Council of Türkiye (TUBITAK) under the Grant Number 123C327 and 224Z063. The authors thank to TUBITAK for their supports.

ORCID:
Kübra Solak: 0000-0001-6643-3368

References:
Ko, M. J., Min, S., Hong, H., Yoo, W., Joo, J., Zhang, Y. S., ... & Kim, D. H. (2024). Magnetic nanoparticles for ferroptosis cancer therapy with diagnostic imaging. Bioactive Materials, 32, 66-97.
Yang, Y., Wang, Y., Guo, L., Gao, W., Tang, T. L., & Yan, M. (2022). Interaction between macrophages and ferroptosis. Cell death & disease, 13(4), 355.

Keyword: *Ferroptosis, Macrophage polarization, THP-1 cells*

Sustainable Magnetic Biochar Nanozymes

Ece Mavili[1], Mehmetcan Uzuner [* 1], Zeynep Elcim Koru[1], Eren Polat[1], Selin Yavuzhan[1], Gözde Duman[2], Büsra Basol[2], Bugra Gizlenci[2], Suna Timur[1]

[1] Department of Biochemistry, Institute of Natural and Applied Sciences, Ege University, İzmir, Turkey
[2] Ege University Faculty of Science, Department of Chemistry

Nanozymes have emerged as attractive alternatives to natural enzymes due to their improved stability, tunable catalytic properties and relatively low production costs [1,2]. In this study, we developed a sustainable magnetic biochar-based nanozyme using sawdust waste as a biomass source. Biochar obtained by pyrolysis was used as a high-surface-area carrier matrix and combined with magnetic iron oxide nanoparticles, which are well known for their peroxidase-like catalytic behavior [3,4,5]. The composite structure was further modified with chitosan to improve surface functionality and biocompatibility.

The peroxidase-like activity of the biochar/MNP/chitosan hybrid system was evaluated through a colorimetric reaction using hydrogen peroxide (H_2O_2) and ABTS as the chromogenic substrate. The catalytic response was monitored by the formation of the oxidized ABTS product, and the resulting color intensities were analyzed using ImageJ software. The effects of different H_2O_2 and ABTS concentrations were investigated, and the kinetic parameters, including Km and Vmax, were calculated according to the Michaelis–Menten model.The optimum catalytic activity was obtained for the biochar/MNP nanozyme system prepared at a 1:1 ratio within a chitosan matrix. Briefly, the chitosan matrix was prepared using 10 g chitosan in 5.0 mL of 1.0% acetic acid and incorporated with biochar suspension and MNPs at a 1:1 ratio. Michaelis–Menten kinetic analyses revealed Km values of 1.02 mM for ABTS and 0.35 mM for H_2O_2. The corresponding Vmax values were determined as 78.5 µmol/min for ABTS and 75.02 µmol/min for H_2O_2. In addition, the morphology of the resulting matrix and the chemical characteristics of the individual components were investigated and evaluated.

This study presents a simple and environmentally friendly route for preparing magnetic biochar-derived nanozymes. By combining waste-derived biochar, magnetic nanoparticles, and chitosan modification, the developed hybrid system may offer a promising platform for future colorimetric sensing and bioanalytical applications.

References:

[1] Liang, M., & Yan, X. (2019). Nanozymes: From new concepts, mechanisms, and standards to applications. Accounts of Chemical Research, 52(8), 2190–2200.
[2] Huang, Y., Ren, J., & Qu, X. (2019). Nanozymes: Classification, catalytic mechanisms, activity regulation, and applications. Chemical Reviews, 119(6), 4357–4412.
[3] Gao, L., Zhuang, J., Nie, L., Zhang, J., Zhang, Y., Gu, N., Wang, T., Feng, J., Yang, D., Perrett, S., & Yan, X. (2007). Intrinsic peroxidase-like activity of ferromagnetic nanoparticles. Nature Nanotechnology, 2, 577–583.
[4] Chi, Z., Wang, Q., & Gu, J. (2023). Recent advances in colorimetric sensors based on nanozymes with peroxidase-like activity. Analyst, 148, 487–506.
[5] Liu, Q., Zhao, S., Zhang, Y., An, X., Wang, Q., Li, S., Lin, A., Du, Y., & Wei, H. (2022). Biochar nanozyme from silkworm excrement for scavenging vapor-phase free radicals in cigarette smoke. ACS Applied Bio Materials, 5, 1831–1838.

Keyword: *Biochar, Magnetic Nanozyme, Peroxidase-like Activity*

A New-Generation Approach to Tuberculosis Treatment: Synthesis, Characterization, and Investigation of the Antimicrobial Activity of Berberine-Based Nanocomplexes

Nimet Temur [*1], **Ismail Ocsoy**[2]

[1] *Erciyes University, Graduate School of Natural and Applied Sciences, Department of Nanoscience and Nanotechnology, Kayseri, Turkey, 38039*

[2] *Department of Analytical Chemistry, Faculty of Pharmacy, Erciyes University, Kayseri, 3809, Türkiye*

Today, the detection of mycobacteria poses significant challenges due to the lengthy procedures and high costs associated with current diagnostic methods. The methods commonly used in our country have disadvantages such as lengthy preparation processes and delays in obtaining results; furthermore, treatment regimens require the use of multiple drugs, which negatively affects patient compliance due to long treatment durations and the frequency of side effects, and creates conditions conducive to the emergence of drug-resistant forms of tuberculosis. In this context, our project aims to develop innovative strategies to overcome the limitations of current methods in controlling tuberculosis. In particular, we plan to synthesize nanocomposites based on berberine (BBR), a natural alkaloid with a quaternary ammonium structure; the goal is to enhance the inhibitory effect against tuberculosis bacilli by leveraging berberine's antimicrobial, membrane-permeability-enhancing, and DNA-replication-inhibiting effects. In addition, baicalin (an anti-inflammatory and immunomodulatory flavonoid), cinnamic acid (with antioxidant and cell membrane-stabilizing properties), glycyrrhizic acid (with antiviral and immune-modulating effects), and rifampicin (an RNA polymerase inhibitor and a key antibiotic in tuberculosis treatment)—which plays a critical role in current therapy—the aim is to leverage both the pharmacological potential of natural compounds and the high efficacy of existing drugs. This strategy aims to both enhance treatment efficacy and reduce the development of resistance. Within the scope of our project, the synthesis, characterization, and antimicrobial activities of BBR-based nanocomposites against a standard tuberculosis strain were carried out. The results obtained demonstrate that BBR-based nanocomposites were successfully synthesized and that these plant-based nanomedicines exhibit effective antimicrobial activity against tuberculosis strains.

Acknowledgment:
The project was supported by the Erciyes University Scientific Research Office with the project code FDK-2025-15441.

ORCID:
Nimet Temur: 0000-0002-1882-2315
Ismail Ocsoy: 0009-0005-7520-6788

Keyword: *Mycobacterium tuberculosis, nanodrugs based on berberine, antimicrobial activity*

Multiplex Colorimetric Profiling of Lung Cancer Cell-Derived Extracellular Vesicles

Selin Yavuzhan [*] [1], Eren Polat[1], Zeynep Elçim Koru[1], Sude Yılmaz[1], Kerem Tok[1], Emine Güler Çelik[2], Didem Aksu[3], Figen Zihnioğlu[1], Suna Timur[1], Derya Nil Kişin[1]

[1] Department of Biochemistry, Institute of Natural and Applied Sciences, Ege University, İzmir, Turkey
[2] Ege University Faculty of Engineering, Department of Bioengineering
[3] Ege University, Central Research Test and Analysis Laboratory Application and Research Center (MATAL)

Extracellular vesicles (EVs) are small membrane-bound particles released by cells and they are increasingly studied as carriers of disease-related molecular information. Since EVs reflect, at least partly, the biological state of their parental cells, their protein composition may provide useful clues for cancer-related biomarker studies (Kalluri & LeBleu, 2020; Singh et al., 2022).

In this work, we aim to develop a simple multiplex colorimetric platform for the profiling of EVs obtained from lung cancer cell culture models. EVs isolated from A549 lung adenocarcinoma cells and BEAS-2B normal bronchial epithelial cells will be comparatively evaluated. The platform will be designed in a spot-based format to allow simultaneous assessment of selected EV-associated markers. Surface-related markers such as EpCAM, EGFR and tetraspanins will be analyzed on intact EVs.

Colorimetric signal generation will be supported by nanomaterial-based amplification strategies to improve the visibility and sensitivity of the assay (Xu et al., 2020; Wu et al., 2024). The analytical response, reproducibility and discrimination capacity of the platform will be investigated using the two cell-derived EV models. This preliminary study may provide a practical basis for multiplex EV profiling in lung cancer-related biosensor research.

ORCID:
Selin Yavuzhan: 0009-0008-8724-4150

References:
Kalluri, R., & LeBleu, V. S. (2020). The biology, function, and biomedical applications of exosomes. Science, 367, eaau6977.
Singh, S., Podder, P. S., Russo, M., Henry, C., & Cinti, S. (2022). Tailored point-of-care biosensors for liquid biopsy in the field of oncology. Lab on a Chip, 23, 44–61.
Xu, L., Chopdat, R., Li, D., & Al-Jamal, K. T. (2020). Development of a simple, sensitive and selective colorimetric aptasensor for the detection of cancer-derived exosomes. Biosensors and Bioelectronics, 169, 112576.
Wu, Y., Wu, Z., Xu, W., Zeng, R., Weng, J., & Sun, L. (2024). A label-free colorimetric biosensor utilizing natural material for highly sensitive exosome detection. Talanta, 275, 126182.

Keyword: *Extracellular vesicles (EVs), Lung cancer, Colorimetric biosensors*

Next-Generation Sequencing for Early Disease Diagnositcs and Targeted Therapeutics in Rare Diseases

Shams Ismayilova [*] [1], **Afig Berdeli**[1,2,3]

[1] *Department of Stem Cell Sciences, Institute of Health Sciences, Ege University, İzmir, Türkiye*
[2] *Department of Pediatrics, Division of Pediatric Rheumatology, Faculty of Medicine, Ege University, İzmir, Türkiye*
[3] *Department of Molecular Medicine, Faculty of Medicine, Ege University, İzmir, Türkiye*

Nanotechnology is revolutionizing the field of Next-Generation Sequencing (NGS), enabling PCR-free library preparation methods through innovations at the nanoscale such as nanopores (nanopore sequencing), nanobeads, tagmentation, and single-molecule manipulation. These approaches eliminate amplification bias, GC content imbalances, and artifacts seen in traditional PCR-based methods, thereby providing higher accuracy, uniform coverage, and ultra-long reads. Thanks to nanometer-scale pores, direct, label- free, and real-time sequencing of a single DNA/RNA molecule is possible; this enables highly sensitive genomic profiling in samples with low DNA input (even at the nanogram level). The integration of nanotechnology increases sequencing speed, reduces costs, supports point-of-care applications with portable devices, and facilitates the direct detection of epigenetic modifications (such as methylation). These nanoscale advantages provide a critical edge in early disease diagnosis. Rare variants, mutations in inflammatory pathways, and complex genomic structural variations can be detected at an early stage with nanoscale sensitivity, thereby preventing diagnostic delays and enabling molecular subtyping. In terms of targeted therapeutics, nanotechnology-enabled NGS enhances precision medicine. By generating mutation profiles using specific gene panels and high-throughput sequencing, personalized drug selection (e.g., inhibitors, immunotherapies) is optimized, and treatment resistance and clonal evolution can be monitored. Nanoscale control enhances data quality and accelerates the clinical decision-making process. From among the numerous rare disease cases we have diagnosed, we present two published case studies below.

Case 1: A novel mutation associated with the HCK gene was identified in a pediatric patient via NGS, shedding light on the molecular basis of an autoinflammatory disease and pulmonary involvement. A nanotechnology-supported PCR-free approach enabled the acquisition of high-quality data from a limited sample. (https://doi.org/10.1186/s12969-025-01170-8)

Case 2: In a patient carrying a RELA variant, a diagnosis of RELA-associated inflammatory disease (RAID) was established through targeted NGS analysis; this allowed for a targeted understanding of the inflammatory pathogenesis and the formulation of a treatment strategy. (https://doi.org/10.1016/j.genrep.2026.102485)

In conclusion, PCR-free NGS, enhanced by advancements in nanotechnology, plays a transformative role in the field of nanoscale genomics for early diagnosis, personalized treatments, and the management of rare diseases.

ORCID:
Shams Ismayilova: https://orcid.org/0009-0000-2913-6866
Afig Berdeli: https://orcid.org/0000-0002-4791-8367

References:
Katara, A. (2024). Evolution and applications of Next Generation Sequencing and its intricate relations with chromatographic and spectrometric techniques in modern day sciences. Journal of Chromatography Open, 5, 100121. https://doi.org/10.1016/j.jcoa.2024.100121
Berdeli, A., Ismayilova, S., & Gürbüz, N. (2026). Novel HCK-associated mutation causing autoinflammatory disorder with pulmonary manifestations in a pediatric patient. Pediatric Rheumatology, 24, Article 1. https://doi.org/10.1186/s12969-025-01170-8
Zhang, T., et al. (2024). Nanopore sequencing: flourishing in its teenage years. National Science Review. https://pubmed.ncbi.nlm.nih.gov/39293510/
Gürbüz, N., Ismayilova, S., Aksu, G., & Berdeli, A. (2026). A novel RELA variant identified in a patient with RELA-associated inflammatory disease (RAID). Gene Reports, 43, 102485. https://doi.org/10.1016/j.genrep.2026.102485

Keyword: *Nanopore Sequencing, Next-Generation Sequencing (NGS), Rare Diseases*

Amino-Functionalized Carbon Dots as a Cost- Effective Alternative to Fluorescent Dyes for Wound Healing Monitoring

Sümeyye Kozan [*1], **Havva Nur Gürbüz**[2], **Meltem Demirel Kars**[1]

[1] *Department of Biomedical Engineering, Necmettin Erbakan University, Konya, Türkiye*
[2] *Selçuk University, Faculty of Science, Department of Chemistry, Konya, Türkiye*

Nanomaterial science offers unique opportunities to engineer advanced optical and biocompatible properties controlled by the quantum size effect at the nanoscale. A highly efficient and single-step 'bottom-up' hydrothermal synthesis route, fully complying with green chemistry principles, was established to fabricate nitrogen-doped carbon quantum dots (N-CQDs) engineered for prospective cell culture applications. Constructed from molecular precursors through an eco-friendly and sustainable approach, these nanostructures exhibit exceptional potential as robust, cost-effective alternatives to conventional fluorophores cellular imaging, particularly in wound healing monitoring. Within this scope, the N-CQDs were well characterized using different techniques (SEM, EDX, FTIR, and Raman spectroscopy). The characterization profiles successfully verified the nanoscale dimensions of the structures along with their distinctive auto fluorescent properties, confirming their high suitability for advanced optical bioimaging. The biocompatibility of different concentrations of N-CQDs was evaluated on the L929 (mouse fibroblast) cell line. The effects of N-CQD on cell proliferation were demonstrated by MTT analysis at 24, 48, and 72 hours. N-CQDs were applied within the safe dose range to monitor in vitro keratinocyte scratch wound models. Cell viability, migration, and wound closure rates over a 7-day period using both inverted and confocal microscopy were assessed compared to the control group. N-CQDs increased the closure rate in 2D scratch and cell proliferation. Direct interaction of N-CQDs with the cells was successfully confirmed by confocal microscopy proving inherent fluorescence property of N-CQDs. These findings demonstrate the cell proliferation-promoting properties of N-CQDs and highlight the usefulness of advanced in vitro models for evaluating pharmacological agents.

Acknowledgment:
This study was financially supported by the Scientific and Technological Research Council of Türkiye (TÜBİTAK) under the 1002-Quick Support Program (Project No: 225M695).

ORCID:
Sümeyye Kozan: 0009-0004-7045-6940
Havva Nur Gürbüz: 0009-0007-4424-0662
Meltem Demirel Kars: 0000-0002-7300-4075

References:
Song H., Li Y., Shang L., Tang Z., Zhang T., Lu S., 2020, Designed controllable nitrogen-doped carbon dots-loaded MoP nanoparticles for boosting hydrogen evolution reaction in alkaline medium, Nano energy 72;(2020);104730
Niu, L., Zhao, X., Tang, Z., Wu, F., Lei, Q., Wang, J., Wang, X., Liang, W., & Wang, X. (2022). Solid-solid synthesis of covalent organic framework as a support for growth of controllable ultrafine Au nanoparticles. Science of The Total Environment, https://doi.org/https://doi.org/10.1016/j.scitotenv.2022.155423
Sayaner Taşçı, B. N., Kozan, S., Demirel Kars, M., Çetin, K., Karslıoğlu, S., & Kars, G. (2025). Fabrication and In Vitro Evaluation of LL37-Loaded Electrospun PHB/Collagen Nanofibers for Wound Healing. Polymers, 17(18), 2486. https://doi.org/10.3390/polym17182486.

Keyword: *CQDs, wound healing, 2D in vitro model*

Biological Applications of Carbon Quantum Dots Synthesized from Different Organometallic Complexes

Taha Yasin Bayram [*1], Serhat Demirci[1], Ezo Palavan[1], Aslı Yılmaz[1,2], Özlem Gündoğdu Aytaç[3,4], Sertan Aytaç[3,4], Yunus Kara[4], Mehmet Yılmaz[2,4]

[1] *Atatürk University, Department of Molecular Biology and Genetics, Erzurum, Turkiye*
[2] *East Anatolia High Technology Application and Research Center (DAYTAM), Atatürk University, 25240 Erzurum, Türkiye*
[3] *Kırşehir Ahi Evran University, Kaman Vocational School, Department of Food Processing, Food Technology Program, Kırşehir, Türkiye*
[4] *Department of Chemistry, Sciences Faculty, Atatürk University, Erzurum 25240, Turkiye*

The development of novel functional materials has become one of the major research areas in materials science and nanotechnology. In particular, metal complexes are considered important precursor compounds for the synthesis of next-generation nanomaterials due to their easily tunable structures and versatile functional properties. In recent years, carbon quantum dots (CQDs) have attracted considerable attention for various biomedical applications, including bioimaging, biosensing, drug delivery, and photocatalysis, owing to their excellent photostability, tunable fluorescence properties, high biocompatibility, and low toxicity. Among the various synthesis approaches, the hydrothermal method is the most widely preferred bottom-up strategy because of its low cost, simple operation, and easily controllable experimental parameters such as temperature, reaction time, and pressure.

In this study, carbon quantum dots were synthesized via the hydrothermal method using different organometallic complexes as carbon precursors, and the biological properties of the synthesized nanomaterials were comparatively evaluated. The study aims to investigate how the structural differences arising from different metal-centered organometallic complexes influence the biological performance of the resulting CQDs. In this context, the effects of the synthesized CQDs on cell viability were evaluated through cytotoxicity assays. The findings are expected to provide insights into the influence of organometallic precursor selection on the biological behavior of CQDs and contribute to the development of novel carbon quantum dots with enhanced biocompatibility and potential for biomedical applications.

Acknowledgment:
This study was supported by the Scientific Research Projects Coordination Unit (BAP) of Atatürk University under Project No. FBA-2026-16557. The authors sincerely acknowledge this financial support.

ORCID:
Taha Yasin Bayram: 0000-0003-46257429
Serhat Demirci: 0009-0000-7975-1998
Ezo Palavan: 0009-0002-5903-2085
Aslı Yılmaz: 0000-0001-7874-5641
Özlem Gündoğdu Aytaç: 0000-0002-6943-9674
Yunus Kara: 0000-0001-7552-9425
Mehmet Yılmaz: 0000-0003-2687-9167

References:
https://doi.org/10.1016/j.ica.2020.119694
https://doi.org/10.3390/molecules29215138
https://doi.org/10.1021/acs.jpcc.5c01343

Keyword: *Carbon Quantum Dots (CQDs), Organometallic Complexes, Cytotoxic*

Production and Characterization of Electrospun Nanofibers Containing Polycationic Polymers for Controlled Release of Anticancer Drugs

Yağmur Aktepe [*1], Sultan Sacide Gelen[1], Ozan Yesiltepe[2], Dilek Odacı[3]

[1] *Department of Biochemistry, Graduate School of Natural and Applied Sciences, Ege University Izmir/Turkiye*
[2] *Department of Nuclear Applications, Institute of Nuclear Sciences, Ege University Izmir/Turkiye*
[3] *Department of Biochemistry, Faculty of Science, Ege University Izmir/Turkiye*

Nanofibers are widely utilized in biomedical applications due to their high surface area-to-volume ratios, adjustable porosities, and structures that mimic the extracellular matrix. Electrospinning, one of the most common techniques for nanofiber fabrication, enables the controlled conversion of various polymers into fibrous forms (Uhljar et al., 2021; Abdulhussain et al., 2023). Among polymers to form nanofibers, poly-ε-caprolactone (PCL), frequently preferred in biomedical fields, offers significant advantages owing to its biocompatibility, mechanical strength, and slow degradation profile. However, its hydrophobic nature can limit cell–matrix interactions (Scaffaro et al., 2017; Chaudhari et al., 2016). Polycationic polymers, which can enhance cell adhesion, interact with negatively charged cell surfaces through their positively charged amino groups (Fil et al., 2026).

This study aimed to fabricate composite nanofibers via electrospinning using PCL as the primary matrix and a polycationic auxiliary polymer, followed by the physicochemical characterization of the resulting structures. The electrospinning process was conducted under an optimized conditions such as applied voltage, a needle-to-collector distance, and a flow rate. The chemical structures of the fabricated nanofibers were characterized by FTIR, while their morphological attributes were evaluated using SEM and SEM-EDS analyses. Additionally, contact angle measurements were performed, and the wetting behavior was monitored over a 15-minute period. The characterization results demonstrated the successful fabrication of the composite nanofibers. While FTIR analysis confirmed the presence of characteristic functional groups associated with the composite structure, SEM images revealed that the fiber morphology was well-preserved. Contact angle measurements indicated that the incorporation of polycationic polymers significantly influenced the surface properties. Furthermore, the fiber morphology was found to vary depending on the composition of the electrospinning solution. These findings suggest that modifying PCL-based nanofibers with polycationic polymers represents an effective strategy for enhancing surface biofunctionality.

ORCID:
Yağmur Aktepe: 0009-0007-1838-1146
Sultan Sacide Gelen: 0000-0002-0373-0602
Ozan Yesiltepe: 0000-0003-1914-1201
Dilek Odacı: 0000-0002-7954-1381

References:
Abdulhussain, Rand & Adebisi, Adeola & Conway, Barbara & Asare-Addo, Kofi. (2023). Electrospun nanofibers: Exploring process parameters, polymer selection, and recent applications in pharmaceuticals and drug delivery. Journal of Drug Delivery Science and Technology. 90. 105156.
Chaudhari, A. A., Vig, K., Baganizi, D. R., Sahu, R., Dixit, S., Dennis, V., Singh, S. R., & Pillai, S. R. (2016). Future Prospects for Scaffolding Methods and Biomaterials in Skin Tissue Engineering: A Review. International Journal of molecular sciences, 17(12), 1974.
Fil, H., Yesiltepe, O., Er Zeybekler, S., Kozgus, O., Kurbanoglu, S., Medine, E. I., & Odaci, D. (2026). In Vitro Testing of Ibrutinib-Loaded Electrospun Nanofibers for Potential Use as a Transdermal Patch Material. ACS omega, 11(8), 13845–13854.
Scaffaro, R., Lopresti, F., & Botta, L. (2017). Preparation, characterization and hydrolytic degradation of PLA/PCL co-mingled nanofibrous mats prepared via dual-jet electrospinning. European Polymer Journal, 96, 266-277.
Uhljar, L. É., Kan, S. Y., Radacsi, N., Koutsos, V., Szabó-Révész, P., & Ambrus, R. (2021). In vitro drug release, permeability, and structural test of ciprofloxacin-loaded nanofibers. Pharmaceutics, 13(4), 556.

Keyword: *Electrospinning, Nanofibers, Poly-ε-caprolactone (PCL)*

ACE2-Rich Plasma Membrane-Modified Gold Interface as a Bioinspired Sensing Platform

Zeynep Elcim Koru [*1], Eren Polat[1], Sude Yılmaz[1], Kerem Tok[1], Didem Aksu[2], Faezeh Ghorbanizamani[1], Hichem Moulahoum[1], Emine Guler Celik[3], Figen Zihnioglu[1], Suna Timur[1]

[1] *Department of Biochemistry, Institute of Natural and Applied Sciences, Ege University, İzmir, Turkey*
[2] *Ege University Central Research Testing and Analysis Laboratory*
[3] *Ege University, Faculty of Engineering, Department of Bioengineering*

The development of biologically relevant sensing interfaces is important for the selective detection of viral targets. The specific interaction between the SARS-CoV-2 spike protein and the host angiotensin-converting enzyme 2 (ACE2) receptor provides a strong biological recognition mechanism for sensing applications [1–4]. In this study, ACE2-rich plasma membrane isolates derived from ACE2-overexpressing HEK293 cells were investigated as cell membrane-derived recognition layers on gold surfaces.

ACE2-rich plasma membrane vesicles were isolated and purified from ACE2-overexpressing HEK293 cells to obtain a biologically active membrane fraction for surface modification. The membrane fraction was immobilized onto cysteamine-modified gold electrodes via EDC/NHS coupling chemistry, enabling the stabilization of a cell-derived recognition layer on the conductive gold interface. Similar ACE2-rich membrane-based structures have previously been shown to interact effectively with SARS-CoV-2, supporting their potential as bioinspired recognition interfaces [5].

The morphology and surface characteristics of the membrane vesicles and modified gold interfaces were examined by SEM and AFM. Following surface modification, the immobilized ACE2-rich membrane showed specific affinity toward SARS-CoV-2 S1 protein. Analytical studies demonstrated a working range of 5–200 ng/mL and a linear response between 10 and 100 ng/mL for S1 protein.

These findings indicate that ACE2-rich plasma membrane-modified gold interfaces can serve as promising bioinspired sensing platforms. Beyond SARS-CoV-2 detection, this approach highlights the potential of receptor-rich cell membrane architectures as functional nanobiointerfaces for virus-oriented biosensing applications.

Acknowledgment:
This study was supported by the Health Institutes of Türkiye (TÜSEB) under project number 47876.

References:
[1] Angius, F., Puxeddu, S., Zaimi, S., Canton, S., Nematollahzadeh, S., Pibiri, A., Delogu, I., Alvisi, G., Moi, M. L., & Manzin, A. (2025). SARS-CoV-2 Evolution: Implications for Diagnosis, Treatment, Vaccine Effectiveness and Development. Vaccines, 13(1), 17. https://doi.org/10.3390/vaccines13010017
[2] Zabidi, N. Z., Liew, H. L., Farouk, I. A., Puniyamurti, A., Yip, A. J. W., Wijesinghe, V. N., Low, Z. Y., Tang, J. W., Chow, V. T. K., & Lal, S. K. (2023). Evolution of SARS-CoV-2 Variants: Implications on Immune Escape, Vaccination, Therapeutic and Diagnostic Strategies. Viruses, 15(4), 944. https://doi.org/10.3390/v15040944
[3] Charles, J., McCann, N., Ploplis, V. A., & Castellino, F. J. (2023). Spike protein receptor-binding domains from SARS-CoV-2 variants of interest bind human ACE2 more tightly than the prototype spike protein. Biochemical and Biophysical Research Communications, 641, 61–66. https://doi.org/10.1016/j.bbrc.2022.12.011
[4] Li, J., Jia, H., Tian, M., Wu, N., Yang, X., Qi, J., Ren, W., Li, F., & Bian, H. (2022). SARS-CoV-2 and emerging variants: unmasking structure, function, infection, and immune escape mechanisms. Frontiers in Cellular and Infection Microbiology, 12, 869832.
[5] Wang, C., Wang, S., Chen, Y., Zhao, J., Han, S., Zhao, G., Kang, J., Liu, Y., Wang, L., Wang, X., Xu, Y., Wang, S., Huang, Y., Wang, J., & Zhao, J. (2021). Membrane nanoparticles derived from ACE2-rich cells block SARS-CoV-2 infection. ACS Nano, 15(4), 6340–6351. https://doi.org/10.1021/acsnano.0c06836

Keyword: *ACE2, plasma membrane vesicles, bioinspired sensing platform*

Eco-Friendly ZnO Thin Films Produced via Leaf Extract-Assisted Hydrothermal Processing

Fatma Nurgül Çataklı, Beyza Sandık, Berrin İkizler *

Ege University, Department of Chemical Engineering, Bornova, İzmir, Türkiye

This project focuses on the synthesis of ZnO thin films on zinc plates via a one-step hydrothermal method completely based on green chemistry principles, and the investigation of their crystalline, morphological, and optical properties, aiming to develop a sustainable solution to industrial water pollution. Due to the severe operational disadvantages of traditionally used powder-form photocatalysts, such as separation difficulties from the reaction medium, secondary pollution risks, and reuse problems [1,3], the idea of fabricating the catalyst directly in film form on a zinc substrate constitutes the fundamental starting point of this study. The limitations of current film coating methods, such as requiring high-cost equipment or using chemicals hazardous to nature, necessitate the development of entirely eco-friendly and economical synthesis alternatives [2]. Since no study has been encountered in the literature utilizing plant extracts directly in one-step film production, this project aims to address a significant gap in the literature.

ZnO thin films were deposited on zinc plates using hydrothermal method. The plates were cut into dimensions of 20x20 mm and subjected to ultrasonic cleaning in solvent baths of increasing polarity containing acetone, ethanol, and deionized water, respectively. Leaf extracts were obtained after the extraction of leaves in water solvent under continuous magnetic stirring and multi-stage filtration steps. Clean zinc plates and the leaf extract solution were loaded into a Teflon-lined stainless-steel autoclave and subjected to hydrothermal treatment at different temperatures. pH of the medium, reaction duration and calcination temperatures were investigated as parameters to obtain ZnO films. The structural, morphological, and optical properties of the synthesized ZnO thin films were evaluated by XRD, SEM, UV-Vis, and band gap measurements. SEM images confirmed that ZnO was successfully deposited in nanosheet form and exhibited a homogeneous surface coverage. XRD results verify the crystallinity of the films. The band gap values were determined from the reflectance measurements of the films. The results indicate that the films are promising candidates for photocatalytic applications under UVA irradiation.

Acknowledgment:
This work is supported by TÜBİTAK 2209A program by the project number of 1919B012543882

ORCID:
Fatma Nurgül Çataklı: 0009-0000-8953-8023
Beyza Sandık: 0009-0000-8953-8023
Berrin İkizler: 0000-0001-8889-0754

References:
[1]Yudasari, N., Putri, K. Y., Sugiarto, I. T., Taufiq, A., Kim, D.-H., & Djuhana, D., Growth Time Optimization of ZnO Nano-microstructures on Zinc Foil for Enhanced Photocatalytic Treatment of Textile Wastewater. Arabian Journal for Science and Engineering. Journal of Hazardous Materials, 455 (2025) 131567.
[2]İkizler B, Peker M., Growth of highly aligned ZnO nanorod arrays on zinc plates: Morphological and structural characterization. Res. Eng. Struct. Mater. 10 (2024) 623-636.
[3]Taşdemir, A., Akman, N., Akkaya, A., Aydın, R., & Şahin, B., Green and cost-effective synthesis of zinc oxide thin films by L-ascorbic acid (AA) and their potential for electronics and antibacterial applications. Journal of Inorganic and Organometallic Polymers and Materials, 32 (2022) 1234-1245.

Keyword: *ZnO thin films, Green synthesis, Surface coating*

Development of a Novel Biomaterial for Seed Treatments Against Drought Stress

Betul Akkus * **, Nermin Seda Kehr**

İzmir Institute of Technology, Department of Chemistry, İzmir, Türkiye

Climate change, unsustainable water management approaches, and environmental pollution directly affect plant growth by increasing the severity and frequency of soil-related water stress and drought in agriculture [1-3]. There is currently no study that offers a solution to drought stress by simultaneously using nanoparticles, hydrogels, and beneficial bacteria and enabling their controlled interaction with seeds through the resulting synergistic effect. Nanobiotechnological approaches in agriculture aimed at increasing abiotic and biotic stress tolerance, particularly the agricultural applications of hydrogels and various nanomaterials, are attracting significant interest due to their tunable physicochemical properties. Seed priming is one of the methods developed to reduce environmental stress in plants, and in this study, probiotic-containing (biological priming agents) and nanoparticle-containing (chemical priming agents) seed pre-treatments have been used to enhance the tolerance of seeds to drought stress. In this study, proline-modified periodic mesoporous organosilicate (PMO) nanoparticles will be developed as seed pre-treatment agents to regulate osmotic balance under drought conditions and protect cells from dehydration. Additionally, the use of a biological priming agent or plant probiotic in combination with nanoparticles improves plant growth and seed physiological parameters under drought conditions. The synthesized nanobiomaterials are characterized using scanning electron microscopy (SEM), dynamic light scattering (DLS), and zeta potential measurements. Furthermore, seed germination rate, reactive oxygen species (ROS), protein, and antioxidant enzyme activities (e.g., superoxide dismutase (SOD)) are measured and compared with unprimed seed groups. In the synthesis of proline-modified nanoparticles, it has been determined that the nanoparticle size increased from 195.6 ± 2.46 nm to 207.0 ± 1.00 nm and the surface charge is negative from zeta potential measurements. In conclusion, the application of nanomaterials to seeds increases seed germination percentage, promotes the production of the SOD antioxidant enzyme, and decreases ROS inhibition compared to the control group.

Acknowledgment: This work is supported by the Scientific and Technological Research Council of Turkey (TÜBİTAK) under the 2515 - COST Action Members R&D Support Program, Project No.CA24156

Acknowledgment:
This work is supported by the Scientific and Technological Research Council of Turkey (TÜBİTAK) under the 2515 - COST Action Members R&D Support Program, Project No.CA24156

ORCID:
Betul Akkus: https://orcid.org/0000-0002-5297-4136
Nermin Seda Kehr: https://orcid.org/0000-0003-2275-1254

References:
[1] Rezaei EE, Webber H, Asseng S, et al. Climate change impacts on crop yields. Nat Rev Earth Environ. 2023;4(12):831–846. doi:10.1038/s43017-023-00491-0
[2] Islam M, Sandhi A. Heavy metal and drought stress in plants: the role of microbes—a review. Gesunde Pflanzen. 2023;75(4):695-708. doi:10.1007/s10343-022-00762-8
[3] Wahab A, Abdi G, Saleem MH, et al. Plants' physio-biochemical and phyto-hormonal responses to alleviate the adverse effects of drought stress: A comprehensive review. Plants. 2022;11(13):1620. doi:10.3390/plants11131620

Keyword: *nanobiomaterials, seed priming, drought stress*

Design and Characterization of Ionic Liquid Functionalized Magnetic MOF-on-MOF Nanocomposite for Green Extraction Applications

Duygu Totur Pamık [*1], **Serap Seyhan Bozkurt**[2]

[1] *Dokuz Eylul University, Faculty of Engineering, Department of Environmental Engineering, Izmir, Türkiye*
[2] *Dokuz Eylul University, Faculty of Science, Department of Chemistry, Izmir, Türkiye*

In this study, a novel magnetic MOF-on-MOF nanocomposite (IS@Fe_3O_4@Cu-MOF/Fe-MOF) functionalized with an ionic liquid was successfully synthesized and characterized for green extraction applications. In this developed hierarchical structure, the secondary structure, Fe-MOF were integrated into the core magnetically coated Cu-MOF structure Subsequently, the structure was functionalized with an ionic liquid to increase the sorption capacity and surface interactions.

The synthesized MOF-on-MOF nanocomposite was characterized by FTIR, SEM-EDX, and XRD. Thus, its structural and morphological properties were determined. Thanks to this hierarchical structure, this material has a high surface area and synergistic sorption behavior. In addition, the magnetic property of the nanocomposite allows for fast and simple separation during extraction.

Mg(II) and Ca(II) ions were selected as model analytes. The developed material also showed good extraction capacity. The parameters pH, sorbent amount, and extraction time were primarily investigated. The results showed that the developed MOF on-MOF structure has a high extraction capacity and an easy operational procedure. The greenness of the proposed analytical method was evaluated using the AGREE metric. It was shown to be environmentally friendly with simplified extraction steps and reduced solvent consumption.

In summary, the findings show that the ionic liquid-impregnated magnetic MOF-on-MOF nanocomposite offers a suitable material for green extraction and sample preparation applications.

ORCID:
Duygu Totur Pamık: 0000-0003-1411-3500

Keyword: *MOF-on-MOF; Magnetic nanocomposite; Ionic liquid; Mg(II); Ca(II); Green analytical chemistry; AGREE*

Potential of Green-Synthesized and Iodine-131 Radiolabeled Plant-Based Nanoparticles in Biomedical Applications

Duygu Tugce Baran [*] **, Rumeysa Celik, Fazilet Zumrut Biber Muftuler**

Department of Nuclear Application, Institute of Nuclear Science, Ege University, İzmir, Türkiye

Driven by the principles of sustainability and green chemistry, the green synthesis of nanotechnology-based biomedical systems utilizing food and agricultural wastes has emerged as a paradigm-shifting approach in modern nanomedicine. This study aims to synthesize chitosan-silver nanoparticles (Ch/AgNPs) using orange carrot (Daucus carota L.) peels and zinc oxide nanoparticles (ZnONPs) using white radish (Raphanus sativus L.) leaves through a green synthesis approach. Subsequently, each nanoparticle system was individually radiolabeled with Iodine-131 (^{131}I), and their wound healing efficacy and antimicrobial activities were comparatively evaluated. Extracts from Daucus carota peel and Raphanus sativus leaves were used as bio-reactive agents in the reduction and stabilisation of nanoparticles. The physicochemical properties and structural characterisation of the synthesised Ch/AgNPs and ZnONPs were verified using DLS, HPLC, EDX and SEM analyses. The nanoparticles obtained via the green synthesis method were radiolabelled with the ^{131}I isotope, which is widely used in diagnostic and therapeutic applications in nuclear medicine, and analyses of radiochemical purity, stability and lipophilicity were carried out. The antimicrobial activities of ^{131}I-Ch/AgNP and ^{131}I-ZnONP formulations were evaluated against Staphylococcus aureus, Candida albicans, and Methicillin-Resistant Staphylococcus aureus strains. Concurrently, the wound healing potential of the NPs was investigated on the dermal fibroblast cell line (BJ, ATCC CRL-2522). Phytochemical analyses of plant extracts have confirmed the presence of phenolic compounds that play a role in nanoparticle synthesis. Characterization results demonstrated that the particle sizes were 111.8 nm for Ch/AgNPs and 151.2 nm for ZnONPs, indicating that both nanoparticles were stable, possessed a homogeneous size distribution, and were at the nanoscale. Radiolabeling studies with ^{131}I exhibited high radiochemical purity yields of over 95% for both NPs. It was observed that the Ch/AgNP and ZnONP systems created a potent antimicrobial barrier against major pathogens causing wound infections and supported tissue regeneration. This study proves that smart nanoplatforms obtained from the recycling of food wastes can overcome the limitations of conventional radiopharmaceuticals. The developed ^{131}I-Ch/AgNP and ^{131}I-ZnONP systems are next-generation biocompatible theranostic agent candidates with high efficacy and low toxicity in deep wound management through nanotechnology-based approaches. In future studies, the retention of these radiolabeled derivatives will be evaluated.

ORCID:
Duygu Tugce Baran: 0009-0008-5716-2218
Rumeysa Celik: 0009-0006-6440-3097
Fazilet Zumrut Biber Muftuler: 0000-0001-8184-9660

References:

al Awadh, A. A., Shet, A. R., Patil, L. R., Shaikh, I. A., Alshahrani, M. M., Nadaf, R., Mahnashi, M. H., Desai, S. v., Muddapur, U. M., Achappa, S., Hombalimath, V. S., Khan, A. A., Gouse, H. S. M., Iqubal, S. M. S., & Kumbar, V. (2022). Sustainable Synthesis and Characterization of Zinc Oxide Nanoparticles Using Raphanus sativus Extract and Its Biomedical Applications. Crystals 2022, Vol. 12, 12(8). https://doi.org/10.3390/CRYST12081142

Bentivoglio, V., Nayak, P., Varani, M., Lauri, C., & Signore, A. (2023). Methods for Radiolabeling Nanoparticles (Part 3): Therapeutic Use. Biomolecules 2023, Vol. 13, 13(8). https://doi.org/10.3390/BIOM13081241 Hano, C., & Abbasi, B. H. (2021). Plant-Based Green Synthesis of Nanoparticles: Production, Characterization and Applications. Biomolecules 2022, Vol. 12, Page 31, 12(1), 31. https://doi.org/10.3390/BIOM12010031

Shehabeldine, A. M., Salem, S. S., Ali, O. M., Abd-Elsalam, K. A., Elkady, F. M., & Hashem, A. H. (2022). Multifunctional Silver Nanoparticles Based on Chitosan: Antibacterial, Antibiofilm, Antifungal, Antioxidant, and Wound-Healing Activities. Journal of Fungi 2022, Vol. 8, 8(6). https://doi.org/10.3390/JOF8060612

Keyword: *green synthesis, iodine-131, chitosan-silver nanoparticles, zinc oxide nanoparticles, wound healing, antimicrobial Activity.*

Effect of Hydrothermal Carbonization Temperature on the Antioxidant Activity of Carbon Dots Derived from Winery Fermentation Waste

Ecem Köseoğlu * **, Didem Aksu, Gözde Duman Taç**

Ege University

Carbon dots (CDs) have attracted considerable attention due to their unique optical properties, excellent water dispersibility, and promising antioxidant activity. In this study, winery fermentation waste was valorized for the sustainable production of carbon dots through hydrothermal carbonization (HTC). Hydrothermal treatment was carried out at three different temperatures (160, 180, and 200 °C) for 2 h. Following HTC, the liquid products were filtered through a 0.22 μm membrane, purified by dialysis to remove low-molecular-weight impurities, frozen at −80 °C, and subsequently freeze-dried to obtain purified carbon dots.

The antioxidant activity of the obtained carbon dots was evaluated using the DPPH radical scavenging assay. All samples were analyzed at a 400-fold dilution, and the antioxidant capacity was expressed as ascorbic acid equivalents (AAE). The carbon dots produced at 160 °C exhibited the highest radical scavenging activity (73.1%), corresponding to an antioxidant capacity of 3.67 M AAE. Increasing the HTC temperature to 180 and 200 °C decreased the DPPH scavenging efficiencies to 59.4% and 47.9%, respectively, corresponding to antioxidant capacities of 2.68 and 1.86 M AAE. These findings indicate that hydrothermal carbonization temperature has a significant influence on the antioxidant properties of carbon dots. Lower HTC temperatures better preserve the surface functional groups responsible for radical scavenging, resulting in enhanced antioxidant activity. This study demonstrates that winery fermentation waste is a promising renewable feedstock for producing antioxidant carbon dots through an environmentally friendly and sustainable process.

ORCID:
Ecem Köseoğlu: 0009-0008-9358-7598
Didem Aksu: 0000-0002-7184-4011
Gözde Duman Taç: 0000-0002-9427-8235

Keyword: *Winery waste valorization, Biomass-derived carbon dots, Green Synthesis*

Conversion of Nitrates into Ammonia Using Nanostructured Metal–Organic Framework-Based Catalysts

Eray Tabak [*] [1,2], **Ali Furkan Albora**[1], **Eren Özbay**[1], **Aslı Sare Gürsu**[1], **Şahika Sena Bayazit**[1]

[1] *Istanbul University-Cerrahpasa, Institute of Nanotechnology and Biotechnology, 34500, Istanbul, Türkiye*
[2] *Istanbul Techical University, Graduate School, Nano Science and Nano Engineering Programme, 34469, Istanbul, Türkiye*

Nitrate pollution is a major environmental concern affecting surface water, groundwater, and wastewater systems due to its detrimental impacts on human health and aquatic ecosystems. Conventional nitrate removal methods, including ion exchange, reverse osmosis, and biological denitrification, are often associated with high operational costs, secondary waste generation, and additional treatment requirements. Therefore, the development of sustainable technologies that simultaneously remove nitrate and generate value-added products is of great importance. In this study, titanium (Ti)- and zirconium (Zr)-based metal-organic frameworks (MOFs) were synthesized and evaluated as catalysts for nitrate reduction. Owing to their high surface area, tunable porosity, and enhanced mass-transfer properties, these materials offer significant advantages for catalytic applications. The nitrate reduction performance of the synthesized MOFs was investigated in potassium nitrate (KNO_3) solutions with concentrations of 100 and 200 ppm using catalyst loadings of 20, 30, and 50 mg. Ammonia formation (Ct) was monitored as a function of reaction time to evaluate the effects of catalyst loading and nitrate concentration on reaction efficiency. The results demonstrated that both catalyst loading and nitrate concentration significantly influenced ammonia production. Among the tested conditions, 30 mg catalyst loading exhibited the highest ammonia yields at both nitrate concentrations. In contrast, 50 mg catalyst loading provided stable ammonia production in 200 ppm KNO_3 solution but showed limited active-site utilization at 100 ppm due to insufficient substrate availability. Overall, higher nitrate concentrations combined with moderate catalyst loadings enhanced ammonia generation. These findings highlight the potential of Ti- and Zr-based MOFs as efficient catalysts for nitrate valorization and provide a promising approach for integrating wastewater treatment with renewable ammonia production.

Acknowledgment:
This work was supported by the Scientific Research Projects Coordination Unit of Istanbul University-Cerrahpaşa (IUC-BAP) within the scope of the Research Universities Support Program (ADEP), Project Number FBA-2024-37600.

ORCID:
Eray Tabak: 0009-0001-6674-8025

Keyword: *MOFs, water treatment, nitrate conversion*

From Bio-Silica to Radionuclide Sorbent: κ-Carrageenan/Diatomite Composites for Sr(II) Removal

Ikbal Gozde Kaptanoglu *

Ege University, Institute of Nuclear Sciences

Strontium-90 (^{90}Sr, $t_{1/2} \approx 28.8$ years), a major fission product released in nuclear accidents and legacy waste streams, poses long-term radiological risks owing to its bone-seeking behavior and prolonged biological retention. Stable Sr(II) serves as a non-radioactive chemical analogue in laboratory-scale adsorption studies, enabling safe mechanistic investigation of sorbent materials intended for ^{90}Sr remediation. In this work, κ-carrageenan/diatomite composite hydrogels were prepared via solution casting without toxic crosslinkers and assessed for Sr(II) uptake from aqueous solutions.

Three formulations incorporating increasing diatomite loadings (0.25–0.75 g per 1 g κ-carrageenan) were synthesized and screened. The best-performing composite (KD-75) was characterized by XRD, FT-IR, SEM–EDX, XPS, and TGA. XRD and FT-IR results indicated non-covalent integration of diatomite within the biopolymer network through hydrogen bonding, with no new crystalline phase formation. SEM images showed a dense, morphologically transformed surface with well-dispersed diatomite particles embedded in the hydrogel matrix.

Batch adsorption experiments were conducted over a range of pH, contact time, initial Sr(II) concentration, and temperature. Removal efficiency peaked at pH 5 and equilibrium was reached within 60 min. Among the tested isotherm models, the nonlinear Freundlich model provided the best fit, suggesting heterogeneous surface adsorption, while the Langmuir-derived maximum capacity of KD-75 (32.52 mg g^{-1}) considerably exceeded that of raw diatomite (18.43 mg g^{-1}). Adsorption kinetics were consistent with the pseudo-second-order model, pointing to surface-reaction control.

XPS spectra recorded before and after Sr(II) loading revealed complete disappearance of the K 2p signal alongside the emergence of Sr 3d peaks at 133.45 and 134.93 eV, indicating that K^+/Sr^{2+} ion exchange is the primary uptake pathway. Shifts in the O 1s region further implicated electrostatic interactions involving –OH and $–SO_3^-$ groups. Desorption with 0.5 M HCl recovered 88.8% of adsorbed Sr(II) over three consecutive cycles. In competitive adsorption experiments with Cu(II), Fe(III), Pb(II), and Cd(II), KD-75 retained partial selectivity for Sr(II). Taken together, the results support κ-carrageenan/diatomite composites as recyclable, bio-based sorbents with a well-characterized uptake mechanism, relevant to the development of materials for radioactive strontium remediation.

Acknowledgment:
This work was supported by the Scientific Research Projects Coordination Unit of Ege University (Project No. 32576).

ORCID:
Ikbal Gozde Kaptanoglu: 0000-0002-3852-9853

Keyword: *κ-Carrageenan, Diatomite, Radionuclide remediation*

Valorization of Grape Pomace for the Green Synthesis of TiO2 Nanoparticles as Nano-biopesticide Against Tuta absoluta

Faezeh Ghorbanizamani, Tugba Oztekin, Kerem Tok, Lale Aktaş * , Ahmet Hatipoglu, Suna Timur, Figen Zihnioğlu, Hichem Moulahoum

Ege university

The sustainable valorization of agro-industrial residues offers an attractive strategy for developing environmentally friendly nanomaterials for agricultural applications. In this study, grape pomace was investigated as a renewable phytochemical source for the green synthesis of titanium dioxide (TiO_2) nanoparticles intended for crop protection. Extraction with 70% ethanol provided the highest recovery (85.6-88.0%) and produced extracts rich in phenolic compounds (up to 44.7 mg GAE/g extract), antioxidant activity (~33.5 mM Trolox equivalents/g), and flavonoids (1.48 mg QE/g). Comprehensive LC-QTOF-MS/MS profiling revealed a phytochemical fingerprint dominated by procyanidins, catechin and epicatechin derivatives, quercetin glycosides, anthocyanins, and the stilbene r-viniferin, supporting their role as natural reducing and capping agents during nanoparticle synthesis. The optimized grape-derived TiO_2 nanoparticles were successfully characterized by UV-Vis spectroscopy, DLS, SEM-EDS, FTIR, XRF, and XRD, exhibiting an average hydrodynamic diameter of 193.5 (PDI=0.341) while preserving the crystalline anatase phase. Preliminary insecticidal evaluation against second-instar larvae of Tuta absoluta demonstrated dose-dependent toxicity, with mortality increasing from 13.3% at 200 ppm to 83.3% at 2000 ppm after 72 h of exposure. Probit analysis yielded an LC_{50} of 789 ppm and an LC_{90} of 2820 ppm, outperforming both lemon-derived and commercial TiO_2 nanoparticles under the same experimental conditions. In addition to increased mortality, treated larvae exhibited abnormal feeding behavior and reduced gallery formation, suggesting that grape-derived TiO_2 nanoparticles may exert both toxic and feeding-inhibitory effects. These findings demonstrate that grape pomace can be transformed into functional TiO_2 nanomaterials with promising potential as sustainable nano-bio-pesticides for future agricultural applications.

Acknowledgment:
The authors thank The Scientific and Technological Research Council of Turkey (TUBITAK) (Project number: 124Z322).

ORCID:
Lale Aktaş: 0000-0003-0815-8470

References:
Tok, K., Oztekin, T., Yilmaz, S., Aktas, L. Y., Hatipoglu, A., Ghorbanizamani, F., Timur, S., Zihnioglu, F., Moulahoum, H. (2025). Safe-by-design green nanopesticides as a sustainable approach for pest management, plant health, and environmental safety. Science of The Total Environment, 994, 180077.

Keyword: *grape pomace; green synthesis; TiO2NPs; Tuta absoluta; pest management*

Encapsulation of Peppermint Essential Oil in a Chitosan Nanosystem and Evaluation of the Particle Size of Encapsulated Nanoparticles

Rezvan Shaddel * **, Sara Jalaei Moghaddam, Younes Zahedi, Bahram Fathi Achachlouei**

Department of Food Science and Technology, Faculty of Agriculture and Natural Resources, University of Mohaghegh Ardabili, Ardabil, Iran

Chitosan-based nanosystems are recognized as suitable carriers for plant essential oils due to their biocompatibility and high capacity to protect sensitive compounds. Peppermint essential oil, rich in bioactive constituents such as menthol, possesses remarkable antimicrobial and antioxidant properties. However, its high sensitivity to light, temperature, and oxygen limits its direct application. Therefore, encapsulation of this essential oil within nanoscale matrices can be an effective strategy to preserve its functional properties and enhance the shelf life of food products. In the present study, peppermint essential oil was encapsulated in chitosan nanoparticles with the aim of improving its stability, reducing volatility, and enhancing encapsulation characteristics. First, peppermint essential oil was extracted from the plant material, and its chemical composition was identified using Gas Chromatography–Mass Spectrometry (GC–MS). Subsequently, chitosan nanoparticles were prepared by the ionic gelation method, and peppermint essential oil was loaded into the nanochitosan structure. After encapsulation, particle size and polydispersity index (PDI) were evaluated using Dynamic Light Scattering (DLS). The incorporation of peppermint essential oil reduced the particle size from 96.4 to 81.2 nm and decreased the PDI from 0.419 to 0.286. These findings indicate improved particle uniformity and enhanced stability of the essential oil-loaded nanocapsules.

Keyword: *Nanochitosan, Peppermint Essential Oil, Encapsulation*

Carbon Dot-Loaded 3D PAN/ES Electrospun Nanofibrous Sponges for Efficient Methylene Blue Removal and Photoinduced Antibacterial Water Treatment

Timur Tongur [*1], **Altangerel Amarjargal**[2], **Viraj P. Nirwan**[2], **Rebecca Hengsbach**[2], **Amir Fahmi**[2], **Seda Demirel Topel**[3]

[1] *Akdeniz University*
[2] *Rhine-Waal University*
[3] *Antalya Bilim University*

Industrial wastewater containing untreated pollutants, particularly synthetic dyes, poses a major global environmental challenge by threatening ecosystems, water resources, and human health. Among these pollutants, methylene blue (MB) is of particular concern due to its widespread industrial use, persistence at even low concentrations, and toxic effects, making its removal from wastewater essential prior to environmental discharge [1]. In this study, anionic three-dimensional (3D) polyacrylonitrile/ Eudragit S100 (PAN/ES) nanofibrous sponges encapsulating carbon dots (CDs) were fabricated via sustainable one-step electrospinning [2] and characterized by scanning electron microscopy (SEM) and Fourier-transform infrared (FTIR) spectroscopy. The resulting 3D PAN/ES-CDs sponges demonstrated highly efficient adsorption of MB, a cationic dye, from aqueous solution at physiological pH (7.4), achieving a removal efficiency of ≥95%. The adsorption kinetics were evaluated using pseudo-first-order and pseudo-second-order models, while equilibrium data were analyzed using Langmuir and Freundlich isotherm models. Both kinetic and isotherm results were best described by the pseudo-second-order model and the Langmuir isotherm, respectively, suggesting chemisorption and monolayer adsorption on the adsorbent surface. The maximum adsorption capacity of 3D PAN/ES-CDs was determined to be 55.56 $mg.g^{-1}$. Reusability was assessed over five adsorption–desorption cycles, with both materials retaining good desorption efficiencies of ≥73%, confirming their practical regenerability. Beyond adsorption, the embedded CDs functioned as singlet oxygen ($^1O_2$) generators under LED irradiation, as confirmed by monitoring the photobleaching of 1,3-diphenylisobenzofuran (DPBF) as a trap molecule via UV-vis spectroscopy. A singlet oxygen quantum yield of $\Phi_\Delta = 0.76$ was obtained, indicating significant photosensitizing activity that confers additional antibacterial potential to the composite material for water treatment applications. These findings highlight the dual functionality of the 3D PAN/ES-CDs composite as a promising water treatment platform, simultaneously achieving efficient MB removal through adsorption and imparting antibacterial activity via CD-mediated singlet oxygen generation under visible light irradiation.

Acknowledgment:
This study was supported by the Scientific and Technological Research Council of Türkiye (TUBITAK) under the Grant Number 125N193 and the German Academic Exchange Service (DAAD). The authors thank TUBITAK and DAAD for their support.

References:
[1] Umesh A.S., Puttaiahgowda, Y.M., Thottathil S. “Enhanced Adsorption: Reviewing the Potential of Reinforcing Polymers and Hydrogels with Nanomaterials for Methylene Blue Dye Removal” Surfaces and Interfaces, 2024, 51, 104670.
[2] Amarjargal A., Nirwan V.P., Hengsbach R., Fahmi A. “Sustainable One-Step Electrospinning of 3D Nanofiber Sponge with Ultrahigh Oil Sorption Capacity” Materials Letters, 2026, 412, 140394.

Keyword: *methylene blue, 3D nanofibrous sponges, carbon dot*

Green Synthesis of Bio-Compatible Quantum Dots and Their Interactions with Plant-Derived Photosynthetic Pigments

Özge İbiş * **, Caner Ünlü**

İstanbul Technical University

Quantum dots (QDs) have attracted considerable attention as nanomaterials capable of enhancing light harvesting and photocatalytic processes in biological systems. In particular, biocompatible and heavy-metal-free QDs offer promising opportunities for agricultural applications by improving the efficiency of photosynthetic pigments under various environmental stress conditions. In this study, environmentally friendly aqueous synthesis routes were employed to prepare different classes of biocompatible quantum dots, including ZnSe, ZnSeS, ZnAgSe, and $CuInSe_2$/ZnS nanocrystals. The synthesized QDs were characterized using UV–Vis absorption spectroscopy, photoluminescence spectroscopy, FTIR, XRD, TEM, XPS, and time-resolved photoluminescence (TRPL) measurements.

To investigate QD–photosynthetic pigment interactions, chlorophyll pigments extracted from spinach leaves were combined with the synthesized QDs to form hybrid assemblies. Spectroscopic analyses revealed that the optical response of chlorophyll strongly depended on the composition and surface chemistry of the QDs. ZnSeS quantum dots significantly enhanced chlorophyll absorption capacity and enabled modulation of chlorophyll spectral responses. Furthermore, TRPL studies on $CuInSe_2$/ZnS–chlorophyll assemblies demonstrated ligand-dependent excited-state interactions, indicating efficient energy-transfer and/or charge-transfer processes between chlorophyll molecules and quantum dots. Surface ligands such as 3-mercaptopropionic acid (3-MPA), N-acetyl-L-cysteine (NAC), and L-glutathione (L-GSH) were found to play a critical role in regulating these photophysical interactions.

The results demonstrate that rationally designed biocompatible QDs can effectively manipulate the light-harvesting behavior of photosynthetic pigments. These findings provide valuable insights into the development of artificial photosynthetic systems and highlight the potential of quantum-dot-based nanomaterials for sustainable agricultural technologies, enhanced photosynthetic efficiency, and future light-management applications.

ORCID:
Özge İbiş: 0000-0001-5448-6489
Caner Ünlü: https://orcid.org/0000-0002-0612-3111

References:
İbiş, Ö., Ük, N., Nar, I., & Ünlü, C. (2025). Manipulation of defect state emission in Zn chalcogenide quantum dots and their effects on chlorophyll spectral response. Spectrochimica Acta Part A: Molecular and Biomolecular Spectroscopy, 327, 125348. https://doi.org/10.1016/J.SAA.2024.125348
İbiş, Ö., Jahangiri, H., Almammadov, T., & Ünlü, C. (2026). Room-temperature aqueous ZnAgSe alloyed quantum dots: Zn-assisted defect passivation for bright NIR emission and biointerface-ready colloids. Journal of Materials Chemistry C, 14(7), 2758–2776. https://doi.org/10.1039/D5TC03700J
İbiş, Ö., Jahangiri, H., Çeltek, E., & Ünlü, C. (Accepted/In press). Surface-Ligand-Dependent Excited-State Dynamics in Aqueous CuInSe2/ZnS Quantum Dot–Chlorophyll Assemblies. Advanced Materials Interfaces. https://doi.org/10.1002/admi.70549

Keyword: *quantum dots, chlorophyll, hybrid systems*

Nanostructured Metal-Organic Framework Aerogel Composites (MOFACs) with Hierarchical Porosity for Enhanced Molecular CO2 Capture

Ayça Tüter Semercioğlu [*1], Hamed Yousefzade[2], Emre Morkaya[1], Prof. Can Erkey[1,3]

[1] *Department of Chemical and Biological Engineering, Koç University, Rumelifeneri Yolu, Istanbul 34450, Türkiye*
[2] *Department of Chemical Engineering, Yeditepe University, Atasehir, Istanbul, Türkiye*
[3] *Koç University Hydrogen Technologies Center (KUHyTech), Koç University, Istanbul 34450, Türkiye*

Energy-intensive industries such as cement, steel, and chemical manufacturing are major contributors to global CO_2 emissions, driving the need for advanced materials capable of efficient carbon capture. Among emerging solutions, metal-organic frameworks (MOFs) have attracted significant attention due to their high intrinsic microporosity and strong molecular affinity for CO_2. However, their practical engineering implementation is often limited by poor mechanical stability and challenges associated with macroscopic shaping, as conventional binders and drying methods can lead to pore blockage, structural collapse, and restricted access to active nanoscale adsorption sites.

In this context, the present work focuses on the development of nanostructured aerogel based composite adsorbents. Highly porous alginate aerogels serve as lightweight, structurally supportive, and continuous matrices for embedded MOF nanoparticles, specifically MIL-160 (Al) and MIL-53 (Al). By employing supercritical CO_2 drying after gelation, the solvent within the meso-microporous network is removed without inducing capillary stresses. This preserves the delicate nanoscale pore architecture and prevents the structural collapse that typically accompanies conventional drying methods. This drying approach enables the formation of mechanically robust composites while maintaining the intrinsic crystallinity and microporosity of the active adsorbent phase. Structural, morphological, and texturing analyses confirmed that the amorphous aerogel framework does not interfere with the crystalline integrity of the embedded MOF nanoparticles, achieving a highly homogeneous dispersion throughout the aerogel matrix.

The resulting nanocomposites feature a preserved hierarchical pore structure and significantly improved accessibility to nanoscale adsorption sites, leading to enhanced molecular CO_2 uptake demonstrated by both static and dynamic measurements. The confinement of MIL-160(Al) within the aerogel matrix leads to a pronounced synergistic enhancement in CO_2 adsorption performance. MOFACs containing 25, 50, and 75 wt% MIL-160 achieved CO_2 uptakes of 0.43, 0.70, and 0.98 mmol g^{-1}, respectively, at 150 mbar and 25 °C. Similarly, MOFACs containing 25, 50, and 75 wt% MIL-53 achieved CO_2 uptakes of 0.15, 0.26 and 0.35 mmol g^{-1} under the same measurement conditions. The dynamic adsorption behavior of AlgMIL-160 and AlgMIL-53 was evaluated using a binary gas mixture containing 15% CO_2 and 85% N_2. The observed adsorption capacities were comparable to those obtained under single-component CO_2 conditions, with only a slight reduction in uptake, indicating competitive adsorption between CO_2 and N_2 molecules.

Overall, this study demonstrates that nanoscale engineering via aerogel shaping and supercritical fluid processing is an effective strategy for producing lightweight, mechanically stable, and high-performance hybrid nanomaterials, offering a promising pathway toward scalable and efficient carbon capture technologies.

References:

[1] Liu, Z.; Deng, Z.; Davis, S. J.; Ciais, P. Global carbon emissions in 2023. Nat. Rev. Earth Environ. 2024, 5 (4), 253−254.

Keyword: *Metal-organic frameworks (MOFs), Aerogel composites, Nanostructured hybrids*

Identification of Organic and Inorganic Surface Contaminants on ZnS Substrates and Development of Safe Cleaning Protocols Before Photolithography

Berkay Tözendemir [*] [1,2], **Ahmet Toprak**[1], **Tolga Yelboğa**[1], **Murat Alp Şahin**[1,2]

[1] *ASELSAN Inc., Ankara, Türkiye*

[2] *Department of Metallurgical and Materials Engineering, Middle East Technical University, Ankara, Türkiye*

Zinc sulfide (ZnS) is a material widely used in infrared (IR) optical window applications and is valued primarily for the transparency it provides in the long-wave infrared (LWIR) (8–12 μm) spectral range and as an alternative to germanium as an optical material. This work focused on surface preparation of ZnS substrates as part of an ongoing effort to integrate Electromagnetic Interference (EMI)/Electromagnetic Compatibility (EMC) shielding functionality via photolithography and metallization. Surface contamination and process-induced modifications are known to degrade resist spreading, patterning quality, metal adhesion, and LWIR transmission — making controlled, non-destructive cleaning a critical process step. Six protocols were tested: a standard solvent sequence using acetone/isopropyl alcohol (IPA)/deionized (DI) water as baseline, dimethyl sulfoxide (DMSO)-based TecniStrip MicroD350, potassium hydroxide (KOH)-based AZ400K, sodium hydroxide (NaOH)-based AZ351B, oxygen (O_2) descum plasma, and argon (Ar) descum plasma. Surfaces were analyzed using atomic force microscopy (AFM), scanning electron microscopy (SEM) in both secondary electron (SE) and backscattered electron (BSE) modes, optical microscopy, water contact angle (WCA) measurements, and LWIR transmission spectroscopy. Roughness values measured by AFM spanned 0.852 nm to 2.30 nm across protocols — a nanoscale range that proved highly sensitive to the chemistry of each treatment. SE imaging in SEM captured distinct surface signatures for each process. Residual organic films were visible on solvent and DMSO-treated samples, with BSE confirming their low atomic number (low-Z) character. KOH flattened the surface to arithmetic average roughness (Ra) = 0.852 nm but left localized crystalline precipitates and showed no improvement in wettability. NaOH created visible nanometric etch features — striations and small dissolution craters — alongside a moderate WCA reduction to 31.9°. O_2 plasma drove WCA down to ~12.7° and maintained Ra at 0.875 nm; SE images showed scattered surface modifications pointing to localized chemistry changes, possibly zinc oxide (ZnO)-like domain formation. Ar plasma also lowered WCA to 15.2°, but the mechanism was different — ion bombardment roughened the surface to 2.30 nm and SE images revealed craters and elevated features typical of preferential sputtering, suggesting Wenzel-regime wetting rather than genuine activation. On the optical side, NaOH gave the highest LWIR optical transmission at 61.36%, and no protocol dropped below 59%. Taken together, these results show that a single metric like WCA is not sufficient to assess surface readiness for lithography. A combined look at nanoscale morphology, wettability, and optical performance is needed — and the right choice of protocol depends on which trade-off matters most for the target process. These findings establish a nanoscale surface engineering framework for ZnS substrates, contributing to the development of novel nanostructured surface applications in advanced IR optical and photonic systems.

Acknowledgment:
The authors would like to thank the ASELSAN MEOS team for their support in surface characterization measurements, including SEM and AFM analyses conducted at ASELSAN facilities. This work was carried out as part of an internal R&D project at ASELSAN A.Ş.

ORCID:
Berkay Tözendemir: 0009-0005-9232-5762
Ahmet Toprak: 0009-0003-4553-0507
Tolga Yelboğa: 0090-0000-4927-6460
Murat Alp Şahin: 0009-0002-1486-3344

Keyword: *Zinc Sulfide (ZnS), Nanoscale Surface Characterization, Plasma Surface Treatment*

Plasmonic Nanostructures Integrated Electrically Driven Phase Transition Soft Actuators

Elif Kose * [1], **Gokhan Demirel**[2]

[1] *Graduate School of Natural and Applied Sciences, Gazi University, Ankara, Türkiye*
[2] *Department of Chemistry, Gazi University, Ankara, Türkiye*

Soft actuators based on liquid-vapor phase transitions have emerged as promising platforms in soft robotics, offering large deformation, low weight, and straightforward system integration. These systems generate mechanical motion through volumetric expansion triggered by externally induced phase transitions. To date, most implementations rely on pneumatic or electrically driven architectures, while electrothermal strategies remain comparatively underexplored. In parallel, although advanced materials such as liquid crystal elastomers have been widely investigated, the role of heat transfer optimization in governing actuation performance has received limited attention. Here, we present an electrothermally driven soft actuator that incorporates silver nanostructures with tailored morphologies, including nanowires, nanoflakes, and nanoprisms to enhance heat transfer and actuation efficiency. The influence of nanostructure morphology on heat distribution was systematically evaluated through the mechanical response of the actuators, demonstrating morphology-dependent improvements in actuation speed and motion behavior under varying applied voltages. In addition, the surface-enhanced Raman scattering (SERS) activity of the fabricated platforms was investigated, indicating a direct correlation between morphology-dependent hotspot formation and signal intensity.

Acknowledgment:
This work was supported by the Scientific and Technological Research Council of Türkiye (TUBITAK) (grant no: 22AG056)

ORCID:
Elif Kose: https://orcid.org/0009-0006-9354-0963
Gokhan Demirel: https://orcid.org/0000-0002-9778-917X

References:
Wei, F., Yang, L., Lv, Z., & Yao, L. (2024). Response speed of phase change based soft actuator enhanced by antagonistic effect. ACS Applied Electronic Materials, 7(1), 471-479.
Miriyev, A., Stack, K., & Lipson, H. (2017). Soft material for soft actuators. Nature communications, 8(1), 596.
Ai, W., Wu, J., Long, Y., & Song, K. (2025). A Rolling Light-Driven Pneumatic Soft Actuator Based on Liquid–Gas Phase Change. Advanced Materials, 37(11), 2418218.
Li, Y., Wang, Z., Lu, Y., Li, H., Weng, Z., Sun, J., ... & Wang, X. S. (2025). Thermal gradient-driven heterogeneous actuation of liquid crystal elastomers for a crawling robot. ACS Applied Materials & Interfaces, 17(6), 9992-10003.
Fonseca, D., & Neto, P. (2025). Electrically-driven phase transition actuators to power soft robot designs. Nature Communications, 16(1), 3920.

Keyword: *Liquid–Vapor Phase Transition, Silver Nanoparticles, Electrothermal Actuation*

Fabrication and Characterization of ZnBO-Based Ultrasonic Biosensors for Blood Pressure Monitoring by Destructive and Non-Destructive Methods

Gökhan Ekinci [*] [1], Fatih Mehmet Coşkun[2], Sümeyye Veziroglu[3], Surhan Bozkurt[4]

[1] *Department of Digital Transformation Electronics, Advanced Vocational School, Dogus University, İstanbul, Türkiye*
[2] *Faculty of Engineering and Natural Sciences, Department of Engineering Physics, Istanbul Medeniyet University, İstanbul, Türkiye*
[3] *Marmara University, Faculty of Science, Department of Physics, İstanbul, Türkiye*
[4] *Electrical and Electronics Engineering, Dogus University, İstanbul, Türkiye*

Throughout history, numerous destructive and non-destructive imaging methods have been developed to measure high blood pressure and comprehensively examine the structure of atherosclerotic plaques [1], [2]. Non-destructive methods of blood pressure measurement are more reliable, faster, and require less expertise than destructive methods. However, destructive methods especially intravascular ultrasound imaging provide more comprehensive information in the evaluation of the coronary artery and in the more detailed investigation of abnormalities [3]. Therefore, ultrasonic waves, with their ability to penetrate to sufficient depths for both destructive and non-destructive methods, have drawn the attention of researchers towards ultrasonic bio-sensors. Because of the ability of ultrasonic waves to penetrate tissues, biocompatible, state-of-the-art ultrasonic bio-sensors can provide continuous temporal dynamics without interrupting communication with the skin and tissue surface [4].

In this study, we present nano-sized ZnBO-based ultrasonic biosensors that can be used in destructive and non-destructive cardiovascular blood pressure measurements. The manufacturing processes of ultrasonic biosensors were carried out using Sol-Gel Dip Coating and Magnetron Sputtering methods. In the manufactured ultrasonic biosensors, the ZnBO layer in the device structure acted as a piezoelectric layer.

The structural characterization of the piezoelectric ZnBO layer in the device structure was performed in detail. For this purpose, X-ray diffraction analysis (XRD) was performed to examine the crystal structure of this layer, and cross-sectional measurements were carried out using Scanning Electron Microscopy (SEM) to determine its thickness. Furthermore, elemental analysis and chemical characterization of the ZnBO film structure were comprehensively performed using Energy Dispersive X-ray Analysis (EDX). To demonstrate that the devices function as ultrasonic biosensors, electrical acoustic measurements were performed under atmospheric conditions at room temperature.

ORCID:
Gökhan Ekinci: 0000-0003-1918-1553
Fatih Mehmet Coşkun: 0000-0001-8040-8054
Sümeyye Veziroglu: 0000-0001-9190-4897
Surhan Bozkurt: 57221178829

References:
Wu, H., Tang, Y., Kim, H., Yao, J. & Jiang, X. Fiber based laser ultrasound transducer for intravascular thrombolysis with detective photoacoustic imaging. in 2020 IEEE International Ultrasonics Symposium (IUS) 1–4 (IEEE, 2020).
Wang, C. et al. Monitoring of the central blood pressure waveform via a conformal ultrasonic device. Nat. Biomed. Eng. 2, 687–695 (2018).
Jedrzejewski, D., McFarlane, E., Lacy, P. S. & Williams, B. Pulse Wave Calibration and Implications for Blood Pressure Measurement: Systematic Review and Meta-Analysis. Hypertension 78, 360–371 (2021).
Zhou, Q., Lam, K. H., Zheng, H., Qiu, W. & Shung, K. K. Piezoelectric single crystal ultrasonic transducers for biomedical applications. Prog. Mater. Sci. 66, 87–111 (2014).

Keyword: *Ultrasonic Biosensors, Transducer, ZnBO*

High-Performance Electrochemical Sensing Platform Based on MWCNT/Ni-MOF Nanocomposites for Catechol Detection

Havva Nur Guden [*] [1,2], Saliha Mutlu[3,4], Bülend Ortaç[4], Ali Karatutlu[4,5], Dilek Soyler[1,2], Jelena Lillepäg[6], Volkan Filiz[5], Nergis Arsu[7], Sevil Savaskan Yilmaz[3,4], Saniye Soylemez[1,2]

[1] *Department of Biomedical Engineering, Necmettin Erbakan University, Konya, Türkiye*
[2] *Science Technology Research and Application Center (BITAM), Necmettin Erbakan University, Konya, Türkiye*
[3] *Faculty of Science, Department of Chemistry, Karadeniz Technical University, Trabzon, Türkiye*
[4] *Institute of Materials Science Nanotechnology and National Nanotechnology Research Center (UNAM), Bilkent University, Ankara, Türkiye*
[5] *Engineering Fundamental Sciences, Sivas University of Science and Technology, Sivas, Türkiye*
[6] *Helmholtz-Zentrum Institute of Membrane Research, Geesthacht, Germany*
[7] *Department of Chemistry, Davutpasa Campus, Yildiz Technical University, Istanbul, Türkiye*

Catechol is a hazardous organic pollutant that poses serious risks to human health and aquatic ecosystems through contaminated water and food sources. Therefore, its rapid, sensitive, and reliable detection in environmental samples is of critical importance for public health and environmental monitoring [1]. Electrochemical sensors have emerged as powerful analytical platforms for such applications due to their high sensitivity, low detection limits, rapid response, and cost-effectiveness [2]. Their performance can be further improved through the integration of advanced nanomaterials [3], where metal–organic frameworks (MOFs) provide high surface area and catalytic activity [4], while multi-walled carbon nanotubes (MWCNTs) enhance electron transfer due to their excellent electrical conductivity and large active surface area [5].

In this study, a high-performance electrochemical sensor for catechol detection was developed by modifying a screen-printed electrode (SPE) with MWCNT and CB-Ni-MOF nanocomposites. The sensor was characterized by using cyclic voltammetry (CV), differential pulse voltammetry (DPV), and electrochemical impedance spectroscopy (EIS). The fabricated sensor exhibited a wide linear range (0.5–200 µM), a low detection limit (0.231 µM), and high sensitivity (0.808 µA μM^{-1} cm^{-2}), indicating strong analytical performance. The results demonstrate that the proposed MWCNT/CB-Ni-MOF-based sensor provides a reliable and efficient platform for catechol detection and holds strong potential for environmental monitoring applications.

Acknowledgment:
S.Soylemez acknowledges the Science Academy, Türkiye for the Young Scientist Award Program (BAGEP).

ORCID:
Havva Nur Guden: 0009-0008-6752-6708
Dilek Soyler: 0000-0003-3937-5830
Saniye Soylemez: 0000-0002-8955-133X

References:
[1] Benjelloun, M.; El Messaoudi, N.; Miyah, Y.; Georgin, J.; Franco, D. S. P.; Šehović, E.; Dehmani, Y.; Knani, S. Recent Advances and Environmentally Friendly Methods for Catechol Removal from Wastewater. J. Water Process Eng. 2025, 76, 108115.
[2] Goswami, P. P.; Singh, S. G. Electrochemical Biosensors: A Prospective Insight to Recent Developments and Future Directions. Curr. Opin. Electrochem. 2025, 54, 101776.
[3] Larik, R.; Balouch, A.; Alveroğlu Durucu, E.; Silah, H.; Abdullah; Saqaf Jagirani, M.; Yaqoob soomro, M. Electrochemical Sensor for Catechol Detection: Leveraging ITO@TiO2/RGO/Pt Nanocomposites for Enhanced Water Quality Monitoring. Mater. Sci. Eng. B 2025, 313, 117966.
[4] Arivazhagan, M.; Prabu, S.; Elancheziyan, M.; Jakmunee, J. Recent Advances and Future Perspectives in Electrochemical Sensing of Biomarkers by Using MOF- Based Electrode Materials. Emerg. Mater. 2024 8:2 2024, 8 (2), 1067–1085.
[5] Tang, J.; Li, R.; Mahmood, S.; Li, J.; Yao, S. Carbon Nanotube-Based Chemical Sensors: Sensing Mechanism, Functionalization and Applications. Chemosensors 2025, Vol. 13, 2025, 13 (10).

Keyword: *Electrochemical Sensor, Catechol Sensing, Metal–Organic Frameworks (MOFs)*

Interface-Engineered Diamond-Like Carbon Coatings on ZnS for Durable LWIR Applications

Murat Alp Şahin [*] [1,2], Eylül Demir Sağıroğlu[1], Hasan Hüseyin Güllü[1], Çiğdem Toparlı[2]

[1] *ASELSAN*
[2] *Middle East Technical University*

Zinc sulfide (ZnS) is an infrared optical material that transmits across both the mid-wave (3-5 µm) and long-wave (8-12 µm) atmospheric windows. It is often regarded as an alternative to the more conventional infrared window materials such as silicon, sapphire, and germanium. In recent years, worldwide restrictions on the supply of germanium have made ZnS even more attractive, and together with its relatively low cost and good availability, it has become a popular choice for infrared optical windows, particularly in LWIR applications. However, ZnS is mechanically soft and reacts poorly to environmental factors such as moisture, abrasion, and particle impact. For windows placed on the outer surface of a system, where they face the environment directly, this is a serious limitation, so a durable protective coating is usually needed. Diamond-like carbon (DLC) is a strong candidate for this role, since it is very hard and stays optically transparent across much of the infrared. Its main drawback is that DLC adheres poorly when grown directly onto ZnS, which weakens the coating and shortens its useful life. To address this, an interface layer was introduced between the ZnS substrate and the DLC film, which both improves adhesion and helps optimize the optical performance of the coating. In this work, the DLC layer was deposited by chemical vapor deposition (CVD) and the interface layer by physical vapor deposition (PVD), with both films kept at nanometer-scale thickness. The choice of interface material, along with the thicknesses of both the interface layer and the DLC film, was treated as a design parameter, with the aim of reaching strong adhesion while obtaining the best possible optical performance in the LWIR region. The coated samples were characterized in terms of their optical behavior, including transmittance and reflectance, as well as their structural and mechanical properties, such as hardness, surface morphology, and roughness, in order to understand how the layer design shapes the overall performance. The results show that a suitable interface layer significantly improves the adhesion of DLC on ZnS while also supporting good optical transmittance, and that tuning the thicknesses of both layers makes it possible to balance optical and mechanical performance rather than trading one off for the other. Since the coating is applied to the surface that comes into direct contact with the outside environment, the study further aims to develop a coating that can pass the environmental durability tests required for its intended application area.

Keyword: *Zinc sulfide (ZnS), Diamond-like carbon (DLC), Protective coating*

Encapsulative Molecule Releasing, Quantum Dot Modified Fluorescent, pH Sensitive Multifunctional Nanofiber Mats Combined by Electrospinning Method

Merve Esra Üngör, Gökçe Asan, Osman Arslan *

İstanbul Sabahattin Zaim University, Food Engineering Department

Multifunctional nanomaterials are structures that can exhibit multiple functional properties simultaneously without interfering with each other. By employing bottom-up or top-down nanotechnological approaches, it is possible to manipulate various parameters to develop platforms where multiple functionalities such as sensing, fluorescence, antibacterial properties, photocatalysis, and smart release are integrated uniquely without compromising individual characteristics. Critical to this concept is the selection of the appropriate matrix platform, followed by the systematic incorporation of functionalities either within the matrix or on its surface. Among various matrix structures, nanofibers produced via electrospinning offer significant advantages due to their extensive surface area, as demonstrated by numerous studies. The ability to sequentially add functionalities to electrospun nanofibers makes them exceptional candidates for creating multifunctional structures with broad application potential. This innovative approach paves the way for groundbreaking solutions in various fields, such as sensors, fluorescence-based applications, antibacterial surfaces, photocatalytic processes, superhydrophobic coatings, and controlled release systems. The expansive application potential of these multifunctional nanofibers underscores their significance in advancing nanotechnology and material science, offering a wide array of practical and innovative solutions.

ORCID:
Merve Esra Üngör: 0009-0002-9720-2161
Gökçe Asan: 0009-0008-9378-6108
Osman Arslan: 0000-0002-3011-1663

References:
1-Arslan, O., Belkoura, L., & Mathur, S. (2015). Swift synthesis, functionalization and phase-transfer studies of ultrastable, visible light emitting oleate@ ZnO quantum dots. Journal of Materials Chemistry C, 3(45), 11965-11973.
2-Arslan, O., & Uyar, T. (2017). Multifunctional electrospun polymeric nanofibrous mats for catalytic reduction, photocatalysis and sensing. Nanoscale, 9(27), 9606–9614. https://doi.org/10.1039/c7nr02658g

Keyword: *multifunctional material, electrospinning, molecular release*

Lightweight Dual-Mode CNT-Aerogel Nanocomposite Stack for Anti- / De-Icing of Sub-20 kg UAVs

Uğur Zaimoğlu *

Kılıçoğlu Anatolian High School , Independent Researcher

Ice accretion on unmanned aerial vehicle (UAV) airframes and propulsion surfaces poses a critical operational hazard under low-altitude icing conditions. Even sub-millimetre leading-edge ice accumulation measurably degrades lift, increases drag, and can rapidly decrease aerodynamic stability and control authority [1]. Existing ice protection approaches developed for manned aviation (pneumatic boots, hot-air bleed systems, and conventional open-loop resistive heaters) are incompatible with the strict power budgets, limited thermal mass, and sub-25 kg weight envelopes characteristic of small UAV platforms [2]. A fundamental inefficiency shared by all conventional approaches is symmetric heat delivery: energy is distributed throughout the structure when only the upper ice-interface requires thermal input.

This work presents a six-layer nanocarbon electrothermal composite stack designed for UAV integration, built around the principle of directional heat confinement. The stack consists of, from outer surface inward:

a micro-textured fluoropolymer icephobic coating (100 µm),
a pyrolytic graphite sheet thermal spreading interlayer (20 µm),
a patterned carbon nanotube (CNT) Joule heating element (50 µm) [3],
a silica-fibre-reinforced aerogel insulation core (1250 µm) [4],
a polished aluminium infrared-reflective backing (30 µm),
and a PC-PET structural enclosure hosting an embedded PID sensor layer.

Each layer serves a distinct thermal or structural function co-designed to bias generated heat toward the ice interface rather than the substrate.

The stack's thermal performance is characterised through a three-tier analytical framework: a one-dimensional steady-state resistance network, a transient thermal model with distributed thermal mass, and a two-dimensional finite-volume simulation incorporating the pyrolytic graphite sheet (PGS) interlayer's anisotropic thermal conductivity tensor and an enthalpy-based treatment of latent heat. The directional confinement ratio, defined as the ratio of downward-to-upward thermal resistance, is $\Phi \approx 194$ under clear-surface conditions at the $-30\circ C$, 5 m/s design point, quantifying the designed thermal asymmetry between the ice-facing and substrate paths.

The system operates in two modes. In anti-icing mode, a continuous heat flux of approximately 1.76 kW/m² is estimated to maintain the surface against combined convective, radiative, substrate, and incoming-water thermal loads at the design point. In de-icing mode, a heater flux of 20–30 kW/m² produces an estimated net thermal input of approximately 18.7–28.7 kW/m² after external and substrate losses. The 2D transient ice model predicts complete melting of a 1 mm ice layer in approximately 18–28 seconds under the modeled conditions; actual ice shedding may occur earlier because complete layer melting is not required for release. An embedded PID controller using the PC-PET sensor layer is proposed for closed-loop temperature regulation and adaptive heater duty-cycle control, with the potential to reduce energy consumption relative to open-loop fixed-power operation.

The proposed architecture addresses a gap in the literature: To the authors’ knowledge, few prior systems integrate active Joule heating, directional aerogel thermal confinement, icephobic surface treatment, infrared reflection, and closed-loop embedded sensing within a single consolidated composite structure.

Acknowledgment:
The author gratefully acknowledges the open-source scientific community, including freely accessible academic literature, open-source computational tools (Python, NumPy, SciPy), and publicly available educational resources, without which this work would not have been possible.

ORCID:
Uğur Zaimoğlu: 0009-0004-4369-0125

References:
[1] R. Hann, A. Wenz, K. Gryte, and T. A. Johansen, "Impact of atmospheric icing on UAV aerodynamic performance," in Proc. 2017 Workshop on Research, Education and Development of Unmanned Aerial Systems (RED-UAS), Linköping, Sweden, Oct. 2017, pp. 66–71.
[2] N. C. Müller, B. Løw-Hansen, K. T. Borup, and R. Hann, "UAV icing: Development of an ice protection system for the propeller of a small UAV," Cold Regions Science and Technology, vol. 213, p. 103938, 2023.
[3] X. Yao, S. C. Hawkins, and B. G. Falzon, "A repairable carbon nanotube web-based electro-thermal heater and damage sensor for aerospace applications," The Aeronautical Journal, vol. 125, no. 1292, pp. 1833–1843, 2021.
[4] H. Li, W. Xu, L. Zhu, F. Xiao, Z. Yu, B. Hao, W. Huang, and K. Zhao, "Study on Thermal Insulation Performance of Silica Aerogel Thermal Insulation Blankets," Gels, vol. 10, no. 11, p. 707, 2024.

Keyword: *Nanocomposites, Aerogel, UAV ice protection*

Applicability of Fairness, Accountability, Transparency and Ethics (Fate) to Electrospun Nanofibers In Dermal Applications

Yasin Sahin *

Istanbul Technical Unıversity, Istanbul, Turkiye

Nanotechnology has been investigated branch of science for many decades. On the nanoscale which is billionth of a meter, nanotechnology is the technology handling applications to utilize atoms and molecules to build nanostructures; also known as atomically precise technology due to covering 1-100 nanometer (nm) scale. Nanometer-scale materials show unique properties in electrical, biological, optical, mechanical, thermal and so on. Nanofibers are the fibers in nanometer scale consisting of polymers affecting a wide range of parameters. Electrospinning is a nanofiber fabrication technique that collects as polymer fibers on the collector of polymer solution under the high voltage condition. This technique has some parameters that affect the nanofibers such as concentration, conductivity, molecular weight, and so forth. In the process, these parameters are taken into account and they make it a little bit complex.

Electrospun nanofibers are used in dermal applications. Nanofibrous scaffolds give the conditions of extracellular matrix for usage in tissue regeneration. Cell proliferation and differentiation are triggered thanks to nanofibers' high surface area and porosity on tissue. This high surface-to-volume ratio on electrospun nanofibers allows a nano-drug delivery system from the nanofibers to desired area as controlled and targeted. Electrospun nanofibers show antimicrobial, antibacterial or antiviral as well as biocompatible and bioactive properties for wound healing. For cancer treatment and diagnosis, nanofibers are beneficial in photothermal therapy. Electrospun nanofibers mats fabricated with some ingredients like collagen are effective wrinkles problems on the skin. Nanofiber cleansers and facemasks with medicinal properties are used in dermal defects. Nanoparticles doped nanofibers with silver prevent bacterial and fungal infections.

New materials and processes at the nanoscale are developed due to new theoretical and experimental techniques. With this growth some ethical issues come along. These ethical issues are tackled with ethical frameworks to govern the uncertainties and concerns. Fairness, Accountability, Transparency, and Ethics (FATE) is started to express mainly for artificial intelligence and digital systems as known. On the other hand, from the material selection to clinical usage, in all the technological lifecycle FATE integrates ethical framework. Fairness ensures mitigation bias and prevention prejudice with equal accession to opportunities and representation for different skin problems and conditions. Accountability clarifies the decision-making responsibility on qualification, verification and validation on fabrication process, long-term performance and safety and prolonged influence on the skin. Transparency fosters being open and transparent to shareholders in the process of design, test and usage as well as communication. Ethics emphasizes moral agency and societal responsibility than technique.

FATE has well-oriented potential to govern ethical issues on the responsible fabrication and clinical test for electrospun nanofibers in dermal applications. Novel technologies like nanotechnology require more research and ethical lens in long term applications.

Acknowledgment:
This article is generated for a necessity of LEE 907E – Ethics of Technology at Istanbul Technical University. The author thanks to Prof. Gurcan Kocan, Dr. Gorkem Giray and class debaters.

ORCID:
Yasin Sahin: https://orcid.org/0009-0009-0157-6849

References:
Memarian, B. & Doleck, T. (2023). Fairness, Accountability, Transparency, and Ethics (FATE) in Artificial Intelligence (AI) and Higher Education: A Systematic Review. Computers and Education: Artificial Intelligence, 5, 100152. doi: 10.1016/j.caeai.2023.100152.
Singhal A., Neveditsin N., Tanveer H., & Mago, V. (2024). Toward Fairness, Accountability, Transparency, and Ethics in AI for Social Media and Health Care: Scoping Review. JMIR Medical Informatics, 12, e50048. doi: 10.2196/50048.
Sahin, Y. (2025). Fabrication of TiO2 Nanoparticle Sprayed PAN/PA6 Layer-by-layer Superimposed Composite Nanofiber Membrane for Dye Removal. MSc Thesis, Istanbul Technical University.
Nasrollahzadeh, M., Sajadi, S. M., Sajadi, M. & Issaabadi, Z. (2019). Chapter 1 - An Introduction to Nanotechnology. Interface Science and Technology, 28, 1-27. doi: 10.1016/B978-0-12-813586-0.00001-8.
Nadaf, A., Gupta, A., Hasan, N., Fauziya, Ahmad, S., Kesharwani, P. & Ahmad, F. J. (2022). Recent Update on Electrospinning and Electrospun Nanofibers: Current Trends and Their Applications. RSC Advances, 12, 23808-23828. doi: 10.1039/d2ra02864f.

Keyword: *Nanoethics, Nanofiber, FATE*

Cell Phone-Based Microscopy for Life Science Applications

Bilge Can [*1], Miktat Efe Eyibilen[2], Arif Engin Çetin[3], Zeynep Güneş Özunal[4]

[1] Department of Biomedical Engineering, Atlas University, Istanbul, Türkiye
[2] Department of Bioengineering, Izmir Institute of Technology, Izmir, Türkiye
[3] Department of Biophysics, Faculty of Medicine, Dokuz Eylul University, Izmir, Türkiye
[4] Department of Medical Pharmacology, Faculty of Medicine, Atlas University, Istanbul, Türkiye

Portable bright-field microscopy is increasingly attracting interest for point-of-care diagnostics, educational applications, routine cell culture monitoring, and in vitro drug screening and drug development studies. Although smartphone-based microscopy platforms have significantly reduced the cost and complexity of microscopic imaging, most existing systems primarily provide qualitative visualization without a standardized method for dimensional analysis. The absence of accurate image calibration limits their use in quantitative biological studies.

In this work, we present a compact, lightweight, portable, and low-cost smartphone-based bright-field microscopy platform capable of automatic scale calibration for quantitative microscopic imaging. The platform consists of a smartphone camera, an LED illumination unit, a miniature optical module, and a custom-designed 3D-printed housing that provides stable optical alignment and repeatable image acquisition. Designed for room-temperature operation, the system requires no bulky laboratory equipment, making it suitable for both laboratory and field applications. A calibration procedure based on a stage micrometer was implemented to determine the pixel-to-micrometer conversion factor of the imaging system. Using this calibration, an accurate scale bar is automatically generated for every acquired image without requiring user intervention.

The developed platform enables direct dimensional measurements from bright-field images and supports quantitative evaluation of cellular morphology and microscopic structures. Compared with conventional laboratory microscopes, the proposed system offers substantially lower cost, portability, lightweight construction, and ease of use while maintaining sufficient imaging quality for routine biological observations. The automatic scale calibration improves measurement reliability and reproducibility by eliminating manual estimation of image dimensions.

The proposed approach demonstrates that smartphone-based microscopy can be extended beyond qualitative visualization toward standardized quantitative imaging. Owing to its compact design, room-temperature operation, portability, and low manufacturing cost, the platform has the potential to support cell culture monitoring, in vitro drug testing, drug development studies, laboratory education, and biomedical research, particularly in resource-limited environments. Future work will focus on integrating automated image-processing algorithms, including cell counting, confluency estimation, and morphological analysis, to establish a complete portable quantitative microscopy platform.

References:

Breslauer D.N., Maamari R.N., Switz N.A., Lam W.A., Fletcher D.A. "Mobile phone based clinical microscopy for global health applications." PLoS ONE, 2009.
Ozcan A., McLeod E. "Lensless imaging and sensing." Annual Review of Biomedical Engineering, 2016.
Avci M.B., Kurul F., Turkan M., Cetin A.E. "Automated smartphone based cell analysis platform." npj Imaging, 2025.

Keyword: *Smartphone microscopy, Bright-field microscopy, Life science*

Light–Matter Interactions of Fluorescent Molecular Rotors Inside Resonant Microcavities

Eren Toker * **, Wonmi Ahn**

UNAM - National Nanotechnology Research Center, Bilkent University, Ankara, Türkiye

Fluorescent molecular rotors are important molecular systems for investigating the relationship between molecular motion and intramolecular charge transfer. Their emission behavior is sensitive to changes in molecular rotation and optical confinement, making them suitable candidates for studying cavity-controlled light–matter interactions. In this study, 4-(Dicyanomethylene)-2-methyl-6-(4-dimethylaminostyryl)-4H-pyran (DCM) fluorescent molecular rotor is used as a model platform to explore its optical response modified by Fabry–Pérot microcavities. The work focuses on Fabry–Pérot microcavities formed by silver mirrors and dielectric spacer layers containing DCM molecules embedded in a poly(methyl methacrylate) (PMMA) matrix. Different cavity configurations are designed to tune the optical environment experienced by the fluorescent molecular rotors. This provides a platform to study how cavity modes affect the optical response of DCM molecules. The cavity systems are characterized using fluorescence spectroscopy, fluorescence lifetime measurements, Fourier-transform infrared spectroscopy (FTIR), ellipsometry, and transfer-matrix method (TMM) simulations. Fluorescence spectroscopy is used to examine the emission behavior of DCM molecular rotors inside and outside the cavity, while lifetime measurements provide information about cavity-dependent excited-state relaxation. FTIR spectroscopy and infrared dispersion mapping are used to study the vibrational-region optical response of the Fabry–Pérot cavities. Ellipsometry is included as an additional optical characterization method for investigating the optical properties of the thin-film and cavity structures. Together, these experimental measurements are compared with TMM simulations to understand the optical response of the DCM fluorescent molecular rotors inside resonant microcavities.

Keyword: *light–matter interaction, Fabry-Pérot cavities, fluorescent molecular rotors*

Plasmon-Coupled Gold-BODIPY Nanocomposites as High-Efficiency Agents for Combined Photodynamic and Photothermal Therapy

Gülden Yıldız Şengüler [*1], Elif Yıldız[2], Fazlı Sözmen[3], Umay Koparan[4], Açelya Yılmazer Aktuna[4], Ayhan Elmalı[2], Sevim Naseri[3], Ahmet Karatay[2]

[1] Department of Physics Engineering, Graduate School of Natural and Applied Sciences, Ankara University, Ankara, Türkiye.
[2] Department of Physics Engineering, Ankara University, Ankara, Türkiye.
[3] Department of Nanotechnology Engineering, Sivas Cumhuriyet University, Sivas, Türkiye.
[4] Department of Biomedical Engineering, Ankara University, Ankara, Türkiye.

Combining the unique photophysical properties of metal nanoparticles and organic dyes in a synergistic architecture, nanocomposites provide potent, dual-functional theranostic platforms for simultaneous bioimaging and therapy (photodynamic/photothermal). Among organic dyes, boron-dipyrromethene (BODIPY) derivatives are prominent owing to their exceptional optical attributes, including high absorption coefficients (>70.000 $M^{-1}cm^{-1}$) high fluorescence quantum efficiencies, and strong photostability. Additionally, introducing various side groups to the BODIPY core induces triplet excited states, making these molecules outstanding photosensitizers for photodynamic therapy (1). Clarifying how plasmon-molecule coupling between the organic dye and gold nanoparticles (AuNPs) affects electron and/or energy transfer dynamics in these hybrid nanostructures is critical to optimizing their therapeutic efficiency.

This study investigates the linear absorption and emission properties of BODIPY dyes and their gold nanoparticle nanocomposites (NC1–NC4) based on plasmon-molecule coupling. Femtosecond pump-probe (transient absorption) spectroscopy was utilized to track real-time energy and electron transfer mechanisms. Excitation of the NC2 (AuNP-BOD1-BOD2) nanostructure at 500 nm induced a strong saturation signal at 560 nm, revealing rapid electron transfer from BOD-1 to BOD-2. Furthermore, a positive signal initially located around 700 nm exhibited a distinct blueshift over time. This time-resolved shift characterizes the T_1–T_n triplet-triplet absorption resulting from the $S_1 \rightarrow T_1$ intersystem crossing. These findings elucidate the kinetics of plasmon-enhanced energy transfer in hybrid nanostructures, highlighting their strong potential as multifunctional agents in advanced bioimaging and photodynamic therapy (PDT).

The in vitro photothermal (PTT) and photodynamic (PDT) therapy efficacies of the nanocomposite structures were evaluated via an LDH (lactate dehydrogenase) cytotoxicity assay on the 4T1 mouse breast cancer cell line. The cells were treated under three experimental conditions: 520 nm illumination ($NC2_{520nm}$), 850 nm illumination ($NC2_{850nm}$), and a dark control. The results revealed significant cytotoxicity at an extremely low concentration of 0.01 µg/mL, particularly for the NC2 and NC4 nanocomposites under 520 nm light exposure. These findings highlight the potential of these materials to deliver high therapeutic efficacy at minimal doses.

Acknowledgment:
This study is supported by the Scientific and Technological Research Council of Türkiye (TÜBİTAK) under project number 124F168, and by TÜBİTAK-BİDEB under the 2211-A National PhD Scholarship Program.

References:
(1) Rahman, Atikur, et al. "Gold–BODIPY Nanoparticles with Luminescence and Photosensitization Properties for Photodynamic Therapy and Cell Imaging." ACS Applied Nano Materials 5.5 (2022): 6532-6542.

Keyword: *Nonlinear optics, Au-NP, Nanocomposites, Pump-probe, PDT, PTT.*

Electric Field Engineering via Floating Guard Ring Optimization for Edge Breakdown Suppression in PLANAR INGAAS/INP SAGCM APDS

Habibe Keleş [*1], Mert Satılmış[2], Çağrı Tok[3], Aydan Yeltik[4], Fikri Oğuz[2], Ekmel Özbay[5]

[1] *Micro and Nanotechnology Department, TOBB University of Economics and Technology, Ankara, Turkey, Nanotechnology Research Center (NANOTAM), Bilkent University, Ankara, Turkey*

[2] *Nanotechnology Research Center (NANOTAM), Bilkent University, Ankara, Turkey*

[3] *Nanotechnology Research Center (NANOTAM), Bilkent University, Ankara, Turkey, Department of Physics Engineering, Ankara University,Ankara, Turkey*

[4] *Micro and Nanotechnology Department, TOBB University of Economics and Technology, Ankara, Turkey, Material Science and Nanotechnology Engineering, TOBB University of Economics and Technology, Ankara, Turkey*

[5] *Nanotechnology Research Center (NANOTAM), Ankara, Turkey, Department of Physics, Bilkent University, Ankara, Turkey, Department of Electrical and Electronics Engineering, Bilkent University, Ankara, Turkey*

InGaAs/InP separated absorption, graded, charge, and multiplication (SAGCM) avalanche photodiodes (APDs) are widely utilized in optical communication, LiDAR, and low-light detection applications due to their high internal gain characteristics. However, in planar APD structures, electric field crowding at the junction periphery leads to premature edge breakdown, which significantly limits device performance. In this study, the effect of floating guard ring (FGR) structures on electric field redistribution and edge breakdown suppression was experimentally investigated.

The InGaAs/InP SAGCM APD structures were grown by Metal-Organic Chemical Vapor Deposition (MOCVD) and fabricated using planar diffusion processes. To optimize the electric field distribution, different FGR spacings (FS), FGR thicknesses (FT), and attached floating guard ring (AFGR) numbers were systematically varied. In addition, the influence of attached guard ring (AGR) structures on FGR performance was also evaluated.

Experimental results demonstrated that FGR structures effectively reduced electric field crowding at the active region edge and significantly improved breakdown characteristics. Particularly, optimized FS and FT values enabled a more controlled electric field distribution toward the peripheral regions. On the other hand, excessively large FGR structures introduced additional high-field regions, negatively affecting device performance. The optimum configuration was achieved with a 2 µm AGR, 8 µm FS, 5 µm FT, and 2 AFGR structures, resulting in an increase in breakdown voltage from 43.9 V to 57.6 V.

The obtained results indicate that FGR geometry plays a critical role in suppressing premature edge breakdown and improving the reliability of planar InGaAs/InP SAGCM APD structures.

ORCID:
Habibe Keleş: https://orcid.org/0009-0002-6691-3972
Mert Satılmış: https://orcid.org/0000-0001-7913-2708
Çağrı Tok: https://orcid.org/0000-0002-6864-8298
Aydan Yeltik: https://orcid.org/0000-0001-6976-4680
Fikri Oğuz: https://orcid.org/0000-0002-5443-3472
Ekmel Özbay: orcid logo https://orcid.org/0000-0003-2953-1828

References:
Y. Liang et al., "Low-Timing-Jitter GHz-Gated InGaAs/InP Single-Photon Avalanche Photodiode for LIDAR," in IEEE Journal of Selected Topics in Quantum Electronics, vol. 28, no. 2: Optical Detectors, pp. 1-7, March-April 2022, Art no. 3801807, doi: 10.1109/JSTQE.2021.3109584.
Chen, Y.-C.; Yan, R.-H.; Huang, H.-C.; Nieh, L.-H.; Lin, H.-H. Guard Ring Design to Prevent Edge Breakdown in Double-Diffused Planar InGaAs/InP Avalanche Photodiodes. Materials 2023, 16, 1667. https://doi.org/10.3390/ma16041667
S. R. Cho et al., "Suppression of avalanche multiplication at the periphery of diffused junction by floating guard rings in a planar InGaAs-InP avalanche photodiode," in IEEE Photonics Technology Letters, vol. 12, no. 5, pp. 534-536, May 2000, doi: 10.1109/68.841277
Y. Liu, S. R. Forrest, J. Hladky, M. J. Lange, G. H. Olsen and D. E. Ackley, "A planar InP/InGaAs avalanche photodiode with floating guard ring and double diffused junction," in Journal of Lightwave Technology, vol. 10, no. 2, pp. 182-193, Feb. 1992, doi: 10.1109/50.120573

Keyword: *InGaAs/InP APD, SAGCM, Edge Breakdown Floasting Guard Ring (FGR), Attached Guard Ring (AGR), Planar Diffusion*

Fano Resonances in Metal−Organic Framework ZIF-8

Naz Ülkem [*1], Sümeyye Meryem Çöpür[2], Ozan Baran Orhan[2], Tuğçe Küçüktartar[3], Sinan Balcı[2], Fadime Mert Balcı[3]

[1] *Department of Physics, Izmir Institute of Technology*
[2] *Department of Photonics, Izmir Institute of Technology*
[3] *Department of Chemistry, Izmir Institute of Technology*

Metal–organic frameworks have recently emerged as promising dielectric platforms for investigating light–matter interactions due to their tunable optical properties and highly porous architectures. In this work, we demonstrate the observation of Fano resonances in microporous ZIF-8 thin films uniformly coated with J-aggregate dyes. The emergence of asymmetric Fano line shape arises from the interference between the narrow excitonic resonance of the J-aggregates and the broad continuum of scattering modes provided by the highly scattering dielectric ZIF-8 framework. Consequently, the hybrid structures exhibit a distinct spectral-shift and a strong asymmetric profile compared to the Lorentzian line shape of bare J-aggregates. We experimentally and computationally show that the morphology and density of the ZIF-8 films strongly modulate the underlying scattering landscape, directly influencing the Fano asymmetry parameter q and the overall coupling strength.
Specifically, as the ZIF-8 particles approach one another, they begin to exhibit strong near-field coupling, shifting their behavior away from that of isolated particles to an interconnected cluster that acts as a unified system. This transition gives rise to collective modes, resulting in broadband scattering and distinctive transmission behavior. Finite-difference time-domain (FDTD) simulations reinforce these findings and reveals a clear spectral evolution from a Lorentzian-like to a Fano line profile as increasing the dielectric particle size systematically strengthens the continuum background. Furthermore, the microporous structure of ZIF-8 promotes electromagnetic field localization within the crystals, enhancing exciton–photon interactions while remaining within the weak coupling regime.
These hybrid systems are anticipated to exhibit enhanced sensitivity when disturbed by external perturbations, thereby offering unique opportunities for biosensing applications. Ultimately, these findings highlight the potential of J-aggregate-coated ZIF-8 films as versatile dielectric nanophotonic platforms and provide new avenues for engineering light–matter interactions for future photonic and sensing applications.

Acknowledgment:
This study was supported by Scientific and Technological Research Council of Turkey (TUBITAK) under the Grant Number 123F014. The authors also thank the Izmir Institute of Technology Center for Material Research for SEM and XRD analyses.

References:
Limonov, M. F.; Rybin, M. V.; Poddubny, A. N.; Kivshar, Y. S. Fano Resonances in Photonics. Nat. Photonics 2017, 11 (9), 543− 554.
Lu, Y.; Li, M.; Feng, Y.; Xu, Y.; Zhou, Y.; Xu, J.; Wang, J. Tuning the Optical Properties of Transparent ZIF-8 Thin Films by Adjusting the Crystal Morphology. Opt. Mater. 2024, 154, 115714.
Conteduca, D.; Khan, S. N.; Martínez Ruiz, M. A.; Bruce, G. D.; Krauss, T. F.; Dholakia, K. Fano Resonance-Assisted All-Dielectric Array for Enhanced Near-Field Optical Trapping of Nanoparticles. ACS Photonics 2023, 10 (12), 4322−4328.
Fano, U. Effects of Configuration Interaction on Intensities and Phase Shifts. Phys. Rev. 1961, 124 (6), 1866−1878.
Demir, S.; Kucuktartar, T.; Orhan, O. B.; Tan, M.; Balci, S.; Balci, F. M. Fano Resonances in Metal–Organic Framework ZIF-8 Derived from Liquid-Crystal-Templated Nanoporous ZnO Films. Chemistry of Materials 2026, 38 (8), 4066–4075. https://doi.org/10.1021/acs.chemmater.5c03276.

Keyword: *Metal–organic framework ZIF-8, Asymmetric Fano line shape, Collective modes*

Investigations of laser-material interactions using Finite Element Method for the creation of laser-inscribed units of photonic integrated circuits.

Okan Uslu [*1], **Mahmut Çağlayan**[1], **Timuçin Emre Tabaru**[1], **Ali Karatutlu**[1,2]

[1] *Sivas University of Science and Technology*

[2] *Institute of Materials Science and Nanotechnology, National Nanotechnology Research Center (UNAM), Bilkent University, Ankara, 06800, Turkey*

Fabrication of photonic integrated circuits (PICs) requires not only complex procedures such as growth, lithography, and etching but also a large number of different components, reaching more than 100 components in one packaged item [1]. On the other hand, silicon (Si) photonics can still offer low-cost and densely integrated components for optical communications and quantum information [2]. In this study, we report laser & material interaction conducted using the Finite Element Method in Comsol MultiPhysics software. The studies demonstrate that one can form simple and complex units of photonic integrated circuits by continuous and pulsed lasers. In continuous lasers, we are limited to laser power, scanning rate, and beam diameter, whereas in pulsed lasers, different laser parameters such as pulsed duration, pulse shape, repetition rate, and peak power can be included in the simulation. We will show that how Si surface could be modified to form couplers, waveguides, and Y-splitters, which are crucial components of PICs.

Acknowledgment:
We would like to thank the infrastructural support provided by the Photonics Innovation and Technology Research Center (FITAM) at Sivas University of Science and Technology.

ORCID:
Ali Karatutlu: 0000-0002-8819-4916

References:
Murphy, E. J. . Integrated Optical Circuits and Components : Design and Applications. (CRC Press, 2020).
Ma, C. et al. Silicon photonic transmitter for polarization-encoded quantum key distribution. Optica 3, 1274 (2016).

Keyword: *Laser writing, waveguide, photonic integrated circuits*

Ultrafast Lattice Dynamics of Layered Material Surfaces

Alp Akbıyık * **, Felix Kurtz, Hannes Böckmann, Claus Ropers**

Max Planck Institute for Multidisciplinary Sciences - Göttingen - Am Faßberg 11 D-37077 Germany

Relaxation of photoexcited carriers into the lattice is a fundamental process that governs how excited quantum materials return to equilibrium. In this work, we study this process in Td-WTe_2 using ultrafast low-energy electron diffraction (ULEED) and momentum-resolved diffuse scattering, techniques that allow us to track how vibrational energy evolves at the material surface. After optical excitation, the lattice response proceeds in two distinct stages, while the diffuse scattering reveals an initial anisotropic population of phonons followed by a redistribution of energy into low-energy acoustic modes. These results show that energy is first coupled into particular phonon modes before spreading throughout the lattice. More generally, this work demonstrates the potential of ULEED and diffuse scattering to probe ultrafast surface dynamics in nanoscale and quantum materials, offering new insights into energy flow and nonequilibrium processes at surfaces.

Acknowledgment:
This work is funded by the European Research Council (ERC Advanced Grant “ULEEM,” ID: 101055435).

Keyword: *Ultrafast dynamics, Layered materials, Phonons*

Ion-Implanted Silicon PIN Photodiodes: Design and Electrical Characterization

Emre Doganci [*1], Ozan Yilmaz[2]

[1] *Department of Radiotheraphy, Vocational School of Health Services, Fenerbahçe University, Istanbul, Turkey*
[2] *Faculty of Arts and Science, Bolu Abant Izzet Baysal University, Bolu, Turkey*

A silicon PIN photodiode with an active area of 5 × 5 mm² was designed and analyzed in this study. The device structure was developed using Silvaco Athena for process simulation, while Silvaco Atlas was employed for device-level electrical simulation. Ion implantation was utilized to precisely form the p and n regions with controlled doping profiles. The process simulation ensured proper junction formation and optimized carrier transport properties. The electrical and optoelectronic characteristics of the device were systematically evaluated. Current–voltage (I–V) analysis demonstrated a low dark current of approximately 3 nA at a reverse bias of 60 V, indicating good junction quality and minimal leakage current. Capacitance–voltage (C–V) analysis revealed a capacitance value of approximately 20 pF, suggesting a well-defined depletion region and stable junction behavior. Additionally, the spectral response of the photodiode was analyzed to evaluate its wavelength-dependent sensitivity, confirming its suitability for photodetection applications. The results demonstrate that precise ion implantation enables effective control over doping profiles, leading to low leakage current and stable device performance. These findings highlight the potential of the proposed silicon PIN photodiode for radiation detection and optical sensing applications.

Keyword: *Silicon PIN Photodiode, Radiation Detection, Dark Current*

Piezoelectric Phononic Crystal Enabled Acoustofluidics for Low-Voltage Microparticle Patterning

Nurseli Seda Genç [*1], Ahmet Cicek[2], Ayşe Erol[1], Furkan Kuruoğlu[1]

[1] *Department of Physics, Faculty of Science, Istanbul University, Vezneciler, 34134 Istanbul, Turkey*
[2] *Department of Physics, Faculty of Arts and Sciences, Mehmet Akif Ersoy University,15100 Burdur, Turkey*

Surface acoustic wave (SAW)-based acoustofluidic platforms enable contactless and label-free microparticle manipulation; however, conventional standing SAW systems commonly require opposed transducers and relatively high excitation voltages [1]. Here, we demonstrate a low-voltage acoustofluidic platform employing a passive piezoelectric phononic crystal (PPnC), monolithically patterned on a YX-128° lithium niobate substrate, as an acoustic reflector. The PPnC reflects waves generated by a single chirped interdigital transducer, forming a standing surface acoustic wave field within an adjacent microfluidic channel without requiring a second active transducer. Finite-element simulations confirm phononic-bandgap-mediated wave confinement and the formation of periodic pressure nodes, while experimental transmission measurements reveal a pronounced response near 85 MHz. Simulations of the acoustic pressure, Gor'kov potential, and radiation force demonstrate stable trapping positions at the pressure nodes. Under excitation at 85 MHz, 4.5 µm polystyrene microparticles migrate toward these nodes and form well-defined periodic patterns with efficiencies exceeding 80% at an applied voltage of only 0.6 V_{pp}. Compared with an internally benchmarked dual-transducer configuration, the PPnC-assisted platform enables microparticle patterning at an approximately twenty-fold lower excitation voltage. These findings establish monolithic phononic band engineering as an effective strategy for compact, low-voltage, and controllable acoustofluidic manipulation.

Acknowledgment:
This work is funded by The Scientific and Technological Research Council of Turkey (TUBITAK) (Project Number: 120F337) and the Scientific Research Projects Coordination Unit of İstanbul University (Project Number: FYL-2024-41154). AC acknowledges support from Turkish Academy of Sciences (TÜBA) within the framework of The Outstanding Young Scientist Award Program (GEBİP-2018).

ORCID:
Nurseli Seda Genç: 0009-0001-5301-177X
Ahmet Cicek: 0000-0002-7686-0045
Ayşe Erol: 0000-0003-4196-1791
Furkan Kuruoğlu: 0000-0002-5314-4441

References:
Y. Ai, C. K. Sanders, and B. L. Marrone, "Separation of Escherichia coli Bacteria from Peripheral Blood Mononuclear Cells Using Standing Surface Acoustic Waves," Analytical Chemistry, vol. 85, no. 19, pp. 9126–9134, 2013, doi: 10.1021/ac4017715.

Keyword: *acoustofluidics, phononic crystals, particle patterning*

Magnetic Susceptibility and ESR Characterization of a Cu(II) Paddle-Wheel Complex with 6 Amonihexonic Acid

Onur Ercem [*1], **Simon Pasqualon**[2], **Jana Chrappová**[2], **Erik Rakovský**[2], **Dmytro Kamenskyi**[1], **Mamoun Hemmida**[1], **Hans-Albrecht Krug von Nidda**[1], **Svitlana Vitushkina**[2]

[1] *University of Augsburg*
[2] *Comenius University Bratislava*

The dinuclear Cu(II) paddle-wheel complex $Cu_2(6\text{-}AHA)_4Cl_2](NO_3)_2.2H_2O$ (6-AHA = 6-aminohexanoic acid) was synthesized by isothermal evaporation from an aqueous-ethanolic solution of $CuCl_2 \cdot 2H_2O$, 6-aminohexanoic acid, and HNO_3 at molar ratio 1:4:2. The compound was characterized by X-ray single-crystal structure analysis and infrared spectroscopy. The crystal structure reveals a centrosymmetric dinuclear complex cation in which two Cu(II) centers are bridged by four bidentate carboxylate groups of 6-AHA ligands in zwitterionic form, with chloride ligands occupying the axial positions and a Cu···Cu distance of 2.6625 Å.

Electron spin resonance (ESR) spectroscopy was employed to probe the magnetic properties of the complex. At elevated temperature ESR spectroscopy reveals a characteristic excited triplet state (S=1) configuration of the dinuclear Cu(II) centers, evidenced by pronounced crystal-field splitting and a well-resolved hyperfine splitting pattern. At low temperature the ESR signal vanishes due to the singlet (S=0) ground state. g-tensor anisotropy and the antiferromagnetic exchange coupling constant J have been determined.

These results contribute to the understanding of magnetostructural correlations in Cu(II) paddle-wheel complexes, where axial ligand identity and Cu···Cu distance are known to modulate spin-spin interactions. The present complex represents a promising model system for further investigation of magnetic behavior in amino acid-based coordination compounds.

ORCID:
Onur Ercem: https://orcid.org/0009-0005-7169-4657

References:
Groom C. R., Bruno I. J., Lightfoot M. P. et al., (2016) Acta Cryst. B72, p. 171
Petra L. (2013) Preparation and characterization of new organoils containing amino acids. (Master's thesis) Comenius University in Bratislava

Keyword: *paddle-wheel complexes Cu(II), Electron Spin Resonance, Magnetic Susceptibility*

Different Wavelength LED Array Integrated Wireless System for Enhanced Photobiomodulation-Assisted PVA Hydrogel-Based Skin Wound Healing

Yusuf Aksu [*1], **Seda Demirel Topel**[2]

[1] *Department of Electrical and Electronics Engineering, Faculty of Engineering and Natural Sciences, Antalya Bilim University, 07190 Doşemealti, Antalya, Türkiye*
[2] *Antalya Bilim University*

Chronic and acute wound management remains a critical challenge in regenerative medicine, necessitating advanced therapeutic strategies that synergize biomaterial design with physical stimulation modalities [1] . In this study, we present an integrated optoelectronic-biomaterial platform comprising a wirelessly controlled, multi-wavelength LED array system coupled with carbon dot (CD)-loaded polyvinyl alcohol (PVA) hydrogel wound dressings to enhance photobiomodulation (PBM)-assisted skin wound healing. The PVA hydrogels were fabricated via the freeze-thaw method and thoroughly characterized using scanning electron microscopy (SEM), Fourier-transform infrared (FTIR) spectroscopy, and thermogravimetric analysis (TGA) to confirm structural integrity, chemical composition, and thermal stability. CDs were successfully incorporated into the hydrogel matrix, serving as photoactive agents capable of generating singlet oxygen ($^1O_2$) upon light irradiation. The $^1O_2$ quantum yields (Φ_Δ) of the CD-loaded PVA hydrogels were determined using 1,3-diphenylisobenzofuran (DPBF) as a trap molecule, monitored by UV-Vis spectroscopy, confirming the photosensitizing capacity of the composite system. The LED array system delivers wavelength-tunable irradiation precisely matched to the optical absorption characteristics of distinct hydrogel formulations, thereby maximizing the therapeutic light-CD interaction and enhancing localized $^1O_2$ generation at the wound site. Wireless communication via integrated Wi-Fi and Bluetooth modules enables real-time, remote adjustment of irradiation wavelength, intensity, and exposure duration, allowing fully personalized and adaptable treatment protocols tailored to specific wound conditions and hydrogel compositions. The core innovation of this work lies in the intelligent coupling of on-demand $^1O_2$ release from PVA hydrogel scaffolds with targeted, wirelessly controlled LED irradiation- creating a closed-loop smart wound care system that bridges photochemistry, biomaterials engineering, and wireless bioelectronics. This platform offers a clinically translatable, next-generation approach to wound management, with the potential to simultaneously address microbial contamination through photodynamic antibacterial action and accelerate tissue regeneration through PBM.

References:

Cai W., Hamushan M., Zhang Y., Xu Z., Ren Z., Du J., Ju J., Cheng P., Tan M., Han P. "Synergistic Effects of Photobiomodulation Therapy with Combined Wavelength on Diabetic Wound Healing In Vitro and In Vivo" Photobiomodulation, Photomedicine, and Laser Surgery, 2022, 40(1), 13–24

Keyword: *photobiomodulation, LED, hydrogel, wound dressing, singlet oxygen, wireless wound care*

Controlled Synthesis and Characterization of Silver Nanoplatelets for Biosensor Applications

Emine Eflin Koç [*] [1], Ülkü Anık[2]

[1] *Faculty of Science, Chemistry Department, Mugla Sitki Kocman University, 48000 Kotekli, Mugla, Türkiye*

[2] *Research Laboratory Center, Mugla Sitki Kocman University, Sensors, Biosensors and Nano-Diagnostic Systems Laboratory, Kotekli-Mugla, Türkiye*

Silver nanoplatelets have attracted significant attention in biosensor design due to their unique physicochemical properties. Their large surface-to-volume ratio and distinctive surface chemistry provide a high density of active binding sites, enabling strong and stable interactions with biomolecules (Zeng et al., 2014). This high bioaffinity allows efficient immobilization of biological agents such as antibodies and enzymes while preserving their functional activity. These characteristics make silver nanoplatelets promising nanomaterials for the development of sensitive and reliable biosensing platforms (Li & Xia, 2022).

In this study, silver nanoplatelets were successfully synthesized by controlling key experimental parameters, resulting in the formation of silver solutions exhibiting distinct color variations. The ability to tune these optical properties reflects the controlled formation of nanoplatelet structures.

The synthesized nanostructures were characterized using scanning electron microscopy (SEM), X-ray diffraction (XRD), and Fourier-transform infrared spectroscopy (FTIR), confirming their morphology, crystalline structure, and surface functional groups . (Wiley et al., 2005).

To evaluate their applicability in biosensing, a biosensor system that is based on FGF-2 Fibroblast Growth Factor-2 (FGF-2)/Heparan sulfate (HS) interaction was developed based on these silver nanoplatelets. The interaction between the nanoplatelets and the target analyte was monitored through UV–Vis absorption spectroscopy by tracking changes in optical properties (Li & Xia, 2022).

The results demonstrate that silver nanoplatelets, owing to their high bioaffinity and abundance of active binding sites, can serve as effective and sensitive signal transducers in optical biosensor platforms. These findings highlight their strong potential for future biosensor applications.

References:

Li, H., & Xia, J. (2022). Silver nanoplate-based colorimetric and plasmonic biosensors for clinical and environmental analysis. Biosensors and Bioelectronics, 202, 113980.

• Wiley, B., Sun, Y., Mayers, B., & Xia, Y. (2005). Shape-controlled synthesis of metal nanocrystals: The case of silver. Chemistry–A European Journal, 11(2), 454-463.

Zeng, S., Baalayan, S., Yong, K. T., & Ho, H. P. (2014). A review on functionalized gold and silver nanoplates for biosensing applications. Analyst, 139(23), 6061-6075.).

Keyword: *nano materials, silver nano plates, biosensing*

Magnetically Actuated Triboelectric Fiber for Self-Powered Sensing Applications

Sk. Rahat Ali * **, Mustafa Ordu**

UNAM – National Nanotechnology Research Center and Institute of Materials Science and Nanotechnology, Bilkent University, Ankara 06800, Türkiye

Self-powered wearable sensors capable of converting external stimuli into electrical signals are attracting significant attention for next-generation human-machine interfaces, healthcare monitoring, and energy harvesting applications. In this study, we present a multifunctional magnetic triboelectric fiber fabricated through a thermal drawing process by integrating neodymium-iron-boron (NdFeB) magnetic particles into a highly stretchable styrene-ethylene-butylene-styrene (SEBS) matrix and employing polyvinylidene fluoride (PVDF) as the triboelectric layer. The resulting fiber combines magnetic responsiveness with triboelectric energy conversion within a single fiber architecture. Upon exposure to an external magnetic field, the embedded magnetic particles induce mechanical deformation of the fiber, generating periodic contact and separation within the triboelectric structure. This magnetically driven motion enables direct conversion of magnetic stimuli into electrical signals without requiring an external power source. Electrical characterization demonstrated an output voltage of approximately 500 mV under magnetic actuation. The fiber also exhibits excellent flexibility and mechanical compliance, making it suitable for wearable and soft electronic applications. The combination of magnetic actuation and triboelectric sensing in a thermally drawn fiber platform offers a promising approach for remote, wireless, and self-powered sensing systems.

Keyword: *Magnetic actuation, Nanogenerator, Self-power sensing*

Innovative Biodegradable Films in Chitosan Matrix: Towards Therapeutic Dressings

Berkay Bektaş [*] [1], Pelin Pehlivanoğlu[2], Ateş Batıkan Özdamar[1], Gizem Tezeren[1], Hürriyet Polat[2]

[1] İzmir Institute of Technology, Department of Chemical Engineering, Urla 35430, Izmir
[2] İzmir Institute of Technology, Department of Chemistry, Urla 35430, Izmir

Wound healing is a complex biological process that requires dressings offering both physical protection and active biochemical support. The aim of this study is to develop chitosan-based biofilms enriched with bioactive compounds to address infection, inflammation and oxidative stress in chronic wounds. To achieve this, a low molecular weight chitosan, known as a biocompatible and biodegradable polysaccharide, was dissolved in dilute lactic acid to prepare 2% w/v polymeric solution. To systematically evaluate the component interactions, a total of nine distinct film formulations were fabricated via an O/W emulsion technique followed by solvent casting. The experimental methodology included a chitosan only control and composite films with varying concentrations of St. John's Wort oil (0.5% and 1.0% v/v), prepared either with or without the biocompatible triblock copolymer P-123 and curcumin. Finally, the prepared films were characterized using ATR-FTIR, SEM, surface hydrophobicity measurements and biological activity assays to evaluate their potential as wound dressing materials.

ORCID:
Hürriyet Polat: 0000-0002-1573-0351

Keyword: *Chitosan, Wound dressing, Biofilm*

Development of Berberine-Antibiotic Nanocomplexes and Investigation of Their In Vitro Antimicrobial Activities

Cemile Yilmaz * **, Ismail Ocsoy**

Department of Analytical Chemistry, Faculty of Pharmacy, Erciyes University, Kayseri 38039, Türkiye

The widespread and indiscriminate use of antibiotics is accelerating the development of multi-drug resistance (MDR) and leading to serious limitations in the fight against infectious diseases. The rise in MDR is reducing treatment success rates, particularly in intensive care units and for nosocomial infections; it is leading to increased mortality rates for systemic infections such as sepsis, pneumonia, and pneumonitis. The reduced effectiveness of antimicrobial agents against bacterial and fungal pathogens is increasing the need for new alternatives in clinical practice. As part of this research, new nanocomplexes have been developed using the “self-assembly” method with berberine (BBR)—a key bioactive component of traditional medicine with proven efficacy—and antibacterial agents (ampicillin, meropenem, ciprofloxacin) and antifungal (fluconazole) agents. BBR is an isoquinoline alkaloid with proven antimicrobial activity that disrupts DNA replication and cell integrity. Without the need for a polymeric carrier, bioactive components and therapeutic agents spontaneously self-assemble through intermolecular physical interactions (π-π stacking, hydrogen bonds, hydrophobic interactions, etc.) to form nanoscale structures. The aim of these formulations is to achieve synergistic antimicrobial activity against major bacterial and fungal strains that have developed resistance—including Klebsiella pneumoniae, Acinetobacter baumannii, Escherichia coli, Staphylococcus aureus, and Candida albicans—and to overcome existing resistance mechanisms. The resulting nanocomplexes were characterized using analytical techniques, and their efficacy was tested in vitro against microorganisms both during the active infection phase and during resistant stages in which they form biofilm-like protective structures. The potential of BBR-based nanodrugs in combating MDR has been demonstrated, leading to the development of new biocompatible nanopharmaceutical products.

Acknowledgment:
This work was supported by Erciyes University Scientific Research Projects Coordination Unit with Project Number TDK-2026-15646.

ORCID:
Cemile Yilmaz: 0009-0001-6947-2773
Ismail Ocsoy: 0000-0002-5991-3934

References:
Eren, E. E., Karagoz, N., Saglam, H., Sav, H., Diksac, S., Deveci, K., & Celik, I. (2025). Yogun Bakim Unitelerinde Kandidemi Etkenlerinin Dagilimi ve Antifungal Duyarliliklarin Alti Yillik Analizi. Mediterranean Journal of Infection, Microbes and Antimicrobials, 14(S1), 106-108.
Huang, X., Wang, P., Li, T., Tian, X., Guo, W., Xu, B., ... & Lei, H. (2019). Self-assemblies based on traditional medicine berberine and cinnamic acid for adhesion-induced inhibition multidrug-resistant Staphylococcus aureus. ACS applied materials & interfaces, 12(1), 227-237.
Fu, S., Yi, X., Li, Y., Li, Y., Qu, X., Miao, P., & Xu, Y. (2024). Berberine and chlorogenic acid-assembled nanoparticles for highly efficient inhibition of multidrug-resistant Staphylococcus aureus. Journal of Hazardous Materials, 473, 134680.
Zheng, T., Chen, H., Wu, C., Wang, J., Cui, M., Ye, H., ... & Dong, Z. (2023). Fabrication of Co-assembly from berberine and tannic acid for multidrug-resistant bacteria infection treatment. Pharmaceutics, 15(7), 1782.
WHO publishes list of bacteria for which new antibiotics are urgently needed: [https://www.who.int/news/item/27-02-2017-who-publishes-list-of-bacteria-for-which-new-antibiotics-are-urgently-needed] Erişim Tarihi: 31.10.2025

Keyword: *self-assembly, nanodrug, multi drug resistance*

Investigation of the Potential of Quercetin-Loaded Lipid Nanoparticles (LipQueNPs) to Enhance Quercetin Bioavailability and Their Applicability in Breast Cancer Treatment

Demet Yalçın [*1], **Mehmet Aytar**[1], **Gülen Melike Demirbolat**[2], **Özge Çevik**[3]

[1] *ADU-Science and Technology Application and Research Center, Aydın Adnan Menderes University, Aydın, Turkey*
[2] *Department of Pharmaceutical Technology, Faculty of Pharmacy, Acibadem Mehmet Ali Aydınlar University, İstanbul, Turkey*
[3] *Department of Medicinal Biochemistry, School of Medicine, Aydin Adnan Menderes University, Aydin, Turkey*

Quercetin is a naturally occurring bioactive compound that suppresses cell proliferation, induces apoptosis, and can inhibit metastatic processes in various cancer types. Breast cancer remains one of the most common malignancies in women, and despite current treatment approaches, drug resistance, systemic toxicity, and disease recurrence remain significant clinical problems. However, its low solubility, poor bioavailability, and limited stability under physiological conditions prevent it from fully utilizing its therapeutic potential, significantly limiting its clinical applications. Therefore, the development of novel drug delivery systems that can enhance the therapeutic efficacy of quercetin is of great importance. In this study, a liposomal formulation was developed using L-α-phosphatidylcholine, cholesterol, and quercetin, and LipQueNPs nanoparticles were created. LipQueNPs were characterized by particle size, zeta potential, and TEM morphological imaging. LipQueNPs encapsulation efficiency, quercetin loading capacity, and release amount were calculated. MCF-7 is a low-aggression, ER+/PR+ Luminal A type breast cancer cell line. In this study, LipQueNPs were investigated for uptake, cell viability (24-72h), colony formation, and Annexin-V/PI apoptosis using flow cytometry. LipQueNPs were found to be 222±16 nm in size, have a charge below -30 mV, and a spheroidal structure. It was observed that LipQueNPs could release more than 50% of the loaded amount of quercetin after 6 hours. In MCF7 cells, LipQueNPs were found to halt cell proliferation at 24 hours, effectively reduce it after 48 hours, and induce early apoptosis. After 72 hours, changes in colonization patterns and decreased cellular interaction were observed. This indicates that the effects of LipQueNPs are not only due to acute cytotoxicity but can also inhibit the long-term proliferation capacity of tumor cells. The developed LipQueNPs nanoparticle system demonstrates that it is a promising drug delivery platform that enhances the anticancer efficacy of quercetin. By helping to overcome the low solubility and bioavailability problems of quercetin, LipQueNPs may offer an alternative or complementary therapeutic approach in breast cancer treatment.

Acknowledgment:
Financial support by the Adnan Menderes University Research Grants (TPF-25051) is acknowledged.

ORCID:
Demet Yalçın: 0000-0003-3255-3753
Mehmet Aytar: 0000-0002-8083-7358
Gülen Melike Demirbolat: 0000-0001-5621-5818
Özge Çevik: 0000-0002-9325-3757

Keyword: *Breast Cancer, Quercetin, Liposome*

Investigation of The Impact of The Second Disulphide Bond In HIV-1 Capsid Binding Nanobody

Dilan İrem Açan [*] [1], **Gamze Terlemez**[2], **Hümeyra Taşkent Sezgin**[3]

[1] *Biotechnology Master's Program, Izmir Institute of Technology, İzmir, Türkiye*
[2] *Medical Biotechnology Doctoral Program, Izmir Institute of Technology, İzmir, Türkiye*
[3] *Bioengineering Department, Izmir Institute of Technology, İzmir, Türkiye*

A nanobody (Nb) is the variable domain of the naturally occurring heavy-chain-only antibody in camelids. Due to their small size (~15 kDa), exceptional thermal and chemical stability, and ease of recombinant production, nanobodies have emerged as promising alternatives to conventional monoclonal antibodies in diagnosis, therapeutics, and biotechnology. One key structural feature contributing to the exceptional stability of nanobodies is the presence of a conserved pair of cysteine (Cys) amino acids forming a disulfide bond between framework regions (FR1 and FR3). Analyses of nanobody sequences from the single domain antibody database (sdAb-DB) revealed that 11.7% of nanobodies have more than two cysteine amino acids and around 1.4% has two more cysteines in CDR3. The nanobody in this study is reported to bind HIV-1 capsid protein. This nanobody has four cysteine amino acids, two of them are in the CDR3 region. We investigated the effect of the second disulfide bond in the CDR3 region of this nanobody to the protein's stability and binding affinity to its antigen.

In this study, the two cysteines at 98 and 107 were mutated to alanine, resulting a double mutant protein. The wild-type (Nb-WT) and double-mutant Nb (Nb-AA) were expressed in Escherichia coli BL21(DE3) cells and were purified using various chromatographic methods. Mutant protein yield was less than the wild-type nanobody protein yield. Melting temperature of Nb-WT with its cysteines in oxidized and reduced form were 75.8 and 71.2ºC, respectively. Melting temperature of the Nb-AA mutant with its cysteines in oxidized and reduced forms was 65.7 and 64.7ºC, respectively. Surprisingly, the absence of the second disulfide bond, even though it is between close-by Cys residues in the CDR3 region, thermally destabilized the protein by 10.1ºC. The dissociation constant (Kd) of the Nb proteins to the antigen, HIV-1 capsid was investigated using surface plasmon resonance. Nb-WT has 130 pM dissociation constant, whereas the Nb-AA mutant has 250 pM. There is a slight decrease in the binding capacity of the Nb protein with the removal of the second disulfide bond. In the literature, disulfide bonds connecting two distant sites are known to have a significant contribution to the stability of proteins, but we determined that a disulfide bond between 98th and 107th position have a measurable impact on stability and on the binding of nanobody to its target antigen.

Acknowledgment:
I would like to thank the Turkish Scientific and Technological Research Council (TUBITAK) for supporting my thesis work with the 2210-A Domestic General Master's Scholarship Program, which is part of the 2211-Master's Scholarship Programs.

ORCID:
Dilan İrem Açan: 0009-0005-9316-2408

Keyword: *Biotechnology, Nanobody, Disulphide bond*

Development of Gold Nanoparticle-Modified, Charge-Tunable Semi-IPN Hydrogels Based On ZEIN, 2-Hydroxyethyl Methacrylate and Vinylimidazole for Controlled Drug Delivery Systems

Elif Sultan Karabayır * **, Pınar Ilgın, İlknur Atlı, Hava Özay, Özgür Özay**

Çanakkale Onsekiz Mart University

For centuries, drugs have been used to treat various diseases; however, their low solubility in blood, rapid clearance from circulation, and potential systemic toxicity negatively affect therapeutic efficiency (1). These limitations highlight the importance of developing controlled drug delivery systems. Among these systems, polymeric hydrogels are widely used in biomedical applications. Thanks to their three-dimensional network structures, hydrogels can encapsulate therapeutic components thousands of times their own mass. Moreover, their properties can be tailored for targeted applications through the selection of suitable monomers and polymers (2,3).

In this study, semi-IPN hydrogel systems containing zein, a corn protein-based natural polymer, together with the synthetic monomers 2-hydroxyethyl methacrylate (HEMA) and vinylimidazole (VI) were synthesized for the first time by free-radical polymerization. In addition, a protonation process was applied to modify the surface charge, swelling behavior, and drug loading/release performance of the synthesized hydrogels, thus also synthesizing cationic hydrogels. Moreover, to enhance the functionality of these synthesized drug delivery systems, gold nanocomposites were prepared using a green synthesis method with polyphenol-rich cherry laurel (Prunus laurocerasus L.) fruit extract. The physicochemical and morphological properties of all these synthesized hydrogel systems were comprehensively characterized by FTIR, TGA, XRD, SEM, and TEM analyses, as well as swelling and pH sensitivity tests in different simulated body fluids. Two different model drugs (cefazolin with antibacterial effect and sodium diclofenac with anti-inflammatory effect) were used to investigate controlled drug release behaviors and kinetics. In vitro drug release studies performed in phosphate buffer solution and simulated gastric fluid environments showed that protonation and gold nanoparticle incorporation significantly enhanced both drug loading capacity and cumulative release percentage. Furthermore, the total phenolic content and antioxidant capacity were determined, and the antimicrobial activities of the prepared systems were evaluated against different microorganisms. The results demonstrated that the incorporation of gold nanoparticles green-synthesized using cherry laurel (Prunus laurocerasus L.) extract enhanced the antioxidant and antimicrobial properties of the hydrogels.

The study results showed that these polymeric hydrogel systems, which have charge-tunable behavior and contain green-synthesized gold nanoparticles, are promising biomaterials for controlled drug delivery and wound dressing applications.

Acknowledgment:
Çanakkale Onsekiz Mart University and TÜBİTAK 2224-B Yurtiçi Bilimsel Etkinlik Katılma Desteği

ORCID:
Elif Sultan Karabayır: 0000-0003-1152-120X
Pınar Ilgın: 0000-0001-7071-0575
İlknur Atlı: 0009-0003-1804-4036
Hava Özay: 0000-0002-4184-7801
Özgür Özay: 0000-0001-6589-9844

References:
Gao, J., Karp, J. M., Langer, R., & Joshi, N. (2023). The future of drug delivery. Chemistry of Materials, 35(2), 359-363. https://doi.org/10.1021/acs.chemmater.2c03003
Fatimi, A., Damiri, F., El Arrach, N., Hemdani, H., Musuc, A. M., & Berrada, M. (2025). Hydrogel-Based Biomaterials: A Patent Landscape on Innovation Trends and Patterns. Gels, 11(3), 216. https://doi.org/10.3390/gels11030216
Ma, X. K., Cao, B., & Liu, X. (2025). Microenvironment-responsive peptide hydrogels: molecular mechanisms, design and frontiers. Frontiers in Bioengineering and Biotechnology, 13, 1692319. https://doi.org/10.3389/fbioe.2025.1692319

Keyword: *Zein, Charge-tunable hydrogels, Green-synthesized gold nanoparticles*

A Novel Microfluidics Immunotherapy-On-Chip to Decipher Paracrine Communication Between Colorectal Cancer Spheroids and Tumor-Associated Macrophages

Gurkan Yesiloz [*1,2], **Eylul Tabel**[1], **Servin Bagheralmoosavi**[1]

[1] *1. Yesiloz Research Laboratory, National Nanotechnology Research Center (UNAM) - Bilkent University, 06800, Cankaya-Ankara, Türkiye.*
[2] *2. Institute of Materials Science and Nanotechnology, Bilkent University, 06800, Cankaya-Ankara, Türkiye.*

Tumor-associated macrophages (TAMs) are central regulators of colorectal cancer progression, shaping an immunosuppressive and pro-tumorigenic microenvironment that limits therapeutic efficacy. However, dissecting TAM-driven paracrine signaling in physiologically relevant yet controllable settings remains challenging using conventional in vitro or animal models. Here, we present a microfluidics-enabled immunotherapy-on-chip platform designed to model close-range paracrine communication between three-dimensional colorectal cancer spheroids and macrophages, while preserving spatial compartmentalization for independent analysis[1-2].

The platform integrates a macrophage-adherent microfluidic chamber with a custom spheroid insert positioned approximately 300 µm away, enabling continuous exchange of soluble factors without direct cell contact. Using this system, tumor-associated macrophages derived from THP-1 monocytes were co-cultured with HT-29 colorectal cancer spheroids and treated with a macrophage-targeted immunotherapeutic formulation of liposomal resiquimod (LipRes). LipRes was engineered to exploit size-selective phagocytosis by macrophages and achieved high encapsulation efficiency and temporal stability under culture conditions.

Functional analyses demonstrated that LipRes effectively re-educated TAMs from a tumor-supportive phenotype toward a pro-inflammatory, anti-tumoral state, evidenced by morphological reversal, restoration of CD86 expression, reduction of CD163 levels, decreased reactive oxygen species, and suppressed IL-6 secretion. Critically, TAM re-education resulted in pronounced inhibition of spheroid growth, attenuation of epithelial–mesenchymal transition markers, and reduced migratory behavior of colorectal cancer cells, both on-chip and in complementary off-chip assays[3].

This work introduces a versatile tumor-microenvironment-on-chip model that enables real-time, compartment-resolved investigation of immune–tumor crosstalk under dynamic perfusion. By combining microfluidic precision with macrophage-selective immunotherapy, the platform offers a powerful tool for mechanistic studies of TAM plasticity and preclinical screening of immunomodulatory strategies. The modular design further allows integration of biosensors and additional stromal components, positioning this approach as a scalable and translational framework for next-generation cancer immunotherapy research.

Acknowledgment:
Dr. Gurkan Yesiloz gratefully acknowledge the support from the Scientific and Technological Research Council of Türkiye (TUBITAK) (2232-Grant No: 118C263 & 221M575 & 123E157) and TUSEB (Group C-Grant No: 34150).

References:
[1] Zafar, A., Khan, M. J., Abu, J. & Naeem, A. (2024). Mol. Biol. Rep. 51, 219. DOI: 10.1007/s11033-023-09096-8
[2] Verona, F. et al.(2025). Front. Immunol. 16, 1529847. DOI: 10.3389/fimmu.2025.1529847
[3] Nahon, D. M. et al. (2024). Nat. Biomed. Eng. 2024 88 8, 941–962. DOI: 10.1038/s41551-024-01236-0

Keyword: *Microfluidics*, *Organ-on-Chips*, *Immunotherapy-on-chip*

Development and Characterization of Extracellular Vesicle–Liposome Hybrid Nanoparticles for Nucleic Acid Delivery

Khayala Rasulova [*] [1], Deniz Bozdağ[1], İsmail Altıntop[2], Irmak Bayazıt[1,3], Gülşah Erel Akbaba[1]

[1] *Department of Pharmaceutical Biotechnology, Faculty of Pharmacy, Izmir Katip Celebi University, İzmir, Turkey*
[2] *Faculty of Pharmacy, İzmir Katip Çelebi University, İzmir 35620, Turkey*
[3] *Department of Pharmaceutical Biotechnology, Faculty of Pharmacy, Ege University, İzmir, Turkey*

Extracellular vesicles (EVs) and liposomes are widely investigated nanocarriers for nucleic acid delivery [1]. Hybrid EV–liposome nanoparticles have emerged as a promising strategy to integrate the biological advantages of EVs with the physicochemical versatility of liposomes for gene delivery applications [2]. In this study, EV-liposome hybrid nanoparticles were developed and characterized to combine the advantages of both systems and establish a potential platform for future mRNA delivery applications.

Liposomes with different lipid compositions were prepared and evaluated in terms of particle size, surface charge, stability, nucleic acid complexation capacity, and protection against enzymatic degradation. The optimized formulation successfully formed complexes with plasmid DNA, protected the genetic cargo from DNase I-mediated degradation, and enabled efficient gene delivery in HEK293T cells. EVs isolated from HEK293T cells were characterized by dynamic light scattering (DLS), nanoparticle tracking analysis (NTA), and Western blotting. Hybridization of EVs with liposomes resulted in nanoparticles exhibiting increased particle size and altered surface charge, confirming successful hybrid nanoparticle formation.

Both liposomal and EV-liposome hybrid formulations demonstrated high biocompatibility, maintaining cell viability above 70% at the highest tested concentration. The hybrid nanosystems exhibited favorable physicochemical properties, including an average particle size of approximately 204 nm, low polydispersity, and a positive surface charge, supporting their suitability for nucleic acid transport.

These findings demonstrate that EV-liposome hybrid nanoparticles provide a biocompatible and versatile delivery platform for nucleic acid therapeutics and represent a promising strategy for future mRNA-based applications.

Acknowledgment:
This study was supported by TÜBİTAK 2247-D National Leading Researchers Program under Project No. 123C597.

ORCID:
Khayala Rasulova: 0000-0001-9773-3240
Deniz Bozdağ: 0000-0003-3082-1582
İsmail Altıntop: 0009-0009-6883-1939
Irmak Bayazıt: 0009-0009-9037-8085
Irmak Bayazıt: 0009-0009-9037-8085
Gülşah Erel Akbaba: 0000-0003-3287-5277

References:
Fraczek, W., Szmidt, M., Kregielewski, K. & Grodzik, M. Liposomes and Extracellular Vesicles as Distinct Paths Toward Precision Glioma Treatment. IJMS 26, 6775 (2025).
Li, Q. et al. Extracellular Vesicle-Based mRNA Therapeutics and Vaccines. Exploration 5, 20240109 (2025).

Keyword: *extracellular vesicles, liposomes, hybrid nanoparticles, gene delivery*

Development of Lung Surfactant-Biomimetic Lipid Nanoparticles for Co-Delivery of Paclitaxel and Nintedanib

Melike Belenli Gümüş [*] [1], Kadir Sinan Arslan[2], Hasan Ümit Öztürk[1], Müge Serhatlı[1], Seda Kızılel[3], Hilal Yazıcı Malkoçoğlu[1]

[1] *Biotechnology Research Group, Climate and Life Sciences, Marmara Research Center (MAM), The Scientific and Technological Research Council of Turkey (TÜBİTAK), Kocaeli, Turkey*

[2] *Biotechnology Research Group, Climate and Life Sciences, Marmara Research Center (MAM), The Scientific and Technological Research Council of Turkey (TÜBİTAK), Kocaeli, Türkiye*

[3] *Chemical and Biological Engineering, Koç University, Rumelifeneri Yolu, Sariyer, Istanbul 34450, Turkey*

Lung cancer remains the leading cause of cancer-related mortality worldwide, and pulmonary fibrosis can further aggravate disease progression by creating a pro-tumorigenic and fibrotic lung microenvironment. Since fibrosis and lung cancer share key pathological mechanisms, including extracellular matrix remodeling, TGF-β signaling, and epithelial–mesenchymal transition, dual-action therapeutic strategies may offer a rational approach for patients with overlapping malignant and fibrotic lung pathology[1]

The biocompatibility, structural versatility, and high drug loading capacities of lipid-based nanosystems make them ideal candidates for drug delivery applications. In this study, we developed lung surfactant-biomimetic lipid nanoparticles for the co-delivery of paclitaxel[2], a chemotherapeutic agent, and nintedanib[3], an antifibrotic drug. The nanosystems were prepared and physicochemically characterized by dynamic light scattering (DLS) to determine hydrodynamic size, polydispersity index, and colloidal stability. Morphological evaluation by transmission electron microscopy (TEM) is being performed to confirm particle architecture. Drug encapsulation efficiency and loading capacity will be quantified by high-performance liquid chromatography (HPLC) for both paclitaxel and nintedanib. Following characterization, in vitro studies will evaluate cytotoxicity, therapeutic efficacy, and potential antifibrotic activity in lung cancer and fibrosis-relevant cellular models.

Overall, this study presents a surfactant-biomimetic lipid nanoparticle platform designed for combined anticancer and antifibrotic drug delivery, targeting the biological interface between lung cancer and pulmonary fibrosis.

“This publication was created by benefiting from the 2236-B Marie Sklodowska-Curie Actions (MSCA) Cofund Scholarship Programs Contribution Fund Program (TUBITAK project ID: 123C460) and Horizon Europe MSCA Cofund Postdoctoral Program (EU project ID: 101126492). Views and opinions expressed are, however, those of the author(s) only and do not necessarily reflect those of the European Union or TUBITAK. Neither the European Union nor the granting authority can be held responsible for them.”

Acknowledgment:
This publication was created by benefiting from the 2236-B Marie Sklodowska-Curie Actions (MSCA) Cofund Scholarship Programs Contribution Fund Program (TUBITAK project ID: 123C460) and Horizon Europe MSCA Cofund Postdoctoral Program (EU project ID: 101126492). Views and opinions expressed are, however, those of the author(s) only and do not necessarily reflect those of the European Union or TUBITAK. Neither the European Union nor the granting authority can be held responsible for them. The authors gratefully acknowledge Prof. Dr. İlknur Dağ, Assoc. Prof. Dr. Bükay Yenice Gürsu, and Assoc. Prof. Dr. Betül Yılmaz Öztürk at Eskişehir Osmangazi University (ESOGU), Central Research Laboratory Application and Research Center (ARUM), for acquiring Cryo-TEM images.

References:
Samarelli AV, Masciale V, Aramini B, et al. Molecular Mechanisms and Cellular Contribution from Lung Fibrosis to Lung Cancer Development. Int J Mol Sci. 2021;22(22):12179. doi:10.3390/ijms222212179
Bayón-Cordero L, Alkorta I, Arana L. Application of Solid Lipid Nanoparticles to Improve the Efficiency of Anticancer Drugs. Nanomaterials. 2019;9(3):474. doi:10.3390/nano9030474
Li D, Zhao A, Zhu J, et al. Inhaled Lipid Nanoparticles Alleviate Established Pulmonary Fibrosis. Small. 2023;19(30). doi:10.1002/smll.202300545

Keyword: *Lung Cancer, Pulmonary Fibrosis, Biomimetic Lipid Nanoparticles*

Investigation of Biomedical Applications of Boron Nitride-Doped Superabsorbent Hydrogels

Nurgul Turker Yildiz [*] [1], **Ozgur Ozay**[2]

[1] *Department of Bioengineering, School of Graduate Studies, Canakkale Onsekiz Mart University, Canakkale, Turkey*
[2] *Department of Bioengineering, Faculty of Engineering, Canakkale Onsekiz Mart University, Canakkale, Turkey*

Nanomaterials have a wide range of applications in the biomedical field. Specifically, the incorporation of metallic nanoparticles into hydrogel structures enhances the efficiency of therapeutic processes in tissue engineering and controlled drug delivery systems. Hydrogels are highly preferred as smart biomaterials due to their porous architecture, high water-retention capacity, and biocompatibility. However, the mechanical limitations of pure hydrogels and their poor control over release kinetics necessitate the development of multifunctional, hybrid nanocomposite systems. Monomers and high-surface-area nanomaterials provide precise control over swelling behavior and offer a prolonged and controlled release profile by limiting the initial burst release of therapeutic agents.

In this study, semi-interpenetrating polymer network (semi-IPN) nanocomposite hydrogels were synthesized. To optimize the structural integrity of the system, a semi-IPN structure was formed using poly(vinyl alcohol) (PVA) and 3-sulfopropyl acrylate potassium salt (SPA), an anionic monomer exhibiting strong sulfonate functionality. To mechanically reinforce the hydrogel matrix at the molecular level and increase the therapeutic loading capacity, hexagonal boron nitride (h-BN) was integrated into the network. The π-π stacking interactions between the h-BN layers and aromatic model drugs created a secondary protective barrier, successfully limiting the initial burst release.

The swelling behaviors of the synthesized hydrogels were evaluated in different media, including deionized water, phosphate-buffered saline (PBS), and simulated gastric fluid (SGF). To impart antibacterial properties, silver nanoparticles (AgNPs) were incorporated into the system via in-situ green synthesis. To eliminate toxic chemicals during synthesis, Myrtus communis extract, which is rich in polyphenolic compounds, was utilized as a reducing and stabilizing agent.

The synthesized hydrogels and nanocomposites were characterized structurally, thermally, and morphologically using FT-IR, TGA, XRD, SEM-EDX, and TEM analyses. The loading and release kinetics of model chemotherapeutic agents were monitored via UV-Vis spectrophotometry to model the release mechanisms. Furthermore, the antioxidant capacities of the developed platforms were determined, and their in vitro biocompatibility and biological activities were evaluated using the MTT assay on target cell lines.

ORCID:
Nurgul Turker Yildiz: 0009-0002-8292-2000
Ozgur Ozay: 0000-0001-6589-9844

Keyword: *Hexagonal boron nitride, Silver nanoparticles, Myrtus communis extract*

Development and Characterization of Tunable Elastin-Peg/Gelma Hydrogels for Topical Drug Delivery

Osman Doğan [*1,2], Aslı Kara[3], Naile Öztürk[4], Yakup Gültekin[5], Şeyma Nigiz[6], Ceren Özkul Koçak[6], Naciye Dilara Zeybek[7], İmran Vural[2]

[1] *Department of Pharmaceutical Technology,Faculty of Pharmacy, Baskent University*
[2] *Department of Pharmaceutical Technology, Faculty of Pharmacy, Hacettepe University*
[3] *Department of Molecular Biology Hitit University*
[4] *Department of Pharmaceutical Technology, Faculty of Pharmacy, Inonu University*
[5] *Department of Pharmaceutical Technology, Faculty of Pharmacy Selçuk University*
[6] *Department of Pharmaceutical Microbiology, Faculty of Pharmacy, Hacettepe University*
[7] *Department of Histology and Embryology, Hacettepe University Faculty of Medicine, Ankara, Turkey*

Ideal hydrogels for topical drug delivery must be highly absorbent, mechanically compatible with human skin, and easily customizable (1). Methacrylated gelatin (GelMA) and elastin composites mimic the dermal extracellular matrix and offer an attractive biomaterial platform; however, the physicochemical properties for a topical delivery must first be specified (2). The preparation of soluble elastin from insoluble elastin was carried out according to the methodology proposed by Partridge et al. (3) To this end, elastin based GelMA hydrogel was developed and characterization tests were carried out.

In this study, bovine elastin was mixed with oxalic acid and This mixture was boiled for 1 hour and then centrifuged at 4000rpm. This cycle was continued until the pellet was completely dissolved. We functionalized soluble elastin with acryloyl-poly(ethylene glycol)-N-hydroxysuccinimide (acryloyl-PEG-NHS) to introduce acrylate groups rendering it photochemically crosslinkable. Fourier-transform infrared (FTIR) spectroscopy was used for confirmation of conjugation. FTIR results demonstrated bands corresponding to C–H stretching, C–O–C ether groups, and acrylate C=C deformation appeared in the spectra.

To select the optimal formulation, four different formulations were developed using varying ratios of GelMA and elastin. Four GelMA-based formulations (GELMA1–GELMA4) were characterized by oscillatory rheology and swelling analysis. Strain sweep analysis showed that each gel maintained a wide linear viscoelastic plateau before undergoing a controlled decline in modulus. Frequency sweep analysis demonstrated that the storage modulus (G') was largely independent of frequency and consistently exceeded the loss modulus (G'') confirming the formation of a crosslinked network. As the amount of elastin in the structure increased, G' value decreased from 370 to 53 Pa. During temperature sweeps, the gels softened progressively as heating proceeded and approached a plateau around 40 °C, demonstrating that the hydrogels remain stable across standard skin temperatures. Considering the balance of skin-compatible stiffness, rapid and stable swelling, thermal stability, and a broad linear viscoelastic region, GELMA3 was identified as the optimal candidate for a topical drug-delivery carrier compared to other formulations. Drug loading and controlled-release profiling of this formulation are planned as future work.

Acknowledgment:
This study was supported by Health Institutes of Türkiye (TÜSEB-GROUP B R&D PROJECTS-34358).

ORCID:
Osman Doğan: 0000-0003-2314-6793

References:
1- Liang, Y., He, J., & Guo, B. (2021). Functional Hydrogels as Wound Dressing to Enhance Wound Healing. ACS nano, 15(8), 12687–12722. https://doi.org/10.1021/acsnano.1c04206
2- Tian, D. M., Wan, H. H., Chen, J. R., Ye, Y. B., He, Y., Liu, Y., Tang, L. Y., He, Z. Y., Liu, K. Z., Gao, C. J., Li, S. L., Xu, Q., Yang, Z., Lai, C., Xu, X. J., Ruan, C. S., Xu, Y. S., Zhang, C., Luo, L., & Yan, L. P. (2022). In-situ formed elastin-based hydrogels enhance wound healing via promoting innate immune cells recruitment and angiogenesis. Materials today. Bio, 15, 100300. https://doi.org/10.1016/j.mtbio.2022.100300
3- Palumbo, F. S., Pitarresi, G., Fiorica, C., Rigogliuso, S., Ghersi, G., & Giammona, G. (2013). Chemical hydrogels based on a hyaluronic acid-graft-α-elastin derivative as potential scaffolds for tissue engineering. Materials science & engineering. C, Materials for biological applications, 33(5), 2541–2549. https://doi.org/10.1016/j.msec.2013.02.015

Keyword: *Methacrylated gelatin, Elastin, Hydrogel*

Isotonic, hypotonic and hypertonic solutions and their differentiation with optical biosensors

İsmail Celil Haskoloğlu[1,2], Oya Akca [* 3], Melih Erol Ceyhan[4], A. Berk Tuzcu[5], Selim Unlu[5,6,7], Zeynep Güneş Özünal[2]

[1] Department of Pharmacology, Faculty of Pharmacy, Near East University, 99138 Nicosia, Cyprus
[2] Department of Medical Pharmacology, Faculty of Medicine, Istanbul Atlas University, Kagithane, Anadolu Cad. No: 40, Istanbul 34408, Türkiye
[3] Department of Medical Biology, Faculty of Medicine, Istanbul Atlas University, Kagithane, Anadolu Cad. No: 40, Istanbul 34408, Türkiye
[4] Faculty of Medicine, Istanbul Atlas University, Kagithane, Anadolu Cad. No: 40, Istanbul 34408, Türkiye
[5] Department of Electrical and Computer Engineering, Boston University, 8 St. Mary's St., Boston, MA, 02125, USA
[6] IRIS Kinetics, 650 Albany St., Boston, MA, 02118, USA
[7] Department of Biomedical Engineering, Boston University, 8 St. Mary's St., Boston, MA, 02125, USA

Optical biosensors are widely used in research and in vitro diagnostic applications because they provide rapid, safe, and sensitive measurements. Biological sample analysis is important for diagnosis, disease monitoring, and clinical decision-making processes related to pharmacotherapy. Common clinical specimens such as hematological samples, bodily secretions, tissues containing genetic material, and urine may differ in terms of their physicochemical properties, including pH, density, protein content, ionic composition, viscosity, sodium levels, and tonicity.

Although many biological fluids are normally maintained close to isotonic conditions, various clinical conditions and medications may alter sodium-water balance, causing samples to acquire hypotonic or hypertonic characteristics. Cardiovascular diseases, endocrine disorders, renal failure, uremia/diuresis and medications disrupt electrolyte balance may alter sample tonicity; this may consequently affect the accuracy and reliability of optical biosensor-based analytical measurements.

The aim of this study is to evaluate the possible effects of tonicity changes on optical biosensor measurements and to investigate whether isotonic, hypotonic, and hypertonic solutions can be differentiated according to optical signal alterations. For this purpose, three different solutions were prepared: 0.45% NaCl was used as the hypotonic solution, 0.9% NaCl as the isotonic solution, and 3.0% NaCl as the hypertonic solution. The assay was performed using silicon dioxide (SiO_2) chips within an Interferometric Reflectance Imaging Sensor (IRIS) with real-time label free measurement setup.

The solutions prepared under different tonicity conditions were analyzed using an optical biosensor system. Signal value and reference value were recorded throughout sequential measurement steps for different sensor tags. Background measurements were excluded from the analysis. The main evaluation parameters were determined as signal value, reference value, and the signal/reference ratio. These parameters were used to compare optical signal changes, signal drift, and possible tonicity-related differences.

This approach allows the evaluation of how matrix-related properties such as tonicity, density, ionic strength, and viscosity may affect optical biosensor performance independently of the target analyte. Comparing signal values with reference values may help identify systematic signal changes caused by altered sample conditions. The results of this study are expected to contribute to the optimization of optical biosensor-based measurements in biological samples and to increase the reliability of in vitro diagnostic results under varying conditions.

Acknowledgment:
The authors would like to thank Ennur Ak for valuable technical assistance and support in laboratory procedures throughout the study.

References:

vci, O., Lortlar Ünlü, N., Yalçın Özkumur, A., & Ünlü, M. S. (2015). Interferometric Reflectance Imaging Sensor (IRIS)—A platform technology for multiplexed diagnostics and digital detection. Sensors, 15(7), 17649–17665. doi: 10.3390/s150717649

Chen, C., & Wang, J. (2020). Optical biosensors: An exhaustive and comprehensive review. Analyst, 145(5), 1605–1628. doi: 10.1039/C9AN01998G

Marn, A. M., Chiodi, E., & Ünlü, M. S. (2021). Bulk-effect-free method for binding kinetic measurements enabling small-molecule affinity characterization. ACS Omega, 6(10), 6836–6841. doi: 10.1021/acsomega.0c05994

Braun, M. M., Barstow, C. H., & Pyzocha, N. J. (2015). Diagnosis and management of sodium disorders: Hyponatremia and hypernatremia. American Family Physician, 91(5), 299–307.

Keyword: *optical biosensor, isotonic solution, hypotonic solution, hypertonic solution, tonicity, biological samples, signal/reference ratio, in vitro diagnostics*

Nanodelivery Systems of Thymoquinone for Enhanced Bioavailability

Rezvan Shaddel [* 1], Ali Rashidinejad[2], Mohammad Mahdi Karimkhani[3], Ozgur Tarhan[4], Seid Mahdi Jafari[5]

[1] *Department of Food Science and Technology, Faculty of Agriculture and Natural Resources, University of Mohaghegh Ardabili, Ardabil, Iran*

[2] *Riddet Institute, Massey University, Private Bag 11222, Palmerston North 4442, New Zealand*

[3] *Center of Environmental Researchers, University of Qom, Qom, Iran*

[4] *Food Engineering Department, Engineering Faculty, Us¸ak University, 1 Eylul Campus, Us¸ak 64100, Türkiye*

[5] *Department of Food Materials and Process Design Engineering, Gorgan University of Agricultural Sciences and Natural Resources, Gorgan, Iran*

Thymoquinone (TQ), a hydrophobic bioactive compound from Nigella sativa, exhibits strong antioxidant and anti-inflammatory properties, but its application is restricted by poor solubility, instability, photosensitivity, rapid metabolism, and low bioavailability. Nanotechnology-based delivery systems offer promising solutions to these challenges. Lipid-based carriers (e.g., nano-liposomes, nano-emulsions, solid lipid nanoparticles) and biopolymeric systems (e.g., nano-hydrogels and cyclodextrin complexes) have shown significant potential in enhancing TQ stability, solubility, and controlled release. These nanocarriers improve bioavailability and therapeutic performance, making TQ more effective for food and biomedical applications. However, large-scale production and regulatory limitations still hinder their practical implementation. Overall, lipid-based and biopolymeric nanocarriers emerge as the most viable strategies for efficient TQ delivery, particularly in oral and functional formulations.

Keyword: *Thymoquinone, Nanodelivery systems, Bioavailability enhancement*

Evaluation of the Bioactive Properties of Silver Nanoparticles Produced by Green Synthesis Using Hericium erinaceus (Lion's Mane Mushroom)

Selcen Çakır [*1], **Özgür Özay**[2], **İlknur Atlı**[3]

[1] *Department of Medical Services and Techniques, Vocational School of Health Services, Çanakkale Onsekiz Mart University, Çanakkale, Türkiye*

[2] *Department of Bioengineering, Faculty of Engineering, Çanakkale Onsekiz Mart University, Çanakkale, Türkiye*

[3] *Department of Bioengineering, School of Graduate Studies, Çanakkale Onsekiz Mart University, Çanakkale, Türkiye*

Green synthesis approaches have attracted considerable attention in recent years due to their ability to produce environmentally friendly, sustainable, and biocompatible silver nanoparticles (AgNPs) using biological resources [1,2]. Hericium erinaceus (lion's mane mushroom) is a valuable medicinal mushroom rich in bioactive compounds [3]. In this study, AgNPs were synthesized through an environmentally friendly green synthesis approach using an aqueous extract of H. erinaceus, and the bioactive properties of the synthesized nanoparticles were evaluated.

The physicochemical properties of the synthesized AgNPs were characterized using UV–Visible spectroscopy, Fourier-transform infrared spectroscopy (FTIR), scanning and transmission electron microscopy (SEM/TEM), X-ray diffraction (XRD), dynamic light scattering (DLS), and zeta potential analysis. The antioxidant capacity of the nanoparticles was determined using the in vitro DPPH free radical scavenging assay. In addition, the total phenolic and flavonoid contents were analyzed, enabling a comprehensive evaluation of the bioactive properties of the synthesized AgNPs. This study contributes to the development of environmentally friendly and multifunctional nanobiomaterials by integrating the natural bioactive compounds of Hericium erinaceus with the functional properties of AgNPs.

Acknowledgment:
This study was supported by Scientific and Technological Research Council of Türkiye (TUBITAK) under the Grant Number 225Z301. The authors thank to TUBITAK for their supports.

References:
[1] İ. Atli, P. Ilgin, O. Ozay, Green synthesis of multifunctional responsive hydrogel embedded with silver, based on Xanthan gum, N-isopropylacrylamide, vinyl imidazole, and Luffa cylindrica for wound healing. J. Macromol. Sci. Chem. A 61(11), 953–965 (2024). https://doi.org/10.1080/10601325.2024.2417176
[2] Kulabas, S.S., Atli, I., Atalay, H.N. et al. Gold and silver nanoparticle decorated biocompatible and antibacterial xanthan gum/poly (HEMA-co-APTMACl) hydrogels for wound healing. emergent mater. 8, 6601–6617 (2025). https://doi.org/10.1007/s42247-025-01225-2
[3] Thongbai, B., Rapior, S., Hyde, K.D. et al. Hericium erinaceus, an amazing medicinal mushroom. Mycol Progress 14, 91 (2015). https://doi.org/10.1007/s11557-015-1105-4

Keyword: *Green synthesis, Hericium erinaceus, Silver nanoparticles (AgNPs)*

Biomedical Applications of Al_2O_3-Doped Hydrogels and Composites

Sema Nur Belen * **, Ozgur Ozay**

Laboratory of Biomaterials Research, Department of Bioengineering, Faculty of Engineering, Çanakkale Onsekiz Mart University

In this study, Al_2O_3-reinforced composite hydrogels were synthesized using biocompatible hydroxyethyl starch (HES) and 2-hydroxyethyl methacrylate (HEMA) via free-radical polymerization. N,N′-methylenebisacrylamide (MBA) was employed as the crosslinking agent, while APS/TEMED was used as the redox initiator system. Gold nanoparticles used to modify the composite hydrogels were synthesized in situ within the hydrogel matrix via a green synthesis approach using butterfly pea flower extract (Clitoria ternatea), and their antibacterial properties were investigated.

The swelling behavior of the synthesized hydrogels was evaluated in isotonic solution, simulated body fluid (SBF, pH 7.4), and an infected wound environment (pH 8.3). The hydrogel and composite structures were characterized by transmission electron microscopy (TEM), scanning electron microscopy (SEM), X-ray diffraction (XRD), Fourier-transform infrared spectroscopy (FT-IR), thermogravimetric analysis (TGA), and swelling studies.

The results revealed higher swelling capacities under alkaline conditions simulating an infected wound environment, indicating their potential for effective wound exudate absorption. Antibacterial analyses demonstrated that the gold nanoparticle-containing composite hydrogels exhibited significant antibacterial activity against the tested microorganisms. Overall, the findings suggest that the synthesized AuNP-Al_2O_3-reinforced p(HEMA)/HES semi-interpenetrating polymer network (s-IPN) composite hydrogels are promising materials for wound dressings, controlled drug delivery, and other biomedical applications.

Acknowledgment:
I extend my appreciation to the Scientific and Technological Research Council of Türkiye (TÜBİTAK) for the financial support provided through the 2224-B Domestic Scientific Event Participation Support Program.

ORCID:
Sema Nur Belen: 0000-0002-4870-7377
Ozgur Ozay: 0000-0001-6589-9844

References:
Ozay, O., Ilgın, P., Özay, H., Güngör, Z., Yılmaz, B., & Kıvanç, M. R. (2020). The preparation of various shapes and porosities of hydroxyethyl starch/p(HEMA-co-NVP) IPN hydrogels as programmable carrier for drug delivery. Journal of Macromolecular Science, Part A, 57(5), 379–387.
Şeref, E., Ilgın, P., Ozay, O., & Ozay, H. (2024). A new candidate for wound dressing materials: s-IPN hydrogel-based highly elastic and pH-sensitive drug delivery system containing pectin and vinyl phosphonic acid. European Polymer Journal, 207, 112824.
Kulabaş, S. S., Atlı, İ., Atalay, H. N., Boyunegmez Tümer, T., Ozay, H., & Ozay, Ö. (2025). Gold and silver nanoparticle decorated biocompatible and antibacterial xanthan gum/poly(HEMA-co-APTMACl) hydrogels for wound healing. Scientific Reports, 15, Article 6601–6617.

Keyword: *p(HEMA)/HES hydrogel, Aluminum oxide (Al_2O_3), Biomedical applications*

Computational Analysis of Doxorubicin Release Kinetics from Carboxymethylcellulose-Modified Superparamagnetic Iron Oxide Nanoparticles

Sıla Nur Soyat * **, Seda Demirel Topel**

Department of Electrical and Electronics Engineering, Faculty of Engineering and Natural Sciences, Antalya Bilim University, Dösemealti, 07190 Antalya, Turkiye

Carboxymethylcellulose (CMC)-coated superparamagnetic iron oxide nanoparticles (Fe_3O_4) have emerged as promising nanocarriers for targeted anticancer drug delivery [1]. This study presents a computational investigation of doxorubicin (Dox) release kinetics to elucidate diffusion behavior, release mechanisms, and pH-responsive therapeutic performance. Spherical CMC-Fe_3O_4 nanoparticles with an average diameter of 15 ± 5 nm and saturation magnetization (Ms) of 58 emu/g were evaluated. A Python-based computational pipeline was developed to process cumulative in vitro Dox release data obtained at pH 3.6 (tumor-mimicking acidic environment), pH 5.5 (endosomal condition), and pH 7.4 (physiological condition). Following automated preprocessing and unit normalization, release profiles were fitted using four kinetic models: pseudo-first-order, pseudo-second-order, Higuchi, and Korsmeyer–Peppas models through linear regression analysis.[2] The nanoparticles exhibited pronounced pH-dependent release characteristics. Maximum cumulative Dox release reached 11.77 ppm at pH 3.6, compared with 6.30 ppm at pH 5.5 and 3.56 ppm at pH 7.4, corresponding to a 3.3-fold enhancement under acidic conditions relative to physiological pH. At pH 3.6, the first-order kinetic model demonstrated the best fit (R^2 = 0.974), while the Korsmeyer–Peppas release exponent (n = 0.339) indicated a Fickian diffusion-controlled mechanism. This suggests that protonation of the CMC matrix in acidic media weakens drug–carrier interactions and facilitates rapid diffusion of Dox molecules from the nanoparticle surface. In contrast, Higuchi (R^2 = 0.987) and first-order (R^2 = 0.979) models best described the release behavior at pH 5.5 and pH 7.4, respectively. Corresponding Korsmeyer–Peppas exponents (n = 0.561 and 0.612) suggested a transition toward anomalous non-Fickian transport at higher pH values. The results confirm that Dox-loaded CMC-Fe_3O_4 nanocarriers preferentially release the drug under tumor-mimicking acidic conditions, highlighting their potential for pH-responsive precision cancer therapy. Furthermore, the extracted kinetic parameters provide a structured dataset for future machine learning-assisted inverse design of nanocarrier systems with tailored nanoscale release profiles.

References:

Sánchez-Orozco J.L., Meléndez-Ortiz H.I., Puente-Urbina B.A., Rodríguez-Fernández O.S., Martínez-Luévanos A., García-Cerda L.A. "Synthesis and Characterization of a pH- and Temperature-Sensitive Fe_3O_4-SiO_2-Poly(NVCL-co-MAA) Nanocomposite for Controlled Delivery of Doxorubicin Anticancer Drug." Polymers, 2023, 15(4), 968. https://doi.org/10.3390/polym15040968

Javanbakht S., Mohammadi R., Shokri M. "Carboxymethyl cellulose/ hydroxyapatite/ Fe_3O_4 bio-nanocomposite hydrogel beads: an efficient oral pH-responsive carrier for doxorubicin delivery." Chemical Papers, 2025, 79(4), 2461–2470. https://doi.org/10.1007/s11696-025-03944-6

Keyword: *Doxorubicin, Superparamagnetic, Drug release kinetics, Inverse design, Machine learning*

Investigation of Biomedical Applications of N-Vinylcaprolactam-Based Hydrogels and Their Composites

Tılsım Ayris Albay [*] [1], **Ozgur Ozay**[2]

[1] *Department of Bioengineering, School of Graduate Studies, Çanakkale Onsekiz Mart University, Çanakkale, Türkiye*
[2] *Department of Bioengineering, Faculty of Engineering, Çanakkale Onsekiz Mart University, Çanakkale Türkiye*

Today, traditional drug methods have some problems. They cannot control drug release and dosage. Because of this, treatment success is low. Also, old wound dressings have disadvantages. They cannot control moisture and cannot stop infections. Therefore, we need better biomaterials for controlled drug release and wound healing.Hydrogels are very popular in biomedical fields. They have high water capacity, biocompatibility, and adjustable mechanical properties. In this study, we aimed to develop functional hydrogels for biomedical use. We synthesized a hydrogel system using poly(vinyl alcohol) (PVA), 2-hydroxyethyl methacrylate (HEMA), and N-vinylcaprolactam (NVCL). We added Plantago ovata extract to this hydrogel. This extract improves the flexibility, water capacity, and functional properties of the hydrogel.We also added gold (Au) nanoparticles to increase the antimicrobial effect. We did not use toxic chemicals for this process. Instead, we used a green synthesis method. We chose kumquat (Citrus japonica) extract as a natural reducer because it has high polyphenol content.We tested the swelling behavior of the hydrogels in different liquids: deionized water, simulated gastric fluid (SGF), simulated saliva fluid (SSF), simulated body fluid (SBF), phosphate-buffered saline (PBS), and different pH conditions.In the second part, we designed another composite hydrogel system. We added zeolite clay to the hydrogel structure for wound dressing applications. We aimed to see the effects of this zeolite system on wound healing.Furthermore, we investigated antimicrobial and antioxidant activities to see the biological properties. A model drug was used to test the drug release system and the wound dressing material. For structural and morphological characterization, we used FTIR, XRD, TGA, SEM-EDX, and TEM analyses. We also used point of zero charge (PZC) analysis to find the surface charge properties.In conclusion, these new hydrogel systems show great potential. They can be alternative biomaterials for controlled drug release and wound dressing applications.

ORCID:
Tılsım Ayris Albay: 0009-0000-0962-1901
Ozgur Ozay: 0000-0001-6589-9844

Keyword: *Biomaterials, Hydrogels, N-vinylcaprolactam (NVCL)*

Development of Metal Organic Framework (MOF) Based Material for the Treatment of Triple Negative Breast Cancer

Zehra Canbulat Altun [*1,2], Beyza Nur Karakoc[3], Zafer Eroğlu[3,4], Melek Sermin Ozer[3], Gozde Korkmaz[1,5], Onder Metin[3]

[1] Koc University, Research Center for Translational Medicine (KUTTAM), Istanbul, Türkiye
[2] Graduate School of Health Sciences, Koc University, Istanbul, Turkiye
[3] Department of Chemistry, College of Sciences, Koç University, Istanbul, Türkiye
[4] Kocaeli University, Faculty of Arts and Sciences, Department of Chemistry, Kocaeli, Türkiye
[5] Koc University, School of Medicine, Istanbul, Türkiye

Triple-negative breast cancer (TNBC) is one of the deadliest cancers seen among women worldwide due to its aggressive nature and high metastatic risk. The absence of targetable hormone receptors makes conventional chemotherapies the primary treatment option, although it has limited efficacy and significant side effects. In this context, photodynamic therapy, which relies on molecular oxygen, a photosensitizer, and light, offers a promising alternative to current treatments, as it is a local and minimally invasive treatment option.

Within this framework, PCN222 heterostructured with Bismuthene (Bismuthene/PCN222) was synthesized and characterized by TEM, photoluminscence (PL), and UV-DRS analyses. In addition, its singlet oxygen generation was evaluated under 660 nm light irradiation. After confirming its photophysical properties and ROS-generating capability, in vitro studies were conducted in MDA-MB-231 cells to determine the optimum light exposure time and material concentration.

According to the initial results, a concentration of 50 µg/ml combined with 10 minutes of 660 nm light exposure at 25 mW/cm² was identified as the optimal condition. These parameters were further validated on a larger scale using the CellTiter-Glo and colony formation assays. Both assays demonstrated that Bismuthene/PCN22 exhibited cytotoxicity and anti-proliferative effects only under light irradiation, with no effects observed under dark conditions.

In addition, to the therapeutic potential of the nanoplatform, its gene delivery capacity was investigated using a gel retardation assay. Although our platform was not able to sufficiently bind plasmid DNA, surface modification with poly-l-lysine (PLL) enabled complex formation, indicating that the system can be adapted for possible gene delivery applications

Keyword: *Photodynamic Therapy, Triple Negative Breast Cancer, Metal Organic Frameworks*

Cell Count Optimization Using a Label-Free Interferometric Reflectance Imaging Sensor (IRIS)

Zg Özünal [*] [1], Ae Çetin[2], Ab Tuzcu[3], S Unlu[3], A Bilir[4]

[1] *İstanbul Atlas University, Faculty of Medicine, Department of Medical Pharmacology*
[2] *Dokuz Eylul University, Faculty of Medicine, Department of Biophysics*
[3] *Boston University, Department of Electrical and Computer Engineering*
[4] *İstanbul Atlas University, Faculty of Medicine, Department of Histology and Embryology*

Reliable cell quantification is essential in drug discovery, toxicity assessment, anticancer research, and tissue engineering. Conventional cell counting methods frequently rely on dyes, fluorescent labels, colorimetric reagents, or viability assays. While widely used, these approaches may interfere with cellular physiology, affect cell viability, increase experimental costs, and generate chemical waste. Furthermore, colored compounds and drug candidates can interfere with assay readouts, limiting analytical accuracy. The increasing emphasis on translational drug development, reduction of animal experiments, and sustainable laboratory practices highlights the need for objective, non-destructive, and label-free cell analysis technologies. Interferometric Reflectance Imaging Sensor (IRIS) technology is a label-free optical biosensing platform capable of detecting biological particles through changes in reflected light intensity on a silicon dioxide substrate. Beyond its established applications in biomolecular detection, IRIS has the potential to provide real-time cellular analysis under dynamic flow conditions. The aim of this study was to evaluate the feasibility of an IRIS-based microfluidic platform for in vitro cell count optimization and real-time cell monitoring without the use of labels or chemical reagents. The sensor consisted of a silicon/silicon dioxide (Si/SiO_2) chip containing laser-drilled inlet and outlet ports. Chips were cleaned, coated with MCP-2 polymer, and assembled into a microfluidic flow chamber. Human gingival fibroblast (HGF-1) cells were cultured in Dulbecco's Modified Eagle Medium (DMEM) under standard conditions (37°C, 5% CO_2). Cell suspensions with predefined concentrations were prepared and quantified using a Thoma hemocytometer prior to analysis. Cells were introduced into the microfluidic chamber, and the sensor surface was continuously perfused with culture medium at a controlled flow rate. Images were acquired every 1–3 seconds, enabling dynamic visualization and quantification of cells passing through the sensing area. Cell counts obtained from IRIS image analysis were compared with reference counts generated by the Thoma hemocytometer. The platform successfully detected and quantified cells in real time without requiring fluorescent dyes, viability markers, or additional chemical reagents. By combining continuous image acquisition with known flow parameters, the system enabled quantitative assessment of cell passage and optical signal generation while preserving cell integrity. These findings demonstrate that IRIS-based cell counting represents a non-destructive, reagent-free, and environmentally sustainable alternative to conventional cell counting methods. The integration of optical biosensing with microfluidics offers a promising approach for automated cell analysis and translational drug development, supporting more objective and greener in vitro testing strategies for future biomedical and nanotechnology applications.

Acknowledgment:
The authors would like to thank Ennur Ak for valuable technical assistance and support in laboratory procedures throughout the study.

ORCID:
Zg Özünal: 0000-0002-3060-1507

References:
Avci, O., Lortlar Ünlü, N., Yalçın Özkumur, A., & Ünlü, M. S. (2015). Interferometric reflectance imaging sensor (IRIS)—a platform technology for multiplexed diagnostics and digital detection. Sensors, 15(7), 17649-17665.
Martinez-Banderas A, Malki A, Froehlich T ... High-performance nanobiosensing technologies for future diagnostic needs Trends in Biotechnology, 2025; 43, 3088-3104

Keyword: *label-free cell counting, optical biosensor, fibroblast*

Design and Development of Magnetic and Thermo-Responsive Polymeric Nanomaterials for Hyperthermia-Induced Controlled Drug Delivery

Muhammad Arsyik Kurniawan, Önder Topel *

Department of Chemistry, Faculty of Sciences, 07058, Akdeniz University, Antalya TÜRKİYE

This study explains in detail the development of magnetic and temperature-responsive polymeric nanomaterials designed for hyperthermia-induced drug delivery applications. Magnetic nanoparticles (MNPs), synthesized via a co-precipitation method to act as supports, were successfully modified with temperature-responsive poly(ethylene glycol)–b–poly(2–(dimethylamino)ethyl methacrylate) (PEG–b–PDMAEMA) block copolymers. The structural, morphological, and magnetic properties of the MNPs were thoroughly characterized using DLS, TEM, XRD, VSM, FTIR, and TGA. The PEG–b–PDMAEMA copolymers with different block lengths were synthesized via Atom Transfer Radical Polymerization (ATRP) and confirmed by FTIR, ^{1}H-NMR, and GPC analyses. Lower Critical Solution Temperature (LCST) measurements identified PEG_{44}–b–$PDMAEMA_{93}$ as the most compatible formulation for MNP modification. Successful surface encapsulation provided a protective polymer shell approximately 5 nm thick, accounting for 5.26 wt% of the composite nanomaterial. Additionally, the ATRP polymerization mechanism and the specific MNP-copolymer coordination pathways were theoretically analyzed and validated using Density Functional Theory (DFT) calculations. Hyperthermia performance under an alternating current magnetic field (ACMF) at 0.745 kA/m and 120 kHz was optimized for both bare and modified MNPs at 25°C and 37°C. Finally, the controlled release profiles of doxorubicin (DOX) under hyperthermia conditions were investigated at pH 5.5 and 7.4. The engineered nanocarrier demonstrated highly efficient, pH-dependent release profiles, achieving maximum cumulative release value of 43.06% for DOX under acidic tumor-mimicking environments (pH 5.5). This smart nanoplatform exhibits excellent potential for advanced magneto-chemotherapeutic systems.

Acknowledgment:
The authors acknowledge the Akdeniz University Coordination Unit of Scientific Research Projects (project no. FBA-2024-6519) for their financial support.

ORCID:
Muhammad Arsyik Kurniawan: 0000-0001-5463-4074
Önder Topel: ondertopel@akdeniz.edu.tr

Keyword: *Magnetic nanoparticles, ATRP, Temperature-responsive copolymer, Magnetic Hyperthermia, Drug delivery*

The use of poly(3-sulfopropyl acrylate-co-1-vinyl imidazole)/xanthan gum@Ag nanocomposites modified with cationic groups in wound healing

Özgür Özay [*1], **Dilara Gokkaya**[2]

[1] *Laboratory of Biomaterials Research, Department of Bioengineering, Faculty of Engineering, Çanakkale Onsekiz Mart University, Çanakkale, Türkiye.*

[2] *Laboratory of Biomaterials Research, Department of Bioengineering, School of Graduate Studies, Çanakkale Onsekiz Mart University, Çanakkale, Türkiye*

Effective wound management requires multifunctional biomaterials rather than single-target approaches. This study introduces a smart, pH-responsive hydrogel matrix designed to address the dynamic microenvironment of healing tissues. A poly(3-sulfopropyl acrylate-co-1-vinyl imidazole)/xanthan gum [p(SPA-co-VI)/XG] semi IPN hydrogel network was synthesized, where the selective protonation of the vinyl imidazole moieties imparted smart pH-responsive characteristics to the matrix. To integrate antimicrobial and antioxidant properties, spherical silver nanoparticles (12.3±2.9 nm) were successfully synthesized in situ within the matrix using a green, Echinacea purpurea-mediated plant-mediated synthesis method. Comprehensive structural and thermal characterizations confirmed the stable integration of nanocomposite architecture. Dual-drug delivery studies revealed complementary release behavior: penicillin followed zero-order kinetics suitable for immediate antimicrobial action (77.1% release), whereas diclofenac exhibited a controlled, sustained release profile (25.5%) driven by matrix swelling and relaxation dynamics over 12 hours. The resulting wound dressing demonstrated selective, contact-active antibacterial efficacy against Gram-positive pathogens (B. subtilis and S. aureus) alongside strong antioxidant activity. By combining pH-responsiveness, targeted dual-drug release, and oxidative stress control within a single matrix, this biocompatible platform offers a holistic and sustainable strategy for advanced wound care.

Acknowledgment:
TUBİTAK (Program 2224-B)

ORCID:
Özgür Özay: 0000-0001-6589-9844
Dilara Gokkaya: 0009-0007-5679-2907

Keyword: *Drug release, Nanocomposite, Cationic hydrogel*

Development of Colon-Targeted Fe3O4-Loaded Alginate Hydrogel Beads Containing Brassica oleracea L. Extract and 5-Fluorouracil for Enhanced Anticancer Activity

İlknur Atlı [*] [1], Selcen Cakır[2], Tılsım Ayris Albay[1], Ozgur Ozay[3]

[1] *Department of Bioengineering, School of Graduate Studies, Çanakkale Onsekiz Mart University, Çanakkale, Türkiye*
[2] *School of Health Services Vocational College, Medical Services and Techniques, Canakkale Onsekiz Mart University*
[3] *Department of Bioengineering, Faculty of Engineering, Çanakkale Onsekiz Mart University, Çanakkale, Türkiye*

Colon cancer remains one of the leading causes of cancer-related mortality worldwide, while the efficacy of conventional chemotherapy is often limited by systemic toxicity and inadequate drug accumulation at the tumor site. In this study, developed was a novel magnetic hydrogel bead system based on alginate for the co-delivery of 5-fluorouracil (5-FU) and Brassica oleracea L. extract. Incorporated into the hydrogel matrix were Fe_3O_4 magnetic nanoparticles, providing magnetic responsiveness together with controlled drug release capability. Confirmed by SEM and TEM analyses were the successful formation of the hydrogel beads and the effective incorporation of magnetic nanoparticles within the polymeric network. Demonstrated by VSM measurements was the superparamagnetic behavior of the developed formulation. Evaluated in simulated gastrointestinal fluids (SGF, SIF, and SCF) were the swelling and drug release behaviors of the hydrogel beads. Minimal release was observed under gastric conditions and limited release in the intestinal environment, whereas enhanced and sustained release occurred under simulated colonic conditions. Supported by these findings was the colon-targeting potential of the developed carrier system. Assessed on HT-29 human colon cancer cells was the antiproliferative activity of the formulation using the MTT assay. Significantly reduced cell viability was observed following treatment with the dual-loaded magnetic hydrogel beads when compared with untreated controls. Suggested by the results was a synergistic anticancer effect between 5-FU and Brassica oleracea extract. Presented herein is a promising colon-targeted drug delivery platform capable of combining controlled release, magnetic guidance, and chemo-phytotherapeutic activity for the treatment of colorectal cancer.

Acknowledgment:
The authors gratefully acknowledge the financial support provided by the TÜBİTAK 2224-B Domestic Scientific Events Participation Support Program for conference participation.

ORCID:
İlknur Atlı: 0009-0003-1804-4036
Selcen Cakır: 0000-0002-6474-9032
Tılsım Ayris Albay: 0009-0000-0962-1901
Ozgur Ozay: 0000-0001-6589-9844

Keyword: *Colorectal cancer, Brassica oleracea L. extract, magnetic hydrogel beads*

An Innovative Approach to Opioid Overdose Emergency Intervention: Development of Naloxone-Loaded ZIF-8 Nanoplatform

İrem Avcı * **, Gülümsernur Can, Mustafa Nakipoglu**

Department of Molecular Biology and Genetics, Faculty of Science, Bartın University, 74100, Bartın, Türkiye

Opioid overdose, which has evolved into a global public health crisis, causes hundreds of thousands of deaths annually. The clinical efficacy of naloxone, the gold standard antidote, is severely limited by its short half-life (30-90 minutes). The prolonged effect of opioids in the body leads to the recurrence of respiratory depression and necessitates multiple naloxone doses, thereby increasing the risk of toxicity. To overcome this clinical bottleneck, this study aims to develop a biocompatible nanocarrier system that will provide a long-acting (20-24 hours) and controlled release of naloxone through a single-dose administration. As the carrier platform, Zeolitic Imidazolate Framework-8 (ZIF-8) metal-organic frameworks (MOFs) were selected due to their exceptional specific surface area, tunable pore architecture, and biocompatibility. ZIF-8 nanoparticles were successfully synthesized at room temperature in a methanol medium using zinc nitrate and 2-methylimidazole precursors. X-ray diffraction (XRD) analyses conclusively proved that the synthesized material exhibits high purity and the characteristic ZIF-8 crystal structure. N_2 adsorption/desorption (BET) isotherms revealed that the nanoplatform possesses an excellent microporous structure (Type I isotherm), reaching a specific surface area of 1368.1 m^2/g and a total pore volume of 0.50 cm^3/g. Furthermore, an average pore radius of ~1.68 nm (16.86 Å) confirms that this high-capacity porous network offers an ideal thermodynamic environment for the highly efficient encapsulation of naloxone molecules. Scanning electron microscopy (SEM) examinations demonstrated that the particles are distributed at the nanoscale with a homogeneous morphology. This pioneering study, representing the first use of ZIF-8 for naloxone delivery in the scientific literature, highlights the potential of smart nanomaterials in emergency medicine applications. Following in vitro release optimizations, this molecularly designed, innovative detoxification system is projected to translate into a commercializable, next-generation emergency intervention product.

Acknowledgment:
This work was funded by Health Institutes of Türkiye (TÜSEB) under project number 44688.

ORCID:
İrem Avcı: 0009-0009-9093-8898
Gülümsernur Can: 0009-0007-1779-5099
Mustafa Nakipoglu: 0000-0001-6423-2917

References:

Boyer, E. W. (2012). Management of Opioid Analgesic Overdose. New England Journal of Medicine, 367(2), 146–155. https://doi.org/10.1056/NEJMra1202561

Giliopoulos, D., Zamboulis, A., Giannakoudakis, D., Bikiaris, D., & Triantafyllidis, K. (2020). Polymer/Metal Organic Framework (MOF) Nanocomposites for Biomedical Applications. Molecules, 25(1), 185. https://doi.org/10.3390/molecules25010185

Kerensky, T., & Walley, A. Y. (2017). Opioid overdose prevention and naloxone rescue kits: what we know and what we don't know. Addiction Science & Clinical Practice, 12(1), 4. https://doi.org/10.1186/s13722-016-0068-3

Britch, S. C., & Walsh, S. L. (2022). Treatment of opioid overdose: current approaches and recent advances. Psychopharmacology, 239(7), 2063–2081. https://doi.org/10.1007/s00213-022-06125-5

Madison, C. A., Arora, M., Kumar, M. N. V. R., & Eitan, S. (2020). Novel Oral Nanoparticle Formulation of Sustained Release Naloxone with Mild Withdrawal Symptoms in Mice. ACS Chemical Neuroscience, 11(13), 1955–1964. https://doi.org/10.1021/acschemneuro.0c00141

Keyword: *Emergency medicine, Metal organic framework, Naloxone*

Generation of Bilayer Oxygen Delivery Antimicrobial Hydrogels for Wound Dressing Applications

Dilek Tepeli * **, Nermin Seda Kehr**

Department of Chemistry, İzmir Institute of Technology, Urla, İzmir, Türkiye

Generation of Bilayer Oxygen Delivery Antimicrobial Hydrogels for Wound Dressing Applications

Traditional wound dressings are often inadequate for addressing bacterial infections, persistent inflammation, and severe oxygen deficiency in wounds. In chronic wounds, impaired vascularization limits oxygen delivery, while increased oxygen consumption by pathogens and immune cells creates hypoxic conditions (<1% O_2). This oxygen deficiency is a major factor contributing to delayed wound healing. This study introduces a multifunctional bilayer hydrogel wound dressing designed to address these challenges by integrating oxygen production, oxygen transport, and antibacterial properties within a 3D-printed bilayer hydrogel system. The system consists of an upper alginate layer loaded with oxygen-releasing CaO_2 and a lower antibacterial polymer layer containing perfluorocarbon-based oxygen-adsorbing and transporting nanoparticles (PMOF). The synthesized PMOF nanoparticles were characterized using scanning electron microscopy (SEM), dynamic light scattering (DLS), and zeta potential analysis. The resulting scaffold demonstrates 3D printability as well as improved mechanical strength and degradation properties. Under hypoxic conditions, the system achieves continuous oxygen release. The bilayer hydrogel exhibits strong antibacterial activity against Gram-positive S. aureus and moderate activity against Gram-negative E. coli. In vitro studies demonstrated that the bilayer scaffold supported cell viability under hypoxic conditions while maintaining oxidative cellular compatibility. Furthermore, the scaffold promoted wound healing by accelerating wound closure in both normoxic and hypoxic environments.

ORCID:
Dilek Tepeli: https://orcid.org/0000-0002-5347-7254

Keyword: *Bilayer hydrogel, antimicrobial agent, oxygen delivery, hypoxia, wound dressing*

Plasmonic-Enabled Edible Soft Biorobots for Targeted Sampling and Molecular Detection

Hayrettin Oner [*] [1,2], Gorkem Liman[2], Gokhan Demirel[2]

[1] *Graduate School of Natural and Applied Sciences, Gazi University, Ankara, Türkiye*
[2] *Department of Chemistry, Gazi University, Ankara, Türkiye*

Soft robotics is increasingly moving toward biocompatible and even edible systems. However, combining controlled actuation, targeted sampling, and molecular diagnostics within a single platform remains challenging. Here, we report an edible, magnetically controllable soft biorobotic platform based on egg white protein (EWP) for active in-situ molecular sensing. The structural matrix is derived from EWP, providing excellent biocompatibility and tunable mechanical properties. Magnetic actuation is achieved by incorporating strontium hexaferrite ($SrFe_{12}O_{19}$) microparticles, enabling programmable and reversible motion under external magnetic fields. Mechanical stiffness is further tuned through secondary ionic crosslinking with multivalent cations (i.e., Na^{+}, K^{+}, Ca^{2+}, Mg^{2+}, Fe^{3+}, and Al^{3+}). For molecular sensing, the sharp tips of the screw-shaped robots are functionalized with plasmonic nanostructures, including gold nanoparticles, gold nanostars, and PVD-deposited gold nanofilms. Under magnetic fields, the platforms exhibit stable directional movement in fluids with a wide range of viscosity (1–100 cP) and can penetrate hydrogel targets, enabling minimally invasive sampling. Surface-enhanced Raman spectroscopy (SERS) measurements show strong signal enhancement and high signal-to-noise ratios for model analytes such as methylene blue, rhodamine 6G, and malachite green, directly at the sampling site. Additionally, the EWP-based platforms undergo controlled enzymatic degradation in the presence of pepsin. Overall, this work demonstrates a multifunctional edible biorobotic system that integrates magnetic actuation with plasmonic sensing. The platform offers a promising, minimally invasive approach for targeted sampling and real-time molecular diagnostics, addressing key limitations of current soft robotic systems.

Acknowledgment:
This work was supported by the Scientific and Technological Research Council of Türkiye (TUBITAK) (grant no: 22AG056)

ORCID:
Hayrettin Oner: https://orcid.org/0009-0000-0691-0003
Gorkem Liman: https://orcid.org/0000-0002-0778-9783
Gokhan Demirel: https://orcid.org/0000-0002-9778-917X

References:
Kim, Y., & Zhao, X. (2022). Magnetic soft materials and robots. Chemical reviews, 122(5), 5317-5364
Ceylan, H., Dogan, N. O., Yasa, I. C., Musaoglu, M. N., Kulali, Z. U., & Sitti, M. (2021). 3D printed personalized magnetic micromachines from patient blood–derived biomaterials. Science advances, 7(36), eabh0273
Zhang, S., Kwak, B., Zhu, R., Pankhurst, M., Zhang, L., Boom, R. M., & Floreano, D. (2025). Edible aquatic robots with Marangoni propulsion. Nature Communications, 16(1), 4238
Floreano, D., Kwak, B., Pankhurst, M., Shintake, J., Caironi, M., Annese, V. F. & Boom, R. M. (2024). Towards edible robots and robotic food. Nature Reviews Materials, 9(8), 589-599
Gervasoni, S., Terzopoulou, A., Franco, C., Veciana, A., Pedrini, N., Burri, J. T. & Pané, S. (2020). CANDYBOTS: a new generation of 3D-printed sugar-based transient small-scale robots. Advanced Materials, 32(52), 2005652

Keyword: *In Situ Molecular Sensing*, *Soft Robotics*, *Edible Robots*

Interactions and Adhesion Capabilities of Extracellular Vesicles Produced by Probiotic Bacteria in Bladder Cancer Cells

Mehmet Aytar [*1], **Demet Yalcin**[1], **Gulen Melike Demirbolat**[2], **Ozge Cevik**[3]

[1] *ADU-Science and Technology Application and Research Center, Aydin Adnan Menderes University, Aydin, Turkey*
[2] *Department of Pharmaceutical Technology, Faculty of Pharmacy, Acibadem Mehmet Ali Aydınlar University, İstanbul, Turkey*
[3] *Department of Medicinal Biochemistry, School of Medicine, Aydin Adnan Menderes University, Aydin, Turkey*

Bacterial cells communicate not only through direct contact but also by secreting metabolites, lipoglycans, quorum sensing peptides, nucleic acids, proteins, and bacterial extracellular vesicles (BEVs). BEVs, which are spherical and membrane-bound particles ranging in diameter from 20-400 nm, transport a portion of the host bacterium's biological content into the extracellular environment. In this study, the interactions of BEVs from Lactobacillus sakei, Lactobacillus plantarum, and Pediococcus acidilactici strains with bladder tumor cells were investigated. BEVs from Lactobacillus sakei, Lactobacillus plantarum, and Pediococcus acidilactici strains were purified by ultracentrifugation and subjected to zeta-size analysis. The microscopic interactions, cell viability, and adhesion percentages of these BEVs and bacteria were determined in non-muscle-invasive bladder tumor (UM-UC-3) cells. The BEVs were found to have dimensions below 200 nm and charges close to -30 mV. All three bacteria were observed to interact with UMUC-3 cells, with P. acidilactici showing the highest adhesion percentage. The BEVs of lactic acid bacteria strains were found to have a significant effect on bacterial adhesion in bladder tumor cells.

In conclusion, BEVs have been shown to be an effective tool for evaluating adhesion tendencies, particularly in the treatment of non-muscle invasive bladder cancer types, and in terms of mammalian cell-bacterial interaction. In this context, probiotic bacteria and the EVs released from them, with their superior natural structures and cellular interaction capacities, can be a tool that supports the development of innovative and reliable therapeutic approaches in bladder cancers. Specifically, BEVs produced by probiotic bacteria can shed light on innovative approaches for bladder cancers, such as vaccine development and targeted delivery of therapeutic molecules.

Acknowledgment:
Financial support by the partly TUBITAK-(124S213) is acknowledged.

ORCID:
Mehmet Aytar: 0000-0002-8083-7358
Demet Yalcin: 0000-0003-3255-3753
Gulen Melike Demirbolat: 0000-0001-5621-5818
Ozge Cevik: 0000-0002-9325-3757

Keyword: *Extracellular vesicles, bladder cancer, probiotic, extracellular environment, cell-bacterial interaction*

Development of Gelatin-Based Hydrogel Inks Loaded with Silver Nanoparticles for 3D Printing

Melike Tuncer [*] [1], **Kemal Çetin**[2], **Gökalp Özmen Güler**[3]

[1] *Department of Biomedical Engineering, Institute of Science, Necmettin Erbakan University, Konya, Türkiye*
[2] *Department of Biotechnology, Faculty of Science, Necmettin Erbakan University, Konya, Türkiye*
[3] *Department of Biology Education, Ahmet Kelesoglu Faculty of Education, Necmettin Erbakan University, Konya, Türkiye*

Hydrogels are widely used in biomedical and tissue engineering applications due to their high water content and structural similarity to the natural extracellular matrix (ECM) [3]. Casting and molding, which are traditional hydrogel production methods, generally provide limited control over the structure's geometry and the internal structure of the hydrogels [5]. In contrast, 3D printing enables the precise fabrication of custom-designed structures, driving an increasing demand for advanced biomaterial inks with enhanced functionality [2]. Among various hydrogel systems, gelatin-based biomaterials have attracted considerable attention due to their excellent biocompatibility and their ability to mimic the native extracellular matrix [4]. Furthermore, the incorporation of functional additives can improve the performance of hydrogel-based platforms for biomedical applications. Silver nanoparticles (AgNPs) are particularly attractive due to their well-known antimicrobial activity [1]. In recent years, green synthesis approaches have emerged as sustainable alternatives to conventional nanoparticle production methods by minimizing the use of hazardous chemicals and reducing environmental impact. In this study, AgNPs were synthesized using an environmentally friendly green synthesis approach and incorporated into gelatin-based hydrogel formulations developed for extrusion-based 3D printing applications. The synthesized nanoparticles were characterized using UV–Vis spectroscopy, X-ray diffraction (XRD), zeta potential analysis, field-emission scanning electron microscopy (FE-SEM), and energy-dispersive X-ray spectroscopy (EDX/EDS). UV–Vis analysis revealed a characteristic surface plasmon resonance (SPR) absorption peak at approximately 425 nm, confirming the successful formation of AgNPs. XRD analysis further verified the crystalline structure of the nanoparticles, with characteristic diffraction peaks observed at 2θ values of 38.40°, 64.44°, and 77.30°, corresponding to the (111), (220), and (311) crystal planes, respectively. Furthermore, the synthesized AgNPs exhibited a zeta potential value of −46.17 mV, indicating excellent colloidal stability and a low tendency toward agglomeration. EDX analysis revealed a distinct silver signal at approximately 3 keV, further confirming the presence of silver nanoparticles. The results confirmed the successful synthesis of AgNPs with suitable physicochemical properties and good colloidal stability. Following nanoparticle synthesis, AgNP-containing hydrogel formulations were prepared and optimized for 3D printing. Physicochemical and structural characterization studies are currently being conducted to evaluate the properties of the developed constructs. Overall, the integration of green-synthesized AgNPs into printable hydrogel systems represents a promising and sustainable strategy for the development of multifunctional bioinks and advanced biofabrication platforms for future biomedical applications.

This study was financially supported by the Scientific Research Projects Coordination Unit of Necmettin Erbakan University (Project No. 24GAP19011).

Acknowledgment:
This study was financially supported by the Scientific Research Projects Coordination Unit of Necmettin Erbakan University (Project No. 24GAP19011).

ORCID:
Melike Tuncer: 0009-0008-7769-1176
Kemal Çetin: 0000-0002-7393-7377
Gökalp Özmen Güler: 0000-0003-4771-2489

References:

1. Ashtariyan, H. Mollania, N. Annabestani, N. Mollania, F. Malayjerdi, M. Dolatabadi, E. R. Ghomi, A. Khoshsima, and R. E. Neisiany, "Synergistic effect of Cydonia oblonga and its extracted silver nanoparticles for improving antioxidant and antibacterial activity of 3D printed alginate-based hydrogel as wound dressing," International Journal of Biological Macromolecules. 2024.
2. Z. Chen, D. Zhao, B. Liu, G. Nian, X. Li, J. Yin, S. Qu, and W. Yang, "3D printing of multifunctional hydrogels," Advanced Functional Materials. 2019.
3. G. Guan, Q. Lv, S. Liu, Z. Jiang, C. Zhou, and W. Liao, "3D-Bioprinted peptide coupling patches for wound healing," Materials Today Bio. 2022.
4. P. Guan, C. Liu, D. Xie, S. Mao, Y. Ji, Y. Lin, Z. Chen, Q. Wang, L. Fan, and Y. Sun, "Exosome-loaded extracellular matrix-mimic hydrogel with anti-inflammatory property facilitates/promotes growth plate injury repair," Bioactive Materials. 2022.
5. J. Liu, J. Garcia, L. M. Leahy, R. Song, D. Mullarkey, B. Fei, A. Dervan, I. V. Shvets, P. Stamenov, W. Wang, F. J. O'Brien, J. N. Coleman, and V. Nicolosi, "3D printing of multifunctional conductive polymer composite hydrogels," Advanced Functional Materials. 2023.

Keyword: *3D printing, Biomaterial ink, Green synthesis, Hydrogel, Silver nanoparticles*

Phage Display-Selected Mineral-Forming Peptides for Biomimetic Enamel Remineralization

Mert Can Akyol * **, Deniz Tanıl Yücesoy, Hümeyra Taşkent Sezgin**

Bioengineering Department, Izmir Institute of Technology, İzmir, Türkiye

Dental diseases are among the most prevalent diseases worldwide. Among these, white spot lesions (WSLs) are the early enamel lesions caused by the demineralization of the enamel tissue, the outermost layer of tooth. If left untreated they progress to cavitated lesions that may end up with aesthetic concerns and ultimately tooth loss. Enamel demineralization is characterized by the progressive loss of hydroxyapatite, the primary calcium phosphate mineral of dental enamel mainly due to bacterial activity and acidic dietary exposure. Therefore, restoring lost enamel mineral before irreversible damage occurs, is of great clinical importance. This study aimed to investigate the reversibility of enamel demineralization and to develop a biomimetic peptide-based strategy for enamel remineralization. Mineral-forming peptides were identified using a phage display-based peptide screening. Four biopanning rounds of phage display were performed to enrich phages displaying peptides with high mineral-forming ability. 50 individual plaques selected from the enriched phage clones of the fourth round of biopanning were propagated in bacterial culture, and DNA from each selected phage was isolated. The peptides from these 50 phages were sequenced. Mineralization kinetics of the 50 peptides on phages were monitored using UV-Vis spectroscopy. 11 unique peptide sequences exhibited mineral-forming activity through different kinetic mechanisms. Subsequently, minerals formed by these 11 peptides were characterized with scanning electron microscopy (SEM), X-ray diffraction (XRD) and Fourier transform infrared spectroscopy (FTIR) to determine their morphology, composition and crystallinity. The identified peptides demonstrate potential of biomimetic peptide-mediated mineralization as a promising strategy for enamel remineralization and the prevention of early-stage white spot lesions.

ORCID:
Mert Can Akyol: 0009-0005-6923-1135

Keyword: *Dental Diseases, Phage Display, Biomaterials*

Development of Cellulose Nanocrystal Reinforced Hydroxyapatite/Chitosan/Gelatin Nanobiocomposite Scaffolds for Bone Tissue Engineering Applications

Nazli Buket Yilmaz [*1], **Deniz Genc**[2], **Elif Vargun**[1]

[1] *Mugla Sitki Kocman University, Faculty of Science, Chemistry Department, Mugla, Türkiye*
[2] *Mugla Sitki Kocman University, Faculty of Health Science, Department of Pediatric Nursery, Mugla, Türkiye*

The development of biocompatible, biodegradable, and mechanically robust scaffold systems is of great importance in bone tissue engineering (1,2). In this study, hydroxyapatite (HAp), chitosan, and gelatin-based nanobiocomposite scaffolds were fabricated, and the effects of cellulose nanocrystal (CNC) and tannic acid (TA) incorporation at different concentrations on scaffold properties were investigated. In addition, the contribution of glutaraldehyde (GA) crosslinking agent to the structural integrity and mechanical properties of scaffolds was investigated. The fabrication of advanced biomimetic composite scaffolds was targeted by utilizing the high surface area and reinforcing capability of CNC (3), the antioxidant property of tannic acid, and the crosslinking mechanism provided by GA. The scaffolds were produced using solution mixing followed by freeze-drying.

The chemical, morphological, thermal, and mechanical properties of the fabricated scaffolds were characterized by Fourier-transform infrared spectroscopy (FTIR), scanning electron microscopy (SEM), thermogravimetric analysis (TGA), differential scanning calorimetry (DSC), and mechanical testing. FTIR analyses confirmed the molecular interactions among scaffold components and the tannic acid-mediated crosslinking mechanism. SEM observations revealed highly interconnected porous structures, while CNC incorporation contributed to the formation of a more homogeneous and integrated microstructure. TGA and DSC results demonstrated that the addition of CNC and tannic acid improved the thermal and structural stability of the scaffolds. Furthermore, mechanical analyses indicated that CNC acted as an effective reinforcing nanomaterial, significantly enhancing the mechanical performance of the composite structures, consistent with previous reports on nanocellulose-reinforced biomaterials (3).

In conclusion, the developed CNC- and tannic acid-reinforced HAp/chitosan/gelatin-based scaffolds exhibited improved physical, thermal, and mechanical properties, highlighting their potential for bone tissue engineering applications (1,2). These findings suggest that the developed nanobiocomposite scaffolds are promising candidates for future biomedical applications.

This study was supported by the Scientific Research Projects Coordination Office of Muğla Sıtkı Koçman University under Graduate Thesis Project No. YLTP-25/53.

Acknowledgment:
We gratefully acknowledge the support of the Scientific Research Projects Coordination Office of Muğla Sıtkı Koçman University through Graduate Thesis Project No. YLTP-25/53.

ORCID:
Nazli Buket Yilmaz: 0009-0007-7755-0843
Deniz Genc: https://orcid.org/0000-0003-0351-2805
Elif Vargun: https://orcid.org/0000-0003-4555-3699

References:
Bose, S., Roy, M., & Bandyopadhyay, A. (2012). Recent advances in bone tissue engineering scaffolds. Trends in Biotechnology, 30(10), 546–554. https://doi.org/10.1016/j.tibtech.2012.07.005
George, J., & Sabapathi, S. N. (2015). Cellulose nanocrystals: Synthesis, functional properties, and applications. Nanotechnology, Science and Applications, 8, 45–54. https://doi.org/10.2147/NSA.S64386
Lin, N., & Dufresne, A. (2014). Nanocellulose in biomedicine: Current status and future prospect. European Polymer Journal, 59, 302–325. https://doi.org/10.1016/j.eurpolymj.2014.07.025

Keyword: *Bone tissue engineering, scaffold, cellulose nanocrystal*

Anodization of Ti13Nb13Zr Alloy for Total Hip Replacement Applications

Olgu Çağan Özonuk [*1], Muhammed Zahid Doğan[2], Merve Gültekinoğlu[2], Eylül Yarar[2,3], Cem Bayram[2], Batur Ercan[1,4]

[1] *Department of Metallurgical and Materials Engineering, Middle East Technical University, 06800 Ankara, Turkeyy*
[2] *Hacettepe University, Graduate School of Science and Engineering, Department of Nanotechnology and Nanomedicine, Ankara*
[3] *OSTİM Technical University, Department of Nanotechnology Engineering, Ankara, Türkiye*
[4] *BIOMATEN, METU Center of Excellence in Biomaterials and Tissue Engineering, 06800 Ankara, Turkey*

Titanium and its alloys are widely used in orthopedic applications due to their excellent corrosion resistance and favorable mechanical properties. However, their bioinert nature necessitates further surface modifications to enhance osseointegration and long-term implant stability [1]. Among various surface modification techniques, anodization is a promising approach for improving the biological performance of titanium alloys by producing nanostructured oxide layers that enhance cellular interactions [2]. Ti13Nb13Zr is a dual-phase titanium alloy with a significantly lower elastic modulus than commercially pure titanium and most conventional titanium alloys, thereby reducing the stress shielding effect in orthopedic applications [3]. In this study, a nanoporous oxide layer was fabricated on Ti13Nb13Zr alloy by anodization, and its surface characteristics and biological performance were investigated for orthopedic applications. Anodization was performed in an ethylene glycol electrolyte containing 0.3 M NH_4F at 40, 50, 60, and 70 V for 4 min. The anodized surfaces were characterized using SEM (Scanning Electron Microscopy), XPS (X-ray Photoelectron Spectroscopy), TEM (Transmission Electron Microscopy), AFM (Atomic Force Microscopy), and WCA (water contact angle) measurements. For the biological evaluation, MC3T3-E1 cells were cultured in Dulbecco's Modified Eagle Medium (DMEM) supplemented with 10% fetal bovine serum (FBS), 1% penicillin–streptomycin, and 1% L-glutamine under standard culture conditions (37 °C, 5% CO_2). Before cell seeding, the samples were sterilized by immersion in 70% ethanol for 15 min, followed by ultraviolet irradiation for 30 min. Cell viability was evaluated after 1, 3, and 5 days using the MTT assay, while cell morphology was examined by staining F-actin filaments and nuclei with rhodamine and DAPI, respectively. Nanoporous oxide layers were successfully fabricated on the Ti13Nb13Zr surfaces, with average pore diameters of 51.0 ± 9.1, 55.9 ± 8.6, 62.4 ± 12.7, and 74.8 ± 16.2 nm for the 40, 50, 60, and 70 V samples, respectively. The nanoscale roughness increased nearly four-fold, with RMS values of 1.37 ± 0.08 nm for the as-polished surface and 5.12 ± 1.51 nm for the 40 V anodized surface. Moreover, the MTT assay confirmed that the anodized Ti13Nb13Zr surfaces exhibited no cytotoxicity toward MC3T3-E1 cells during the 5-day culture period. In addition, MC3T3-E1 cells showed improved spreading and proliferation on the anodized surfaces compared with the non-anodized alloy. These findings demonstrate that anodization effectively enhances the surface characteristics and cytocompatibility of Ti13Nb13Zr alloy, highlighting its potential for orthopedic implant applications.

Acknowledgment:
We would like to acknowledge TUBITAK project no 22AG049 for funding.

References:
[1] Abd-Elaziem W. et al., 2024, doi.org/10.1016/j.matdes.2024.112850
[2] Webster T.J. et al., 2003, doi.org/10.1016/j.biomaterials.2003.12.002
[3] Cvijovic-Alagic et al., 2014, doi.org/10.1016/j.corsci.2014.02.017

Keyword: *Osseointegration, Anodization, Orthopedic Implants*

Handheld Electrospinning-Assisted In Situ Deposition of Silk Fibroin Fibrous Dressings for Wound Healing Applications

Rumeysa Bilginer Kartal [*] [1,2], **Burçin İzbudak**[2,3], **Ayça Bal Öztürk**[1,2,4]

[1] *Stem Cell and Tissue Engineering Application and Research Center (ISUKOK), Istinye University, Istanbul, 34396, Turkey*
[2] *AdBioInk Biosystem Technology, Kocaeli,Turkey,41470*
[3] *Department of Stem Cell and Tissue Engineering, Institute of Graduate Education, Istinye University, Istanbul, 34396, Turkey*
[4] *Faculty of Pharmacy, Department of Analytical Chemistry, Istinye University, Istanbul, 34396, Turkey*

Wound dressing materials are expected to provide biocompatibility, adequate mechanical integrity, controlled fluid exchange, and a microenvironment that supports cell migration and tissue regeneration. In situ electrospinning has emerged as a promising strategy for wound dressing applications, as it enables the direct deposition of fibrous matrices onto wound sites and provides effective surface coverage. When appropriately formulated, electrospun fibrous structures can create a favorable microenvironment that supports wound healing. In this context, natural biomaterials have attracted considerable attention due to their inherent biocompatibility and bioactive properties. Among them, silk fibroin (SF) stands out as a promising candidate owing to its remarkable biocompatibility, suitability for fibrous scaffold fabrication, and potential to support cellular responses involved in tissue repair. In this study, SF-based fibrous wound dressing was developed using a handheld electrospinning technique to evaluate its potential as a wound dressing material. Commercially developed silk fibroin (AdBioInk Biyosystem Technology) solution was utilized as the starting material. In situ electrospinning process optimization was carried out by varying silk fibroin concentration, needle-to-collector distance, applied voltage, and syringe flow rate using handheld electrospinning device (AdBioInk Biyosystem Technology). The morphology of the resulting mats was examined using optical microscopy and scanning electron microscopy (SEM), and fiber diameters were quantified using ImageJ software. The physicochemical properties of the electrospun mats were characterized by FTIR, while surface wettability and moisture management properties were evaluated by measuring the water contact angle (WCA) and water vapor transmission rate (WVTR), respectively. To assess biological performance, cytotoxicity was evaluated using the MTT assay with dermal fibroblasts. The wound healing potential of the mats was investigated through an in vitro scratch assay by monitoring cell migration at defined time points. Hemocompatibility was further examined using a hemolysis assay to determine the compatibility of the developed dressings. The handheld electrospinning device enabled the in situ deposition of SF-based fibrous wound dressing successfully. SEM analysis confirmed the formation of homogeneous fiber morphology. FTIR spectra verified the successful incorporation of SF in wound dressing. Water contact angle measurements indicated improved hydrophilicity of the wound dressings, supporting their ability to maintain a moist wound environment. Furthermore, WVTR values were found to be within the optimal range required for wound healing. Cytocompatibility assessment revealed the biocompatibility of the developed wound dressings. In addition, İn vitro scratch assay results demonstrated enhanced fibroblast migration and more rapid wound closure compared with the control groups. Hemolysis assay results indicated favorable hemocompatibility, with hemolysis rates remaining within acceptable limits for wound dressing applications. Overall, this study highlights the potential of handheld electrospinning-assisted SF mat fabrication as a biocompatible and functionally adaptable fibrous platform for in situ development of next-generation wound care materials.

Acknowledgment:
The authors gratefully acknowledge TÜBİTAK 2224-B for its support.

Keyword: *Silk fibroin, Wound dressing, Handheld electrospinning*

Development of Superparamagnetic NIR Carbon Dots for Theranostic Applications

Selin Alptekin * **, Berke Ayevi, Alphan Sennaroğlu, H. Funda Yağcı Acar**

Department of Chemistry, Faculty of Science, Koç University, Istanbul, Türkiye

Cancer remains one of the leading causes of mortality worldwide, arising from uncontrolled cell proliferation. Conventional therapeuticstrategies, including chemotherapy, radiotherapy, and surgery, are often limited by adverse side effects, drug resistance, and insufficientselectivity. In this context, nanoparticle-mediated photothermal therapy has emerged as a promising alternative, as it enables efficientlight-to-heat conversion for targeted tumor ablation while minimizing damage to healthy tissues. Herein, we report the development of indocyanine green (ICG)-integrated poly(acrylic acid) (PAA)-coated superparamagnetic iron oxide nanoparticles (SPIONs) as amagnetofluorescent theranostic system.

PAA-coated SPIONs were synthesized via a co-precipitation approach, yielding stable nanoparticles with abundant surface carboxylgroups for further modification. ICG was incorporated through a carbonization-assisted strategy in order to improve its stability. Thenanoparticles were characterized using UV–Vis, PL, DLS, and FTIR techniques, confirming their optical properties, size distribution,and successful surface modification. The resulting hybrid nanostructures exhibit strong near-infrared (NIR) absorption, making themsuitable for photothermal applications.

The photothermal properties of the samples were investigated under 808 nm laser irradiation. The results showed effective light-to-heatconversion. In addition, repeated heating and cooling cycles demonstrated that the system has good photothermal stability.

The presence of SPIONs also provides magnetic properties, which may be useful for future targeting or imaging applications. Overall,this study presents a simple approach to prepare a multifunctional nanoparticle system with potential use in photothermal therapy.

Acknowledgment:
The authors gratefully acknowledge Prof. Uğur Ünal for TEM analysis.

References:
Bilici, K., Muti, A., Demir Duman, F., Sennaroğlu, A., & Yağci Acar, H. (2018). Investigation of the factors affecting the photothermal therapy potential of small iron oxide nanoparticles over the 730-840 nm spectral region. Photochemical and Photobiological Sciences, 17(11), 1787-1793.
Doughty, A. C., Hoover, A. R., Layton, E., Murray, C. K., Howard, E. W., & Chen, W. R. (2019). Nanomaterial applications in photothermal therapy for cancer. Materials, 12(5), 779.
Jiang, Y., Tan, Z., Zhao, T., Wu, J., Li, Y., Jia, Y., & Peng, Z. (2023). Indocyanine green derived carbon dots with significantly enhanced properties for efficient photothermal therapy. Nanoscale, 15(4), 1925-1936.

Keyword: *indocyanine green, magnetofluorescent nanoparticles, photothermal therapy*

Development and in vitro Analysis of Immunological Cell-Derived Nano Extracellular Vesicle Added Injectable Hydrogel

Umut Doğu Seçkin [*1], **Aylin Şendemir**[2,3]

[1] *Ege University, Graduate School of Natural and Applied Sciences, Department of Bioengineering, Bornova, Izmir, 35040, Turkiye*
[2] *Ege University, Engineering Faculty, Department of Bioengineering, Bornova, Izmir, 35040, Turkiye*
[3] *Ege University, Graduate School of Natural and Applied Sciences, Department of Biomedical Technologies, Bornova, Izmir, 35040, Türkiye*

Tissue engineering is a complex system that includes cells, signals, and scaffolds. This system means that cells are cultured in a three-dimensional scaffold that plays the role of ECM for cell growth (Eftekhari et al. 2020). Signals are used for cell growth and differentiation, resulting in greater cellular adhesion. Bones are responsible for providing mechanical support and protecting internal organs. They also form the body skeleton, which stores red and white blood cells and minerals. The completion of restoration of a damaged bone requires mechanical stability and the presence of periosteal cells and inflammatory cells at the defect site (Temenoff and Mikos 2000). The three key factors for bone reconstruction are to trigger calcification by cells and to synthesize the extracellular matrix. Enhanced and co-substituted hydroxyapatite is an alternative option to increase osteoconduction and osteogenesis. Hydrogels are nanoporous, three-dimensional networks that can absorb large amounts of water. Hydrogels are widely used for tissue engineering due to their similar structure to macromolecular-based components in the body (Temenoff and Mikos 2000).

In this study, it was aimed to develop a biodegradable and injectable hydrogel system with nanomaterial additives for use in bone tissue engineering and to evaluate the cellular effects of this system in the osteoimmune microenvironment in vitro. The developed system was prepared by adding biphasic calcium phosphate (BCP) to gelatin-based hydrogels and cross-linking with glutaraldehyde. The hydrogels were characterized by turbidimetric, UV-Vis absorbance, injectability, area scanning, homogeneity and ISO 10993-5 compatible cytotoxicity tests.

Within the scope of the study; extracellular vesicles (EVs) were isolated from M0 and M2 phenotype macrophages derived from THP-1 and U937 cell lines and characterized by dynamic light spectrophotometry (DLS) size analysis, BCA protein determination and polydispersity index analysis; it was determined that M2-derived EVs in particular had higher protein content and more regular distribution. EVs were applied to SAOS-2 osteoblast cells and their osteogenic activities were evaluated by ALP activity, Fluo 4 NW staining after 14 days, and calcification by Alizarin Red staining after 21 days. In addition, SAOS-2 osteoblast cells cultured with combined ceramic, EV-containing hydrogels were stained with Alizarin Red and Von Kossa after 28 days.

It was observed that the combination of EV and BCP increased osteoblastic activity. Especially the BCP-gel structures combined with M2-EV showed an enhancing effect on advanced osteoblastic differentiation. The findings indicated that the potential of these nanomaterial-containing hydrogels to be used minimally invasively is promising in terms of osteogenesis and immune-cell interaction modulation.

ORCID:
Umut Doğu Seçkin: 0000-0002-0123-0284
Aylin Şendemir: 0000-0003-1818-6651

References:
1. Eftekhari, A., Maleki Dizaj, S., Sharifi, S., Salatin, S., Rahbar Saadat, Y., Zununi Vahed, S., and Cucchiarini, M. (2020). The use of nanomaterials in tissue engineering for cartilage regeneration; current approaches and future perspectives. International journal of molecular sciences, 21(2), 536.
Temenoff, J. S., & Mikos, A. G. (2000). Injectable biodegradable materials for orthopedic tissue engineering. Biomaterials, 21(23), 2405-2412.
Ressler, A., Žužić, A., Ivanišević, I., Kamboj, N., & Ivanković, H. (2021). Ionic substituted hydroxyapatite for bone regeneration applications: A review. Open Ceramics, 6, 100122.

Keyword: *Nanomaterial, Extracelluler vesicle, Hydrogel*

The Effect of Cornelıan Cherry and Cısplatın-Loaded Nanofıbers on Skın Cancer Cells

Zeynep Gergin [*] [1], Aysegul Tiryaki[2], Songul Ulag[3], Ali Sahin[4]

[1] Department of Nanoscience and Nanoengineering, Istanbul Technical University, Istanbul, Türkiye
[2] Department of Bioengineering, Faculty of Chemical and Metallurgical Engineering, Yildiz Technical University, Istanbul, Türkiye
[3] Biomaterials Research and Development Laboratory (BRD-Lab), Faculty of Technology, Marmara University, Istanbul, Türkiye
[4] Genetic and Metabolic Diseases Research and Investigation Center, Marmara University, Istanbul, Türkiye

Polyurethanes are polymer biomaterials of interest to biomedical engineering because their mechanical behavior, degradation profiles, and biological responses can be appropriately modified. Their structure provides versatility in terms of adjustable mechanical, physicochemical, and biological properties, as well as blood and tissue compatibility and biodegradability. While polyurethanes are generally used as biologically stable and inert materials in catheters, heart valves, prostheses, and vascular grafts, these materials have recently begun to be preferred in drug delivery systems. These developments have become noteworthy in cancer research. Thanks to their structures that can provide controlled drug release, polyurethane-based systems can offer a suitable platform for more effective delivery of anticancer agents to target cells and the development of local treatment approaches [1]. Cisplatin is a chemotherapy drug used in many types of cancer. Cisplatin may exhibit anticancer activity by activating apoptotic pathways in tumor cells due to its disruption of DNA replication and repair processes [2]. Cornelian cherry (Cornus mas L.), which is rich in anthocyanins, has anti-inflammatory properties, and it is effective in regulating apoptosis [3]. In this study, based on the information given above, three groups were formed (polyurethane+cornelian cherry, polyurethane+cisplatin, and polyurethane+ cisplatin+cornelian cherry), and the swelling and degradation behaviors, chemical, mechanical, and morphological properties were evaluated.

ORCID:
Zeynep Gergin: 0009-0007-9695-2215

References:
[1] Sobczak, M., & Kędra, K. (2022). Biomedical Polyurethanes for Anti-Cancer Drug Delivery Systems: A Brief, Comprehensive Review. International journal of molecular sciences, 23(15), 8181. https://doi.org/10.3390/ijms23158181
[2]. Dasari, S., & Tchounwou, P. B. (2014). Cisplatin in cancer therapy: molecular mechanisms of action. European journal of pharmacology, 740, 364–378. https://doi.org/10.1016/j.ejphar.2014.07.025
[3]. Szot, I., Łysiak, G. P., Sosnowska, B., & Chojdak-Łukasiewicz, J. (2024). Health-Promoting Properties of Anthocyanins from Cornelian Cherry (Cornus mas L.) Fruits. Molecules (Basel, Switzerland), 29(2), 449. https://doi.org/10.3390/molecules29020449

Keyword: *Polyurethaane*, *Cisplatin*, *Cranberry*

Oleuropein-Rich Olive Leaf Extract-Incorporated PAN/CA Nanofibrous Membranes via Electrospinning: Characterization and In Vitro Biocompatibility for Wound Healing

Çağla McKenzie [*1], Amarjargal Altangerel[2], Timur Tongur[3], Viraj P. Nirwan[4], Rebecca Hengsbach[4], Suray Pehlivanoğlu[5], Amir Fahmi[4], Seda Demirel Topel[6]

[1] *Department of Gastronomy and Culinary Arts, Faculty of Tourism, Antalya Bilim University*
[2] *Faculty of Technology and Bionics, Rhine-Waal University of Applied Science, Power Engineering School, Mongolian University of Science and Technology*
[3] *Department of Chemistry, Faculty of Sciences, Akdeniz University*
[4] *Faculty of Technology and Bionics, Rhine-Waal University of Applied Science*
[5] *Department of Molecular Biology and Genetics, Faculty of Sciences, Necmettin Erbakan University*
[6] *Department of Electrical and Electronics Engineering, Faculty of Engineering and Natural Sciences, Antalya Bilim University*

Olive leaves (Olea europaea L.) are an abundant and largely underutilized agricultural byproduct rich in bioactive polyphenolic compounds, most notably oleuropein, which possesses well-documented antioxidant, anti-inflammatory, and antimicrobial properties [1,2]. Despite their therapeutic potential, the incorporation of olive leaf bioactives into functional biomaterials for wound care applications remains underexplored. In this study, oleuropein-rich extracts were obtained via maceration using two solvent systems, pure ethanol and ethanol:water (1:1, v/v), and their phytochemical profiles were comparatively evaluated using HPLC. For fabrication of functional wound dressing materials, olive leaf extracts were incorporated into a polyacrylonitrile/cellulose acetate (PAN/CA) polymer matrix dissolved in dimethylformamide (DMF) at concentrations of 5%, 10%, and 15% (w/w), and their nanofibers were produced via electrospinning. SEM morphological analysis revealed that increasing extract concentration progressively influenced fiber diameter and surface uniformity, with higher loadings tending to increase average fiber diameter and introduce minor bead formation, likely due to changes in solution viscosity and conductivity. FTIR spectroscopy confirmed successful integration of the olive leaf extract within the nanofibers, evidenced by characteristic absorption bands corresponding to hydroxyl, carbonyl, and aromatic functional groups of the polyphenolic constituents alongside the polymer backbone signals. The release profile of the olive leaf extract was studied using zero-order, first order, Higuchi and Korsmeyer Peppas models. The biocompatibility of the nanofibrous membranes was evaluated using L929 mouse fibroblast cells through the MTT assay in vitro. The findings establish a strong foundation for the application of PAN/CA-olive leaf extract nanofibers as bioactive wound dressing platforms, with future work directed toward evaluating wound healing acceleration through in vitro scratch assays and in vivo wound models.

Acknowledgment:
This study was supported by the Scientific and Technological Research Council of Türkiye (TUBITAK) under the Grant Number 125N193 and the German Academic Exchange Service (DAAD). The authors thank TUBITAK and DAAD for their support.

References:
[1] Tarchi, I., Olewnik-Kruszkowska, E., Aït-Kaddour, A., & Bouaziz, M. (2025). Innovative Process for the Recovery of Oleuropein-Rich Extract from Olive Leaves and Its Biological Activities: Encapsulation for Activity Preservation with Concentration Assessment Pre and Post Encapsulation. ACS Omega, 10, 6135 - 6146. https://doi.org/10.1021/acsomega.4c10858.
[2] Topuz, S., & Bayram, M. (2021). Oleuropein extraction from leaves of three olive varieties (Olea europaea L.): Antioxidant and antimicrobial properties of purified oleuropein and oleuropein extracts. Journal of Food Processing and Preservation. https://doi.org/10.1111/jfpp.15697.

Keyword: *Oleuropein, electrospinning, wound dressing, cytotoxicity, release kinetics*

Development and Characterization of Biocompatible Fe_3O_4 Nanoparticles for Magnetically Controlled Microrobotic Applications

Özge Akbülbül [*1], Şeyma Özkan[2], Barış Oğuz Gürses[1], Bekir Özkan[3], Arif Altan Selçuk[4], Edin Yilmaz[1]

[1] Ege University Mechanical Engineering Department, İzmir/Turkey
[2] Dokuz Eylül University, The Graduate School of Natural and Applied Sciences Department of Chemistry, İzmir/Turkey , Ege University Central Research, Test and Analysis Laboratory Application and Research Center, İzmir/Turkey
[3] Ege University Institute of Nuclear Sciences, İzmir/Turkey
[4] Ege University Department of Biology, İzmir/Turkey

Magnetic micro- and nanorobots have become an important research topic in various fields, including biomedical engineering, targeted drug delivery, minimally invasive surgery, and smart manufacturing technologies, owing to their ability to be remotely manipulated using external magnetic fields without physical contact. One of the key factors determining the performance of these systems is the biocompatibility, colloidal stability, and controllable motion of magnetic nanoparticles. Therefore, biocompatible surface modification represents a critical strategy for enhancing the performance of robotic systems.

In this study, the suitability of phosphocholine-coated Fe_3O_4 nanoparticles for robotic applications was investigated. The nanoparticles were synthesized, and their particle size, surface characteristics, and magnetic properties were characterized. Subsequently, their maneuverability under an external magnetic field was evaluated to assess their potential as components of microrobotic systems.

ORCID:
Özge Akbülbül: 0000-0002-7892-6458

Keyword: *magnetic particles, phosphocholine, magnetic manipulation*

Two-Dimensional Nanomaterial–Reinforced Hydrocarbon Membranes for High-Performance Aqueous Organic Redox Flow Batteries

Amina Ben Ayed [*1], Rumman Zaidi[1], Mina Namvari[1], Barun K. Chackrabarti[1], Lukas Pachernegg-Mair[2], Gutmann Torsten[3], Stefan Spirk[4], Tülay Y. İnan[1]

[1] *Sabanci University Nanotechnology Research and Application Center (SUNUM), Tuzla 34956, Istanbul, Türkiye*
[2] *Ecolyte GmbH, TU Graz Campus Inffeldgasse, Inffeldgasse 21b, 8010, Graz, Austria*
[3] *3Department of Chemistry, Physical Chemistry, University Paderborn, Warburger Straße 100, 33098 Paderborn, Germany*
[4] *Austria, Graz University of Technology - Institute of Bioproducts and Paper Technology, Austria, Ecolyte GmbH, TU Graz Campus Inffeldgasse, Inffeldgasse 21b, 8010, Graz*

Redox flow batteries (RFBs) have attracted noticeable attention as encouraging large-scale energy storage technologies because of their scalability, operational flexibility, and enhanced safety characteristics. Despite the maturity of vanadium redox flow batteries, their deployment is limited by high material costs and supply chain volatility, motivating the development of organic redox flow batteries (ORFB). Aqueous organic redox flow batteries (AORFB) offer a sustainable route by using earth-abundant, structurally tunable redox-active molecules such as benzoquinone disulfonic acid (1,2-dihydrobenzoquinone-3,5-disulfonic acid (BQDS)) [1,2]. However, the performance of these systems is still constrained by membranes selectivity, ionic transport resistance, and crossover of active species.

Herein, non-fluorinated hydrocarbon ion-exchange membranes reinforced with two-dimensional (2D) nanomaterials are developed for application in AORFBs. The incorporation of 2D nanosheets into the polymer matrix forms a confined transport network that enhances proton conductivity while suppressing BQDS crossover. The resulting composite membranes exhibit a favorable balance between ionic conductivity and selectivity, leading to improved electrochemical stability under cycling conditions. Compared with conventional perfluorinated membranes, the proposed hydrocarbon/2D composites provide a lower-cost and environmentally more sustainable alternative. This approach demonstrates a promising pathway toward high-performance membrane engineering for next-generation RFB systems, with further optimization required in long-term durability and scalable processing.

References:

[1] Ghotli, R. A., Kudaş, Z., Chaudhuri, S., Çelik, S., İnan, T. Y., Soytaş, S. H., Çobandede, Z., Bayazıt, M. K., Puerto, A. P., Hirn, Ü., Spirk, S., & Chakrabarti, B. K. (2026). Electrophoretic deposition of nanomaterial catalysts on carbon cloth electrodes for Aqueous-Organic flow batteries. In Proceedings in Technology Transfer (pp. 209–220). https://doi.org/10.1007/978-981-95-7817-7_16.
[2] Lee, W., Park, G., & Kwon, Y. (2019). Alkaline aqueous organic redox flow batteries of high energy and power densities using mixed naphthoquinone derivatives. Chemical Engineering Journal, 386, 123985. https://doi.org/10.1016/j.cej.2019.123985

Keyword: *two-dimensional (2D) nanomaterials, Aqueous organic redox flow batteries, Hydrocarbon membranes*

Investigation of the Layer and Substrate Dependency of the Thermal Conductivity of MoS_2

Elanur Hut * **, Ayşe Erol, Fahrettin Sarcan**

Istanbul University, Faculty of Science, Department of Physics, Istanbul, Türkiye

In recent years, two-dimensional (2D) transition metal dichalcogenides (TMDs) have gained attention as promising candidates for thermoelectric applications. Their layered structures and high surface-to-volume ratios inherently lead to low thermal conductivity and improved thermoelectric performance compared to bulk materials. In this context, understanding how heat is transported in 2D TMDs is essential for evaluating their potential in thermoelectric and nanoelectronic devices.

In this study, the thermal response of mechanically exfoliated MoS_2 flakes with different layer numbers was investigated on SiO_2/Si, Si_3N_4 membrane and PDMS substrates using optothermal Raman spectroscopy. The layer numbers of the samples were determined by photoluminescence (PL) measurements and atomic force microscopy (AFM). Temperature-dependent Raman measurements were performed to obtain the first-order temperature coefficients of the E^1_{2g} and A_{1g}phonon modes, while laser power-dependent Raman measurements were used to evaluate local heating effects.

The thermal conductivity/effective thermal conductivity values were obtained from the Raman peak shifts induced by changes in temperature and laser powerThe highest thermal conductivity was observed for 1L MoS_2 on the SiO_2/Si substrate, with a value of 63.5 W $m^{-1}.K^{-1}$, while the values decreased to 27.5 and 22.8 W m^{-1} K^{-1} for 4L and bulk MoS_2, respectively.On the Si_3N_4 membrane values were obtained as 22.5, 23.4 and 37.8 W $m^{-1}.K^{-1}$, while on the PDMS substrate were obtained as 20.8, 22.3 and 25.9 W $m^{-1}.K^{-1}$ for 1L, 4L and bulk MoS_2, respectively.

The results showed that the thermal transport behavior of MoS_2 strongly depends on both the substrate material and the layer number. For monolayer MoS_2, the highest thermal conductivity was obtained on the SiO_2/Si substrate, while lower values were observed on Si_3N_4 and PDMS substrates. This difference was mainly attributed to exciton–phonon coupling, which may preserve phonon coherence, rather than to the direct thermal effect of the substrate**.**In addition, the change in layer number caused noticeable variations in the thermal conductivity values, indicating that phonon transport in MoS_2 is affected by both layer-dependent structural properties and substrate coupling.

These findings demonstrate that the thermal conductivity of 2D materials is not only affected by the thermal properties of the substrates, but is also influenced by the strength of exciton–phonon coupling.

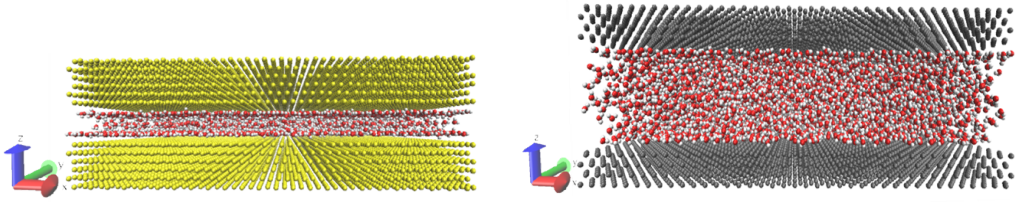
Keyword: *MoS_2, Thermal conductivity, Two-dimensional materials*

Molecular Dynamics Simulation of 2D Water Confined Between Metal Surfaces

Gamze Ozgunes * **, Mine Ilk Capar**

Ege University, Faculty of Science, Department of Physics, Izmir, Turkey

Understanding the diffusion and viscosity properties of two-dimensional (2D) water is important for the design of nanochannels, metal coatings, sensors, and micro/nanofluidic systems. These findings contribute to the development of more efficient materials, membranes, and surface technologies by providing insight into the control of water transport between surfaces. In this project, molecular dynamics (MD) simulations were performed for systems containing two-dimensional water confined between iron (Fe) and gold (Au) metal surfaces. In the simulation systems, the iron surface was constructed as a BCC Fe(110) crystal surface, while the gold surface was constructed as an FCC Au(111) crystal surface, and they were placed parallel to the xy plane. The distance between the metal surfaces was regularly increased from 3 Å to 200 Å, and the space between them was filled with water molecules to obtain 2D water layers with different thicknesses. The MD simulations were performed using the OPLS (Optimized Potential for Liquid Simulations) [1] force field with the GROMACS 2024 program [2]. The TIP3P [3] water model was used. The computer simulations were carried out using computer clusters within the TÜBİTAK TRUBA infrastructure. By changing the channel width formed by the metal surfaces, the diffusion and viscosity coefficients of the water molecules were calculated.



(a) **(b)**

Figure 1. Representative snapshots of water confined between (a) Au surfaces with a ~5 Å water layer and (b) Fe surfaces with a ~21 Å water layer. Au atoms are shown in yellow, Fe atoms in gray, H atoms in white, and O atoms in red.

The results showed that the diffusion coefficients of water molecules interacting with Fe surfaces were lower than those in systems with Au surfaces. In all systems, the D_xy diffusion coefficient in the direction parallel to the metal surface was found to be greater than the D_z diffusion coefficient in the direction perpendicular to the surface. This indicates that 2D water exhibits anisotropic diffusion behavior between metal surfaces. The viscosity values calculated in the systems with Au surfaces were found to be approximately 100 times greater than those obtained in the systems with Fe surfaces. For both metal surfaces, it was observed that as the channel width increased, the diffusion coefficients of 2D water increased, while the viscosity coefficient decreased.

Acknowledgment:
In this study, the simulations and some numerical calculations were performed at the TÜBİTAK ULAKBİM, High Performance and Grid Computing Center (via TRUBA resources). This work was supported by TÜBİTAK under the 2209-A program with project number 1919B012454560.

ORCID:
Gamze Ozgunes: 0009-00009-1734-9712
Mine Ilk Capar: 0000-0001-6184-3026

References:
[1]Jorgensen, W. L., Maxwell, D. S., & Tirado-Rives, J. (1996). Development and testing of the OPLS all-atom force field on conformational energetics and properties of organic liquids. Journal of the American Chemical Society, 118(45), 11225–11236.
[2]Hess, B., Kutzner, C., Van Der Spoel, D., & Lindahl, E. (2008). GROMACS 4: Algorithms for highly efficient, load-balanced, and scalable molecular simulation. Journal of Chemical Theory and Computation, 4(3), 435–477.
[3]Jorgensen, W. L., Chandrasekhar, J., Madura, J. D., Impey, R. W., & Klein, M. L. (1983). Comparison of simple potential functions for simulating liquid water. The Journal of Chemical Physics, 79(2), 926–935.

Keyword: *2D water, dynamics properties, simulation*

Synthesis of Large-Area Single- to Few-Layered MoS2 With Liquide Phase Mechanism

Gizem Gülistan Bozkurt Akın * **, Cumhur Gökhan Ünlü, Aleyna Akçay Tataroğlu, Ayten Cantaş Bağdaş, Hatice Dilay Yazıcı**

Pamukkale Üniversitesi

Molybdenum disulfide (MoS_2), a prominent member of the two-dimensional transition metal dichalcogenide family, has attracted significant attention due to its tunable bandgap, atomically thin structure, and exceptional electronic and optoelectronic properties. However, achieving large-area, high-quality, and controllable growth of MoS_2 remains a major challenge for its practical implementation in next-generation devices.

In this study, the growth behavior of MoS_2 thin films synthesized by NaCl-assisted chemical vapor deposition was investigated. Optical characterization revealed the formation of distinctive concentric ring patterns accompanied by flower-like MoS_2 crystal morphologies. These observations suggest that NaCl plays a crucial role beyond that of a conventional growth promoter. The observed growth features indicate the formation of transient liquid domains during the synthesis process, which act as localized transport media and significantly influence nucleation and crystal evolution. The resulting radial growth from droplet-centered nucleation sites points to a liquid-phase-assisted growth mechanism.

Raman and optical analyses demonstrated that the incorporation of NaCl enhances nucleation density, promotes lateral crystal growth, and improves film continuity. The findings provide valuable insight into the role of alkali halide additives in tailoring the growth dynamics of two-dimensional materials. Furthermore, the proposed liquid-phase-assisted growth mechanism offers a promising route for the scalable synthesis of high-quality MoS_2 and other two-dimensional semiconductors, paving the way for their integration into future electronic, optoelectronic, and sensing technologies.

ORCID:
Gizem Gülistan Bozkurt Akın: 0009-0004-1049-9631
Cumhur Gökhan Ünlü: 0000-0003-2554-5886
Aleyna Akçay Tataroğlu: 0000-0001-6719-4688
Ayten Cantaş Bağdaş: 0000-0002-6536-5516
Hatice Dilay Yazıcı: 0000-0001-6264-0036

Keyword: *MoS2, Chemical Vapor Deposition, Liquid Phase Growth Mechanism*

Conductive Network Formation and EMI Shielding in MXene/PVA Composites

Nevzat Duman[1], Muhittin Aktaş[1], Göktürk Torun [* 1], Teng Zhang[1], Kadri Aydınol[2], Goknur Cambaz Buke[1,3,4]

[1] Materials Science and Nanotechnology Engineering, Micro and Nanotechnology Program, TOBB University of Economics and Technology
[2] Metallurgical and Materials Engineering Department, Middle East Technical University (METU), Ankara, Turkey
[3] A.J. Drexel Nanomaterials Institute, Drexel University, Philadelphia, PA, USA
[4] UNAM — National Nanotechnology Research Center and Institute of Materials Science and Nanotechnology, Bilkent University, Ankara, Turkey

The design of MXene-based electromagnetic interference (EMI) shielding materials has largely focused on increasing electrical conductivity to maximize shielding effectiveness. However, highly conductive materials often exhibit reflection-dominated shielding, which limits electromagnetic energy dissipation within the material. Understanding how conductive network formation influences the balance between transmission, reflection, and absorption remains critical for the development of next-generation EMI shielding systems.

In this study, MXene/PVA composites containing 1–16 wt% MXene were fabricated using a blade-casting approach to investigate the relationship between conductive network formation and electromagnetic energy partitioning. Structural evolution was examined by cross-sectional SEM, effective in-plane and out-of-plane electrical conductivities were measured via Solartron Modulab XM potentiostat and X-band (8.2–12.4 GHz) shielding performance was evaluated using Keysight E5063A Vector Network Analyzer. Reflection (R), transmission (T) coefficients were derived from the measured S-parameters. Absorption was calculated as A = 1 - R - T.

The results reveal a pronounced transition in shielding behavior associated with conductive network formation. As MXene loading increased, transmission decreased from 97.1% to 0.3%, while reflection increased from 0.7% to 95.3%. In contrast, absorption exhibited a non-monotonic dependence on MXene concentration, reaching a maximum value of 17.0% at 4 wt% MXene before decreasing at higher loadings. This concentration range coincided with the onset of rapid conductivity growth, indicating the formation of a percolated conductive network. Maximum absorption does not occur at maximum conductivity, but near the conductive network formation threshold where electromagnetic waves can still penetrate the material while interacting with emerging conductive pathways. The results provide new insight into the design of MXene-based EMI shielding materials by highlighting conductive network engineering as a strategy for controlling shielding mechanisms rather than simply maximizing conductivity.

Acknowledgment:
This study was supported by the Air Force Office of Scientific Research, grant numbers FA9550-22-1-0358 and FA9550-21-1-0202.

ORCID:
Nevzat Duman: 0009-0005-6717-4931
Muhittin Aktaş: 0009-0001-1210-1226
Göktürk Torun: 0009-0009-3532-6610

Keyword: *MXene, Nanocomposite, EMI shielding*

Fabrication and Optoelectronic Characterization of a Lithography-Free Gr/4H-SiC-Based UV Photodetector Array

Melike Gözek * **, Cem Çelebi**

İzmir Institute of Technology, Faculty of Science, Department of Physics, Urla, 35430, İzmir, Turkey

Ultraviolet (UV) photodetectors have great potential for applications in fields such as environmental monitoring, space applications, optical communications [1]. These applications necessitate low dark current, high UV sensitivity and responsivity, fast response speed and stable operation. Wide bandgap semiconductors are broadly used in UV photodetectors due to their ability to detect short-wavelength UV light and stability under harsh environmental conditions [1]. Silicon carbide (SiC), which is one of these materials, stands out as a convenient semiconductor for UV detection applications due to its wide bandgap (~ 3.26 eV), high thermal stability and radiation resistance [2]. In addition, graphene can be used as a transparent conductive electrode in Schottky junction photodetectors owing to its two dimensional structure, high electrical conductivity and excellent optical transparency [2,3].

In this study, a four-element Gr/4H-SiC based UV photodetector array (PDA) was fabricated without using any lithography technique and its electrical and optical properties were investigated. The device was fabricated on a 4H-SiC substrate where graphene formed the active Schottky contact while the NiO layer isolated the diodes from each other both electrically and optically. The electrical behavior of the produced photodetector array was examined by dark current-voltage (I-V) measurements, while its UV detection capability was determined through photocurrent measurements under 280 nm LED illumination. In addition, spectral response and time-dependent photocurrent measurements were carried out to investigate the wavelength-dependent photoresponse and response speed of the device. The optical crosstalk effect, which is a key parameter for array-structured devices, was analyzed by comparing the signals from neighboring diodes. Raman spectroscopy and mapping measurements verified the presence of the graphene and provided information on its spatial distribution.

The obtained results indicate that the fabricated Gr/4H-SiC photodetector array using a lithography-free production approach demonstrates potential for UV detection applications. It is anticipated that the further optimization of the NiO isolation layer and graphene homogeneity could enhance the overall device performance. This study provides a simplified fabrication process for the SiC based multi-element UV photodetectors.

ORCID:
Melike Gözek: 0009-0008-6708-5981

References:
[1] Zou, Y., Zhang, Y., Hu, Y., & Gu, H. (2018). Ultraviolet Detectors Based on Wide Bandgap Semiconductor Nanowire: A Review. Sensors, 18(7), 2072. https://doi.org/10.3390/s18072072
[2] Jehad, A. K., Unverdi, O., & Celebi, C. (2023). High voltage response of graphene/4H-SiC UV photodetector with low level detection. Journal of Alloys and Compounds, 969, 172288. https://doi.org/10.1016/j.jallcom.2023.172288
[3] Nair, R. R., Blake, P., Grigorenko, A. N., Novoselov, K. S., Booth, T. J., Stauber, T., Peres, N. M. R., & Geim, A. K. (2008). Fine structure constant defines visual transparency of graphene. Science, 320(5881), 1308. https://doi.org/10.1126/science.1156965

Keyword: *Graphene, Silicon Carbide (SiC), UV Photodetector Array*

Structural Quality vs. Transferability in CVD-Grown Graphene

Oyku Sude Uluturhan [*1], Gokturk Torun[1], Eren Atli[1], Elif Okay[1], Erhan Gurpinar[1], Emre Ozan Polat[2,3], Goknur Cambaz Buke[1,3,4]

[1] *Micro and Nanotechnology, Graduate School of Engineering and Science TOBB University of Economics and Technology, Ankara, Turkey*
[2] *Department of Physics, Bilkent University, Ankara, Turkey*
[3] *UNAM – National Nanotechnology Research Center and Institute of Materials Science and Nanotechnology, Bilkent University, Ankara, Turkey*
[4] *A.J. Drexel Nanomaterials Institute, Drexel University, Philadelphia, USA*

Graphene synthesized by chemical vapor deposition (CVD) on copper is widely considered one of the most promising materials for large-area electronic applications. However, achieving high structural quality alone is insufficient for practical device integration, as successful transfer onto target substrates is equally critical. In this study, the influence of growth pressure and temperature on graphene quality, transferability, and electrical performance was systematically investigated.

Graphene was synthesized on Cu foils using atmospheric-pressure CVD (APCVD) and low-pressure CVD (LPCVD) systems at 1000°C and 1100°C. The synthesized films were characterized by optical microscopy, scanning electron microscopy (SEM), Raman spectroscopy, and Raman mapping. Controlled oxidation was employed to visualize graphene coverage and assess film continuity. Subsequently, graphene films were transferred onto Si and glass substrates using a photoresist-assisted wet transfer process.

Raman mapping revealed that increasing the growth temperature to 1100°C resulted in a more homogeneous graphene distribution and reduced defect density. However, operation above the melting point of Cu required the use of a tungsten support substrate. During wet transfer, the graphene/photoresist film detached non-uniformly from the tungsten support, resulting in shrinkage, tearing, and severe degradation of film integrity. In contrast, graphene synthesized at 1000°C on solid Cu foils exhibited lower structural uniformity but significantly improved transferability.

All investigated conditions were transferred onto large-area glass and silicon substrates, and also the APCVD-grown graphene synthesized at 1000°C could be successfully electrically characterized. Hall-effect measurements yielded a sheet resistance of 960 Ω/sq, carrier concentration of 2.5×10^{13} cm^{-2}, and carrier mobility of 258 $cm^2V^{-1}s^{-1}$. The results demonstrate that optimizing graphene growth solely based on structural quality may be misleading and highlight the importance of considering transferability and device integration when identifying optimum synthesis conditions.(This study is supported by The Scientific and Technological Research Council of Turkey (TUBITAK), project no: 1919B012424851)

Acknowledgment:
This study is supported by The Scientific and Technological Research Council of Turkey (TUBITAK), project no: 1919B012424851

Keyword: *Graphene, CVD, Electrical Characterization*

Synthesis of Molybdenum Boride (MoB) via Different Hydrothermal Routes: Structural and Morphological Characterization

Sevda Jafari Aghdam [*1,2], **Aytekin Uzunoglu**[2]

[1] *Sabancı University, Faculty of Eng. & Natural Sci., Istanbul 34956, Turkiye*
[2] *Department of Materials and Metallurgical Engineering, Istanbul Technical University, Istanbul, Türkiye*

Molybdenum borides (MoB) have become important precursor materials for 2D MBene fabrication, yet a direct comparison of how different synthesis routes shape their phase purity and morphology is still absent from the literature. Selective etching inside an autoclave is notoriously hard to control. The problem is compounded by the fact that temperature, reaction time, and chemical medium all interact, and understanding that interplay, in our view, is what will make reproducible MoB preparation possible.

To address this, we tracked the structural evolution of MoB powders across four distinct hydrothermal routes. In Method 1, we etched 0.5 g of a MAB phase precursor with LiF and 12 M HCl (10 mL) under stirring at 300 rpm for 30 minutes, then sealed the mixture in a Teflon-lined autoclave at 90°C for 144 hours. After washing the powder to pH 4–5 and vacuum-drying it at 60°C for 24 hours, we finished the processing via room-temperature ultrasonication (2 hours), centrifugation (1000 rpm, 5–10 min), and a 6-day freeze-drying cycle. Method 2 ran differently: we dissolved MoAlB in HCl, stirred for 10 minutes, and treated it hydrothermally at 45°C for 48 hours. Method 3 used 3N HCl, autoclaved at room temperature for 48 hours. Method 4 moved fully into alkaline territory: 2 M KOH, 80°C, 24 hours.

We characterized all four products using XRD and SEM. XRD patterns directly showed how processing conditions altered phase purity and crystal structure, while SEM imaging revealed a clear morphological contrast between the acidic and alkaline runs. These findings indicate that MoB synthesis allows for much greater flexibility than typically assumed. The same target phase is accessible through quite different chemical routes, which is worth bearing in mind for groups working on catalysis, sensing, or energy storage electrodes.

Acknowledgment:
"The authors would like to thank Istanbul Technical University for providing the necessary research facilities and technical support during this work.

ORCID:
Sevda Jafari Aghdam: 0009-0004-3667-0185
Aytekin Uzunoglu: 0000-0002-2726-3930

Keyword: *Molybdenum Boride (MoB), Autoclave Processing, Hydrothermal Synthesis, Phase Stability, X-ray Diffraction (XRD), Scanning Electron Microscopy (SEM)*

Solution-Phase Delamination of Magnesium Diboride Facilitated by EDTA

Sibel Şentürk [*1], Cansu Yıldırım[1,2], Alara Efsun Canlı[1], Hale Gürbüz[1], Hüseyin Enis Karahan[1,3]

[1] *Department of Chemical Engineering, Istanbul Technical University, Maslak 34469, Istanbul, Türkiye*
[2] *Polymer Science and Technology Graduate Program, Istanbul Technical University, Maslak 34469, Istanbul, Türkiye*
[3] *Synthetic Fuels & Chemicals Technology Center (ITU-SENTEK), Istanbul Technical University, Maslak 34469, Istanbul, Türkiye*

Synthesis of graphene paved the way for intense exploration of two-dimensional (2D) materials (2DMs). However, boron-based nanosheets and related systems (shortly, borophenes) are still overlooked as a sub-family of 2DMs despite the first successful liquid-phase exfoliation of magnesium diboride (MgB_2) being reported over ten years ago [1]. Going forward, it is now established that liquid-phase exfoliation of metal diborides into borophene-like structures is not limited to MgB_2, as similar observations have been made in aluminum diboride and titanium diboride [2,3], in both water [4] and acetonitrile [5]. Nevertheless, the mechanism of solvent-based metal diboride delamination is poorly understood. To better understand the process, we have explored the delamination behavior of MgB_2 in deionized water (DIW), acetonitrile (ACN), and DIW-ACN mixtures. In a matter of a few hours, MgB_2 undergoes a stark color change in DIW from dark brown to light yellow dispersion with higher stability, as verified by the Tyndall effect and dynamic light scattering observations. In contrast, the color change was absent in ACN, but the colloidal stability of MgB_2 was still high. Moreover, surprisingly, DIW-ACN mixtures neither induced color change nor supported colloidal stability. Notably, bubble formation, which indicates hydrogen gas release (a known sign of delamination), was also absent in these solvent mixtures. Considering that the leaching out of metal ions from metal diborides is the most plausible underlying mechanism of the observed delamination process, we also tested the impact of ethylenediaminetetraacetic acid (EDTA), a well-known chelating agent, to explore the process further. In the presence of EDTA, the color change was rapid (at the natural pH of the system), and the Tyndall effect was profound with no visible precipitation. Crucially, the addition of EDTA in the DIW-ACN mixture resulted in a change of color (light yellow) and enhanced dispersion. Based on Fourier-transform infrared spectroscopy and scanning electron microscopy observations, we concluded DIW itself and EDTA are successful in delaminating MgB_2 into Mg-deficient boron nanosheets, while ACN gives Mg-rich particles. We believe our fundamental observations will yield improved borophene synthesis routines with potential implications in various fields, ranging from catalysis to energy conversion and storage, to name a few.

Acknowledgment:
We thank Dr. Selçuk Acar (of PavTec) for generously donating magnesium diboride samples.

ORCID:
Sibel Şentürk: 0009-0007-8116-673X
Cansu Yıldırım: 0000-0003-1023-4030
Hüseyin Enis Karahan: 0000-0002-7753-1024

References:
[1] Das, S. K., Bedar, A., Kannan, A., & Jasuja, K. (2015). Aqueous dispersions of few-layer-thick chemically modified magnesium diboride nanosheets by ultrasonication assisted exfoliation. Scientific Reports, 5, 1–11. https://doi.org/10.1038/srep10522
[2] James, A. L., & Jasuja, K. (2017). Chelation assisted exfoliation of layered borides towards synthesizing boron based nanosheets. RSC Advances, 7(4), 1905–1914. https://doi.org/10.1039/c6ra26658d
[3] John, S. K., & Anappara, A. A. (2019). Aqueous dispersions of highly luminescent boron-rich nanosheets by the exfoliation of polycrystalline titanium diboride. New Journal of Chemistry, 43(25), 9953–9960. https://doi.org/10.1039/c9nj01502g
[4] Gunda, H., Das, S. K., & Jasuja, K. (2018). Simple, green, and high-yield production of boron-based nanostructures with diverse morphologies by dissolution and recrystallization of layered magnesium diboride crystals in water. ChemPhysChem, 19(7), 880–891. https://doi.org/10.1002/cphc.201701033
[5] Nishino, H., Fujita, T., Cuong, N. T., Tominaka, S., Miyauchi, M., Iimura, S., Hirata, A., Umezawa, N., Okada, S., Nishibori, E., Fujino, A., Fujimori, T., Ito, S. I., Nakamura, J., Hosono, H., & Kondo, T. (2017). Formation and characterization of hydrogen boride sheets derived from MgB2 by cation exchange. Journal of the American Chemical Society, 139(39), 13761–13769. https://doi.org/10.1021/jacs.7b06153

Keyword: *exfoliation, solvent, nanosheet*

MXene-Coated Glass Veil Interlayers for EMI Shielding in Lightweight Glass Fiber Composite Panels for Electrical/Hybrid Vehicles

Sinan Şen [*1], Mert Özdoğan[1], Berke Kesici[1], Suat Bahar Baştürk[1], Gülnur Başer[2], Melisa Yeke[2]

[1] *Manisa Celal Bayar University*
[2] *Metyx-Telateks Corp.*

Electromagnetic interference (EMI) has become an important engineering problem in electric and hybrid vehicles due to the increasing use of power electronics, battery management systems, sensors, communication modules, and electronic control units. These components can generate or be affected by unwanted electromagnetic waves, leading to signal distortion, performance loss, and reliability problems. Conventional metallic shielding materials such as aluminum, copper, and steel provide high shielding performance; however, their high density, limited design flexibility, corrosion tendency, and reflection-dominated shielding behavior restrict their use in lightweight vehicle structures [1,2]. Therefore, polymer matrix composites containing conductive functional interlayers are being investigated as alternative EMI shielding materials [3,4].

In this study, lightweight glass fiber/epoxy composite panels containing MXene-coated glass veil interlayers were developed and evaluated. $Ti_3C_2T_x$ MXene is a two-dimensional transition metal carbide with high electrical conductivity, large specific surface area, hydrophilic surface chemistry, and strong potential for interfacial interaction with polymer-based systems [5]. Owing to its layered structure and high aspect ratio, MXene can support the formation of conductive networks at relatively low loading levels and can contribute to electromagnetic wave attenuation through reflection, absorption, and multiple internal reflection mechanisms [3,4]. Similar conductive filler strategies, including graphene- and carbon-based systems, have also been widely investigated for improving EMI shielding behavior in polymer composites.

$Ti_3C_2T_x$ MXene was deposited onto glass veil substrates by dip-coating at different theoretical areal densities, including 4, 8, and 12 g/m². Silane-treated glass veil samples were also prepared to improve interfacial compatibility and coating stability. The coated veils were integrated into composite laminates using vacuum infusion and hot-pressing of prepreg layers. The produced panels were characterized by Archimedes density measurement, interlaminar shear strength testing according to ASTM D2344, three-point bending testing according to ASTM D790, and vector network analyzer measurements in the X-band frequency range.

The results showed that coating cycle number and theoretical MXene areal density affected MXene retention on the glass veil surface. The 12 g/m² condition provided the highest retained MXene amount. Mechanically, prepreg-based laminates showed higher ILSS values than vacuum-infused MXene-coated panels, while 4 and 12 g/m² vacuum-infused samples maintained acceptable flexural strength levels. EMI measurements showed limited shielding improvement compared with the carbon fiber reinforced reference panel. These findings indicate that MXene-coated glass veil interlayers are promising for lightweight multifunctional composites, but coating homogeneity, MXene retention, and conductive network continuity require further optimization.

Acknowledgment:
We would like to express our sincere gratitude to our esteemed Academic Advisor Assoc. Prof. Dr. Suat Bahar Baştürk, Prof. Dr. Mustafa Seçmen from Yaşar University, and our Industry Advisor Dr. Gülnur Başer, as well as all the employees of Metyx.

ORCID:
Sinan Şen: 0009-0004-6503-7290
Mert Özdoğan: 0009-0000-8228-6548
Berke Kesici: 0009-0000-9699-0333
Suat Bahar Baştürk: 0000-0002-4027-1935
Gülnur Başer: 0009-0003-5976-9666
Melisa Yeke: 0000-0001-9502-3990

References:
[1] Pai, A. R., Puthiyaveettil Azeez, N., Thankan, B., Gopakumar, N., Jaroszewski, M., Paoloni, C., & Thomas, S. (2022). Recent progress in electromagnetic interference shielding performance of porous polymer nanocomposites—A review. Energies, 15(11), 3901.
[2] Sezer Hicyilmaz, A., & Celik Bedeloglu, A. (2022). Electromagnetic interference shielding thermoplastic composites reinforced with carbon based hybrid materials: A review. Composite Interfaces, 29(13), 1413–1470.
[3] Bheema, R. K., Gopu, J., Bhaskaran, K., Verma, A., Chavali, M., & Etika, K. C. (2024). A review on recent progress in polymer composites for effective electromagnetic interference shielding properties–structures, process, and sustainability approaches. Nanoscale Advances, 6(23), 5773
[4] Hareesh, M. S., Joseph, P., & George, S. (2025). Electromagnetic interference shielding: a comprehensive review of materials, mechanisms, and applications. Nanoscale Advances, 7(15), 4510-4534.
[5] Hussain, S., Siddique, R., Nadeem, M., Zafar, E., Manzoor, S., & Darr, J. A. (2025). Unlocking exceptional EMI shielding in Ti 3 C 2 T x MXenes through controled microstructure and surface chemistry. Nanoscale advances, 7(19), 6179-6195.

Keyword: *MXene, Electromagnetic Interference Shielding, Glass Veil Interlayer*

Structural Characterization of Polycarbonate+MoS_2/MWCNT Nanocomposites

Habiba Shirinova[1], Jeyran Sultanova[2], Turkan Musayeva [* 1], Huseyn Mammadov[3], B.G. Pashayev[4]

[1] Department of Chemical Physics of the Nanomaterials, Baku State University, Baku AZ 1148, Azerbaijan
[2] Department of Physics, Azerbaijan State Oil and Industry University
[3] Department of Physical Electronics, Baku State University
[4] Department of Optics and Molecular Physics, Baku State University, Baku AZ 1148, Azerbaijan

In this work, polycarbonate (PC)-based nanocomposites reinforced with MoS_2 and multi-walled carbon nanotubes (MWCNT) were prepared in order to investigate their structural and chemical characteristics. The MoS_2+MWCNT nanosystem was incorporated into a polycarbonate solution prepared in tetrahydrofuran (THF), followed by homogenization using magnetic stirring to ensure a uniform dispersion of the nanofillers. After solvent evaporation at room temperature, the obtained materials were additionally dried in a vacuum oven to remove residual solvent and obtain stable nanocomposite samples.

The structural and chemical properties of the prepared nanocomposites were investigated by X-ray diffraction (XRD) and Fourier-transform infrared (FTIR) spectroscopy. XRD analysis revealed that the neat polycarbonate matrix exhibited a characteristic broad amorphous diffraction maximum in the $2\theta \approx 15–20°$ range. Following the incorporation of MoS_2 nanoparticles, distinct diffraction peaks corresponding to the (002), (100), (101), (103), (006), (105), and (110) crystallographic planes of the hexagonal 2H-MoS_2 phase were identified, confirming the successful incorporation of the layered nanofiller into the polymer matrix. Furthermore, as the MoS_2 content increased, a corresponding increase in the intensity of the characteristic diffraction peaks was observed.

For hybrid nanocomposites on the base of MoS_2+MWCNT, the diffraction peaks associated with MoS_2 became broader and partially overlapped with the amorphous halo of polycarbonate. This behavior suggests improved dispersion of the nanofillers and a more homogeneous distribution throughout the polymer matrix owing to the combined effect of the two nanofillers. Moreover, no additional diffraction peaks corresponding to new crystalline phases were detected, demonstrating that the preparation method did not induce chemical transformation or structural degradation of the polymer matrix.

FTIR spectra confirmed that the characteristic absorption bands of polycarbonate were preserved in all samples. The absorption bands observed at 1774–1781 cm^{-1} (C=O stretching of the carbonate group), 1500–1400 cm^{-1} (aromatic ring vibrations), and 1288–1080 cm^{-1} (carbonate C–O–C stretching vibrations) remained clearly visible after the incorporation of the nanofillers. Increasing the MoS_2 concentration caused only slight variations in the intensity and position of several absorption bands, while no additional peaks were observed. These findings indicate that the chemical structure of the polymer matrix remained unchanged during composite preparation and that the interaction between polycarbonate and the nanofillers is predominantly physical rather than chemical. Overall, results demonstrate the successful preparation of PC+MoS_2/MWCNT nanocomposites with homogeneous filler dispersion and good compatibility between the polymer matrix and the incorporated nanofillers, making them promising candidates for advanced multifunctional polymer-based materials.

Keyword: *MoS_2, 2D nanomaterials, polymer nanocomposites*

Determination and Evaluation of Rheological Properties of Solid Lubricants on Lithium Greases

Alize Pınar * **, Sevda Atar, Semih Koç, İbrahim Alkaya**

Petrol Ofisi, POTEM (R&D Center), Kocaeli, Turkiye

Lithium greases are among the most widely used lubricants in industry due to their mechanical stability, water resistance, and high-temperature performance. However, their properties can be further enhanced through the incorporation of solid lubricants. Solid lubricants are often employed to improve tribological and rheological performance, particularly in demanding applications.

In this study, molybdenum disulfide (MoS_2), one of the most commonly used solid lubricants in industrial practice, was selected to investigate its effects on lithium greases. Solid lubricants were added to lithium grease formulations prepared in our laboratory at concentrations of 0%, 0.5%, 1%, 3%, 5%, 7%, 10%, and 20%.

The rheological and performance effects of molybdenum disulfide were then evaluated by measuring parameters such as mechanical stability, consistency changes, and flow behavior. The results were reported to demonstrate the impact of solid lubricant concentration on the overall performance of lithium greases.

This research aims to provide insights into the optimization of lithium grease formulations with solid lubricants, contributing to the development of high-performance lubricants for industrial applications.

ORCID:
Alize Pınar: 0009-0009-4370-4036

Keyword: *lithium greases, molibdenum disulfide, rheological properties*

Dynamic and Electrically Tunable Electromagnetic Shielding via Phase-Engineered MoS2

Atalay Bozdoğan [*1], Hakan Eroğlu[2], Muharrem Karaaslan[2], Mustafa Akyol[1]

[1] *Adana Alparslan Türkeş Science and Technology University, Department of Materials Science and Engineering, 01250 Adana, Türkiye*
[2] *İskenderun Technical University, Department of Electrical and Electronic Engineering, 31200 Hatay, Türkiye*

Controlling electromagnetic (EM) wave reflection and absorption is crucial for advanced defense technologies and safeguarding high-frequency electronics [1, 2]. Traditional static electromagnetic interference (EMI) shielding materials typically demand multi-millimeter thicknesses, heavily restricting their integration into compact electronic systems [1, 2]. To overcome this limitation, this study introduces a sub-millimeter-thick, electrically reconfigurable EMI shielding platform utilizing phase-engineered molybdenum disulfide (MoS_2) heterostructures. Through a controlled hydrothermal approach, flower-like MoS_2 nanosheets featuring distinct metallic (1T) to semiconducting (2H) crystalline phase ratios (0.27, 0.93, and 2.77) were successfully synthesized. These active nanostructures were subsequently integrated into symmetric device configurations separated by a flexible polyvinyl alcohol and potassium hydroxide (PVA+KOH) gel electrolyte. Electrochemical characterization demonstrated that the configuration utilizing the highest 1T phase ratio (Device I) yielded superior capacitive performance, achieving a specific capacitance of 361 mF/cm^2 at 5 mV/s.

The active electromagnetic wave attenuation and reconfigurable capabilities of the fabricated devices were evaluated across the X-band spectrum (8–12 GHz) under external electric fields ranging from -40 to +40 V/cm. The experimental results reveal a profound correlation between the internal 1T/2H phase balance and the field-responsive tuning behavior. As a result, Device II demonstrated highly pronounced electrically switchable shielding properties. While it exhibited low shielding (11–12 dB) in its unbiased state, applying an external electric field dramatically increased its SE to 28–35 dB. This switchable mechanism is driven by agile ion migration within the electrolyte layer and dynamic charge accumulation at the MoS_2 interfaces. These findings establish a composition-driven design principle for developing next-generation adaptive, lightweight, and smart microwave shielding devices.

Acknowledgment:
This work was supported by the Scientific and Technological Research Council of Türkiye (TÜBİTAK) under Project Number: 223M012.

ORCID:
Atalay Bozdoğan: https://orcid.org/0009-0001-6559-4992
Muharrem Karaaslan: https://orcid.org/0000-0003-0923-1959
Mustafa Akyol: https://orcid.org/0000-0001-8584-0620

References:
Yan, Y., Zhang, K., Qin, G., Gao, B., Zhang, T., Huang, X., & Zhou, Y. (2024). Phase engineering on MoS2 to realize dielectric gene engineering for enhancing microwave absorbing performance. Advanced Functional Materials, 34(32), 2316338.
Ma, G., Li, J., Yan, Y., Ramasubramanian, B., Ramakrishna, S., & Huang, X. (2025). External Field-Driven Adaptive Electromagnetic Wave Response Material: From Mechanisms to Applications. Small, 21(34), 2501879.

Keyword: *MoS2, Phase Engineering, Electromagnetic wave absorbing*

Fabrication and Electrical Characterization of Laterally a-Si:H Photodiodes for Scintillator-Based Radiation Imaging

Leyla Başak Büklü [*1], Hanife Baş[2], Alp Osman Kodolbaş[3,4]

[1] *Istanbul Okan University*
[2] *Koç University*
[3] *Tübitak MAM*
[4] *KDE Bilişim Elektronik ve Güvenlik Teknolojileri San. ve Tic. A.Ş.*

The increasing use of high-energy radiation, including X-rays and gamma rays, as well as ionizing particles such as alpha, beta, and neutrons, in applications such as medical imaging, food sterilization, industrial inspection, security, defense, and space exploration has created a growing demand for low cost, high-performance radiation stable imaging detectors.

Unlike the conventional vertically structured p-i-n photodiodes widely reported in the literature, the proposed lateral architecture is designed to provide low dark current, high detection sensitivity, low power consumption, long-term operational stability, and cost-effective large-area fabrication.

In this study, laterally structured hydrogenated amorphous silicon (a-Si:H) photodiodes were deposited by Plasma -Enhanced Chemical Vapor Deposition (PECVD), photolithography, wet chemical etching and Inductively Coupled Plasma Reactive Ion Etching (ICP-RIE) process were employed in patterning photodiodes with square and circular geometries compatible with scintillator-based radiation imaging systems.

The electrical characteristics of the fabricated photodiodes were investigated by current–voltage (I–V) measurements at 300K and 80K. The saturation current (I_0), barrier height (Φ_B), and ideality factor (n) were calculated from the I–V characteristics.

Results, demonstrate that the proposed laterally structured a-Si:H photodiodes are promising candidates for integration into scintillator-based indirect radiation imaging systems, offering a practical approach toward the realization of low-cost, large-area radiation detector arrays.

* **Corresponding Author:** Leyla Başak Büklü, e-mail: leyla.buklu@okan.edu.tr

References:

Gupta V., Madaan N. et al. 2013. “Hydrogen Plasma Treatment of Silicon Dioxide for Improved Silane Deposition“, Langmuir, 29, 3604−3609.
He L. et al. 1995. “Vibrational Properties of SiO and SiH in Amorphous SiOx:H films prepared by Plasma-enhanced Chemical Vapor Deposition”, Journal of Non-crystalline Solids, 185, 249-261.
Kavasoplu, S., Birgi O., et al. 2011. “Electrical Characterization of a-Si:H(n)/c-Si(p) Structure”, Journal of Alloys and Compounds, 509, 9394–939.

Keyword: *lateral p-i-n photodiodes, Plasma -Enhanced Chemical Vapor Deposition (PECVD)*

Power beam combining of quantum cascade lasers using high-reflective distributed Bragg gratings for sensing and defense applications

Mahmut Çağlayan [*1], **Ali Aytaç Seymen**[2,3], **Timuçin Emre Tabaru**[1], **Bülend Ortaç**[3], **Ali Karatutlu**[1,3]

[1] *Sivas University of Science and Technology*

[2] *EA Teknoloji LLC Bilkent CyberPark, 06800, Ankara, Turkey*

[3] *Institute of Materials Science and Nanotechnology, National Nanotechnology Research Center (UNAM), Bilkent University, Ankara, 06800, Turkey*

Mid-infrared (mid-IR) high-power laser sources are crucial for different applications, including greenhouse gas sensing and defence applications [1,2]. Yet, access to such high-power lasers is limited and cannot be reached readily. In this study we report finite element simulation of distributed Bragg gratings not only for mid-IR sensing for carbon dioxide and methane but also for defence applications such as Directed Infrared Counter Measures (DIRCM). We report that power beam combining using high-reflective distributed Bragg gratings could be used to obtain W-level mid-IR laser sources in Zemax. We also demonstrate the design of novel mid-IR DBRs using our recently published and patented silicon oxynitride-doped silicon layers [3] alternated with silica layers using the finite element method by Comsol Multiphysics.

Acknowledgment:
We would like to thank the financial support by the Scientific Research Projects Coordination Office at Sivas University of Science and Technology.

ORCID:
Ali Karatutlu: https://orcid.org/0000-0002-8819-4916

References:
Joe, H. E., Yun, H., Jo, S. H., Jun, M. B. G. & Min, B. K. A review on optical fiber sensors for environmental monitoring. Int. J. Precis. Eng. Manuf. - Green Technol. 5, 173–191 (2018).
Swiderski, J. Recent Development of Mid-Infrared Supercontinuum Generation in Fluoroindate Glass Fibers. Appl. Sci. 12, 4927 (2022).
Karatutlu, A., Tabaru, T. E. & Ortaç, B. Low-Temperature Synthesis of Silicon Oxynitride-Doped Si for Tunable Bragg Gratings Homogeneously Deposited on Si, SiO2, and Borosilicate Substrates and the tip of SM and PM Optical Fibers (Advanced Optical Materials 12/2023). Adv. Opt. Mater. 11, 2370039 (2023).

Keyword: *Quantum Cascade Lasers, Greenhouse, Beam combining using high-reflective DBRs*

Development of a Photocatalytic Nano-TiO_2 Functional Coating for Self-Cleaning PVC Synthetic Leather Used in Public Transportation

Remziye Yıldız Ceyhan * **, Sevda Manav**

Güzelcan Suni Deri Teks.San Tic.A.Ş., 35860, İzmir, Turkiye

The ability of self-cleaning surfaces based on titanium dioxide (TiO_2) photocatalysis to remove organic pollutants under light irradiation has captured a lot of interest, providing useful advantages in terms of maintaining hygiene and extending material service life. Nevertheless, it is still very difficult to integrate photocatalytic TiO_2 nanoparticles into flexible polymeric substrates while maintaining structural integrity and industrial processability. To address interior upholstery applications in public transportation vehicles, a unique multilayer polyvinyl chloride (PVC) synthetic leather incorporating nano-TiO_2 was fabricated in this work using an industrially suitable transfer coating approach. To determine the best configuration for surface functionality and industrial viability, three incorporation strategies—introducing TiO_2 nanoparticles into polyurethane (PU), PVC plastisol, and lacquer layers—were methodically examined. To enhance surface durability and long-term photocatalytic efficacy, hydrophobic additives and UV stabilizers were also added.

Under industrial production environments, prototype samples were produced and tested against representative organic pollutants such as mustard, ketchup, tomato paste, mayonnaise, and cooking oil while exposed to up to 100 hours of natural sun radiation. Spectrophotometric color difference (ΔE) measurements and absorbance–wavelength analysis were used to quantify self-cleaning performance. The findings showed that while homogenous nanoparticle dispersion was effectively accomplished inside PVC plastisol and lacquer systems without structural damage, TiO_2 embedding into the polyurethane layer caused unwanted surface flaws. The enhanced nanostructured coating started to visibly degrade stains within the first five hours of sunlight exposure and reached more than 85% contaminant removal efficiency after 100 hours. Spectroscopic examination validated a notable decrease in absorbance intensity due to the photocatalytic breakdown of organic substances, whereas the unmodified reference synthetic leather showed minimal self-cleaning activity under the same conditions. The developed nanostructured material combines photocatalytic activity, hydrophobic surface characteristics, and stain resistance within an industrially scalable platform, offering a sustainable and viable solution for next-generation transportation, automotive, marine, furniture, and outdoor applications.

Acknowledgement

This work was supported by the Scientific and Technological Research Council of Turkey (TÜBİTAK 1501) under the project number:3240866.

Acknowledgment:
This work was supported by the Scientific and Technological Research Council of Turkey (TÜBİTAK 1501) under the project number:3240866..

ORCID:
Remziye Yıldız Ceyhan: https://orcid.org/0000-0001-9363-7219
Sevda Manav: https://orcid.org/0009-0008-6985-3868

Keyword: *Synthetic Leather, Nano TiO2, Self -Cleaning Surfaces, Surface Engineering*

Comparative Wear Performance and Surface Residue Characterization of Zirconia-Based Grinding Media Used in the Paint Industry

Rüştü Alper Taştekin *

Kansai Paint, R&D Laboratory, İzmir, Türkiye

Grinding media is a crucial factor in bead milling processes used in the paint industry, that has effect on milling efficiency, product quality and operational costs. In coatings systems, achieving effective particle size reduction of pigments and extenders provides advantages in rheological behavior, color, gloss and stability. Achieving these properties depends on efficient milling of pigment and filler pastes in bead mills. Depending on grinding media size and operating conditions, particle size reduction can be achieved over a broad range extending from nanometer to micron scale. To obtain a more homogeneous particle size distribution, grinding media wear resistance is a critical parameter. In this study, durability and surface behavior of three commercially relevant ceramic grinding media types were comparatively evaluated under laboratory milling conditions: zirconium silicate, cerium-stabilized zirconia, and yttria-stabilized zirconia beads.

A high abrasive pigment paste was processed in a laboratory bead mill for a duration to simulate industrial conditions. Mass and volumetric measurements were done to determine wear. Electron microscopy and EDX was used to examine morphological and surface changes before and after milling.

Results indicated differences in wear resistance among the tested media. Stabilized zirconia-based beads showed improved durability compared with zirconium silicate media under milling. Microscopic observations supported the wear data by revealing surface degradation and edge rounding.

During pre-test cleaning of the grinding beads, turbidity was observed in the washing solvent of zirconium silicate and cerium-stabilized zirconia beads, whereas no turbidity was detected for yttria-stabilized zirconia beads. To identify the source of turbidity, the collected precipitates were analyzed using FTIR and SEM-EDX techniques. Elemental and structural analyses indicates the presence of inorganic species containing Zr, Ce, Ca, and Si, along with polyolefin-like organic polymeric components transferred into the washing solvent medium.

These findings demonstrate that grinding media selection should consider not only wear resistance but also potential surface-derived contamination. Further studies will focus on the influence of long-term grinding media wear on pigment paste particle size distribution and milling performance. The study provides insight about the importance of material composition in ensuring both milling efficiency and product purity in advanced coating formulations. Moreover, the use of smaller beads in nanoscale pigment dispersion presents a further challenge in evaluating wear resistance as function of bead size.

Keyword: *Grinding Media, Bead Milling, Pigment Dispersion*

A Multiscale DFT and Ab Initio Molecular Dynamics Study of LiBOB Tuned Li+ Solvation in Multicomponent Carbonate Electrolytes, Validated by ATR-FTIR

Abdül Kahar Baruğ [*1], Didem Ketenoğlu[1], Bahadır Boyacıoğlu[1], Hande Toffoli[2]

[1] *Ankara University*
[2] *Middle East Technical University*

The electrochemical stability of the electrolyte governs the lifetime, safety, and energy density of lithium-ion batteries, yet the molecular mechanism by which functional additives reshape the Li^+ solvation shell remains poorly understood. Lithium bis(oxalato)borate (LiBOB) is known to build robust interphases and to improve high-temperature stability, but how, and to what extent, it enters the primary coordination sphere and rearranges cation–anion–solvent interactions in realistic, multicomponent solvents is unresolved. Unlike prior studies that, for tractability, focus on single or standard binary solvents and largely neglect the anion, no systematic work has combined experiment and theory to resolve the additive-ratio dependence across binary and ternary carbonate mixtures.

This work establishes an atoms-to-applications, multiscale workflow that bridges static quantum chemistry, finite-temperature dynamics, and experiment to explain LiBOB action in 1 M $LiPF_6$ electrolytes across EC:DMC, EC:PC, PC:DMC and EC:PC:DMC at 0, 1, 2 and 5 wt% additive.

At the electronic-structure scale, optimized $Li^+(solvent)_n(PF_6^-)/(BOB^-)$ clusters are treated with DFT (B3LYP/6-311++G(d,p), PCM) in Gaussian16 to obtain binding energies, frontier-orbital (HOMO–LUMO) gaps, global reactivity descriptors, dipole/polarizability and scaled vibrational spectra. To capture the dynamic, temperature-dependent solvation that static clusters cannot represent, the study is extended with ab initio molecular dynamics in Quantum ESPRESSO on periodic, explicitly solvated boxes. AIMD yields radial distribution functions, Li^+ coordination numbers, additive residence times, and the populations of solvent-separated, contact-ion-pair and aggregate (SSIP/CIP/AGG) configurations as a function of LiBOB content. Both computational scales are reconciled with high-resolution ATR-FTIR, focusing on the C=O (1700–1800 cm^{-1}) and C–O (1000–1300 cm^{-1}) bands, whose shifts, splittings and intensity changes are direct fingerprints of Li^+ coordination.

By coupling static descriptors, dynamic statistics and vibrational signatures, this study delivers a quantitative, experimentally validated picture of how LiBOB redistributes coordination and stabilizes the electrolyte. Linking solvation structure to interphase (SEI) formation, the electrochemical stability window and ion transport, it turns additive selection from trial-and-error into rational, data-ready design. Spanning 16 systematically varied electrolytes, the combined descriptors, dynamic statistics and validated spectra form a structured, reusable dataset linking composition to coordination and stability, laying the groundwork for data-driven screening of carbonate electrolyte formulations.

Acknowledgment:
This work was carried out with the support of the Scientific and Technological Research Council of Türkiye (TÜBİTAK) under the 2209-A University Students Research Projects Support Program

References:
Holomb, R., Xu, W., Markusson, H., Johansson, P., & Jacobsson, P. (2006). Vibrational spectroscopy and ab initio studies of lithium bis(oxalato)borate (LiBOB) in different solvents. The Journal of Physical Chemistry A, 110(40), 11467–11472.
Borodin, O., & Jow, T. R. (2010). Quantum chemistry studies of the oxidative stability of carbonate, sulfone and sulfonate-based electrolytes for Li-ion batteries. The Journal of Physical Chemistry C, 114(19), 8786–8796.
Korsun, O. M., Kalugin, O. N., Fritsky, I. O., & Prezhdo, O. V. (2016). Ion association in aprotic solvents for lithium ion batteries requires discrete-continuum approach: lithium bis(oxalato)borate in ethylene carbonate based mixtures. The Journal of Physical Chemistry C, 120(29), 16545–16552.

Keyword: *LiBOB, ab initio molecular dynamics, ATR-FTIR*

First-Principles Investigation of CO and CO2 Capture on Group IVB Metal Diboride Monolayers

Ahmet Selim Gözükara * **, Duygu Şentürk, Ongun Özçelik**

Materials Science and Nano Engineering Program, Sabanci University, Istanbul, 34956, Turkey.

Two-dimensional (2D) transition metal diborides of group IVB metals (TiB2, ZrB2, and HfB2) combine metallic conductivity with a robust hexagonal MB2-type lattice, making them promising candidates for gas-capture and filtration applications. In this work, quantum chemical simulations based on first-principles density functional theory (DFT) were employed to systematically investigate CO and CO2 adsorption vacuum-separated TiB2, ZrB2, and HfB2 monolayers.

For each monolayer, CO and CO2 molecules were positioned at high-symmetry adsorption sites directly above the metal atom and above the B–B bridge site and relaxed toward their energetically favorable configurations. Binding energies were calculated for each site and distance to identify the most stable adsorption geometry for both molecules on each of the three diboride surfaces. Projected density of states (PDOS) and Bader charge analysis were performed for both CO and CO2 to characterize the nature of the adsorbate–substrate bonding and the extent of charge transfer driving the adsorption. These analyses reveal how the choice of metal atom and adsorption site influences the strength and character of the molecule–surface interaction. For CO2 adsorption, the hollow-flat configuration in which the molecule lies parallel to the surface above the boron hollow site is identified as the most stable geometry across all three diborides, with binding energies of 1.96, 2.90, and 3.03 eV for TiB2, HfB2, and ZrB2, respectively. For CO adsorption on pristine monolayers, ZrB2 again exhibits the strongest interaction, with a binding energy of 2.80 eV. Introduction of metal vacancies was found to slightly reduce the adsorption strength for CO relative to the pristine surfaces, indicating that the intrinsic diboride lattice already provides a favorable electronic environment for CO capture without structural modification. Across both molecules, ZrB2 consistently outperforms TiB2 and HfB2 in binding strength, establishing it as the most promising candidate among the group IVB metal diborides for selective CO and CO2 capture applications.

Acknowledgment:
This work was supported by Sabanci University President’s Research Grant under project No F.A.CF-24-02901. Computational resources have been provided by Sabanci University, High Performance Computing Center, and by the National Center for High Performance Computing of Turkey (UHeM) under grant number 1013432022.

Keyword: *DFT,, Carbon Capture, 2D Metal Diborides*

Quantum Mechanical Assessment of Adsorption Dynamics in Lisinopril-Single Walled Carbon Nanotube Complexes as Drug Delivery System

Celal Yıldıray Köylü * **, Harun Nalçakan, Müşerref Önal**

Ankara University

The rational design of carbon-based nanomaterials for targeted Drug Delivery Systems (DDS) requires a deep, atomic-level understanding of interfacial phenomena. In this contribution, we present a robust computational framework that establishes a critical baseline for the non-covalent adsorption dynamics of lisinopril, a widely prescribed antihypertensive agent, onto a pristine single-walled carbon nanotube (SWCNT) with a length of approximately 20 Å. All electronic structure calculations were mapped using the Gaussian 16 software package. Density Functional Theory (DFT) at the high-level M06-2X/6-311G(d,p) framework was systematically employed, incorporating Grimme's D3 empirical dispersion correction (GD3) to accurately capture long-range van der Waals interactions. To simulate physiological conditions, these fundamental interactions were investigated within an implicit aqueous environment using the Solvation Model based on Density (SMD). Furthermore, to accurately model the extreme structural rigidity of the carbon lattice while allowing the flexible drug molecule to identify its global energy minimum, a partial optimization strategy was utilized by keeping the SWCNT coordinates frozen. Our preliminary Molecular Electrostatic Potential (MEP) analyses firmly validate the chemical rationale of the system, indicating that lisinopril's highly nucleophilic and electrophilic terminals are driven outward toward the aqueous continuum by a remarkably high permanent dipole moment of 7.94 Debye. This strong electrostatic topology allows the structurally neutral phenyl ring to act as a primary anchoring site, establishing parallel-displaced π−π and CH-π stacking with the pristine nanotube surface. Upon complexation, the initial thermodynamic evaluations of the solution interaction energy (ΔE_{ads}) confirm a highly stable and spontaneous physisorption mechanism, driven predominantly by these dispersion forces at a well-defined van der Waals interfacial distance.

Acknowledgment:
This work was supported by the Ankara University Scientific Research Projects (BAP) Coordination Office under Project No: FBG-2025-4390.

ORCID:
Celal Yıldıray Köylü: 0009-0006-0755-7671
Harun Nalçakan: 0000-0003-3821-8681
Müşerref Önal: 0000-0002-1540-8389

Keyword: *M06-2X functional, Drug Delivery Systems, Van der Waals interactions*

Computational Surface Modeling of Lunar Ilmenite for CO_2 Capture toward In-Situ Resource Utilization

Harun Nalçakan * **, Celal Yıldıray Köylü, Müşerref Önal**

Ankara University

Ilmenite ($FeTiO_3$) is a common iron–titanium oxide mineral found in both terrestrial and lunar settings, yet the two differ in fundamental ways. Terrestrial ilmenite contains ferric iron (Fe^{3+}) through solid solution with hematite, whereas lunar ilmenite is fully reduced, incorporates magnesium via the geikielite ($MgTiO_3$) end-member, and hosts structural oxygen vacancies generated by the Moon's strongly reducing environment. With concentrations reaching 10–15 wt% in high-Ti mare basalt regions, ilmenite is among the most abundant minerals in the lunar regolith and has long been studied as a target for in-situ resource utilization. In the context of future crewed lunar missions, CO_2 management at a lunar outpost is an emerging concern: orbital measurements have confirmed the existence of solid CO_2 cold traps near the lunar south pole, and CO_2 is increasingly recognized as a potential feedstock for carbon, fuel, and oxygen production on the lunar surface. Understanding how CO_2 interacts with lunar mineral surfaces at the atomic level is therefore a critical step toward evaluating indigenous materials as adsorbents or reactive substrates in future life-support and resource-utilization systems. In this study, we construct a physically realistic surface model of lunar ilmenite using first-principles methods. Starting from the bulk $FeTiO_3$ crystal structure obtained from the Materials Project database, a 2×2×1 supercell slab was built with approximately 20 Å of vacuum to simulate the surface environment. The model incorporates Mg substitution at an Fe site and a surface oxygen vacancy to reproduce the chemical characteristics of lunar ilmenite, including the associated Ti^{3+} defect states arising from the Moon's reducing conditions. CO_2 molecules were subsequently positioned above distinct surface sites in a linear adsorption geometry. All models were constructed and validated using VESTA and prepared in VASP-compatible format for DFT+U calculations with Quantum ESPRESSO. The resulting surface models provide a well-defined computational framework for investigating CO_2 adsorption on lunar ilmenite, capturing the key structural and chemical features that distinguish the lunar mineral from its terrestrial counterpart.

Acknowledgment:
This work was supported by the Ankara University Scientific Research Projects (BAP) Coordination Office under Project No: FBG-2025-4390.

ORCID:
Harun Nalçakan: 0000-0003-3821-8681
Celal Yıldıray Köylü: 0009-0006-0755-7671

Keyword: *CO2 Adsorption, DFT, Lunar Ilmenite*

Heterostructure Engineering of p- and n-Type P3HT Polymers for Enhanced Organic Photovoltaic Performance

Can Çoruh, Somayyeh Alidoust * , Ali Kumralbaş, V. Ongun Özçelik

Materials Science and Nano Engineering Program, Sabanci University, Istanbul, 34956, Turkey.

Functionalization and heterostructure engineering offer effective approaches for tailoring the electronic properties of conjugated polymers for organic photovoltaic applications. In this work, quantum chemical simulations based on density functional theory (DFT) were performed to systematically examine the effects of alkali metal (Li, Na, and K) and halogen (F and Cl) functionalization of monolayer poly(3-hexylthiophene-2,5-diyl) (P3HT) and the P3HT/biphenylene heterostructure. Single-, double-, and multi-atom functionalization configurations were considered to evaluate the influence of atom type and concentration on the structural and electronic characteristics of P3HT. The results indicate that alkali metals act as electron donors, inducing n-type behavior, whereas halogens extract electrons and promote p-type characteristics. Among the investigated functional groups, Li and F exhibit the strongest interactions with P3HT among alkali metals and halogens, respectively. Band structure analysis reveals pronounced Fermi-level shifts and the emergence of metallic behavior at the studied functionalization levels. Multi-atom functionalization shows distinct concentration-dependent trends. Li exhibits reduced charge transfer per atom due to interatomic interactions, while F preserves nearly constant charge withdrawal behavior. For the P3HT/biphenylene heterostructure, functionalization modifies interfacial charge redistribution. Projected density of states calculations confirm donor-state formation near the Fermi level for alkali metals and localized valence states for halogens. Overall, these findings provide atomistic insights into controlling the electronic structure and charge-transfer characteristics of P3HT through functionalization and heterostructure design.

Acknowledgment:
This work was supported by the Scientific and Technological Research Council of Turkey (TUBITAK) under project No 123F264.
Computational resources have been provided by TUBITAK ULAKBIM, High Performance and Grid Computing Center, and by the National Center for High Performance Computing of Turkey (UHeM) under grant number 1013432022.

Keyword: *P3HT; Density functional theory (DFT); Functionalization; Biphenylene heterostructure; Charge transfer*

Mechanisms Of Kapton Polyimide Degradation Under Atomic Oxygen Exposure In Low Earth Orbit

Tugay Kaya [*1], İrem Böbrek[1], Gozde Ozaydin İnce[1,2,3], V. Ongun Özçelik[1]

[1] *Materials Science and Nanoengineering Program, Faculty of Engineering and Natural Sciences, Sabanci University, Istanbul 34956, Turkey*
[2] *Nanotechnology Research and Application Center (SUNUM), Sabanci University, Istanbul 34956, Turkey*
[3] *Center of Excellence for Functional Surfaces and Interfaces (EFSUN), Sabanci University, Istanbul 34956, Turkey*

Kapton is a highly preferred material for spacecraft and satellites due to its high thermal stability and electrical insulation properties. However, it is subjected to material degradation and surface erosion, as a result of highvelocity atomic oxygen (AO) bombardment, ultraviolet (UV) radiation, and thermal cycling in low Earth orbit (LEO), which hosts most of the spacecrafts. Here, to clarify the degradation pathways of Kapton under AO bombardment and the conductivity damage of the degradation at the atomistic level, multiscale simulation studies are combined with an oxygen plasma experiment, and we propose a thermostat layer configuration strategy for realistic AO bombardment simulations. By performing quantum chemical simulations based on Density Functional Theory (DFT), weak bonds, mainly the C-H bond in the phenyl ring, were identified through Crystal Orbital Hamilton Populations (COHP) analysis of the Kapton structure. AO binding energy analysis was performed for reactive sites determined by the Fukui function. Density of states results were obtained for the C-H (phenylene), C-C (imide), and C-N (imide) cases where degradation was observed. With ReaxFF/QTPIE MD dynamics, OH formation and unstable intermediates occurred during early-stage degradation. Molecular, CO and CO_2 emerged as erosion products in the later degradation stages. The reaction dynamics findings and erosion yield values obtained from the simulation were correlated with the experimental Fourier transform infrared (FT-IR) and Raman spectroscopy observation data of the oxygen plasma degradation, demonstrating that the fundamental degradation mechanisms remain consistent despite the kinetic energy disparity.

Acknowledgment:
This work is supported by US Air Force Office of Scientific Research (AFOSR) through grant number FA9550- 24-1-0192. Computational resources have been provided by TUBITAK ULAKBIM, High Performance and Grid Computing Center, and by the National Center for High Performance Computing of Turkey (UHeM) under grant number 1013432022.

Keyword: *Kapton Polyimide, Erosion mechanism, Atomic Oxygen (AO)*

Monobee: Micro-Dispensing-Based Fabrication of Flexible Heaters Using Silver and Carbon Conductive Inks

Yaren Özdemir * **, Kaan Yapıcı, Ömer Faruk Güleç**

Beespenser Teknoloji Anonim Şirketi

This study presents the fabrication and thermal characterization of multilayer flexible heaters on PET substrates using silver and carbon conductive inks. The heaters were produced using Monobee, micro-dispensing platform for direct deposition of conductive and functional materials. Silver ink was used for conductive tracks and contacts, while carbon ink formed the resistive heating layer. Two different heater geometries were fabricated to investigate geometry-dependent thermal behavior.

The fabrication process demonstrates Monobee's capability for multi-material and multilayer printed electronics prototyping. After printing and curing the silver layer, reference markers were used for alignment, allowing the carbon layer to be deposited accurately over the corresponding conductive structures. This approach enables rapid fabrication of multilayer functional devices without photolithography, etching, or mask-based processes.

Thermal imaging showed distinct heating behaviors and temperature distributions for the two printed geometries. The results demonstrate the potential of micro-dispensing for rapid prototyping of flexible resistive heaters and highlight Monobee as a versatile platform for applications including wearable electronics, localized thermal management, smart packaging, and defogging or de-icing systems.

Keyword: *micro-dispensing, printed electronics, flexible heater*

Theoretical Investigation of Size, Ligand, and Functional Effects on the Excited-State Properties of Silver Nanoclusters

Fahri Alkan, Zeynep Başocak *

Bilkent University, Department of Chemistry, Ankara, Türkiye

Metal nanoclusters are an emerging class of ultra-small nanomaterials, typically under 2 nm in core size, that bridge the structural and electronic gap between isolated atoms and bulk metals. Due to strong quantum confinement effects, metal nanoclusters do not exhibit the continuous band structure of bulk metals and instead exhibit discrete, molecule-like electronic transitions. These unique optical and electronic properties have positioned noble metal nanoclusters as promising candidates for applications in optoelectronics, chemical sensing, and nanomedicine. However, the theoretical investigation of their optical properties is often hindered by the immense computational cost associated with excited-state calculations. In this work, we investigate the geometric and electronic structural changes upon photoexcitation in silver nanoclusters using time-dependent density functional theory (TDDFT) and its highly efficient, approximate variant, which employs the tight-binding approximation (TD-DFT+TB). We systematically analyze the impact of ligand substitution by interchanging -H and -CH_3 functional groups shell-by-shell. Notably, a consistent red shift in the emission spectra is observed for both ligands, shedding light on the underlying photophysical mechanisms and ligand-core interactions. Furthermore, to evaluate the performance and accuracy of the theoretical models, we benchmarked several density functionals, including B3LYP, BHandHLYP, PBE0, and BP86. Our comparative analysis highlights how the approximate TD-DFT+TB method, when combined with ground-state DFT descriptions, reliably captures key optical trends at a fraction of the computational cost. These findings provide critical insights for the rational, cost-effective design of silver nanoclusters with precisely tailored optical functionalities.

Acknowledgment:
This work is funded by TÜBİTAK. (122N449)

ORCID:
Fahri Alkan: 0000-0002-4046-9044
Zeynep Başocak: 0000-0003-4504-4624

Keyword: *TDDFT, tight-binding, silver nanoclusters, excited-state calculations, electronic structure*

Carbazole-Based Polymers: Promising Emitters for High-Performance Solution-Processable Oleds

Dilara Naz Günaydın [*1], Gökçe Kadeş[2], Semih Can Çakmaktepe[1], Gönül Hızalan Özsoy[3], Ali Çırpan[1,2,3,4]

[1] *Department of Chemistry, Middle East Technical University (METU), 06800, Ankara,Türkiye*
[2] *Department of Polymer Science and Technology, Middle East Technical University (METU), 06800, Ankara,Türkiye*
[3] *ODTU - GUNAM, Middle East Technical University, Ankara, 06800, Türkiye*
[4] *Department of Micro and Nanotechnology, Middle East Technical University (METU), 06800, Ankara,Türkiye*

Organic light-emitting diodes (OLEDs) have gained significant attention as a superior alternative to inorganic LEDs due to their high contrast ratio, excellent color purity, and lightweight nature [1]. In recent years, third-generation thermally activated delayed fluorescence (TADF) emitters have emerged as potent candidates for high-efficiency OLEDs. TADF emitters can utilize triplet excitons via reverse intersystem crossing (RISC) alongside singlet excitons, theoretically achieving 100% internal quantum efficiency (IQE). While both small molecules and polymers can serve as emitter materials, small molecules often exhibit limited solubility and poor film-forming properties in common solvents, which restricts their industrial scalability. To overcome this limitation, polymeric TADF emitters have become highly promising candidates. Their excellent solubility in organic solvents enables cost-effective, large-area processing techniques such as spin coating, inkjet printing, and blade coating. Furthermore, to maximize external quantum efficiency (EQE) and color purity, incorporating these emitters into mixed-host systems is highly preferred over using neat polymer emissive layers to improve charge transfer [2]. In this study, a mixed-host emissive layer consisting of a TCTA (0.65): TAPC (0.25): Polymer (0.10) blend was developed to facilitate efficient light generation. An OLED device with the configuration of ITO / PEDOT: PSS / TCTA:TAPC:Polymer / TmPyPB / LiF / Al was fabricated and characterized using a Keithley 2400 SMU and an EnliTech Quantum Efficiency Measurement System. The optimized device demonstrated a maximum luminance (L_{max}) of 12,020 cd/m² and a maximum current efficiency (CE_{max}) of 4.864 cd/A. The device exhibited an emission corresponding to CIE chromaticity coordinates of (0.49, 0.44) and achieved a peak external quantum efficiency (EQE_{max}) of 1.07%. These results demonstrate that solution-processable polymeric TADF OLEDs utilizing mixed-host systems hold strong potential for scalable, efficient, and low-cost display and lighting applications.

Acknowledgment:
This study was supported by ADEP (Research Universities Support Program) under the project code: ADEP-103-2025-11626. The authors thank ADEP for their support.

ORCID:
Semih Can Çakmaktepe: 0009-0005-1962-8118
Gönül Hızalan Özsoy: 0000-0002-3308-404X
Ali Çırpan: 0000-0003-3051-8380

References:
Sain, N., Sharma, D., & Choudhary, P. (2020). A review paper on: Organic light-emitting diode (Oled) technology and applications. International Journal of Engineering Applied Sciences and Technology, 04(11), 587-591. https://doi.org/10.33564/ijeast.2020.v04i11.103
Liu, Y., Wang, Y., Li, C., Ren, Z., Ma, D., & Yan, S. (2018). Efficient thermally activated delayed fluorescence conjugated polymeric emitters with tunable nature of excited states regulated via carbazole derivatives for solution-processed OLEDs. Macromolecules, 51(12), 4615-4623. https://doi.org/10.1021/acs.macromol.8b00565

Keyword: *Solution processable, TADF OLED, Polymer*

Development and Characterization of Isocyanate-Free Polyurethane (NIPU)-Based Hybrid Coatings Synthesized by Sol-Gel Method

Feride Demir [*1], **Ömer Kesmez**[2]

[1] *Akdeniz Üniversitesi, Institute of Science, Department of Chemistry*
[2] *Akdeniz Üniversitesi, Faculty of Science, Department of Chemistry*

Increasing environmental regulations and health concerns regarding traditional polyurethane (PU) coatings have accelerated the development of sustainable isocyanate-free polyurethane (NIPU) systems. While NIPUs eliminate the use of toxic isocyanates and phosgene-derived feedstocks, their relatively low mechanical performance and limited crosslinking densities remain significant obstacles to widespread industrial application. In this study, a novel sol-gel strategy is developed to produce highly cross-linked organic-inorganic hybrid NIPU (HNIPU) coatings by integrating aminosilane-derived NIPU precursors with an inorganic siloxane network. The resulting hybrid nanostructured coatings are designed to improve mechanical, thermal, optical, and surface properties while maintaining a green and catalyst-free synthesis pathway [1]. NIPU precursor systems were synthesized via room-temperature aminolysis of five-membered cyclic carbonates, namely ethylene carbonate (EC), propylene carbonate (PC), and 1,2-butylene carbonate (BC), using amino-functionalized alkoxysilanes including (3-aminopropyl)trimethoxysilane (AMMO), (3-aminopropyl)triethoxysilane (AMEO), and [3-(methylamino)propyl]trimethoxysilane (MAMMO). The synthesized precursors were then hybridized with tetraethyl orthosilicate (TEOS) via acid-catalyzed hydrolysis and condensation reactions to obtain transparent Class II organic-inorganic hybrid coatings in which the NIPU matrix is covalently integrated with a Si–O–Si network [1]. The precursor systems were characterized by FTIR spectroscopy to evaluate the aminolysis reaction and chemical transformation. The hybrid coatings were investigated using SEM-EDS, TGA, DSC, optical measurements, and mechanical performance tests. Among all formulations, the EC-AMMO precursor showed the highest chemical conversion at 96.2%. The corresponding EC-AMMO/HNIPU coating exhibited superior mechanical performance, achieving a 9H pencil hardness, 14N scratch resistance, and a 5B maximum adhesion classification [2]. To further improve surface properties, the optimum formulation was modified using fluorinated and non-fluorinated alkylsilanes. The modified coatings were successfully applied to wood, stainless steel, aluminum, ceramic, and polycarbonate substrates, providing significantly increased hydrophobicity and easy cleanability while maintaining excellent transparency [3]. This study represents the first report of 5CC-Aminosilane/HNIPU coatings prepared by catalyst-free aminolysis and sol-gel process. Integration of the nanometer-scale siloxane network into the NIPU matrix significantly improved coating performance without compromising the environmentally friendly nature of the system. These multifunctional hybrid coatings demonstrate significant potential for advanced protective coatings, sustainable surface engineering, and high-performance coating technologies.

ORCID:
Feride Demir: https://orcid.org/0009-0005-2062-9759
Ömer Kesmez: https://orcid.org/0000-0003-0107-8558

References:
[1] M. L. Chaudhary and R. K. Gupta, "Non-Isocyanate Polyurethanes (NIPU): An Introduction," in Non-Isocyanate Polyurethanes: Chemistry, Progress, and Challenges, ACS Symposium Series, vol. 1507. Washington, DC, USA: American Chemical Society, 2025, ch. 3, pp. 31–57, doi: 10.1021/bk-2025-1507.ch003.
[2] P. Zhang, G. Zhang, J. Pan, C. Ma, and G. Zhang, "Non-isocyanate Polyurethane Coating with High Hardness, Superior Flexibility, and Strong Substrate Adhesion," ACS Applied Materials & Interfaces, vol. 15, no. 4, pp. 5998–6004, Feb. 2023, doi: 10.1021/acsami.2c22433.
[3] O. Kesmez, "Preparation of hybrid nanocomposite coatings via sol-gel method for hydrophobic and self-cleaning properties," Journal of Molecular Structure, vol. 1205, Art. no. 127572, Apr. 2020, doi: 10.1016/j.molstruc.2019.127572

Keyword: *Organic-Inorganic Hybrid Coating, Sol-Gel Method, Non-Isocyanate Polyurethane*

Opto-Electronic Properties of Carbazole-Phenothiazine Donor Polymers with Pendent Diphenyl Sulfone for Solution-Processable TADF-Based OLED Applications

Gökçe Kadeş [*1], Dilara Naz Günaydın[2], Semih Can Çakmaktepe[2], Oğuzhan Karakurt[2], Ali Çırpan[1,2,3,4]

[1] *Middle East Technical University, Department of Polymer Science and Technology,Ankara, 06800, Turkey*
[2] *Middle East Technical University, Department of Chemistry, Ankara, 06800, Turkey*
[3] *Middle East Technical University, ODTU GUNAM, Ankara, 06800, Turkey*
[4] *Middle East Technical University, Department of Micro and Nanotechnology, Ankara, 06800, Turkey*

The need for sustainable, energy-efficient lighting materials has grown in recent years alongside accelerating technological developments and their adverse environmental impacts. Organic Light Emitting Diodes (OLEDs) have come into prominence due to their superior properties such as low energy consumption, flexibility, and high contrast ratio (Karakurt et al., 2024). The performance of OLED devices is significantly influenced by the chemical structure of the emissive layer, which consists of conjugated organic semiconductor materials that emit light upon electrical excitation. Thermally activated delayed fluorescence (TADF) has gained considerable interest as an exciton harvesting mechanism due to its high internal quantum efficiency. TADF materials utilize reverse intersystem crossing (RISC), whereby triplet excitons are thermally upconverted to the singlet state, allowing both singlet and triplet excitons to contribute to light emission and thereby maximizing energy efficiency (Wang et al., 2024).

This study aims to develop solution-processable TADF OLED materials with high efficiency and processability. A polymer compatible with cost-effective deposition techniques, including spin coating and spray coating, was designed using the Backbone-Donor Pendent-Acceptor (BDPA) molecular design strategy, which minimizes the energy gap and facilitates the RISC mechanism (Zhang & Cheng, 2018). To ensure high solubility and good film-forming ability, an alkyl-substituted copolymer incorporating carbazole and phenothiazine as backbone donor units and diphenyl sulfone as a pendent acceptor unit was synthesized. Monomers were characterized by NMR and HRMS, while the polymer's optoelectronic and electrochemical properties were evaluated by PL, UV-Vis, GPC, and CV. The results demonstrate that the synthesized TADF polymer is a promising candidate for OLED applications, offering both high efficiency and excellent processability.

Acknowledgment:
This study was supported by Research Universities Support Program (ADEP) under the Grant Number 103-2025-11626. The authors thank ADEP for their supports.

References:
Karakurt, O., Demirgezer, E. F., Dastemir, M., Cakmaktepe, S. C., Miranda-Salinas, H., Aksoy, E., Danos, A., Monkman, A., Yildirim, E., & Cirpan, A. (2024a). Design and performance of sulfur and selenium-substituted triarylboron d3-a TADF emitters for OLED applications. Organic Electronics, 134, 107130. https://doi.org/10.1016/j.orgel.2024.107130
Wang, T., Cheng, Y., & Yang, C. (2024). Thermally activated delayed fluorescence polymers and their application in organic light-emitting diodes. Progress in Polymer Science.
Zhang, B., & Cheng, Y. (2018). Recent advances in conjugated TADF polymer featuring in backbone-donor/pendant-acceptor structure: Material and device perspectives. The Chemical Record, 19(8), 1624–1643. https://doi.org/10.1002/tcr.201800152

Keyword: *Organic Light Emitting Diode (OLED), Thermally Activated Delayed Fluorescence (TADF), Reverse İntersystem Crossing (RISC), Backbone-Donor Pendent-Acceptor (BDPA)*

Theoretical and Photophysical Evaluation of a Novel Ethynyl-Bridged Hot Exciton Emitter for OLEDs

Ozan Tekin [*1], Esra Yenidoğan[1], Cem Maraşlıoğlu[2], Gönül Hızalan Özsoy[3], Selçuk Gümüş[4], Erkan Aksoy[5], Ali Çırpan[1,2,3,6]

[1] Middle East Technical University, Department of Chemistry, Ankara, 06800, Türkiye
[2] Middle East Technical University, Department of Polymer Science and Technology, Ankara, 06800, Türkiye
[3] Middle East Technical University, ODTU GUNAM, Ankara, 06800, Türkiye
[4] Bartın University, Faculty of Engineering, Architecture and Design, Department of Basic Sciences, Bartın, 74110, Türkiye
[5] Bartın University, Rectorate, Project and Technology Office, Bartın, 74100, Türkiye
[6] Middle East Technical University, Department of Micro and Nanotechnology, Ankara, 06800, Türkiye

The development of high-efficiency Organic Light-Emitting Diodes (OLEDs) relies on materials capable of harvesting both singlet and triplet excitons to overcome the theoretical 25% internal quantum efficiency limit of conventional fluorescent emitters. While thermally activated delayed fluorescence (TADF) typically operates via reverse intersystem crossing (RISC) from T_1 to S_1, the "hot exciton" mechanism offers an alternative pathway by utilizing high-lying triplet states (T_n, $n \geq 2$) to achieve rapid upconversion to S_1 [1]. This pathway circumvents the strict requirement of an extremely small singlet-triplet energy gap (ΔE_{ST}), opening new avenues for efficient metal-free organic emitters.

This work aims to design, synthesize, and photophysically evaluate a novel small-molecule donor-acceptor (D-A) architecture, designated as D-A1. The molecule features a carbazole-based donor unit linked via a rigid ethynyl bridge to a customized acceptor core, aimed at tuning electronic coupling and molecular conformation [2]. Structural integrity of D-A1 and its synthetic intermediates were confirmed by NMR spectroscopy and HRMS. Photophysical, electrochemical, and thermal properties were investigated using UV-Vis absorption, photoluminescence (PL) spectroscopy, CV, and TGA. Although the framework was initially targeted for conventional TADF behavior, quantum chemical calculations revealed a relatively large ΔE_{ST} between S_1 and T_1, hindering traditional TADF channels. However, energy alignment calculations identified a higher-lying triplet state (T_n) nearly degenerate with S_1. This energetic alignment, combined with favorable spin-orbit coupling, strongly supports an efficient hRISC pathway consistent with the hot exciton mechanism. The rigid ethynyl spacer effectively regulates conjugation and dihedral angles, facilitating the necessary orbital overlap for this process. Overall, this study demonstrates that ethynyl-bridged D-A systems are promising structural platforms for high-efficiency hot exciton emitters in next-generation OLED applications.

Acknowledgment:
This study was supported by Scientific and Technological Research Council of Turkey (TUBITAK) under the Grant Number 124F400. The authors thank TUBITAK for their support.

References:
Hu, D., & Ma, Y. (2018). "The 'hot exciton' mechanism for organic light-emitting diodes: Challenges and prospects." Chemical Society Reviews, 47(13), 4553-4565.
Wong, M. Y., & Zysman-Colman, E. (2017). "Purely organic thermally activated delayed fluorescence materials for organic light-emitting diodes." Advanced Materials, 29(22), 1605444.

Keyword: *Thermally Activated Delayed Fluorescence (TADF), Hot Exciton Mechanism, Donor-Acceptor Small Molecule*

Sustainable Cellulose/MXene/CuO Hybrid Composites Derived from Forestry Waste for Electromagnetic Interference Shielding Applications

Rumman Zaidi * **, Amina Ben Ayed, Tülay Yılmaz İnan**

Sabanci University Nanotechnology Research and Application Center (SUNUM), 34956, Tuzla-İstanbul, Turkey

Electronic devices have become indispensable in modern society; however, the rapid increase in wireless communication systems, portable electronics, and miniaturized devices has significantly intensified electromagnetic interference (EMI), leading to concerns regarding device malfunction, signal disturbance, and potential health risks. Therefore, the development of lightweight, sustainable, multifunctional, and high-performance EMI shielding materials has become increasingly important.

In this study, sustainable cellulose-based hybrid composites containing MXene and CuO are being developed for EMI shielding applications in the X-band frequency region. Cellulose derived from forestry waste is utilized as a renewable matrix material due to its biodegradability, low density, flexibility, high aspect ratio, and network-forming capability. MXene is incorporated to construct conductive pathways and improve electromagnetic attenuation, while CuO nanoparticles are introduced to enhance interfacial polarization, dielectric loss, and microwave absorption behavior. Composite systems including cellulose/MXene, cellulose/CuO, and cellulose/MXene-CuO with different MXene loadings (10–40 wt%) are being fabricated through a dispersion-assisted processing approach. The resulting composites will be systematically characterized using Fourier transform infrared spectroscopy (FTIR), X-ray diffraction (XRD), scanning electron microscopy (SEM), thermogravimetric analysis (TGA), and EMI shielding measurements. The synergistic interaction between cellulose, MXene, and CuO is expected to improve conductive network formation, thermal stability, interfacial interactions, and electromagnetic wave dissipation. The developed hybrid structures are anticipated to provide environmentally friendly and lightweight alternatives for next-generation EMI shielding applications in flexible electronics, wearable systems, aerospace technologies, and advanced communication devices.

Acknowledgment:
This work was supported by TÜBİTAK COST Action Project No. 2515-223M347.

ORCID:
Rumman Zaidi: https://orcid.org/0000-0001-7692-6692

References:
1. K. Liu, H. Du, T. Xu, C. Si, and X. Pan, “Hierarchical Cellulose/MXene Aerogel Films with Coral-Like Polyaniline Skin for Absorption-Led Broadband EMI Shielding.” Advanced Functional Materials36, no. 31 (2026): e74562. https://doi.org/10.1002/adfm.74562
2. Shuaijie Liu, Tianyi Zhang, Bowen Tan, Jinglun Guo, Wei Zhong, Nannan Chen, Han Zou, Le Cao, Xuqing Liu, “Dual-network aramid nanofibers/cellulose Nanofibers/MXene aerogels for lightweight, pulse electromagnetic interference shielding.” Composites Science and Technology, no. 272, (2025):111373, https://doi.org/10.1016/j.compscitech.2025.111373

Keyword: *Electromagnetic interference shielding, Cellulose nanocomposites, Copper oxide nanoparticles*

Synthesis of Fluorene-Containing DBPA-Type Polymeric TADF Emitters

Semih Can Çakmaktepe [*1], Dilara Naz Günaydın[1], Gökçe Kadeş[1], Oğuzhan Karakurt[1], Ali Çırpan[1,2,3,4]

[1] *Middle East Technical University, Department of Chemistry, 06800, Ankara, Turkey*
[2] *Middle East Technical University, ODTU GUNAM, Ankara, 06800, Turkey*
[3] *Middle East Technical University, Department of Polymer Science and Technology, Ankara, 06800, Turkey*
[4] *Middle East Technical University, Department of Micro and Nanotechnology, Ankara, 06800, Turkey*

Organic Light-Emitting Diodes (OLEDs) are a cutting-edge technology in the lighting and display fields [1]. Their advantages over inorganic counterparts, such as high efficiency, a wider color gamut, higher contrast, vivid colors, and flexibility, make OLEDs promising candidates for next-generation display technology [2]. OLEDs are commonly classified into three generations: fluorescent, phosphorescent, and thermally activated delayed fluorescent (TADF) OLEDs. The first generation fluorescent OLEDs, harvesting only singlet excitons which is 25% of the all excitons, limiting their efficiency, shortening device lifetime, and causing heating problems [3]. Phosphorescent OLEDs were developed to overcome these limitations by incorporating heavy-metal atoms such as Ir, Pt, and Os, which enable efficient triplet harvesting. However, the use of these metals leads to high material costs and environmental sustainability concerns. In contrast, TADF OLEDs aim to reduce costs by using purely organic materials with a small singlet–triplet energy gap (ΔE_{ST}), enabling reverse intersystem crossing (RISC). This approach reduces material costs while maintaining high efficiency. However, many TADF materials suffer from low solubility [4], often making vacuum deposition more practical. Polymeric TADF OLEDs are a class of materials that can be processed by solution-processing techniques and are suitable for large-area coating applications. While the donor-backbone–pendant-acceptor strategy enables efficient RISC, alkylated backbone units help increase polymer solubility. This study aims to synthesize an emitter polymer containing geminally alkylated fluorene units to enhance solubility, benzophenone units as acceptors, and phenothiazine units as donors for TADF OLED applications.

Acknowledgment:
This project is funded by Middle East Technical University, with project ID ADEP-103-2025-11626

ORCID:
Semih Can Çakmaktepe: 0009-0005-1962-8118
Oğuzhan Karakurt: 0000-0002-1856-0503
Ali Çırpan: 0000-0003-3051-8380

References:
R. Liguori, F. Nunziata, S. Aprano, and M. G. Maglione, “Overcoming Challenges in OLED Technology for Lighting Solutions,” Apr. 01, 2024, Multidisciplinary Digital Publishing Institute (MDPI). doi: 10.3390/electronics13071299.
O. Karakurt et al., “Design and performance of sulfur and selenium-substituted triarylboron D3-A TADF emitters for OLED applications,” Org. Electron., vol. 134, Nov. 2024, doi: 10.1016/j.orgel.2024.107130.
X. Yang, G. Mu, K. Weng, and X. Tang, “Advances in High-Efficiency Blue OLED Materials,” Sep. 01, 2024, Multidisciplinary Digital Publishing Institute (MDPI). doi: 10.3390/photonics11090864.
E. Witkowska, G. Wiosna-Salyga, I. Glowacki, T. H. Ke, P. Malinowski, and P. Heremans, “Effect of TADF assistance on performance enhancement in solution processed green phosphorescent OLEDs,” Polymers (Basel)., vol. 13, no. 7, Apr. 2021, doi: 10.3390/polym13071148.

Keyword: *TADF, OLED, Polymer*

Shrimp-Derived Chitosan-Activated Carbon Composite for Methylene Blue Removal

Hamed Yousefzadeh * **, Dila Selin Cubukcuoglu, Azra Zeynep Ture**

Department of Chemical Engineering, Yeditepe University, Ataşehir 34755, İstanbul, Türkiye

Crosslinking in polymer-based adsorbents not only improves the chemical and mechanical properties of the adsorbent, but also affects its adsorption performance. In this study, shrimp-shell-derived chitosan/activated carbon composite beads (ChAc) and glutaraldehyde-crosslinked beads (ChAcG) were prepared and comparatively evaluated for methylene blue (MB) removal from water to reveal the effect of crosslinking on adsorption behavior. FTIR confirmed crosslinking via imine-related features, while adsorption tests showed clear effects of pH, dosage, contact time, and temperature (298–318 K). Equilibrium uptake generally increased from 298 to 308 K, indicating an overall endothermic uptake in this range, and the isotherm data were described by Langmuir/Freundlich models. ChAc exhibited a high maximum adsorption capacity of 327.5 mg g^{-1} at 298 K, whereas crosslinking reduced the accessible capacity to 115.2 mg g^{-1}, consistent with partial consumption of amine sites and network densification, which limits site accessibility and transport. Overall, ChAc provides higher capacity, while ChAcG offers improved structural robustness at the expense of adsorption performance due to glutaraldehyde crosslinking.

ORCID:
Hamed Yousefzadeh: 0000-0002-3292-5783

Keyword: *Adsorption, Methylene Blue, Activated Carbon*

Additive-Dependent Triboelectric Performance of Polystyrene Composites against Polytetrafluoroethylene

Ahmet Tulumtas[1], Ahmet Korkmaz [* 1], Barkin Bayram[1], Onur Demircioglu[1], Fatih Ozcan[2], Mehmet Gursoy[1,3], Husnu Emrah Unalan[1]

[1] Middle East Technical University
[2] Selcuk University
[3] Konya Technical University

Triboelectric nanogenerators (TENGs) have attracted increasing attention as sustainable technology for self-powered sensing and energy harvesting applications. In this study, to investigate their influence on energy conversion efficiency, polystyrene (PS) based composite samples were cast by incorporating different additives: hexagonal boron nitride (h-BN), hexagonal boron carbide (h-BC), and graphene. The triboelectric performance of the samples was systematically evaluated using polytetrafluoroethylene (PTFE) as the counter triboelectric material. The measurements were conducted in a vertical contact separation mode. The results showed that the type of additive had a significant effect on the electrical output of the system during the continuous cycles. Among the investigated composites, the h-BN containing sample exhibited the highest triboelectric response, generating a peak voltage of 30 V and a short circuit current of 70 nA. This was followed by the h-BC containing sample, which produced 18 V and 50 nA, while the graphene containing one showed the lowest performance, yielding only 1 V and 7 nA. The better performance of h-BN can be attributed to its insulating nature, dielectric properties, and possible contribution to charge trapping at the polymer filler interface. In contrast, the relatively low output of the graphene containing composite may be related to rapid charge dissipation due to its highly conductive character and possible filler aggregation within the polymer matrix. These findings provide valuable insights for the design and optimization of promising performance composite triboelectric materials, showing great potential for future applications in flexible electronics and self-powered autonomous sensor systems.

Acknowledgment:
This work was supported by The Scientific and Technological Research Council of Türkiye 124C127.

ORCID:
Ahmet Tulumtas: 0009-0003-7938-4907
Ahmet Korkmaz: 0009-0006-4564-0118
Barkin Bayram: 0009-0000-3552-323X
Onur Demircioglu: 0000-0002-1136-0357
Fatih Ozcan: 0000-0002-3922-7902
Mehmet Gursoy: 0000-0003-2275-9096
Husnu Emrah Unalan: 0000-0003-3667-179X

Keyword: *TENG, Polystyrene, Additives*

GO/CNT-Modified DGEBA-Based Epoxy Systems: Thermal, Curing, and Spectroscopic Evaluation

Berke Sayınman [*1,2], **Elif Okutan**[1]

[1] *Department of Chemistry, Gebze Technical University, Kocaeli, Türkiye*
[2] *Aksa Carbon, R&D Center, Yalova, Türkiye*

Graphene oxide (GO) and carbon nanotubes (CNTs) can influence the thermal stability and cure behavior of epoxy resins through their surface functionalities, nanoscale morphology, and interactions with the polymer matrix. However, the combined effects of these nanofillers depend strongly on their concentration, dispersion quality, and interfacial interactions. In this study, the effects of GO loading and COOH-functionalized multi-walled carbon nanotube (MWCNT-COOH) addition were systematically investigated in DGEBA-based epoxy formulations at both the intermediate mixture stage and in the fully formulated resin systems.

GO-modified epoxy intermediates containing 0.25, 0.50, and 0.75 phr GO were prepared, while the corresponding hybrid formulations additionally incorporated 0.50 phr COOH-functionalized carbon nanotubes (CNTs). To isolate the effects of the nanofillers, uncured intermediate mixtures without polyethersulfone (PES) or hardener were first investigated. Selected intermediates were then incorporated into DGEBA/PES/4,4′-diaminodiphenyl sulfone epoxy systems. FT-IR spectroscopy was used for the structural characterization, whereas TGA, DSC, and isothermal rheological measurements were employed to evaluate the thermal stability and curing behavior of the epoxy systems.

These findings demonstrate that the thermal stability and curing behavior of GO/CNT-modified epoxy systems are governed not only by nanofiller concentration but also by the dispersion state, interfacial interactions, and the nanofiller architecture developed within the epoxy matrix.

Acknowledgment:
The authors acknowledge Aksa Carbon for providing access to the laboratory infrastructure, resin-processing facilities, and rheological characterization equipment used in the study.

ORCID:
Berke Sayınman: 0009-0006-4418-4827
Elif Okutan: 0000-0002-6576-4453

References:
Qi, Z., Tan, Y., Zhang, Z., Gao, L., Zhang, C., & Tian, J. (2018). Synergistic effect of functionalized graphene oxide and carbon nanotube hybrids on mechanical properties of epoxy composites. RSC Advances, 8, 38689–38700. https://doi.org/10.1039/C8RA08312F
Li, S., Liu, X., Fang, C., Liu, N., & Liu, D. (2018). Surface modification and thermal performance of a graphene oxide/novolac epoxy composite. RSC Advances, 8, 20505–20516. https://doi.org/10.1039/C8RA02847H
Wan, Y.-J., Tang, L.-C., Gong, L.-X., Yan, D., Li, Y.-B., Wu, L.-B., Jiang, J.-X., & Lai, G.-Q. (2014). Grafting of epoxy chains onto graphene oxide for epoxy composites with improved mechanical and thermal properties. Carbon, 69, 467–480. https://doi.org/10.1016/j.carbon.2013.12.050
Yang, S.-Y., Lin, W.-N., Huang, Y.-L., Tien, H.-W., Wang, J.-Y., Ma, C.-C. M., Li, S.-M., & Wang, Y.-S. (2011). Synergetic effects of graphene platelets and carbon nanotubes on the mechanical and thermal properties of epoxy composites. Carbon, 49, 793–803. https://doi.org/10.1016/j.carbon.2010.10.014

Keyword: *Epoxy Nanocomposites; Graphene Oxide; Carbon Nanotubes; Thermal Stability; Cure Behavior; Hybrid Nanofillers*

Multi-Analytical Characterization of Silica Nanoparticles for Paint and Coating Applications

Ece Sağkol * **, Seçil Sevim Ünlütürk, Adalet Ayça Biçen İbik, Necati Güdümcüoğlu**

Kansai Altan Paint Company, 35730, Izmir, Turkey

Abstract

Silica nanoparticles are widely employed as functional additives in paint and coating formulations to enhance mechanical durability, scratch resistance, rheological performance, and thermal stability. However, their effectiveness within polymer matrices is strongly influenced by their physicochemical, morphological, and surface chemical properties. This study aims to comparatively characterize different grades of silica nanoparticles using complementary analytical techniques to elucidate their structural features, surface chemistry, thermal behavior, and colloidal stability in liquid media.

Fourier transform infrared spectroscopy (FTIR) will be used to identify characteristic silanol groups and organic functionalities associated with surface modification. An FTIR system equipped with a thermogravimetric analysis attachment (FTIR-TGA) will be employed to monitor temperature-dependent mass loss and characterize volatile decomposition products released from the nanoparticle surfaces. Solvent extraction will also be applied to isolate extractable organic species associated with the silica surfaces. Comparative evaluation of the extracted fractions and residual silica particles is expected to provide insight into physically adsorbed components and more strongly bound surface modifications.

Dynamic light scattering (DLS) and zeta potential measurements will be conducted to determine solvodynamic particle size distribution, polydispersity index, zeta potential and aggregation tendency. Scanning electron microscopy coupled with energy-dispersive X-ray spectroscopy (SEM-EDX) will be used to evaluate particle morphology, spatial organization, and elemental composition.

The resulting analytical framework is expected to establish relationships among surface functionality, extractable organic content, particle size distribution, morphology, thermal behavior, and dispersion stability. The outcomes may support the comparative assessment and rational selection of silica nanoparticles for targeted paint and coating applications.

Acknowledgment:
The authors gratefully acknowledge Kansai Altan Paint Company for providing the materials, laboratory facilities, and analytical support for this study.

ORCID:
Ece Sağkol: 0000-0002-9179-1463
Seçil Sevim Ünlütürk: 0000-0001-8300-3837
Adalet Ayça Biçen İbik: 0000-0002-4156-6575
Necati Güdümcüoğlu: 0000-0001-6563-4870

References:
Gun'ko, V. M., et al. "A New Route for Preparation of Hydrophobic Silica Nanoparticles Using a Mixture of Poly(dimethylsiloxane) and Diethyl Carbonate." Polymers, 2018.
Park, E. J., et al. "Fabrication of Superhydrophobic Thin Films on Various Substrates Using SiO_2 Nanoparticles Coated with Polydimethylsiloxane." RSC Advances, 2015.
Zheng, B., Li, W., Liu, L., Wang, X., Chen, C., Yu, Z., & Li, H. Determination of phenol isomers in water by a novel nanosilica/polydimethylsiloxane-coated stirring bar combined with high-performance liquid chromatography–Fourier transform infrared spectroscopy. Scientific Reports, 2017, 7, 8697.
Protsak, I., Pakhlov, E., Tertykh, V., Le, Z.-C., & Dong, W. A new route for preparation of hydrophobic silica nanoparticles using a mixture of poly(dimethylsiloxane) and diethyl carbonate. Polymers, 2018, 10, 116.
Kulyk, K., Zettergren, H., Gatchell, M., Alexander, J. D., Borysenko, M., Palianytsia, B., Larsson, M., & Kulik, T. Dimethylsilanone generation from pyrolysis of polysiloxanes filled with nanosized silica and ceria/silica. ChemPlusChem, 2016, 81, 1003–1013.

Keyword: *Silica Nanoparticles, Surface Modification, Coatings*

Correlation Between Microstructural Characteristics and Mechanical Properties of Selective Laser Melted Ti-6Al-4V Alloy Fabricated in Different Build Orientations

Uğurcan Güncan *

Department of Mechanical Engineering, Izmir Institute of Technology, Izmir, Türkiye

Ti-6Al-4V is one of the most widely used titanium alloys due to its high specific strength, excellent corrosion and oxidation resistance, and superior biocompatibility, making it suitable for aerospace, biomedical, defense, and space applications. Among metal additive manufacturing technologies, Selective Laser Melting (SLM), a laser powder bed fusion process, has attracted considerable attention because of its ability to fabricate complex components with high dimensional accuracy and design flexibility. Ti-6Al-4V is a dual-phase (α+β) alloy, however, the rapid heating and cooling rates together with repeated thermal cycles inherent to the SLM process promote the formation of an acicular α′ martensitic microstructure. Furthermore, steep thermal gradients and the layer-by-layer manufacturing strategy produce orientation-dependent microstructural features that directly influence the mechanical behavior of the alloy. Although numerous studies have investigated the microstructure and mechanical properties of SLM-fabricated Ti-6Al-4V, the correlation between build orientation, microstructural characteristics, and mechanical behavior has not been fully clarified. In this study, Ti-6Al-4V specimens were fabricated by SLM in vertical and horizontal build orientations. After fabrication, stress-relief heat treatment was applied to reduce residual stresses and promote microstructural stabilization. Tensile, compression, and hardness tests were performed to evaluate the mechanical behavior of the specimens. Scanning Electron Microscopy (SEM) was used to characterize the microstructure and investigate the deformation and fracture mechanisms. The relationship between microstructural characteristics and mechanical behavior was evaluated by combining the mechanical test results with SEM observations. The mechanical test results showed that horizontally fabricated specimens exhibited higher yield strength and strain capacity during tensile testing, whereas the ultimate tensile strength was nearly identical for both build orientations. Compression tests also showed higher compressive yield strength and maximum true stress values for the horizontal specimens. In contrast, hardness measurements revealed no significant difference between the two build orientations. SEM observations identified orientation-dependent differences in α-lath morphology and fracture characteristics, supporting the interpretation of the mechanical behavior. Overall, the results demonstrate that build orientation plays a key role in the relationship between microstructural characteristics and the mechanical performance of SLM-fabricated Ti-6Al-4V.

Acknowledgment:
would like to express my sincere gratitude to my advisor, Dr. Benay Uzer, and my co-advisor, Prof. Dr. Mustafa Güden, for their invaluable guidance, knowledge, and continuous support throughout every stage of this study. I would also like to thank 149 (Advanced Materials Laboratory / Izmir Institute of Technology) for providing laboratory facilities and technical assistance. I would like to extend my special thanks to Hatice İrem Ertem, a Ph.D. student involved in the project, for her valuable support and contributions throughout this study. I am also grateful to my colleagues and peers for the insightful discussions and collaboration during the course of this research. Lastly, I would like to express my appreciation to TÜBİTAK for the opportunity to participate in Project No. 22AG053.

Keyword: *Ti-6Al-4V; Selective Laser Melting (SLM); Build Orientation; Scanning Electron Microscopy (SEM); Mechanical Properties*

A Cascade Nanozyme Platform for Synergistic Glioblastoma Therapy

Serhat Hacıibrahimoğlu [*1], Esin Akbay Çetin[2], İrem Yağmur Gök[3], Gökçe Çoban[4], Burcu Gökçal Kapucu[4], Çiğdem Kip[4], Mustafa Polat[5], Mehmet Ali Onur[2,3], Ali Tuncel[1,3,4]

[1] *Hacettepe University, Division of Nanotechnology and Nanomedicine, Ankara, Turkey*
[2] *Hacettepe University, Department of Biology, Ankara, Turkey*
[3] *Hacettepe University, Division of Bioengineering, Ankara, Turkey*
[4] *Hacettepe University, Chemical Engineering Department, Ankara, Turkey*
[5] *Hacettepe University, Department of Physics Engineering, Ankara, Turkey*

Glioblastoma remains one of the most lethal primary brain tumors, where the hypoxic and glutathione-rich tumor microenvironment critically undermines the efficacy of single-modality therapeutic approaches. To simultaneously address these challenges, polydopamine-based multifunctional nanoparticles were engineered through in-situ reduction of noble metals onto polydopamine nanoparticles.

The nanoparticles operate through a self-reinforcing therapeutic cascade centered on chemodynamic and photothermal modalities. The intrinsic catalase-like nanozyme activity continuously decomposes intratumoral H_2O_2 into molecular oxygen, simultaneously relieving tumor hypoxia and restoring oxygen availability within the tumor microenvironment. This enzyme mimetic activity additionally facilitates glutathione depletion within the tumor microenvironment, neutralizing a key antioxidant defense mechanism and thereby sensitizing tumor cells to oxidative stress, further amplifying the overall chemodynamic therapeutic effect.

Under near-infrared (NIR) irradiation, the exceptional photothermal conversion ability of the polydopamine-noble metal nanoplatform induces direct thermal cytotoxicity against glioblastoma cells. Crucially, the local hyperthermia generated simultaneously upregulates nanozyme catalytic rates, accelerating H_2O_2 decomposition and sustaining intratumoral oxygen replenishment, while further potentiating oxidative stress within the already glutathione-depleted tumor microenvironment, locking the system into a positive feedback loop that synergistically enhances chemodynamic therapy. This photothermal chemodynamic interplay ensures that each modality reinforces the other, overcoming the limitations associated with monotherapy approaches in the immunosuppressive and reductive tumor microenvironment.

Preliminary in vitro evaluation against T98G glioblastoma cells demonstrated highly promising synergistic anticancer activity, with notable suppression of tumor cell viability, migration, and proliferation. These proof-of-concept findings position polydopamine-based noble metal-loaded nanospheres as a compelling multifunctional nanoplatform warranting further investigation for next-generation glioblastoma therapy.

Acknowledgment:
This study was supported by the Scientific and Technological Research Council of TURKEY (TUBITAK) under the Grant Number 22AG004, Next Generation Biomaterial Technologies Research Network for Healthy Life. The authors thank to TUBITAK for their support.

ORCID:
Serhat Hacıibrahimoğlu: https://orcid.org/0009-0008-6468-9544
Esin Akbay Çetin: https://orcid.org/0000-0002-0797-8322
İrem Yağmur Gök: https://orcid.org/0000-0001-4131-2479
Burcu Gökçal Kapucu: https://orcid.org/0000-0002-3364-9100
Çiğdem Kip: https://orcid.org/0000-0003-0491-2616
Mustafa Polat: https://orcid.org/0000-0002-9437-864X
Mehmet Ali Onur: https://orcid.org/0000-0002-3630-7982
Ali Tuncel: https://orcid.org/0000-0002-4341-1286

Keyword: *Nanozyme, Synergistic Therapy, Polydopamine*

Author Index

Abasov, H. 117
Abdolhosseinzadeh, S. 18
Abdubakir, A. 220
Abofoul, A. 78, 85, 181, 228
Acar, H.F.Y. 382
Acar, S.Ş. 266
Achachlouei, B.F. 326
Açan, D.İ. 355
Adeel, M. 66
Afacan, R.S.U. 284
Aghamaliyev, A. 203
Aghdaei, Y.F. 240
Aghdam, S.J. 394
Ağalar, A.A. 276
Ağrı, E. 277
Ahmed, H. 57
Ahmed, I. 102, 165
Ahmetoglu, C.V. 9
Ahn, W. 340
Aissa, B. 88
Ajala, O.J. 142, 179, 218
Akan, T. 232
Akbaba, G.E. 358
Akbaba, H. 304
Akbayrak, S. 282, 283, 288
Akbıyık, A. 345
Akbulut, Ö. 196, 197
Akbülbül, Ö. 386
Akca, O. 362
Akdeniz, D. 246
Akdogan, O. 197
Akdogan, Y. 139
Akdoğan, E. 189
Aker, V. 175

Akgündoğdu, A. 258
Akgür, S.A. 188
Akın, G.G.B. 390
Akıncı, Ü. 90
Akin, L.D. 290
Akinoglu, E.M. 141
Akkoyun, S. 86
Akkus, B. 319
Akman, E. 47
Akpınar, S. 45
Aksan, O.A. 76
Aksoy, E. 53, 415
Aksoy, F. 35, 114, 138, 234
Aksu, D. 305, 312, 317, 322
Aksu, P. 151
Aksu, Y. 349
Akşener, A.E. 225
Aktas, O.C. 250
Aktaş, L. 65, 325
Aktaş, M. 391
Aktepe, Y. 316
Aktuna, A.Y. 341
Aktürk, E.Z. 210
Akyol, M. 399
Akyol, M.C. 378
Akyüz, S.A. 190
Alakent, B. 259
Alal, O. 235
Albay, T.A. 367, 372
Albayrak, A.Z. 250
Albora, A.F. 323
Aleinawi, M.H. 229
Alev, O. 111
Ali, S.R. 74, 101, 351
Alidoust, S. 200, 408
Alkan, F. 198, 411

Alkaya, İ. 398
Alptekin, D.A. 262, 263, 265, 266, 267, 268
Alptekin, S. 382
Altangerel, A. 385
Altay, L. 44
Altınapa, S. 123
Altıntop, İ. 358
Altıok, E. 87
Altun, Z.C. 368
Altunbek, M. 110
Altuntaş, E. 137
Altuntepe, A. 82, 162
Alves, F. 57
Alves, F.S. 136
Amarjargal, A. 327
Amasya, G. 96
Anbar, D. 204
Andaç, T. 63
Anık, Ü. 8, 299, 299, 350
Anik, U. 233, 233
Anlaş, B. 79
Ansuini, A. 260
Antanavičė, A. 273
Arabacı, E.D. 41, 243, 246
Arapoglu, M.A. 249
Aras, T.S. 164
Arda, M. 87
Arıcan, S. 171
Arıduman, K. 286, 295
Arikan, B. 84
Arslan, A.A. 71
Arslan, G. 238
Arslan, H. 18
Arslan, K.S. 359
Arslan, L.Ç. 76
Arslan, O. 134, 335

Arslan, Y. 224
Arsu, N. 333
Asan, G. 335
Asil, D. 174
Aslan, F. 157
Aslan, R. 188
Aslım, B. 251
Asmafiliz, N. 85
Atak, G. 92, 146, 255
Ataman, D.S. 112
Atar, S. 398
Atay, M. 94, 217
Atilla, D.Ç. 261
Atlı, E. 168
Atlı, İ. 33, 356, 364, 372
Atli, E. 393
Atmaca, B. 210
Avcı, İ. 373
Avcıoğlu, S. 223
Avci, M.B. 71, 300
Aydemir, N. 204
Aydın, F. 214
Aydın, M. 274
Aydın, N. 166
Aydın, O. 182
Aydın, S. 119
Aydınol, K. 391
Aydin, E. 285
Aydogan, D. 50, 281
Aydoğdu, M. 274
Ayed, A.B. 387, 416
Ayevi, B. 382
Aygun, S.C. 84
Aygün, S.Ç. 77
Aytaç, Ö.G. 221, 315
Aytaç, S. 221, 315

Aytar, M. 354, 376
Aytas, S. 241
Aytuna, Ç.U. 210
Ayyıldız, B. 155
Azhari, S. 135
Bagheralmoosavi, S. 114, 357
Baghirov, M.B. 40
Bağdaş, A.C. 390
Bakbak, H.E. 125
Bakhshpour-Yücel, M. 113, 298
Bakır, S.E. 291
Bakırsoy, T. 223
Balcı, F.M. 343
Balcı, S. 343
Balki, H.B. 294
Baran, D. 4
Baran, D.T. 321
Baran, E. 243
Baran, G. 118
Barandır, T.K. 59, 261
Barlas, F.B. 95, 97, 116
Baruğ, A.K. 404
Basaran, B. 133
Baskan-Bayrak, H. 165
Basol, B. 310
Basol, M. 139, 139
Basu, S. 91
Baş, H. 400
Baş, S. 286, 295
Başer, G. 396
Başocak, Z. 411
Başol, B. 279
Baştürk, S.B. 396
Bauerdick, S. 144
Bayat, F.E. 213
Bayazıt, I. 358, 358

Bayazıt, Ş.S. 116
Bayazit, Ş.S. 95, 323
Bayrak, H.B. 102
Bayram, B. 107, 419
Bayram, C. 38, 380
Bayram, T.Y. 221, 315
Baysoy, E. 72
Behram, Z.S. 67
Beker, L. 294
Bekin, M. 144
Bekkevold, J.M. 11
Bektaş, B. 352
Belek, E.N. 181
Belen, S.N. 365
Berdeli, A. 313
Berdiyorov, G. 88
Bhaskar, S. 27, 290
Bıçak, T.C. 286
Bibin, B. 209
Bigalı, A. 201
Bikbaeva, G. 7
Bildirici, B.B. 118
Bilge, S. 68, 78, 85, 181, 228
Bilgi, E. 222
Bilir, A. 369
Bilisik, E. 125
Bilişik, K. 125
Birgun, N. 165, 165
Boccacini, A.R. 106
Bostancı, K. 87
Boyacıgil, S. 203
Boyacıoğlu, B. 237, 404
Boyacioglu, B. 236
Bozdağ, D. 358
Bozdoğan, A. 399
Bozkurt, P.A. 129, 213

Bozkurt, S. 332
Bozkurt, S.S. 81, 320
Böbrek, İ. 409
Böckmann, H. 345
Braniste, T. 227
Buke, G. 205
Buke, G.C. 167, 167, 167, 391, 393
Bulut, U. 282
Burgaz, S.H. 163
Busharov, Y. 74
Buyukcakir, O. 254
Büke, G.C. 168
Büklü, L.B. 400
Büküşoğlu, E. 39, 63
Bülbül, A. 278
Bütüner, B.D. 109
Büyükcakir, O. 249
Büyükçakır, O. 231
Büyükköse, S. 76, 111
Büyükserin, F. 180, 252
Büyüksungur, S. 178
Cagnetta, F. 260
Cahay, M. 167, 167
Cakan-Akdogan, G. 139, 139
Cakır, S. 372
Cakir, D. 52, 205, 272
Can, B. 339
Can, G. 373
Can, G.K. 72
Canlı, A.E. 395
Canpolat, N. 45
Cansever, M. 171
Canturk, B.S. 249, 254
Cantürk, B.S. 231
Capar, M.I. 389
Carenza, L. 60

Carenza, L.N. 63, 260
Castro-Méndez, A. 242
Cebeci, F.Ç. 103, 104
Celik, E.G. 100, 285, 287, 292, 301, 302, 317
Celik, R. 321
Celik, S. 110
Cemaloğlu, R. 85
Ceran, R.N. 192
Cetin, A.E. 20, 50, 71, 281, 300
Cetinkaya, A. 296
Cevik, O. 376
Ceyhan, M.E. 362
Ceyhan, R.Y. 402
Ceyirdekci, V. 100, 285, 287, 292, 302
Ceylan, M. 276
Chackrabarti, B.K. 387
Chakra, M.A. 23
Chananonnawathorn, C. 300
Chatterjee, A. 237
Cheffena, M. 111
Chen, Y. 64
Cho, J. 64
Chrappová, J. 348
Cicek, A. 347
Ciloglu, F.U. 27, 27, 290, 290
Cirpan, A. 283
Coskun, S. 84
Coşkun, F.M. 80, 332
Coşkun, İ.Y. 51
Cörüt, S. 149
Cross, G.L.W. 58
Cubukcuoglu, D.S. 418
Cunningham, B.T. 27, 290
Czaplewski, D.A. 64
Czelej, K. 127
Çağlayan, M. 344, 401

Çakır, S. 364
Çakır, T. 36
Çakmaktepe, S.C. 283, 412, 414, 417
Çamcı, P. 87
Çataklı, F.N. 318
Çay, A. 188
Çaylayık, N.S. 299
Çelebi, C. 59, 143, 163, 261, 392
Çelik, C. 79
Çelik, E.G. 99, 312
Çelik, S. 26, 86
Çetin, A. 369
Çetin, A.E. 339
Çetin, E.A. 423
Çetin, K. 377
Çetinel, A. 115
Çetiner, B. 18
Çetiner, F. 86
Çetintürk, K. 97, 116
Çevik, B. 245
Çevik, E. 41
Çevik, Ö. 354
Çırpan, A. 1, 41, 41, 41, 41, 53, 53, 53, 53, 55, 55, 55, 55, 119, 119, 119, 119, 145, 145, 145, 145, 172, 172, 172, 172, 238, 238, 238, 238, 243, 243, 243, 243, 246, 246, 246, 246, 247, 247, 247, 247, 412, 414, 415, 415, 415, 415, 417
Çiçek, Ş. 97
Çitil, B.E. 299
Çoban, G. 423
Çok, S.S. 126
Çoruh, C. 48, 408
Çotaoğlu, E.M.Z. 194
Çöpür, S.M. 343
Çubukcuoğlu, S. 87
Dadi, S. 289
Dağdeviren, H.D.Y. 106
Dalkılıç, B. 181

Dalkilic, F. 289
Danış, N. 276
Davut, K. 270
Değirmenci, E. 146
Demir, A. 57
Demir, F. 413
Demir, M. 185, 235
Demir, N.Y. 39
Demir, Y.D. 156
Demir, Z.A. 284
Demirbilek, N. 207
Demirbolat, G.M. 354, 376
Demirci, E. 151
Demirci, S. 221, 315
Demircioglu, O. 419
Demircioğlu, A. 229
Demirel, G. 71, 253, 331, 375
Demirel, G.B. 214, 244, 245, 251
Demirhan, A. 303
Demirkol, İ.N. 78
Demirtas, B. 84
Deniz, E. 202
Deniz, M. 87
Denizli, A. 278
Dereli, M. 252
Derici, Z.S. 276
Deveci, D.G. 59, 256, 261
Dias, R.A. 136
Dilbar, A. 220
Dilci, E.G. 37
Dinçer, O. 77
Dinu, M. 178
Dirican, E. 227
Dirican, N.E. 74
Doganay, D. 84
Doganci, E. 346

Doğan, G. 90
Doğan, H. 185
Doğan, M.Z. 380
Doğan, O. 361
Doğan, S. 165
Doğan, Ü. 274, 277
Dolanbay, S.N. 251
Dolenko, T. 7
Dolu, İ.B. 209
Dönmez, Ö. 274, 274
Dragomir, A.V. 178
Duatepe, F.P.G. 98
Dudás, Z. 126
Duman, D.C. 96, 306
Duman, G. 279, 310
Duman, N. 391
Duman, S. 49
Duman, Ş. 89
Dumoulin, F. 6
Duran, E.C. 13
Duran, T. 210
Durgun, E. 62
Durmaz, Y.Y. 23
Durukan, M.B. 107
Duygulu, Ö. 12
Dülcel, A.M. 143
Ebil, Ö. 248
Efe, E. 262
Egorova, A. 7
Eker, E.B. 33
Eker, F. 275
Ekinci, E. 307
Ekinci, G. 80, 332
Eksik, O. 204
El-Hout, S.I. 228
Elçioğlu, E.B. 121, 164, 201

Elgörmüş, N. 298
Elmalı, A. 341
Elmas, E.N. 288
Eminoğlu, H.F. 274, 274
Emre, A.E. 259
Emre, F.B. 307
Eray, M. 265
Erbey, D.N. 206
Ercan, B. 107, 158, 176, 178, 208, 380
Ercem, O. 348
Erdali, A.D. 202
Erdem, E. 21, 142, 179, 218, 219, 229
Erdem, Z.S. 189
Erdemir, E. 291
Erdogan, G. 125
Erdogmus, M. 249, 254
Erdoğan, T. 99
Erdoğan, U. 79
Erdoğan, Y.K. 158
Erdoğan, Z.K. 206
Erdoğmuş, M. 231
Eren, M.Ç. 216
Erez, O. 139
Ergen, O. 127
Ergen, S. 253
Erikli, T.E. 171
Erkey, C. 36
Erkey, P.C. 329
Eroğlu, H. 399
Eroğlu, Z. 368
Erol, A. 274, 274, 347, 388
Ershadrad, S. 193
Ersoy, S. 79, 209, 223
Ertaş, F.N. 188
Ertemcoz, G. 292
Eskandari, Z. 31

Eşit, Ö.F. 37
Evran, S. 302
Eyibilen, M.E. 339
Fafal, T. 130
Fahmi, A. 327, 385
Fasy, B.J. 60
Fatima, A. 173
Filiz, A. 97, 116
Filiz, V. 333
Fuerkaiti, F. 114
Gaber, A. 78, 228
Ganız, M. 238
Garcia, I. 57
Garcia, I.S. 136
Gecalp, Y. 249, 254
Geçalp, Y. 231
Gelen, S.S. 316
Genc, D. 379
Genç, M.K. 188
Genç, N.S. 347
Gergin, Z. 384
Ghasemi, M. 182
Ghorbanizamani, F. 100, 317, 325
Gizer, T.D. 118
Gizlenci, B. 279, 310
Gogotsi, Y. 205
Gok, C. 50
Gokkaya, D. 371
Goksel, T. 100
Goktas, T. 250
Gouveia, M. 60
Gök, İ.Y. 423
Göreli, M.C. 223
Görkan, T. 62
Gözek, M. 143, 392
Gözükara, A.S. 405

Guden, H.N. 333
Gul-Mete, A. 139, 139
Guler, S. 84
Gultekin, B. 133
Gunes, O.C. 250
Gurpinar, E. 167, 393
Gursoy, M. 419
Güçlü, A.D. 170
Güden, M. 270
Güdümcüoğlu, N. 421
Gül, T.F. 186, 241
Güleç, Ö.F. 410
Güler, G.Ö. 377
Gülgün, M.A. 225
Güllü, H.H. 334
Gülseroğlu, S. 252
Gültekin, Y. 361
Gültekinoğlu, M. 38, 380
Gümrah, Ö. 129, 213
Gümüş, M.B. 359
Gümüş, S. 53, 415
Gümüşkaya, İ.T. 107, 208
Günaydın, D.N. 412, 414, 417
Güncan, U. 422
Gündoğdu, V. 109
Güneysu, Z.S. 37
Güngör, A. 142, 179
Güngörmüşler, M. 183
Gür, S.D. 298
Gürbüz, H. 395
Gürbüz, H.N. 293, 314
Gürmen, S. 127
Gürsel, S.A. 18
Gürses, A. 45
Gürses, B.O. 112, 386
Gürsoy, A. 243

Gürsu, A.S. 323
Güven, S. 276
Güvenç, T.A.A. 132
Güzel, U. 233
Hacıefendioğlu, T. 174
Hacıibrahimoğlu, S. 423
Hafızoğlu, E.D. 18
Haghmoradi, N. 18
Hajri, E.A. 102, 165
Hall, S. 23
Hanay, M.S. 136
Hanay, S. 57
Hanedar, B.A. 48, 269
Harder, M. 236, 237
Hasanah, K.M. 65
Hasırcı, N. 178
Hasin, H.S. 203
Haskoloğlu, İ.C. 362
Hatipoglu, A. 325
Helvacı, Ş.Ş. 212
Hemmida, M. 348
Hengsbach, R. 327, 385
Heppekcan, N. 252
Hincheeranan, W. 300
Horprathum, M. 300
Hosseini, S.F. 31
Hosseinjany, A. 42
Hoyer, K. 270
Hsu, C. 28
Huang, C. 28
Hukum, K.O. 253
Hut, E. 388
Hürkul, M. 296
Igdır, M.J.A. 47
Ikemoto, S. 135
Iken, T. 52, 272

Ilgın, P. 356
Irmak, G.O. 12
Ismayilova, S. 313
Issatayev, N. 74
İbik, A.A.B. 421
İbiş, Ö. 211, 328
İkizler, B. 212, 318
İldeş, C. 232
İnan, T.Y. 387, 416
İnanç, M. 199
İnce, G.O. 409
İnce, G.Ö. 42
İpek, S. 149
İzbudak, B. 381
Jafari, S.M. 363
Jahangir, R. 234
Jamoliddin, R. 220
Jarczewski, S. 239
Jovanović, S. 296
Jungmann, G. 83
Kabak, M. 229
Kabay, N. 87, 241
Kadeş, G. 412, 414, 417
Kahraman, M. 26
Kala, E.D. 223
Kalaycioglu, G.D. 31
Kalimuldina, G. 74
Kalkan, H. 70
Kamenskyi, D. 348
Kamoladdin, S. 220
Kaplan, B.Y. 18
Kaptanoglu, I.G. 324
Kapucu, B.G. 423
Kara, A. 32, 278, 309, 361
Kara, Y. 221, 315
Karaaslan, M. 399

Karabayır, E.S. 356
Karabıyık, M. 248
Karaca, S. 214
Karacali, A. 61, 135
Karacan, E.N. 76
Karacaoğlu, M.A. 86
Karahan, H.E. 203, 240, 286, 295, 395
Karakaş, Y.E. 267
Karakeçili, A. 68
Karakoc, B.N. 368
Karakurt, O. 41, 247, 283, 414, 417
Karakuş, C.Ö. 17, 222
Karakuş, E. 207, 291
Karatay, A. 341
Karatutlu, A. 224, 333, 344, 401
Karausta, A. 63
Karav, S. 275
Kardiyen, F. 251
Karimkhani, M.M. 363
Karman, F.O. 112
Kars, M.D. 314
Kartal, R.B. 381
Katı, A. 95, 116
Kats, M.A. 64
Kavukcu, B. 133
Kaya, C. 79, 209
Kaya, D. 235
Kaya, İ. 26
Kaya, İ.D. 208
Kaya, K. 229
Kaya, M. 216, 275
Kaya, Ş. 242
Kaya, T. 409
Kayaci, H.U. 84
Kayalar, H. 130
Kazancıoğlu, B. 145

Kehr, N.S. 156, 319, 374
Keleş, H. 342
Kelle, K. 128
Kelleci, S.O. 37
Kermen, E. 128
Keserci, A.Z. 172
Kesici, B. 396
Keskin, N.O.S. 131
Kesmez, Ö. 413
Ketenoğlu, D. 236, 237, 404
Khakimjan, B. 220
Khalid-Salako, F. 75, 75
Khurshid, S. 220
Kılıc, K. 194
Kılıç, A. 76, 111
Kılıç, M.D. 188
Kılıç, T.I. 112
Kılıçarslan, B. 38
Kıran, S.B. 177, 222
Kırlıoğlu, A.C. 18
Kızıldağ, N. 76
Kızılel, S. 359
Kibar, G. 160, 308
Kimizuka, K. 135
Kip, Ç. 423
Kiraz, A. 289
Kişin, D.N. 312
Kivrak, E. 294
Kivshar, Y. 64
Koc, B. 110
Koca, C. 137
Koca, F.A. 263
Kocak, Y. 202
Kochan, E. 301
Koç, E.E. 350
Koç, F. 212

Koç, S. 251, 398
Koçak, C.Ö. 361
Koçhan, E. 287
Kodolbaş, A.O. 400
Koh, Y. 176
Kol, M. 151
Kolay, İ. 174, 262, 263, 265, 266, 267, 268
Kolbusz, P. 239
Kolesnikov, I. 7
Kolukısa, A. 279
Kopar, E.E. 128
Koparan, U. 341
Korkmaz, A. 419
Korkmaz, B. 68
Korkmaz, G. 368
Korkmaz, M. 94, 125
Koru, Z.E. 279, 305, 310, 312, 317
Kose, E. 331
Kose, Y. 128
Koşar, A. 5, 219
Kotmakçı, M. 109
Kozan, S. 314
Köken, D. 103, 104
Köroğlu, D. 43
Köse, K. 159
Köse, M.D. 212
Kösebay, Ö.N. 48
Köseoğlu, E. 322
Köylü, C.Y. 152, 406, 407
Köytepe, S. 307
Kucuk, E. 294
Kucukcobanoglu, Y. 65
Kumar, B. 64
Kumralbaş, A. 408
Kurniawan, M.A. 370
Kurt, A. 296

Kurt, H. 75, 75
Kurtz, F. 345
Kuruoğlu, F. 64, 347
Kuş, A.G. 255
Kutman, U.B. 67
Küçük, S. 91
Küçüktartar, T. 343
Lang, F. 242
Lau, D.T. 290
Lertvanithphol, T. 300
Leuchs, G. 2
Lillepäg, J. 333
Liman, G. 253, 375
Liou, J. 28
Liu, C. 203
Liu, W. 290
Luo, Z. 141
Macit, S. 23
Madenoğlu, T.G. 87
Maldonado, E.A.L. 186
Malkoçoğlu, H.Y. 359
Mammadov, H. 397
Man, E. 302
Manav, S. 402
Manshina, A. 7
Mansoor, M. 127, 127, 127, 184, 184, 184
Mansuroğlu, B.A. 251
Maraşlıoğlu, C. 415
Mariya, P. 220
Marzi, M. 129
Mavi, A. 32, 309
Mavili, E. 310
Maziukiene, M. 273
McKenzie, Ç. 385
Mech, K. 239
Memioğlu, D. 176

Menceloğlu, Y. 30
Mercan, S. 188
Mermer, H. 264
Mertol, Ş. 116
Mesudiyeli, E. 170
Metin, O. 368
Milićević, M. 296
Milosevic, M.V. 62
Misirlioglu, F.B. 179
Mittal, S. 290
Moghaddam, S.J. 326
Mojarrad, N.R. 18
Moradi, O. 196, 219, 229
Morkaya, E. 329
Moulahoum, H. 100, 317, 325
Muftuler, F.Z.B. 321
Munir, I. 138
Munoz, C. 52
Muradov, M. 40
Musayeva, T. 397
Mustafa, M.S.M. 115
Mustafa, W. 23
Mustafaoglu, N. 118
Mutlu, B. 89
Mutlu, P. 96, 306
Mutlu, S. 333
Mutlu, V.N. 18
Muzhen, X. 61
Naguib, M. 205
Nakipoglu, M. 373
Nakipoğlu, B. 155
Nalçakan, H. 152, 406, 407
Namvari, M. 110, 387
Narang, J. 292, 302
Naser, I. 23
Naseri, S. 341

Nasser, H. 182
Navarrete, J. 167
Nazir, F. 138
Negro, G. 60, 260
Nguyen, M. 290
Nidda, H.K.V. 348
Nigiz, Ş. 361
Nirwan, V.P. 327, 385
Ocak, B. 133
Ocsoy, I. 289, 311, 353
Odabaş, Ö.C. 12
Odacı, D. 316
Oğur, E. 132
Oğuz, F. 342
Okan, B.S. 102, 102, 165, 165, 171
Okay, E. 393
Okcu, E. 170
Okutan, E. 420
Olğar, M.A. 162
Olim, R. 220
Onan, D. 304
Onbaşlı, K. 69
Oncel, N. 52, 272
Oner, H. 375
Onur, M.A. 308, 423
Onuralp, D.B. 74
Oral, B.E.B. 98
Ordu, M. 10, 74, 93, 101, 173, 227, 351
Orhan, O.B. 343
Orhon, A. 183
Ortaç, B. 224, 333, 401
Ouzaid, Z. 137
Ova, A.Ö. 177
Ozay, O. 360, 365, 367, 372
Ozbayrak, I. 84
Ozcan, F. 419

Ozcubukcu, S. 297
Ozdemir, Y. 303
Ozdil, Z.C.C. 190
Ozdogan, M. 52, 272
Ozel, F. 47
Ozel, S. 47
Ozer, M.S. 368
Ozgunes, G. 389
Ozkan, S.A. 296
Ozmen, O.T. 280
Oztas, M. 308
Oztekin, T. 65, 325
Ozufuklar, O. 100, 285, 287, 292, 302
Ökçün, A. 277
Ölçeroğlu, B. 95, 97, 116
Önal, M. 152, 406, 407
Önel, S. 37
Ören, E.E. 192
Öz, E. 236, 237
Öz, M.N. 248
Özay, H. 356
Özay, Ö. 33, 356, 364, 371
Özay, S. 132
Özbay, E. 323, 342
Özbey, D.H. 62
Özcan, M. 269
Özçelik, O. 405
Özçelik, V.O. 43, 200, 408, 409
Özdamar, A.B. 108, 352
Özdemir, B. 67
Özdemir, E. 96, 306
Özdemir, O. 76
Özdemir, Y. 410
Özdilek, Ş. 277
Özdoğan, M. 396
Özer, H. 89

Özer, H.Ö. 58, 169, 256
Özkan, B. 386
Özkan, G. 215
Özkan, M. 212
Özkan, S.A. 14
Özkan, Ş. 112, 386
Özkaya, B. 197
Özkaynak, Y. 286
Özlen, K. 164
Özonuk, O.Ç. 380
Özsaltık, C. 196
Özsoy, G.H. 53, 55, 119, 145, 238, 412, 415
Öztekin, Y. 293
Öztürk, A. 176, 206
Öztürk, A.B. 381
Öztürk, H.Ü. 359
Öztürk, M. 151
Öztürk, N. 361
Özunal, Z.G. 339
Özünal, Z. 369
Özünal, Z.G. 362
Pachernegg-Mair, L. 387
Palancı, H.S. 137
Palavan, E. 315
Pamık, D.T. 320
Pamik, D.T. 81
Pamuk, U. 72
Pana, I. 178
Parau, A.C. 178
Park, J. 176, 176
Parlak, B. 112
Parlak, O. 22
Parmaksiz, O. 102, 102
Parto, D.B. 274
Pashayev, B. 397
Pasqualon, S. 348

Patır, B. 18
Pehlivan, S. 180
Pehlivan, Z.S. 75
Pehlivanoğlu, P. 352
Pehlivanoğlu, S. 385
Peker, H.U. 133
Pekerten, B. 148
Pınar, A. 398
Pilip, A. 7
Piravadili, S. 185
Polat, B. 244
Polat, E. 279, 305, 310, 312, 317
Polat, E.O. 46, 150, 393
Polat, G. 158
Polat, H. 108, 216, 352
Polat, M. 108, 216, 423
Porrang, S. 118
Qasem, H.A. 224
Rad, M.E. 30
Rahman, M. 93, 227
Rakovský, E. 348
Rashidinejad, A. 363
Rasulova, K. 358
Razmarafar, R. 260
Ropers, C. 345
Rosas, S. 64
Rouhi, S. 127, 184
Ruzgar, S.T. 128
Saçlı, E.Ü. 112
Sağıroğlu, E.D. 334
Sağkol, E. 421
Sağlam, Ö. 183
Sahin, A. 384
Sahin, A.B. 118
Sahin, D. 133
Sahin, Y. 338

Sakar, N. 217, 250
Salhi, A. 88
Samad, Y.A. 102, 102, 165, 165
Sandık, B. 318
Sanyal, B. 193
Sarcan, F. 388
Sargın, G.Ö. 120
Sarıboğa, F. 112
Sarıkanat, M. 44
Sarıtaş, E. 229
Sarkmaz, Y.E. 112
Satılmış, M. 342
Saurabh, K. 153
Savacı, U. 56
Savru, İ. 226
Say, Z. 202
Sayın, Ç. 42
Sayınman, B. 420
Scala, G. 16
Seçkin, T. 307
Seçkin, U.D. 105, 383
Seki, Y. 44
Selçuk, A.A. 112, 386
Selvi, E. 26
Semercioğlu, A.T. 329
Senger, R.T. 49
Sennaroğlu, A. 382
Senturk, B. 34, 280
Serhatlı, M. 359
Serim, T.M. 96
Sert, Ş. 166
Sevik, C. 62
Sevinçli, H. 170
Seyitdanlıoğlu, P. 70
Seymen, A.A. 401
Sezgin, H.T. 355, 378

Shaddel, R. 326, 363
Shahid, K.F. 72
Shavkat, M. 220
Shirinova, H. 397
Silva, P.P. 136
Simsek, S. 300
Singh, V.P. 74, 227
Sisman, Z. 186, 241
Siyah, P. 97
Siyahjani-Gultekin, S. 133
Skvorcinskiene, R. 273
Snee, P.T. 258
Socaciu-Siebert, L. 140
Solak, K. 32, 309
Solovchuk, D.R. 28
Solovchuk, M. 153
Soyat, S.N. 366
Soydan, D.A. 214
Soydaner, K. 191
Soyer, F. 177
Soylemez, S. 122, 282, 283, 288, 297, 333
Soyler, D. 122, 283, 297, 333
Soytaş, S.H. 67, 271
Sozer, Y. 297
Sönmez, E. 286
Sönmez, S.N. 58, 256
Sönmezoğlu, S. 227
Sözer-Demirdas, S.C. 139
Sözmen, F. 341
Spiekermann, G. 236, 237
Spirk, S. 387
Suleiman, A.A. 54, 191, 199
Sultanova, J. 397
Suna, G. 291
Surucu, O. 29
Suyolcu, Y.E. 24

Süleymanzade, U. 156
Şahin, C. 193
Şahin, E. 45, 177
Şahin, M. 252, 291, 293
Şahin, M.A. 330, 334
Şahin, O. 77
Şahin, Ö. 293
Şahin, T.E. 156
Şahinaslan, S. 41, 247
Şaylıgil, Ö. 121
Şen, S. 131, 215, 226, 396
Şendemir, A. 105, 206, 206, 383
Şengüler, G.Y. 341
Şensoy, Ö. 23
Şentürk, D. 405
Şentürk, S. 203, 395
Şişman, N. 161, 175
Tabak, E. 323
Tabaru, T.E. 191, 224, 344, 401
Tabel, E. 357
Taç, G.D. 322
Tamukoh, H. 135
Tan, E. 258
Tanaka, H. 61, 135
Tanatar, B. 91
Tantiwanichapan, K. 300
Tarhan, O. 363
Tarım, T.G. 177
Tas, B. 280
Taşkıran, T. 193
Taştekin, R.A. 403
Tataroğlu, A.A. 390
Tavukçu, E.E. 207
Tekin, E.D. 154
Tekin, N.D. 92
Tekin, O. 53, 415

Tekkalmaz, M.S. 237
Temelli, B. 70
Temur, L.Ö. 261
Temur, N. 289, 311
Tepeli, D. 374
Terlemez, G. 355
Tezcan, D. 233
Tezeren, G. 352
Tırpan, E.S. 209
Timur, S. 100, 127, 279, 285, 287, 292, 302, 305, 310, 312, 317, 325
Tiryaki, A. 384
Titko, D. 144
Toffoli, H. 404
Tok, Ç. 342
Tok, K. 305, 312, 317, 325
Toker, E. 340
Tokgoz, M.M. 44
Tongur, T. 327, 385
Top, A. 215, 226
Top, C.B. 214
Topal, G.R. 194
Toparlı, Ç. 334
Topcu, A.B. 202
Topel, Ö. 370
Topel, S.D. 327, 349, 366, 385
Topkaya, S.N. 50, 281
Toplu, G. 162
Toppare, L. 257
Toprak, A. 330
Toptan, F. 132
Torsten, G. 387
Torun, G. 391, 393
Tözendemir, B. 330
Tufan, Y. 176
Tulumtas, A. 419
Tuncel, A. 423

Tuncer, M. 377
Turan, R. 84, 182
Ture, A.Z. 418
Turhan, S.M. 213
Tuzcu, A. 369
Tuzcu, A.B. 362
Türkatar, M. 55
Türkmen, G. 133
Türköz, N. 212
Türkpençesi, B.İ. 270
Türktaş, M. 251
Ulag, S. 384
Uluca, A. 58
Ulusel, M. 77
Uluturhan, O.S. 393
Umrao, S. 290
Unalan, H.E. 84, 419
Unlu, M.S. 298
Unlu, N.L. 113
Unlu, S. 362, 369
Unver, S.K. 84
Unveroglu, B. 289
Urlu, Y.C. 161
Usami, Y. 61, 135
Uslu, O. 344
Utlu, G. 163
Uvak, İ. 197
Uyanık, Y.E. 237
Uzer, B. 177, 270
Uzuner, B.E. 145
Uzuner, M. 310
Uzunoglu, A. 394
Üçüncü, D. 252
Ülkem, N. 343
Ümekkan, K. 236
Ünal, H. 67

Ünal, N. 144
Ünalan, H.E. 15, 41, 107
Üngör, M.E. 134, 335
Ünlü, C. 51, 211, 328
Ünlü, C.G. 390
Ünlü, F.Y. 211
Ünlü, M.S. 3, 113
Ünlü, N.L. 298
Ünlütürk, S.S. 421
Ünüvar, Ü. 157
Ünver, H. 237
Ünverdi, A. 277
Ünverdi, Ö. 59, 124, 143, 256, 261
Ürgen, M. 127
Ürküt, N. 295
Vargun, E. 379
Verma, A. 159
Veziroglu, S. 80, 332
Vitelaru, C. 178
Vitushkina, S. 348
Vlaisavljevich, E. 23
Vorotinskiene, L. 273
Vural, İ. 361
Wang, X. 290
Wang, Y. 159
Yaghmur, A. 31
Yağız, G. 248
Yakut, Ş. 274
Yalcin, D. 376
Yalçın, D. 354
Yalçın, M.E. 259
Yalçinkaya, T.T. 188
Yalvaç, D. 55
Yaman, Ş.Ö. 129
Yanasık, S. 287
Yanasik, S. 301

Yanaz, Ö. 196
Yapıcı, K. 195, 271, 410
Yarar, E. 380
Yardim, A. 100, 302
Yavuzhan, S. 279, 305, 310, 312
Yayla, S. 296
Yazıcı, H.D. 390
Yeke, M. 396
Yelboğa, T. 330
Yeltik, A. 199, 342
Yenen, B. 256
Yener, Y. 79
Yenidoğan, E. 53, 415
Yeniterzi, D. 122, 282, 288
Yerci, S. 145, 145, 145
Yesilkoy, F. 64
Yesiloz, G. 35, 114, 138, 234, 357
Yesiltepe, O. 316
Yetiş, K. 178
Yetişkin, E. 307
Yıldırım, C. 203, 240, 286, 295, 395
Yıldırım, D.H. 257
Yıldırım, E. 53, 155, 257
Yıldırım, F.N. 169
Yıldırım, G. 247
Yıldırım, I.D. 179, 219
Yıldırım, İ.D. 142
Yıldız, A.A. 106
Yıldız, A.E. 150
Yıldız, E. 341
Yıldız, M. 236, 237
Yılmaz, A. 117, 221, 315
Yılmaz, A.E. 213
Yılmaz, E.P. 119
Yılmaz, F. 278
Yılmaz, G. 133

Yılmaz, G.Z. 240
Yılmaz, H.N. 300
Yılmaz, M. 221, 315
Yılmaz, S. 305, 312, 317
Yılmaz, S.N. 274
Yılmaz, Y. 225
Yılmaz, Y.E. 223
Yılmaz, Z.K. 251
Yılmaz, Z.S. 130
Yiğit, M. 215
Yildiz, E. 71
Yildiz, N.T. 360
Yilmaz, C. 73, 289, 353
Yilmaz, E. 386
Yilmaz, N.B. 379
Yilmaz, O. 346
Yilmaz, S.S. 333
Yin, S. 64
Yorgancılar, M.H. 297
Yorulmaz, Y. 103, 104
Youngblood, J.P. 159
Yousefzade, H. 329
Yousefzadeh, H. 36, 418
Yuce, M. 30
Yunt, E. 25
Yurdakul, O.C. 84
Yurddaskal, M. 94, 217
Yusan, S. 34, 186, 241, 280
Yüce, M. 75
Yücel, M. 39
Yücesoy, D. 177, 284
Yücesoy, D.T. 378
Yüksel, A.E. 227
Yürekli, Y. 206
Yürüm, A. 18
Zahedi, Y. 326

Zahidov, A. 18
Zahrabi, M. 110
Zaid, A. 185
Zaidi, R. 387, 416
Zaimoğlu, U. 336
Zan, R. 162
Zaraee, N. 298
Zeybek, N.D. 361
Zhang, T. 391
Zheng, K. 106
Zırhlı, O. 103, 104
Zihnioglu, F. 305, 317
Zihnioğlu, F. 312, 325
Zulfikar, B. 204
Zuraiqi, K. 147



Organizing Office

ARBER Conference Solutions

meetinghand
Conference Management Software

www.nanotr.org